MEMOIRS
of the
American Mathematical Society
ISSN 0065-9266 (print)
ISSN 1947-6221 (online)
Number 1645

Surgery Exact Triangles in Involutive Heegaard Floer Homology

Kristen Hendricks
Jennifer Hom
Matthew Stoffregen
Ian Zemke

July 2026 • Volume 323 • Number 1645 (first of 5 numbers)

AMS American Mathematical Society

MEMOIRS
of the
American Mathematical Society
ISSN 0065-9266 (print)
ISSN 1947-6221 (online)

Number 1645

Surgery Exact Triangles in Involutive Heegaard Floer Homology

Kristen Hendricks
Jennifer Hom
Matthew Stoffregen
Ian Zemke

July 2026 • Volume 323 • Number 1645 (first of 5 numbers)

AMS American Mathematical Society

Library of Congress Cataloging-in-Publication Data

Cataloging-in-Publication Data has been applied for by the AMS.
See http://www.loc.gov/publish/cip/.

DOI: https://doi.org/10.1090/memo/1645

Memoirs of the American Mathematical Society

This journal is devoted entirely to research in pure and applied mathematics.

Subscription information. Beginning in 2024, Memoirs will be published monthly through 2026. Memoirs is also accessible from www.ams.org/journals. The 2026 subscription begins with volume 317 and consists of twelve mailings, each containing one or more numbers. Individual subscription prices for 2026 are as follows. For electronic only: US$1075. For paper delivery: US$1233. Add US$100 for delivery within the United States; US$235 for surface delivery outside the United States. Upon request, subscribers to paper delivery of this journal are also entitled to receive electronic delivery. For information on institutional pricing, please visit `https://www.ams.org/publications/journals/subscriberinfo`. Subscription renewals are subject to late fees. See `www.ams.org/journal-faq` for more journal subscription information. Each number may be ordered separately; please specify number when ordering an individual number.

Back number information. For back issues see `www.ams.org/backvols`.

Subscriptions and orders should be addressed to the American Mathematical Society, P. O. Box 845904, Boston, MA 02284-5904 USA. *All orders must be accompanied by payment.* Other correspondence should be addressed to 201 Charles Street, Providence, RI 02904-2213 USA.

Copying and reprinting. Individual readers of this publication, and nonprofit libraries acting for them, are permitted to make fair use of the material, such as to copy select pages for use in teaching or research. Permission is granted to quote brief passages from this publication in reviews, provided the customary acknowledgment of the source is given.

Republication, systematic copying, or multiple reproduction of any material in this publication is permitted only under license from the American Mathematical Society. Requests for permission to reuse portions of AMS publication content are handled by the Copyright Clearance Center. For more information, please visit `www.ams.org/publications/pubpermissions`.

Send requests for translation rights and licensed reprints to `reprint-permission@ams.org`.

Excluded from these provisions is material for which the author holds copyright. In such cases, requests for permission to reuse or reprint material should be addressed directly to the author(s). Copyright ownership is indicated on the copyright page, or on the lower right-hand corner of the first page of each article within proceedings volumes.

Memoirs of the American Mathematical Society (ISSN 0065-9266 (print); 1947-6221 (online)) is published bimonthly (each volume consisting usually of more than one number) by the American Mathematical Society at 201 Charles Street, Providence, RI 02904-2213 USA. Periodicals postage paid at Providence, RI. Postmaster: Send address changes to Memoirs, American Mathematical Society, 201 Charles Street, Providence, RI 02904-2213 USA.

©2026 Kristen Hendricks, Jennifer Hom, Matthew Stoffregen, and Ian Zemke. All rights reserved.

This publication is indexed in *Mathematical Reviews*®, *Zentralblatt MATH*, *Science Citation Index*®, *Science Citation Index*™*-Expanded*, *ISI Alerting Services*℠, *SciSearch*®, *Research Alert*®, *CompuMath Citation Index*®, *Current Contents*®*/Physical, Chemical & Earth Sciences*.
This publication is archived in *Portico* and *CLOCKSS*.
Printed in the United States of America.

⊗ The paper used in this book is acid-free and falls within the guidelines established to ensure permanence and durability.
Visit the AMS home page at `https://www.ams.org/`

10 9 8 7 6 5 4 3 2 1 31 30 29 28 27 26

This is a free offprint provided to the author by the publisher. Copyright restrictions may apply.

Contents

Chapter 1. Introduction 1
1.1. Involutive surgery exact sequences 1
1.2. The involutive mapping cone formula 2
1.3. Knots in S^3 3
1.4. An application to the homology cobordism group 5
1.5. The involutive hypercube of a surgery triad 7
1.6. The doubling model of the involution 8
1.7. Organization 8

Chapter 2. Involutive Heegaard Floer homology 11
2.1. 3-manifolds 11
2.2. Knots 12
2.3. Twisted 3-manifold complexes 13

Chapter 3. Iota complexes and mapping cones 15
3.1. ι-complexes 15
3.2. Local equivalence 16
3.3. Almost ι-complexes and almost local equivalence 16
3.4. ι_K-complexes 18
3.5. The algebraic involutive mapping cone 20
3.6. The algebraic cone is an iota-complex 26
3.7. The local equivalence class of surgeries 33
3.8. Correction terms of integer surgeries 39

Chapter 4. An application to the homology cobordism group 43
4.1. Some tensor products 43
4.2. The ι_K-complex of $-2T_{6,7}\#T_{6,13}\# - T_{2,3;2,5}$ 49
4.3. Surgery along $-2T_{6,7}\#T_{6,13}\# - T_{2,3;2,5}$ 54
4.4. Almost local equivalence classes and $S^3_{+1}(-2T_{6,7}\#T_{6,13}\# - T_{2,3;2,5})$ 56

Chapter 5. Hypercubes and hyperboxes 59
5.1. Hyperboxes of chain complexes 59
5.2. Stacking and compressing hyperboxes 60
5.3. Mapping cones and hyperboxes 62
5.4. Hypercubes and involutive complexes 64
5.5. Hyperboxes of attaching curves 65
5.6. Pairing hypercubes of attaching curves 66
5.7. Hypercubes with twisted coefficients 67
5.8. Low dimensional notation 67

This is a free offprint provided to the author by the publisher. Copyright restrictions may apply.

Chapter 6. Doubled Heegaard diagrams and the involution 69
6.1. Doubled Heegaard diagrams 69
6.2. Doubled diagrams for knots 70
6.3. The involution via doubling 71
6.4. Doubling and the involutive hypercube of a triad 72
6.5. Admissibility and doubled diagrams 73

Chapter 7. Moduli spaces and almost complex structures 77
7.1. Almost complex structures for holomorphic disks 77
7.2. Moduli spaces of disks 77
7.3. Moduli spaces with matching conditions 78
7.4. Expected dimensions 79
7.5. Cylindrical boundary degenerations 81
7.6. Boundary degenerations and split almost complex structures 82
7.7. Boundary degenerations and generic almost complex structures 82
7.8. Boundary degenerations for generic almost complex structures 83
7.9. Holomorphic polygons and related constructions 86
7.10. Compactifications via holomorphic combs 88

Chapter 8. Degenerating connected sum tubes 91
8.1. Connected sums and matched moduli spaces 91
8.2. Matched chain complexes for connected sums 92
8.3. Maximally pinched families of almost complex structures 93

Chapter 9. Stabilizing Heegaard multi-diagrams 95
9.1. Stabilizing Heegaard diagrams 95
9.2. Stabilizing Heegaard triples 96
9.3. Stabilizing Heegaard quadruples 96
9.4. Index tuples 97

Chapter 10. Stabilizations and holomorphic curves 101
10.1. Stabilizations and holomorphic disks 101
10.2. Stabilizations and holomorphic triangles 102
10.3. Stabilizations and holomorphic quadrilaterals 105
10.4. Lens space stabilizations of Heegaard diagrams 107
10.5. Lens space stabilizations and holomorphic triangles 108
10.6. Lens space stabilizations and holomorphic rectangles 109

Chapter 11. Holomorphic triangles and nearest point maps 111
11.1. Vertex multiplicities 111
11.2. Approximating triangle classes 112
11.3. Proof of Proposition 11.1 113
11.4. Small isotopies and Heegaard quadruples 114

Chapter 12. Input from Ozsváth and Szabó's surgery exact sequence 117
12.1. Surgery quadruples 117
12.2. Heegaard Floer homology of lens spaces 117
12.3. Cobordism maps for disk bundles over S^2 118
12.4. The length 1 maps on the top and bottom of the main hypercube 119
12.5. The length 2 maps along the top and bottom of the main hypercube 120

This is a free offprint provided to the author by the publisher. Copyright restrictions may apply.

12.6. Heegaard quadruples related to disk bundles 120

Chapter 13. Hypercubes for changing the almost complex structure 123

Chapter 14. Hypercubes for stabilization 127
14.1. Singular stabilization hypercubes 127
14.2. Desingularization hypercubes 129

Chapter 15. The first 2-handle hypercube 131

Chapter 16. The central hypercube 135
16.1. Almost complex structures 135
16.2. Standard curves in the surgery region 135
16.3. The hypercube $\mathcal{C}^{(1)}_{\mathrm{cen}}$ 136
16.4. The hypercube $\mathcal{C}^{(2)}_{\mathrm{cen}}$ 139
16.5. The hypercube $\mathcal{C}^{(3)}_{\mathrm{cen}}$ 144
16.6. Constructing $\mathcal{C}_{\mathrm{cen}}$ 150
16.7. Compatibility with the involution 151

Chapter 17. The second 2-handle hypercube 153
17.1. Heegaard diagrams for $\mathcal{C}^2_{2\text{-h}}$ 153
17.2. Constructing $\mathcal{C}^2_{2\text{-h}}$ 154

Chapter 18. The tautological and flip-map hypercubes 157
18.1. The tautological hypercube 157
18.2. The flip-map 158
18.3. More hypercubes with twisted coefficients 159
18.4. The flip-map hypercube 160

Chapter 19. Constructing the null-homotopy H_E 167
19.1. The endomorphism E 167
19.2. Vector fields for deformations 168
19.3. Local degree theory 171
19.4. The connected sum formula by deforming the matching 173
19.5. Deformed stabilizations 178
19.6. Deformed stabilizations and holomorphic triangles 179
19.7. Deforming E 180
19.8. Proof of Proposition 19.12 184

Chapter 20. The involutive mapping cone formula and surgery exact sequence 209
20.1. Truncations 210
20.2. Filling hypercubes 211
20.3. Gradings 213
20.4. Proof of Theorem 20.1 217
20.5. Proof of Theorems 1.2 and 1.3 221

Chapter 21. The strong cone formula for L-spaces 223
21.1. Overview of the proof of Theorem 21.1 223
21.2. The hypercube $\mathcal{K}_{\mathfrak{r}_s}$ 226
21.3. The hypercubes $\mathcal{K}_{1\text{-h};\mathfrak{y}_s}$, $\mathcal{K}^1_{2\text{-h};\mathfrak{y}_s}$, $\mathcal{K}^2_{2\text{-h};\mathfrak{y}_s}$ and $\mathcal{K}_{3\text{-h};\mathfrak{y}_s}$ 230
21.4. The hypercube $\mathcal{K}^{(1)}_{\mathrm{cen};\mathfrak{y}_s}$ 234

This is a free offprint provided to the author by the publisher. Copyright restrictions may apply.

21.5. The hypercube $\mathcal{K}^{(2)}_{\mathrm{cen};\mathfrak{y}_s}$ 237
21.6. The hypercube $\mathcal{K}^{(3)}_{\mathrm{cen};\mathfrak{y}_s}$ 240
21.7. The hypercubes $\mathcal{K}_{\eta;\mathfrak{y}_s}$ and $\mathcal{K}_{\mathfrak{F};\mathfrak{y}_s}$ 241

Chapter 22. Rational surgeries and 0-surgeries 245
22.1. Rationally null-homologous knots 245
22.2. Spin^c structures 246
22.3. The cobordism $W_{\lambda,\lambda+m}$ 248
22.4. Negative surgeries 250
22.5. Knot Floer homology and rationally null-homologous knots 251
22.6. Ozsváth and Szabó's mapping cone formula for rationally null-homologous knots 252
22.7. The involutive mapping cone formula for rationally null-homologous knots 255
22.8. Rational surgeries 256
22.9. 0-surgeries 260

Bibliography 261

This is a free offprint provided to the author by the publisher. Copyright restrictions may apply.

Abstract

We establish a surgery exact triangle for involutive Heegaard Floer homology by using a doubling model of the involution. We use this exact triangle to give an involutive version of Ozsváth-Szabó's mapping cone formula for knot surgery. As an application, we use this surgery formula to give examples of integer homology spheres that are not homology cobordant to any linear combination of Seifert fibered spaces.

Received by the editor November 13, 2020, and, in revised form, November 13, 2023, January 7, 2025, and July 1, 2025.

Article electronically published on September 28, 2026.

DOI: https://doi.org/10.1090/memo/1645

2020 *Mathematics Subject Classification.* Primary 57K18, 57K31, 57R58.

KH was partially supported by NSF grant DMS-2019396 and a Sloan Research Fellowship.

JH was partially supported by NSF grant DMS-1552285.

MS was partially supported by NSF grant DMS-1702532.

IZ was partially supported by NSF grant DMS-1703685.

We would like to thank Sherry Gong, Tye Lidman, Robert Lipshitz, Ciprian Manolescu, and JungHwan Park for helpful conversations. We would like to thank Danny Ruberman for helpful comments on an earlier draft. We are grateful to the Frontiers in Floer Homology Workshop at Boston College in August 2019, the University of Oregon Floer Homotopy Workshop in August 2019, and the Geometry and Topology Workshop at UCLA in January 2020, where parts of this work were completed. Finally, we are grateful to the anonymous referees for their thoughtful reading and helpful comments.

©2026 Kristen Hendricks, Jennifer Hom, Matthew Stoffregen, and Ian Zemke

This is a free offprint provided to the author by the publisher. Copyright restrictions may apply.

This is a free offprint provided to the author by the publisher. Copyright restrictions may apply.

CHAPTER 1

Introduction

Heegaard Floer homology, defined by Ozsváth-Szabó [**OS04b**], is a powerful suite of invariants for studying 3-manifolds, knots inside of them, and 4-manifold cobordisms between them. The first author and Manolescu [**HM17**] put additional structure on this package of invariants, in the form of a homotopy involution, leading to involutive Heegaard Floer homology. Their refinement was motivated by Manolescu's resolution of the triangulation conjecture. Galewski-Stern [**GS80**] and Matumoto [**Mat78**] reduced the triangulation conjecture in dimension at least 5 to the assertion that there exists an integral homology sphere with Rokhlin invariant one that is of order two in $\Theta^3_{\mathbb{Z}}$, the 3-dimensional integral homology cobordism group. Manolescu [**Man16**] used a Pin(2)-equivariant version of Seiberg-Witten Floer homology to show that there exists no such homology sphere, proving that there exist manifolds in every dimension ≥ 5 that cannot be triangulated.

The involutive Heegaard Floer package has been particularly useful in studying $\Theta^3_{\mathbb{Z}}$; see, for example, [**HHL21**], [**DHST23**]. To a closed 3-manifold Y, the first author and Manolescu [**HM17**] associate a homotopy involution

$$\iota\colon CF^-(Y) \to CF^-(Y).$$

The pair $(CF^-(Y), \iota)$ is called an *ι-complex* and, up to homotopy equivalence, is an invariant of Y. Hendricks, Manolescu, and Zemke [**HMZ18**] show that up to a weaker notion of equivalence, called *local equivalence*, the pair $(CF^-(Y), \iota)$ is an invariant of the homology cobordism class of Y.

The goal of this paper is to extend various properties of Heegaard Floer homology, such as the surgery exact triangle and mapping cone formula, to the involutive setting. We show that up to local equivalence, the involutive mapping cone formula simplifies dramatically, paving the way for effective computations. As an application, we use this formula to prove:

THEOREM 1.1. *Seifert fibered spaces do not generate the homology cobordism group $\Theta^3_{\mathbb{Z}}$.*

1.1. Involutive surgery exact sequences

One particularly useful feature of Heegaard Floer homology is the surgery exact triangle. Given a framed knot in a closed 3-manifold Y, Ozsváth-Szabó [**OS04c**] prove that there are exact triangles

$$\cdots \to \boldsymbol{HF}^-(Y) \to \boldsymbol{HF}^-(Y_0(K)) \to \boldsymbol{HF}^-(Y_1(K)) \to \cdots \tag{1.1}$$

where $\boldsymbol{HF}^-(Y)$ denotes the minus flavor of Heegaard Floer homology with completed coefficients.

Our paper centers on establishing the surgery exact triangle for involutive Heegaard Floer homology:

This is a free offprint provided to the author by the publisher. Copyright restrictions may apply.

THEOREM 1.2. *Suppose that Y is a closed 3-manifold and K is a framed knot. There is an exact triangle*

$$\cdots \to \boldsymbol{HFI}^-(Y) \to \boldsymbol{HFI}^-(Y_0(K)) \to \boldsymbol{HFI}^-(Y_1(K)) \to \cdots.$$

The same holds for the plus version.

The surgery exact triangle was previously been established by the first author and Lipshitz [**HL19**, Theorem 7.1] for the hat version of involutive Heegaard Floer homology, but remained elusive for the minus theory. Our exact sequence mirrors the exact sequence of Ozsváth and Szabó [**OS04c**, Theorem 9.1] in ordinary Heegaard Floer homology, as well as Lin's exact sequence for Pin(2)-equivariant Monopole Floer homology [**Lin17**, Theorem 1].

Additionally, we prove the following analog of [**OS08b**, Theorem 3.1] for involutive Heegaard Floer homology:

THEOREM 1.3. *Suppose that Y is an integer homology 3-sphere, and K is a knot. For any $n \in \mathbb{Z}$ and $m \geq 1$, there is an exact triangle*

$$\cdots \to \boldsymbol{HFI}^-(Y_n(K)) \to \boldsymbol{HFI}^-(Y_{n+m}(K)) \to \underline{\boldsymbol{HFI}}^-(Y) \to \cdots.$$

In Theorem 1.3, $\underline{\boldsymbol{HFI}}^-(Y)$ denotes a twisted version of involutive Heegaard Floer homology. Furthermore,

$$\underline{\boldsymbol{HFI}}^-(Y) \cong \bigoplus_{i=1}^{N} \boldsymbol{HFI}^-(Y) \oplus \bigoplus_{i=1}^{M} (\boldsymbol{HF}^-(Y)[-1] \oplus \boldsymbol{HF}^-(Y)), \tag{1.2}$$

where

$$(N, M) = \begin{cases} (1, (m-1)/2) & \text{if } m \text{ is odd,} \\ (0, m/2) & \text{if } m \text{ is even and } n \text{ is odd,} \\ (2, (m-2)/2) & \text{if } m \text{ and } n \text{ are even.} \end{cases}$$

1.2. The involutive mapping cone formula

The exact triangle in Theorem 1.3 is a key ingredient in establishing Ozsváth and Szabó's mapping cone formula [**OS08b**] for the Heegaard Floer homology of surgery along a knot. The mapping cone formula gives a powerful relation between the knot Floer complex and the Heegaard Floer complex of surgeries. We first recall the formula, and then discuss the involutive counterparts we prove in our present work.

Given a knot K in an integer homology 3-sphere Y, define $A_s^- \subseteq CFK^\infty(Y, K)$ to be the subcomplex generated over $\mathbb{F}[U]$ by elements $[\mathbf{x}, i, j]$ with $i \leq 0$ and $j \leq s$, which satisfy $A(\mathbf{x}) - j + i = 0$, where A denotes the Alexander grading. We write $\boldsymbol{A}_s^-$ for its completion over $\mathbb{F}[\![U]\!]$. Define B_s^- to be the subcomplex generated by elements $[\mathbf{x}, i, j]$ satisfying the same Alexander grading restriction, and $i \leq 0$, and write $\boldsymbol{B}_s^-$ for its completion. Define

$$\mathbb{A}^- := \prod_{s \in \mathbb{Z}} \boldsymbol{A}_s^- \quad \text{and} \quad \mathbb{B}^- := \prod_{s \in \mathbb{Z}} \boldsymbol{B}_s^-.$$

Ozsváth and Szabó [**OS08b**] construct a map $D_n \colon \mathbb{A}^- \to \mathbb{B}^-$ so that

$$\boldsymbol{CF}^-(Y_n(K)) \simeq \mathbb{X}_n^- := \mathrm{Cone}(D_n \colon \mathbb{A}^- \to \mathbb{B}^-). \tag{1.3}$$

We prove the following analog of (1.3) for involutive Heegaard Floer homology:

This is a free offprint provided to the author by the publisher. Copyright restrictions may apply.

THEOREM 1.4. *Suppose $n \geq 1$, and K is a knot in Y, an integer homology 3-sphere. Then $\boldsymbol{CFI}^-(Y_n(K))$ is homotopy equivalent over the ring $\mathbb{F}[\![U]\!][Q]/Q^2$ to a complex of the form:*

$$\mathbb{XI}_n^-(Y,K) := \begin{array}{ccccc} \mathbb{A}^- & & \xrightarrow{D_n} & & \mathbb{B}^- \\ \downarrow{\scriptstyle Q(\mathrm{id}+\iota_{\mathbb{A}})} & \searrow & & & \downarrow{\scriptstyle Q(\mathrm{id}+\iota_{\mathbb{B}})} \\ & & \searrow{\scriptstyle QH} & & \\ Q\mathbb{A}^- & & \xrightarrow{D_n} & & Q\mathbb{B}^-. \end{array}$$

Here D_n is the map in Ozsváth and Szabó's mapping cone formula, $\iota_{\mathbb{A}}$ is a map which is determined by the knot involution on $CFK^\infty(K)$, $\iota_{\mathbb{B}}$ is a map which is determined by the 3-manifold involution on $CF^-(Y)$, and H is a homogeneously graded map making the diagram into a chain complex. Equivalently, the iota-complex $(CF^-(Y_n(K)), \iota)$ is homotopy equivalent (as an iota-complex) to $\mathbb{X}_n^-$, equipped with the involution $\iota_{\mathbb{A}} + H + \iota_{\mathbb{B}}$.

A more detailed version of Theorem 1.4 is proven in Chapter 20. Theorem 1.4 also has a refinement over Spin^c structures, which we briefly summarize. There is a natural identification of Spin$^c(Y_n(K))$ with $\mathbb{Z}_n$, where Spin^c conjugation is identified with the map $i \mapsto -i$. Of most interest to involutive Heegaard Floer homology are the *self-conjugate* Spin^c structures, which are the ones satisfying $i \equiv -i \mod n$. If n is odd, there is one self-conjugate Spin^c structure on $Y_n(K)$, and if n is even, there are two. The complex $\mathbb{XI}_n^-$ naturally splits over conjugacy classes of Spin^c structures on $Y_n(K)$, giving the involutive Heegaard Floer homology of $Y_n(K)$ in each conjugacy class. See Chapter 20 for more details.

1.3. Knots in S^3

One of the most useful properties of Ozsváth and Szabó's mapping cone formula is that for a knot K in S^3, the map D_n is computable up to chain homotopy from the chain complex $CFK^\infty(K)$. For knots in other 3-manifolds, computation of D_n usually requires knowledge of additional holomorphic curves, beyond those used to compute the knot Floer complex. We prove a similar result for the involutive mapping cone formula:

THEOREM 1.5. *If K is a knot in S^3, and $r \in \mathbb{Q}$, then $CFI^-(S^3_r(K))$ is computable from the pair $(CFK^\infty(K), \iota_K)$.*

We briefly describe what goes into Theorem 1.5. If K is a knot in an integer homology 3-sphere, then the pair $(CFK^\infty(Y,K), \iota_K)$ may naturally be viewed as an object in a category of algebraic *ι_K-complexes*; see Chapter 3 for more details. These consist of chain complexes C_K over a two-variable polynomial ring $\mathbb{F}[\mathscr{U}, \mathscr{V}]$, equipped with an endomorphism ι_K, which together satisfy a list of algebraic properties satisfied by any knot Floer complex. We say that an ι_K-complex is of *L-space type* if it algebraically looks like the knot Floer complex of a knot in a 3-manifold Y satisfying $HF^-(Y) \cong \mathbb{F}[U]$. Concretely, this amounts to requiring that $H_*(B_s) \cong \mathbb{F}[U]$. In Section 3.5, we construct an algebraically defined map

$$\mathbb{XI}_n^{\mathrm{alg}} \colon \frac{\{\iota_K\text{-complexes of L-space type}\}}{\iota_K\text{-homotopy equivalence}} \to \frac{\{\iota\text{-complexes}\}}{\iota\text{-homotopy equivalence}},$$

This is a free offprint provided to the author by the publisher. Copyright restrictions may apply.

which gives the maps D_n, $\iota_{\mathbb{A}}$, $\iota_{\mathbb{B}}$, and H, appearing in Theorem 1.4, via a specified procedure. We call $\mathbb{XI}^{\mathrm{alg}}_n$ the *algebraic* involutive mapping cone. The map $\mathbb{XI}^{\mathrm{alg}}_n$ enjoys several functoriality properties, with respect to morphisms of ι_K-complexes.

The key property that characterizes $\mathbb{XI}^{\mathrm{alg}}_n$ is that the maps D_n and H admit a factorization though the inclusions of A^-_s into B^-_s and A^-_s into $\widetilde{B}^-_s$, where $\widetilde{B}^-_s$ denotes the subcomplex of $CFK^\infty(K)$ generated over $\mathbb{F}$ by elements $[\mathbf{x}, i, j]$ with $j \leq s$.

In Chapter 21 we prove that

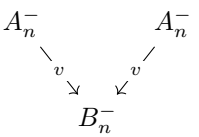
$$(\boldsymbol{CF}^-(S^3_n(K), \iota)) \simeq \mathbb{XI}^{\mathrm{alg}}_n(CFK^\infty(K), \iota_K).$$

Although Theorem 1.5 allows for algorithmic computation of $CFI^-(S^3_n(K))$ whenever the ι_K-complex $(CFK^\infty(K), \iota_K)$ is known, it often produces very large chain complexes. For applications to homology cobordism, it is sufficient to work with the local equivalence class of $CFI^-(S^3_n(K))$. We prove the following:

THEOREM 1.6. *Suppose K is a knot in S^3 and $n > 0$ is an integer.*

(1) *The ι-complex $CFI^-(S^3_n(K), [0])$ is locally equivalent to $(A^-_0(K), \iota_K)$. Here, $[0]$ is the self-conjugate* Spin^c *structure of $S^3_n(K)$ corresponding to $[0] \in \mathbb{Z}/n$ under the standard correspondence* Spin$^c(S^3_n(K)) \cong \mathbb{Z}/n$.

(2) *The ι-complex $(CF^-(S^3_{2n}(K), [n]), \iota)$ is locally equivalent to the complex*



with the involution which swaps the two copies of A^-_n, and fixes B^-_n.

The fact that for $n > 0$ the local equivalence class of $CFI^-(S^3_n(K), [0])$ is determined by $(A^-_0(K), \iota_K)$ is perhaps unsurprising in light of [**NW15**, Proposition 1.6], where Ni–Wu show that $d(S^3_n(K), [0])$ (which can be thought of as the local equivalence class of $CF^-(S^3_n(K), [0])$ in the non-involutive setting) is determined by $A^-_0(K)$. Theorem 1.6 also has an analog for rational surgeries. See Proposition 22.9 for a precise statement.

In [**HM17**], the first author and Manolescu use involutive Heegaard Floer homology to associate two new correction terms $\underline{d}(Y, \mathfrak{s})$ and $\overline{d}(Y, \mathfrak{s})$ to a rational homology sphere Y with a conjugation invariant Spin^c structure $\mathfrak{s}$, and two related knot concordance invariants $\underline{V}_0(K)$ and $\overline{V}_0(K)$. (The definitions of these invariants are reviewed in Sections 2.1 and 2.2.) As a consequence of Theorem 1.6, and its analog for rational surgeries, we compute the involutive correction terms of p/q surgery in terms of p/q and the involutive concordance invariants.

PROPOSITION 1.7. *Suppose that $p, q > 0$ are relatively prime integers and K is a knot in S^3.*

(1) *If p and q are odd, then there is one self-conjugate* Spin^c *structure $[0]$ on $S^3_{p/q}(K)$, and furthermore*

$$\underline{d}(S^3_{p/q}(K), [0]) = d(L(p,q), [0]) - 2\underline{V}_0(K),$$
$$\overline{d}(S^3_{p/q}(K), [0]) = d(L(p,q), [0]) - 2\overline{V}_0(K).$$

This is a free offprint provided to the author by the publisher. Copyright restrictions may apply.

(2) *If p is even and q is odd, then there are two self-conjugate* Spin^c *structures, which we denote* $[0]$ *and* $[p/2q]$*. The correction terms for* $[0]$ *are the same as the previous case, while*

$$\underline{d}(S^3_{p/q}(K), [p/2q]) = d(S^3_{p/q}(K), [p/2q]),$$
$$\overline{d}(S^3_{p/q}(K), [p/2q]) = d(L(p,q), [p/2q]).$$

(3) *If p is odd and q is even, then there is just one self-conjugate* Spin^c *structure* $[p/2q]$*, and*

$$\underline{d}(S^3_{p/q}(K), [p/2q]) = d(S^3_{p/q}(K), [p/2q]),$$
$$\overline{d}(S^3_{p/q}(K), [p/2q]) = d(L(p,q), [p/2q]).$$

Note that Proposition 1.7 is a generalization of [**HM17**, Theorem 1.6], which is the case $q = 1$ and $p \geq g(K)$. Proposition 1.7 has a particularly simple form for $+1$ surgeries:

COROLLARY 1.8. *If K is a knot in S^3, then*

$$\underline{d}(S^3_{+1}(K)) = -2\underline{V}_0(K) \quad \text{and} \quad \overline{d}(S^3_{+1}(K)) = -2\overline{V}_0(K).$$

1.4. An application to the homology cobordism group

In the 1950s, the Rokhlin homomorphism

$$\mu\colon \Theta^3_{\mathbb{Z}} \to \mathbb{Z}/2\mathbb{Z},$$

showed that $\Theta^3_{\mathbb{Z}}$ is non-trivial. Since then significant progress has been made in understanding the structure of the 3-dimensional homology cobordism group, starting with Fintushel-Stern's proof [**FS85**], using techniques from Donaldson's proof of the diagonalization theorem, that the Poincaré homology sphere has infinite order in $\Theta^3_{\mathbb{Z}}$. Subsequently, Fintushel-Stern [**FS90**] and Furuta [**Fur90**] established that $\Theta^3_{\mathbb{Z}}$ contains a $\mathbb{Z}^\infty$-subgroup, using Yang-Mills gauge theory; the third author [**Sto17**] has given an alternate proof of this fact using Pin(2)-equivariant Seiberg-Witten theory.

Dai, Hom, Stoffregen and Truong [**DHST23**] described a homomorphism

$$\hat{h}\colon \Theta^3_{\mathbb{Z}} \to \hat{\mathfrak{I}},$$

where $\hat{\mathfrak{I}}$ denotes the group of *almost ι-complexes*; roughly, $\hat{\mathfrak{I}}$ consists of ι-complexes up to a slightly weaker version of local equivalence. They construct an infinite family of linearly independent surjective homomorophisms

$$\phi_n\colon \hat{\mathfrak{I}} \to \mathbb{Z}$$

to show that $\Theta^3_{\mathbb{Z}}$ contains a direct summand isomorphic to $\mathbb{Z}^\infty$.

Despite this progress in understanding the structure of $\Theta^3_{\mathbb{Z}}$, there has been relatively less progress on understanding exactly which kinds of manifolds can represent a given class $\xi \in \Theta^3_{\mathbb{Z}}$.

The first results about this question were in the positive direction. Livingston [**Liv81**] showed that any class in $\Theta^3_{\mathbb{Z}}$ is represented by an irreducible integer homology sphere. Later, Myers [**Mye83**] proved that in fact any class admits a hyperbolic representative.

In the negative direction, Frøyshov (in unpublished work), F. Lin [**Lin17**], and the third author [**Sto20**] constructed classes $\xi \in \Theta^3_{\mathbb{Z}}$ that are not represented by

This is a free offprint provided to the author by the publisher. Copyright restrictions may apply.

any Seifert fibered spaces. However, none of these proofs suffices to establish that a homology cobordism class is not represented by a *connected sum* of Seifert spaces. The classes constructed by Frøyshov and in [**Sto20**] are both connected sums of Seifert spaces: the proofs proceeded by describing, respectively, the behavior of mod 2 instanton homology and Pin(2)-equivariant Seiberg-Witten Floer homology of connected sums, as well as the Floer homologies of Seifert spaces. The class ξ constructed by Lin is surgery on a certain alternating knot, but has Floer homology consistent with it being representable as a connected sum of Seifert spaces. All of these arguments depend on the fact that instanton Floer homology and Seiberg-Witten Floer homology of Seifert fibered spaces are relatively easy to understand, and then using that these theories can be understood under connected sum.

The group $\hat{\mathfrak{I}}$ admits $\hat{h}(\Theta_{SF})$ as a summand [**DHST23**, Figure 14], where Θ_{SF} denotes the span of Seifert fibered homology 3-spheres in $\Theta^3_{\mathbb{Z}}$. Furthermore, building on [**DM19**], [**DS19**] and [**Dai19**], Dai-Hom-Stoffregen-Truong prove $\hat{h}(\Theta_{SF}) \cong \mathbb{Z}^\infty$, and that $\hat{h}(\Theta_{SF})$ is a proper subgroup of $\hat{\mathfrak{I}}$. Due to the challenging nature of performing computations, they were unable to produce an integer homology 3-sphere Y such that $\hat{h}(Y) \notin \hat{h}(\Theta_{SF})$. Using Theorems 1.5 and 1.6, we prove the following:

THEOREM 1.9. *Let* $Y = S^3_{+1}(-2T_{6,7}\#T_{6,13}\#T_{-2,3;2,5})$. *Then* $n[Y]$ *is non-trivial in* $\Theta^3_{\mathbb{Z}}/\Theta_{SF}$ *for any non-zero* $n \in \mathbb{Z}$.

Note that Theorem 1.1 follows immediately from Theorem 1.9. The proof of Theorem 1.9 relies on the fact from [**DHST23**, Theorem 8.1] (cf. the proof of [**Dai19**, Theorem 1.1]) that the almost-local equivalence class of linear combinations of Seifert fibered spaces takes on a particularly simple form. Note that the manifold Y in Theorem 1.9 is somewhat ad hoc, and does not immediately generalize to show that $\Theta^3_{\mathbb{Z}}/\Theta_{SF}$ is infinitely generated. We plan to address this question in future work.

REMARK 1.10. More generally, one can consider Θ_{AR}, the subgroup of $\Theta^3_{\mathbb{Z}}$ generated by almost-rationally plumbed 3-manifolds. (For the precise definition of an almost-rational plumbing, see [**Ném05**].) Note that Seifert fibered spaces are almost-rationally plumbed. By [**DS19**, Theorem 1.1], $\hat{h}(\Theta_{SF}) = \hat{h}(\Theta_{AR})$, so the proof of Theorem 1.9 actually shows that $n[Y]$ is non-trivial in $\Theta^3_{\mathbb{Z}}/\Theta_{AR}$; that is, almost-rationally plumbed 3-manifolds do not generate $\Theta^3_{\mathbb{Z}}$.

Theorem 1.9 also has the following corollary, which was suggested to us by Tye Lidman.

COROLLARY 1.11. *The Montesinos knots do not generate the smooth concordance group* $\mathcal{C}$.

PROOF. Recall that the double branched cover of a Montesinos knot is a Seifert fibred space, and that furthermore the operation of taking branched double covers of knots sends connected sums of knots to connected sums of 3-manifolds and concordant knots to spin rational homology cobordant 3-manifolds. The local equivalence class and almost local equivalence class of the pair $(CF^-(Y), \iota)$ for a 3-manifold Y are invariant under not only integer homology cobordism but spin rational homology cobordism [**HMZ18**, **DHST23**]. Therefore it suffices to show that the manifold Y of Theorem 1.9 is a double branched cover. Torus knots are strongly

This is a free offprint provided to the author by the publisher. Copyright restrictions may apply.

invertible, and connected sums of strongly invertible knots are strongly invertible [**Sak86**]. Moreover, cables of strongly invertible knots are strongly invertible, see for example [**Wat11**], so $K = -2T_{6,7}\#T_{6,13}\#T_{-2,3;2,5}$ is a strongly invertible knot. Therefore $Y = S^3_{+1}(K)$ is a double branched cover $\Sigma(K')$ of some knot K' [**Mon75**]. Hence K' is not concordant to any connected sum of Montesinos knots. □

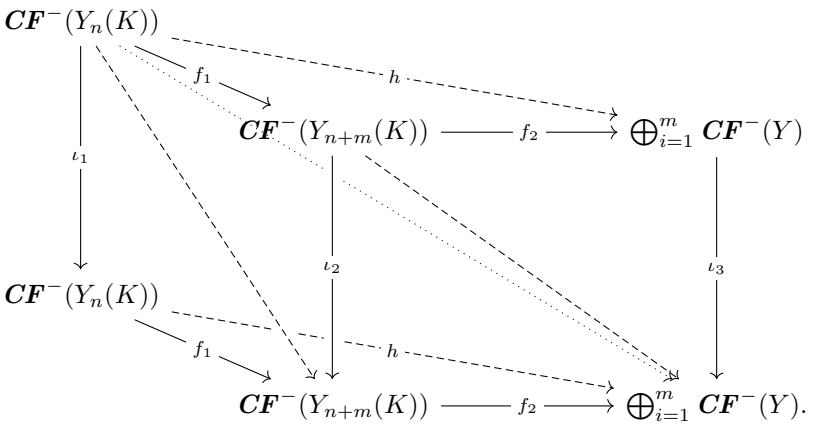
REMARK 1.12. An alternate proof of Corollary 1.11 can be obtained as follows. Lowrance [**Low08**, Theorem 1.1] (see also [**SS22**, Corollary 1.3]) proved that Montesinos knots have thickness at most one, from which it follows that if K is a Montesinos knot, then $\varphi_n(K) = 0$ for $n > 2$, where φ_n is the concordance invariant from [**DHST21**]. Since $\bigoplus_{n\in\mathbb{N}} \varphi_n \colon \mathcal{C} \to \mathbb{Z}^\infty$ is a surjective homomorphism, it follows that Montesinos knots do not generate the concordance group.

REMARK 1.13. A similar computation to the proof of Theorem 1.9 shows the following. We recall from [**HL19**, Remark 9.7] that a homology sphere Y is $\widehat{HFI}$-*trivial* if $\widehat{HFI}(Y) \cong \widehat{HF}(Y) \oplus \mathbb{F}$, where Q vanishes on $\widehat{HF}$ and is non-vanishing on the remaining generator. Heretofore, no 3-manifolds have been shown to be $\widehat{HFI}$-non-trivial. In Section 4.3, we compute that $+1$ surgery on $-2T_{4,5}\#T_{4,9}$ is $\widehat{HFI}$-non-trivial.

1.5. The involutive hypercube of a surgery triad

Theorems 1.2, 1.3 and 1.4 all follow from the existence of a certain *hypercube of chain complexes*. See Chapter 5 for the definition of a hypercube of chain complexes. The relevant version of the hypercube necessary for Theorems 1.3 and 1.4 is the following:

THEOREM 1.14. *Suppose that K is a knot in an integer homology 3-sphere Y, $m, n \in \mathbb{Z}$ and $m \geq 1$. Then there is a hypercube of chain complexes of the following form*



Furthermore, the maps f_1, f_2 and h are the ones appearing in Ozsváth and Szabó's exact sequence [**OS08b**].

In Theorem 1.14, the complexes $\boldsymbol{CF}^-(Y_n(K))$ and $\boldsymbol{CF}^-(Y_{n+m}(K))$ are the ordinary Heegaard Floer complexes, summed over all Spin^c structures, and with coefficients in the power series ring $\mathbb{F}[\![U]\!]$. The maps ι_1 and ι_2 are chain homotopic to the ordinary involutions on Heegaaard Floer homology. The map ι_3 interchanges

This is a free offprint provided to the author by the publisher. Copyright restrictions may apply.

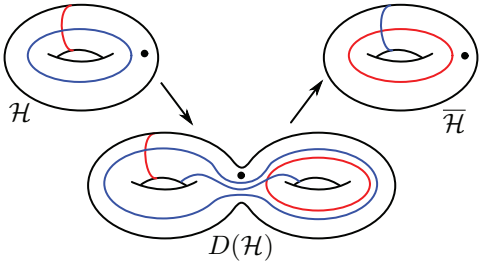


FIGURE 1.1. Realizing the involution on S^3 by doubling.

the summands of $\bigoplus_{i=1}^{m} \boldsymbol{CF}^-(Y)$, but can otherwise be identified with the involution on $\boldsymbol{CF}^-(Y)$.

1.6. The doubling model of the involution

The involution in [**HM17**] is given using an arbitrary sequence of Heegaard moves from $\mathcal{H}$ to $\overline{\mathcal{H}}$. In this paper, we make use of a special sequence of moves connecting $\mathcal{H}$ and $\overline{\mathcal{H}}$, which we call the *doubling* model of the involution. The key observation is that if Σ is a Heegaard splitting of Y, containing a basepoint w, then we can construct another Heegaard splitting $D(\Sigma)$ of Y, with $D(\Sigma) \cong \Sigma \# \overline{\Sigma}$, which is embedded as the boundary of a regular neighborhood of $\Sigma \setminus N(w)$. We think of $D(\Sigma)$ as lying half-way between Σ and $\overline{\Sigma}$. Attaching curves for doubled diagrams are described in Chapter 6. A schematic example is shown in Figure 1.1. One helpful property of the doubling operation is that if $\mathcal{H}$ is a diagram for Y, and $D(\mathcal{H})$ is a double, then the maps from naturality relating $CF^-(\mathcal{H})$ and $CF^-(D(\mathcal{H}))$ have a conceptually simple form, and similarly for the maps from $CF^-(D(\mathcal{H}))$ to $CF^-(\overline{\mathcal{H}})$; see Proposition 6.1.

In the context of Heegaard Floer homology, doubled diagrams have been studied in [**Zem21**], [**JZ20**] and [**JZ24**]. We note that a doubled Heegaard diagram can also be thought of as a diagram obtained by gluing together two bordered Heegaard diagrams [**LOT18**] for genus g handlebodies.

Finally, we note that the doubling model has an interesting topological relation to work of Hass, Thompson and Thurston; see [**HTT09**, p. 2032]. If Σ is a Heegaard surface in Y, it follows from the Reidemeister–Singer theorem that Σ and $\overline{\Sigma}$ become isotopic as oriented surfaces after some number of stabilizations. The doubling model shows that $g = g(\Sigma)$ stabilizations is always sufficient. According to [**HTT09**, Theorem 1.1], for each $g > 1$, there is a closed, oriented 3-manifold with a genus g Heegaard surface Σ which does not become isotopic to $\overline{\Sigma}$ until at least g stabilizations.

1.7. Organization

The paper is organized as follows. We begin by recalling some background on involutive Heegaard Floer homology and Heegaard Floer homology with twisted coefficients in Chapter 2. In Chapter 3, we describe the algebraic framework of ι-complexes and ι_K-complexes, and define an algebraic operation which takes an algebraic ι_K-complex $\mathscr{C}$, and gives an algebraically defined model for the involutive mapping cone $\mathbb{X}\mathbb{I}_n^{\mathrm{alg}}(\mathscr{C})$. In Chapter 4, we use the involutive mapping cone formula

This is a free offprint provided to the author by the publisher. Copyright restrictions may apply.

to prove Theorem 1.9. In Chapter 5, we present some background on homological algebra, in particular hyperboxes of chain complexes. Next, in Chapter 6, we describe the operation of doubling a Heegaard diagram, use this operation to give a conceptually simple formula for the involution, and sketch the construction of the main hypercube used to prove Theorem 1.14. In Chapter 7, we deal with some of the analytic input, and in Chapter 8, we describe a neck-stretching technique that will be particularly helpful to us. In Chapter 9, we describe several stabilization operations for Heegaard diagrams, triples and quadruples, and in Chapter 10, we describe their interaction with the counts of holomorphic curves. In Chapter 11, we consider Heegaard triples where one set of attaching curves is obtained via a small isotopy of another and show that in favorable circumstances, the counts of holomorphic triangles are appropriately simple. In Chapter 12, we review some background on Ozsváth and Szabó's surgery exact sequence [**OS08b**] and describe the maps which appear along the top and bottom faces of our main hypercube. Chapters 13–18 deal with the construction of different pieces of the main hypercube, and Chapter 19 deals with a technical detail from Chapter 16.6. In Chapter 20, we use the involutive hypercube to prove Theorem 1.4 and Theorem 1.3. In Chapter 21, we prove that for a knot K in L-space integer homology sphere Y, the algebraic involutive mapping cone from Chapter 3 computes $\mathit{HFI}^-(Y^3_n(K))$. Finally, in Chapter 22, we consider rational surgery as well as 0-surgery.

This is a free offprint provided to the author by the publisher. Copyright restrictions may apply.

This is a free offprint provided to the author by the publisher. Copyright restrictions may apply.

CHAPTER 2

Involutive Heegaard Floer homology

In this chapter, we recall background on *involutive Heegaard Floer homology*, due to the first author and Manolescu [**HM17**], as well as some variations which are relevant to the exact sequences and knot surgery formula.

2.1. 3-manifolds

If $\mathcal{H} = (\Sigma, \boldsymbol{\alpha}, \boldsymbol{\beta}, w)$ is a Heegaard diagram of a 3-manifold Y, then $\overline{\mathcal{H}} := (\overline{\Sigma}, \boldsymbol{\beta}, \boldsymbol{\alpha}, w)$ is also a Heegaard diagram for Y, where $\overline{\Sigma}$ denotes Σ, with its orientation reversed. We say $\mathcal{H}$ and $\overline{\mathcal{H}}$ are *conjugate*. If $\varpi \subseteq \mathrm{Spin}^c(Y)$ denotes a conjugacy class of Spin^c structures, and $\mathcal{H}$ is a Heegaard diagram, we write

$$CF^-(\mathcal{H}, \varpi) := \bigoplus_{\mathfrak{s} \in \varpi} CF^-(\mathcal{H}, \mathfrak{s}).$$

Note that ϖ either consists of one Spin^c structure $\mathfrak{s}$ satisfying $\mathfrak{s} = \overline{\mathfrak{s}}$, or is a 2-element set of the form $\{\mathfrak{s}, \overline{\mathfrak{s}}\}$.

There is a tautological chain isomorphism

$$\eta\colon CF^-\left(\overline{\mathcal{H}}, \overline{\mathfrak{s}}\right) \to CF^-\left(\mathcal{H}, \mathfrak{s}\right).$$

There is additionally a chain homotopy equivalence

$$\Psi_{\mathcal{H} \to \overline{\mathcal{H}}}\colon CF^-\left(\mathcal{H}, \mathfrak{s}\right) \to CF^-\left(\overline{\mathcal{H}}, \mathfrak{s}\right),$$

obtained by picking a set of Heegaard moves connecting $\overline{\mathcal{H}}$ and $\mathcal{H}$, and using the induced map from naturality.

Hendricks and Manolescu study the involution $\iota\colon CF^-(\mathcal{H}, \varpi) \to CF^-(\mathcal{H}, \varpi)$ defined as the composition $\iota := \eta \circ \Psi_{\mathcal{H} \to \overline{\mathcal{H}}}$. They define the involutive Heegaard Floer chain complex to be

$$CFI^-(Y, \varpi) := \mathrm{Cone}\left(Q \cdot (\iota + \mathrm{id})\colon CF^-(\mathcal{H}, \varpi) \to Q \cdot CF^-(\mathcal{H}, \varpi)\right),$$

where Q is a formal variable, which we view as satisfying $Q^2 = 0$.

Note that if $\varpi = \{\mathfrak{s}, \overline{\mathfrak{s}}\}$ where $\mathfrak{s} \neq \overline{\mathfrak{s}}$, then

$$HFI^-(Y, \varpi) \cong HF^-(Y, \mathfrak{s})[-1] \oplus HF^-(Y, \overline{\mathfrak{s}}).$$

See [**HM17**, Proposition 4.5]. For a conjugation invariant Spin^c structure, Hendricks and Manolescu extract two involutive correction terms $\underline{d}(Y, \mathfrak{s})$ and $\overline{d}(Y, \mathfrak{s})$ defined via

$$\underline{d}(Y, \mathfrak{s}) = \max\{r \mid \exists\, x \in HFI^-_r(Y, \mathfrak{s}), \forall\, n,\ U^n x \neq 0 \text{ and } U^n x \notin \mathrm{Im}(Q)\} - 1$$

and

$$\overline{d}(Y, \mathfrak{s}) = \max\{r \mid \exists\, x \in HFI^-_r(Y, \mathfrak{s}), \forall\, n, U^n x \neq 0; \exists\, m \geq 0 \text{ s.t. } U^m x \in \mathrm{Im}(Q)\}.$$

Involutive Heegaard Floer homology also has a connected sum formula [**HMZ18**], extending Ozsváth and Szabó's connected sum formula for ordinary

This is a free offprint provided to the author by the publisher. Copyright restrictions may apply.

Heegaard Floer homology [**OS04c**, Theorem 1.5]. If Y_1 and Y_2 are two 3-manifolds, equipped with self-conjugate Spin^c structures $\mathfrak{s}_1$ and $\mathfrak{s}_2$, then

$$(CF^-(Y_1\#Y_2,\mathfrak{s}_1\#\mathfrak{s}_2),\iota_{Y_1\#Y_2})\simeq(CF^-(Y_1)\otimes CF^-(Y_2),\iota_{Y_1}\otimes\iota_{Y_2}), \tag{2.1}$$

where $\simeq$ denotes homotopy equivalence of iota-complexes.

2.2. Knots

If K is a null-homologous knot in an integer homology 3-sphere Y, Hendricks and Manolescu also describe a skew-filtered homotopy automorphism

$$\iota_K\colon CFK^\infty(Y,K)\to CFK^\infty(Y,K)$$

[**HM17**, Section 6.1], which we describe presently.

We recall that a Heegaard diagram for (Y,K) consists of a tuple $\mathcal{H}=(\Sigma,\boldsymbol{\alpha},\boldsymbol{\beta},w,z)$ such that the following hold:

(KD-1) $(\Sigma,\boldsymbol{\alpha},\boldsymbol{\beta})$ is a Heegaard diagram for Y. In particular $Y\setminus\Sigma$ is the disjoint union of two handlebodies U_α and U_β.
(KD-2) $K\cap\Sigma=\{w,z\}$, and furthermore K intersects Σ positively at z and negatively at w.
(KD-3) The tangles $K\cap U_\alpha$ and $K\cap U_\beta$ are boundary parallel.

If $\mathcal{H}=(\Sigma,\boldsymbol{\alpha},\boldsymbol{\beta},w,z)$ is a diagram for (Y,K), then $\overline{\mathcal{H}}:=(\overline{\Sigma},\boldsymbol{\beta},\boldsymbol{\alpha},z,w)$ is also a diagram for (Y,K). There is a tautological isomorphism

$$\eta_K\colon CFK^\infty(\overline{\mathcal{H}})\to CFK^\infty(\mathcal{H})$$

given by $\eta_K([\mathbf{x},i,j])=[\mathbf{x},j,i]$.

The two diagrams $\overline{\mathcal{H}}$ and $\mathcal{H}$ both represent (Y,K). However, there is an additional subtlety that the roles of the basepoints have been reversed, and the naturality theorem of [**JTZ21**] holds only for *based* knots and links. Nonetheless, we may pick an automorphism ψ of (Y,K), which is supported in a neighborhood of K, and which switches w and z via a half twist along K. Then $\psi_*(\mathcal{H})$ and $\overline{\mathcal{H}}$ are both diagrams for (Y,K), with the same basepoints. Hence there is a naturality map

$$\Psi_{\psi_*(\mathcal{H})\to\overline{\mathcal{H}}}\colon CFK^\infty(\psi_*(\mathcal{H}))\to CFK^\infty(\overline{\mathcal{H}}). \tag{2.2}$$

Hendricks and Manolescu define the knot involution ι_K as

$$\iota_K:=\eta_K\circ\Psi_{\psi_*(\mathcal{H})\to\overline{\mathcal{H}}}\circ\psi_*.$$

Note that technically ι_K is not an involution, since ι_K^2 is homotopic to Sarkar's map $\mathrm{id}+\Phi\Psi$ (cf. [**Sar15**]); however, it is a convention to refer to ι_K as the knot involution.

One key property established by Hendricks and Manolescu is the relation of the involutive knot Floer complex to the involutive Heegaard Floer complex of surgeries. If K is a knot in S^3, then according to [**HM17**, Theorem 1.5], $(CF^-(S^3_n(K),[0]),\iota_{S^3_n(K)})$ is equivariantly homotopy equivalent to the iota-complex $(A_0(K),\iota_K)$ for $n\gg 0$ (in fact, $n\geq g_3(K)$ is sufficient). Here $[0]$ represents the conjugation invariant Spin^c structure identified with $[0]$ in the usual identification of Spin^c structures on $S^3_n(K)$ with $\mathbb{Z}/n\mathbb{Z}$.

This is a free offprint provided to the author by the publisher. Copyright restrictions may apply.

From involutive knot Floer homology, Hendricks and Manolescu extract two concordance invariants $\underline{V}_0(K)$ and $\overline{V}_0(K)$, which may be defined via the formula

$$\underline{d}(S^3_n(K),[0]) = \frac{n-1}{4} - 2\underline{V}_0(K), \qquad \overline{d}(S^3_n(K),[0]) = \frac{n-1}{4} - 2\overline{V}_0(K).$$

Finally, involutive knot Floer homology enjoys a connected sum formula, similar to (2.1). If K_1 and K_2 are two knots in S^3, then the knot involution $\iota_{K_1\#K_2}$ on $CFK^\infty(K_1\#K_2) \cong CFK^\infty(K_1)\otimes CFK^\infty(K_2)$ is homotopic to

$$\iota_1\otimes\iota_2 + \Phi\iota_1\otimes\Psi\iota_2,$$

where Φ and Ψ are the two *formal derivative* maps, which are endomorphisms of knot Floer homology. See [**Zem19a**, Theorem 1.1] for more details.

2.3. Twisted 3-manifold complexes

If K is a knot in a 3-manifold Y, then there is a twisted version of the complex $CF^-(Y)$, which naturally appears in the proof of the mapping cone formula [**OS08b**]. In this section, we describe its definition, as well as define an involution. To simplify the discussion, we focus on the case that Y is an integer homology sphere. We will revisit the construction for rational homology 3-spheres in Chapter 22, when we consider rational surgeries.

Definition 2.1. Suppose (K,w,z) is a doubly pointed knot. An *enhanced orientation* $\hat{\mathfrak{o}} = (\mathfrak{o},p)$ on K consists of an orientation $\mathfrak{o}$ on K, together with a choice of special basepoint $p\in\{w,z\}$.

We write $\mathcal{H}_{\hat{\mathfrak{o}}}$ or $\mathcal{H}_{\mathfrak{o},p}$ for a doubly pointed Heegaard diagram, equipped with an enhanced orientation of the underlying knot.

Suppose $\mathcal{H} = (\Sigma,\boldsymbol{\alpha},\boldsymbol{\beta},w,z)$ is a diagram for K in Y, and further, suppose K is equipped with an enhanced orientation $\hat{\mathfrak{o}}$. We now describe the complex $\underline{\boldsymbol{CF}}^-(\mathcal{H}_{\hat{\mathfrak{o}}})$. We define $\underline{\boldsymbol{CF}}^-(\mathcal{H}_{\hat{\mathfrak{o}}})$ to be the free $\mathbb{F}[\![U]\!]\otimes\mathbb{F}[\mathbb{Z}/m]$-module generated by intersection points $\mathbf{x}\in\mathbb{T}_\alpha\cap\mathbb{T}_\beta$. If $a\in\mathbb{Z}/m$, write T^a for the corresponding element of the group ring $\mathbb{F}[\mathbb{Z}/m]$. We equip $\underline{\boldsymbol{CF}}^-(\mathcal{H}_{\hat{\mathfrak{o}}})$ with the differential

$$\partial\mathbf{x} = \sum_{\mathbf{y}\in\mathbb{T}_\alpha\cap\mathbb{T}_\beta}\sum_{\substack{\phi\in\pi_2(\mathbf{x},\mathbf{y})\\ \mu(\phi)=1}} \#(\mathcal{M}(\phi)/\mathbb{R})\cdot U^{n_p(\phi)}T^{n_z(\phi)-n_w(\phi)}\cdot\mathbf{y}, \tag{2.3}$$

where $p\in\{w,z\}$ is the special point of $\hat{\mathfrak{o}}$. Note that the ordering of the basepoints in the exponent of T is induced by the orientation of K. More precisely, z is the basepoint of K corresponding to a positive intersection of K and Σ, and w is the basepoint of K corresponding to the negative intersection.

It is convenient also to have some additional notation. We will also write $(\Sigma,\boldsymbol{\alpha},\boldsymbol{\beta},\hat{w},z)$ or $(\Sigma,\boldsymbol{\alpha},\boldsymbol{\beta},w,\hat{z})$ for a diagram of a knot with an enhanced orientation. The order of the basepoints indicates the orientation, through the convention in (*KD*-2), and the hat indicates the special basepoint.

There is a trivialization

$$\theta_p\colon \underline{\boldsymbol{CF}}^-(\mathcal{H}_{\mathfrak{o},p}) \to \boldsymbol{CF}^-(\Sigma,\boldsymbol{\alpha},\boldsymbol{\beta},p)\otimes\mathbb{F}[\mathbb{Z}/m] \tag{2.4}$$

given by

$$\theta_p(T^s\cdot\mathbf{x}) = T^{s+A_{w,z}(\mathbf{x})}\cdot\mathbf{x}.$$

extended equivariantly over the action of U. Here, $A_{w,z}(\mathbf{x})$ denotes the absolute Alexander grading of $\mathbf{x}$, as an element of $\widehat{CFK}(\Sigma,\boldsymbol{\alpha},\boldsymbol{\beta},w,z)$. (Recall that the

This is a free offprint provided to the author by the publisher. Copyright restrictions may apply.

relative Alexander grading is given by $A_{w,z}(\mathbf{x},\mathbf{y}) = n_z(\phi) - n_w(\phi)$ where ϕ is any class in $\pi_2(\mathbf{x},\mathbf{y})$.)

LEMMA 2.2. *The map θ_p is a chain isomorphism.*

PROOF. The map θ_p is obviously an isomorphism of modules, so it is sufficient to show that it is a chain map. Suppose that $\phi \in \pi_2(\mathbf{x},\mathbf{y})$ is a class with Maslov index 1. Then ϕ contributes a summand of

$$\#(\mathcal{M}(\phi)/\mathbb{R}) \cdot U^{n_p(\phi)} T^{A_{w,z}(\mathbf{y})+n_z(\phi)-n_w(\phi)} \cdot \mathbf{y} \tag{2.5}$$

to $(\theta_p \circ \partial)(\mathbf{x})$, and a summand of

$$\#(\mathcal{M}(\phi)/\mathbb{R}) \cdot U^{n_p(\phi)} T^{A_{w,z}(\mathbf{x})} \cdot \mathbf{y} \tag{2.6}$$

to $(\partial \circ \theta_p)(\mathbf{x})$. Equations (2.5) and (2.6) are clearly equal, so $\theta_p\partial + \partial\theta_p = 0$. □

Writing $\overline{\mathcal{H}} = (\overline{\Sigma}, \boldsymbol{\beta}, \boldsymbol{\alpha}, z, w)$, there is a tautological map

$$\underline{\eta}\colon \underline{\boldsymbol{CF}}^-(\overline{\mathcal{H}}_{\hat{\mathfrak{o}}}) \to \underline{\boldsymbol{CF}}^-(\mathcal{H}_{\hat{\mathfrak{o}}}), \tag{2.7}$$

given by the formula

$$\underline{\eta}(U^i T^j \cdot \mathbf{x}) = U^i T^{-j} \mathbf{x}.$$

It is straightforward to see that $\underline{\eta}$ is a chain isomorphism. Note that in (2.7), the diagram $\overline{\mathcal{H}}_{\hat{\mathfrak{o}}}$ denotes $\overline{\mathcal{H}}$ decorated with the enhanced orientation $\hat{\mathfrak{o}}$. In particular, the enhanced orientation is the same in the domain and codomain of $\underline{\eta}$.

The last ingredient of the involution is the *flip-maps*, which change the special point of an enhanced orientation. These take the form of maps

$$\mathfrak{F}_{w\to z}\colon \underline{\boldsymbol{CF}}^-(\mathcal{H}_{\mathfrak{o},w}) \to \underline{\boldsymbol{CF}}^-(\mathcal{H}_{\mathfrak{o},z}) \quad \text{and}$$
$$\mathfrak{F}_{z\to w}\colon \underline{\boldsymbol{CF}}^-(\mathcal{H}_{\mathfrak{o},z}) \to \underline{\boldsymbol{CF}}^-(\mathcal{H}_{\mathfrak{o},w}).$$

which we describe presently.

There is diffeomorphism map

$$\phi_*\colon \boldsymbol{CF}^-(\Sigma, \boldsymbol{\alpha}, \boldsymbol{\beta}, z) \to \boldsymbol{CF}^-(\Sigma, \boldsymbol{\alpha}, \boldsymbol{\beta}, w),$$

obtained by moving z to w along a subarc of K, and then composing with the change of diagram maps from naturality. In principle, there is a dependence on the choice of subarc, however in all cases we will make a specific choice. The flip map $\mathfrak{F}_{z\to w}$ is defined via the formula

$$\mathfrak{F}_{z\to w} := T^n \cdot \theta_w^{-1} \circ \left(\phi_* \otimes \mathrm{id}_{\mathbb{F}[\mathbb{Z}/m]}\right) \circ \theta_z. \tag{2.8}$$

(Here n is the surgery coefficient that appears in the exact sequence). The other flip map $\mathfrak{F}_{w\to z}$ is defined via the formula

$$\mathfrak{F}_{w\to z} := T^{-n} \cdot \theta_z^{-1} \circ \left((\phi^{-1})_* \otimes \mathrm{id}_{\mathbb{F}[\mathbb{Z}/m]}\right) \circ \theta_w. \tag{2.9}$$

Finally, we define the involution $\underline{\iota}$ of $\underline{\boldsymbol{CF}}^-(\Sigma, \boldsymbol{\alpha}, \boldsymbol{\beta}, w, z)$ via the formula

$$\underline{\iota} := \mathfrak{F}_{z\to w} \circ \underline{\eta} \circ \Psi_{\psi(\mathcal{H})\to\overline{\mathcal{H}}} \circ \psi_*. \tag{2.10}$$

We note that in Theorem 1.14, we are identifying $\bigoplus_{i=1}^m \boldsymbol{CF}^-(Y)$ with $\underline{\boldsymbol{CF}}^-(\mathcal{H}_{\mathfrak{o},w})$, for a Heegaard diagram $\mathcal{H}$ of (Y,K), as well as a fixed orientation $\mathfrak{o}$ on K. Furthermore, the map labeled ι_3 therein is the map $\underline{\iota}$ in this notation.

This is a free offprint provided to the author by the publisher. Copyright restrictions may apply.

CHAPTER 3

Iota complexes and mapping cones

In this chapter, we describe the algebraic framework of ι-complexes and ι_K-complexes, and define an algebraic operation which takes an algebraic ι_K-complex $\mathscr{C}$, and gives an algebraically defined model for the involutive mapping cone $\mathbb{XI}_n^{\mathrm{alg}}(\mathscr{C})$. In this chapter, we focus on the case that n is a non-zero integer. The construction has natural analogs for rational surgeries and 0-surgeries. See Sections 22.8 and 22.9.

3.1. ι-complexes

We begin by defining ι-complexes and ι_K-complexes. Compare the following to [**HMZ18**, Definition 8.1]:

Definition 3.1. An *ι-complex* is a chain complex (C, ∂), which is free and finitely generated over $\mathbb{F}[U]$, equipped with an endomorphism ι. Furthermore, the following hold:

(1) C is equipped with a $\mathbb{Z}$-grading, such that U has grading -2. We call this grading the *Maslov* or *homological* grading.
(2) There is a grading preserving isomorphism $U^{-1}H_*(C) \cong \mathbb{F}[U, U^{-1}]$.
(3) ι is a grading preserving chain map and $\iota^2 \simeq \mathrm{id}$.

Remark 3.2. We will usually abuse notation and refer to the involutive mapping cone $\mathbb{XI}_n^{\mathrm{alg}}(\mathscr{C}) = (\mathbb{X}_n(\mathscr{C}), \iota_{\mathbb{X}})$, constructed in Section 3.5, as an ι-complex. However, the reader should recall that $\mathbb{X}_n$ is defined over $\mathbb{F}[\![U]\!]$, is infinitely generated, and also satisfies $U^{-1}H_*(\mathbb{X}_n) \cong \bigoplus^n \mathbb{F}[\![U, U^{-1}]\!]$.

Definition 3.3. If (C, ι) and (C', ι') are two ι-complexes, an *ι-homomorphism* is a homogeneously graded, $\mathbb{F}[U]$-equivariant chain map $F\colon C \to C'$ such that $F\iota + \iota' F \simeq 0$. Two ι-complexes (C, ι) and (C', ι') are *ι-homotopy equivalent* if there exist ι-homomorphisms $F\colon (C, \iota) \to (C', \iota')$ and $G\colon (C', \iota') \to (C, \iota)$ such that $FG \simeq \mathrm{id}$ and $GF \simeq \mathrm{id}$.

We write Iota for the category whose objects are ι-complexes, and whose morphisms are ι-homomorphisms. Note that Iota is naturally a preadditive category, but is not naturally a dg-category. There is a related category $\underline{\mathsf{Iota}}$, which we call the category of ι-complexes with *enhanced morphisms*, as follows:

Definition 3.4. If (C, ι) and (C', ι') are ι-complexes, we define the group of *enhanced ι-morphisms* to be

$$\underline{\mathrm{Mor}}((C, \iota), (C', \iota')) := \mathrm{Hom}_{\mathbb{F}[U]}(C, C') \oplus \mathrm{Hom}_{\mathbb{F}[U]}(C, C')[1],$$

where $[1]$ denotes a grading shift. We define

$$\partial_{\underline{\mathrm{Mor}}}(F, h) = (\partial' F + F\partial, F\iota + \iota' F + \partial' h + h\partial),$$

This is a free offprint provided to the author by the publisher. Copyright restrictions may apply.

which makes $\underline{\mathsf{Iota}}$ into a dg-category. An enhanced ι-*homo*morphism is an enhanced ι-morphism (F,h) satisfying $\partial_{\underline{\mathrm{Mor}}}(F,h)=0$. An *enhanced ι-homotopy equivalence* is an enhanced ι-homomorphism (F,h), such that there exists an enhanced ι-homomorphism (G,k) such that $(G,k)\circ(F,h)$ and $(F,h)\circ(G,k)$ both differ from $(\mathrm{id},0)$, the identity enhanced ι-morphism, by a boundary in $\underline{\mathrm{Mor}}$.

Remark 3.5.

(1) Note that an enhanced ι-homomorphism (F,h) consists of a chain map $F\colon C\to C'$ such that $F\iota+\iota' F\simeq 0$ via the chain homotopy h.
(2) We will see later that an enhanced ι-homomorphism (F,h) is an enhanced ι-homotopy equivalence if and only if F is an ordinary homotopy equivalence of chain complexes over $\mathbb{F}[U]$. See Lemma 5.5.

Composition of enhanced ι-morphisms is given by

$$(F,h)\circ(G,k)=(FG,hG+Fk).$$

The group of enhanced ι-morphisms (F,h) is canonically isomorphic to

$$\mathrm{Hom}_{\mathbb{F}[U,Q]/Q^2}\left(\mathrm{Cone}(C\xrightarrow{Q(1+\iota)}QC),\mathrm{Cone}(C'\xrightarrow{Q(1+\iota')}QC')\right) \tag{3.1}$$

via $(F,h)\mapsto F+Qh$.

3.2. Local equivalence

To study the homology cobordism group, we consider a special type of ι-morphism, called a *local map*:

Definition 3.6. Suppose (C,ι) and (C',ι') are two ι-complexes.

(1) A *local map* from (C,ι) to (C',ι') is a grading preserving ι-homomorphism $F\colon C\to C'$, which induces an isomorphism from $U^{-1}H_*(C)$ to $U^{-1}H_*(C')$.
(2) We say that (C,ι) are (C',ι') are *locally equivalent* if there is a local map from (C,ι) to (C',ι'), as well as a local map from (C',ι') to (C,ι).

The set of local equivalence classes forms an abelian group, denoted $\mathfrak{I}$, with group structure given by

$$(C,\iota)*(C',\iota')=(C\otimes C',\iota\otimes\iota'). \tag{3.2}$$

See [**HMZ18**, Section 8]. According to [**HMZ18**, Theorem 1.8], the map

$$Y\mapsto[(CF^-(Y),\iota)]$$

determines a homomorphism from $\Theta^3_{\mathbb{Z}}$ to $\mathfrak{I}$.

Given an ι-complex (C,ι), we may define correction terms $d(C)$, $\underline{d}(C)$, and $\overline{d}(C)$ as in Section 2.1, all of which are preserved by local equivalence.

3.3. Almost ι-complexes and almost local equivalence

There is an additional, weaker, equivalence relation between iota complexes, as follows.

Definition 3.7 ([**DHST23**, Definition 3.1]). Let C_1 and C_2 be free, finitely generated chain complexes over $\mathbb{F}[U]$, such that each C_i has an absolute $\mathbb{Q}$-grading

This is a free offprint provided to the author by the publisher. Copyright restrictions may apply.

and a relative $\mathbb{Z}$-grading with respect to which U has grading -2. Two grading-preserving $\mathbb{F}[U]$-module homomorphisms

$$f, g\colon C_1 \to C_2$$

are *homotopic mod* U, denoted $f \simeq g \mod U$, if there exists an $\mathbb{F}[U]$-module homomorphism $H\colon C_1 \to C_2$ such that H increases grading by one and

$$f + g + H \circ \partial + \partial \circ H \in \operatorname{im} U.$$

DEFINITION 3.8 ([**DHST23**, Definition 3.2]). An *almost ι-complex* is a chain complex (C, ∂), which is free and finitely generated over $\mathbb{F}[U]$, equipped with an endomorphism $\overline{\iota}$. Furthermore, the following hold:

(1) C has an absolute $\mathbb{Z}$-grading, such that U has grading -2.
(2) There is a grading preserving isomorphism $U^{-1}H_*(C) \cong \mathbb{F}[U, U^{-1}]$.
(3) $\overline{\iota}$ is a grading-preserving, $\mathbb{F}[U]$-module homomorphism $\overline{\iota}\colon C \to C$ such that

$$\overline{\iota} \circ \partial + \partial \circ \overline{\iota} \in \operatorname{im} U \qquad \text{and} \qquad \overline{\iota}^2 \simeq \mathrm{id} \mod U.$$

It will often be convenient to consider the map

$$\omega = 1 + \overline{\iota}.$$

Of course, every ι-complex has an associated almost ι-complex. Note that the definition of an almost ι-complex is obtained from the definition of an ι-complex by relaxing every statement about ι to merely be true mod U.

DEFINITION 3.9 ([**DHST23**, Definition 3.4]). An *almost ι-homomorphism* from $\mathcal{C}_1 = (C_1, \overline{\iota}_1)$ to $\mathcal{C}_2 = (C_2, \overline{\iota}_2)$ is a grading-preserving, $\mathbb{F}[U]$-equivariant chain map

$$f\colon C_1 \to C_2$$

such that

$$f \circ \overline{\iota} \simeq \overline{\iota} \circ f \mod U.$$

DEFINITION 3.10 ([**DHST23**, Definition 3.5]).

(1) If $(C, \overline{\iota})$ and $(C', \overline{\iota}')$ are almost ι-complexes, an *almost local map* is a degree preserving almost ι-homomorphism $F\colon C \to C'$, which induces an isomorphism from $U^{-1}H_*(C)$ to $U^{-1}H_*(C')$.
(2) We say that $(C, \overline{\iota})$ are $(C', \overline{\iota}')$ are *almost locally equivalent* if there is an almost local map from $(C, \overline{\iota})$ to $(C', \overline{\iota}')$, as well as an almost local map from $(C', \overline{\iota}')$ to $(C, \overline{\iota})$.

According to [**DHST23**, Theorem 3.25], the set of almost local equivalence classes forms a totally ordered abelian group, denoted $\widehat{\mathfrak{I}}$. As with the local equivalence group, the group structure is given by

$$(C, \overline{\iota}) * (C', \overline{\iota}') = (C \otimes C', \overline{\iota} \otimes \overline{\iota}'). \tag{3.3}$$

There are homomorphisms

$$\Theta^3_{\mathbb{Z}} \to \mathfrak{I} \to \widehat{\mathfrak{I}}$$

The structure of the group $\widehat{\mathfrak{I}}$ is recalled in further detail in Chapter 4.

This is a free offprint provided to the author by the publisher. Copyright restrictions may apply.

3.4. ι_K-complexes

There is a refinement of the notion of an ι-complex for knots, called an ι_K-complex. Before stating the definition, we state some algebraic background. Suppose that (C_K, ∂) is a free, finitely generated complex over the ring $\mathbb{F}[\mathscr{U}, \mathscr{V}]$. There are two naturally associated maps

$$\Phi, \Psi \colon C_K \to C_K,$$

as follows. We write ∂ as a matrix with respect to a free $\mathbb{F}[\mathscr{U}, \mathscr{V}]$-basis of C_K. We define Φ to be the endomorphism obtained differentiating each entry of this matrix with respect to $\mathscr{U}$. We define Ψ to be the endomorphism obtained by differentiating each entry with respect to $\mathscr{V}$. These maps naturally appear in the context of knot Floer homology, see [**Sar11**, **Zem17**, **Zem19c**]. The maps Φ and Ψ are independent of the choice of basis, up to $\mathbb{F}[\mathscr{U}, \mathscr{V}]$-equivariant chain homotopy [**Zem19a**, Corollary 2.9].

We say an $\mathbb{F}$-linear map $F \colon C_K \to C'_K$ is *skew-$\mathbb{F}[\mathscr{U}, \mathscr{V}]$-equivariant* if

$$F \circ \mathscr{V} = \mathscr{U} \circ F \quad \text{and} \quad F \circ \mathscr{U} = \mathscr{V} \circ F.$$

We may view a free complex over $\mathbb{F}[\mathscr{U}, \mathscr{V}]$ also as an infinitely generated complex over $\mathbb{F}[U]$, where U acts diagonally via $U = \mathscr{U}\mathscr{V}$. Concretely, if $B = \{\mathbf{x}_1, \dots, \mathbf{x}_n\}$ is an $\mathbb{F}[\mathscr{U}, \mathscr{V}]$-basis, then an $\mathbb{F}[U]$-basis is given by the elements $\mathscr{U}^i \cdot \mathbf{x}_k$ and $\mathscr{V}^j \cdot \mathbf{x}_k$, ranging over all $i \geq 0$, $j \geq 0$ and $k \in \{1, \dots, n\}$.

Compare the following to [**HM17**, Definition 6.2] and [**Zem19a**, Definition 2.2].

Definition 3.11.

(1) An *ι_K-complex* (C_K, ∂, ι_K) is a finitely generated, free chain complex (C_K, ∂) over $\mathbb{F}[\mathscr{U}, \mathscr{V}]$, equipped with a skew-equivariant endomorphism ι_K satisfying
$$\iota_K^2 \simeq \mathrm{id} + \Phi\Psi.$$
(2) We say an ι_K-complex (C_K, ∂, ι_K) is of *$\mathbb{Z}HS^3$-type* if there are two $\mathbb{Z}$ valued gradings, $\mathrm{gr}_{\mathbf{w}}$ and $\mathrm{gr}_{\mathbf{z}}$, such that $\mathscr{U}$ and $\mathscr{V}$ have $(\mathrm{gr}_{\mathbf{w}}, \mathrm{gr}_{\mathbf{z}})$-bigrading $(-2, 0)$ and $(0, -2)$, respectively. We assume ∂ has $(\mathrm{gr}_{\mathbf{w}}, \mathrm{gr}_{\mathbf{z}})$-bigrading $(-1, -1)$, and that ι_K switches $\mathrm{gr}_{\mathbf{w}}$ and $\mathrm{gr}_{\mathbf{z}}$. Furthermore, we assume that $A := \frac{1}{2}(\mathrm{gr}_{\mathbf{w}} - \mathrm{gr}_{\mathbf{z}})$ is integer valued. We call A the *Alexander* grading, and we call $\mathrm{gr}_{\mathbf{w}}$ and $\mathrm{gr}_{\mathbf{z}}$ the *Maslov* gradings. Writing $\mathcal{A}_s \subseteq C_K$ for the subspace in Alexander grading s, we assume that there is a grading preserving isomorphism $U^{-1}H_*(\mathcal{A}_s) \cong \mathbb{F}[U, U^{-1}]$ for all $s \in \mathbb{Z}$.
(3) We say an ι_K-complex (C_K, ∂, ι_K) is of *L-space type* if it is of $\mathbb{Z}HS^3$-type and additionally $H_*(\mathcal{B}_s) \cong \mathbb{F}[U]$, where $\mathcal{B}_s$ is the subset of $\mathscr{V}^{-1}C_K$ in Alexander grading s.

In Definition 3.11, an ι_K-complex of $\mathbb{Z}HS^3$-type is equipped with two Maslov gradings, $\mathrm{gr}_{\mathbf{w}}$ and $\mathrm{gr}_{\mathbf{z}}$. We note that in the literature, usually one considers just the $\mathrm{gr}_{\mathbf{w}}$-grading, which is referred to as the homological grading.

Remark 3.12. If (C_K, ∂, ι_K) is an ι_K-complex, then ι_K commutes with $U = \mathscr{U}\mathscr{V}$, and hence we can view C_K as an (infinitely generated) complex with an $\mathbb{F}[U]$-equivariant endomorphism ι_K.

If K is a knot in an integer homology 3-sphere Y, then we obtain an ι_K-complex in the sense of Definition 3.11 by considering the version of the knot Floer complex

This is a free offprint provided to the author by the publisher. Copyright restrictions may apply.

generated by monomials $\mathscr{U}^i\mathscr{V}^j\cdot\mathbf{x}$, for $i,j\geq 0$, where $\mathscr{U}$ counts the basepoint w and $\mathscr{V}$ counts the basepoint z. This contains equivalent information to the more standard version of the knot Floer complex generated by tuples satisfying $[\mathbf{x},i,j]$ with $A(\mathbf{x})-j+i=0$. The correspondence is given by

$$\mathscr{U}^i\mathscr{V}^j\cdot\mathbf{x}\longleftrightarrow[\mathbf{x},-i,-j]. \tag{3.4}$$

Analogous to Definitions 3.3 and 3.4, we have the following notions of morphism of ι_K-complexes:

DEFINITION 3.13. Suppose that $\mathscr{C}=(C_K,\partial,\iota_K)$ and $\mathscr{C}'=(C'_K,\partial',\iota'_K)$ are ι_K-complexes.

(1) An *ι_K-homomorphism* from $\mathscr{C}$ to $\mathscr{C}'$ consists of an $\mathbb{F}[\mathscr{U},\mathscr{V}]$-equivariant chain map $F\colon C_K\to C'_K$, which satisfies $\iota'_KF+F\iota_K\approx 0$ (where $\approx$ denotes skew-equivariantly chain homotopy equivalence).
(2) The group of *enhanced ι_K-morphisms* is

$$\underline{\mathrm{Mor}}(\mathscr{C},\mathscr{C}'):=\mathrm{Hom}_{\mathbb{F}[\mathscr{U},\mathscr{V}]}(C_K,C'_K)\oplus\overline{\mathrm{Hom}}_{\mathbb{F}[\mathscr{U},\mathscr{V}]}(C_K,C'_K)[1,1],$$

where $\overline{\mathrm{Hom}}_{\mathbb{F}[\mathscr{U},\mathscr{V}]}(C_K,C'_K)$ denotes the group of $\mathbb{F}[\mathscr{U},\mathscr{V}]$-skew-equivariant maps. The differential on $\underline{\mathrm{Mor}}(\mathscr{C}_K,\mathscr{C}'_K)$ is given by

$$\partial_{\underline{\mathrm{Mor}}}(F,g)=(F\partial+\partial'F,F\iota_K+\iota'_KF+\partial'g+g\partial).$$

We say (F,g) is an enhanced ι_K-*homo*morphism if $\partial_{\underline{\mathrm{Mor}}}(F,g)=0$. Two enhanced ι_K-morphisms are ι_K-*homotopic* if their sum is a boundary in $\underline{\mathrm{Mor}}(\mathscr{C}_K,\mathscr{C}'_K)$.

We write Iota_K for the category of ι_K-complexes, with morphism set equal to the set of ι_K-homomorphisms. We write $\underline{\mathsf{Iota}}_K$ for the category of ι_K-complexes with enhanced ι_K-morphisms.

There is also a natural notion of local equivalence of ι_K-complexes:

DEFINITION 3.14. Suppose that $\mathscr{C}=(C_K,\partial,\iota_K)$ and $\mathscr{C}'=(C'_K,\partial',\iota'_K)$ are ι_K-complexes of $\mathbb{Z}HS^3$-type.

(1) A local map from $\mathscr{C}$ to $\mathscr{C}'$ is a $(\mathrm{gr}_{\mathbf{w}},\mathrm{gr}_{\mathbf{z}})$-preserving, $\mathbb{F}[\mathscr{U},\mathscr{V}]$-linear chain map $F\colon C_K\to C'_K$, which satisfies $F\iota_K+\iota'_KF\approx 0$, and which induces an isomorphism from $H_*(U^{-1}\mathcal{A}_s)$ to $H_*(U^{-1}\mathcal{A}'_s)$ for all s.
(2) We say $\mathscr{C}$ and $\mathscr{C}'$ are *locally equivalent* if there are local maps in both directions.

According to [**Zem19a**, Theorem 1.5], the set of local equivalence classes of ι_K-complexes forms a group, denoted $\mathfrak{I}_K$. The group operation is given by

$$(C_K,\partial,\iota_K)*(C'_K,\partial',\iota'_K)\mapsto(C_K\otimes_{\mathbb{F}[\mathscr{U},\mathscr{V}]}C'_K,\partial\otimes 1+1\otimes\partial',\iota_K\otimes\iota'_K+\iota_K\Phi\otimes\iota'_K\Psi).$$

Furthermore, the map

$$K\mapsto[(\mathcal{CFK}^-(K),\iota_K)]$$

determines a homomorphism from the concordance group to $\mathfrak{I}_K$, where $\mathcal{CFK}^-(K)$ denotes the version of knot Floer homology generated by monomials $\mathscr{U}^i\mathscr{V}^j\cdot\mathbf{x}$, where $i,j\geq 0$.

This is a free offprint provided to the author by the publisher. Copyright restrictions may apply.

3.5. The algebraic involutive mapping cone

In this section, we define the algebraic involutive mapping cone

$$\mathbb{XI}_n^{\mathrm{alg}}(\mathscr{C}) = (\mathbb{X}_n(\mathscr{C}), \iota_{\mathbb{X}})$$

of an ι_K-complex $\mathscr{C}$ of L-space type. The $\mathbb{F}[\![U]\!]$ complex $\mathbb{X}_n(\mathscr{C})$ coincides with the minus version of the mapping cone complex constructed by Ozsváth and Szabó [**OS08b**]. If $(F,g)\colon \mathscr{C} \to \mathscr{C}'$ is an enhanced ι_K-homomorphism, then we will also construct an enhanced ι-homomorphism,

$$\mathbb{XI}_n^{\mathrm{alg}}(F,g)\colon \mathbb{XI}_n^{\mathrm{alg}}(\mathscr{C}) \to \mathbb{XI}_n^{\mathrm{alg}}(\mathscr{C}'),$$

which is well defined up to homotopy of enhanced ι-morphisms. We now summarize the important properties of $\mathbb{XI}_n^{\mathrm{alg}}$:

Proposition 3.15. *Let $\mathscr{C}$ and $\mathscr{C}'$ be ι_K-complexes of L-space type.*

1. *The pair $\mathbb{XI}_n^{\mathrm{alg}}(\mathscr{C}) = (\mathbb{X}(\mathscr{C}), \iota_{\mathbb{X}})$ is an ι-complex, which is well defined up to ι-homotopy equivalence.*
2. *If (F,g) is an enhanced ι_K-homomorphism from $\mathscr{C}$ to $\mathscr{C}'$, then $\mathbb{XI}_n^{\mathrm{alg}}(F,g)$ is an enhanced ι-homomorphism from $\mathbb{XI}_n^{\mathrm{alg}}(\mathscr{C})$ to $\mathbb{XI}_n^{\mathrm{alg}}(\mathscr{C}')$. If (F_1,g_1) and (F_2,g_2) are two enhanced ι_K-morphisms which are ι_K-homotopic, then $\mathbb{XI}_n^{\mathrm{alg}}(F_1,g_1)$ and $\mathbb{XI}_n^{\mathrm{alg}}(F_2,g_2)$ are ι-homotopic.*
3. *If (F,g) is an enhanced ι_K-homomorphism, such that F is an ι_K-homotopy equivalence, then $\mathbb{XI}_n^{\mathrm{alg}}(F,g)$ is an enhanced ι-homotopy equivalence.*
4. *If (F,g) is an enhanced ι-homomorphism, such that F is a local map, then $\mathbb{XI}_n^{\mathrm{alg}}(F,g)$ is also a local map.*

In this section, we describe the constructions of $\mathbb{XI}_n^{\mathrm{alg}}(\mathscr{C}) = (\mathbb{X}_n(\mathscr{C}), \iota_{\mathbb{X}})$ and $\mathbb{XI}_n^{\mathrm{alg}}(F,g)$, and prove parts part (2)–(4) of Proposition 3.15. In the subsequent Section 3.6, we prove part (1).

Recall that A_s denotes the subset of $(\mathscr{U},\mathscr{V})^{-1}C_K$ generated by monomials $\mathscr{U}^i\mathscr{V}^j\cdot\mathbf{x}$ satisyfing $A(\mathbf{x}) + j - i = 0$, $i \geq 0$ and $j \geq -s$. Recall also that B_s denotes the subset of $(\mathscr{U},\mathscr{V})^{-1}C_K$ generated by monomials $\mathscr{U}^i\mathscr{V}^j\cdot\mathbf{x}$ satisfying $A(\mathbf{x}) + j - i$, and $i \geq 0$, but with no restriction on j. We define $\widetilde{B}_s$ to be the subcomplex generated by $\mathscr{U}^i\mathscr{V}^j\cdot\mathbf{x}$ satisfying $A(\mathbf{x}) + j - i = 0$, and $j \geq -s$, but with no restriction on i.

Note that in the literature, A_s is often given the equivalent definition of being generated by $[\mathbf{x},i,j]$ with $A(\mathbf{x}) - j + i = 0$, $i \leq 0$ and $j \leq s$, and similarly for B_s. The correspondence between the two definitions is given in (3.4).

We define $\boldsymbol{A}_s$ and $\boldsymbol{B}_s$ to be the completions over $\mathbb{F}[\![U]\!]$ of A_s and B_s. We set

$$\mathbb{A} := \prod_{s\in\mathbb{Z}} \boldsymbol{A}_s \quad \text{and} \quad \mathbb{B} := \prod_{s\in\mathbb{Z}} \boldsymbol{B}_s.$$

Remark 3.16. Here and throughout, we slightly extend the notion of a graded ring to allow for infinite sums of homogeneously graded elements, so that $\mathbb{F}[\![U]\!]$ is a graded ring over which A_s and B_s are graded modules, and likewise for analogous cases.

Next, we let $\mathfrak{A}$ be the $\mathbb{F}[\![\mathscr{U},\mathscr{V}]\!]$-module obtained by completing C_K with respect to the actions of $\mathscr{U}$ and $\mathscr{V}$. We let $\mathfrak{B}$ be defined as the $\mathbb{F}[\![\mathscr{U},\mathscr{V}]\!]$-completion of the

This is a free offprint provided to the author by the publisher. Copyright restrictions may apply.

module $\mathscr{V}^{-1} \cdot C_K$, and we let $\widetilde{\mathfrak{B}}$ be the completion of the module $\mathscr{U}^{-1} \cdot C_K$. There is a canonical *shift map*

$$\mathscr{S} \colon \mathfrak{A} \to \mathbb{A}, \tag{3.5}$$

which is an $\mathbb{F}[\![U]\!]$-equivariant chain isomorphism, as we now describe. The map $\mathscr{S}$ sends $\mathcal{A}_s$ to A_s, via multiplication by V^{-s}. This uniquely determines a map on the completion. There are similar isomorphisms between $\mathfrak{B}$ and $\mathbb{B}$, and $\widetilde{\mathfrak{B}}$ and $\widetilde{\mathbb{B}}$. Abusing notation slightly, we denote these isomorphisms also by $\mathscr{S}$.

Next, we pick a homogeneously graded chain homotopy equivalence

$$\mathfrak{F} \colon \widetilde{B}_s \to B_{s+n},$$

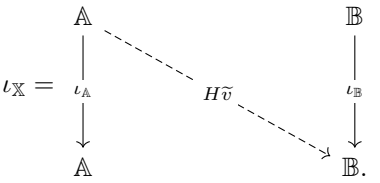
which exists since $\mathscr{C}$ is of L-space type. We set $\mathbb{X}_n(\mathscr{C})$ to be the mapping cone

$$\mathbb{X}_n(\mathscr{C}) := \mathrm{Cone}(D_n \colon \mathbb{A} \to \mathbb{B}),$$

where $D_n := v + \mathfrak{F}\widetilde{v}$. Here, v denotes the inclusion of A_s into B_s, and $\widetilde{v}$ denotes the inclusion of A_s into $\widetilde{B}_s$. The map $\mathfrak{F}\widetilde{v}$ coincides with the map h in Ozsváth and Szabó's notation [**OS08b**].

We now construct the involution $\iota_{\mathbb{X}}$, which will have the form shown in (3.6).

(3.6)



The map $\iota_{\mathbb{A}}$ is induced by ι_K and the shift isomorphism $\mathscr{S}$, as we now describe. By definition, ι_K sends $\mathcal{A}_s$ to $\mathcal{A}_{-s}$. Hence, with respect to the canonical shift isomorphisms $A_s \cong \mathcal{A}_s$ and $A_{-s} \cong \mathcal{A}_{-s}$, given by multiplication by $\mathscr{V}^{-s}$ and $\mathscr{V}^s$, respectively, the map $\iota_{\mathbb{A}}$ is defined on A_s to be

$$\iota_{\mathbb{A}} := U^s \iota_K.$$

The map $\iota_{\mathbb{B}}$ is defined on B_s to be

$$\iota_{\mathbb{B}} := \mathfrak{F} U^s \iota_K.$$

Note, ι_K sends B_s to $\widetilde{B}_0$, U^s sends $\widetilde{B}_0$ to $\widetilde{B}_{-s}$, and $\mathfrak{F}$ sends $\widetilde{B}_{-s}$ to B_{-s+n}.

We now define the map H appearing in (3.6). We will construct it to send $\widetilde{B}_s$ to B_{-s}. Consider the map

$$N := D_n \iota_{\mathbb{A}} + \iota_{\mathbb{B}} D_n,$$

which sends A_s to $B_{-s} \oplus B_{-s+n}$. The component of N which maps A_s to B_{-s+n} consists of

$$\Pi_{-s+n} N_s = \mathfrak{F}\widetilde{v} U^s \iota_K + \mathfrak{F} U^s \iota_K v, \tag{3.7}$$

where Π_{-s+n} denotes projection of $\mathbb{B}$ onto B_{-s+n}. Since ι_K is skew-equivariant, we have

$$U^s \iota_K v = \widetilde{v} U^s \iota_K, \tag{3.8}$$

as maps from A_s to $\widetilde{B}_{-s}$, so (3.7) vanishes. We now consider the component of N which maps A_s to B_{-s}. This takes the form

$$\Pi_{-s} N_s = v U^s \iota_K + \mathfrak{F} U^s \iota_K \mathfrak{F}\widetilde{v}. \tag{3.9}$$

This is a free offprint provided to the author by the publisher. Copyright restrictions may apply.

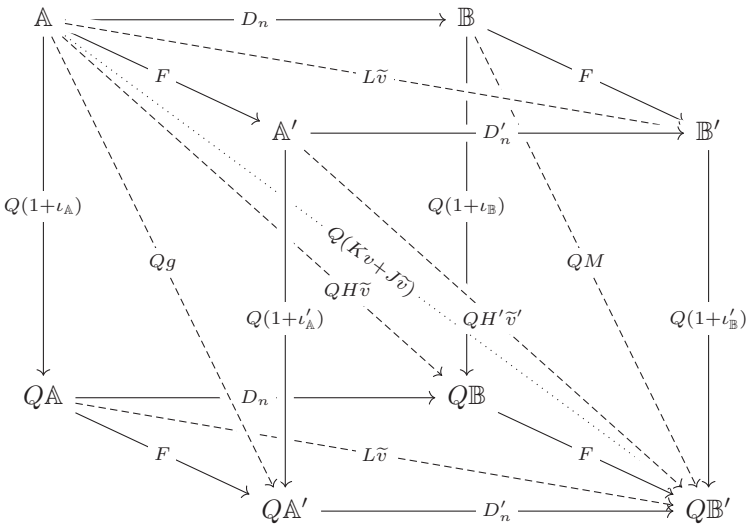


FIGURE 3.1. A diagram encoding $\mathbb{XI}_n^{\mathrm{alg}}(F,g)$.

Using (3.8), we see that (3.9) is equal to $(U^s\iota_K + \mathfrak{F}U^s\iota_K\mathfrak{F})\widetilde{v}$. The maps $U^s\iota_K$ and $\mathfrak{F}U^s\iota_K\mathfrak{F}$ are both homogeneously graded, $\mathbb{F}[U]$-equivariant chain homotopy equivalences from $\widetilde{B}_s$ to B_{-s}. Since C_K is of L-space type, $U^s\iota_K$ and $\mathfrak{F}U^s\iota_K\mathfrak{F}$ must be chain homotopic over $\mathbb{F}[U]$, as maps from $\widetilde{\mathbb{B}}$ to $\mathbb{B}$. We define the map H appearing in (3.6) to be any $+1$ graded chain homotopy between $U^s\iota_K$ and $\mathfrak{F}U^s\iota_K\mathfrak{F}$, which sends $\widetilde{B}_s$ to B_{-s}.

The construction above gives a map $\iota_{\mathbb{X}}$ which is clearly a chain map from $\mathbb{X}_n(\mathscr{C})$ to itself. Hence, we may view $\mathbb{XI}_n^{\mathrm{alg}}(\mathscr{C})$ as inducing a chain complex over $\mathbb{F}[\![U]\!][Q]/Q^2$ (though we have not established that $\iota_{\mathbb{X}}^2 \simeq \mathrm{id}$).

Before addressing the well-definedness of $\mathbb{XI}_n^{\mathrm{alg}}(\mathscr{C})$, it is helpful to first address functoriality of the construction, from which well-definedness will follow easily. The description of enhanced ι-morphisms in (3.1) implies that the notion of an enhanced ι-morphism is independent from whether $\iota_{\mathbb{X}}^2 \simeq \mathrm{id}$, and hence we can tackle parts (2)–(4) of Proposition 3.15 before considering part (1).

Suppose that $\mathscr{C}$ and $\mathscr{C}'$ are ι_K-complexes, and $(F,g)\colon \mathscr{C} \to \mathscr{C}'$ is an enhanced ι_K-homomorphism. Let $\mathfrak{F}$ and H be choices of maps used in the construction of $\mathbb{XI}_n^{\mathrm{alg}}(\mathscr{C})$, and let $\mathfrak{F}'$ and H' be analogous choices for $\mathbb{XI}_n^{\mathrm{alg}}(\mathscr{C}')$.

Our goal will be to construct length 2 and 3 maps which turn the diagram in Figure 3.1 into a chain complex. (Such a diagram is called a *hypercube of chain complexes*; see Chapter 5). Along the left face of Figure 3.1, we use the maps F and g (technically, we are implicitly conjugating with the shift map in (3.5), though we suppress this from the notation).

We first describe the map L, appearing in Figure 3.1. The sum of length 1 compositions along the top face (as well as the bottom face) is $FD_n + D_n'F$, which expands to

$$Fv + F\mathfrak{F}\widetilde{v} + v'F + \mathfrak{F}'\widetilde{v}'F. \tag{3.10}$$

Here, v and $\widetilde{v}$ denote the inclusion maps for $\mathscr{C}$, while v' and $\widetilde{v}'$ denote the inclusion maps for $\mathscr{C}'$. Since F is induced by an $\mathbb{F}[\mathscr{U},\mathscr{V}]$-equivariant map, we have $Fv = v'F$

This is a free offprint provided to the author by the publisher. Copyright restrictions may apply.

and $\widetilde{v}'F = F\widetilde{v}$. Hence, (3.10) simplifies to

$$(F\mathfrak{F} + \mathfrak{F}'F)\widetilde{v}.$$

As maps from $\widetilde{\mathbb{B}}$ to $\mathbb{B}'$, the maps $F\mathfrak{F}$ and $\mathfrak{F}'F$ have the same grading, and map $\widetilde{B}_s$ to B'_{s+n}. Since $\widetilde{B}_s$ and B'_{s+n} are homotopy equivalent to $\mathbb{F}[U]$, and $\mathfrak{F}$ and $\mathfrak{F}'$ are homotopy equivalences, it follows that the maps $F\mathfrak{F}$ and $\mathfrak{F}'F$ are homotopic to each other. We let L be a $+1$ graded map such that

$$[\partial, L] = F\mathfrak{F} + \mathfrak{F}'F.$$

We now construct the map M, appearing on the right side of the cube in Figure 3.1. We let M be any $\mathbb{F}[U]$-equivariant, homogeneously $+1$ graded map which sends B_s to B'_{-s+n}, and satisfies

$$[\partial, M] = F\iota_{\mathbb{B}} + \iota'_{\mathbb{B}}F.$$

The existence of M follows from the fact that B_s and B'_s are homotopy equivalent to $\mathbb{F}[U]$, using the same logic that gave the existence of L.

We now construct the maps K and J appearing along the length 3 arrow (dotted) in Figure 3.1. We wish to choose these maps so that the total diagram is a chain complex (or equivalently, so that the maps make the diagram into a hypercube of chain complexes; see Chapter 5).

Let N denote the composition of the length 1 and 2 maps which feature in the length 3 hypercube relation, i.e.:

$$N := MD_n + \iota'_{\mathbb{B}}L\widetilde{v} + H'\widetilde{v}'F + FH\widetilde{v} + D'_n g + L\widetilde{v}\iota_{\mathbb{A}}. \tag{3.11}$$

First, an easy computation shows that $[\partial, N] = 0$ (in fact, this is automatic from the length 1 and 2 relations of the diagram in Figure 3.1).

We expand N, and use the fact that F is induced by an $\mathbb{F}[\mathscr{U}, \mathscr{V}]$-equivariant map, and ι_K and g are induced by skew-equivariant maps, to obtain that

$$N = qv + r\widetilde{v},$$

where

$$q = M + \mathfrak{F}'g + L\iota_{\mathbb{A}}, \quad \text{and} \quad r = M\mathfrak{F} + \iota'_{\mathbb{B}}L + H'F + FH + g.$$

We note that qv maps A_s to B'_{-s+n} while $r\widetilde{v}$ maps A_s to B'_{-s}. It is easy to check that both q and r are $+1$ graded chain maps. Since $\mathscr{C}$ and $\mathscr{C}'$ are of L-space type, every $+1$ graded map from B_s to B'_{-s+n}, or from $\widetilde{B}_s$ to B'_{-s} is a boundary, since $\mathrm{Hom}_{\mathbb{F}[U]}(\mathbb{F}[U], \mathbb{F}[U])$ is $\{0\}$ in gradings greater than 0. Hence, q and r are both chain homotopic to zero. We pick K and J to be any $+1$ graded null-homotopies of q and r which send B_s to B'_{-s+n} and $\widetilde{B}_s$ to B'_{-s}, respectively.

We now address the well-definedness of $\mathbb{XI}^{\mathrm{alg}}_n(F, g)$ from the choices made in the construction:

Proof of Part (2) of Proposition 3.15. Suppose that (F_1, g_1) and (F_2, g_2) are two enhanced homomorphisms from $\mathscr{C}$ to $\mathscr{C}'$, which are ι_K-homotopic as enhanced morphisms. We wish to show that the maps $\mathbb{XI}^{\mathrm{alg}}_n(F_1, g_1)$ and $\mathbb{XI}^{\mathrm{alg}}_n(F_2, g_2)$ are enhanced ι-chain homotopic. (Our argument when $(F_1, g_1) = (F_2, g_2)$ will prove that $\mathbb{XI}^{\mathrm{alg}}_n(F, g)$ is independent of the choices in the construction, up to enhanced ι-homotopy).

Let $\mathfrak{F}$ and H be the maps used to construct $\mathbb{XI}^{\mathrm{alg}}_n(\mathscr{C})$, and let $\mathfrak{F}'$ and H' be the maps used to construct $\mathbb{XI}^{\mathrm{alg}}_n(\mathscr{C}')$. Let L_1, M_1, J_1 and K_1 be the maps used

This is a free offprint provided to the author by the publisher. Copyright restrictions may apply.

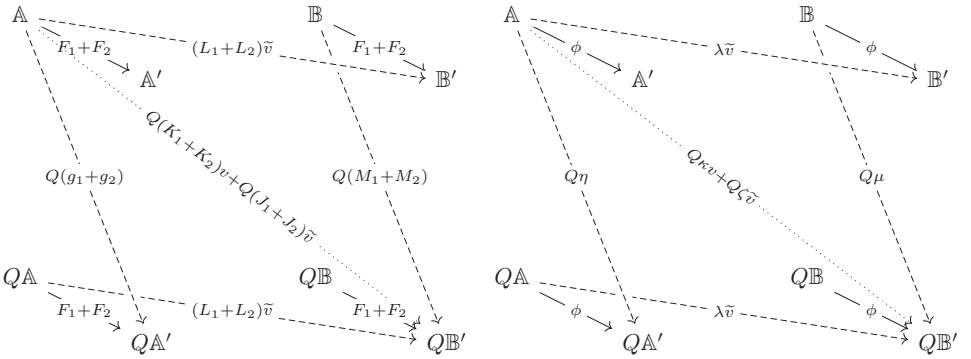


FIGURE 3.2. The enhanced ι-morphisms $\mathbb{XI}_n^{\mathrm{alg}}(F_1, g_1) + \mathbb{XI}_n^{\mathrm{alg}}(F_2, g_2)$ (left) and $\mathcal{E}$ (right).

in the construction of $\mathbb{XI}_n^{\mathrm{alg}}(F_1, g_1)$, and let L_2, M_2, J_2 and K_2 be the analogs for $\mathbb{XI}_n^{\mathrm{alg}}(F_2, g_2)$.

We now wish to construct an enhanced ι-morphism $\mathcal{E}$ from $\mathbb{XI}_n^{\mathrm{alg}}(\mathscr{C})$ to $\mathbb{XI}_n^{\mathrm{alg}}(\mathscr{C}')$ such that

$$\partial_{\underline{\mathrm{Mor}}}(\mathcal{E}) = \mathbb{XI}_n^{\mathrm{alg}}(F_1, g_1) + \mathbb{XI}_n^{\mathrm{alg}}(F_2, g_2).$$

First, we pick $(\phi, \eta) \in \underline{\mathrm{Mor}}(\mathscr{C}_1, \mathscr{C}_2)$ such that $\partial_{\underline{\mathrm{Mor}}}(\phi, \eta) = (F_1 + F_2, g_1 + g_2)$, which exists by hypothesis.

The relation

$$\partial_{\underline{\mathrm{Mor}}}(\mathcal{E}) = \mathbb{XI}_n^{\mathrm{alg}}(F_1, g_1) + \mathbb{XI}_n^{\mathrm{alg}}(F_2, g_2) \tag{3.12}$$

can be compactly restated as follows. Consider the $\mathbb{F}[\![U]\!]$-module M appearing on the right side of Figure 3.2 (consisting of the direct sum of $\mathbb{A}$, $\mathbb{B}$, $\mathbb{A}'$, $\mathbb{B}'$ and so forth). We build an endomorphism $\hat{\mathcal{E}}$ of M, as follows. We begin with $\mathcal{E}$ as show on the right side of Figure 3.2, and add $H\widetilde{v}$, D_n, $Q(1 + \iota_{\mathbb{A}})$, $Q(1 + \iota_{\mathbb{B}})$ to the back face of the cube, and also add the corresponding maps to the front face. Then, we add the internal differentials of $\mathbb{A}$, $\mathbb{B}$, and so forth. Equation (3.12) is equivalent to the relation

$$\hat{\mathcal{E}}^2 = \mathbb{XI}_n^{\mathrm{alg}}(F_1, g_1) + \mathbb{XI}_n^{\mathrm{alg}}(F_2, g_2). \tag{3.13}$$

We now construct λ, μ, κ and ζ. Our construction will be similar to our construction of the maps $\mathbb{XI}_n^{\mathrm{alg}}(F_i, g_i)$.

We begin by noting that (3.13) is already satisfied along the left face of the cube, since the desired relations are

$$F_1 + F_2 = [\partial, \phi] \quad \text{and} \quad g_1 + g_2 + \iota_{\mathbb{A}'}\phi + \phi\iota_{\mathbb{A}} = [\partial, \eta],$$

which is equivalent to $\partial_{\underline{\mathrm{Mor}}}(\phi, \eta) = (F_1, g_1) + (F_2, g_2)$.

Next, we wish λ to satisfy

$$D_n'\phi + \phi D_n + (L_1 + L_2)\widetilde{v} = [\partial, \lambda\widetilde{v}]. \tag{3.14}$$

Rearranging, and using the fact that ϕ is induced by an $\mathbb{F}[\mathscr{U}, \mathscr{V}]$-equivariant map, we see (3.14) is equivalent to

$$(\phi\mathfrak{F} + \mathfrak{F}'\phi + L_1 + L_2)\widetilde{v} = [\partial, \lambda]\widetilde{v}.$$

This is a free offprint provided to the author by the publisher. Copyright restrictions may apply.

The map $\phi\mathfrak{F}+\mathfrak{F}'\phi+L_1+L_2$ is a $+1$ graded chain map from $\widetilde{\mathbb{B}}$ to $\mathbb{B}'$, which sends $\widetilde{B}_s$ to B_{s+n}, and hence is null-homotopic. We let λ be any $+2$ graded homotopy, which sends $\widetilde{B}_s$ to B_{s+n}.

Next, we construct μ. The desired length 2 relation for the right face of the cube is

$$\phi\iota_{\mathbb{B}}+\iota_{\mathbb{B}'}\phi+M_1+M_2=[\partial,\mu].$$

It is straightforward to check that $\phi\iota_{\mathbb{B}}+\iota_{\mathbb{B}'}\phi+M_1+M_2$ is a $+1$ graded chain map which sends B_s to B_{-s+n}, and hence is null-homotopic. We let μ be any $+2$ graded null-homotopy, which also sends B_s to B_{-s+n}.

Finally, we construct κ and ζ. The desired equality is

(3.15)
$$H'\widetilde{v}'\phi+D'_n\eta+\mu D_n+\phi H\widetilde{v}+\iota_{\mathbb{B}'}\lambda\widetilde{v}+\lambda\widetilde{v}\iota_{\mathbb{A}}+(K_1+K_2)v+(J_1+J_2)\widetilde{v}=[\partial,\kappa v+\zeta\widetilde{v}].$$

It is easy to check that the left hand side of (3.15) decomposes as a sum $qv+r\widetilde{v}$, where q sends B_s to B'_{-s+n} and r sends $\widetilde{B}_s$ to B'_{-s}. Furthermore both q and r are $+2$ graded chain maps, and hence are null-homotopic, since $\mathrm{Hom}_{\mathbb{F}[U]}(\mathbb{F}[U],\mathbb{F}[U])$ is trivial in grading $+2$. We let κ and ζ be $+3$ graded null-homotopies.

The above relations show exactly that $\partial_{\underline{\mathrm{Mor}}}(\mathcal{E})=\mathbb{XI}^{\mathrm{alg}}_n(F_1,g_1)+\mathbb{XI}^{\mathrm{alg}}_n(F_2,g_2)$, so the proof is complete. □

We now consider the behavior of $\mathbb{XI}^{\mathrm{alg}}_n$ with respect to ι_K-homotopy equivalences, and local maps:

Proof of parts (3) and (4) of Proposition 3.15. We begin with part (3). Suppose (F,g) is an enhanced ι_K-homomorphism from $\mathscr{C}$ to $\mathscr{C}'$, such that F is a homotopy equivalence of chain complexes over $\mathbb{F}[\mathscr{U},\mathscr{V}]$. Clearly, the map F induces a homotopy equivalence of chain complexes over $\mathbb{F}[\![U]\!]$ from $\mathbb{A}$ to $\mathbb{A}'$. Similarly, F also induces a homotopy equivalence between $\mathbb{B}$ and $\mathbb{B}'$. We pick a map $L\colon\mathbb{B}\to\mathbb{B}'$, as in the construction of $\mathbb{XI}^{\mathrm{alg}}_n(F,g)$. The same argument as in Lemma 5.5 implies that the map induced by F and L is a homotopy equivalence from $\mathbb{X}_n(\mathscr{C})$ to $\mathbb{X}_n(\mathscr{C}')$, for any choice of L. Lemma 5.5 now implies that the map from $\mathbb{XI}^{\mathrm{alg}}_n(\mathscr{C})$ to $\mathbb{XI}^{\mathrm{alg}}_n(\mathscr{C}')$ is an ι-homotopy equivalence, completing the proof of part (3).

Next, we consider part (4). For concreteness, we focus on the case that $n>0$, as the case that $n<0$ is a minor modification. Suppose that (F,g) is an enhanced ι_K-homomorphism, such that F is a local map. We want to show that the map from $\mathbb{X}_n(\mathscr{C})$ to $\mathbb{X}_n(\mathscr{C}')$ induced by F and L becomes an isomorphism after inverting U. One should note that there is some subtlety in that localization at U does not naturally commute with infinite direct products, so we need to argue somewhat carefully. First, we truncate the mapping cone and consider the quotient complex $\mathbb{X}_n(\mathscr{C})\langle b\rangle$ generated by A_i for $-b\le i\le b$ and B_i for $-b+n\le i\le b$, for some large b. Analogously to [**OS08b**, Lemma 4.3], the projection maps onto the quotient complexes $\mathbb{X}_n(\mathscr{C})\langle b\rangle$ and $\mathbb{X}_n(\mathscr{C}')\langle b\rangle$ are quasi-isomorphisms. Since these are finite direct sums, we may invert U on each summand. Each summand is homotopy equivalent to $\mathbb{F}[\![U,U^{-1}]$. Furthermore, both v_s and $\mathfrak{F}\widetilde{v}_s$ become quasi-isomorphisms after inverting U. From this description, we see that projection of $U^{-1}\mathbb{X}_n(\mathscr{C})\langle b\rangle$ onto $U^{-1}A_0\oplus\cdots\oplus U^{-1}A_{n-1}$ is a quasi-isomorphism. Furthermore, under the projection map onto these summands, the map F is intertwined with the identity map from $\mathbb{F}[\![U,U^{-1}]$ to itself. In particular, the map induced by F is an isomorphism from $U^{-1}H_*(\mathbb{X}_n(\mathscr{C}))$ to $U^{-1}H_*(\mathbb{X}_n(\mathscr{C}'))$, completing the proof. □

This is a free offprint provided to the author by the publisher. Copyright restrictions may apply.

3.6. The algebraic cone is an iota-complex

In this section, we prove part (1) of Proposition 3.15, i.e. that the pair $(\mathbb{X}_n(\mathscr{C}), \iota_{\mathbb{X}})$ is an iota complex whenever $\mathscr{C}$ is an ι_K-complex of L-space type. We begin by proving that the algebraic analogs of the large surgery complexes are iota-complexes:

LEMMA 3.17. *Suppose $\mathcal{C}_K = (C_K, \partial, \iota_K)$ is an ι_K-complex. Then $\mathcal{C}_K$ is also an ι-complex, if we view C_K instead as a chain complex over $\mathbb{F}[U]$. In particular $\iota_K^2 \simeq \mathrm{id}$, $\mathbb{F}[U]$-equivariantly, on each $\mathcal{A}_s$.*

PROOF. We will write $\mathcal{C} = (C, \partial, \iota)$, for $\mathcal{C}_K$, viewed as a complex over $\mathbb{F}[U]$. We will write down a $+1$ graded endomorphism of $\mathbb{F}[U]$-modules $H\colon C \to C$ which satisfies

$$\iota^2 + \mathrm{id} = [\partial, H].$$

The map H we write down will not in general be a map of $\mathbb{F}[\mathscr{U}, \mathscr{V}]$-modules.

First, it is sufficient to write down a homotopy between $\Phi\Psi$ and 0, since by definition, $\iota_K^2 \simeq \Phi\Psi + \mathrm{id}$. There is an $\mathbb{F}[U]$-equivariant map

$$\Omega\colon C \to C,$$

defined similarly to Φ and Ψ, except keeping track of the changes of the U variable. More concretely, if $\mathbf{x}$ and $\mathbf{y}$ are basis elements of an $\mathbb{F}[U]$-basis of C, and $\partial(\mathbf{x})$ contains a summand of $U^k \cdot \mathbf{y}$, then $\Omega(\mathbf{x})$ contains a summand of $kU^{k-1} \cdot \mathbf{y}$. In terms of our original $\mathbb{F}[\mathscr{U}, \mathscr{V}]$-basis of C_K, Ω has the following description. If $\langle \partial(\mathscr{U}^i\mathscr{V}^j \cdot \mathbf{x}), \mathbf{y}\rangle = \mathscr{U}^{i+m}\mathscr{V}^{j+n}$, then

$$\langle \Omega(\mathscr{U}^i\mathscr{V}^j \cdot \mathbf{x}), \mathbf{y}\rangle := (\min(i+m, j+n) - \min(i,j))\, \mathscr{U}^{i+m-1}\mathscr{V}^{j+n-1}.$$

There is an $\mathbb{F}[U]$-equivariant map $H_{\Omega^2}\colon C \to C$, of homogeneous grading $+1$, which satisfies

$$\Omega^2 = [\partial, H_{\Omega^2}]. \tag{3.16}$$

If $\langle \partial(\mathbf{x}), \mathbf{y}\rangle = \mathscr{U}^m\mathscr{V}^n$,

$$\langle H_{\Omega^2}(\mathscr{U}^i\mathscr{V}^j \cdot \mathbf{x}), \mathbf{y}\rangle = \frac{\ell(\ell-1)}{2} \cdot \mathscr{U}^{i+m-2}\mathscr{V}^{j+n-2},$$

where $\ell = \min(i+m, j+n) - \min(i,j)$. Equation (3.16) follows from the same argument as in [**Zem15**, Lemma 14.18].

We make the following claims:

$$\begin{aligned} \Phi + \mathscr{V}\Omega &= [\partial, H_\Phi] \\ \Psi + \mathscr{U}\Omega &= [\partial, H_\Psi], \end{aligned} \tag{3.17}$$

where

$$\begin{aligned} H_\Phi(\mathscr{U}^i\mathscr{V}^j \cdot \mathbf{x}) &= \max(0, i-j)\mathscr{U}^{i-1}\mathscr{V}^j \cdot \mathbf{x}, \quad \text{and} \\ H_\Psi(\mathscr{U}^i\mathscr{V}^j \cdot \mathbf{x}) &= \max(0, j-i)\mathscr{U}^i\mathscr{V}^{j-1} \cdot \mathbf{x}. \end{aligned}$$

It is easy to check that H_Φ and H_Ψ give well defined endomorphisms of C_K (in particular, there are no negative exponents when applied to elements $\mathscr{U}^i\mathscr{V}^j \cdot \mathbf{x}$ with $i, j \geq 0$).

This is a free offprint provided to the author by the publisher. Copyright restrictions may apply.

We now prove the first equation of (3.17). Suppose that $\langle \partial(\mathbf{x}), \mathbf{y}\rangle = \mathscr{U}^m\mathscr{V}^n$. We compute directly from the definitions that

$$\begin{aligned}
\langle \Phi(\mathscr{U}^i\mathscr{V}^j \cdot \mathbf{x}), \mathbf{y}\rangle &= m \cdot \mathscr{U}^{i+m-1}\mathscr{V}^{j+n},\\
\langle \mathscr{V}\Omega(\mathscr{U}^i\mathscr{V}^j \cdot \mathbf{x}), \mathbf{y}\rangle &= (\min(i+m, j+n) - \min(i,j)) \cdot \mathscr{U}^{i+m-1}\mathscr{V}^{j+n},\\
\langle \partial H_\Phi(\mathscr{U}^i\mathscr{V}^j \cdot \mathbf{x}), \mathbf{y}\rangle &= \max(0, i-j) \cdot \mathscr{U}^{i+m-1}\mathscr{V}^{j+n},\\
\langle H_\Phi\partial(\mathscr{U}^i\mathscr{V}^j \cdot \mathbf{x}), \mathbf{y}\rangle &= \max(0, i+m-j-n) \cdot \mathscr{U}^{i+m-1}\mathscr{V}^{j+n}.
\end{aligned}$$

Hence, to prove the first equation of (3.17), it is sufficient to show that if i, j, m, n are integers, then

(3.18)
$$\max(0, i-j)+\min(i,j)+\max(0, i+m-j-n)+\min(m+i, n+j)+m \equiv 0 \pmod 2.$$

Note that $\max(i+m-j-n, 0) = \max(i+m, j+n) - j - n$ and $\max(0, i-j) = \max(i,j) - j$. Furthermore, $\max(a,b) + \min(a,b) = a+b$, for any a and b. Hence, we manipulate the left hand side of (3.18), as follows:

$$\begin{aligned}
&\max(i,j) + \min(i,j) + \max(i+m, j+n) + \min(i+m, j+n) - j + m - n - j\\
&\qquad = (i+j) + (i+m+j+n) - j + m - n - j\\
&\qquad \equiv 0 \pmod 2,
\end{aligned}$$

establishing (3.18), and hence the first relation of (3.17). The second relation of (3.17) follows by an easy modification.

Combining (3.16), (3.17) and the $\mathbb{F}[\mathscr{U}, \mathscr{V}]$-equivariance of Φ, we conclude

$$\begin{aligned}
\Phi\Psi &\simeq \Phi\mathscr{U}\Omega\\
&= \mathscr{U}\Phi\Omega\\
&\simeq \mathscr{U}\mathscr{V}\Omega\Omega\\
&\simeq 0.
\end{aligned} \tag{3.19}$$

□

The maps $\iota_{\mathbb{A}}$ and ι_K are conjugate under $\mathscr{S}$. Hence, we obtain the following corollary:

Corollary 3.18. *The map $\iota_{\mathbb{A}}\colon \mathbb{A} \to \mathbb{A}$ satisfies $\iota_{\mathbb{A}}^2 \simeq \mathrm{id}$.*

We now investigate the homotopy constructed in Lemma 3.17 in more detail. We write

$$H_{\mathfrak{A}}\colon \mathfrak{A} \to \mathfrak{A}$$

for the null-homotopy of $\Phi\Psi$ constructed in Lemma 3.17. Concretely,

$$H_{\mathfrak{A}} := \Phi H_\Psi + \mathscr{U} H_\Phi \Omega + \mathscr{U}\mathscr{V} H_{\Omega^2}. \tag{3.20}$$

It is helpful now to abuse notation slightly, and write v for the inclusion of $\mathfrak{A}$ into $\mathfrak{B}$, and $\widetilde{v}$ for the inclusion of $\mathfrak{A}$ into $\widetilde{\mathfrak{B}}$.

In our proof of part (1) of Proposition 3.15, we will encounter the expressions $vH_{\mathfrak{A}}$ and $\widetilde{v}H_{\mathfrak{A}}$. The general algebraic strategy is to factor the maps through an initial factor of v or $\widetilde{v}$. Hence, one might optimistically hope that

$$vH_{\mathfrak{A}} = H_{\mathfrak{B}}v, \quad \text{and} \quad \widetilde{v}H_{\mathfrak{A}} = H_{\widetilde{\mathfrak{B}}}\widetilde{v}, \tag{3.21}$$

for some $\mathbb{F}[U]$-equivariant maps $H_{\mathfrak{B}}\colon \mathfrak{B} \to \mathfrak{B}$ and $H_{\widetilde{\mathfrak{B}}}\colon \widetilde{\mathfrak{B}} \to \widetilde{\mathfrak{B}}$. Such maps do not exist in general, as we illustrate in Example 3.19.

This is a free offprint provided to the author by the publisher. Copyright restrictions may apply.

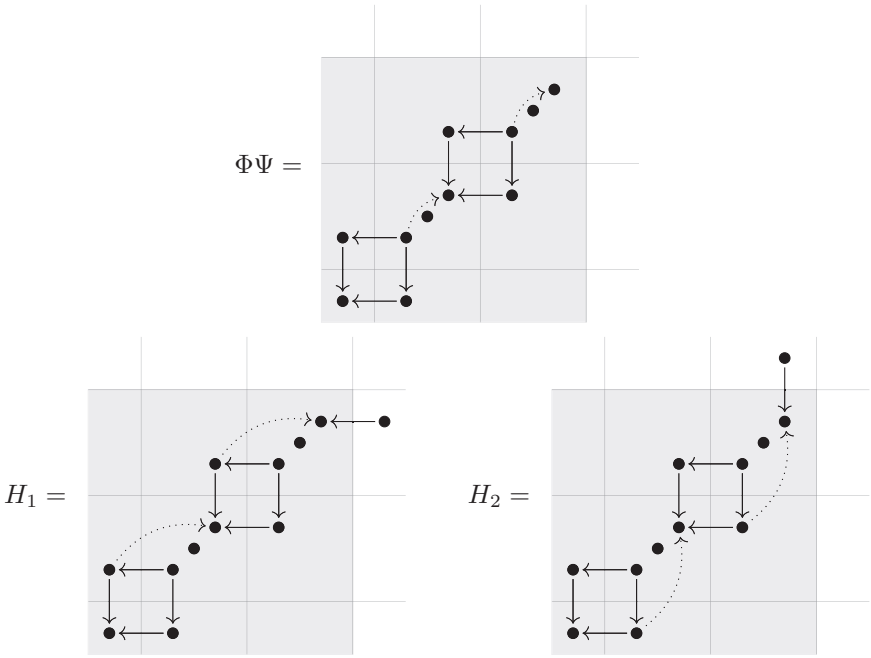


FIGURE 3.3. Two null-homotopies of $\Phi\Psi$ for the figure-8. The solid arrows are differentials of CFK^∞, and the dotted arrows denote $\Phi\Psi$, H_1 or H_2. The shaded region is A_0.

EXAMPLE 3.19. Consider the figure-8 knot. The complex A_0, and the map $\Phi\Psi$ are shown in Figure 3.3, as well as two natural choices of null-homotopies, H_1 and H_2, of $\Phi\Psi$. The map H_2 extends to a $\mathbb{F}[U]$-equivariant map over B_0, and the map H_1 extends to a map over $\widetilde{B}_0$. There is no $\mathbb{F}[U]$-equivariant null-homotopy of $\Phi\Psi$ on A_0 which extends over both B_0 and $\widetilde{B}_0$.

Despite Example 3.19, it turns out that we may construct maps $H_{\mathfrak{B}}$ and $H_{\widetilde{\mathfrak{B}}}$ which satisfy (3.21) up to a further chain homotopy, as we now describe.

We define $H_{\mathfrak{B}}\colon \mathfrak{B} \to \mathfrak{B}$ via the formula

$$H_{\mathfrak{B}} := \Phi H_\Psi + \mathscr{V}^{-1}\mathscr{U}\Phi H_\Phi + \mathscr{V}^{-1}\mathscr{U} H_{\Phi^2}. \tag{3.22}$$

Note that $\mathscr{V}$ is invertible on $\mathfrak{B}$. The map H_{Φ^2} in (3.22) is defined similarly to H_{Ω^2}, as follows. If $\langle \partial(\mathbf{x}), \mathbf{y}\rangle = \mathscr{U}^m\mathscr{V}^n$, then

$$\langle H_{\Phi^2}(\mathscr{U}^i\mathscr{V}^j \cdot \mathbf{x}), \mathbf{y}\rangle = \frac{m(m-1)}{2} \cdot \mathscr{U}^{i+m-2}\mathscr{V}^{j+n}.$$

Thinking 2-categorically, we think of the map $H_{\mathfrak{B}}$ as being constructed from the following sequence of homotopies:

$$\Phi\Psi \xrightarrow{\Phi H_\Psi} \Phi\mathscr{U}\Omega = \mathscr{V}^{-1}\mathscr{U}\Phi\mathscr{V}\Omega \xrightarrow{\mathscr{V}^{-1}\mathscr{U}\Phi H_\Phi} \mathscr{V}^{-1}\mathscr{U}\Phi^2 \xrightarrow{\mathscr{V}^{-1}\mathscr{U}H_{\Phi^2}} 0.$$

(Here, an arrow denotes a homotopy between the maps at the two ends). It is straightforward to check that the expression in equation (3.22) gives a well-defined map from $\mathfrak{B}$ to $\mathfrak{B}$.

This is a free offprint provided to the author by the publisher. Copyright restrictions may apply.

Next, we define $H_{\widetilde{\mathfrak{B}}}\colon \mathfrak{A} \to \widetilde{\mathfrak{B}}$ via the formula

$$H_{\widetilde{\mathfrak{B}}} := H_{\Phi}\Psi + \mathscr{U}^{-1}\mathscr{V}H_{\Psi}\Psi + \mathscr{U}^{-1}\mathscr{V}H_{\Psi^2}. \tag{3.23}$$

Here, H_{Ψ^2} is the map which satisfies

$$\langle H_{\Psi^2}(\mathscr{U}^i\mathscr{V}^j \cdot \mathbf{x}), \mathbf{y}\rangle = \frac{n(n-1)}{2} \cdot \mathscr{U}^{i+m}\mathscr{V}^{j+n-2},$$

if $\langle \partial(\mathbf{x}), \mathbf{y}\rangle = \mathscr{U}^m\mathscr{V}^n$. We think of $H_{\widetilde{\mathfrak{B}}}$ as being associated to the following sequence of homotopies:

$$\Phi\Psi \xrightarrow{H_{\Phi}\Psi} \mathscr{V}\Omega\Psi = \mathscr{U}^{-1}\mathscr{V}\mathscr{U}\Omega\Psi \xrightarrow{\mathscr{U}^{-1}\mathscr{V}H_{\Psi}\Psi} \mathscr{U}^{-1}\mathscr{V}\Psi\Psi \xrightarrow{\mathscr{U}^{-1}\mathscr{V}H_{\Psi^2}} 0.$$

The maps $H_{\mathfrak{B}}$ and $H_{\widetilde{\mathfrak{B}}}$ satisfy

$$[\partial, H_{\mathfrak{B}}] = \Phi\Psi \quad \text{and} \quad [\partial, H_{\widetilde{\mathfrak{B}}}] = \Phi\Psi.$$

The following technical lemma relates $H_{\mathfrak{A}}$, $H_{\mathfrak{B}}$ and $H_{\widetilde{\mathfrak{B}}}$:

LEMMA 3.20. *Suppose that (C_K, ∂, ι_K) is an ι_K-complex of L-space type.*

(1) *There is an $\mathbb{F}[U]$-equivariant map $h_{\mathfrak{A},\mathfrak{B}}\colon \mathfrak{A} \to \mathfrak{B}$ satisfying*

$$[\partial, h_{\mathfrak{A},\mathfrak{B}}] = vH_{\mathfrak{A}} + H_{\mathfrak{B}}v.$$

Furthermore, $h_{\mathfrak{A},\mathfrak{B}}$ may be taken to have homogeneous grading $+2$, and send $\mathcal{A}_s$ to $\mathcal{B}_s$.

(2) *There is an $\mathbb{F}[U]$-equivariant map $h_{\mathfrak{A},\widetilde{\mathfrak{B}}}\colon \mathfrak{A} \to \widetilde{\mathfrak{B}}$ satisfying*

$$[\partial, h_{\mathfrak{A},\widetilde{\mathfrak{B}}}] = \widetilde{v}H_{\mathfrak{A}} + H_{\widetilde{\mathfrak{B}}}\widetilde{v}.$$

Furthermore, $h_{\mathfrak{A},\widetilde{\mathfrak{B}}}$ may be taken to have homogeneous grading $+2$ and send $\mathcal{A}_s$ to $\widetilde{\mathcal{B}}_s$.

PROOF. We begin by investigating part (1). We consider the sum $vH_{\mathfrak{A}} + H_{\mathfrak{B}}v$. Using the formulas in (3.20) and (3.22), we compute that if $\langle \partial(\mathbf{x}), \mathbf{y}\rangle = \mathscr{U}^m\mathscr{V}^n$, then

$$\begin{aligned}
&\langle (vH_{\mathfrak{A}} + H_{\mathfrak{B}}v)(\mathscr{U}^i\mathscr{V}^j \cdot \mathbf{x}), \mathbf{y}\rangle \\
=&\Bigg(\max(0, m+i-n-j) \cdot (\min(m+i, n+j) - \min(i,j)) \\
&+ \frac{(\min(m+i, n+j) - \min(i,j))(\min(m+i, n+j) - \min(i,j) - 1)}{2} \\
&+ \max(0, i-j)m + \frac{m(m-1)}{2}\Bigg) \mathscr{U}^{i+m-1}\mathscr{V}^{j+n-1}.
\end{aligned} \tag{3.24}$$

To simplify (3.24), we introduce some notation. Write

$$\mathbf{X} := \mathscr{U}^i\mathscr{V}^j \cdot \mathbf{x} \quad \text{and} \quad \mathbf{Y} := \mathscr{U}^{i+m}\mathscr{V}^{j+n} \cdot \mathbf{y}. \tag{3.25}$$

Define

$$\epsilon(\mathbf{X}) := \max(i-j, 0) \quad \text{and} \quad \epsilon(\mathbf{Y}) := \max(m+i-n-j, 0),$$

which we view as elements of $\mathbb{Z}$. Note that

$$\begin{aligned}
\min(m+i, n+j) - \min(i,j) &= \min(0, n+j-m-i) + m + i - \min(0, j-i) - i \\
&= -\epsilon(\mathbf{Y}) + \epsilon(\mathbf{X}) + m,
\end{aligned}$$

This is a free offprint provided to the author by the publisher. Copyright restrictions may apply.

since $\min(0,a) = -\max(0,-a)$ for all $a \in \mathbb{Z}$. Hence, the coefficient of $\mathscr{U}^{i+m-1}\mathscr{V}^{j+n-1}$ in (3.24) becomes

$$\begin{aligned}&\epsilon(\mathbf{Y})(-\epsilon(\mathbf{Y})+\epsilon(\mathbf{X})+m)+\frac{(-\epsilon(\mathbf{Y})+\epsilon(\mathbf{X})+m)(-\epsilon(\mathbf{Y})+\epsilon(\mathbf{X})+m-1)}{2}\\&+m\epsilon(\mathbf{X})+\frac{m(m-1)}{2}\\&\equiv\frac{\epsilon(\mathbf{Y})(\epsilon(\mathbf{Y})-1)}{2}+\frac{\epsilon(\mathbf{X})(\epsilon(\mathbf{X})-1)}{2}\pmod 2.\end{aligned}$$

In particular, $vH_{\mathfrak{A}}+H_{\mathfrak{B}}v=[\partial,h_{\mathfrak{A},\mathfrak{B}}]$, where

$$h_{\mathfrak{A},\mathfrak{B}}(\mathbf{X})=U^{-1}\cdot\frac{\epsilon(\mathbf{X})(\epsilon(\mathbf{X})-1)}{2}\cdot\mathbf{X}.$$

It is easy to check that $h_{\mathfrak{A},\mathfrak{B}}$ is $\mathbb{F}[U]$-equivariant and maps $\mathcal{A}_s$ to $\mathcal{B}_s$.

We now consider part (2) of the main claim. The argument is similar to part (1), as we now describe. Similar to the previous case, using (3.20) and (3.23), we compute that if $\langle\partial(\mathbf{x}),\mathbf{y}\rangle=\mathscr{U}^m\mathscr{V}^n$, then

$$\begin{aligned}&\langle(\widetilde{v}H_{\mathfrak{A}}+H_{\widetilde{\mathfrak{B}}}\widetilde{v})(\mathscr{U}^i\mathscr{V}^j\cdot\mathbf{x}),\mathbf{y}\rangle\\&=\Big(m\max(0,j-i)+\max(0,m+i-n-j)(\min(m+i,n+j)-\min(i,j))\\&+\frac{(\min(m+i,n+j)-\min(i,j))(\min(m+i,n+j)-\min(i,j)-1)}{2}\\&+n\max(0,i+m-j-n+1)+n\max(0,j+n-1-m-i)\\&+\frac{n(n-1)}{2}\Big)\cdot\mathscr{U}^{i+m-1}\mathscr{V}^{j+n-1}.\end{aligned}\tag{3.26}$$

We let $\mathbf{X}$ and $\mathbf{Y}$ be as in (3.25), and define

$$\nu(\mathbf{X}):=\max(0,j-i)\quad\text{and}\quad\nu(\mathbf{Y}):=\max(0,n+j-m-i).$$

Noting that $\min(m+i,n+j)-\min(i,j)=-\nu(\mathbf{Y})+\nu(\mathbf{X})+n$, and also that $\max(0,a)+\max(0,-a)\equiv a \mod 2$, for any a, modulo 2 the coefficient of the right hand side of (3.26) becomes

$$\begin{aligned}&m\nu(\mathbf{X})+(m+i-n-j)(-\nu(\mathbf{Y})+\nu(\mathbf{X})+n)+\nu(\mathbf{Y})(-\nu(\mathbf{Y})+\nu(\mathbf{X})+n)\\&+\frac{(-\nu(\mathbf{Y})+\nu(\mathbf{X})+n)(-\nu(\mathbf{Y})+\nu(\mathbf{X})+n-1)}{2}\\&+n(i+m-j-n)+n+\frac{n(n-1)}{2}.\end{aligned}\tag{3.27}$$

Rearranging (3.27), we obtain

$$\begin{aligned}&-\frac{\nu(\mathbf{Y})(\nu(\mathbf{Y})-1)}{2}+\frac{\nu(\mathbf{X})(\nu(\mathbf{X})-1)}{2}\\&+(n+m)\nu(\mathbf{X})+(m+i-n-j)(-\nu(\mathbf{Y})+\nu(\mathbf{X}))+n\\&+n(n-1)+2n(m+i-n-j).\end{aligned}\tag{3.28}$$

Noting that, modulo 2, $(i-j)\nu(\mathbf{X})=\nu(\mathbf{X})$ and $(m+i-n-j)\nu(\mathbf{Y})=\nu(\mathbf{Y})$, we see that, modulo 2, (3.28) is equal to

$$\frac{\nu(\mathbf{Y})(\nu(\mathbf{Y})+1)}{2}+\frac{\nu(\mathbf{X})(\nu(\mathbf{X})+1)}{2}+n.\tag{3.29}$$

This is a free offprint provided to the author by the publisher. Copyright restrictions may apply.

We define

$$h(\mathbf{X}) := U^{-1} \cdot \frac{\nu(\mathbf{X})(\nu(\mathbf{X})+1)}{2} \cdot \mathbf{X} \quad \text{and} \quad k(\mathscr{U}^i \mathscr{V}^j \cdot \mathbf{x}) := j \cdot \mathscr{U}^{i-1} \mathscr{V}^{j-1} \cdot \mathbf{x}.$$

Note that h is $\mathbb{F}[U]$-equivariant, while k is not. Also note that h maps $\mathcal{A}_s$ to $\widetilde{\mathcal{B}}_s$.

The above manipulation shows that

$$\widetilde{v} H_{\mathfrak{A}} + H_{\widetilde{\mathfrak{B}}} \widetilde{v} = [\partial, h] + [\partial, k]. \tag{3.30}$$

We note that $[\partial, k] = \mathscr{U}^{-1}\Psi\widetilde{v}$. The map $\mathscr{U}^{-1}\Psi$ is $\mathbb{F}[U]$-equivariant, maps $\widetilde{\mathcal{B}}_s$ to $\widetilde{\mathcal{B}}_s$, and shifts both $\mathrm{gr}_{\mathbf{w}}$ and $\mathrm{gr}_{\mathbf{z}}$ by $+1$ (recall that $\mathrm{gr}_{\mathbf{w}} = \mathrm{gr}_{\mathbf{z}} + 2s$ on $\widetilde{\mathcal{B}}_s$). Since C_K is of L-space type, there is an $\mathbb{F}[U]$-equivariant map $h_0 \colon \widetilde{\mathcal{B}}_s \to \widetilde{\mathcal{B}}_s$ such that $\mathscr{U}^{-1}\Psi = [\partial, h_0]$, as endomorphisms of $\widetilde{\mathcal{B}}_s$. We extend h_0 to an endomorphism of all of $\widetilde{\mathfrak{B}}$, by declaring h_0 to be equivariant with respect to $\mathscr{U}$ and $\mathscr{V}$. We set $h_{\mathfrak{A},\widetilde{\mathfrak{B}}}$ to be

$$h_{\mathfrak{A},\widetilde{\mathfrak{B}}} := h + h_0 \widetilde{v},$$

which manifestly satisfies $[\partial, h_{\mathfrak{A},\widetilde{\mathfrak{B}}}] = \widetilde{v} H_{\mathfrak{A}} + H_{\widetilde{\mathfrak{B}}} \widetilde{v}$, completing the proof. □

Proposition 3.21. *If $\mathscr{C} = (C_K, \partial, \iota_K)$ is an ι_K-complex of L-space type, then $\mathbb{XI}^{\mathrm{alg}}_n(\mathscr{C})$ is an ι-complex.*

Proof. Let H and $\mathfrak{F}$ denote the maps chosen in the construction of $\iota_{\mathbb{X}}$. We compute that

$$\iota^2_{\mathbb{X}} + \mathrm{id} = \begin{array}{ccc} \mathbb{A} & & \mathbb{B} \\ \downarrow{\scriptstyle \iota^2_{\mathbb{A}}+\mathrm{id}} & \searrow^{H\iota_{\mathbb{A}} v + \iota_{\mathbb{B}} H \widetilde{v}} & \downarrow{\scriptstyle \iota^2_{\mathbb{B}}+\mathrm{id}} \\ \mathbb{A} & & \mathbb{B}. \end{array} \tag{3.31}$$

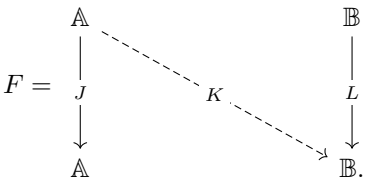
Here we have implicitly used the relation $U^s \iota_K v = \widetilde{v} U^s \iota_K$, which follows since ι_K is $\mathbb{F}[\mathscr{U}, \mathscr{V}]$-equivariant. Our proof of the main claim will be to show that

$$\iota^2_{\mathbb{X}} + \mathrm{id} \simeq \begin{array}{ccc} \mathbb{A} & & \mathbb{B} \\ \downarrow{\scriptstyle 0} & \searrow^{qv + r\widetilde{v}} & \downarrow{\scriptstyle 0} \\ \mathbb{A} & & \mathbb{B} \end{array} \tag{3.32}$$

where $q \colon \mathbb{B} \to \mathbb{B}$ and $r \colon \widetilde{\mathbb{B}} \to \mathbb{B}$ are $\mathbb{F}[\![U]\!]$-equivariant maps such that q sends B_s to B_s and r sends $\widetilde{B}_s$ to B_{s+n}, such that q and r are $+1$ graded. Note that if this is the case, then q and r must be chain maps. Furthermore, $q \simeq 0$ and $r \simeq 0$, since $\mathscr{C}$ is of L-space type. We obtain a homotopy giving the relation $\iota^2_{\mathbb{X}} + \mathrm{id} \simeq 0$, by defining a map from $\mathbb{X}_n(\mathscr{C})$ to $\mathbb{X}_n(\mathscr{C})$ which puts this null-homotopy of $qv + r\widetilde{v}$ along the diagonal.

This is a free offprint provided to the author by the publisher. Copyright restrictions may apply.

More generally, suppose that $F\colon \mathbb{X}_n(\mathscr{C}) \to \mathbb{X}_n(\mathscr{C})$ is a grading preserving map which is filtered with respect to the mapping cone filtration, i.e., F takes the following form:



We say that F is *simple* if the diagonal map K decomposes as

$$K = qv + r\widetilde{v},$$

where $q\colon \mathbb{B} \to \mathbb{B}$ and $r\colon \widetilde{\mathbb{B}} \to \mathbb{B}$ are homogeneously graded, $\mathbb{F}[\![U]\!]$-equivariant maps, such that q sends B_s to B_s, and r sends $\widetilde{B}_s$ to B_{s+n}. Equation (3.31) implies that $\iota_{\mathbb{X}}^2 + \mathrm{id}$ is simple.

Given an $\mathbb{F}[\![U]\!]$-equivariant chain map $F\colon \mathbb{X}_n(\mathscr{C}) \to \mathbb{X}_n(\mathscr{C})$, which is filtered with respect to the mapping cone filtration, it is natural to change the maps J, K and L individually. We make the following observations:

(κ-1) If F' is obtained by replacing L with $[\partial_{\mathbb{B}}, \kappa]+L$ and replacing K with $K+\kappa D_n$, for a $+1$ graded map $\kappa\colon \mathbb{B} \to \mathbb{B}$, then $F' \simeq F$. If F is simple and κ sends B_s to B_s, then F' is also simple.

(κ-2) If F' is obtained by replacing J with $J + [\partial_{\mathbb{A}}, \kappa]$, where $\kappa\colon \mathbb{A} \to \mathbb{A}$ is a $+1$ graded map, and also replacing K with $K + D_n\kappa$, then

$$F' \simeq F.$$

Furthermore, F' is simple if F is simple and $D_n\kappa$ decomposes as $jv + k\widetilde{v}$, for homogeneously graded maps $j\colon \mathbb{B} \to \mathbb{B}$ and $k\colon \widetilde{\mathbb{B}} \to \mathbb{B}$ such that j maps B_s to B_s and g maps $\widetilde{B}_s$ to B_{s+n}, and q and r are grading preserving (with respect to the mapping cone grading).

(κ-3) If F' is obtained from F by adding $[\partial, \kappa]$ to the diagonal map K, where $\kappa\colon \mathbb{A} \to \mathbb{B}$ is any $+1$ graded map of $\mathbb{F}[\![U]\!]$-modules, then $F' \simeq F$.

All of the above observations are straightforward to prove.

We return to the expression for $\iota_{\mathbb{X}}^2 + \mathrm{id}$ in equation (3.31). Firstly, $\iota_{\mathbb{B}}^2 \simeq \mathrm{id}$ on $\mathbb{B}$ (automatically, since $\mathscr{C}$ is L-space type), so using observation (κ-1), $\iota_{\mathbb{X}}^2 + \mathrm{id}$ is chain homotopic to a simple map which maps $\mathbb{A}$ to $\mathbb{A}$ via $\iota_{\mathbb{A}}^2 + \mathrm{id}$, and maps $\mathbb{B}$ to $\mathbb{B}$ via 0.

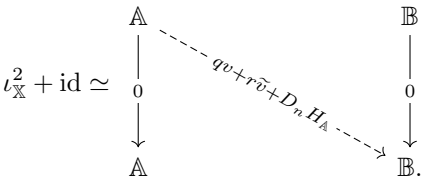
Next, we take an $\mathbb{F}[\mathscr{U}, \mathscr{V}]$-equivariant map κ satisfying $[\partial, \kappa] = \iota_K^2 + \mathrm{id} + \Phi\Psi$ on C_K. Conjugating with the shift isomorphism, we obtain a map from $\mathbb{A}$ to $\mathbb{B}$, which we also denote by κ (abusing notation slightly). Since κ is induced by an $\mathbb{F}[\mathscr{U}, \mathscr{V}]$-equivariant map, we have

$$D_n\kappa = (v + \mathfrak{F}\widetilde{v})\kappa = \kappa v + \mathfrak{F}\kappa\widetilde{v}.$$

By (κ-2), we may replace the component of $\iota_{\mathbb{X}}^2 + \mathrm{id}$ mapping $\mathbb{A}$ to $\mathbb{A}$ (which takes the form $\iota_{\mathbb{A}}^2 + \mathrm{id}$) with $\Phi\Psi$, while retaining simplicity of the map.

This is a free offprint provided to the author by the publisher. Copyright restrictions may apply.

By Lemma 3.17, there is an $\mathbb{F}[\![U]\!]$-equivariant map $H_{\mathbb{A}}\colon \mathbb{A} \to \mathbb{A}$ which satisfies $\Phi\Psi = [\partial_{\mathbb{A}}, H_{\mathbb{A}}]$. By ($\kappa$-2)



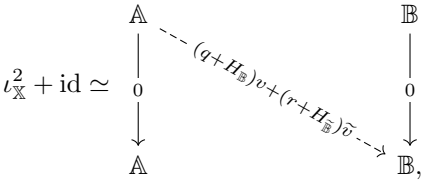
Note that

$$D_n H_{\mathbb{A}} = vH_{\mathbb{A}} + \mathfrak{F}\widetilde{v}H_{\mathbb{A}}.$$

Conjugating the maps constructed in Lemma 3.20 with the shift map $\mathscr{S}$, we obtain maps $H_{\mathbb{B}}\colon \mathbb{B} \to \mathbb{B}$ and $H_{\widetilde{\mathbb{B}}}\colon \widetilde{\mathbb{B}} \to \widetilde{\mathbb{B}}$ such that

$$vH_{\mathbb{A}} \simeq H_{\mathbb{B}}v \quad \text{and} \quad \widetilde{v}H_{\mathbb{A}} \simeq H_{\widetilde{\mathbb{B}}}\widetilde{v}.$$

Hence, by (κ-3)



which completes the proof, since we have reduced to the form described in (3.32). □

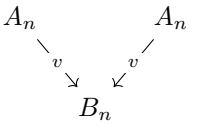
3.7. The local equivalence class of surgeries

In this section, we prove that the local equivalence class of $\mathbb{XI}_n^{\mathrm{alg}}(\mathscr{C})$ has a simple form:

PROPOSITION 3.22. *Suppose $\mathscr{C}$ is an ι_K-complex of L-space type and $n > 0$.*

(1) *Then $\mathbb{XI}_n^{\mathrm{alg}}(\mathscr{C}, [0])$ is locally equivalent to $A_0(\mathscr{C})$.*
(2) *Furthermore, $\mathbb{XI}_{2n}^{\mathrm{alg}}(\mathscr{C}, [n])$ is locally equivalent to the complex*

(3.33)



with the involution which swaps the two copies of A_n, and fixes B_n.

We split the proof of Proposition 3.22 into two parts:

PROOF OF PART (1) OF PROPOSITION 3.22. We assume $n = 1$, to simplify the notation. Projection gives a local map from $\mathbb{XI}_{+1}^{\mathrm{alg}}(\mathscr{C})$ to $A_0(\mathscr{C})$, so it suffices to construct a local map

$$F\colon \mathbb{XI}_{+1}^{\mathrm{alg}}(\mathscr{C})\langle k\rangle \to \mathbb{XI}_{+1}^{\mathrm{alg}}(\mathscr{C})\langle k+1\rangle.$$

On the summands $A_{-k+1}, \dots, A_{k-1}, B_{-k+1}, \dots, B_k$, we define F to be the identity. On the remaining summands, we define F as in Figure 3.4, where α, β, and γ are maps which we define shortly.

This is a free offprint provided to the author by the publisher. Copyright restrictions may apply.

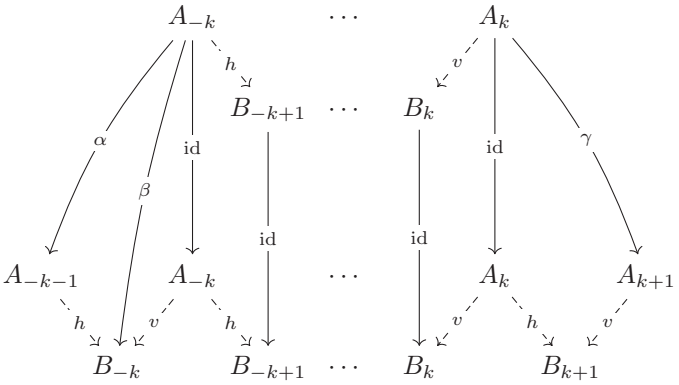


FIGURE 3.4. The map $F\colon \mathbb{XI}^{\mathrm{alg}}_{+1}(\mathscr{C})\langle k\rangle \to \mathbb{XI}^{\mathrm{alg}}_{+1}(\mathscr{C})\langle k+1\rangle$. Solid arrows denote F, while dashed arrows denote internal differentials of $\mathbb{XI}^{\mathrm{alg}}_{+1}(\mathscr{C})\langle k\rangle$ and $\mathbb{XI}^{\mathrm{alg}}_{+1}(\mathscr{C})\langle k+1\rangle$.

We recall that $h_s\colon A_s \to B_{s+1}$ is the composition of $\mathfrak{F}_s\widetilde{v}_s$, where $\mathfrak{F}_s\colon \widetilde{B}_s \to B_{s+1}$ is a choice of homogeneously graded homotopy equivalence, and $\widetilde{v}_s$ is the inclusion of A_s into $\widetilde{B}_s$. The choice of $\mathfrak{F}_s$ does not affect the homotopy type of the mapping cone complex, so we make the following convenient choice of $\mathfrak{F}_s$:

$$\mathfrak{F}_s := U^s\iota_K. \tag{3.34}$$

In (3.34), ι_K gives a homotopy equivalence between $\widetilde{B}_s = C(j \le s)$ and $C(i \le s)$, and U^s gives a chain isomorphism between $C(i \le s)$ and $B = C(i \le 0)$. With these definitions, the involutions take the form

$$\iota_{\mathbb{B}} = \iota_K^2 \quad \text{and} \quad \iota_{\mathbb{A},s} := U^s\iota_K.$$

(The formula for $\iota_{\mathbb{B}}$ looks odd, but follows from the definition $\iota_{\mathbb{B},s} := \mathfrak{F}_sU^{-s}\iota_K$).

With this choice of $\mathfrak{F}$, the property of F being a chain map is equivalent to the relations

$$\begin{aligned} [\partial,\alpha] &= 0,\\ h\alpha + v &= [\partial,\beta],\\ [\partial,\gamma] &= 0,\\ v\gamma + h &= 0. \end{aligned} \tag{3.35}$$

In (3.35), the maps are to be applied only to A_{-k} or A_k, as appropriate, and also ∂ denotes the internal differential of the summands A_s and B_s (in particular, not the mapping cone differential, which includes v and h). We set

$$\alpha = U^{k+1}\iota_K \quad \text{and} \quad \gamma = U^k\iota_K.$$

These are clearly chain maps, so the first and third relations of (3.35) are satisfied. The fourth is also satisfied, since $h_k = U^k\iota_K\widetilde{v}_k$. The second relation of (3.35), which involves α and β, is equivalent to

$$(\iota_K^2 + \mathrm{id})v = [\partial,\beta].$$

This is a free offprint provided to the author by the publisher. Copyright restrictions may apply.

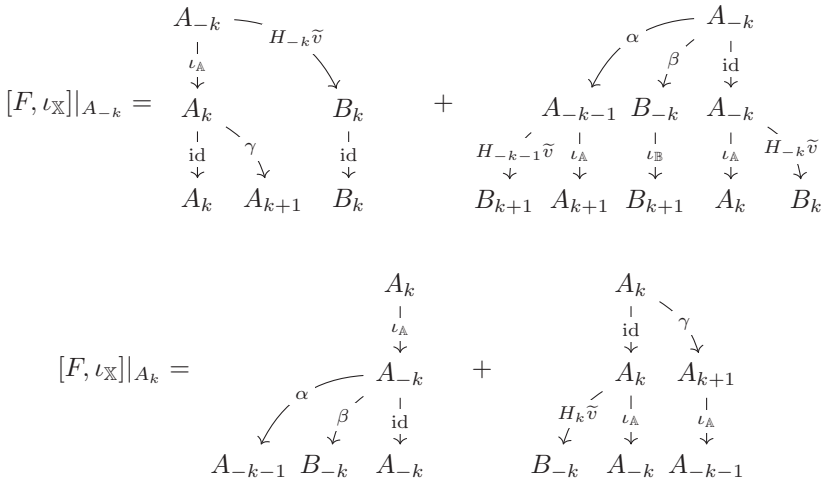


FIGURE 3.5. Computing $[F,\iota_{\mathbb{X}}]$ on A_{-k} (top row) and A_k (bottom row).

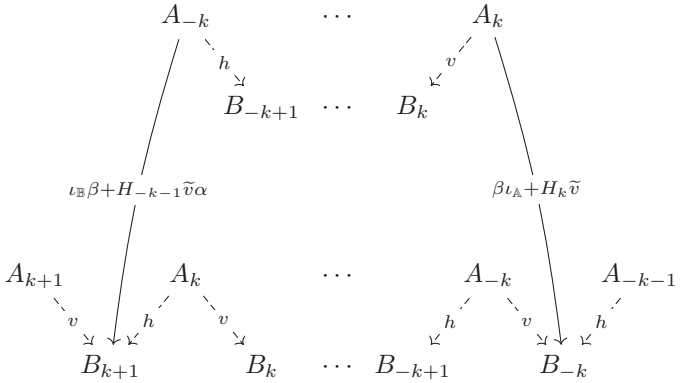


FIGURE 3.6. The commutator $[F,\iota_{\mathbb{X}}]$ (solid arrows). Note that the order of the indices is reversed along the bottom row. Dashed arrows denote internal differentials of $\mathbb{X}_n(\mathscr{C})$.

We pick any $\mathbb{F}[U]$-equivariant, homogeneously $+1$ graded map $J\colon B_s \to B_s$ satisfying $[\partial, J] = \iota_K^2 + \mathrm{id}$, which exists because $B_s \simeq \mathbb{F}[U]$. We define

$$\beta = Jv. \tag{3.36}$$

With these definitions, F becomes a chain map. Furthermore, F is homogeneously graded with respect to the grading on the mapping cone, and clearly becomes an isomorphism on homology after inverting U.

It remains to show that

$$F\iota_{\mathbb{X}} + \iota_{\mathbb{X}}F \simeq 0. \tag{3.37}$$

Note that $F\iota_{\mathbb{X}} + \iota_{\mathbb{X}}F = 0$ on all of the summands of $\mathbb{X}\mathbb{I}_{+1}(\mathscr{C})\langle k\rangle$ except for A_{-k} and A_k. On A_k and A_{-k}, we expand out $[F,\iota_{\mathbb{X}}]$ schematically in Figure 3.5.

After removing and canceling terms, we obtain the description of $[F,\iota_{\mathbb{X}}]$ shown in Figure 3.6.

This is a free offprint provided to the author by the publisher. Copyright restrictions may apply.

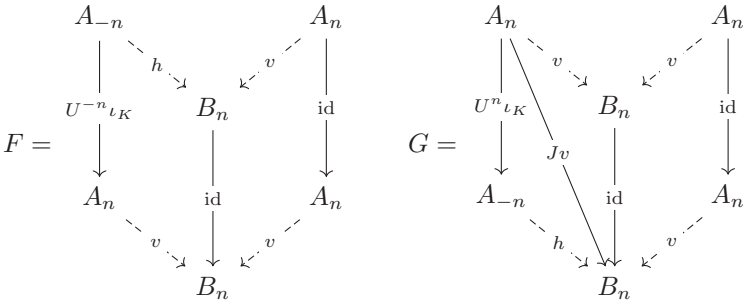


FIGURE 3.7. The maps F and G (solid arrows).

Hence, it is sufficient to show that the maps

$$\iota_{\mathbb{B}}\beta + H_{-k-1}\widetilde{v}\alpha\colon A_{-k} \to B_{k+1} \quad \text{and} \quad \beta\iota_{\mathbb{A}} + H_k\widetilde{v}\colon A_k \to B_{-k}$$

are null-homotopic. (Given such null-homotopies, we form a null-homotopy of $[F, \iota_{\mathbb{X}}]$ by putting these null-homotopies in the same positions as in Figure 3.4). Expanding out the definitions, we obtain

$$\iota_{\mathbb{B}}\beta + H_{-k-1}\widetilde{v}\alpha = (\iota_K^2 J + H_{-k-1}U^{k+1}\iota_K)v.$$

The map $(\iota_K^2 J + H_{-k-1}U^{k+1}\iota_K)$ is a $+1$ graded chain map from B_{-k} to B_{k+1}, and is hence null-homotopic, since both B_{-k} and B_{k+1} are homotopy equivalent to $\mathbb{F}[U]$, with 1 supported in the same grading.

Similarly,

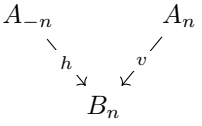
$$\beta\iota_{\mathbb{A}} + H_k\widetilde{v} = JU^k\iota_K\widetilde{v} + H_k\widetilde{v},$$

which is null-homotopic by the same reasoning. This concludes the claim about the Spin^c structure [0]. □

We now consider the local class of even surgeries:

PROOF OF PART (2) OF PROPOSITION 3.22. The proof of part (1) carries over to show that $\mathbb{XI}^{\mathrm{alg}}_{2n}(\mathscr{C}, [n])$ is locally equivalent to the truncation of $\mathbb{XI}^{\mathrm{alg}}_{2n}(\mathscr{C}, [n])$ shown in (3.38), with the involution induced by $\mathbb{XI}^{\mathrm{alg}}_{2n}(\mathscr{C})$.

(3.38)



As before, we can choose $\mathfrak{F}_{-n} = U^{-n}\iota_K$, so that $h = U^{-n}\iota_K\widetilde{v}$, in (3.38).

We define chain maps F and G between (3.33) and (3.38) in Figure 3.7. Here, Jv is the same map as in (3.36). We compute $[F, \iota]$ and $[G, \iota]$ in Figure 3.8.

In Figure 3.8,

$$L = H_{-n}U^n\iota_K + \iota_K^2 J.$$

This is a free offprint provided to the author by the publisher. Copyright restrictions may apply.

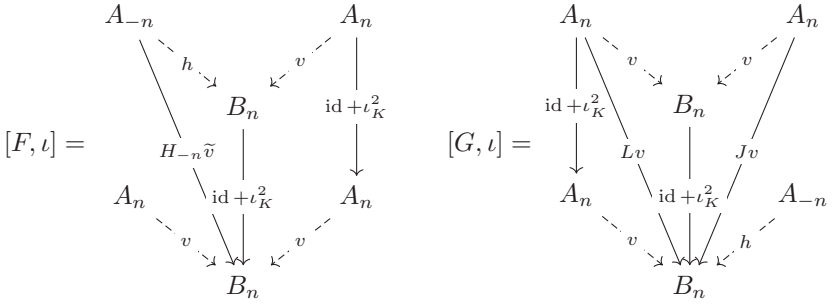
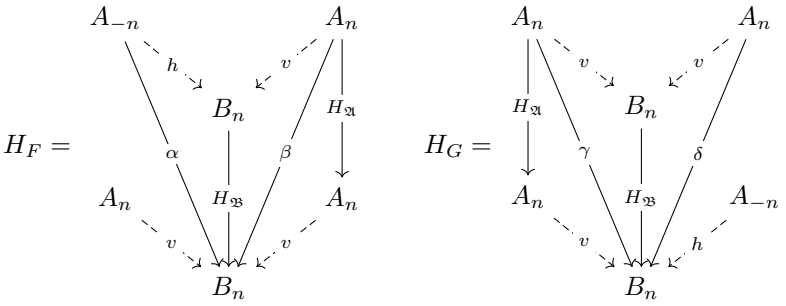


FIGURE 3.8. The commutators $[F,\iota]$ and $[G,\iota]$.

We claim that $[F,\iota]$ and $[G,\iota]$ are both null-homotopic. We construct null-homotopies of $[F,\iota]$ and $[G,\iota]$ in (3.39).

(3.39)



In (3.39) we write $H_{\mathfrak{B}}$ and $H_{\mathfrak{A}}$ for the homotopies constructed in Section 3.6 (plus an $F[\mathscr{U},\mathscr{V}]$-equivariant homotopy between $\mathrm{id}+\iota_K^2$ and $\Phi\Psi$, which we suppress from the notation). The relation $[F,\iota]=[\partial_{\mathbb{X}},H_F]$ is equivalent to the relations

$$\begin{aligned}\mathrm{id}+\iota_K^2 &= [\partial, H_{\mathfrak{A}}],\\ \mathrm{id}+\iota_K^2 &= [\partial, H_{\mathfrak{B}}],\\ H_{\mathfrak{B}}h + H_{-n}\widetilde{v} &= [\partial,\alpha],\\ H_{\mathfrak{B}}v + vH_{\mathfrak{A}} &= [\partial,\beta],\end{aligned} \tag{3.40}$$

(applied only to A_n or A_{-n}, as appropriate). The first and second relations of (3.40) follow from the constructions of $H_{\mathfrak{A}}$ and $H_{\mathfrak{B}}$. The existence of a β satisfying the fourth relation of (3.40) follows from Lemma 3.20. The existence of α which satisfies the third relation follows since $H_{\mathfrak{B}}h+H_{-k}\widetilde{v}$ is a $+1$ graded chain map which factors through $\widetilde{v}$.

Similarly, $[G,\iota]=[\partial_{\mathbb{X}},H_G]$ is equivalent to the relations

$$\begin{aligned}\mathrm{id}+\iota_K^2 &= [\partial, H_{\mathfrak{A}}],\\ \mathrm{id}+\iota_K^2 &= [\partial, H_{\mathfrak{B}}],\\ H_{\mathfrak{B}}v + Jv &= [\partial,\delta],\\ Lv + vH_{\mathfrak{A}} + H_{\mathfrak{B}}v &= [\partial,\gamma].\end{aligned} \tag{3.41}$$

The first two relations are immediate. The existence of δ which satisfies the third relation follows since $H_{\mathfrak{B}}v + Jv$ is a $+1$ graded chain map which factors through v. The existence of γ satisfying the fourth relation is as follows. By Lemma 3.20,

This is a free offprint provided to the author by the publisher. Copyright restrictions may apply.

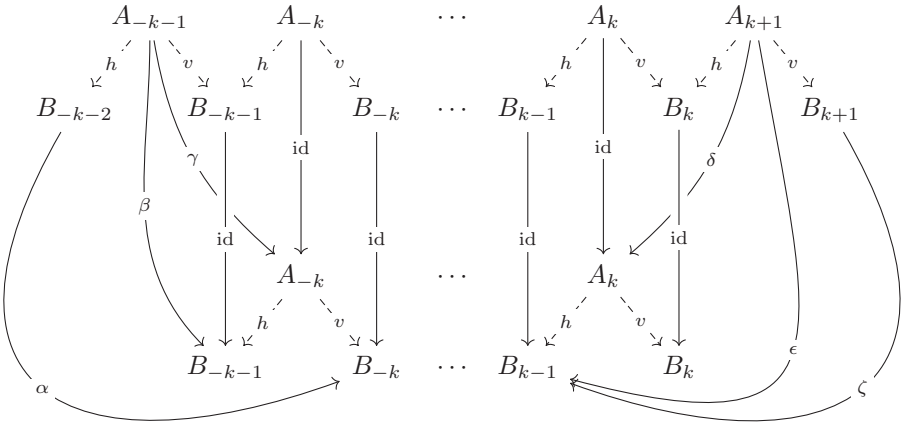


FIGURE 3.9. The local equivalence $F\colon \mathbb{XI}^{\mathrm{alg}}_{-1}(\mathscr{C})\langle k+1\rangle \to \mathbb{XI}^{\mathrm{alg}}_{-1}(\mathscr{C})\langle k\rangle$.

$vH_{\mathfrak{A}} \simeq H_{\mathfrak{B}}v$. Furthermore, L is a $+1$ graded chain map from B_n to B_n, so is null-homotopic. The proof is complete. □

For negative surgery coefficients, we have the following analog of Proposition 3.22:

PROPOSITION 3.23. *The local equivalence class of* $\mathbb{XI}^{\mathrm{alg}}_{-n}(\mathscr{C},[0])$ *coincides with the local class of* $(A_0(-\mathscr{C}),\iota_K)^\vee$*, where* $\vee$ *denotes the dual* ι*-complex, and* $-\mathscr{C}$ *denotes the dual* ι_K*-complex.*

PROOF. The proof is very similar to the proof of Proposition 3.22, so we only sketch the important details. As before, we focus on the case that $n=1$. Inclusion gives a local map from $\mathbb{XI}^{\mathrm{alg}}_{-1}(\mathscr{C},[0])\langle k\rangle$ to $\mathbb{XI}^{\mathrm{alg}}_{-1}(\mathscr{C},[0])\langle k+1\rangle$, so it suffices to construct a local map F in the opposite direction, which we do in Figure 3.9.

The necessary relations for F to be a chain map are

$$\begin{aligned}
[\partial,\alpha] &= 0,\\
[\partial,\gamma] &= 0,\\
\alpha h + v\gamma &= 0,\\
v + h\gamma &= [\partial,\beta],\\
[\partial,\delta] &= 0,\\
[\partial,\zeta] &= 0,\\
h\delta + \zeta v &= [\partial,\epsilon],\\
h + v\delta &= 0.
\end{aligned} \tag{3.42}$$

In (3.42), the third and fourth relations have domain A_{-k-1}, while the last two have domain A_{k+1}. Toward (3.42), we make the following definitions:

$$\alpha := U^{2k+1}\,\mathrm{id}, \quad \gamma := U^k\iota_K, \quad \delta = U^{k+1}\iota_K, \quad \text{and} \quad \zeta = U^{2k+1}\,\mathrm{id}\,. \tag{3.43}$$

It is easily checked that with the definitions in (3.43), maps β and ϵ may be found so that (3.42) is satisfied. Thus, F is a homogeneously graded chain map, and clearly sends $\mathbb{F}[U]$-non-torsion cycles to $\mathbb{F}[U]$-non-torsion cycles.

This is a free offprint provided to the author by the publisher. Copyright restrictions may apply.

The proof of Proposition 3.22 extends easily to show that $[F, \iota_{\mathbb{X}}]$ is null-homotopic. We conclude that $\mathbb{XI}^{\mathrm{alg}}_{-1}(\mathscr{C}, [0])$ is locally-equivalent to the complex

$$\begin{array}{ccccc} & & A_0 & & \\ & \swarrow^{h} & & \searrow^{v} & \\ B_{-1} & & & & B_0 \end{array} \tag{3.44}$$

with involution induced by $\mathbb{XI}^{\mathrm{alg}}_{-1}$. An argument analogous to the proof of part (2) of Proposition 3.22 shows that (3.44) is locally equivalent to the complex

$$\begin{array}{ccccc} & & A_0 & & \\ & \swarrow^{\widetilde{v}} & & \searrow^{v} & \\ \widetilde{B}_0 & & & & B_0 \end{array} \tag{3.45}$$

with the involution which is ι_K on A_0, and is also ι_K on the B-summands, switching B_0 and $\widetilde{B}_0$. We now claim that the complex in (3.45) is homotopy equivalent to the subcomplex A_0^{big} of $CFK^\infty(K)$ generated by $[\mathbf{x}, i, j]$ with $\min(i, j) \leq 0$ and $A(\mathbf{x}) + i - j = 0$. To see this, note that the complex in (3.45) is $\mathrm{Cone}(\widetilde{v} \oplus v \colon A_0 \to \widetilde{B}_0 \oplus B_0)$. Note $A_0 = \widetilde{B}_0 \cap B_0$ and $A_0^{\mathrm{big}} = \widetilde{B}_0 + B_0$. We obtain an exact sequence

$$0 \to A_0 \xrightarrow{\widetilde{v} \oplus v} \widetilde{B}_0 \oplus B_0 \xrightarrow{\Sigma} A_0^{\mathrm{big}} \to 0, \tag{3.46}$$

which manifestly induces a chain map Φ from $\mathrm{Cone}(\widetilde{v} \oplus v) \to A_0^{\mathrm{big}}$. A chain map Ψ in the opposite direction is given by basic homological algebra. Namely, we may construct $\mathbb{F}[U]$-equivariant, splittings $f \colon A_0^{\mathrm{big}} \to \widetilde{B}_0 \oplus B_0$ and $g \colon \widetilde{B}_0 \oplus B_0 \to A_0$ of the exact sequence in (3.46) because A_0^{big} is a free module over $\mathbb{F}[U]$. In general, f and g will not be chain maps. There is an induced map $\Psi \colon A_0^{\mathrm{big}} \to A_0 \oplus \widetilde{B}_0 \oplus B_0 = \mathrm{Cone}(\widetilde{v} \oplus v)$ given by $\Psi(x) = (g\partial f x, fx)$. Basic homological algebra shows that Φ and Ψ are chain maps, and furthermore, homotopy inverses. The map Φ commutes with the involution, and hence it follows automatically that Ψ commutes with the involution up to homotopy.

Furthermore, it is not hard to see that $(A_0^{\mathrm{big}}(\mathscr{C}), \iota_K(\mathscr{C}))$ is canonically isomorphic to $(A_0(-\mathscr{C}), \iota_K(-\mathscr{C}))^\vee$, where $\vee$ denotes the dual ι-complex, completing the proof. □

Remark 3.24. For ι_K-complexes induced by knots in S^3, Proposition 3.23 follows from Proposition 3.22, together with the observation that $S^3_{-n}(K) = -S^3_{+n}(m(K))$. A similar statement holds more generally for null-homologous knots in L-spaces.

3.8. Correction terms of integer surgeries

Proposition 3.22 has the following implication for the involutive correction terms of surgeries, which is the restriction of Proposition 1.7 to integer surgeries:

Proposition 3.25. *Suppose K is a knot in S^3 and $n > 0$. Then*

$$\begin{aligned} &\underline{d}(S^3_n(K), [0]) = d(L(n,1), [0]) - 2\underline{V}_0(K) \\ \text{and} \quad &\overline{d}(S^3_n(K), [0]) = d(L(n,1), [0]) - 2\overline{V}_0(K), \end{aligned} \tag{3.47}$$

This is a free offprint provided to the author by the publisher. Copyright restrictions may apply.

and

$$\underline{d}(S^3_{2n}(K),[n]) = d(S^3_{2n}(K),[n]), \quad \text{and} \quad \overline{d}(S^3_{2n}(K),[n]) = d(L(2n,1),[n]). \tag{3.48}$$

We begin with a lemma which will allow us to pass to a smaller model of $\mathbb{X}$, where $B_s = \mathbb{F}[U]$:

LEMMA 3.26. *Let (C,ι) be an ι-complex. Then for any chain complex C' homotopy equivalent to C, there exists a homotopy involution $\iota'\colon C' \to C'$ such that the ι-complex (C',ι') is homotopy equivalent to (C,ι).*

PROOF. Suppose that $f\colon C \to C'$ and $g\colon C' \to C$ such that $g\circ f \simeq \mathrm{id}$ via a homotopy H. Then it is straightforward to verify that $\iota' = f\circ\iota\circ g$ gives a homotopy involution on C' and that $f\circ\iota \simeq \iota'\circ f$ via $f\circ\iota\circ H$ and $g\circ\iota' \simeq \iota\circ g$ via $H\circ\iota\circ g$. □

REMARK 3.27. Note that if $\mathbb{A} \simeq \mathbb{A}'$ via $f_s\colon A_s \to A'_s$ and $f'_s\colon A'_s \to A_s$ where $f'_s f_s \simeq \mathrm{id}$ via H_s, and $\mathbb{B} \simeq \mathbb{B}'$ via $g_s\colon B_s \to B'_s$ and $g'_s\colon B'_s \to B_s$ where $g'_s g_s \simeq \mathrm{id}$ via J_s, then $\mathbb{X} := \mathrm{Cone}(D\colon \mathbb{A} \to \mathbb{B}) \simeq \mathrm{Cone}(gDf'\colon \mathbb{A} \to \mathbb{B}) =: \mathbb{X}'$ via the homotopy equivalence

$$\begin{aligned} F&\colon \mathbb{X} \to \mathbb{X}' \\ &(a,b) \mapsto (f(a), gDH(a) + g(b)) \end{aligned}$$

with homotopy inverse

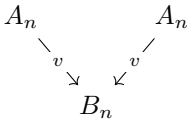
$$\begin{aligned} G&\colon \mathbb{X}' \to \mathbb{X} \\ &(a',b') \mapsto (f'(a'), JDf'(a') + g'(b')). \end{aligned}$$

(It's straightforward to verify that $G\circ F \simeq \mathrm{id}_{\mathbb{X}}$. Furthermore, one can see that $F\circ G$ is homotopic to a chain isomorphism, i.e., an upper triangular matrix with ones along the diagonal, which we will denote ϕ. Hence $F\circ G\circ\phi^{-1} \simeq \mathrm{id}_{\mathbb{X}'}$. Then $G \simeq G\circ F\circ G\circ\phi^{-1} \simeq G\circ\phi^{-1}$.) In particular, if we replace each A_s and B_s with homotopy equivalent complexes A'_s and B'_s respectively, then the induced mapping cone $\mathbb{X}'$ still has the form as in Theorem 20.1.

We now prove Proposition 3.25, our computation of the correction terms of surgeries:

PROOF OF PROPOSITION 3.25. The first claim about the correction terms in the Spin^c structure corresponding to [0] is an immediate consequence of Proposition 3.22, together with the definition of the absolute grading on the mapping cone complex (see [**OS08b**, Section 4]), the large surgery formula for involutive Heegaard Floer homology, and the definition of the involutive concordance invariants.

We now investigate the second claim, concerning even surgeries. Let C be the complex



with involution ι which swaps the two copies of A_n and is the identity on B_n. This represents the local equivalence class of $\mathbb{XI}^{\mathrm{alg}}_{2n}(\mathscr{C},[n]) \simeq CF^-(S^3_{2n}(Y),[n])$.

For any element $x \in A_n$, let x^ℓ denote the copy of x in the lefthand copy of A_n and x^r the copy in the righthand copy of A_n. By Lemma 3.26, we may replace B_n with an appropriately-graded copy of $\mathbb{F}[U]$. More precisely, using Remark 3.27

This is a free offprint provided to the author by the publisher. Copyright restrictions may apply.

we choose some chain maps $g\colon B_n \to \mathbb{F}[U]$ and $g'\colon \mathbb{F}[U] \to B_n$, and a homotopy J between $g'g$ and the identity map on B_n. Then taking the maps f_s and f'_s in the statement of the remark to be identity maps and the homotopy H to be identically zero, we see that replacing B_n by $\mathbb{F}[U]$ replaces ι by $F \circ \iota \circ G$, where F and G are chain homotopy equivalences in the remark. We see that

$$\begin{aligned}(F \circ \iota \circ G)(x^\ell) &= x^r + Jv(x^r)\\ (F \circ \iota \circ G)(x^r) &= x^\ell + Jv(x^\ell)\\ (F \circ \iota \circ G)(b) &= b\end{aligned}$$

where the last term is forced by the fact that $b \in \mathbb{F}[U]$. Let $M = Jv$, so that ι is replaced by $\iota + M$. Notice, in particular, that the element $x^\ell + x^r$ is always fixed by the replacement involution.

Let a_n be a tower generator of A_n. That is, a_n is a cycle of maximal grading such that $U^m[a_n] \neq 0$ for $m \geq 0$ in $H_*(A_n)$. Let b_n be a generator of B_n. Then $v(a_n) = U^{V_n} b_n$. The element $[a_n^\ell + a_n^r]$ is then a tower generator in $H_*(C)$. By [**OS08b**, Section 4] and [**NW15**, Proposition 1.6]

$$\begin{aligned}\operatorname{gr}(b_n) &= d(L(2n,1),[n]) - 1\\ \operatorname{gr}(a_n^\ell) = \operatorname{gr}(a_n^r) &= d(S^3_{2n}(K),[n]) = d(L(2n,1),[n]) - 2V_n(K).\end{aligned}$$

We now turn our attention to the computation of the involutive correction terms. Let ∂_A denote the differential in the complex A_n and ∂_C denote the differential in the complex C. Consider the involutive complex

$$CI = (C[-1] \otimes \mathbb{F}[Q]/(Q^2), \partial^\iota = \partial_C + Q(1+\iota)).$$

Note that, as elements of CI, we have

$$\operatorname{gr}(b_n) = d(L(2n,1),[n]) \qquad \operatorname{gr}(a_n^\ell) = \operatorname{gr}(a_n^r) = d(S^3_{2n}(K),[n]) + 1$$

because of the upward grading shift. Observe that $U^m(a_n^\ell + a_n^r)$ is ι-invariant and is nonzero in $H_*(CI)$ for all $m \geq 0$. Therefore $[a_n^\ell + a_n^r]$ generates a copy of $\mathbb{F}[U]$ in $H_*(CI)$ in gradings of the same parity $d(S^3_{2n}(K),[n]) + 1$ modulo two, which must therefore be contained in the first tower in $H_*(CI)$. Hence $\underline{d}(C)$ must be no less than

$$\operatorname{gr}(a_n^\ell + a_n^r) - 1 = d(S^3_{2n}(K),[n]) + 1 - 1 = d(S^3_{2n}(K),[n]).$$

Since $d(S^3_{2n}(K),[n]) = d(C)$ is also an upper bound on $\underline{d}(C)$, we conclude that $[a_n^\ell + a_n^r]$ generates the first tower in $H_*(CI)$ and

$$\underline{d}(C) = d(S^3_{2n}(K),[n]).$$

We now locate the second tower in $H_*(CI)$. We claim that the class $[b_n]$ generates the tower. First we check that $U^m[b_n] \neq 0$ for $m \geq 0$. For if not, then $U^m b_n$ lies in the image of ∂^ι for some m. Since $\partial^\iota(B_n[-1] \otimes \mathbb{F}[Q]/(Q^2))$ lies entirely in $\operatorname{Im}(Q)$, we see that there must exist some $x_1, x_2, x_3, x_4 \in A_n$ such that

$$U^m b_n = \partial^\iota(x_1^\ell + (x_2^\ell + x_2^r) + Qx_3^\ell + Q(x_4^\ell + x_4^r)).$$

Then

$$\begin{aligned}U^m b_n &= v(x_1^\ell) + \partial_A x_1^\ell + Q(x_1^\ell + x_1^r) + QM(x_1^\ell) + (\partial_A x_2^\ell + \partial_A x_2^r)\\ &\quad + Qv(x_3^\ell) + Q\partial_A x_3^\ell + Q(\partial_A x_4^\ell + \partial_A x_4^r)\\ &= v(x_1^\ell) + \partial_A x_1^\ell + (\partial_A x_2^\ell + \partial_A x_2^r) + Q(v(x_3^\ell) + \partial_A x_3^\ell\end{aligned}$$

This is a free offprint provided to the author by the publisher. Copyright restrictions may apply.

$$+ (x_1^\ell + x_1^r) + (\partial_A x_4^\ell + \partial_A x_4^r) + M x_1^\ell)$$

We see that we must have $v(x_1^\ell) = U^m b_n$ and $\partial_A x_4^r = x_1^r$. But then

$$\begin{aligned}\partial_C^2(x_4^r) &= \partial_C(x_1^r) + \partial_C(v(x_4^r)) \\ &= \partial_A(x_1^r) + v(x_1^r) + 0 \\ &= \partial_A(x_1^r) + U^m b_n \\ &\neq 0.\end{aligned}$$

This is a contradiction, so $U^m[b_n] \neq 0$ for all $m \geq 0$. It remains to be shown that $[b_n] \neq U[\eta]$ for some $\eta \in CI$. Since b_n is an element of maximal grading in $B_n[-1] \otimes \mathbb{F}[Q]/(Q^2)$, the element η must lie in $(A_n \oplus A_n)[-1] \otimes \mathbb{F}[Q]/(Q^2)$. Suppose that

$$\begin{aligned}b_n + U\eta &= \partial^\iota(x_1^\ell + (x_2^\ell + x_2^r) + Q x_3^\ell + Q(x_4^\ell + x_4^r)) \\ &= v(x_1^\ell) + \partial_A(x_1^\ell) + Q(x_1^\ell + x_1^r) + QM(x_1^\ell) + (\partial_A x_2^\ell + \partial_A x_2^r) \\ &\quad + Qv(x_3^\ell) + Q\partial_A x_3^\ell + Q(\partial_A x_4^\ell + \partial_A x_4^r).\end{aligned}$$

We observe that $v(x_1^\ell) = b_n$ and $v(x_3^\ell) = 0$. We then have

$$U\eta = \partial_A(x_1^\ell) + (\partial_A x_2^\ell + \partial_A x_2^r) + Q\partial_A x_3^\ell + Q((x_1^\ell + \partial_A x_4^\ell) + (x_1^r + \partial_A x_4^r)) + QM(x_1^\ell)$$

Since $U\eta$ is in the image of U, in particular $x_1^r + \partial_A x_4^r = Ux^r$ for some $x \in A_n$. However, then

$$\begin{aligned}Uv(x^r) &= v(Ux^r) \\ &= v(x_1^r + \partial_A x_4^r) \\ &= v(x_1^r) + \partial_B v(x_4^r) \\ &= b_n + 0 \\ &= b_n.\end{aligned}$$

This is a contradiction since b_n is not in the image of U. We conclude that $[b_n]$ generates the second tower in $H_*(CI)$, and that

$$\overline{d}(C) = \mathrm{gr}(b_n) = (d(L(2n,1),[n]) - 1) + 1 = d(L(2n,1),[n]). \qquad \square$$

This is a free offprint provided to the author by the publisher. Copyright restrictions may apply.

CHAPTER 4

An application to the homology cobordism group

The goal of this chapter is to use the involutive mapping cone formula to prove Theorem 1.9, that is, to find examples of homology spheres which are not homology cobordant to linear combinations of Seifert fibered spaces. Our proof begins by computing the ι_K-complexes of certain linear combinations of torus knots and their cables, in order to compute the almost-local equivalence class of $Y = S^3_{+1}(-2T_{6,7}\#T_{6,13}\# - T_{2,3;2,5})$. We then use these calculations to show that $n[Y]$ is non-trivial in $\Theta^3_{\mathbb{Z}}/\Theta_{SF}$ for any non-zero integer n. The proof relies on the fact from [**DHST23**, Theorem 8.1] (cf. the proof of [**Dai19**, Theorem 1.1]) that the almost-local equivalence class of linear combinations of Seifert fibered spaces takes on a particularly simple form.

Let $T_{p,q;r,s}$ denote the (r,s)-cable of the (p,q)-torus knot, where r denotes the longitudinal winding. The goal of this chapter is to compute the local equivalence class of the ι-complex associated to $S^3_{+1}(K)$, where $K = -2T_{6,7}\#T_{6,13}\# - T_{2,3;2,5}$, in order to prove that $S^3_{+1}(K)$ is not homology cobordant to a linear combination of Seifert fibered spaces.

In Section 4.1, we compute some tensor products of abstract ι_K-complexes. In Section 4.2, we identify some of these abstract ι_K-complexes with the ι_K-complexes of specific knots in S^3. In Section 4.3, we use Proposition 3.22 to compute the local equivalence class of $(CF^-(S^3_{+1}(K)), \iota)$. In Section 4.4, we use these calculations to prove Theorem 1.9.

4.1. Some tensor products

We begin by computing the local equivalence classes of several tensor products of ι_K-complexes. Throughout, we describe ι_K-complexes as finitely generated chain complexes over $\mathbb{F}[U, U^{-1}]$; that is, following Remark 3.12, we consider $\mathcal{A}_0$ as a chain complex over $\mathbb{F}[U]$ with an $\mathbb{F}[U]$-equivariant endomorphism ι_K and localize at U.

LEMMA 4.1. *Let C_1 be the complex in Figure 4.1 generated by a, b, c, d, e with Maslov gradings*

$$M(a) = M(b) = 0, \quad M(c) = M(d) = -1, \quad M(e) = -2,$$

differential

$$\partial a = 0, \quad \partial b = c + d, \quad \partial c = e, \quad \partial d = e, \quad \partial e = 0,$$

and ι_K (which we denote by ι_1)

$$\iota_1(a) = a + U^{-1}e, \quad \iota_1(b) = b + a, \quad \iota_1(c) = d, \quad \iota_1(d) = c, \quad \iota_1(e) = e.$$

Let C_2 be the complex in Figure 4.1, together with the endomorphism ι_2

$$\iota_2(x_i) = x_{4-i}, \quad 0 \le i \le 4.$$

This is a free offprint provided to the author by the publisher. Copyright restrictions may apply.

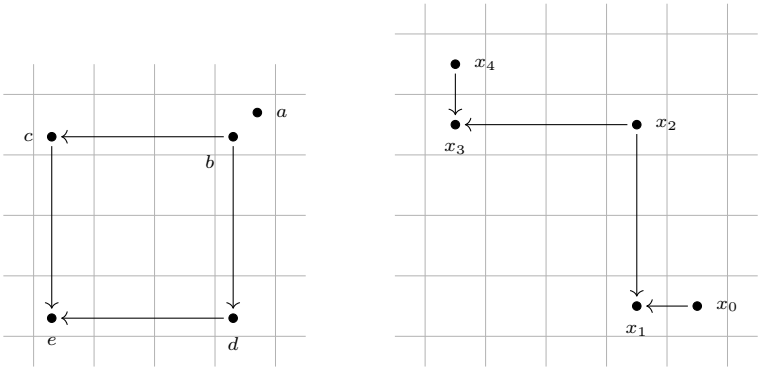


FIGURE 4.1. Left, the complex C_1. Right, the complex C_2.

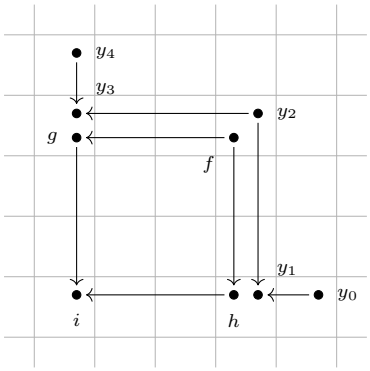


FIGURE 4.2. The complex C_3, which is locally equivalent to $C_1 \otimes C_2$.

The tensor product $C_1 \otimes C_2$ is locally equivalent to the complex C_3 in Figure 4.2, where ι_3 is given by

$$\begin{aligned}
\iota_3(y_i) &= y_{4-i}, \quad i \neq 2\\
\iota_3(y_2) &= y_2 + U^{-1}i\\
\iota_3(f) &= f + y_2\\
\iota_3(g) &= h + y_1\\
\iota_3(h) &= g + y_3\\
\iota_3(i) &= i.
\end{aligned}$$

PROOF. Let (C_1, ι_1) and (C_2, ι_2) be as above. Recall from [**Zem19a**, Theorem 1.1] that

$$\iota_{C_1 \otimes C_2} \colon C_1 \otimes C_2 \to C_1 \otimes C_2$$

is given by

$$\iota_1 \otimes \iota_2 + (\Phi_1 \otimes \Psi_2) \circ (\iota_1 \otimes \iota_2).$$

This is a free offprint provided to the author by the publisher. Copyright restrictions may apply.

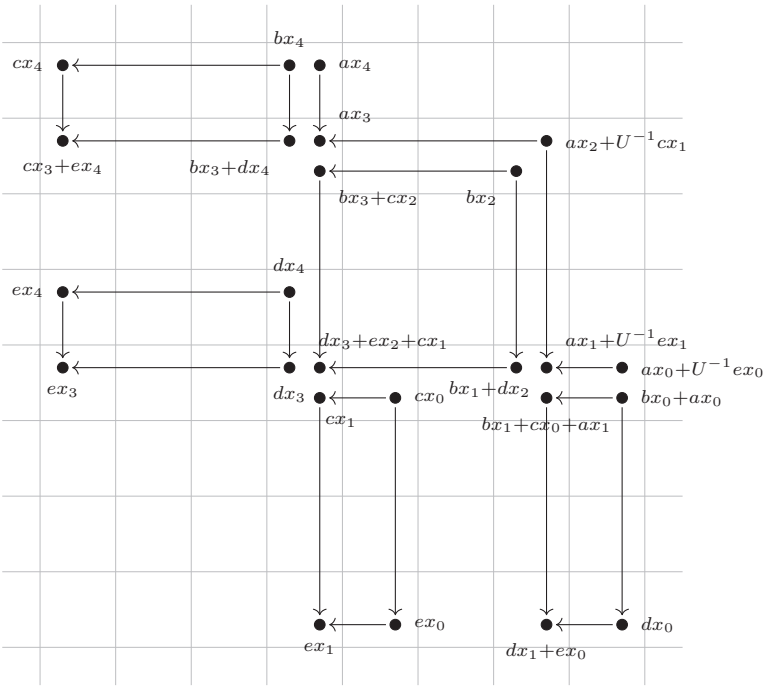


FIGURE 4.3. The complex $C_1 \otimes C_2$.

where Φ_1 and Ψ_2 are the formal derivatives of ∂. (In practice, after fixing a basis, $(\Phi_1 \otimes \Psi_2)(x \otimes y)$ counts arrows leaving x that point an odd number of units to the left and arrows leaving y that point an odd number of units down, together with an overall factor of U^{-1}.) For simplicity, we will denote $\iota_{C_1 \otimes C_2}$ by ι_{12}. We find that ι_{12} is given by

$$\begin{aligned}
\iota_{12}(ax_0) &= ax_4 + U^{-1}ex_4,\\
\iota_{12}(ax_1) &= ax_3 + U^{-1}ex_3,\\
\iota_{12}(ax_2) &= ax_2 + U^{-1}ex_2,\\
\iota_{12}(ax_3) &= ax_1 + U^{-1}ex_1,\\
\iota_{12}(ax_4) &= ax_0 + U^{-1}ex_0,\\
\iota_{12}(bx_0) &= bx_4 + ax_4 + U^{-1}cx_3,\\
\iota_{12}(bx_1) &= bx_3 + ax_3,\\
\iota_{12}(bx_2) &= bx_2 + ax_2 + U^{-1}cx_1,\\
\iota_{12}(bx_3) &= bx_1 + ax_1,\\
\iota_{12}(bx_4) &= bx_0 + ax_0,\\
\iota_{12}(cx_0) &= dx_4 + U^{-1}ex_3,\\
\iota_{12}(cx_1) &= dx_3,\\
\iota_{12}(cx_2) &= dx_2 + U^{-1}ex_1,
\end{aligned}$$

This is a free offprint provided to the author by the publisher. Copyright restrictions may apply.

$$\begin{aligned}
\iota_{12}(cx_3) &= dx_1,\\
\iota_{12}(cx_4) &= dx_0,\\
\iota_{12}(dx_0) &= cx_4,\\
\iota_{12}(dx_1) &= cx_3,\\
\iota_{12}(dx_2) &= cx_2,\\
\iota_{12}(dx_3) &= cx_1,\\
\iota_{12}(dx_4) &= cx_0,\\
\iota_{12}(ex_0) &= ex_4,\\
\iota_{12}(ex_1) &= ex_3,\\
\iota_{12}(ex_2) &= ex_2,\\
\iota_{12}(ex_3) &= ex_1,\\
\iota_{12}(ex_4) &= ex_0.
\end{aligned}$$

Consider the change of basis shown in Figure 4.3. It is straightforward to verify that we may ι_{12}-equivariantly decompose $C_1 \otimes C_2$ as

$$C_1 \otimes C_2 = X_1 \oplus X_2 \oplus X_3,$$

where X_1 consists of the "staircase" together with the three-by-three box (namely, the span of $ax_0+U^{-1}ex_0, ax_1+U^{-1}ex_1, ax_2+U^{-1}cx_1, ax_3, ax_4, bx_2, bx_3+cx_2, bx_1+dx_2, dx_3+ex_2+cx_1$), X_2 consists of the upper left and lower right rectangle (the span of $bx_4, cx_4, bx_3+dx_4, cx_3+ex_4, bx_0+ax_0, bx_1+cx_0+ax_1, dx_0, dx_1+ex_0$), and X_3 consists of the remaining two rectangles (the span of $dx_4, ex_4, dx_3, ex_3, cx_0, cx_1, ex_0, ex_1$).

Since X_1 supports HF^∞, it follows that $C_1 \otimes C_2$ is locally equivalent to X_1, which is isomorphic to (C_3, ι_3) as described in the statement of the lemma. □

LEMMA 4.2. *Let C_4 be the complex in Figure 4.4 together with*

$$\iota_4(z_i) = z_{20-i}, \quad 0 \le i \le 20.$$

The tensor product of (C_1, ι_1) and (C_4, ι_4) is locally equivalent to C_5 in Figure 4.5, where ι_5 is given by

$$\begin{aligned}
\iota_5(w_i) &= w_{20-i}, \quad i \neq 10\\
\iota_5(w_{10}) &= w_{10} + U^{-1}m\\
\iota_5(j) &= j + w_{10}\\
\iota_5(k) &= l + w_9\\
\iota_5(l) &= k + w_{11}\\
\iota_5(m) &= m.
\end{aligned}$$

PROOF. The proof is analogous to the proof of Lemma 4.1. □

LEMMA 4.3. *Let C_6 be the complex in Figure 4.6 with*

$$\iota_6(v_i) = v_{10-i}, \quad 0 \le i \le 10.$$

Then $C_6 \otimes C_6$ is locally equivalent to (C_5, ι_5), where ι_5 is as described in Lemma 4.2.

This is a free offprint provided to the author by the publisher. Copyright restrictions may apply.

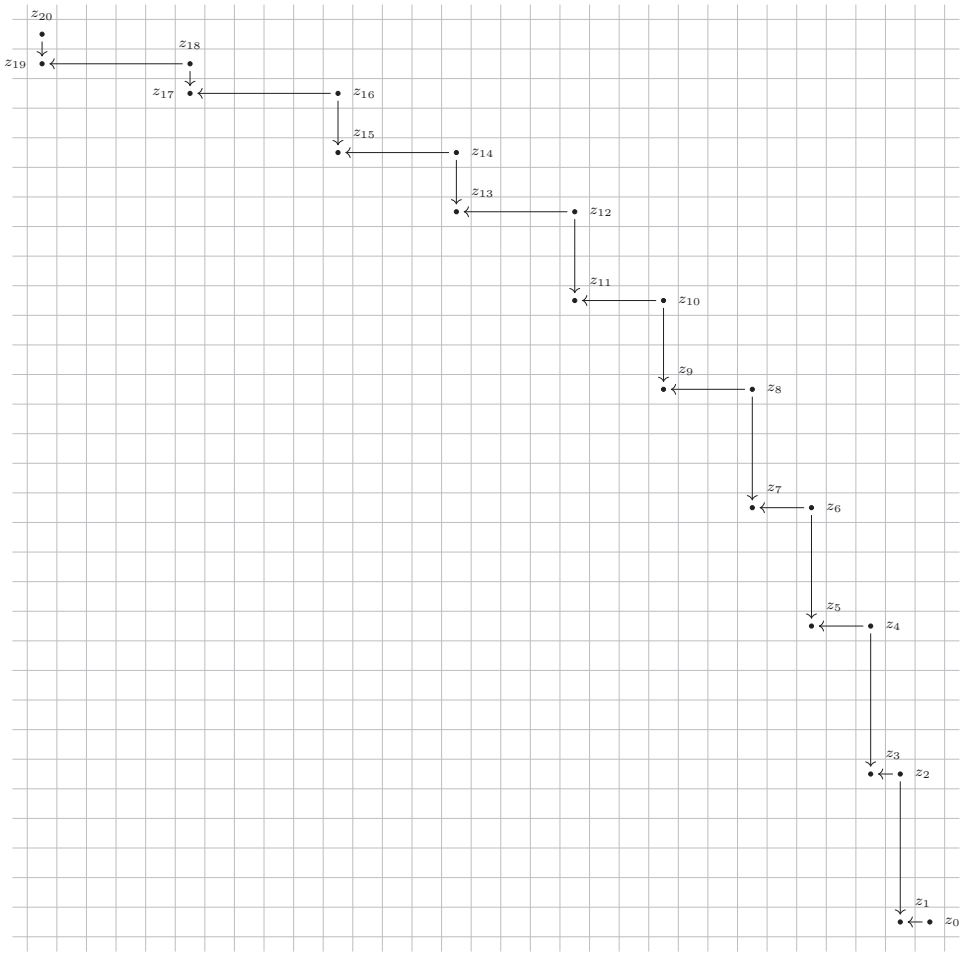


FIGURE 4.4. The complex $C_4 = CFK^\infty(-T_{6,13})$.

PROOF. After a change of basis, we have that $C_6 \otimes C_6$ splits as in Figure 4.7. Moreover, this splitting may be chosen to be equivariant with respect to $\iota_{C_6 \otimes C_6} = \iota_6 \otimes \iota_6 + (\Phi_6 \otimes \Psi_6) \circ (\iota_6 \otimes \iota_6)$. The "staircase" together with the three-by-three box along the diagonal form a direct summand that is isomorphic to C_5, under the identification

$$\begin{aligned}
w_0 &= v_0 v_0, \\
w_1 &= v_0 v_1 + v_1 v_0, \\
w_2 &= v_0 v_2 + v_2 v_0 + U^{-1} v_1 v_1, \\
w_3 &= v_0 v_3 + v_1 v_2 + v_2 v_1 + v_3 v_0, \\
w_4 &= v_0 v_4 + v_2 v_2 + v_4 v_0, \\
w_5 &= v_0 v_5 + v_1 v_4 + v_2 v_3 + v_3 v_2 + v_4 v_1 + v_5 v_0, \\
w_6 &= v_0 v_6 + v_2 v_4 + v_4 v_2 + v_6 v_0 + U^{-1}(v_1 v_5 + v_5 v_1), \\
w_7 &= v_0 v_7 + v_1 v_6 + v_2 v_5 + v_3 v_4 + v_4 v_3 + v_5 v_2 + v_6 v_1 + v_7 v_0,
\end{aligned}$$

This is a free offprint provided to the author by the publisher. Copyright restrictions may apply.

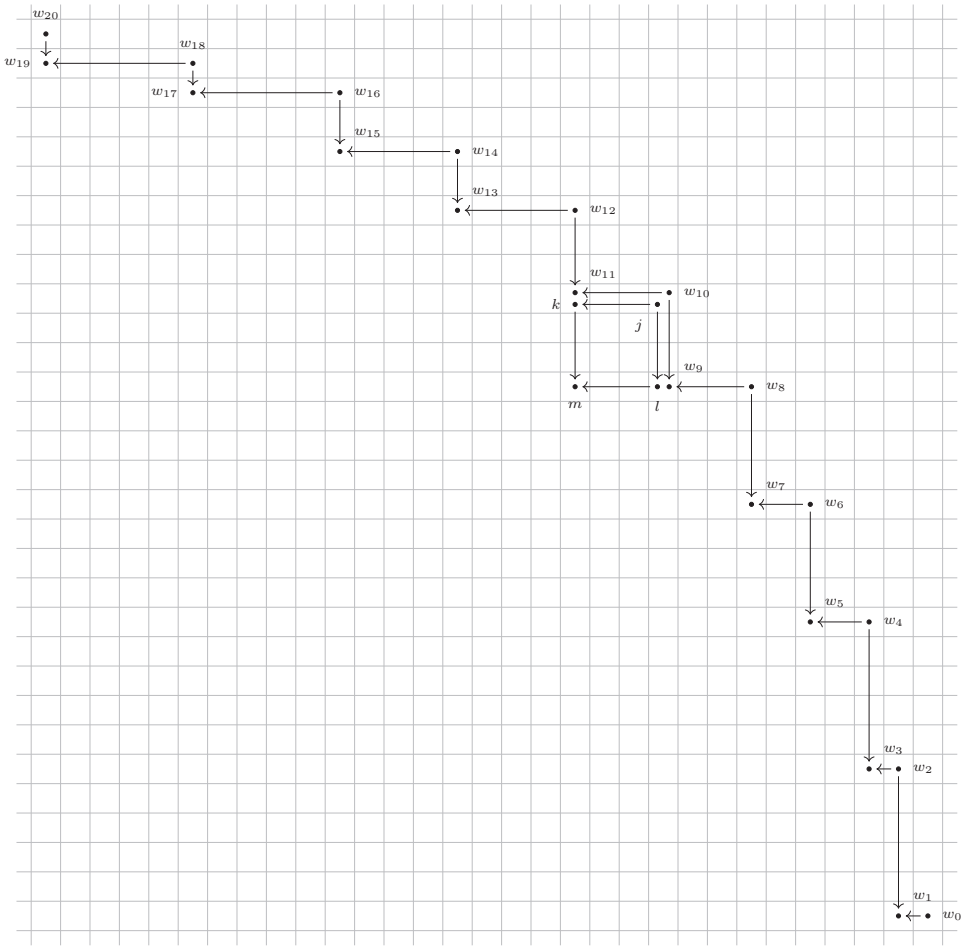


FIGURE 4.5. The complex C_5.

$$
\begin{aligned}
w_8 &= v_0v_8 + v_2v_6 + v_4v_4 + v_6v_2 + v_8v_0,\\
w_9 &= v_0v_9 + v_1v_8 + v_2v_7 + v_3v_6 + v_4v_5 + v_5v_4 + v_6v_3 + v_7v_2 + v_8v_1 + v_9v_0,\\
w_{10} &= v_0v_{10} + v_2v_8 + v_4v_6 + v_6v_4 + v_8v_2 + v_{10}v_0 + U^{-1}(v_1v_9 + v_5v_5),\\
w_{11} &= v_1v_{10} + v_2v_9 + v_3v_8 + v_4v_7 + v_5v_6 + v_6v_5 + v_7v_4 + v_8v_3 + v_9v_2 + v_{10}v_1,\\
w_{12} &= v_2v_{10} + v_4v_8 + v_6v_6 + v_8v_4 + v_{10}v_2,\\
w_{13} &= v_3v_{10} + v_4v_9 + v_5v_8 + v_6v_7 + v_7v_6 + v_8v_5 + v_9v_4 + v_{10}v_3,\\
w_{14} &= v_4v_{10} + v_6v_8 + v_8v_6 + v_{10}v_4,\\
w_{15} &= v_5v_{10} + v_6v_9 + v_7v_8 + v_8v_7 + v_9v_6 + v_{10}v_5,\\
w_{16} &= v_6v_{10} + v_8v_8 + v_{10}v_6,\\
w_{17} &= v_7v_{10} + v_8v_9 + v_9v_8 + v_{10}v_7,\\
w_{18} &= v_8v_{10} + v_{10}v_8,\\
w_{19} &= v_9v_{10} + v_{10}v_9,
\end{aligned}
$$

This is a free offprint provided to the author by the publisher. Copyright restrictions may apply.

$$\begin{aligned} w_{20} &= v_{10}v_{10}, \\ j &= v_6v_4 + v_8v_2 + v_{10}v_0, \\ k &= v_6v_5 + v_7v_4 + v_8v_3 + v_9v_2 + v_{10}v_1, \\ l &= v_5v_4 + v_6v_3 + v_7v_2 + v_8v_1 + v_9v_0, \\ m &= v_5v_5, \end{aligned}$$

as shown in Figure 4.8. Indeed, it is straightforward to verify that $\iota_{C_6\otimes C_6}$ maps the span of $\{w_1, \dots, w_{20}, j, k, l, m\}$ into itself. It is then sufficient to show that the basis in Figure 4.7 can be chosen so that none of $w_1, \dots, w_{20}, j, k, l, m$ appear in $\iota_{C_6\otimes C_6}$ of any of the other basis elements. Since $\iota_{C_6\otimes C_6}$ is grading-preserving and skew-filtered, it is sufficient to verify this for the vertices along the top and right edges of the rectangles shown in Figure 4.9, as well as for v_2v_8 and v_8v_2, the top right corners of the two squares in Figure 4.9. By a direct computation, one sees that the span of

$$\{v_1v_0, v_1v_1, v_2v_0, v_2v_1 + v_3v_0, v_7v_{10} + v_8v_9, v_8v_{10}, v_9v_9, v_9v_{10}\},$$

that is, the span of the vertices of the upper left and bottom right rectangles in Figure 4.9, forms an $\iota_{C_6\otimes C_6}$ equivariant subcomplex. Similarly, one sees that the span of

$$\begin{aligned} \{v_3v_2 + v_4v_1 + v_5v_0, v_3v_3, v_4v_2 + v_6v_0 + U^{-1}v_5v_1, v_4v_3 + v_5v_2v_6v_1 + v_7v_0, v_3v_3, \\ v_3v_{10} + v_4v_9 + v_5v_8 + v_6v_7, v_4v_{10} + v_6v_8, v_5v_{10}v_6v_9 + v_7v_8, v_7v_7, \} \end{aligned}$$

that is, the span of the vertices of the middle two rectangles in Figure 4.9, also forms an $\iota_{C_6\otimes C_6}$-equivariant subcomplex. Lastly, one sees that $\iota_{C_6\otimes C_6}(v_2v_8) = v_8v_2 + U^{-1}v_9v_1$ and $\iota_{C_6\otimes C_6}(v_8v_2) = v_2v_8$. (Alternatively, there is a change of basis such that all of the rectangles in Figure 4.9 except the central 3×3 square are "paired" with their symmetric mate by $\iota_{C_6\otimes C_6}$.)

Thus, the span of $\{w_1, \dots, w_{20}, j, k, l, m\}$, which is isomorphic to C_5 in Figure 4.5, forms an $\iota_{C_6\otimes C_6}$-equivariant summand of $C_6 \otimes C_6$. Since this summand supports HF^∞, it follows that $C_6 \otimes C_6$ is locally equivalent to C_5, as desired. □

4.2. The ι_K-complex of $-2T_{6,7}\#T_{6,13}\# - T_{2,3;2,5}$

Recall that $K \subseteq S^3$ is an *L-space knot* if $S^3_r(K)$ is an L-space for some $r > 0$. We say that K is a *negative L-space knot* if $S^3_{-r}(K)$ is an L-space for some $r > 0$. The following lemma, combining results of [**OS05**] and [**HM17**], describes the ι_K-complex associated to a negative L-space knot K in terms of the Alexander polynomial $\Delta_K(t)$.

LEMMA 4.4. *Let K be a negative L-space knot with Alexander polynomial*

$$\Delta_K(t) = \sum_{i=0}^{n} (-1)^i t^{a_i},$$

where $(a_i)_{i=0}^n$ is a decreasing sequence of integers and n is even. Then $CFK^\infty(K)$ is generated over $\mathbb{F}[U, U^{-1}]$ by $x_i, 0 \le i \le n$, with Maslov gradings

$$\begin{aligned} M(x_i) &= 0, \quad i \text{ even} \\ M(x_i) &= -1, \quad i \text{ odd} \end{aligned}$$

This is a free offprint provided to the author by the publisher. Copyright restrictions may apply.

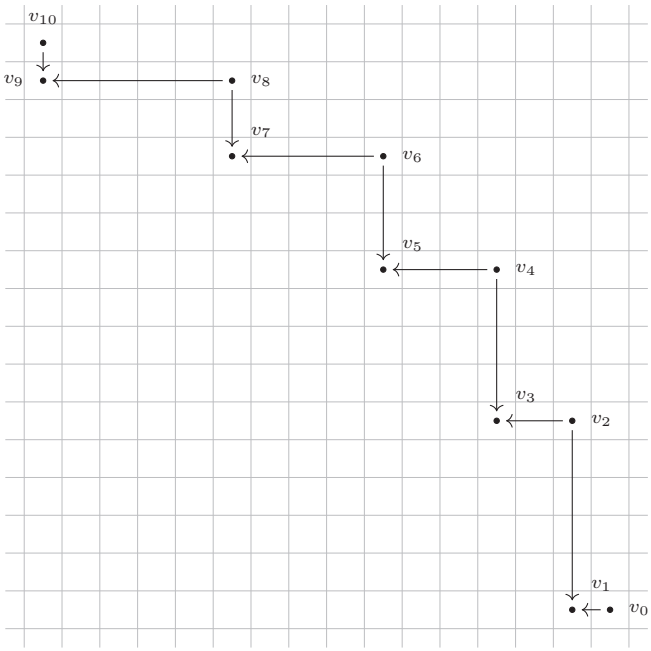


FIGURE 4.6. The complex $C_6 = CFK^\infty(-T_{6,7})$.

where the $\mathbb{Z} \oplus \mathbb{Z}$-filtration level of x_0 is $\mathcal{F}(x_0) = (0, -g(K))$ and relative filtration of x_i, x_{i+1} is

$$\mathcal{F}(x_i) - \mathcal{F}(x_{i+1}) = (a_i - a_{i+1}, 0), \quad i \text{ even}$$
$$\mathcal{F}(x_i) - \mathcal{F}(x_{i+1}) = (0, a_{i+1} - a_i), \quad i \text{ odd}.$$

The differential is given by

$$\partial x_0 = x_1$$
$$\partial x_i = x_{i-1} + x_{i+1}, \quad 2 \leq i \leq n-2 \text{ even}$$
$$\partial x_n = x_{n-1}$$
$$\partial x_i = 0, \quad i \text{ odd}.$$

The endomorphism ι_K is given by

$$\iota_K(x_i) = x_{n-i}, \quad 0 \leq i \leq n.$$

PROOF. The description of $CFK^\infty(K)$ follows from [**OS05**, Theorem 1.2] (cf. [**OSS17**, Theorem 2.10]). The description of ι_K follows from [**HM17**, Section 7]. □

LEMMA 4.5. *We have the following identifications:*

1. *The complex (C_2, ι_2) in Figure 4.1 where $\iota_2(x_i) = x_{4-i}$ is the ι_K-complex associated to $-T_{2,3;2,5}$.*
2. *The complex (C_4, ι_4) in Figure 4.4 where $\iota_4(z_i) = z_{20-i}$ is the ι_K-complex associated to $-T_{6,13}$.*
3. *The complex (C_6, ι_6) in Figure 4.6 where $\iota_5(v_i) = v_{10-i}$ is the ι_K-complex associated to $-T_{6,7}$.*

This is a free offprint provided to the author by the publisher. Copyright restrictions may apply.

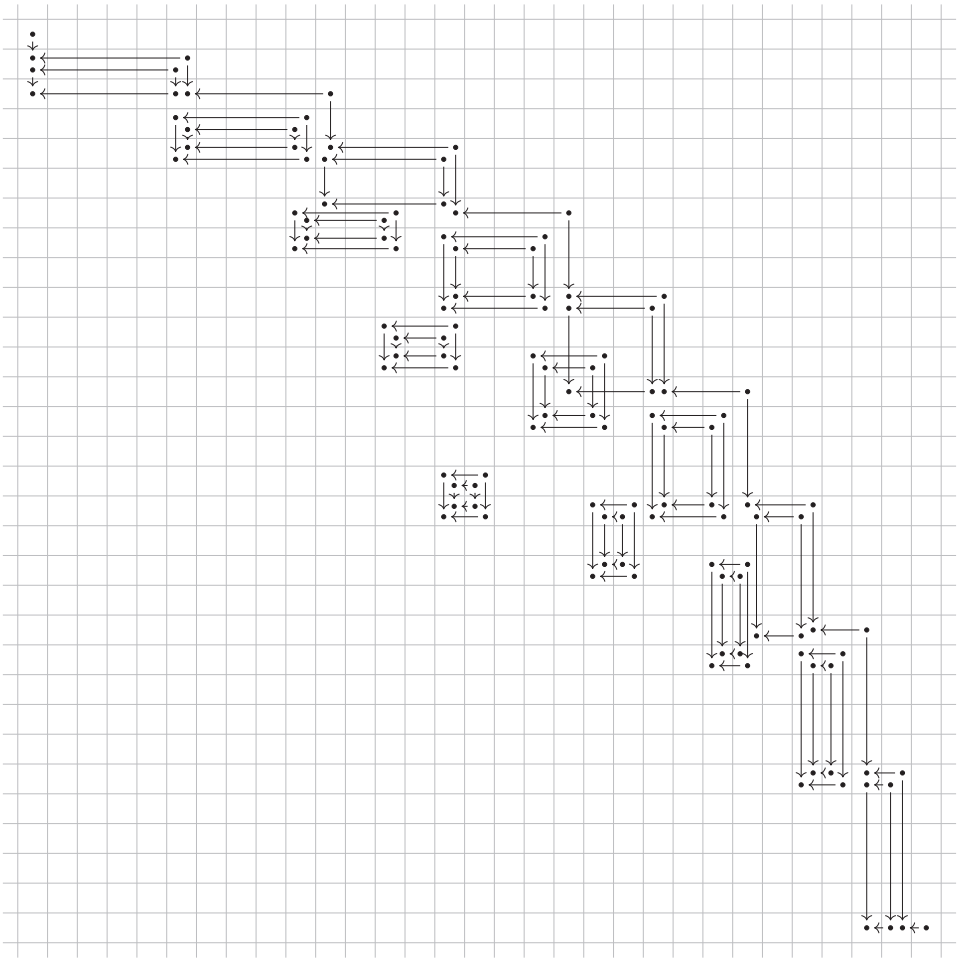


FIGURE 4.7. The complex $C_6 \otimes C_6$, after a change of basis.

PROOF. The Alexander polynomial of $-T_{2,3;2,5}$ is

$$\Delta_{-T_{2,3;2,5}}(t) = t^8 - t^7 + t^4 - t + 1,$$

the Alexander polynomial $\Delta_{-T_{6,13}}(t)$ is

$$t^{60} - t^{59} + t^{54} - t^{53} + t^{48} - t^{46} + t^{42} - t^{40} + t^{36} - t^{33} + t^{30}$$
$$- t^{27} + t^{24} - t^{20} + t^{18} - t^{14} + t^{12} - t^7 + t^6 - t + 1,$$

and the Alexander polynomial of $-T_{6,7}$ is

$$\Delta_{-T_{6,7}}(t) = t^{30} - t^{29} + t^{24} - t^{22} + t^{18} - t^{15} + t^{12} - t^8 + t^5 - t + 1.$$

Recall that negative torus knots admit negative L-space surgeries, as does $-T_{2,3;2,5}$ [**Hed09**, Theorem 1.10] (cf. [**Hom11**]). The result now follows from Lemma 4.4. □

We now combine Lemma 4.5 with the computations of Section 4.1 to compute the ι_K-complex of $K = -2T_{6,7}\#T_{6,13}\# - T_{2,3;2,5}$.

This is a free offprint provided to the author by the publisher. Copyright restrictions may apply.

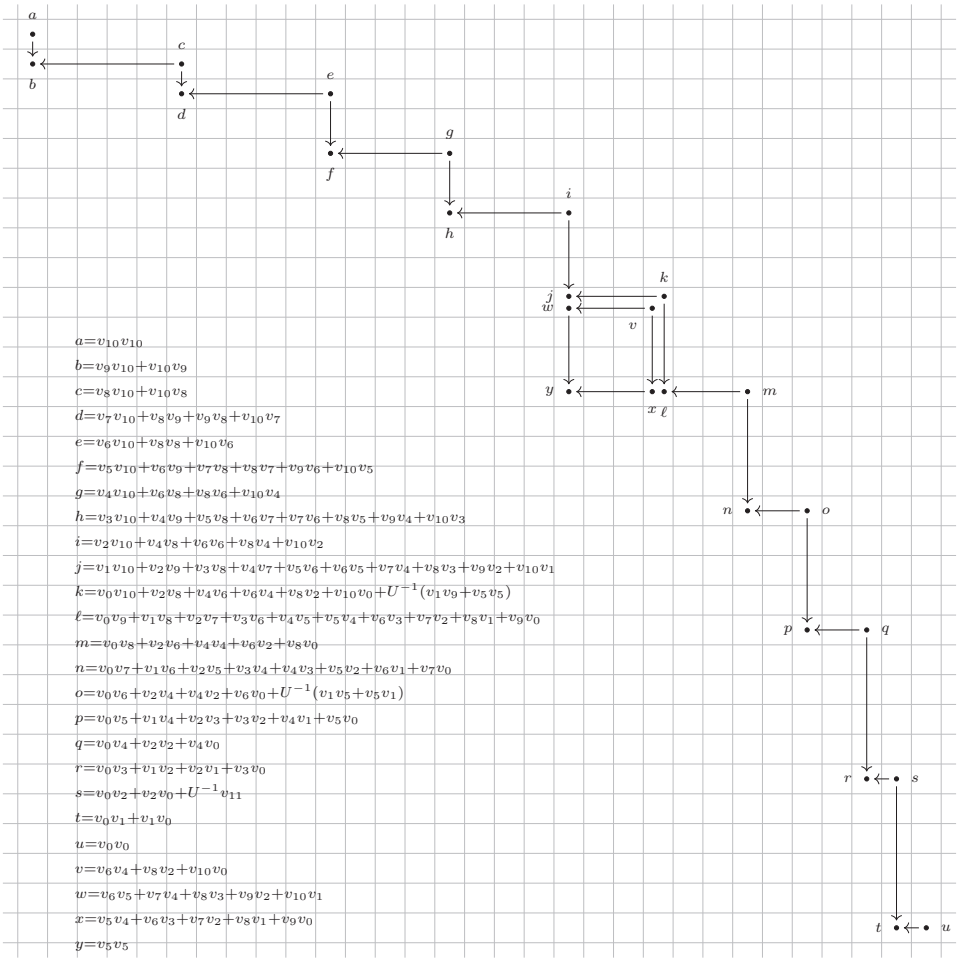


FIGURE 4.8. The summand of $C_6 \otimes C_6$ that is isomorphic to C_5.

PROPOSITION 4.6. *The ι_K-complex of $K = -2T_{6,7}\#T_{6,13}\# - T_{2,3;2,5}$ is locally equivalent to the complex (C_3, ι_3) in Figure 4.2, where ι_3 is given by*

$$\begin{aligned}
\iota_3(y_i) &= y_{4-i}, \quad i \neq 2 \\
\iota_3(y_2) &= y_2 + U^{-1}i \\
\iota_3(f) &= f + y_2 \\
\iota_3(g) &= h + y_1 \\
\iota_3(h) &= g + y_3 \\
\iota_3(i) &= i.
\end{aligned}$$

PROOF. By Lemma 4.5 and the Künneth formula for ι_K-complexes, we have that the ι_K-complex of K is $C_6 \otimes C_6 \otimes C_4^* \otimes C_2$.

This is a free offprint provided to the author by the publisher. Copyright restrictions may apply.

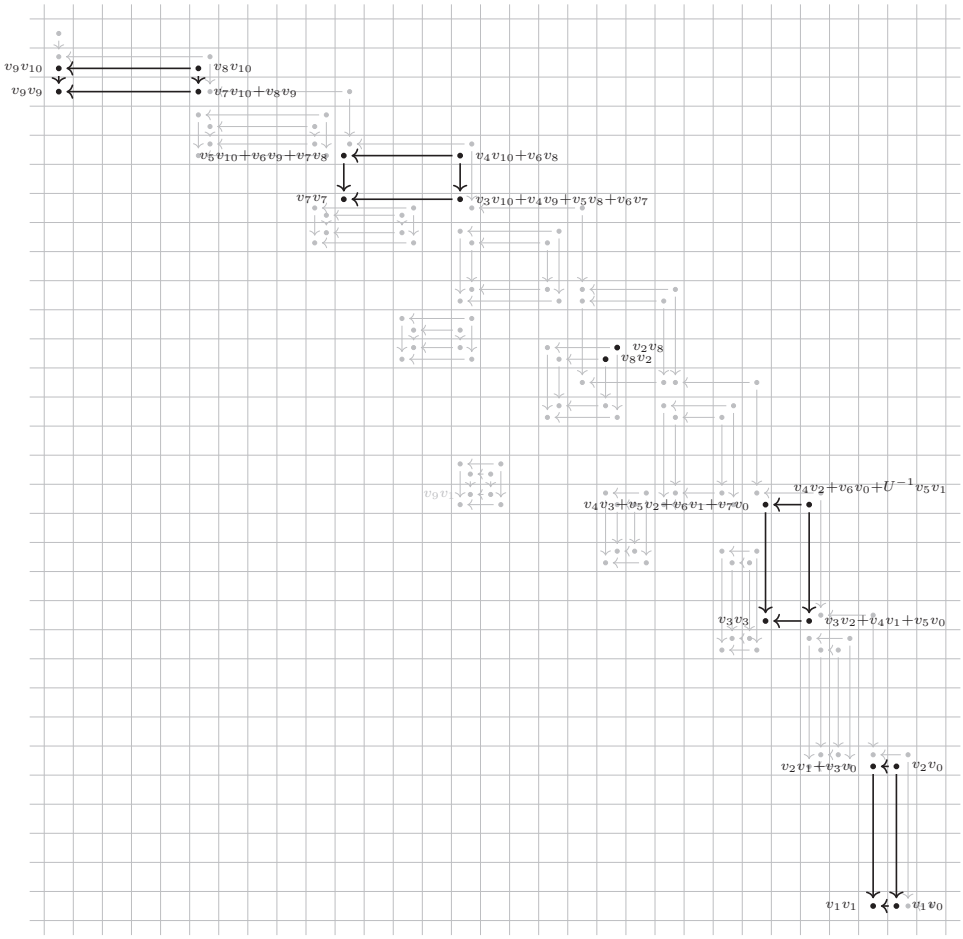


FIGURE 4.9. The complex $C_6 \otimes C_6$, after a change of basis, with some basis elements labelled.

We have the following sequence of equivalences, where $\simeq$ denotes local equivalence:

$$\begin{aligned} C_6 \otimes C_6 \otimes C_4^* \otimes C_2 &\simeq C_6 \otimes C_6 \otimes C_4^* \otimes C_1^* \otimes C_1 \otimes C_2 \\ &\simeq C_5 \otimes C_5^* \otimes C_1 \otimes C_2 \\ &\simeq C_1 \otimes C_2 \\ &\simeq C_3, \end{aligned}$$

where the first and third equivalences follow from the fact that C_i and C_i^* are inverses in the local equivalence group of ι_K-complexes, the second equivalence follows from Lemmas 4.3 and 4.2 (and duality, in the latter case), and the fourth equivalence follows from Lemma 4.1. □

This is a free offprint provided to the author by the publisher. Copyright restrictions may apply.

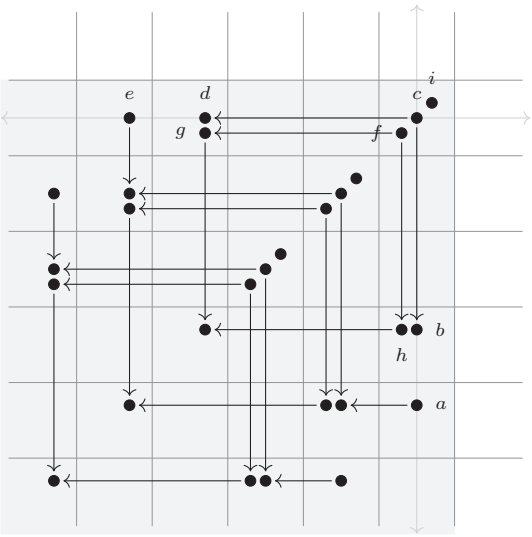


FIGURE 4.10. The complex A_0^- associated to C_3 with (appropriate U-powers of) y_1, y_2, y_3, y_4, y_5 renamed a, b, c, d, e respectively.

4.3. Surgery along $-2T_{6,7}\#T_{6,13}\# - T_{2,3;2,5}$

In this section, we employ Proposition 3.22 to compute the local equivalence class of $(CF^-(S^3_{+1}(K)), \iota)$, where $K = -2T_{6,7}\#T_{6,13}\# - T_{2,3;2,5}$.

PROPOSITION 4.7. *Let $K = -2T_{6,7}\#T_{6,13}\# - T_{2,3;2,5}$. Then $(CF^-(S^3_{+1}(K)), \iota)$ is locally equivalent to (C, ι_C) where C is generated by x_0, x_1, x_2, x_3, x_4 where*

$$\begin{aligned} \partial x_0 &= 0 & \omega x_0 &= 0 \\ \partial x_1 &= U x_2 & \omega x_1 &= x_0 \\ \partial x_2 &= 0 & \omega x_2 &= 0 \\ \partial x_3 &= U^3 x_4 & \omega x_3 &= x_2 \\ \partial x_4 &= 0 & \omega x_4 &= 0, \end{aligned}$$

where $\omega = 1 + \iota_C$.

In particular, in the notation of Section 4.4, the almost local equivalence class of $S^3_{+1}(K)$ is $(+, -1, +, -3)$.

PROOF. By Proposition 4.6, we have that $(CFK^\infty(K), \iota_K)$ is locally equivalent to (C_3, ι_3). Let (A_0^-, ι_K) denote $C_3\{\max(i, j) \leq 0\}$ with the homotopy involution induced by ι_3. Proposition 3.22 implies that (A_0^-, ι_K) is locally equivalent to $(CF^-(S^3_{+1}(K)), \iota)$. Thus it suffices to show that (A_0^-, ι_K) is locally equivalent to the ι-complex (C, ι_C) in the statement of Proposition 4.7.

We have that (A_0^-, ι_K) is generated over $\mathbb{F}[U]$ by $a, b, c, d, e, f, g, h, i$ with

$$\begin{aligned} \partial a &= Ub, & \iota_K(a) &= e, & \omega(a) &= a + e, \\ \partial b &= 0, & \iota_K(b) &= d, & \omega(b) &= b + d, \\ \partial c &= b + d, & \iota_K(c) &= c + U^2 i, & \omega(c) &= U^2 i, \end{aligned}$$

This is a free offprint provided to the author by the publisher. Copyright restrictions may apply.

$$\begin{aligned}
\partial d &= 0, & \iota_K(d) &= b, & \omega(d) &= b + d,\\
\partial e &= Ud, & \iota_K(e) &= a, & \omega(e) &= a + e,\\
\partial f &= h + g, & \iota_K(f) &= f + c, & \omega(f) &= c,\\
\partial g &= U^3 i, & \iota_K(g) &= b + h, & \omega(g) &= b + g + h,\\
\partial h &= U^3 i, & \iota_K(h) &= d + g, & \omega(h) &= d + g + h,\\
\partial i &= 0, & \iota_K(i) &= i, & \omega(i) &= 0,
\end{aligned}$$

as shown in Figure 4.10, where $y_0, U^{-1}y_1, U^{-1}y_2, U^{-1}y_3, y_4$ have been renamed a, b, c, d, e respectively, f, g, h have been shifted by U^{-1}, and i has been shifted by U^{-4}. (We include $\omega = \mathrm{id} + \iota_K$ above in order to aid with verifying the calculations below.)

Consider $\psi\colon A_0^- \to C$ defined to be

$$\begin{aligned}
\psi(a) &= x_1,\\
\psi(b) &= x_2,\\
\psi(c) &= 0,\\
\psi(d) &= x_2,\\
\psi(e) &= x_0 + x_1,\\
\psi(f) &= 0,\\
\psi(g) &= x_3,\\
\psi(h) &= x_3,\\
\psi(i) &= x_4.
\end{aligned}$$

It is straightforward to verify that ψ is a chain map and that $\omega\psi = \psi\omega$. Moreover, since $[a + Uc + e]$ is a U-nontorsion cycle in $H_*(A_0^-)$ and $[x_0]$ is a U-nontorsion cycle in $H_*(C)$, it follows that ψ induces an isomorphism on $U^{-1}H_*$.

Now consider $\phi\colon C \to A_0^-$ defined to be

$$\begin{aligned}
\phi(x_0) &= a + Uc + e,\\
\phi(x_1) &= a,\\
\phi(x_2) &= b,\\
\phi(x_3) &= g,\\
\phi(x_4) &= i.
\end{aligned}$$

It is straightforward to verify that ϕ is a chain map. We have that $\omega\phi \simeq \phi\omega$ via $H\colon C \to A_0^-$ defined by

$$\begin{aligned}
H(x_0) &= g,\\
H(x_1) &= 0,\\
H(x_2) &= c,\\
H(x_3) &= f,\\
H(x_4) &= 0.
\end{aligned}$$

Moreover, since $[x_0]$ is $\mathbb{F}[U]$-non-torsion in $H_*(C)$ and $[a+Uc+e]$ is $\mathbb{F}[U]$-non-torsion in $H_*(A_0^-)$, it follows that ϕ induces an isomorphism on $U^{-1}H_*$.

This is a free offprint provided to the author by the publisher. Copyright restrictions may apply.

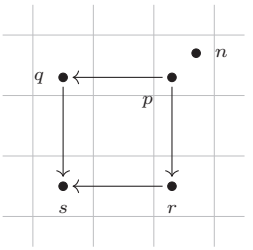


FIGURE 4.11. The complex C_7.

Hence ψ and ϕ provide the desired local equivalence between (A_0^-, ι_K) and (C, ι_C). (In fact, $\psi\phi = \mathrm{id}_{C_3}$ and $\phi\psi \simeq \mathrm{id}_{A_0^-}$ via the homotopy J defined by $J(d) = c, J(h) = f$, and $J(y) = 0$ if $y \neq d, h$.) □

REMARK 4.8. Recall from [**HL19**, Remark 9.7] that a homology sphere Y is called *$\widehat{HFI}$-trivial* if $\widehat{HFI}(Y) \cong \widehat{HF}(Y) \oplus \mathbb{F}$ where $Q \cdot \widehat{HF}(Y) = 0$ and Q is non-vanishing on the remaining generator. Let $J = -2T_{4,5}\#T_{4,9}$. Similar computations to those in Sections 4.1 and 4.2 can show that $Y = S^3_{+1}(J)$ is not $\widehat{HFI}$-trivial. Indeed, we have that $(CFK^\infty(J), \iota_J)$ decomposes ι_J-equivariantly as $C_7 \oplus C_8$ where C_7 the complex in Figure 4.11 where the Maslov gradings of the generators are

$$M(n) = M(p) = 0, \quad M(q) = M(r) = -1, \quad M(s) = -2,$$

and ι_7 is given by

$$\begin{aligned}
\iota_7(n) &= n,\\
\iota_7(p) &= p + n,\\
\iota_7(q) &= r,\\
\iota_7(r) &= q,\\
\iota_7(s) &= s
\end{aligned}$$

and C_8 consists of an even number of rectangles which are paired by ι_8 much like the (non-square) rectangles in Figure 4.3 are. (Compare this to the computation of $-2T_{6,7}\#T_{6,13}$, which is locally equivalent to C_1 in Figure 4.1.) An application of the involutive mapping cone then shows that $\widehat{HFI}(S^3_{+1}(J)) \cong \widehat{HF}(Y) \oplus \mathbb{F}^3$ and where $Q \cdot \widehat{HF}(Y) = 0$ and Q is non-vanishing on the remaining generators.

4.4. Almost local equivalence classes and $S^3_{+1}(-2T_{6,7}\#T_{6,13}\# - T_{2,3;2,5})$

The goal of this section is to prove Theorem 1.9. We begin by recalling some some terminology and notation.

Recall from [**DHST23**, Section 4.1] that to a sequence $(a_1, b_2, a_3, b_4, \ldots, a_{2m-1}, b_{2m})$, where $a_i \in \{\pm\}$ and $b_i \in \mathbb{Z}\backslash\{0\}$, we may associate an almost ι-complex, called the *standard complex of type* $(a_1, b_2, a_3, b_4, \ldots, a_{2m-1}, b_{2m})$, as follows. (We will abuse notation and let (a_i, b_i) denote both a sequence and the associated standard complex.) The standard complex is generated over $\mathbb{F}[U]$ by $t_0, t_1, \ldots, t_{2m}$. For each symbol a_i, we introduce an ω-relation between t_{i-1} and t_i as follows:

- If $a_i = +$, then $\omega t_i = t_{i-1}$.
- If $a_i = -$, then $\omega t_{i-1} = t_i$.

This is a free offprint provided to the author by the publisher. Copyright restrictions may apply.

For each symbol b_i, we introduce an ∂-relation between t_{i-1} and t_i as follows:

- If $b_i > 0$, then $\partial t_i = U^{|b_i|}t_{i-1}$.
- If $b_i < 0$, then $\partial t_{i-1} = U^{|b_i|}t_i$.

We begin with a few lemmas about tensor products of standard complexes.

LEMMA 4.9. *Let $k \geq 2$ and let*

$$S_n = (+, -1, +, -k, +, -1, +, -k, \dots, +, -1, +, -k)$$

where the right-hand side consists of $+, -1, +, -k$ repeated n times. There is an almost local map from S_n to $S_1 \otimes S_{n-1}$.

PROOF. Let the complex S_n be generated by $x_0, x_1, \dots, x_{4n}$, the complex S_1 by $y_0, y_1, \dots, y_4$ and the complex S_{n-1} by $z_0, z_1, \dots, z_{4n-4}$. Define $f\colon S_n \to S_1 \otimes S_{n-1}$ to be

$$f(x_i) = \begin{cases} y_i \otimes z_0 & \text{if } 0 \leq i \leq 4 \\ y_4 \otimes z_{i-4} & \text{if } 5 \leq i \leq 4n. \end{cases}$$

It is straightforward to verify that f is an almost local map. □

LEMMA 4.10. *Let $k \geq 2$ and let*

$$-S_n = (-, 1, -, k, -, 1, -, k, \dots, -, 1, -, k)$$

where the right-hand side consists of $-, 1, -, k$ repeated n times. There is an almost local map from $-S_n$ to $-S_1 \otimes -S_{n-1}$.

PROOF. Let the complex $-S_n$ be generated by $x_0, x_1, \dots, x_{4n}$, the complex $-S_1$ by $y_0, y_1, \dots, y_4$ and the complex $-S_{n-1}$ by $z_0, z_1, \dots, z_{4n-4}$. Define $f\colon -S_n \to -S_1 \otimes -S_{n-1}$ to be

$$\begin{aligned}
f(x_0) &= y_0 \otimes z_0, \\
f(x_1) &= y_0 \otimes z_1 + y_1 \otimes z_0 + y_1 \otimes z_1, \\
f(x_2) &= y_0 \otimes z_2 + y_2 \otimes z_0 + y_1 \otimes z_2, \\
f(x_3) &= y_0 \otimes z_3 + y_1 \otimes z_2 + y_2 \otimes z_1 + y_3 \otimes z_0 + y_3 \otimes z_1, \\
f(x_4) &= y_0 \otimes z_4 + U^{k-1}y_2 \otimes z_2 + y_4 \otimes z_0 + y_4 \otimes z_1, \\
&\vdots \\
f(x_{4i+1}) &= y_0 \otimes z_{4i+1} + y_1 \otimes z_{4i} + U^{k-1}y_2 \otimes z_{4i-1} + U^{k-1}y_3 \otimes z_{4i-2}, \\
&\quad + y_4 \otimes z_{4i-3} + U^{k-1}y_3 \otimes z_{4i-1} + y_1 \otimes z_{4i+1}, \\
f(x_{4i+2}) &= y_0 \otimes z_{4i+2} + y_2 \otimes z_{4i} + y_4 \otimes z_{4i-2} + y_3 \otimes z_{4i} + y_1 \otimes z_{4i+2}, \\
f(x_{4i+3}) &= y_0 \otimes z_{4i+3} + y_1 \otimes z_{4i+2} + y_2 \otimes z_{4i+1} + y_3 \otimes z_{4i} + y_4 \otimes z_{4i-1}, \\
f(x_{4i+4}) &= y_0 \otimes z_{4i+4} + U^{k-1}y_2 \otimes z_{4i+2} + y_4 \otimes z_{4i}, \\
&\vdots \\
f(x_{4n-3}) &= y_1 \otimes z_{4n-4} + U^{k-1}y_2 \otimes z_{4n-5} + U^{k-1}y_3 \\
&\quad \otimes z_{4n-6} + y_4 \otimes z_{4n-7} + U^{k-1}y_3 \otimes z_{4n-5}, \\
f(x_{4n-2}) &= y_2 \otimes z_{4n-4} + y_4 \otimes z_{4n-6} + y_3 \otimes z_{4n-4}, \\
f(x_{4n-1}) &= y_3 \otimes z_{4n-4} + y_4 \otimes z_{4n-5},
\end{aligned}$$

This is a free offprint provided to the author by the publisher. Copyright restrictions may apply.

$$f(x_{4n}) = y_4 \otimes z_{4n-4}$$

where $i = 1, \dots, n-2$. It is straightforward to verify that f is an almost local map. □

LEMMA 4.11. *Let $k \geq 2$. Then, in the notation of Lemmas* 4.9 *and* 4.10*, we have that $S_1^{\otimes n}$ is locally equivalent to S_n.*

PROOF. By Lemma 4.9, we have that $S_n \leq S_1 \otimes S_{n-1}$ and by Lemma 4.10, we have that $-S_n \leq -S_1 \otimes -S_{n-1}$, or equivalently, $S_n \geq S_1 \otimes S_{n-1}$. Since $\leq$ is a partial order on the set of almost local equivalence classes (see [**DHST23**, Definition 3.19]), it follows that $S_n = S_1 \otimes S_{n-1}$, where equality denotes almost local equivalence. Hence by induction, $S_1^{\otimes n} = S_n$. □

REMARK 4.12. In Lemmas 4.9 and 4.10, the complexes S_n and $-S_n$ are in fact iota complexes (not just almost iota complexes), and the maps are in fact local maps (not just almost local maps). Hence $S_1^{\otimes n}$ and S_n are in fact locally equivalent (not just almost locally equivalent).

We are now ready to prove Theorem 1.9.

PROOF OF THEOREM 1.9. Let $Y = S^3_{+1}(-2T_{6,7} \# T_{6,13} \# -T_{2,3;2,5})$. By Proposition 4.7, we have that the almost local equivalence class of $(CF^-(Y), \iota)$ is $(+, -1, +, -3)$. Then by Lemma 4.11, the almost local equivalence class of $(CF^-(nY), \iota)$ is $(+, -1, +, -3, +, -1, +, -3, \dots, +, -1, +, -3)$, that is, the sequence $(+, -1, +, -3)$ repeated n times.

Suppose (a_i, b_i) represents the almost local equivalence class of a linear combination of Seifert fibered spaces. By [**DHST23**, Theorem 8.1] (cf. the proof of [**Dai19**, Theorem 1.1]), if $a_i = +$ for all i, then $b_i \geq b_{i+1}$ for all i. Hence nY, for $n \neq 0$, is not homology cobordant to any linear combination of Seifert fibered spaces. □

This is a free offprint provided to the author by the publisher. Copyright restrictions may apply.

CHAPTER 5

Hypercubes and hyperboxes

In this chapter, we present some background on homological algebra.

5.1. Hyperboxes of chain complexes

We recall the notion of a hyperbox of chain complexes, due to Manolescu and Ozsváth [**MO10**]. We let $\mathbb{E}_n$ denote the unit cube in $\mathbb{R}^n$:

$$\mathbb{E}_n := \{0,1\}^n.$$

More generally, if $\mathbf{d} = (d_1, \dots, d_n) \in \mathbb{Z}^n_{\geq 0}$, we define the cube of size $\mathbf{d}$ to be

$$\mathbb{E}(\mathbf{d}) = \prod_{i=1}^{n} \{0, \dots, d_i\}.$$

If $\varepsilon = (\varepsilon_1, \dots, \varepsilon_n) \in \mathbb{E}(\mathbf{d})$, we write

$$\|\varepsilon\| = \varepsilon_1 + \cdots + \varepsilon_n.$$

Definition 5.1. An n-dimensional *hyperbox of chain complexes* of size $\mathbf{d} = (d_1, \dots, d_n) \in \mathbb{Z}^n_{\geq 0}$ consists of a collection of $\mathbb{Z}$-graded $\mathbb{F}$-vector spaces

$$(C^\varepsilon)_{\varepsilon \in \mathbb{E}(\mathbf{d})},$$

together with a collection of maps

$$D^\varepsilon_{\varepsilon_0} \colon C^{\varepsilon_0}_* \to C^{\varepsilon_0+\varepsilon}_{*-1+\|\varepsilon\|},$$

indexed over pairs $(\varepsilon_0, \varepsilon) \in \mathbb{E}(\mathbf{d}) \times \mathbb{E}_n$ such that $\varepsilon_0 + \varepsilon \in \mathbb{E}(\mathbf{d})$. Furthermore, if $\varepsilon \in \mathbb{E}_n$ and $\varepsilon_0 \in \mathbb{E}(\mathbf{d})$, then

$$\sum_{\substack{\varepsilon' \in \mathbb{E}_n \\ \varepsilon' \leq \varepsilon}} D^{\varepsilon - \varepsilon'}_{\varepsilon_0 + \varepsilon'} \circ D^{\varepsilon'}_{\varepsilon_0} = 0, \tag{5.1}$$

whenever ε_0 and $\varepsilon_0 + \varepsilon$ are both in $\mathbb{E}(\mathbf{d})$.

If $H = (C^\varepsilon, D^\varepsilon_{\varepsilon_0})$ is a hyperbox of chain complexes of size $\mathbf{d}$, we write C for the total space

$$C := \bigoplus_{\varepsilon \in \mathbb{E}(\mathbf{d})} C^\varepsilon.$$

Similarly, the maps $D^\varepsilon_{\varepsilon_0}$ may be summed to give an endomorphism

$$D \colon C \to C.$$

Equation (5.1) implies $D^2 = 0$. Similarly, if (C, D) is a hyperbox, and $\varepsilon \in \mathbb{E}_n$, we write D^ε for the direct sum of $D^\varepsilon_{\varepsilon_0}$ over all ε_0 where the map is defined.

A hyperbox of chain complexes of size $\mathbf{d} = (1, \dots, 1) \in \mathbb{Z}^n_{\geq 0}$ is called an n-dimensional *hypercube* of chain complexes.

For this paper, we only consider hyperboxes of dimension $n \leq 3$.

This is a free offprint provided to the author by the publisher. Copyright restrictions may apply.

5.2. Stacking and compressing hyperboxes

In this section, we describe two algebraic operations, called *stacking* and *compressing*.

We begin with the operation of stacking. A hyperbox of size $(1,1,2)$ is the same as two hyperboxes of size $(1,1,1)$, which have chain complexes and maps which coincide along one face. More generally, suppose we have a hyperbox H_1 of size (x,y,d_1) and a hyperbox H_2 of size (x,y,d_2). Suppose further that the restriction of H_1 to $\mathbb{E}(x,y)\times\{d_1\}$ coincides with the restriction of H_2 to $\mathbb{E}(x,y)\times\{0\}$. We form a new hyperbox $\mathrm{St}(H_1,H_2)$, which is a hyperbox of size (x,y,d_1+d_2). A similar description holds for stacking two hypercubes of the same dimension, which coincide along a hyperface.

We now describe *compression*, which is described by Manolescu and Ozsváth [**MO10**, Section 5]. The operation takes an n-dimensional hyperbox $H=(C,D)$ of size $\mathbf{d}$, and yields an n-dimensional hypercube $\widehat{H}=(\widehat{C},\widehat{D})$. The compression operation is fundamental to our construction of the main hypercube from Theorem 1.14. To simplify the exposition, we focus on the compression of hyperboxes size (d), $(1,d)$ or $(1,1,d)$, which will be sufficient for our purposes.

We begin with 1-dimensional hyperboxes of size (d). A hyperbox $H=(C,D)$ of size (d) is a collection of $d+1$ chain complexes $C^0,\dots,C^d$, together with chain maps

$$D^1_i\colon C^i\to C^{i+1}.$$

We depict such a hyperbox as

$$C^0 \xrightarrow{D^1} C^1 \xrightarrow{D^1} \cdots \xrightarrow{D^1} C^d.$$

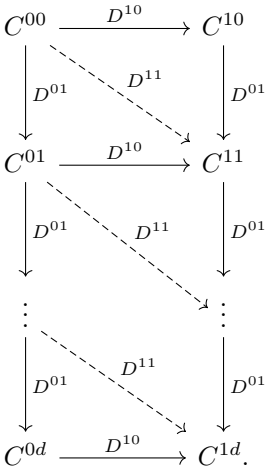
The compression $\widehat{H}=(\widehat{C},\widehat{D})$ has underlying chain complex equal to $C^0\oplus C^d$. The length 0 map $\widehat{D}^0$ is the restriction of the original length 0 map D^0. The length 1 map $\widehat{D}^1$ is the d-fold composition of the original length 1 map, D^1. We depict $\widehat{H}$ as

$$C^0 \xrightarrow{(D^1)^{\circ d}} C^d.$$

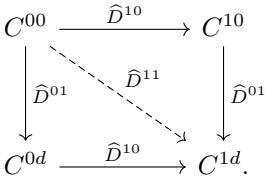
Next, we move on to 2 dimensional hyperboxes of size $(1,d)$. A 2-dimensional hyperbox of size $(1,d)$ consists of $2(d+1)$ chain complexes $(C^\varepsilon)_{\varepsilon\in\{0,1\}\times\{0,\dots,d\}}$, as well as chain maps D^{01} and D^{10}, and a chain homotopy D^{11} between $D^{10}\circ D^{01}$

This is a free offprint provided to the author by the publisher. Copyright restrictions may apply.

and $D^{01} \circ D^{10}$. Schematically, we depict (C, D) as the diagram



The compression $\widehat{H} = (\widehat{C}, \widehat{D})$ is the 2-dimensional hypercube depicted below:



Here

$$\begin{aligned} \widehat{D}^{10} &= D^{10}, \\ \widehat{D}^{01} &= (D^{01})^{\circ d}, \\ \widehat{D}^{11} &= \sum_{\substack{i+j=d-1 \\ i,j\geq 0}} (D^{01})^{\circ j} \circ D^{11} \circ (D^{01})^{\circ i}. \end{aligned} \tag{5.2}$$

The length 2 compressed map $\widehat{D}^{11}$ is shown schematically in Figure 5.1.

We now discuss 3-dimensional hyperboxes and their compressions. Suppose that $H = (C, D)$ is a 3-dimensional hyperbox of size $(1, 1, d)$. The underlying chain complexes of the compressed $\widehat{C}$ are

$$\widehat{C}^{(\varepsilon_1,\varepsilon_2,\varepsilon_3)} := C^{(\varepsilon_1,\varepsilon_2,\varepsilon_3 d)}.$$

The length 1 maps, $\widehat{D}^{100}$, $\widehat{D}^{010}$ and $\widehat{D}^{001}$, as well as the length 2 maps, $\widehat{D}^{110}$, $\widehat{D}^{101}$ and $\widehat{D}^{011}$, are essentially the same as in the 2-dimensional case. See (5.2). The

This is a free offprint provided to the author by the publisher. Copyright restrictions may apply.

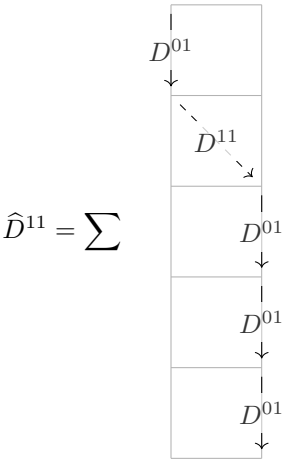


FIGURE 5.1. The length 2 map $\widehat{D}^{11}$ of the compression of a 2-dimensional hyperbox of size $(1, d)$.

length 3 map, $\widehat{D}^{111}$, is given by the formula

$$\begin{aligned}\widehat{D}^{111} := &\sum_{\substack{i+j=d-1\\ i,j\geq 0}} (D^{001})^{\circ j} \circ D^{111} \circ (D^{001})^{\circ i} \\ &+ \sum_{\substack{i+j+k=d-2\\ i,j,k\geq 0}} (D^{001})^{\circ i} \circ D^{101} \circ (D^{001})^{\circ j} \circ D^{011} \circ (D^{001})^{\circ k} \\ &+ \sum_{\substack{i+j+k=d-2\\ i,j,k\geq 0}} (D^{001})^{\circ i} \circ D^{011} \circ (D^{001})^{\circ j} \circ D^{101} \circ (D^{001})^{\circ k}.\end{aligned} \tag{5.3}$$

Equation (5.3) is schematically illustrated in Figure 5.2.

5.3. Mapping cones and hyperboxes

In this section, we describe the relationship between the hyperbox construction of Manolescu and Ozsváth and the more common mapping cone construction. The results of this section will be helpful for deriving the involutive mapping cone formula from the hypercube in Theorem 1.14.

EXAMPLE 5.2. Suppose (C_0, D_0) and (C_1, D_1) are chain complexes, and $F_0^1 \colon C_0 \to C_1$ is a chain map. We may form the mapping cone complex

$$\mathrm{Cone}(F_0^1) := C_0[-1] \oplus C_1,$$

which has differential $D_0 + D_1 + F$. The mapping cone complex is naturally filtered over the set $\{0, 1\}$. The mapping cone complex is a 1-dimensional hypercube of chain complexes, of size (1). If $F_0^1 \colon C_0 \to C_1$ is a chain map, then there is an exact triangle

$$\cdots \to H_*(C_0) \to H_*(C_1) \to H_*(\mathrm{Cone}(F_0^1)) \to H_{*-1}(C_0) \to \cdots .$$

This is a free offprint provided to the author by the publisher. Copyright restrictions may apply.

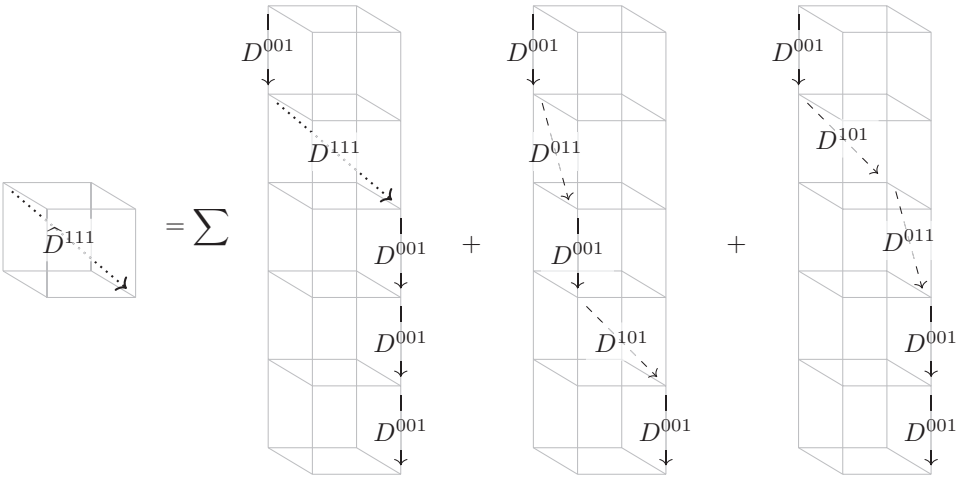


FIGURE 5.2. The length 3 map $\widehat{D}^{111}$ of the compression of a 3-dimensional hyperbox of size $(1, 1, d)$.

EXAMPLE 5.3. Consider a 2-dimensional hypercube $H = (C, D)$ satisfying $C^{10} = 0$. Such a hypercube has the following presentation:

$$\begin{array}{ccc} C^{00} & & \\ {\scriptstyle D^{01}}\downarrow & \searrow^{D^{11}} & \\ C^{01} & \xrightarrow[D^{10}]{} & C^{11}. \end{array}$$

The data of H is equivalent to three chain complexes, two chain maps D^{01} and D^{10}, and a null-homotopy D^{11} of the composition $D^{10} \circ D^{01}$. Equivalently, the hypercube is the same as a chain map from C^{00} to $\mathrm{Cone}(D^{10} \colon C^{01} \to C^{11})$.

More generally, suppose $H = (C, D)$ is an arbitrary 2-dimensional hypercube of chain complexes:

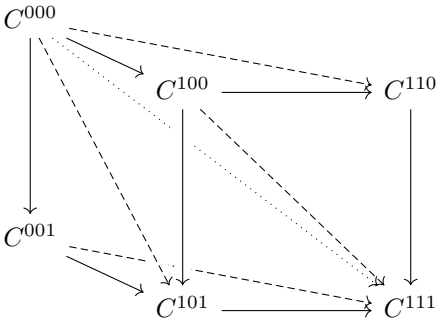
$$\begin{array}{ccc} C^{00} & \xrightarrow{D^{10}} & C^{10} \\ {\scriptstyle D^{01}}\downarrow & \searrow^{D^{11}} & \downarrow{\scriptstyle D^{01}} \\ C^{01} & \xrightarrow[D^{10}]{} & C^{11}. \end{array}$$

The data of the hypercube H is equivalent to a chain map from $\mathrm{Cone}(D^{01}_{00} \colon C^{00} \to C^{01})$ to $\mathrm{Cone}(D^{01}_{10} \colon C^{10} \to C^{11})$ which is filtered with respect to the mapping cone filtrations.

This is a free offprint provided to the author by the publisher. Copyright restrictions may apply.

EXAMPLE 5.4. Suppose that $H = (C, D)$ is a 3-dimensional hypercube, which has the property that C^{010} and C^{011} are both zero. See (5.4).

(5.4)



We can identify the subcomplex generated by C^{100}, C^{110}, C^{101} and C^{111} as the cone of a filtered chain map

$$G\colon \operatorname{Cone}\begin{pmatrix} C^{100} \\ \downarrow \\ C^{101} \end{pmatrix} \to \operatorname{Cone}\begin{pmatrix} C^{110} \\ \downarrow \\ C^{111} \end{pmatrix}.$$

The 3-dimensional hypercube in (5.4) may be interpreted as encoding the data of a chain map

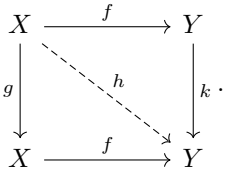
$$\Phi\colon \operatorname{Cone}\begin{pmatrix} C^{000} \\ \downarrow \\ C^{001} \end{pmatrix} \to \operatorname{Cone}(G),$$

which is filtered with respect the last component of the indexing (the vertical direction in our diagrams).

5.4. Hypercubes and involutive complexes

In this section, we describe some helpful algebra for relating the hypercube construction to the algebraic setting of involutive Heegaard Floer homology. Suppose $\mathcal{R}$ is a ring such that $2 = 0$, and that we have a hypercube of chain complexes over $\mathcal{R}$ of following form:

(5.5)



In particular, the complexes and morphisms along the top and bottom coincide. We can view $\operatorname{Cone}(g)$ and $\operatorname{Cone}(k)$ as complexes over $\mathcal{R}[Q]/Q^2$, where Q takes the first copy of X to the second, and similarly for Y.

The diagram in (5.5) determines a map $f + Q \cdot h$ from $\operatorname{Cone}(g)$ to $\operatorname{Cone}(k)$ which is Q-equivariant. We collect the following basic algebraic facts:

LEMMA 5.5. *Suppose that X, Y, f, g, k and h form a hypercube, as in* (5.5). *Suppose that $f\colon X \to Y$ is a homotopy equivalence.*

This is a free offprint provided to the author by the publisher. Copyright restrictions may apply.

(1) *The induced map* $f + Q \cdot h$ *from* $\mathrm{Cone}(g)$ *to* $\mathrm{Cone}(k)$ *is also a homotopy equivalence over* $\mathcal{R}[Q]/Q^2$.
(2) *If* $g^2 \simeq \mathrm{id}$, *then* $k^2 \simeq \mathrm{id}$. *Similarly, if* $g^2 \simeq 0$, *then* $k^2 \simeq 0$.

PROOF. Let $j\colon Y \to X$ be a homotopy inverse to f. We consider the first claim. First, we claim that $jk \simeq gj$. To see this, we begin with the relation $kf \simeq fg$, and pre- and post-compose with j to obtain $jkfj \simeq jfgj$. Using the fact that j and f are homotopy inverses, we obtain that $jk \simeq gj$. If s is a map so that $jk + gj = [\partial, s]$, then $j + Q \cdot s$ is a chain map from $\mathrm{Cone}(k)$ to $\mathrm{Cone}(g)$. Since $jf \simeq \mathrm{id}$, the composition $(j + Q \cdot s) \circ (f + Q \cdot h)$ is chain homotopic to a map of the form $\Psi = (\mathrm{id} + t \cdot Q)$, for some $t\colon X \to X$. The map Ψ is a chain isomorphism, with inverse equal to itself. Hence $\Psi \circ (j + Q \cdot s)$ is a left homotopy inverse of $f + Q \cdot h$. A similar argument shows that $(f + Q \cdot h)$ has a right homotopy inverse. An easy argument shows that if $(f + Q \cdot h)$ has both a left and a right homotopy inverse, then they must be homotopic.

To prove the second claim, suppose first that $g^2 \simeq \mathrm{id}$. We perform the following computation:

$$\begin{aligned} \mathrm{id} &\simeq fj \\ &\simeq (fg)(gj) \\ &\simeq (kf)(jk) \\ &\simeq k^2. \end{aligned}$$

A similar argument shows that if $g^2 \simeq 0$, then $k^2 \simeq 0$. □

5.5. Hyperboxes of attaching curves

Manolescu and Ozsváth also describe a natural analog of a hyperbox for diagrams in the Fukaya category. The main structural difference is that in the Fukaya category, we must include higher compositions into the hypercube relations. We make the following defintion, focusing on the case relevant to Heegaard Floer homology:

DEFINITION 5.6. An n-dimensional *hypercube of beta attaching curves* on (Σ, w) is a collection of attaching curves $\boldsymbol{\beta}^{\varepsilon}$, ranging over $\varepsilon \in \mathbb{E}_n$, together with a distinguished element

$$\Theta_{\beta^{\varepsilon},\beta^{\varepsilon'}} \in \boldsymbol{CF}^-(\boldsymbol{\beta}^{\varepsilon}, \boldsymbol{\beta}^{\varepsilon'}),$$

whenever $\varepsilon < \varepsilon'$. Furthermore, whenever $\varepsilon < \varepsilon'$, the following compatibility condition is satisfied:

$$0 = \sum_{\varepsilon < \varepsilon_1 < \cdots < \varepsilon_k < \varepsilon'} f_{\beta^{\varepsilon},\beta^{\varepsilon_1},\ldots,\beta^{\varepsilon_k},\beta^{\varepsilon'}}(\Theta_{\beta^{\varepsilon},\beta^{\varepsilon_1}}, \ldots, \Theta_{\beta^{\varepsilon_k},\beta^{\varepsilon'}}), \tag{5.6}$$

where $f_{\beta^{\varepsilon},\beta^{\varepsilon_1},\ldots,\beta^{\varepsilon_k},\beta^{\varepsilon'}}$ is the map which counts $2+k$-gons. An n-dimension *hyperbox* of beta attaching curves is defined by the obvious adaptation.

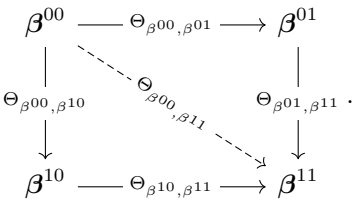
An n-dimensional *hypercube of alpha attaching curves* is a collection of attaching curves $(\boldsymbol{\alpha}^{\nu})_{\nu \in \mathbb{E}_n}$, together with a distinguished chain $\Theta_{\alpha^{\nu'},\alpha^{\nu}} \in \boldsymbol{CF}^-(\boldsymbol{\alpha}^{\nu'}, \boldsymbol{\alpha}^{\nu})$ whenever $\nu < \nu'$. Furthermore, the classes $\Theta_{\alpha^{\nu'},\alpha^{\nu}}$ satisfy the natural adaptation of (5.6).

REMARK 5.7. Manolescu and Ozsváth's definition of a hypercube of beta attaching curves [**MO10**, Section 8.1] assumes that for all $\varepsilon, \varepsilon' \in \mathbb{E}_n$, the curves

This is a free offprint provided to the author by the publisher. Copyright restrictions may apply.

$\boldsymbol{\beta}^{\varepsilon}$ and $\boldsymbol{\beta}^{\varepsilon'}$ are related by a sequence of handleslides and isotopies, whereas ours does not. The additional generality will be useful especially in Section 16 when we construct the central hypercube.

EXAMPLE 5.8. We consider a 2-dimensional hypercube of beta attaching curves, which has the following form:



The compatibility relations are equivalent to the length 1 chains, $\Theta_{\beta^{00},\beta^{01}}$, $\Theta_{\beta^{00},\beta^{10}}$, $\Theta_{\beta^{10},\beta^{11}}$ and $\Theta_{\beta^{01},\beta^{11}}$, being cycles, and to the relation

$$\partial\Theta_{\beta^{00},\beta^{11}} + f_{\beta^{00},\beta^{01},\beta^{11}}(\Theta_{\beta^{00},\beta^{01}}, \Theta_{\beta^{01},\beta^{11}}) + f_{\beta^{00},\beta^{10},\beta^{11}}(\Theta_{\beta^{00},\beta^{10}}, \Theta_{\beta^{10},\beta^{11}}) = 0.$$

REMARK 5.9. Given a collection of attaching curves $(\boldsymbol{\beta}^{\varepsilon})_{\varepsilon\in\mathbb{E}_n}$, and a set of length 1 chains $\Theta_{\beta^{\varepsilon},\beta^{\varepsilon'}}$, ranging over $\varepsilon,\varepsilon'\in\mathbb{E}_n$ such that $|\varepsilon-\varepsilon'|=1$, it is natural to ask when one may pick higher length chains which satisfy the hypercube relations. If, for all $\varepsilon,\varepsilon'\in\mathbb{E}_n$, the attaching curves $\boldsymbol{\beta}^{\varepsilon}$ and $\boldsymbol{\beta}^{\varepsilon'}$ are related by a sequence of handleslides and isotopies, and length 1 cycles are chosen to represent the top degree generators of $\boldsymbol{HF}^-(\Sigma,\boldsymbol{\beta}^{\varepsilon},\boldsymbol{\beta}^{\varepsilon'},w)$, then a procedure of Manolescu and Ozsváth [**MO10**, Lemma 8.6] proves the existence of such a collection of higher length chains which satisfy the hypercube relations.

5.6. Pairing hypercubes of attaching curves

Suppose $\mathcal{L}_{\alpha}=(\boldsymbol{\alpha}^{\nu})_{\nu\in\mathbb{E}_m}$ is a hypercube of alpha attaching curves, and $\mathcal{L}_{\beta}=(\boldsymbol{\beta}^{\varepsilon})_{\varepsilon\in\mathbb{E}_n}$ is a hypercube of beta attaching curves. Furthermore, suppose that the Heegaard multi-diagram with all 2^m+2^n attaching curves has only transverse double point intersections, and is weakly admissible. In this situation, there is a naturally associated $n+m$-dimensional hypercube of chain complexes $\boldsymbol{CF}^-(\mathcal{L}_{\alpha},\mathcal{L}_{\beta})$, as follows.

The chain complex associated to the vertex $(\nu,\varepsilon)\in\mathbb{E}_{m+n}$ is $\boldsymbol{CF}^-(\boldsymbol{\alpha}^{\nu},\boldsymbol{\beta}^{\varepsilon})$. To describe the maps, it is helpful to introduce some notation. If $\nu_1<\cdots<\nu_i$ and $\varepsilon_1<\cdots<\varepsilon_j$, we define the map

$$f^{\beta^{\varepsilon_1}\to\cdots\to\beta^{\varepsilon_j}}_{\alpha^{\nu_1}\to\cdots\to\alpha^{\nu_i}}\colon \boldsymbol{CF}^-(\boldsymbol{\alpha}^{\nu_1},\boldsymbol{\beta}^{\varepsilon_1})\to\boldsymbol{CF}^-(\boldsymbol{\alpha}^{\nu_i},\boldsymbol{\beta}^{\varepsilon_j})$$

via the formula

$$f^{\beta^{\varepsilon_1}\to\cdots\to\beta^{\varepsilon_j}}_{\alpha^{\nu_1}\to\cdots\to\alpha^{\nu_i}}(\mathbf{x}) = f_{\alpha^{\nu_i},\ldots,\alpha^{\nu_1},\beta^{\varepsilon_1},\ldots,\beta^{\varepsilon_j}}\left(\Theta_{\alpha^{\nu_i},\alpha^{\nu_i-1}},\ldots,\Theta_{\alpha^{\nu_2},\alpha^{\nu_1}},\mathbf{x},\Theta_{\beta^{\varepsilon_1},\beta^{\varepsilon_2}},\ldots,\Theta_{\beta^{\varepsilon_{j-1}},\beta^{\varepsilon_j}}\right),$$

extended equivariantly over the action of U. The hypercube map in $\boldsymbol{CF}^-(\mathcal{L}_{\alpha},\mathcal{L}_{\beta})$ from (ν,ε) to (ν',ε') is given by the formula

$$F^{\beta^{\varepsilon}\to\beta^{\varepsilon'}}_{\alpha^{\nu}\to\alpha^{\nu'}} := \sum_{\substack{\nu<\nu_1<\cdots<\nu_i<\nu'\\ \varepsilon<\varepsilon_1<\cdots<\varepsilon_j<\varepsilon'}} f^{\beta^{\varepsilon}\to\beta^{\varepsilon_1}\to\cdots\to\beta^{\varepsilon_j}\to\beta^{\varepsilon'}}_{\alpha^{\nu}\to\alpha^{\nu_1}\to\cdots\to\alpha^{\nu_i}\to\alpha^{\nu'}}. \tag{5.7}$$

This is a free offprint provided to the author by the publisher. Copyright restrictions may apply.

In the notation of Section 5.1, the map $F^{\beta^\varepsilon\to\beta^{\varepsilon'}}_{\alpha^\nu\to\alpha^{\nu'}}$ would be written $D^{(\nu'-\nu,\varepsilon'-\varepsilon)}_{(\nu,\varepsilon)}$. If $\nu=\nu'$, then we will usually write $F^{\beta^\varepsilon\to\beta^{\varepsilon'}}_{\alpha^\nu}$, and similarly if $\varepsilon=\varepsilon'$.

LEMMA 5.10. *If $\mathcal{L}_\alpha$ and $\mathcal{L}_\beta$ are m and n-dimensional hypercubes of attaching curves on (Σ,w), such that the Heegaard multi-diagram consisting of all 2^m+2^n attaching curves is weakly admissible, then the diagram $\boldsymbol{CF}^-(\mathcal{L}_\alpha,\mathcal{L}_\beta)$ is an $(n+m)$-dimensional hypercube of chain complexes.*

Lemma 5.10 follows immediately from the associativity relations for holomorphic polygons, together with the compatibility conditions in (5.6).

5.7. Hypercubes with twisted coefficients

The above notions naturally adapt to give a notion of a hypercube of attaching curves on a doubly pointed surface (Σ,w,z) with twisted coefficients. Assume first that there is a chosen path γ from w to z. A twisted hypercube of alpha attaching curves $\mathcal{L}_\alpha$ is defined similarly to the untwisted case, except all of the Floer complexes have coefficients in $\mathbb{F}[\![U]\!]\otimes\mathbb{F}[\mathbb{Z}/m]$. A holomorphic curve representing a class ϕ is counted with a multiplicity of $U^{n_w(\phi)}T^{n_z(\phi)-n_w(\phi)}$. We may pair two twisted hypercubes $\mathcal{L}_a$ and $\mathcal{L}_\beta$ to form a hypercube of chain complexes over $\mathbb{F}[\![U]\!]\otimes\mathbb{F}[\mathbb{Z}/m]$, denoted

$$\underline{\underline{\boldsymbol{CF}}}^-(\mathcal{L}_\alpha,\mathcal{L}_\beta).$$

We are usually interested in a subcomplex of $\underline{\underline{\boldsymbol{CF}}}^-(\mathcal{L}_\alpha,\mathcal{L}_\beta)$, which we denote by $\underline{\boldsymbol{CF}}^-(\mathcal{L}_\alpha,\mathcal{L}_\beta)$. Suppose that $\mathcal{L}_\alpha$ and $\mathcal{L}_\beta$ are n and m-dimensional, respectively. If $(\varepsilon,\nu)\in\mathbb{E}_n\times\mathbb{E}_m$, we define $\underline{\boldsymbol{CF}}^-(\mathcal{L}_\alpha,\mathcal{L}_\beta)^{(\varepsilon,\nu)}$ to be $\boldsymbol{CF}^-(\boldsymbol{\alpha}^\varepsilon,\boldsymbol{\beta}^\nu)\otimes T^0\cong\boldsymbol{CF}^-(\boldsymbol{\alpha}^\varepsilon,\boldsymbol{\beta}^\nu)$ if

$$\boldsymbol{\alpha}^{\varepsilon'}\cap\gamma=\boldsymbol{\beta}^{\nu'}\cap\gamma=\emptyset\quad\text{whenever}\quad\varepsilon'\le\varepsilon\quad\text{and}\quad\nu'\le\nu,$$

and we define $\underline{\boldsymbol{CF}}^-(\mathcal{L}_\alpha,\mathcal{L}_\beta)^{(\varepsilon,\nu)}=\underline{\boldsymbol{CF}}^-(\boldsymbol{\alpha}^\varepsilon,\boldsymbol{\beta}^\varepsilon)$ otherwise. It is straightforward to see that $\underline{\boldsymbol{CF}}^-(\mathcal{L}_\alpha,\mathcal{L}_\beta)$ is a subcomplex of $\underline{\underline{\boldsymbol{CF}}}^-(\mathcal{L}_\alpha,\mathcal{L}_\beta)$.

5.8. Low dimensional notation

Since we will only be dealing with hypercubes of dimension 3 or less, it is convenient to make some special notation.

(1) We use the characters Θ, λ and ω for length 1, 2 and 3 chains, respectively, in a hypercube of attaching curves.
(2) We use the characters F, H, and P, respectively, for the length 1, 2 and 3 maps in a hypercube of chain complexes.
(3) We use the characters f, h and p to indicate triangle, quadrilateral, and pentagon counting maps, respectively.

As particular examples, if $\boldsymbol{\alpha}'$ and $\boldsymbol{\alpha}$ differ in a single hypercube coordinate, we write $f^{\beta}_{\alpha\to\alpha'}$ for the map $f_{\alpha',\alpha,\beta}(\Theta_{\alpha',\alpha},-)$. Similarly, if $\boldsymbol{\alpha}'$ and $\boldsymbol{\alpha}$ differ in two coordinates, we write $f^{\beta}_{\alpha\to\alpha'}$ for the map $f_{\alpha',\alpha,\beta}(\lambda_{\alpha',\alpha},-)$.

This is a free offprint provided to the author by the publisher. Copyright restrictions may apply.

This is a free offprint provided to the author by the publisher. Copyright restrictions may apply.

CHAPTER 6

Doubled Heegaard diagrams and the involution

In this chapter, we begin by describing the operation of *doubling* a Heegaard diagram of a 3-manifold in Section 6.1. There is an analog for diagrams of knots, which is described in Section 6.2. In Section 6.3, we will see how doubled Heegaard diagrams give a conceptually simple formula for the involution. In Section 6.4, we sketch our construction of the main hypercube, in terms of doubled diagrams. We prove a technical result regarding admissibility of doubled diagrams in Section 6.5.

In this chapter, we focus on the case that Y is an integer homology 3-sphere, which simplifies the discussion of the twisted complexes $\underline{\boldsymbol{CF}}^-(Y)$. This level of generality will be sufficient for our purposes until Chapter 22, when we talk about rational surgeries.

6.1. Doubled Heegaard diagrams

Suppose that $(\Sigma, \boldsymbol{\alpha}, \boldsymbol{\beta}, w)$ is a Heegaard diagram for (Y, w). Let $D \subseteq \Sigma$ be an open disk centered at w. Note that both $N(\Sigma \setminus D)$ and its complement are handlebodies. We construct a new Heegaard surface $D(\Sigma)$ for Y:

$$D(\Sigma) := \partial\left((\Sigma \setminus D) \times [0,1]\right) \cong \Sigma \# \overline{\Sigma}.$$

We now describe a method for constructing attaching curves on $D(\Sigma)$. We may take one set of attaching curves to be $\boldsymbol{\alpha} \cup \overline{\boldsymbol{\beta}}$, where $\boldsymbol{\alpha} \subseteq \Sigma$ and $\overline{\boldsymbol{\beta}} \subseteq \overline{\Sigma}$. (The barring of $\boldsymbol{\beta}$ indicates only that it lives on $\overline{\Sigma}$). A second set of attaching curves may be constructed as follows. Let $I \subseteq \partial D$ be a subinterval. Let $d_1, \dots, d_{2g}$ be a set of pairwise disjoint, properly embedded arcs in $\Sigma \setminus D$, such that $\partial d_i \subseteq I$, and which induce a basis of $H_1(\Sigma \setminus D, I; \mathbb{Z})$. If we view $D(\Sigma)$ as $\Sigma \# \overline{\Sigma}$, we may double the arcs $d_1, \dots, d_{2g}$ to obtain a collection of pairwise disjoint simple closed curves $\boldsymbol{\Delta} = (\Delta_1, \dots, \Delta_{2g})$ on $D(\Sigma)$, which form a set of compressing curves for $D(\Sigma)$. On $\Sigma \# \overline{\Sigma}$, we view the basepoint w as living in a subset of the connected sum region which is complementary to $I \times [0,1]$.

The above construction naturally gives two Heegaard diagrams,

$$D(\mathcal{H}) := \left(\Sigma \# \overline{\Sigma}, \boldsymbol{\alpha} \cup \overline{\boldsymbol{\beta}}, \boldsymbol{\Delta}, w\right) \quad \text{and} \quad \overline{D}(\mathcal{H}) := \left(\overline{\Sigma} \# \Sigma, \boldsymbol{\Delta}, \overline{\boldsymbol{\alpha}} \cup \boldsymbol{\beta}, w\right),$$

which are conjugates of each other.

The transition maps $\Psi_{\mathcal{H} \to D(\mathcal{H})}$ and $\Psi_{D(\mathcal{H}) \to \mathcal{H}}$ have a simple description, as we now describe. Let $\boldsymbol{\beta}'$ be small Hamiltonian translate of $\boldsymbol{\beta}$, such that $|\beta_i \cap \beta_j'| = 2\delta_{ij}$. There is a 1-handle map

$$F_1^{\overline{\beta}, \overline{\beta}'} \colon CF^-(\Sigma, \boldsymbol{\alpha}, \boldsymbol{\beta}) \to CF^-(\Sigma \# \overline{\Sigma}, \boldsymbol{\alpha} \cup \overline{\boldsymbol{\beta}}, \boldsymbol{\beta} \cup \overline{\boldsymbol{\beta}}'),$$

defined by the formula

$$F_1^{\overline{\beta}, \overline{\beta}'}(\mathbf{x}) = \mathbf{x} \times \Theta^+_{\overline{\beta}, \overline{\beta}'}, \tag{6.1}$$

This is a free offprint provided to the author by the publisher. Copyright restrictions may apply.

extended $\mathbb{F}[U]$-equivariantly, where $\Theta^+_{\overline{\beta},\overline{\beta}'}$ is the top degree generator of $CF^-(\overline{\Sigma}, \overline{\boldsymbol{\beta}}, \overline{\boldsymbol{\beta}}')$. Next, we note that $(\Sigma\#\overline{\Sigma}, \boldsymbol{\beta}\cup\overline{\boldsymbol{\beta}}', \boldsymbol{\Delta}, w)$ is the double of $(\Sigma, \boldsymbol{\beta}, \boldsymbol{\beta}', w)$ which is a diagram $(S^1\times S^2)^{\#g}$. Hence, assuming the diagram $(\Sigma\#\overline{\Sigma}, \boldsymbol{\beta}\cup\overline{\boldsymbol{\beta}}', \boldsymbol{\Delta}, w)$ is weakly admissible, there is a cycle

$$\Theta^+_{\beta\cup\overline{\beta}',\Delta} \in CF^-(\Sigma\#\overline{\Sigma}, \boldsymbol{\beta}\cup\overline{\boldsymbol{\beta}}', \boldsymbol{\Delta}, w) \simeq CF^-\left((S^1\times S^2)^{\#g}\right),$$

representing the top degree generator of homology. See Section 6.5 for more on admissibility and doubled diagrams. We define

$$f^{\beta\cup\overline{\beta}'\to\Delta}_{\alpha\cup\overline{\beta}}(\mathbf{x}) := f_{\alpha\cup\overline{\beta},\beta\cup\overline{\beta}',\Delta}\left(\mathbf{x}, \Theta^+_{\beta\cup\overline{\beta}',\Delta}\right).$$

Proposition 6.1. *If $\mathcal{H} = (\Sigma, \boldsymbol{\alpha}, \boldsymbol{\beta}, w)$ is a Heegaard diagram and $D(\mathcal{H}) = (\Sigma\#\overline{\Sigma}, \boldsymbol{\alpha}\cup\overline{\boldsymbol{\beta}}, \boldsymbol{\Delta}, w)$ is a double of $\mathcal{H}$, then*

$$\Psi_{\mathcal{H}\to D(\mathcal{H})} \simeq f^{\beta\cup\overline{\beta}'\to\Delta}_{\alpha\cup\overline{\beta}} \circ F_1^{\overline{\beta},\overline{\beta}'}.$$

Dually,

$$\Psi_{D(\mathcal{H})\to\mathcal{H}} \simeq F_3^{\overline{\beta},\overline{\beta}'} \circ f^{\Delta\to\beta\cup\overline{\beta}'}_{\alpha\cup\overline{\beta}}.$$

In Proposition 6.1, the map $F_3^{\overline{\beta},\overline{\beta}'}$ is the dual of the map $F_1^{\overline{\beta},\overline{\beta}'}$ in (6.1), i.e., it is $\mathbb{F}[U]$-equivariant and satisfies

$$F_3^{\overline{\beta},\overline{\beta}'}(\mathbf{x}\times\Theta) = \begin{cases} \mathbf{x} & \text{if } \Theta = \Theta^-_{\overline{\beta},\overline{\beta}'} \\ 0 & \text{otherwise.} \end{cases}$$

Proposition 6.1 is proven by interpreting the first composition as the cobordism map for a canceling sequence of 1-handles and 2-handles. The second map is similarly interpreted as the cobordism map for a canceling sequence of 2-handles and 3-handles. See [**Zem21**, Proposition 7.2] for further details.

6.2. Doubled diagrams for knots

In this section, we describe an analog of the doubling construction from Section 6.1, for doubly pointed diagrams of knots. We also describe an analog of Proposition 6.1 for the twisted complexes $\underline{\boldsymbol{CF}}^-(\Sigma, \boldsymbol{\alpha}, \boldsymbol{\beta}, \hat{w}, z)$. There is a new source of ambiguity in the construction, since we may add the new 1-handles near either w, or near z.

Suppose $\mathcal{H} = (\Sigma, \boldsymbol{\alpha}, \boldsymbol{\beta}, w, z)$ is a Heegaard diagram for a doubly pointed knot (K, w, z) in Y. We form a diagram $(\Sigma\#\overline{\Sigma}, \boldsymbol{\alpha}\cup\overline{\boldsymbol{\beta}}, \boldsymbol{\Delta}, z, \overline{z})$ by doubling the diagram $\mathcal{H}$, at the basepoint w. In this diagram, we delete w, and add a new basepoint $\overline{z}\in\overline{\Sigma}$, which is the image of z on $\overline{\Sigma}$.

The diagram $(\Sigma\#\overline{\Sigma}, \boldsymbol{\alpha}\cup\overline{\boldsymbol{\beta}}, \boldsymbol{\Delta}, z, \overline{z})$ may naturally be viewed as a diagram for (Y, K), as follows. Let D be an open disk containing the basepoint w, and we embed $\Sigma\#\overline{\Sigma}$ into Y as $\partial(N(\Sigma\setminus D))$. The knot K no longer intersects the Heegaard surface at w, and instead intersects it at $z\in\Sigma$ and $\overline{z}\in\overline{\Sigma}$. See Figure 6.1.

There is a 1-handle map

$$F_1^{\overline{\beta},\overline{\beta}'} : \underline{\boldsymbol{CF}}^-(\Sigma, \boldsymbol{\alpha}, \boldsymbol{\beta}, \hat{w}, z) \to \underline{\boldsymbol{CF}}^-\left(\Sigma\#\overline{\Sigma}, \boldsymbol{\alpha}\cup\overline{\boldsymbol{\beta}}, \boldsymbol{\beta}\cup\overline{\boldsymbol{\beta}}', z, \hat{\overline{z}}\right).$$

We think of $F_1^{\overline{\beta},\overline{\beta}'}$ as corresponding to attaching 1-handles near w, then moving w to the position of $\overline{z}$.

This is a free offprint provided to the author by the publisher. Copyright restrictions may apply.

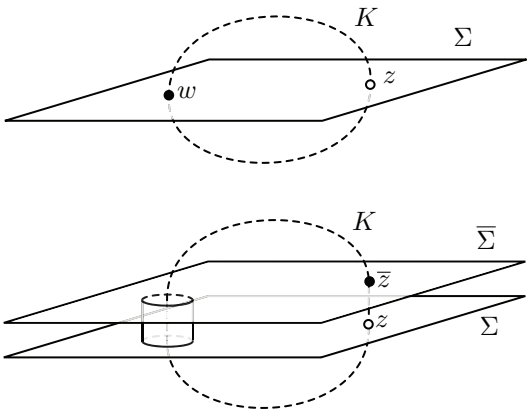


FIGURE 6.1. A Heegaard diagram for a knot (top), and its double (bottom).

We have the following analog to Proposition 6.1, for twisted complexes:

PROPOSITION 6.2. *The composition*

$$f^{\beta\cup\overline{\beta}'\to\Delta}_{\alpha\cup\overline{\beta}}\circ F_1^{\overline{\beta},\overline{\beta}'}:\underline{\boldsymbol{CF}}^-(\Sigma,\boldsymbol{\alpha},\boldsymbol{\beta},\hat{w},z)\to\underline{\boldsymbol{CF}}^-\left(\Sigma\#\overline{\Sigma},\boldsymbol{\alpha}\cup\overline{\boldsymbol{\beta}},\boldsymbol{\Delta},z,\hat{\overline{z}}\right)$$

is chain homotopic to the map for the diffeomorphism which moves w to $\overline{z}$ along a subarc of K, while keeping z fixed, followed by the map from naturality. Dually,

$$F_3^{\overline{\beta},\overline{\beta}'}\circ f^{\Delta\to\beta\cup\overline{\beta}'}_{\alpha\cup\overline{\beta}}:\underline{\boldsymbol{CF}}^-\left(\Sigma\#\overline{\Sigma},\boldsymbol{\alpha}\cup\overline{\boldsymbol{\beta}},\boldsymbol{\Delta},z,\hat{\overline{z}}\right)\to\underline{\boldsymbol{CF}}^-(\Sigma,\boldsymbol{\alpha},\boldsymbol{\beta},\hat{w},z),$$

is chain homotopic to the diffeomorphism map moving $\overline{z}$ to w while fixing z, followed by the map from naturality.

6.3. The involution via doubling

A doubled diagram $D(\mathcal{H})$ may be viewed as the double of both $\mathcal{H}$ and $\overline{\mathcal{H}}$. Hence, the involution may be described as a composition of a doubling map, followed by an un-doubling map, using the formulas from Proposition 6.1 and 6.2. More concretely, if $(\Sigma,\boldsymbol{\alpha},\boldsymbol{\beta},w)$ is a Heegaard diagram, then

$$\iota\simeq\eta\circ F_3^{\alpha,\alpha'}\circ f^{\Delta\to\alpha'\cup\overline{\alpha}}_{\alpha\cup\overline{\beta}}\circ f^{\beta\cup\overline{\beta}'\to\Delta}_{\alpha\cup\overline{\beta}}\circ F_1^{\overline{\beta},\overline{\beta}'}. \tag{6.2}$$

(Recall that η is the tautological chain isomorphism from Section 2.1.)

Similarly, if $(\Sigma,\boldsymbol{\alpha},\boldsymbol{\beta},\hat{w},z)$ is a diagram for an oriented null-homologous knot K in Y, with w marked as the special basepoint, then the twisted involution defined in (2.10) satisfies

$$\underline{\iota}\simeq\mathfrak{F}_{z\to w}\circ\underline{\eta}\circ F_3^{\alpha,\alpha'}\circ f^{\Delta\to\alpha'\cup\overline{\alpha}}_{\alpha\cup\overline{\beta}}\circ f^{\beta\cup\overline{\beta}'\to\Delta}_{\alpha\cup\overline{\beta}}\circ F_1^{\overline{\beta},\overline{\beta}'}.$$

(Recall that $\underline{\eta}$ is the tautological chain isomorphism from Section 2.3.)

REMARK 6.3. At this point we pause for one important note concerning the definition of the knot involution. The choice of which basepoint at which we form the connect sum in Figure 6.1 is not arbitrary; it is instead determined by our choice of flip map $\mathfrak{F}_{z\to w}$. In particular, the choice of basepoint at which we form the connect sum determines the direction in which the basepoint-moving diffeomorphism in the definition of ι_K twists along the knot K. If we take the connected

This is a free offprint provided to the author by the publisher. Copyright restrictions may apply.

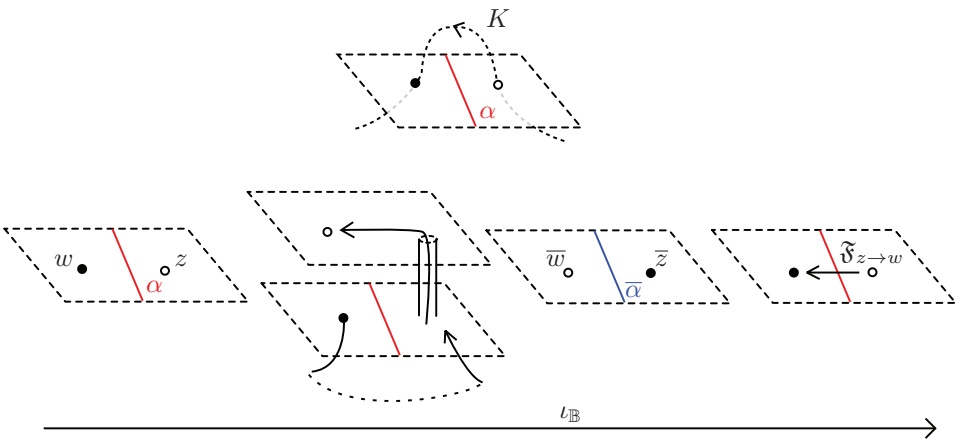


FIGURE 6.2. A schematic of the map $\iota_{\mathbb{B}}$ defined using the wrong choice of connected sum point. The top image indicates the orientation of K, and the bottom row indicates the diagrams which appear in the definition of $\iota_{\mathbb{B}}$. Arrows indicate movement of the basepoints throughout. The diagram on the left is $(\Sigma, \boldsymbol{\alpha}, \boldsymbol{\beta}, w, z)$. The middle-left is the doubled diagram. The middle-right is the diagram $(\Sigma, \overline{\boldsymbol{\beta}}, \overline{\boldsymbol{\alpha}}, \overline{z}, \overline{w})$. The final right-hand diagram indicates the path for the flip map. Note that w is sent through a full loop around K as we go from left to right.

sum near w, the basepoint-moving diffeomorphism from ι_K twists oppositely to the orientation of K, whereas the flip map twists coherently to K. The net effect is that the map $\iota_{\mathbb{B}} := \mathfrak{F}_{z\to w} \circ \iota_K$ carries the basepoint w through a nullhomotopic loop. If we instead take the connected sum near z then both ι_K and $\mathfrak{F}_{z\to w}$ move basepoints positively along K. Hence $\iota_{\mathbb{B}}$ sends the basepoints through a full loop around K, as in Figure 6.2. Our proof of the surgery exact triangle does not carry through with this choice. Concretely, one of the model counts in Lemma 19.23 will fail.

6.4. Doubling and the involutive hypercube of a triad

We now outline our construction of the main hypercube, from Theorem 1.14. We will construct a hyperbox of chain complexes, of size $(1, 1, 7)$, which we show in Figure 6.3. In the subsequent sections, we will construct the hypercubes labeled $\mathcal{C}_{1\text{-h}}$, $\mathcal{C}^1_{2\text{-h}}$, $\mathcal{C}_{\text{cen}}$, $\mathcal{C}^2_{2\text{-h}}$, $\mathcal{C}_{3\text{-h}}$, $\mathcal{C}_\eta$ and $\mathcal{C}_{\mathfrak{F}}$.

We have not drawn any of the length 2 or 3 arrows in any of the hypercubes. The compression of the above hyperbox of chain complexes will be our main hypercube. Our construction is organized as follows:

- $\mathcal{C}_{1\text{-h}}$ and $\mathcal{C}_{3\text{-h}}$ are the *1-handle* and *3-handle hypercubes*. They are special cases of the *hypercubes for stabilization*, constructed in Chapter 14.
- $\mathcal{C}^1_{2\text{-h}}$ and $\mathcal{C}^2_{2\text{-h}}$ are the *2-handle hypercubes*. They are constructed in Chapters 15 and 17.
- $\mathcal{C}_{\text{cen}}$ is the *central hypercube*. It is constructed in Chapter 16.
- $\mathcal{C}_\eta$ is the *tautological hypercube*. It is described in Chapter 18.

This is a free offprint provided to the author by the publisher. Copyright restrictions may apply.

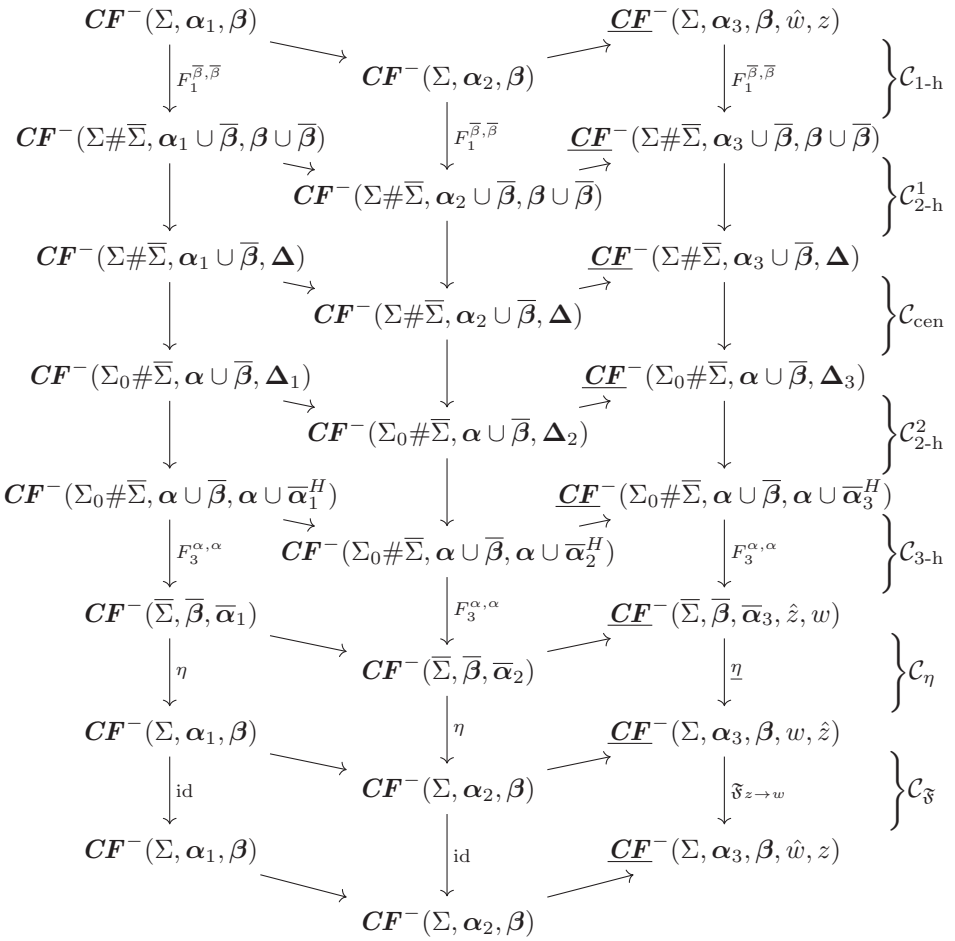


FIGURE 6.3. The hyperbox whose compression is the hypercube in Theorem 1.14. Length 2 and 3 arrows are not shown.

- $\mathcal{C}_{\mathfrak{F}}$ is the *flip-map hypercube*. It is constructed in Chapter 18.

The surface $\Sigma_0\#\overline{\Sigma}$, and the attaching curves $\boldsymbol{\Delta}_i$, $\boldsymbol{\alpha}$ and $\overline{\boldsymbol{\alpha}}_i^H$ will be described in Chapter 15. Note that the columns are not identical to the doubling model described in Section 6.3 (for example, the model described therein did not feature $\Sigma_0\#\overline{\Sigma}$). We prove in Lemma 16.14 that the vertical maps in $\mathcal{C}_{\text{cen}}$ coincide with change of diagram maps. Using this fact, the same logic as in Proposition 6.1 also shows that the composition of each vertical arrow in the columns of Figure 6.3 gives the involution.

6.5. Admissibility and doubled diagrams

In this section, we prove a technical result concerning admissibility of doubled diagrams, which will be used as the model for more complicated admissibility arguments later.

DEFINITION 6.4. Suppose $\mathcal{D} = (\Sigma, \boldsymbol{\gamma}_1, \dots, \boldsymbol{\gamma}_n, w)$ is a Heegaard multi-diagram.

This is a free offprint provided to the author by the publisher. Copyright restrictions may apply.

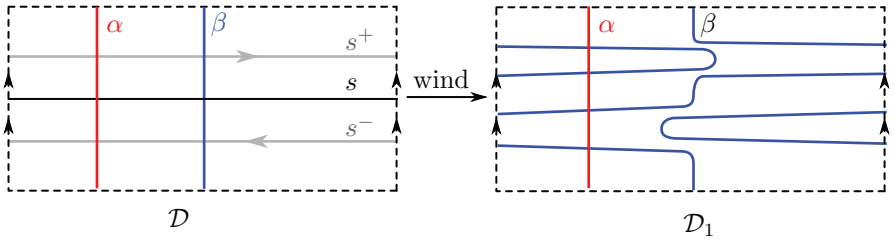


FIGURE 6.4. Winding along s_i once to obtain $\mathcal{D}_1$.

(1) A *(rational) periodic domain* is an integral (resp. rational) 2-chain D on Σ such that ∂D is a (rational) linear combination of the curves in $\boldsymbol{\gamma}_1 \cup \cdots \cup \boldsymbol{\gamma}_n$, and furthermore, $n_w(D) = 0$.
(2) $\mathcal{D}$ is *weakly admissible* if every non-zero periodic domain has both positive and negative multiplicities.

Since we are working over the power series ring $\mathbb{F}[\![U]\!]$, it is sufficient to work with diagrams which are weakly admissible. (See [**OS04b**, Lemma 4.13].) Admissibility is usually achieved by the process of *winding* [**OS04b**, Section 5], which we now sketch. If $(\Sigma, \boldsymbol{\alpha}, \boldsymbol{\beta}, w)$ is a Heegaard diagram, we pick pairwise disjoint, embedded curves $s_1, \dots, s_g$ which are dual to the $\boldsymbol{\beta}$ curves, in the sense that

$$|s_i \cap \beta_j| = \delta_{ij}.$$

We then consider two pushoffs s_i^+ and s_i^- of s_i. We form a diagram $\mathcal{D}_N$ by winding β_i N-times, positively, along s_i^+, and N-times, negatively, along s_i^-. See Figure 6.4.

Ozsváth and Szabó show that if one winds a Heegaard multi-diagram sufficiently, then weak admissibility is obtained [**OS04b**, Lemma 5.4]. In particular, if $(\Sigma \# \overline{\Sigma}, \boldsymbol{\alpha} \cup \overline{\boldsymbol{\beta}}, \boldsymbol{\Delta}, w)$ is a doubled diagram, we may wind $\boldsymbol{\alpha} \cup \overline{\boldsymbol{\beta}}$ to achieve admissibility. This is not quite suitable for our purposes. Instead, we now show that for a doubled diagram, we need only wind $\overline{\boldsymbol{\beta}}$ to achieve admissibility.

We now prove a helpful admissibility result for doubled diagrams where $\boldsymbol{\Delta}$ are adapted to $\boldsymbol{\alpha}$. The following will be a model for proving admissibility of Heegaard multi-diagrams appearing in the construction of the central hypercube.

LEMMA 6.5. *Suppose that $\mathcal{H} = (\Sigma, \boldsymbol{\alpha}, \boldsymbol{\beta}, w)$ is a Heegaard diagram, and $D(\mathcal{H}) = (\Sigma \# \overline{\Sigma}, \boldsymbol{\alpha} \cup \overline{\boldsymbol{\beta}}, \boldsymbol{\Delta}, w)$ is a double of $\mathcal{H}$. Then, after winding the $\overline{\boldsymbol{\beta}}$ curves sufficiently on $\overline{\Sigma}$, the diagram $D(\mathcal{H})$ becomes weakly admissible.*

PROOF. Let $s_1, \dots, s_g \subseteq \overline{\Sigma}$ denote dual curves to the $\overline{\boldsymbol{\beta}}$ curves, along which to wind. Let $D(\mathcal{H})_N$ denote the diagram obtained by winding $\overline{\boldsymbol{\beta}}$ N-times, along positive and negative push-offs of the curves $s_1, \dots, s_g$, as in Figure 6.4.

Let $\mathcal{P}_N^{\mathbb{Q}}$ denote the set of rational periodic domains on $D(\mathcal{H})_N$. It is clearly sufficient to rule out the existence of a nonzero rational periodic domain with non-negative coefficients.

Note that there is a canonical isomorphism

$$\phi_N \colon \mathcal{P}^{\mathbb{Q}} \to \mathcal{P}_N^{\mathbb{Q}},$$

which preserves the multiplicities which are not in the winding region.

We suppose for contradiction that $D(\mathcal{H})_N$ is not weakly admissible, for arbitrarily large N. This means there is a sequence of periodic domains, $\{D_i\}_{i \in \mathbb{N}}$ such

This is a free offprint provided to the author by the publisher. Copyright restrictions may apply.

that D_i is a nonzero periodic domain on $D(\mathcal{H})_{N_i}$ with only nonnegative multiplicities, where $N_i \to \infty$. By rescaling, we assume that

$$\|D_i\|_{L^\infty} = 1,$$

for all i. We consider the domains $D_i' := \phi_{N_i}^{-1}(D_i)$. Noting that the set of multiplicities of D_i' is a subset of the multiplicities of D_i, it follows that $\|D_i'\|_{L^\infty} \leq 1$, for all i. Let D_∞' be the limit of a convergent subsequence of the D_i'. We make the following claims:

- (d-1) D_∞' is nonnegative.
- (d-2) D_∞' is a real periodic domain such that $\partial D_\infty'$ is a linear combination of the $\boldsymbol{\alpha}$ and $\boldsymbol{\Delta}$ curves (in particular, the boundary contains no multiples of $\overline{\boldsymbol{\beta}}$).
- (d-3) $\|D_\infty'\| \geq 1/2$.

Claim (d-1) follows since D_i is nonnegative, and the set of multiplicities of D_i' is a subset of the set of multiplicities of D_i.

To prove claim (d-2), it is sufficient to show that D_∞' has equal multiplicity on either side of a curve β in $\overline{\boldsymbol{\beta}}$. Assume $D_i' \to D_\infty'$. As the difference of D_∞' across β at a point $p \in \beta$ is independent of p, it is sufficient to consider p adjacent to the winding region, but not contained in it. Let x_i^l and x_i^r denote the multiplicities of D_i' on either side of β at p (the order is unimportant). Let x_∞^l and x_∞^r denote the limits (which are the values of D_∞' near p). By construction, D_i has multiplicities of both $x_i^l + N_i(x_i^l - x_i^r)$ and $x_i^r + N_i(x_i^r - x_i^l)$. Since for all i,

$$0 \leq x_i^l + N_i(x_i^l - x_i^r) \leq 1 \quad \text{and} \quad 0 \leq x_i^l \leq 1,$$

we obtain that $x_\infty^l - x_\infty^r = 0$, by taking the limit. In particular, D_∞' has equal multiplicities on both sides of β. Claim (d-2) follows.

We now consider claim (d-3). We claim that each D_i' has a multiplicity which is at least $1/2$. By construction, each D_i has a multiplicity which is 1. If this multiplicity occurs outside of the winding region, then we are done. Suppose that it occurs inside of the winding region for a curve $s \in \{s_1, \dots, s_g\}$ which is dual to $\beta \in \boldsymbol{\beta}$. Let δ denote the coefficient of β in $\partial D_i'$, which is equivalently the difference in multiplicities on the two sides of β. We may assume $\delta \geq 0$ by changing the orientation of β, if necessary. The multiplicities of D_i are exactly $m + k \cdot \delta$, where m is a multiplicity of D_i' and $k \in \{-N_i, \dots, N_i\}$. For $m + k \cdot \delta$ to be the maximal multiplicity of D_i', we must have $k = N_i$. However,

$$0 \leq m - N_i \cdot \delta.$$

Adding $1 = m + N_i \cdot \delta$ and dividing by 2 we obtain $m \geq 1/2$, establishing (d-3).

However, there are no non-trivial, real 2-chains on $\Sigma \# \overline{\Sigma}$ which have multiplicity 0 at w and satisfy (d-1), (d-2) and (d-3). Indeed, such a 2-chain would give a non-trivial linear relation amongst the classes $[\alpha_1], \dots [\alpha_g], [\Delta_1], \dots, [\Delta_{2g}]$ in $H_1(\Sigma \# \overline{\Sigma}; \mathbb{R})$. However, the subspaces

$$\text{Span}([\alpha_1], \dots, [\alpha_g]),\ \text{Span}([\Delta_1], \dots, [\Delta_{2g}]) \subseteq H_1(\Sigma \# \overline{\Sigma}; \mathbb{R})$$

have trivial intersection, and are themselves g and $2g$-dimensional, respectively. □

To ensure certain stabilization results for holomorphic curves, it will be helpful to introduce the following restricted version of a doubled diagram:

This is a free offprint provided to the author by the publisher. Copyright restrictions may apply.

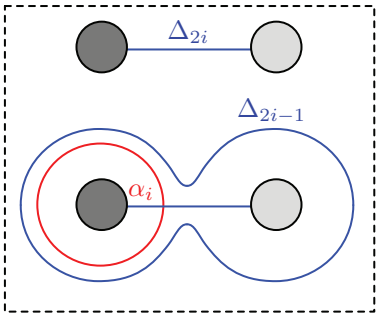


FIGURE 6.5. A schematic of a choice of $\boldsymbol{\Delta} \subseteq \Sigma \# \overline{\Sigma}$, which are adapted to $\boldsymbol{\alpha} \subseteq \Sigma$. Here, Σ is the genus 1 region on the left, and $\overline{\Sigma}$ is the genus 1 region on the right.

DEFINITION 6.6. Suppose that $\mathcal{H} = (\Sigma, \boldsymbol{\alpha}, \boldsymbol{\beta}, w)$ is a Heegaard diagram, and $(\Sigma \# \overline{\Sigma}, \boldsymbol{\alpha} \cup \overline{\boldsymbol{\beta}}, \boldsymbol{\Delta}, w)$ is a double of $\mathcal{H}$. We say that the curves $\boldsymbol{\Delta}$ are *adapted to* $\boldsymbol{\alpha}$ if they are constructed by doubling a basis of arcs $d_1, \dots d_{2g}$ for $H_1(\Sigma \setminus N(w), I; \mathbb{Z})$, where I is a subarc of $\partial N(w)$, as follows. The arcs $d_2, d_4, \dots, d_{2g}$ are chosen (arbitrarily) to satisfy

$$|d_{2i} \cap \alpha_j| = \delta_{ij}.$$

The arc d_{2i} induces two arcs from α_i to $\overline{\alpha}_i$. Let λ_i denote one of these arcs (chosen arbitrarily). We let Δ_{2i-1} be obtained by handlesliding α_i across $\overline{\alpha}_i$, using the arc λ_i as a guide. We assume Δ_{2i-1} is chosen to be disjoint from α_i.

Note that Lemma 6.5 implies that $\boldsymbol{\alpha}$-adapted diagrams may be made weakly admissible by winding $\overline{\boldsymbol{\beta}}$ sufficiently.

This is a free offprint provided to the author by the publisher. Copyright restrictions may apply.

CHAPTER 7

Moduli spaces and almost complex structures

In this chapter, we describe some analytic input we will need. We begin by defining our spaces of almost complex structures and moduli spaces for holomorphic disks in Section 7.1. In Section 7.3 we describe some results on transversality of holomorphic curves with pointwise constraints, including pointwise tangency constraints, which we use frequently. In Sections 7.5–7.8 we describe the necessary input on boundary degenerations, including Proposition 7.9, which has not appeared previously in the literature.

7.1. Almost complex structures for holomorphic disks

Let $\omega = dA + ds \wedge dt$ be a fixed, split symplectic form on $\Sigma \times [0,1] \times \mathbb{R}$. Suppose $p_1, \dots, p_n$ is a fixed collection of points in $\Sigma \backslash (\boldsymbol{\alpha} \cup \boldsymbol{\beta})$, and $D_1, \dots, D_n$ are a collection of small regular neighborhoods of $p_1, \dots, p_n$ in Σ.

DEFINITION 7.1. We say an almost complex structure J on $\Sigma \times [0,1] \times \mathbb{R}$ is *admissible* if it satisfies the following:

- (J-1) J is tamed by ω.
- (J-2) J is split on $(D_1 \cup \dots \cup D_n) \times [0,1] \times \mathbb{R}$.
- (J-3) J is translation invariant under the $\mathbb{R}$-action.
- (J-4) $J\partial/\partial s = \partial/\partial t$.
- (J-5) $T_p\Sigma \oplus \{0\}$ is a complex line in a neighborhood of $(\boldsymbol{\alpha} \cup \boldsymbol{\beta}) \times [0,1] \times \mathbb{R}$, and on $\Sigma \times \{0,1\} \times \mathbb{R}$.

Note that our axioms (J-1)–(J-5) are equivalent to the ones that Lipshitz labels (J-1)–(J-4) and (J-5') (in particular, our numbering does not coincide with his). A similar family of almost complex structures are called *relaxed* in [**LOT18**, p. 229].

7.2. Moduli spaces of disks

Suppose $(\Sigma, \boldsymbol{\alpha}, \boldsymbol{\beta}, w)$ is a Heegaard diagram. Suppose that S is a smooth (not nodal) Riemann surface with boundary and a finite collection of boundary punctures, designated as $+$ or $-$. Suppose J is an almost complex structure on $\Sigma \times [0,1] \times \mathbb{R}$ which satisfies (J-1)–(J-5). We are interested in pairs (u, j), where j is an almost complex structure on S, and u is a smooth map

$$u \colon (S, \partial S) \to (\Sigma \times [0,1] \times \mathbb{R}, (\boldsymbol{\alpha} \times \{1\} \times \mathbb{R}) \cup (\boldsymbol{\beta} \times \{0\} \times \mathbb{R})),$$

representing the homology class ϕ, and satisfying the following:

- (M-1) u is (j, J)-holomorphic.
- (M-2) u is proper.
- (M-3) For each i, $u^{-1}(\alpha_i \times \{1\} \times \mathbb{R})$ and $u^{-1}(\beta_i \times \{0\} \times \mathbb{R})$ each consist of exactly one component of ∂S.
- (M-4) If q is a $+$ puncture of S, then $\lim_{z \to q}(\pi_{\mathbb{R}} \circ u)(z) = +\infty$.

This is a free offprint provided to the author by the publisher. Copyright restrictions may apply.

(M-5) If q is a $-$ puncture of S, then $\lim_{z\to q}(\pi_{\mathbb{R}}\circ u)(z) = -\infty$.
(M-6) u has finite energy.
(M-7) $\pi_{\mathbb{D}}\circ u$ is non-constant on each component of S, where $\pi_{\mathbb{D}}$ denotes the projection onto $[0,1]\times\mathbb{R}$.

Compare [**Lip06**, p. 960], [**LOT18**, p. 63]. We write $\mathcal{M}_J(S,\phi)$ for the set of such pairs, modulo the relation that $(u,j)\sim(u',j')$ if there is a (j,j')-holomorphic diffeomorphism $\phi\colon S\to S$ such that $u'\circ\phi = u$.

The next object of interest is the moduli space of holomorphic curves with marked points. Suppose S is a Riemann surface, as above, and $\mathbf{q} = (q_1,\dots,q_n)$ is an ordered collection of distinct points along S. We write $S^{\mathbf{q}}$ for a surface, equipped with a choice of $\mathbf{q}$. We write $\mathcal{M}_J(S^{\mathbf{q}},\phi)$ for the set of pairs (u,j) satisfying (M-1)–(M-7), except we quotient only by diffeomorphisms $\phi\colon S\to S$ which fix $\mathbf{q}$ pointwise.

We say two marked surfaces $S^{\mathbf{q}}$ and $T^{\mathbf{p}}$ are *equivalent* if there is a diffeomorphism $\phi\colon S\to T$ which takes the positive (resp. negative) punctures to positive (resp. negative) punctures, and restricts to an order preserving bijection between $\mathbf{q}$ and $\mathbf{p}$.

7.3. Moduli spaces with matching conditions

A common construction is to restrict the values obtained by holomorphic curves on their marked points. A refinement of this construction is to consider holomorphic curves with additional tangency constraints at their marked points. In this section, we provide background on the construction.

Suppose that (W,J) is an almost complex manifold and $p\in W$. A *complex r-jet* at p is an equivalence class of germs of J-holomorphic maps

$$g\colon(\mathbb{C},0)\to(W,p),$$

where two germs, g_1 and g_2, are *r-equivalent* if $\left(\frac{\partial^i}{\partial^i x}g_1\right)(0) = \left(\frac{\partial^i}{\partial^i x}g_2\right)(0)$ for all $0\le i\le r$, where (x,y) are the standard coordinates on $\mathbb{C}$. We write $\mathrm{Jet}^r_p(W,J)$ for the set of complex r-jets at p.

Using the local existence of holomorphic curves, one can identify $\mathrm{Jet}^r_p(W^{2n},J)$ with $\mathbb{C}^{rn}$ [**ZZ15**, Proposition 2.1]. By convention, we interpret the 0-jet space as a single point. When $W=\mathbb{C}^n$, coordinates on the jet spaces may be given by coefficients of complex Taylor series.

It is straightforward to identify $\mathrm{Jet}^1_p(W,J)$ with T_pW, and hence $\mathrm{Jet}^1_p(W,J)$ is naturally a complex vector space. For $r>1$, $\mathrm{Jet}^r_p(W,J)$ is not naturally a vector space, however it does have a distinguished point 0, given by the constant map at p. We define

$$\mathrm{Jet}^r(W,J) := \bigcup_{p\in W}\mathrm{Jet}^r_p(W,J),$$

which forms a fiber bundle over W.

If (W_1,J_1) and (W_2,J_2) are two almost complex manifolds and $u\colon W_1\to W_2$ is (J_1,J_2)-holomorphic, there is an r-jet evaluation map

$$J^r_p u\colon\ \mathrm{Jet}^r_p(W_1,J_1)\to\mathrm{Jet}^r_{u(p)}(W_2,J_2),$$

given by $(J^r_p u)(g) = u\circ g$.

This is a free offprint provided to the author by the publisher. Copyright restrictions may apply.

DEFINITION 7.2. We say $M = (M_0, \mathbf{t})$ is a *matching condition* if $M_0 \subseteq ((0,1) \times \mathbb{R})^k$ is a smoothly embedded submanifold, and $\mathbf{t} = (n_1, \dots, n_k, m_1, \dots, m_k)$ is a tuple of nonnegative integers.

If $\mathbf{t} = (n_1, \dots, n_k, m_1, \dots, m_k)$, we write

$$|\mathbf{t}| := n_1 + \cdots + n_k + m_1 + \cdots + m_k.$$

Suppose M is a matching condition, $S^{\mathbf{q}}$ is a marked Riemann surface for disks, $p \in \Sigma \setminus (\boldsymbol{\alpha} \cup \boldsymbol{\beta})$ is a chosen point, and J is an admissible almost complex structure on $\Sigma \times [0,1] \times \mathbb{R}$ which is split in a cylindrical neighborhood of $\{p\} \times [0,1] \times \mathbb{R}$. We define the *moduli space of M-matched disks* to be

(7.1)
$$\mathcal{M}_J(S^{\mathbf{q}}, \phi, M) := \left\{ (u,j) \in \mathcal{M}_J(S,\phi) \;\middle|\; \begin{array}{c} (\pi_\Sigma \circ u)(q_i) = p \\ ((\pi_{\mathbb{D}} \circ u)(q_1), \dots, (\pi_{\mathbb{D}} \circ u)(q_k)) \in M_0, \\ J^{n_i}_{q_i}(\pi_\Sigma \circ u) = 0, \\ J^{m_i}_{q_i}(\pi_{\mathbb{D}} \circ u) = 0, \\ \text{for } i = 1, \dots, k \end{array} \right\}.$$

In (7.1), if $n_i = 0$, we interpret $J^{n_i}_{q_i}(\pi_\Sigma \circ u) = 0$ as holding vacuously.

If $p_1, \dots, p_\ell$ is a collection of special points on $\Sigma \setminus (\boldsymbol{\alpha} \cup \boldsymbol{\beta})$, and we are equipped with a function $f \colon \mathbf{q} \to \{p_1, \dots, p_\ell\}$, then we may also define the moduli space of M-matched disks for $S^{\mathbf{q},f}$ by a simple adaptation of (7.1).

7.4. Expected dimensions

Given a matching condition $M = (M_0, \mathbf{t})$, we will write

$$|M| := \operatorname{codim}(M_0) + 2|\mathbf{t}|.$$

We define the *embedded, matched index* of a pair (ϕ, M) to be

$$\operatorname{ind}_{\mathrm{emb}}(\phi, M) := \mu(\phi) - |M|,$$

where $\mu(\phi)$ denotes the ordinary Maslov index of the class ϕ.

PROPOSITION 7.3. *Suppose that $S^{\mathbf{q}}$ is a Riemann surface with k marked points $\mathbf{q} = (q_1, \dots, q_k)$, and $M = (M_0, \mathbf{t})$ is a matching condition at a point $p \in \Sigma$.*

(1) *For generic J satisfying (J-1)–(J-5), the M-matched moduli space $\mathcal{M}_J(S^{\mathbf{q}}, \phi, M)$ is a smooth manifold of dimension*

$$\operatorname{ind}(u) - |M|,$$

where $\operatorname{ind}(u)$ *denotes the Fredholm index, viewing u as a holomorphic curve with no marked points.*

(2) *Furthermore, the dimension of $\mathcal{M}_J(S^{\mathbf{q}}, \phi, M)$ also coincides with the quantity*

$$\operatorname{ind}_{\mathrm{emb}}(\phi, M) - 2\operatorname{Sing}(u),$$

where $\operatorname{Sing}(u)$ *denotes the singularity number of u.*

In part (2) of Proposition 7.3, the quantity $\operatorname{Sing}(u)$ is the signed count of double points, in an equivalent singularity. An interior (positive) double point contributes 1, and a boundary double point contributes $\frac{1}{2}$.

Proposition 7.3 follows from a standard line of reasoning, as we now sketch. We begin with part (1). In the restricted case that $\mathbf{t} = (0, \dots, 0)$, the result follows from a straightforward combination of the proofs of [**Lip06**, Proposition 3.7] and

This is a free offprint provided to the author by the publisher. Copyright restrictions may apply.

[**MS12**, Proposition 3.4.2]. For a generic J, $\mathcal{M}_J(S^{\mathbf{q}}, \phi)$ is a smooth manifold, and the map $\mathrm{ev}_{\mathbf{q}}$ is transverse to M_0, giving the claimed dimension count immediately.

The case when $|\mathbf{t}| > 0$ is slightly more involved, as we now describe. We note that $J^{n_i}_{q_i}(\pi_\Sigma \circ u)$ lives in $\mathrm{Map}(\mathrm{Jet}^{n_i}_{q_i}(S, j), \mathrm{Jet}^{n_i}_{(\pi_\Sigma \circ u)(q_i)}(\Sigma, j_\Sigma))$, which depends on j. This is slightly inconvenient for computing expected dimensions, and one solution is to pick complex coordinates carefully on S, near $\mathbf{q}$, as we now describe.

Write $\mathcal{J}(S)$ for the set of almost complex structures on S. The *Teichmüller space* of $S^{\mathbf{q}}$, which we denote by $\mathcal{T}(S^{\mathbf{q}})$, is the the quotient of $\mathcal{J}(S)$ by $\mathrm{Diff}_0(S, \mathbf{q})$ (automorphisms of S, which are isotopic to id_S via an isotopy which fixes $\mathbf{q}$). Let us write $\pi \colon \mathcal{J}(S) \to \mathcal{T}(S^{\mathbf{q}})$ for the natural map.

Definition 7.4. If $j_0 \in \mathcal{J}(S)$, a *Teichmüller slice* through j_0 is a subset $\mathcal{T} \subseteq \mathcal{J}(S)$ parametrized by a map

$$\phi \colon (U, 0) \to (\mathcal{J}(S), j_0)$$

where U is an open subset of some Euclidean space, containing 0, such that the composition $\pi \circ \phi \colon U \to \mathcal{T}(S^{\mathbf{q}})$ is a diffeomorphism onto its image. Furthermore, all $j \in \mathcal{T}$ coincide on a neighborhood of $\mathbf{q}$.

See [**Wen10a**, Section 3.1] for information on constructing Teichmüller slices.

Let $\mathcal{B}$ denote the set of $W^{p,1}_\delta$ maps from S to $\Sigma \times [0,1] \times \mathbb{R}$. Fix a Teichmüller slice $\mathcal{T}$ through $j_0 \in \mathcal{J}(S)$. There is a Banach space bundle $\mathcal{E}$ over $\mathcal{T} \times \mathcal{B}$, whose fiber over (j, u) consists of L^p_δ sections of the vector bundle $\Omega^{0,1}(S, j, u) \to S$, whose fiber at p is the vector space

$$\Omega^{0,1}_p(S, j, u) = \overline{\mathrm{Hom}}_{\mathbb{C}}\left((T_pS, j), (T_{u(p)}\Sigma \times [0,1] \times \mathbb{R}, J)\right).$$

We view the operator $\overline{\partial}_J \colon \mathcal{T} \times \mathcal{B} \to \mathcal{E}$, given by

$$\overline{\partial}_J(u) = du + J \circ du \circ j,$$

as giving a section of the bundle $\mathcal{E}$.

Since the almost complex structures $j \in \mathcal{T}$ on S from a Teichmüller slice $\mathcal{T}$ are constant near $\mathbf{q}$, we may pick complex coordinates in a neighborhood of each q_i. For a tuple $(r_1, \ldots, r_k) \in \mathbb{Z}^k_{\geq 0}$, we obtain a jet space evaluation map

$$\mathrm{ev}^{\mathrm{Jet}} \colon \overline{\partial}_J^{-1}(0) \cap (\mathcal{T} \times \mathcal{B}) \to \mathrm{Jet}^{r_1}(\Sigma \times [0,1] \times \mathbb{R}, J) \times \cdots \times \mathrm{Jet}^{r_k}(\Sigma \times [0,1] \times \mathbb{R}, J). \tag{7.2}$$

Write $\overline{\partial}_J^{-1}(0)|_D$ for the set of open subset consisting of marked holomorphic curves whose marked points have evaluation in $D \times [0,1] \times \mathbb{R}$. Furthermore, we may restrict attention to the set of almost complex structures satisfying (J-1)–(J-5) which additionally coincide with $j_D \times j_{\mathbb{D}}$ on $D \times [0,1] \times \mathbb{R}$, for some fixed almost complex structure j_D on D. In this case, the jet evaluation map from (7.2) restricts to a map

$$\mathrm{ev}^{\mathrm{Jet}}_D \colon \overline{\partial}_J^{-1}(0)|_D \to \mathrm{Jet}^{r_1}(D \times [0,1] \times \mathbb{R}) \times \cdots \times \mathrm{Jet}^{r_k}(D \times [0,1] \times \mathbb{R}), \tag{7.3}$$

which has a codomain independent of J.

The matched moduli space in (7.1) is then locally given as the preimage under $\mathrm{ev}^{\mathrm{Jet}}_D$ of a submanifold

$$Z(M) \subseteq \mathrm{Jet}^{r_1}(D \times [0,1] \times \mathbb{R}) \times \cdots \times \mathrm{Jet}^{r_k}(D \times [0,1] \times \mathbb{R}),$$

This is a free offprint provided to the author by the publisher. Copyright restrictions may apply.

where $r_i = \max\{n_i, m_i\}$. We leave it to the reader to write down an explicit formula for $Z(M)$ in terms of M, however we note that it has codimension

$$2k + \operatorname{codim}(M_0) + 2|\mathbf{t}|.$$

DEFINITION 7.5. We say that J is *regular* for M if at every $(u, j) \in \mathcal{M}_J(S^{\mathbf{q}}, \phi, M)$ there is a Teichmüller slice $\mathcal{T}$ through j, such that the map $\overline{\partial}_J$ is transverse to the zero section of the bundle $\mathcal{E} \to \mathcal{T} \times \mathcal{B}$, and the map $\mathrm{ev}_D^{\mathrm{Jet}}$ is transverse to $Z(M)$.

The above regularity condition is independent of the Teichmüller slice $\mathcal{T}$; see [**Wen10b**, Lemma 4.3.2]. Finally, an essentially standard argument shows that there is a dense (Baire) subset of almost complex structures satisfying (J-1)–(J-5) which are regular. The argument can be obtained by combining [**Lip06**, Proposition 4.3] together with one of [**Wen23**, Lemma A.3], [**CM07**, Lemma 6.6] or [**ZZ15**].

Taking the preimage of $Z(M)$ under $\mathrm{ev}_D^{\mathrm{Jet}}$ gives part (1) of Proposition 7.3. Part (2) of Proposition 7.3 follows from part (1), together with the formula

$$\operatorname{ind}(u) = \mu(\phi) - 2\operatorname{Sing}(u). \tag{7.4}$$

Equation (7.4) follows from [**Lip14**, Proposition 4.2']. See also [**LOT18**, Proposition 5.69].

7.5. Cylindrical boundary degenerations

In this section, we recall some notions about cylindrical boundary degenerations. The material is mostly based on [**OS08a**, Section 5] and [**OS04**, Section 5.6], though Proposition 7.9 is new.

DEFINITION 7.6. A *cylindrical beta boundary degeneration* is a smooth map

$$u\colon (S, \partial S) \to (\Sigma \times [0,\infty) \times \mathbb{R}, \boldsymbol{\beta} \times \{0\} \times \mathbb{R}),$$

satisfying the following:

- (N-1) u is (j, J)-holomorphic.
- (N-2) u is proper.
- (N-3) For each $t \in \mathbb{R}$ and $i \in \{1, \dots, n\}$, $u^{-1}(\beta_i \times \{t\})$ consists of a single point.
- (N-4) u has finite energy.
- (N-5) $\pi_{\mathbb{H}} \circ u$ is non-constant on each component of S, where $\pi_{\mathbb{H}}$ denotes the projection onto $[0,\infty) \times \mathbb{R}$.

We define cylindrical alpha boundary degenerations analogously.

If B is a relative 2-cycle on $(\Sigma, \boldsymbol{\beta})$, we write $\mathcal{N}_J(B)$ for the moduli space of cylindrical beta-boundary degenerations representing the homology class B. There is an evaluation map

$$\mathrm{ev}^\infty\colon \mathcal{N}_J(B) \to \mathbb{T}_\beta,$$

obtained by evaluating a boundary degeneration at its punctures. If $\mathbf{x} \in \mathbb{T}_\beta$, we write $\mathcal{N}_J(B, \mathbf{x})$ for $(\mathrm{ev}^\infty)^{-1}(\mathbf{x})$.

The space $\mathcal{N}_J(B, \mathbf{x})$ has an action of $\mathrm{Aut}(\mathbb{H})$, the group of conformal automorphisms of the half plane, which acts pointwise on the $[0,\infty) \times \mathbb{R}$ factor of a curve. We write $\widetilde{\mathcal{N}}_J(B, \mathbf{x})$ for the quotient

$$\widetilde{\mathcal{N}}_J(B, \mathbf{x}) := \mathcal{N}_J(B, \mathbf{x}) / \operatorname{Aut}(\mathbb{H}).$$

This is a free offprint provided to the author by the publisher. Copyright restrictions may apply.

7.6. Boundary degenerations and split almost complex structures

Ozsváth and Szabó prove the following:

THEOREM 7.7 ([**OS08a**, Theorem 5.5]). *Suppose that* $(\Sigma, \boldsymbol{\alpha}, \boldsymbol{\beta}, \mathbf{w})$ *is a Heegaard diagram, and* J *is a generic, split almost complex structure on* $\Sigma \times [0,\infty) \times \mathbb{R}$. *If* B *is a Maslov index 2 class of beta boundary degenerations and* $\mathbf{x} \in \mathbb{T}_\beta$, *then*

$$\#\widetilde{\mathcal{N}}_J(B,\mathbf{x}) \equiv \begin{cases} 1 & \text{if} \quad |\mathbf{w}| > 1 \\ 0 & \text{if} \quad |\mathbf{w}| = 1. \end{cases}$$

Ozsváth and Szabó's proof when $|\mathbf{w}| = 1$ is based on the corresponding result for the symmetric product [**OS04b**, Theorem 3.15], via the *tautological correspondence*. This turns out to not be the most natural setting for our purposes, since it does not rule out curves appearing in codimension 1 degenerations which satisfy only (N-1)–(N-4), but not (N-5). For example, we may always form a holomorphic curve as the union of $\Sigma \times \{pt\}$ together with a constant curve at $\mathbf{x} \in \mathbb{T}_\beta$. The $\overline{\partial}$ operator does not achieve transversality for such curves, as can easily be seen since they violate expected dimension counts; compare Proposition 7.3.

In Sections 7.7 and 7.8, we adapt Lipshitz's proof of stabilization invariance [**Lip06**, Section 12] and consider more general families of almost complex structure where, generically, transversality is achieved for all curves appearing in codimension 1 degenerations. Note that when we do this, we get a different count for the case $|\mathbf{w}| = 1$; see Proposition 7.9.

7.7. Boundary degenerations and generic almost complex structures

In this section, we define the almost complex structures we consider for boundary degenerations. Suppose that $p_1, \dots, p_n$ is a (possibly empty) collection of distinct points in $\Sigma \backslash \boldsymbol{\beta}$, and $D_1, \dots, D_n$ is a collection of small disks in $\Sigma \backslash \boldsymbol{\beta}$, containing $p_1, \dots, p_n$, respectively.

DEFINITION 7.8. We say an almost complex structure J on $\Sigma \times [0,\infty) \times \mathbb{R}$ is *admissible* if it satisfies the following:

- (J'-1) J is tamed by ω.
- (J'-2) J is split on $(D_1 \cup \cdots \cup D_n) \times [0,\infty) \times \mathbb{R}$.
- (J'-3) J is invariant under the action of $\mathrm{Aut}(\mathbb{H})$.
- (J'-4) $J\partial/\partial s = \partial/\partial t$.
- (J'-5) $T_p\Sigma \times \{0\}$ is a complex line in a neighborhood of $\boldsymbol{\beta} \times [0,\infty) \times \mathbb{R}$, and along $\Sigma \times \{0\} \times \mathbb{R}$.

If J is an almost complex structure on $\Sigma \times [0,1] \times \mathbb{R}$, satisfying ($J$-1)–($J$-5), then there is a naturally associated almost complex structure J' on $\Sigma \times [0,\infty) \times \mathbb{R}$, as we now describe. Fix $y_0 \in \{0\} \times \mathbb{R}$. If $r > 0$, write

$$R_{r,y_0} \colon \Sigma \times [0,1] \times \mathbb{R} \hookrightarrow \Sigma \times [0,\infty) \times \mathbb{R}$$

for the embedding $R_{r,y_0}(x,z) = (x, r \cdot (z - y_0))$. We define

$$J' = \lim_{r \to \infty} dR_{r,y_0} \circ J \circ d(R_{r,y_0})^{-1}. \tag{7.5}$$

Note that J' is independent of y_0.

This is a free offprint provided to the author by the publisher. Copyright restrictions may apply.

There is a more concrete description of J' (which in particular makes it clear that the limit exists). With respect to the isomorphism

$$T_{(p,y)}(\Sigma \times [0,1] \times \mathbb{R}) \cong T_p\Sigma \oplus T_y([0,1] \times \mathbb{R}),$$

we may decompose

$$J_{(p,y)} = \begin{pmatrix} (j_\Sigma)_{(p,y)} & 0 \\ Y_{(p,y)} & j_{\mathbb{D}} \end{pmatrix},$$

where the following hold:

- $(j_\Sigma)_{(p,y)}$ is an almost complex structure on $T_p\Sigma$,
- $j_{\mathbb{D}}$ is the standard almost complex structure on $[0,1] \times \mathbb{R}$,
- $Y_{(p,y)} \colon T_p\Sigma \to T_y([0,1] \times \mathbb{R})$ is complex anti-linear.

Equation (7.5) has the more concrete description

$$J'_{(p,y)} = \begin{pmatrix} (j_\Sigma)_{(p,y_0)} & 0 \\ (\partial_y Y)_{(p,y_0)} & j_{\mathbb{H}} \end{pmatrix}, \tag{7.6}$$

where $\partial_y Y$ denotes the directional derivative, in the direction y.

Finally, we note that if a boundary degeneration $u \colon S \to \Sigma \times [0,\infty) \times \mathbb{R}$ appears in the limit of J-holomorphic curves on $\Sigma \times [0,1] \times \mathbb{R}$, then u will be J'-holomorphic. This holds because a boundary degeneration which appears in the limit of a sequence of curves in $\Sigma \times [0,1] \times \mathbb{R}$ is obtained by rescaling the $[0,1] \times \mathbb{R}$ component. Hence, the description in (7.5) makes it clear that the limiting curve will be J'-holomorphic.

7.8. Boundary degenerations for generic almost complex structures

In this section, we count index 2 boundary degenerations, for almost complex structures on $\Sigma \times [0,\infty) \times \mathbb{R}$ which satisfy (J'-1)–(J'-5); compare Theorem 7.7.

A key observation is that for a generic almost complex structure on $\Sigma \times [0,\infty) \times \mathbb{R}$, satisfying ($J'$-1)–($J'$-5), the $\overline{\partial}$ operator achieves transversality at holomorphic maps satisfying (N-1)–(N-4), which have no multiply covered, closed components. The proof may be easily adapted from Lipshitz's proof of the analogous statement for holomorphic disks [**Lip06**, Proposition 3.7].

We now state our main count:

PROPOSITION 7.9. *Suppose $\boldsymbol{\beta} \subseteq \Sigma$ is a collection of attaching curves on Σ, B is a Maslov index 2 class of beta boundary degenerations, and $\mathbf{x} \in \mathbb{T}_\beta$. Then for generic J satisfying (J'-1)–(J'-5),*

$$\#\widetilde{\mathcal{N}}_J(B,\mathbf{x}) \equiv 1 \pmod 2, \tag{7.7}$$

(regardless of whether $|\mathbf{w}| = 1$ or $|\mathbf{w}| > 1$).

PROOF. First, we argue that the mod 2 count of $\widetilde{\mathcal{N}}_J(B,\mathbf{x})$ is independent of the choice of generic J. Indeed if J_0 and J_1 are two generic almost complex structures, then one picks a generic family, $(J_t)_{t\in[0,1]}$, connecting J_0 and J_1. We consider the parametrized moduli space

$$\widetilde{\mathcal{N}}_{J_t,t\in[0,1]}(B,\mathbf{x}) := \bigcup_{t\in[0,1]} \widetilde{\mathcal{N}}_{J_t}(B,\mathbf{x}) \times \{t\}.$$

We claim the ends of $\widetilde{N}_{J_t,t\in[0,1]}(B,\mathbf{x})$ are exactly the curves at $t=0$ and $t=1$. To see this, we consider the possible degenerations away from $t=0$ or $t=1$.

This is a free offprint provided to the author by the publisher. Copyright restrictions may apply.

The source may degenerate along a collection of closed circles and boundary-to-boundary arcs. If the source degenerates along a boundary-to-boundary arc, then (N-3) implies that the limit contains either an additional boundary degeneration, or a *ghost curve* component (i.e. a component which has image equal to a single point). The formation of an additional boundary degeneration is prohibited since every non-trivial boundary degeneration has Maslov index at least 2, so the formation of an additional boundary degeneration would force B to have Maslov index at least 4.

For the moment, consider the components remaining after we trim any ghost components. If there are additional degenerations of the source, then the remaining components of the source have nodal points in their interior. The existence of such curves are prohibited by the analog of Proposition 7.3 for boundary degenerations. In particular, the expected dimension over all t of the space of non-embedded curves representing B is at most 1. After quotienting by $\mathrm{Aut}(\mathbb{H})$, we obtain an expected dimension of -1, so a generic family J_t misses the almost complex structures which support such curves.

Finally, it remains to rule out ghost curves. These are ruled out by an easy adaptation of a standard Fredholm index argument, for which we refer the reader to [**LOT18**, Lemma 5.57] for more details.

Next, it remains to establish the stated count of boundary degenerations. We begin with the $g = 1$ case, when $(\Sigma, \boldsymbol{\beta}) = (\mathbb{T}^2, \beta)$. In this case, we take an embedded, homologically essential closed curve $c \subseteq \mathbb{T}^2 \setminus \beta$. We stretch the neck along c. If we cut $\mathbb{T}^2$ along c, and collapse the two boundary components, we are left with a 2-sphere, with two special points, p_1 and p_2. For large neck-length parameter, by gluing, we may identify $\widetilde{\mathcal{N}}_{J(T)}(B, \mathbf{x})$ with the space of *self-matched boundary degenerations* on (S^2, β), of Maslov index 4. A self-matched boundary degeneration is a boundary degeneration $u\colon S \to S^2 \times [0,\infty) \times \mathbb{R}$, with two marked points, $q_1, q_2 \in S$, satisfying

$$(\pi_\Sigma \circ u)(q_1) = p_1 \quad \text{and} \quad (\pi_\Sigma \circ u)(q_2) = p_2 \quad \text{and} \quad (\pi_{\mathbb{H}} \circ u)(q_1) = (\pi_{\mathbb{H}} \circ u)(q_2).$$

See Figure 7.1.

We deform the space of self-matched boundary degenerations and consider, for $t \in (0,\infty)$, the space of *t-self-matched* cylindrical boundary degenerations, which are Maslov index 4 boundary degenerations with two marked points, q_1 and q_2 on the source, which satisfy

$$(\pi_\Sigma \circ u)(q_1) = p_1 \quad \text{and} \quad (\pi_\Sigma \circ u)(q_2) = p_2 \quad \text{and} \quad (\pi_{\mathbb{H}} \circ u)(q_1) = t \cdot (\pi_{\mathbb{H}} \circ u)(q_2).$$

Here, if $z \in [0,\infty) \times \mathbb{R}$, then $t \cdot z \in [0,\infty) \times \mathbb{R}$ denotes the ordinary product, viewing $[0,\infty) \times \mathbb{R}$ as the right-half plane in $\mathbb{C}$. The ordinary self-matched moduli space coincides with the 1-matched moduli space. Write $\mathcal{N}^t(B, \mathbf{x})$ for the moduli space of t-self-matched boundary degenerations, which we view as a subspace of $\mathcal{N}(B_1 \cup B_2, \mathbf{x})$, where B_1 and B_2 denote the two components of $S^2 \setminus \beta$. Note that the action of $\mathrm{Aut}(\mathbb{H})$ preserves $\mathcal{N}^t(B, \mathbf{x})$ for each t.

Gluing identifies the moduli space $\widetilde{\mathcal{N}}^t(B, \mathbf{x})$ with the cartesian product

$$\widetilde{\mathcal{N}}(B_1, \mathbf{x}) \times \widetilde{\mathcal{N}}(B_2, \mathbf{x}),$$

when t is large, where B_1 and B_2 are the index 2 classes which cover p_1 and p_2, respectively. Hence, it remains to count $\widetilde{\mathcal{N}}(B_i, \mathbf{x})$ individually. These may be counted by arguing the same as [**OS08a**, Theorem 5.5]. Namely, we deform the almost complex structure so that it becomes a product, and then we are counting

This is a free offprint provided to the author by the publisher. Copyright restrictions may apply.

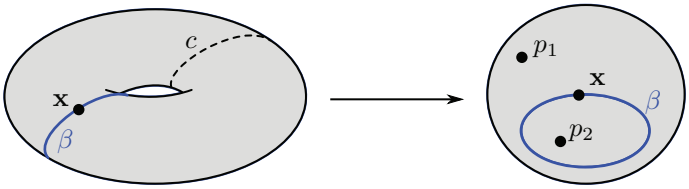


FIGURE 7.1. Stretching the neck along c identifies $\mathcal{N}(B, \mathbf{x})$ with the space of self-matched, Maslov index 4 boundary degenerations on (S^2, β).

holomorphic maps from $\mathbb{H}$ to $\mathbb{H} \times [0, \infty) \times \mathbb{R}$, which are the identity on $\mathbb{H}$, modulo the action of $\mathrm{Aut}(\mathbb{H})$. The count of such curves is clearly 1.

The case when $|\mathbf{w}| = 1$, but $g(\Sigma) > 1$ is proven repeatedly performing a neck-stretching argument, similar to the above one, to reduce to the $g = 1$ case (compare the proof of [**OS08a**, Theorem 5.5]). □

REMARK 7.10. Proposition 7.9 gives an alternative to the last step in Lipshitz's proof of stabilization invariance. In his proof, Lipshitz proves several gluing results [**Lip06**, Appendix A] which reduce the question of stabilization invariance to the claim that

$$\#\mathcal{M}(\phi, d) \equiv 1 \pmod 2,$$

where ϕ is the Maslov index 2 class on a standard genus 1 diagram for S^3, $d \in (0,1) \times \mathbb{R}$. This count may instead be performed by letting d approach a point in $d_0 \in \{1\} \times \mathbb{R}$, along some path γ. By considering the moduli space of curves which match any point along γ, one identifies $\mathcal{M}(\phi, d)$ with the count of beta-boundary degenerations, which is 1, according to our Proposition 7.9.

Another situation that is helpful to understand is that of *matched boundary degenerations* on pairs of diagrams. Suppose that $\mathcal{H}_1 = (\Sigma_1, \boldsymbol{\beta}_1)$ and $\mathcal{H}_2 = (\Sigma_2, \boldsymbol{\beta}_2)$ are two partial Heegaard diagrams, each with a special point $p_i \in \Sigma_i \setminus \boldsymbol{\beta}_i$. Suppose $\mathbf{x}_1 \in \mathbb{T}_{\beta_1}$ and $\mathbf{x}_2 \in \mathbb{T}_{\beta_2}$ are two points. There are unique, non-negative, index 2 classes, B_1 and B_2, which cover p_1 and p_2 once, respectively. For $t \in \mathbb{R}$, we consider the moduli space $\mathcal{NN}^t(B_1, B_2, \mathbf{x}_1, \mathbf{x}_2)$ which consists of pairs (u_1, u_2) of boundary degenerations, each with a marked point, q_1 and q_2, such that

$$\begin{gathered}(\pi_{\Sigma_1} \circ u_1)(q_1) = p_1, \quad (\pi_{\Sigma_2} \circ u_2)(q_2) = p_2, \quad (\pi_{\mathbb{H}} \circ u_1)(q_1) = (\pi_{\mathbb{H}} \circ u_2)(q_2), \\ \mathrm{ev}^\infty(u_1) = \mathbf{x}_1 \quad \text{and} \quad \mathrm{ev}^\infty(u_2) = \mathbf{x}_2.\end{gathered} \tag{7.8}$$

We write $\widetilde{\mathcal{NN}}^t(B_1, B_2, \mathbf{x}_1, \mathbf{x}_2)$ for the quotient by the action of $\mathrm{Aut}(\mathbb{H})$.

LEMMA 7.11. *Suppose $(\Sigma_1, \boldsymbol{\beta}_1)$ and $(\Sigma_2, \boldsymbol{\beta}_2)$ are two partial Heegaard diagrams, each with a special point $p_i \in \Sigma_i \setminus \boldsymbol{\beta}_i$, as above. If B_1 and B_2 are classes described above, and J is a generic almost complex structure on $(\Sigma_1 \sqcup \Sigma_2) \times [0, \infty) \times \mathbb{R}$ which satisfies (J'-1)–(J'-5), then*

$$\#\widetilde{\mathcal{NN}}_J(B_1, B_2, \mathbf{x}_1, \mathbf{x}_2) \equiv 1.$$

The same also holds for alpha boundary degenerations.

This is a free offprint provided to the author by the publisher. Copyright restrictions may apply.

PROOF. The argument follows from the same line of reasoning as Proposition 7.9. For $t \in [1,\infty)$, we consider the moduli space of t-matched boundary degenerations $\mathcal{NN}^t(B_1, B_2, \mathbf{x}_1, \mathbf{x}_2)$, which are defined as in (7.8), except we require

$$(\pi_{\mathbb{H}} \circ u_1)(q_1) = t \cdot (\pi_{\mathbb{H}} \circ u_2)(q_2),$$

where $t\cdot$ denotes the standard action of $\mathbb{R}^{>0}$ on $\mathbb{H}$. We may view $\mathcal{NN}^t(B_1, B_2, \mathbf{x}_1, \mathbf{x}_2)$ as being a subspace of the four dimensional moduli space $\mathcal{N}(B_1, B_2, \mathbf{x}_1, \mathbf{x}_2)$. We note that the action of $\mathrm{Aut}(\mathbb{H})$ preserves the subspace $\mathcal{NN}^t(B_1, B_2, \mathbf{x}_1, \mathbf{x}_2)$, for all t, so we may consider the quotient $\widetilde{\mathcal{NN}}^t(B_1, B_2, \mathbf{x}_1, \mathbf{x}_2)$. Next, we consider the parametrized moduli space

$$\widetilde{\mathcal{N}} = \bigcup_{t\in[1,\infty)} \widetilde{\mathcal{NN}}^t(B_1, B_2, \mathbf{x}_1, \mathbf{x}_2) \times \{t\}.$$

One end of $\widetilde{\mathcal{N}}$ may be identified with $\widetilde{\mathcal{NN}}(B_1, B_2, \mathbf{x}_1, \mathbf{x}_2)$, while the other may be identified with $\widetilde{\mathcal{N}}(B_1, \mathbf{x}_1) \times \widetilde{\mathcal{N}}(B_2, \mathbf{x}_2)$. Additional ends are ruled out as in Proposition 7.9, completing the proof. □

7.9. Holomorphic polygons and related constructions

In this section, we describe the holomorphic polygon counting maps, and their friends, in the cylindrical setting. We write D_n for a disk with n boundary punctures, which we view as an n-gon with cylindrical ends.

DEFINITION 7.12. Suppose that $\mathcal{A} = \{a_1, \dots, a_k\}$ is a collection of compact, properly embedded embedded arcs in D_n. We say that $\mathcal{A}$ is a collection of *decomposing arcs* if no a_i has its endpoints on the same component of ∂D_n. Let $2^{\mathcal{A}}$ denote the power set of $\mathcal{A}$. Suppose X is a smooth, compact manifold with corners. We say $f\colon X \to 2^{\mathcal{A}}$ is a *stratified decomposing map* if it satisfies the following:

- (s-1) f is constant on the interior of each component of the codimension l strata of X, for all l.
- (s-2) $f(x) \equiv \emptyset$ on the codimension 0 strata.
- (s-3) If h is a component of the codimension l strata of X, $x \in h$ and $y \in \partial h$, then $f(x) \subseteq f(y)$.
- (s-4) If $f(x) = \{a_{i_1}, \dots, a_{i_l}\}$, then $a_{i_1}, \dots, a_{i_l}$ are pairwise disjoint.

If $\mathcal{A} = \{a_1, \dots, a_k\}$ is a collection of decomposing arcs in D_n, we pick regular neighborhoods $N(a_1), \dots, N(a_k)$, equipped with identifications $N(a_i) \cong a_i \times [-1,1]$. Further, we assume that if a_i and a_j are disjoint, then $N(a_i)$ and $N(a_j)$ are as well. Additionally, pick a smooth function $\rho\colon [-1,1] \to [0,1]$ such that

1. $\rho(x) = 0$ for x in a neighborhood of -1 and 1.
2. $\rho(0) = 1$, and $\rho(x) < 1$ for $x \neq 0$.

We encourage the reader to compare the following to [**LOT16**, Definition 3.5]:

DEFINITION 7.13. Suppose $\mathcal{A}$ is a set of decomposing arcs for D_n, as above, X is a smooth manifold with corners, and $f\colon X \to 2^{\mathcal{A}}$ is a stratified decomposing map. We say $(J_x)_{x\in X}$ is a *stratified family of almost complex structures* on $\Sigma \times D_n$ if the following hold:

- (J''-1) For each $x \in X$, J_x is an almost complex structure on $\Sigma \times (D_n \setminus f(x))$, which is tamed by the split symplectic form on $\Sigma \times (D_n \setminus f(x))$.

This is a free offprint provided to the author by the publisher. Copyright restrictions may apply.

(J''-2) If h is a component of the codimension l strata of X, and D_m is a component of $D_n \setminus f(x)$, then J_x is constant on the cylindrical ends of D_m, for all $x \in h$. Furthermore, the induced cylindrical almost complex structure on $\Sigma \times [0,1] \times \mathbb{R}$ satisfies (J-1)–(J-5).

(J''-3) J_x preserves TD_n for all $x \in X$. In particular, there is an induced family $(j_{D_n,(x,p)})_{(x,p)\in X\times\Sigma}$ of almost complex structures on D_n. We assume the family $j_{D_n,(x,p)}$ is constant in p.

(J''-4) $T_p\Sigma \oplus \{0\}$ are complex lines on a neighborhood of $(\boldsymbol{\alpha} \cup \boldsymbol{\beta}) \times D_n$, and along $\Sigma \times \partial D_n$.

(J''-5) Roughly, if $x \in X$ and $f(x) = \{a_{i_1}, \dots, a_{i_k}\}$, then for y near x, J_y is obtained by inserting long necks along $a_{i_1}, \dots, a_{i_k}$, consistently with the stratified map f. Precisely, there is a neighborhood $U \subseteq X$ of x and a collection of smooth functions $\tau_1, \dots, \tau_k \colon U \to [0,1]$, satisfying the following:

(a) For all $y \in U$, $\tau_j(y) = 1$ if and only if $a_{i_j} \in f(y)$.

(b) On each $N(a_{i_j})$,

$$J_y \frac{\partial}{\partial s} = (1 - \tau_j(y) \cdot \rho(t)) \frac{\partial}{\partial t},$$

where (s,t) denote the coordinates on $N(a_{i_j}) \cong a_{i_j} \times [-1,1]$.

(c) For each $y \in U$, J_y is invariant on $\Sigma \times N(a_{i_j})$ under the flow of

$$V_y = (1 - \tau_j(y) \cdot \rho(t)) \frac{\partial}{\partial t},$$

and $(J_y)|_{\Sigma\times a_i\times\{-1,1\}}$ is constant for $y \in U$.

(d) If $x_n \to x$, then J_{x_n} approaches J_x on $\Sigma \times D_n \setminus (N(a_{i_1}) \cup \cdots \cup N(a_{i_k}))$ in the C^∞ topology.

The main example is when X is an associahedron. The example that $X = K_4$ is shown in Figure 7.2. Note that the associahedron is not the only example we need; see for example Figure 13.1.

Definition 7.14. We say that a stratified family of almost complex structures $(J_x)_{x\in X}$ on $\Sigma \times D_n$ is *split* if $J_x = j_\Sigma \times j_{D_n,x}$, for a fixed almost complex structure j_Σ on Σ, and a family $(j_{D_n,x})_{x\in X}$ on D_n.

If $J = (J_x)_{x\in X}$ is a stratified family of almost complex structures on $\Sigma \times D_n$, and S is a source curve for n-gons, we define the moduli space $\mathcal{M}_J(S,\phi)$ to be the set of tuples (x,u,j), where x lies in the codimension 0 strata, $j \in \mathcal{J}(S)$ and $u \colon S \to \Sigma \times D_n$ is (j,J_x)-holomorphic and satisfies the analogs of (M-2)–(M-7).

If $\mathcal{D} = (\Sigma, \boldsymbol{\gamma}_1, \dots, \boldsymbol{\gamma}_n, w)$ is a Heegaard n-tuple, then (assuming $\mathcal{D}$ is weakly admissible), there is a cylindrical holomorphic polygon counting map, obtained by picking a stratified family $(J_x)_{x\in X}$, where X is the Deligne-Mumford compactification of the moduli space of n marked points on a disk (or equivalently, X is the associahedron K_{n-1}) and defining

$$F_{\boldsymbol{\gamma}_1,\dots,\boldsymbol{\gamma}_n;J} \colon \boldsymbol{CF}^-(\boldsymbol{\gamma}_1,\boldsymbol{\gamma}_2) \otimes \cdots \otimes \boldsymbol{CF}^-(\boldsymbol{\gamma}_{n-1},\boldsymbol{\gamma}_n) \to \boldsymbol{CF}^-(\boldsymbol{\gamma}_1,\boldsymbol{\gamma}_n),$$

to count curves of Maslov index $3-n$ mapping into $\Sigma\times D_n$ which are J_x-holomorphic for some $x \in \operatorname{int}(X)$. The motivating example is when X is an associahedron, however we also need some variations of this. See Figure 13.1.

This is a free offprint provided to the author by the publisher. Copyright restrictions may apply.

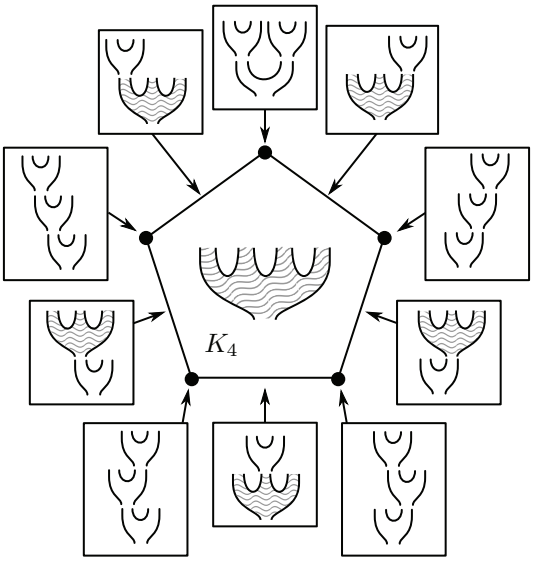


FIGURE 7.2. A stratified family of almost complex structures indexed by the assocediahedron K_4 (a pentagon). We have schematically illustrated how the almost complex structure degenerates on the codimension 1 and 2 strata. The wavy lines indicate where the almost complex structure is allowed to vary along the codimension 0 and 1 strata.

7.10. Compactifications via holomorphic combs

We now describe a compactification of the moduli spaces in Chapter 7 which provides a helpful framework for some of the arguments of this paper (and is used implicitly in Section 7.8). It is based on the compactness results of symplectic field theory [**EGH00**] [**BEH$^+$03**], as well as several related notions in the setting of bordered Floer homology (see especially [**LOT18**, Section 5.4] [**OS04**, Section 7.7]).

DEFINITION 7.15. Suppose that $(\Sigma, \boldsymbol{\alpha}, \boldsymbol{\beta}, w)$ is a Heegaard diagram of genus g.

(1) Let u be a holomorphic curve in $\Sigma \times [0,1] \times \mathbb{R}$ and $\mathbf{P}$ be a set of boundary punctures on the source of u. We say that $\mathbf{P}$ is an *extended fiber of u over $\partial\mathbb{D}$* if $\mathbf{P}$ consists of g punctures $p_1, \dots, p_g$, such that $\lim_{z\to p_i} u(z)$ exists and is in $\Sigma \times \{0,1\} \times \mathbb{R}$ for all i, and the projection to $[0,1] \times \mathbb{R}$ is independent of i. Furthermore, we assume that no two distinct p_i have limit in the same $\boldsymbol{\alpha}$ or $\boldsymbol{\beta}$ curve. We also allow the case that $\lim_{z\to p_i}(\pi_{\mathbb{D}} \circ u)(z) = \pm\infty$.

For a holomorphic curve mapping into $\Sigma \times \mathbb{H}$, we say a set of g boundary punctures is an *extended fiber over $\partial\mathbb{H}$* if the analogous conditions hold, though we also allow the case that $\lim_{z\to p_i}(\pi_{\mathbb{H}} \circ u(z)) = \infty$.

(2) A *holomorphic story* is a collection of holomorphic curves

$$\{b_n, \dots, b_1, u, a_1, \dots, a_m\},$$

as follows:

This is a free offprint provided to the author by the publisher. Copyright restrictions may apply.

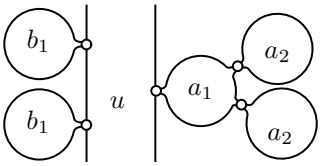


FIGURE 7.3. A holomorphic comb with one story.

(a) For each $i \in \{1, \dots, m\}$, a_i is a finite collection of alpha-boundary degenerations on $(\Sigma, \boldsymbol{\alpha})$, equipped with two sets of boundary punctures, $\mathbf{A}^+(a_i)$ and $\mathbf{A}^-(a_i)$.
(b) For each $i \in \{1, \dots, n\}$, b_i is a finite collection of beta-boundary degenerations on $(\Sigma, \boldsymbol{\beta})$, equipped with two sets of boundary punctures $\mathbf{B}^+(b_i)$ and $\mathbf{B}^-(b_i)$.
(c) u is a holomorphic curve in $\Sigma \times [0,1] \times \mathbb{R}$. The source of u has two g-tuples of boundary punctures labeled $+\infty$ and $-\infty$, which are asymptotic to intersection points $\mathbf{x} \times \{-\infty\}$ and $\mathbf{y} \times \{+\infty\}$ in $(\mathbb{T}_\alpha \cap \mathbb{T}_\beta) \times \overline{\mathbb{D}}$. The source of u also has two sets of boundary punctures, $\mathbf{A}^-(u)$ and $\mathbf{B}^-(u)$. After completing over $\mathbf{A}^-(u)$ and $\mathbf{B}^-(u)$, the curve u satisfies (M-1)–(M-6).

Additionally:

(a) The set $\mathbf{A}^-(u)$ is partitioned into extended $\partial\mathbb{D}$ fibers, which all project to $\{1\} \times \mathbb{R}$, and have distinct projection thereto. The set $\mathbf{B}^-(u)$ are similarly partitioned into extended $\partial\mathbb{D}$ fibers which map to $\{0\} \times \mathbb{R}$, and have distinct projection.
(b) For each a_i, the punctures $\mathbf{A}^+(a_i)$ are partitioned into extended $\partial\mathbb{H}$ fibers (one for each boundary degeneration of a_i), and the projection $\pi_{\mathbb{H}} \circ a_i$ is asymptotic to ∞ at each puncture. The same holds for the punctures $\mathbf{B}^+(b_i)$ on b_i.
(c) The punctures $\mathbf{A}^-(a_i)$ are partitioned into extended $\partial\mathbb{H}$ fibers. Furthermore, any two extended $\partial\mathbb{H}$ fibers on the same boundary degeneration have distinct projection to $\partial\mathbb{H}$. The analogous statement holds for each $\mathbf{B}^-(b_i)$.
(d) There is a chosen bijection between $\mathbf{A}^-(u)$ and $\mathbf{A}^+(a_1)$, which is compatible with the two partitions into extended fibers. Furthermore, each pair of extended fibers which are matched, have equal evaluation in $\mathbb{T}_\alpha$. A similar identification and matching condition holds between $\mathbf{A}^-(a_{i+1})$ and $\mathbf{A}^+(a_i)$. There are analogous identifications and matching conditions between $\mathbf{B}^-(u)$ and $\mathbf{B}^+(b_1)$, and also between $\mathbf{B}^-(b_i)$ and $\mathbf{B}^+(b_{i+1})$.

(3) A *holomorphic comb* is a sequence of holomorphic stories $\mathcal{U}_1, \dots, \mathcal{U}_n$, such that the intersection point at $+\infty$ of $\mathcal{U}_i$ coincides with the intersection point at $-\infty$ of $\mathcal{U}_{i+1}$.

REMARK 7.16.

(1) Definition 7.15 admits a natural extension for holomorphic polygons mapping into $\Sigma \times D_n$. The only complication is that one also has to keep track

This is a free offprint provided to the author by the publisher. Copyright restrictions may apply.

of degenerations of D_n, via a stratified family of almost complex structures on $\Sigma \times D_n$.

(2) Definition 7.15 admits a natural extension to holomorphic combs with marked points.

(3) The set of holomorphic combs (with or without marked points) possesses a natural topology, similar to the one described in [**BEH$^+$03**]. See also [**LOT18**, Definition 5.21].

This is a free offprint provided to the author by the publisher. Copyright restrictions may apply.

CHAPTER 8

Degenerating connected sum tubes

A common tool in gauge theory is the neck-stretching argument. In our paper, it becomes helpful to allow the neck-length parameter to go to ∞, and work with moduli spaces which are defined as a fibered product over an evaluation map. In this chapter, we describe some of these techniques.

8.1. Connected sums and matched moduli spaces

Suppose $\mathcal{H}_1 = (\Sigma_1, \boldsymbol{\alpha}_1, \boldsymbol{\beta}_1, w_1)$ and $\mathcal{H}_2 = (\Sigma_2, \boldsymbol{\alpha}_2, \boldsymbol{\beta}_2, w_2)$ are two Heegaard diagrams, and suppose that J_1 and J_2 are almost complex structures on $\Sigma_1 \times [0,1] \times \mathbb{R}$ and $\Sigma_2 \times [0,1] \times \mathbb{R}$, which are split in a neighborhood of two chosen points $p_1 \in \Sigma_1$ and $p_2 \in \Sigma_2$. In this section, we focus on the case that p_1 and p_2 are immediately adjacent to w_1 and w_2.

Suppose $\phi_1 \in \pi_2(\mathbf{x}_1, \mathbf{y}_1)$ and $\phi_2 \in \pi_2(\mathbf{x}_2, \mathbf{y}_2)$ are homotopy classes of disks on $\mathcal{H}_1$ and $\mathcal{H}_2$, satisfying

$$n_{p_1}(\phi_1) = n_{p_2}(\phi_2).$$

Let us write k for the common value. Suppose $S_1^{\mathbf{q}_1}$ and $S_2^{\mathbf{q}_2}$ are Riemann surfaces, each decorated with an ordered k-tuple of marked points. We define the *matched moduli space of disks*, representing ϕ_1 and ϕ_2, to be

(8.1)

$$\mathcal{MM}_{J_1 \wedge J_2}(S_1^{\mathbf{q}_1}, S_2^{\mathbf{q}_2}, \phi_1, \phi_2)$$
$$:= \left\{ (u_1, u_2) \in \mathcal{M}_{J_1}(S_1^{\mathbf{q}_1}, \phi_1) \times \mathcal{M}_{J_2}(S_2^{\mathbf{q}_2}, \phi_2) \;\middle|\; \begin{array}{c} (\pi_\Sigma \circ u_1)(q_{1,i}) = p_1, \\ (\pi_\Sigma \circ u_2)(q_{2,i}) = p_2, \\ (\pi_{\mathbb{D}} \circ u_1)(q_{1,i}) = (\pi_{\mathbb{D}} \circ u_2)(q_{2,i}), \\ \text{for } i = 1, \dots, k \end{array} \right\}.$$

The construction in (8.1) is a special case of the construction from Section 7.3, for a matching condition $M_\#$ at the points p_1 and p_2. In this case, the associated submanifold M_0 is the diagonal

$$\Delta_{([0,1]\times\mathbb{R})^k} \subseteq ([0,1] \times \mathbb{R})^{2k}.$$

The tuple of tangencies $\mathbf{t}$ is $\{0\} \times \cdots \times \{0\}$. We note that $M_\#$ has a dependence on k, though it is convenient to suppress this from the notation.

By Proposition 7.3, for generic J_1 and J_2, the space $\mathcal{MM}_{J_1 \wedge J_2}(S_1^{\mathbf{q}_1}, S_2^{\mathbf{q}_2}, \phi_1, \phi_2)$ is a smooth manifold of dimension

$$\operatorname{ind}_{\text{emb}}(\phi_1, \phi_2, M_\#) = \mu(\phi_1) + \mu(\phi_2) - 2n_{p_i}(\phi_i),$$

near a pair (u_1, u_2) of embedded curves.

When no confusion may arise, we write $\mathcal{MM}_{J_1 \wedge J_2}(\phi_1, \phi_2)$ for the disjoint union of the matched moduli spaces over all equivalence classes of pairs of marked sources $S_1^{\mathbf{q}_1}$ and $S_2^{\mathbf{q}_2}$, where $|\mathbf{q}_1| = |\mathbf{q}_2| = n_{p_i}(\phi_i)$.

This is a free offprint provided to the author by the publisher. Copyright restrictions may apply.

8.2. Matched chain complexes for connected sums

Suppose that $\mathcal{H}_1$ and $\mathcal{H}_2$ are two singly pointed Heegaard diagrams. The matched moduli spaces $\mathcal{MM}_{J_1\wedge J_2}(\phi_1,\phi_2)$ from Section 8.1 may be used to construct a chain complex $CF^-_{J_1\wedge J_2}(\mathcal{H}_1,\mathcal{H}_2)$, as we now describe.

As a module, $CF^-_{J_1\wedge J_2}(\mathcal{H}_1,\mathcal{H}_2)$ is generated over $\mathbb{F}[U]$ by pairs $\mathbf{x}_1\times\mathbf{x}_2$, where $\mathbf{x}_i$ is a generator on $\mathcal{H}_i$. We define

$$\partial_{J_1\wedge J_2}(\mathbf{x}_1\times\mathbf{x}_2) := \sum_{\substack{\phi_1\in\pi_2(\mathbf{x}_1,\mathbf{y}_1)\\ \phi_2\in\pi_2(\mathbf{x}_2,\mathbf{y}_2)\\ n_{p_1}(\phi_1)=n_{p_2}(\phi_2)\\ \mathrm{ind}_{\mathrm{emb}}(\phi_1,\phi_2,M_\#)=1}} \#(\mathcal{MM}_{J_1\wedge J_2}(\phi_1,\phi_2)/\mathbb{R})\cdot U^{n_w(\phi_1,\phi_2)}\cdot\mathbf{y}_1\times\mathbf{y}_2,$$

where $n_w(\phi_1,\phi_2)$ denotes the multiplicity in the connected sum region.

LEMMA 8.1. *The endomorphism $\partial_{J_1\wedge J_2}$ of $CF^-_{J_1\wedge J_2}(\mathcal{H}_1,\mathcal{H}_2)$ squares to zero.*

PROOF. The argument follows from the usual strategy of proving that $\partial^2=0$ in Floer homology. One considers the ends of the 1-dimensional moduli spaces $\mathcal{MM}_{J_1\wedge J_2}(\phi_1,\phi_2)/\mathbb{R}$, ranging over pairs (ϕ_1,ϕ_2) where $\mathrm{ind}_{\mathrm{emb}}(\phi_1,\phi_2,M_\#)=2$.

Using Proposition 7.3, it is straightforward to adapt [**Lip06**, Lemma 8.2] to show that the ends of the spaces of matched, index 2 flowlines consist exactly of the following broken curves:

(1) 2-level, broken holomorphic disks, where each level satisfies (M-1)–(M-7) and has matched index 1.
(2) Maslov index 4, matched alpha or beta boundary degenerations, together with a constant flowline.

The count of the first type of broken curve gives $\partial^2_{J_1\wedge J_2}(\mathbf{x}_1\times\mathbf{x}_2)$. Hence,

$$\partial^2_{J_1\wedge J_2}(\mathbf{x}_1\times\mathbf{x}_2) = U\cdot\left(\#\widetilde{\mathcal{N}}^\alpha(\mathbf{x}_1\times\mathbf{x}_2)+\#\widetilde{\mathcal{N}}^\beta(\mathbf{x}_1\times\mathbf{x}_2)\right)\cdot\mathbf{x}_1\times\mathbf{x}_2,$$

where $\widetilde{\mathcal{N}}^\alpha(\mathbf{x}_1\times\mathbf{x}_2)$ and $\widetilde{\mathcal{N}}^\beta(\mathbf{x}_1\times\mathbf{x}_2)$ denote the moduli spaces of Maslov index 4, matched alpha and beta degenerations at $\mathbf{x}_1\times\mathbf{x}_2$, modulo the action of $\mathrm{Aut}(\mathbb{H})$. By Lemma 7.11,

$$\#\widetilde{\mathcal{N}}^\alpha(\mathbf{x}_1\times\mathbf{x}_2)\equiv\#\widetilde{\mathcal{N}}^\beta(\mathbf{x}_1\times\mathbf{x}_2)\equiv 1.$$

Hence $\partial^2_{J_1\wedge J_2}=0$, concluding the proof. □

If J is a (non-singular) almost complex structure on $\Sigma_1\#\Sigma_2\times[0,1]\times\mathbb{R}$, satisfying ($J$-1)–($J$-5), we may define a transition map

$$\Psi_{J\to J_1\wedge J_2}\colon CF^-_J(\mathcal{H}_1\#\mathcal{H}_2)\to CF^-_{J_1\wedge J_2}(\mathcal{H}_1,\mathcal{H}_2),$$

by picking a non-cylindrical almost complex structure $\widetilde{J}$ on $\Sigma_1\#\Sigma_2\times[0,1]\times\mathbb{R}$, which for large $T\in\mathbb{R}$, coincides with an almost complex structure $J(T)$ along $\Sigma_1\#\Sigma_2\times[0,1]\times\{T\}$, which has a neck of length T. We define $\Psi_{J\to J_1\wedge J_2}$ to count index 0 $\widetilde{J}$-holomorphic curves in $\Sigma\times[0,1]\times\mathbb{R}$. A map

$$\Psi_{J_1\wedge J_2\to J}\colon CF^-_{J_1\wedge J_2}(\mathcal{H}_1,\mathcal{H}_2)\to CF^-_J(\mathcal{H}_1\#\mathcal{H}_2),$$

is defined similarly.

LEMMA 8.2. *The maps $\Psi_{J\to J_1\wedge J_2}$ and $\Psi_{J_1\wedge J_2\to J}$ are chain maps, and furthermore, are homotopy inverses.*

This is a free offprint provided to the author by the publisher. Copyright restrictions may apply.

PROOF. Suppose $\widetilde{J}$ is an almost complex structure, as above. To see that $\Psi_{J\to J_1\wedge J_2}$ is a chain map, we consider the ends of index 1 families of $\widetilde{J}$-holomorphic matched curves. Using Proposition 7.3, it is straightforward to see that the ends of $\widetilde{J}$-holomorphic matched moduli spaces consist of the following configurations:

(1) An index 1 $J_1 \wedge J_2$-holomorphic matched curve (u_1, u_2), and an index 0 $\widetilde{J}$-holomorphic curve.
(2) An index 0 $\widetilde{J}$-holomorphic curve, and an index 1 J-holomorphic curve.

This implies that $\Psi_{J\to J_1\wedge J_2}$ is a chain map.

Let $\widetilde{I}$ be an almost complex structure which can similarly be used to compute $\Psi_{J_1\wedge J_2\to J}$. A homotopy between $\Psi_{J_1\wedge J_2\to J}\circ\Psi_{J\to J_1\wedge J_2}$ and $\mathrm{id}_{CF^-_J(\mathcal{H}_1\#\mathcal{H}_2)}$ is constructed by picking a 1-parameter family of almost complex structures $(J_t)_{t\in(0,1)}$ on $\Sigma\times[0,1]\times\mathbb{R}$, such that as $t\to 0$, J_t approaches J, and as $t\to 1$, the family J_t approaches the two-level almost complex structure with $\widetilde{J}$ on one level, and $\widetilde{I}$ on the other. Counting the ends of the moduli spaces of index 0, J_t-holomorphic curves, ranging over $t\in(0,1)$, we obtain

$$\Psi_{J_1\wedge J_2\to J}\circ\Psi_{J\to J_1\wedge J_2}+\mathrm{id}=\partial\circ H+H\circ\partial,$$

where H counts index -1 curves which are J_t-holomorphic for some $t\in(0,1)$. A homotopy between $\mathrm{id}_{CF^-_{J_1\wedge J_2}(\mathcal{H}_1,\mathcal{H}_2)}$ and $\Psi_{J\to J_1\wedge J_2}\circ\Psi_{J_1\wedge J_2\to J}$ is constructed in an analogous fashion. □

REMARK 8.3. When $\mu(\phi_1\#\phi_2)=1$, one can identify $\mathcal{MM}_{J_1\wedge J_2}(\phi_1,\phi_2)$ with the ordinary moduli space $\mathcal{M}_{J(T)}(\phi_1\#\phi_2)$ for large T, where $J(T)$ is obtained by joining J_1 and J_2 with neck-length T. Hence we could avoid Lemma 8.1 by just using the normal proof that $CF^-_{J(T)}(\mathcal{H}_1\#\mathcal{H}_2)$ is a chain complex, where $J(T)$ is an almost complex structure with sufficiently long neck. This becomes impractical when working with higher polygon counts, since the polygon counting maps count infinitely many classes, and it is not clear we can pick a single value of T which works for all classes.

8.3. Maximally pinched families of almost complex structures

In Section 8.1, we described moduli spaces of disks for almost complex structures which were stretched along a simple closed curve in the Heegaard surface. The construction therein adapts easily to connected sums of Heegaard n-tuples, however the most straightforward generalization is slightly too restrictive for our purposes. In this section, we describe a more subtle generalization of the connected sum operation which we refer to as a stratified family of almost complex structures on $\Sigma\times D_n$ which is *maximally pinched* along a simple closed curve $S\subseteq\Sigma$. Roughly speaking, this means that if $f\colon X\to 2^{\mathcal{A}}$ is the stratifying map, then J_x has infinite neck length along S on any component of $D_n\setminus f(x)$ whose associated subdiagram of $\mathcal{D}$ has no attaching curves which intersect S. For Heegaard diagrams (with two attaching curves) this reduces to the infinite neck length construction found in Section 8.1, but for Heegaard n-tuples with $n\geq 3$, it is a more flexible generalization.

We begin with some notation. First, let j_0 denote the almost complex structure on $S^1\times[-1,1]$ given by $j_0(\partial/\partial\theta)=\partial/\partial t$. If $\delta\in[0,1)$, we write j_δ for an almost complex structure which is conformally equivalent to $(S^1\times[-1/(1-\delta),1/(1-\delta)],j_0)$. Furthermore, we assume that j_δ is chosen to coincide with j_0 in a neighborhood of $S^1\times\{-1,1\}$. We do not need a concrete formula for j_δ, however we assume that

This is a free offprint provided to the author by the publisher. Copyright restrictions may apply.

sending $\delta \to 1$ corresponds to the almost complex structure collapsing along the circle $S^1 \times \{0\}$.

Next, suppose that $S \subseteq \Sigma$ is a simple closed curve, and $(J_x)_{x\in X}$ is a stratified family of almost complex structures on $\Sigma \times D_n$, which is split on $N(S) \times U$, for some open set $U \subseteq D_n \times X$, where $N(S)$ denotes a regular neighborhood of S. In particular, over $N(S)\times U$, there is an induced almost complex structure j_Σ on $N(S)$, and we assume that $(N(S), j_\Sigma)$ is conformally identified with $(S^1 \times [-1, 1], j_0)$. If $\delta\colon D_n \times X \to [0, 1)$ is a smooth function with support in U, we define a family $(J_x(\delta))_{x\in X}$ by modifying J_x so that it coincides with $j_{\delta(x,y)} \times j_{D_n,x}$ on $N(S) \times U$, and coincides with J_x, outside of $N(S) \times U$.

Definition 8.4. Suppose that $\mathcal{D} = (\Sigma, \boldsymbol{\gamma}_1, \dots, \boldsymbol{\gamma}_n)$ is a Heegaard n-tuple, and S is a closed curve on Σ (possibly intersecting some of the $\boldsymbol{\gamma}_i$). Suppose that $\mathcal{A}$ is a set of decomposing arcs of D_n, X is a compact, smooth manifold with corners, and $f\colon X \to 2^{\mathcal{A}}$ is a stratified decomposing map, as in Definition 7.12. We say a family of (singular) almost complex structures $(J_x)_{x\in X}$ on $\Sigma \times D_n$ is a *stratified family which is maximally pinched along* S if it is constructed via the following procedure:

(Step-1) Pick a stratified family of almost complex structures $(J^0_x)_{x\in X}$ on $\Sigma\times D_n$, such that there is an open set $U \subseteq D_n \times X$, satisfying the following:
  (a) J_x coincides with $j_0 \times j_{D_n,x}$ on $N(S) \times U$.
  (b) Suppose $x \in X$ and $f(x) = \{a_{i_1}, \dots, a_{i_l}\}$. If D_l is a component of $D_n \setminus f(x)$ corresponding to a subdiagram of $\mathcal{D}$, all of whose attaching curves are disjoint from S, and whose boundary contains the arcs arcs $a_{j_1}, \dots, a_{j_s}$, then
  $$(D_l \cup N(a_{j_1}) \cup \cdots \cup N(a_{j_s})) \times \{x\} \subseteq U.$$
  (c) If $\boldsymbol{\gamma}_i$ and $\boldsymbol{\gamma}_{i+1}$ are cyclically consecutive attaching curves on $\mathcal{D}$ which are disjoint from S, then U contains $E_{\gamma_i,\gamma_{i+1}} \times X$, where $E_{\gamma_i,\gamma_{i+1}}$ denotes the cylindrical end of D_n corresponding to $\boldsymbol{\gamma}_i$ and $\boldsymbol{\gamma}_{i+1}$.

(Step-2) Pick a smooth $\delta\colon D_n \times X \to [0, 1]$ (the neck-length parameter) which is supported in U. We assume that $\delta(y, x) = 1$ if and only if $f(x) = \{a_{i_1}, \dots, a_{i_m}\}$ and y is in the closure of a component of $D_n \setminus f(x)$ which corresponds to a subdiagram of $\mathcal{D}$, all of whose attaching curves are disjoint from S. We further assume the following:
  (a) $\delta \to 1$ in the cylindrical ends $E_{\gamma_i,\gamma_{i+1}}$ of D_n, whenever $\boldsymbol{\gamma}_i$ and $\boldsymbol{\gamma}_{i+1}$ are disjoint from S.
  (b) δ is constant along the $[0, 1]$ component of $E_{\gamma_i,\gamma_{i+1}} \cong [0, 1]\times[0, \infty)$.
  (c) For each x, the function $\delta(-, x) : D_n \to [0, 1]$ is constant on $a_i \times \{t\} \subseteq N(a_i)$.

(Step-3) Set $(J_x)_{x\in X}$ to be $(J^0_x(\delta))_{x\in X}$.

If $S_1, \dots, S_k$ is a collection of pairwise disjoint, simple closed curves on Σ, we may similarly define a family $(J_x)_{x\in X}$ to be maximally pinched along $(S_1, \dots, S_k)$ if it constructed by performing the above procedure along each S_i.

This is a free offprint provided to the author by the publisher. Copyright restrictions may apply.

CHAPTER 9

Stabilizing Heegaard multi-diagrams

In this chapter, we describe several stabilization operations for Heegaard diagrams, triples and quadruples. In Chapter 10, we describe their interaction with the counts of holomorphic curves.

9.1. Stabilizing Heegaard diagrams

The most basic way to stabilize a Heegaard diagram is to take the connected sum with a standard genus 1 diagram for S^3. More generally, we may take the connected sum of a Heegaard diagram with a standard diagram for the lens space $L(m,1)$, shown in Figure 10.1. A third operation is related to 1-handles, and involves taking the connected sum at two points with a standard, genus 0, doubly pointed diagram of (S^3, p_1, p_2). See Figure 9.1. We call these *elementary stabilizations*, *elementary lens space stabilizations*, and *elementary 1-handle stabilizations*, respectively.

It is convenient to perform multiple stabilizations at once. We make the following definition:

DEFINITION 9.1. We say a Heegaard diagram $\mathcal{H}_0 = (\Sigma_0, \boldsymbol{\xi}, \boldsymbol{\zeta}, p_0)$ is a *multi-stabilizing diagram* if it is constructed by starting with the diagram (S^2, p_0) (with no attaching curves) and inductively attaching elementary stabilizations and 1-handle stabilizations.

One could also consider multi-stabilizing diagrams which have standard lens space summands, though we will not have a need for such diagrams.

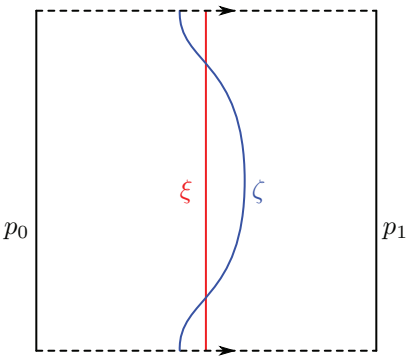


FIGURE 9.1. The standard diagram $(S^2, \xi, \zeta, p_1, p_2)$ for (S^3, p_1, p_2) used for a 1-handle stabilization. The Heegaard surface is obtained by identifying the top and bottom sides, and collapsing the left and right sides each to a point.

This is a free offprint provided to the author by the publisher. Copyright restrictions may apply.

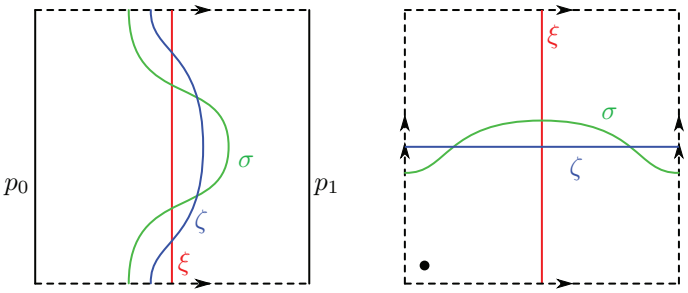


FIGURE 9.2. Left: An elementary 1-handle triple. Right: An elementary stabilization triple. We collapse the solid lines to basepoints, and identify the dashed sides.

9.2. Stabilizing Heegaard triples

We now consider stabilizations of Heegaard triples.

DEFINITION 9.2.

(1) We say a genus 0 triple $(S^2, \xi, \zeta, \sigma, p_0, p_1)$ is an *elementary 1-handle triple*, if ξ, ζ and σ are transverse, pairwise isotopic, and each pair of distinct curves in $\{\xi, \zeta, \sigma\}$ intersects in exactly 2 points.
(2) We say that a genus 1 triple $(\mathbb{T}^2, \xi, \zeta, \sigma, p_0)$ is an *elementary stabilization triple* if (up to cyclic permutation) ζ and σ are pairwise Hamiltonian isotopic, and $|\zeta \cap \sigma| = 2$, while $|\xi \cap \zeta| = |\xi \cap \sigma| = 1$. See Figure 9.2.

DEFINITION 9.3. We say a Heegaard triple $\mathcal{T}_0 = (\Sigma_0, \boldsymbol{\xi}, \boldsymbol{\zeta}, \boldsymbol{\sigma}, p_0)$ is a *multi-stabilizing triple* if it is constructed by starting with the diagram (S^2, p_0), and inductively attaching elementary stabilization triples and elementary 1-handle triples.

9.3. Stabilizing Heegaard quadruples

Finally, we consider stabilizations of quadruples.

DEFINITION 9.4.

(1) We say a genus 0 quadruple $(S^2, \xi, \zeta, \sigma, \tau, p_0, p_1)$ is an *elementary 1-handle quadruple* if ξ, ζ, σ and τ are transverse, pairwise isotopic, and each pair of distinct curves in $\{\xi, \zeta, \sigma, \tau\}$ intersects in exactly 2 points.
(2) We say a genus 1 quadruple $(\mathbb{T}^2, \xi, \zeta, \sigma, \tau, p_0)$ is an *elementary stabilization quadruple* if (up to cyclic permutation) one of the following holds:
   (a) ξ, ζ and σ are pairwise Hamiltonian isotopic, and

$$|\xi \cap \zeta| = |\xi \cap \sigma| = |\zeta \cap \sigma| = 2, \quad \text{while} \quad |\xi \cap \tau| = |\zeta \cap \tau| = |\sigma \cap \tau| = 1.$$

   (b) ξ and ζ are Hamiltonian isotopic, and σ and τ are Hamiltonian isotopic. Furthermore,

$$|\xi \cap \zeta| = |\sigma \cap \tau| = 2 \quad \text{and} \quad |\xi \cap \sigma| = |\zeta \cap \sigma| = |\xi \cap \tau| = |\zeta \cap \tau| = 1.$$

See Figure 9.3 for examples of elementary 1-handle and stabilization quadruples.

This is a free offprint provided to the author by the publisher. Copyright restrictions may apply.

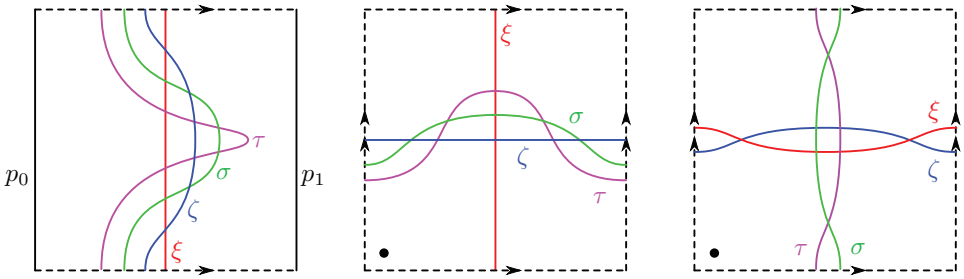


FIGURE 9.3. Left: An elementary 1-handle quadruple. Center and right: Elementary stabilization quadruples.

DEFINITION 9.5. We say that $\mathcal{Q}_0 = (\Sigma_0, \boldsymbol{\xi}, \boldsymbol{\zeta}, \boldsymbol{\sigma}, \boldsymbol{\tau}, p_0)$ is a *multi-stabilizing Heegaard quadruple* if it is constructed by starting with the diagram (S^2, p_0) and inductively attaching elementary 1-handle quadruples and simple 1-handle stabilization quadruples.

9.4. Index tuples

In this section, we define the *index tuple* of a multi-stabilizing triple or quadruple. The index tuple will allow us to efficiently state the holomorphic stabilization formulas in Section 10.

For a multi-stabilizing triple $\mathcal{T}_0$, the index tuple is a triple

$$\mathbf{m}(\mathcal{T}_0) = (m_1(\mathcal{T}_0), m_2(\mathcal{T}_0), m_3(\mathcal{T}_0)).$$

For a multi-stabilizing quadruple $\mathcal{Q}_0$, the index tuple is a 4-tuple

$$\mathbf{m}(\mathcal{Q}_0) = (m_1(\mathcal{Q}_0), m_2(\mathcal{Q}_0), m_3(\mathcal{Q}_0), m_4(\mathcal{Q}_0)).$$

If $\mathcal{T}_0 = (\Sigma_0, \boldsymbol{\xi}, \boldsymbol{\zeta}, \boldsymbol{\sigma}, p_0)$ is a multi-stabilizing triple, we set $m_1(\mathcal{T}_0)$ to be $\mu(\psi)$ for any triangle class $\psi \in \pi_2(\Theta^-_{\xi,\zeta}, \Theta^+_{\zeta,\sigma}, \Theta^+_{\sigma,\xi})$ with $n_{p_0}(\psi) = 0$. (Note that we are using an unusual ordering of the subscripts, and $\Theta^{\pm}_{\sigma,\xi} = \Theta^{\mp}_{\xi,\sigma}$). Similarly, we define $m_2(\mathcal{T}_0)$ to be the Maslov index of any triangle class $\psi \in \pi_2(\Theta^+_{\xi,\zeta}, \Theta^-_{\zeta,\sigma}, \Theta^+_{\sigma,\xi})$ with $n_{p_0}(\psi) = 0$, and $m_3(\mathcal{T}_0)$ is the Maslov index of any triangle class $\psi \in \pi_2(\Theta^+_{\xi,\zeta}, \Theta^+_{\zeta,\sigma}, \Theta^-_{\sigma,\xi})$.

We define the index 4-tuple of a multi-stabilizing quadruple $\mathcal{Q}_0 = (\Sigma_0, \boldsymbol{\xi}, \boldsymbol{\zeta}, \boldsymbol{\sigma}, \boldsymbol{\tau}, p_0)$ as follows. We define $m_1(\mathcal{Q}_0)$ to be the Maslov index of any rectangle class $\psi \in \pi_2(\Theta^-_{\xi,\zeta}, \Theta^+_{\zeta,\sigma}, \Theta^+_{\sigma,\tau}, \Theta^+_{\tau,\xi})$ with $n_{p_0}(\psi) = 0$. Similarly $m_2(\mathcal{Q}_0)$ is the Maslov index of any rectangle class $\psi \in \pi_2(\Theta^+_{\xi,\zeta}, \Theta^-_{\zeta,\sigma}, \Theta^+_{\sigma,\tau}, \Theta^+_{\tau,\xi})$ with $n_{p_0}(\psi) = 0$. The integers $m_3(\mathcal{Q}_0)$ and $m_4(\mathcal{Q}_0)$ are defined similarly.

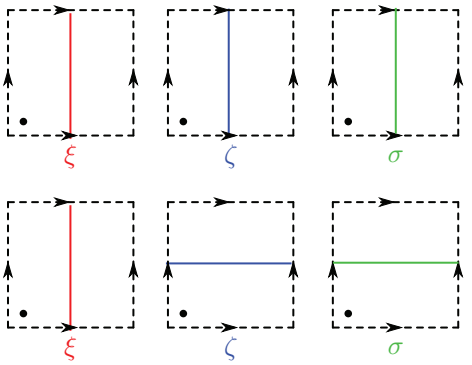
In the subsequent Lemma 9.6, we prove that the definition of index tuples given above is well defined. Before stating the lemma, we note that we use the grading convention that the top degree generator of $CF^-((S^1 \times S^2)^{\#k}, p_0)$ is supported in grading $k/2$.

LEMMA 9.6.

(1) *If $\mathcal{T}_0 = (\Sigma_0, \boldsymbol{\xi}, \boldsymbol{\zeta}, \boldsymbol{\sigma}, p_0)$ is a multi-stabilizing Heegaard triple, and $\psi \in \pi_2(\mathbf{x}, \mathbf{y}, \mathbf{z})$ is a homology class of triangles, then*

$$\mu(\psi) = 2n_{p_0}(\psi) + \mathrm{gr}(\mathbf{x}) + \mathrm{gr}(\mathbf{y}) - \mathrm{gr}(\mathbf{z}) - n/2,$$

This is a free offprint provided to the author by the publisher. Copyright restrictions may apply.



$\mathbf{m}(\mathcal{T}_0) = (0,0,0)$

$\mathbf{m}(\mathcal{T}_0) = (0,-1,0)$

FIGURE 9.4. Top: An elementary stabilization triple. Bottom: An elementary 1-handle triple. The index tuples are labeled.

where $\mathrm{gr}(\mathbf{z})$ *is the absolute grading of* $\mathbf{z}$*, as an element of* $\boldsymbol{CF}^-(\Sigma_0, \boldsymbol{\xi}, \boldsymbol{\sigma})$*, and* $n = |\boldsymbol{\xi}| = |\boldsymbol{\zeta}| = |\boldsymbol{\sigma}|$.

(2) *If* $\mathcal{Q}_0 = (\Sigma_0, \boldsymbol{\xi}, \boldsymbol{\zeta}, \boldsymbol{\sigma}, \boldsymbol{\tau}, p_0)$ *is a multi-stabilizing Heegaard quadruple, and* $\psi \in \pi_2(\mathbf{x}, \mathbf{y}, \mathbf{z}, \mathbf{w})$ *is a homology class of quadrilaterals, then*

$$\mu(\psi) = 2n_{p_0}(\psi) + \mathrm{gr}(\mathbf{x}) + \mathrm{gr}(\mathbf{y}) + \mathrm{gr}(\mathbf{z}) - \mathrm{gr}(\mathbf{w}) - n,$$

where $\mathrm{gr}(\mathbf{w})$ *denotes the Maslov grading of* $\mathbf{w}$ *as an element of* $\boldsymbol{CF}^-(\Sigma_0, \boldsymbol{\xi}, \boldsymbol{\tau})$*, and* $n = |\boldsymbol{\xi}| = |\boldsymbol{\zeta}| = |\boldsymbol{\sigma}| = |\boldsymbol{\tau}|$.

PROOF. Both claims are proven using the same strategy. First, one checks directly that they hold for elementary 1-handle and stabilization triples and quadruples. Next, one argues by induction that the formulas hold when we add an extra elementary 1-handle or stabilization triple or quadruple. We leave the details to the reader. □

LEMMA 9.7. *Suppose* $\mathcal{T}_0 = (\Sigma_0, \boldsymbol{\xi}, \boldsymbol{\zeta}, \boldsymbol{\sigma}, p_0)$ *is a multi-stabilizing triple which is built using elementary triples* $\mathcal{T}_1, \dots, \mathcal{T}_n$.

(1) $m_i(\mathcal{T}_0)$ *is non-positive, for* $i \in \{1,2,3\}$.
(2) $\mathbf{m}(\mathcal{T}_0) = \sum_{i=1}^n \mathbf{m}(\mathcal{T}_i)$.
(3) $m_i(\mathcal{T}_0) = 0$ *if and only if* $m_i(\mathcal{T}_j) = 0$ *for all* $j \in \{1, \dots, n\}$.

The analogous statements hold for multi-stabilizing quadruples.

PROOF. The same argument works for both triples and quadruples, so we focus on triples. Firstly, additivity of $\mathbf{m}(\mathcal{T}_0)$ is immediate from the construction, as the grading is additive under tensor products. For elementary tuples, the relation $m_i(\mathcal{T}_0) \leq 0$ is easily checked. It follows that $m_i(\mathcal{T}_0) \leq 0$ and $m_i(\mathcal{T}_0) = 0$ if and only if each $m_i(\mathcal{T}_j) = 0$ for all j. □

REMARK 9.8. Cyclic permutation of the attaching curves in a multi-stabilizing triple $\mathcal{T}_0$, has the effect on $\mathbf{m}(\mathcal{T}_0)$ of cyclic permuation. The same holds for multi-stabilizing quadruples.

The index tuples of elementary stabilization and 1-handle triples and quadruples are shown in Figures 9.4 and 9.5.

We now state an associativity relation for the index tuples:

This is a free offprint provided to the author by the publisher. Copyright restrictions may apply.

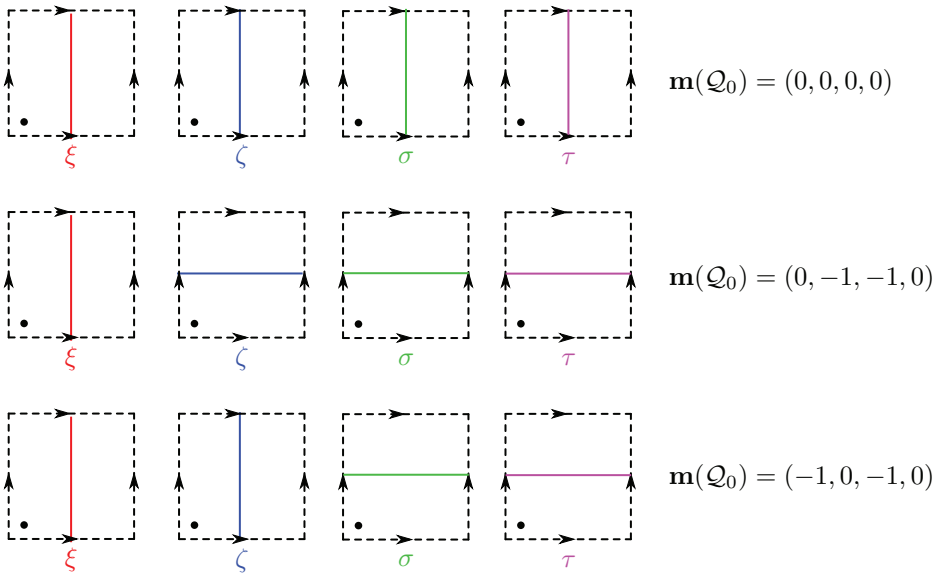


FIGURE 9.5. Elementary 1-handle and stabilization quadruples, and their index tuples.

LEMMA 9.9. *Let $\mathcal{Q}_0 = (\Sigma_0, \boldsymbol{\xi}, \boldsymbol{\zeta}, \boldsymbol{\sigma}, \boldsymbol{\tau}, p_0)$ be a multi-stabilizing quadruple, and let $\mathcal{T}_{\xi,\zeta,\sigma}$ denote the triple $(\Sigma_0, \boldsymbol{\xi}, \boldsymbol{\zeta}, \boldsymbol{\sigma}, p_0)$ (and so forth for the other sub-triples). The following hold:*

(1) $m_1(\mathcal{Q}_0) = m_1(\mathcal{T}_{\xi,\zeta,\sigma}) + m_1(\mathcal{T}_{\xi,\sigma,\tau}) = m_3(\mathcal{T}_{\zeta,\sigma,\tau}) + m_1(\mathcal{T}_{\xi,\zeta,\tau})$.
(2) $m_2(\mathcal{Q}_0) = m_2(\mathcal{T}_{\xi,\zeta,\sigma}) + m_1(\mathcal{T}_{\xi,\sigma,\tau}) = m_1(\mathcal{T}_{\zeta,\sigma,\tau}) + m_2(\mathcal{T}_{\xi,\zeta,\tau})$.
(3) $m_3(\mathcal{Q}_0) = m_3(\mathcal{T}_{\xi,\zeta,\sigma}) + m_2(\mathcal{T}_{\xi,\sigma,\tau}) = m_2(\mathcal{T}_{\zeta,\sigma,\tau}) + m_2(\mathcal{T}_{\xi,\zeta,\tau})$.
(4) $m_4(\mathcal{Q}_0) = m_3(\mathcal{T}_{\xi,\zeta,\sigma}) + m_3(\mathcal{T}_{\xi,\sigma,\tau}) = m_3(\mathcal{T}_{\zeta,\sigma,\tau}) + m_3(\mathcal{T}_{\xi,\zeta,\tau})$.

PROOF. We focus on the first equation of the first claim. We pick triangle classes

$$\psi_{\xi,\zeta,\sigma} \in \pi_2(\Theta^-_{\xi,\zeta}, \Theta^+_{\zeta,\sigma}, \Theta^+_{\sigma,\xi}) \quad \text{and} \quad \psi_{\xi,\sigma,\tau} \in \pi_2(\Theta^-_{\xi,\sigma}, \Theta^+_{\sigma,\tau}, \Theta^+_{\tau,\xi}),$$

which both have zero multiplicity on p_0. The classes $\psi_{\xi,\zeta,\sigma}$ and $\psi_{\xi,\sigma,\tau}$ may be spliced together since $\Theta^+_{\sigma,\xi} = \Theta^-_{\xi,\sigma}$. Using additivity of the index under juxtoposition, as well as the definition of m_i, we obtain the stated equation. The same argument applies for all of the other equations. □

This is a free offprint provided to the author by the publisher. Copyright restrictions may apply.

This is a free offprint provided to the author by the publisher. Copyright restrictions may apply.

CHAPTER 10

Stabilizations and holomorphic curves

In this chapter, we describe how the counts of holomorphic curves interact with the stabilization operations from Chapter 9.

10.1. Stabilizations and holomorphic disks

We now consider multi-stabilizations of Heegaard diagrams. Suppose that $\mathcal{H}_0 = (\Sigma_0, \boldsymbol{\xi}, \boldsymbol{\zeta}, p_0)$ is a multi-stabilizing Heegaard diagram. By construction, there is a top graded intersection point $\Theta^+_{\xi,\zeta} \in \mathbb{T}_\xi \cap \mathbb{T}_\zeta$, as well as a bottom graded intersection point $\Theta^-_{\xi,\zeta}$. We define

$$F_1^{\xi,\zeta} \colon \boldsymbol{CF}^-_J(\mathcal{H}) \to \boldsymbol{CF}^-_{J\wedge J_0}(\mathcal{H}, \mathcal{H}_0) \quad \text{and} \quad F_3^{\xi,\zeta} \colon \boldsymbol{CF}^-_{J\wedge J_0}(\mathcal{H}, \mathcal{H}_0) \to \boldsymbol{CF}^-_J(\mathcal{H})$$

via the formulas

$$F_1^{\xi,\zeta}(\mathbf{x}) = \mathbf{x} \times \Theta^+_{\xi,\zeta} \quad \text{and} \quad F_3^{\xi,\zeta}(\mathbf{x} \times \Theta) = \begin{cases} \mathbf{x} & \text{if } \Theta = \Theta^-_{\xi,\zeta} \\ 0 & \text{otherwise} \end{cases},$$

extended equivariantly over U. Similar to Ozsváth and Szabó's original 1- and 3-handle maps [**OS06**, Section 4.3], we have the following:

LEMMA 10.1. *The maps $F_1^{\xi,\zeta}$ and $F_3^{\xi,\zeta}$ are chain maps.*

PROOF. We focus on the claim for $F_1^{\xi,\zeta}$, as $F_3^{\xi,\zeta}$ is algebraically dual. Suppose $\phi_0 \in \pi_2(\Theta_1, \Theta_2)$ is a class on $\mathcal{H}_0$. By the grading formula, we have

$$\mu(\phi_0) = \mathrm{gr}(\Theta_1, \Theta_2) + 2n_{p_0}(\phi_0).$$

Hence, if $\phi \in \pi_2(\mathbf{x}, \mathbf{y})$ is a class on $\mathcal{H}$, then

$$\mathrm{ind}_{\mathrm{emb}}(\phi, \phi_0, M_\#) = \mu(\phi) + \mathrm{gr}(\Theta_1, \Theta_2). \tag{10.1}$$

(We remind the reader that $\mathrm{ind}_{\mathrm{emb}}(\phi, \phi_0, M_\#) = \mu(\phi \# \phi_0)$). The differential on $\boldsymbol{CF}^-_{J\wedge J_0}(\mathcal{H}, \mathcal{H}_0)$ counts representatives of pairs of classes (ϕ, ϕ_0) with $\mathrm{ind}_{\mathrm{emb}}(\phi, \phi_0, M_\#) = 1$. We note that $\mathrm{gr}(\Theta^+_{\xi,\zeta}, \Theta_2) \geq 0$. Furthermore, transversality for holomorphic curves representing ϕ implies that $\mu(\phi) \geq 0$, with equality if and only if ϕ is a constant class. Hence, any index 1 pair $(\phi, \phi_0) \in \pi_2(\mathbf{x}, \mathbf{y}) \times \pi_2(\Theta^+_{\xi,\zeta}, \Theta_2)$ which admits holomorphic representatives must have one of the following configurations: either $\mu(\phi) = 1$ and $\Theta^+_{\xi,\zeta} = \Theta_2$, or $\mu(\phi) = 0$ and $\mathrm{gr}(\Theta^+_{\xi,\zeta}, \Theta_2) = 1$. The contribution to $\partial(\mathbf{x} \times \Theta^+_{\xi,\zeta})$ of curves satisfying the latter condition coincides with $\mathbf{x} \otimes \hat{\partial}_0(\Theta^+_{\xi,\zeta})$, where $\hat{\partial}_0$ denotes the ordinary differential on the complex $\widehat{CF}(\mathcal{H}_0)$. Since $\Theta^+_{\xi,\zeta}$ is a cycle in $\widehat{CF}(\mathcal{H}_0)$, this contribution is zero. It remains to consider the case where

This is a free offprint provided to the author by the publisher. Copyright restrictions may apply.

$\mu(\phi) = 1$ and $\Theta_1 = \Theta_2 = \Theta^+_{\xi,\zeta}$. In this case, the main claim amounts to showing that if $\mathbf{d} \in ((0,1)\times\mathbb{R})^k$ is a generic k-tuple of points, then

$$\sum_{\substack{\phi_0 \in \pi_2(\Theta^+_{\xi,\zeta}, \Theta^+_{\xi,\zeta}) \\ n_{p_0}(\phi_0) = k}} \#\mathcal{M}(\phi_0, \mathbf{d}) \equiv 1 \pmod 2, \tag{10.2}$$

which is verified in [**Zem21**, Proposition 6.1], by degenerating the set $\mathbf{d}$, adapting an argument of Ozsváth and Szabó [**OS08a**, Lemma 6.4]. □

10.2. Stabilizations and holomorphic triangles

We now describe the interaction of the holomorphic triangle maps with multi-stabilizations.

PROPOSITION 10.2. *Suppose that $\mathcal{T} = (\Sigma, \boldsymbol{\alpha}, \boldsymbol{\beta}, \boldsymbol{\gamma}, w)$ is a Heegaard triple and $\mathcal{T}_0 = (\Sigma_0, \boldsymbol{\xi}, \boldsymbol{\zeta}, \boldsymbol{\sigma}, p_0)$ is a multi-stabilizing triple. We form the wedge product triple $\mathcal{T} \wedge \mathcal{T}_0$ (thought of as a connected sum with infinite neck length), at p_0 and some point in $\Sigma \setminus (\boldsymbol{\alpha} \cup \boldsymbol{\beta} \cup \boldsymbol{\gamma})$. We delete the basepoint p_0, and leave w as a basepoint. With respect to the almost complex structures J and $J \wedge J_0$, we have the following:*

(1) *If $m_1(\mathcal{T}_0) = 0$, then*

$$\begin{aligned} &f_{\mathcal{T}\wedge\mathcal{T}_0;\mathfrak{s}\#\mathfrak{s}_0}(\mathbf{x}\times\Theta^-_{\xi,\zeta}, \mathbf{y}\times\Theta^+_{\zeta,\sigma}) \\ =&f_{\mathcal{T};\mathfrak{s}}(\mathbf{x},\mathbf{y})\otimes\Theta^-_{\xi,\sigma} + \sum_{\substack{\mathbf{z}\in\mathbb{T}_\alpha\cap\mathbb{T}_\gamma \\ \Theta\in\mathbb{T}_\xi\cap\mathbb{T}_\sigma\setminus\{\Theta^-_{\xi,\sigma}\}}} C_{\mathbf{x},\mathbf{y},\mathbf{z},\Theta}\cdot\mathbf{z}\times\Theta, \end{aligned}$$

for some $C_{\mathbf{x},\mathbf{y},\mathbf{z},\Theta} \in \mathbb{F}[U]$.

(2) *If $m_2(\mathcal{T}_0) = 0$, then*

$$\begin{aligned} &f_{\mathcal{T}\wedge\mathcal{T}_0;\mathfrak{s}\#\mathfrak{s}_0}(\mathbf{x}\times\Theta^+_{\xi,\zeta}, \mathbf{y}\times\Theta^-_{\zeta,\sigma}) \\ =&f_{\mathcal{T};\mathfrak{s}}(\mathbf{x},\mathbf{y})\otimes\Theta^-_{\xi,\sigma} + \sum_{\substack{\mathbf{z}\in\mathbb{T}_\alpha\cap\mathbb{T}_\gamma \\ \Theta\in\mathbb{T}_\xi\cap\mathbb{T}_\sigma\setminus\{\Theta^-_{\xi,\sigma}\}}} C_{\mathbf{x},\mathbf{y},\mathbf{z},\Theta}\cdot\mathbf{z}\times\Theta, \end{aligned}$$

for some $C_{\mathbf{x},\mathbf{y},\mathbf{z},\Theta} \in \mathbb{F}[U]$.

(3) *If $m_3(\mathcal{T}_0) = 0$, then*

$$\begin{aligned} &f_{\mathcal{T}\wedge\mathcal{T}_0;\mathfrak{s}\#\mathfrak{s}_0}(\mathbf{x}\times\Theta^+_{\xi,\zeta}, \mathbf{y}\times\Theta^+_{\zeta,\sigma}) \\ =&f_{\mathcal{T};\mathfrak{s}}(\mathbf{x},\mathbf{y})\otimes\Theta^+_{\xi,\sigma}. \end{aligned}$$

Here, $\mathfrak{s}_0 \in \mathrm{Spin}^c(X_{\xi,\zeta,\tau})$ is the one which restricts to the torsion Spin^c structure on each end.

PROOF. We focus on the third claim, since the other two are obtained by cyclically permuting the attaching curves.

Suppose that $\psi\#\psi_0 \in \pi_2(\mathbf{x}\times\Theta^+_{\xi,\zeta}, \mathbf{y}\times\Theta^+_{\zeta,\sigma}, \mathbf{z}\times\Theta)$, for some $\Theta \in \mathbb{T}_\xi \cap \mathbb{T}_\sigma$. By definition of $m_3(\mathcal{T}_0)$,

$$\mu(\psi_0) = m_3(\mathcal{T}_0) + 2n_{p_0}(\psi_0) + \mathrm{gr}(\Theta^+_{\xi,\sigma}, \Theta).$$

Since $m_3(\mathcal{T}_0) = 0$ by assumption, we conclude that

$$\mu(\psi_0) = 2n_{p_0}(\psi_0) + \mathrm{gr}(\Theta^+_{\xi,\sigma}, \Theta). \tag{10.3}$$

This is a free offprint provided to the author by the publisher. Copyright restrictions may apply.

Using (10.3), we have

$$\mathrm{ind}_{\mathrm{emb}}(\psi,\psi_0,M_\#)=\mu(\psi)+\mathrm{gr}(\Theta^+_{\xi,\sigma},\Theta). \tag{10.4}$$

If $\mathcal{MM}_{J\wedge J_0}(\psi,\psi_0)$ is non-empty, then $\mathcal{M}_J(\psi)$ is non-empty by definition, so $\mu(\psi)\geq 0$ by transversality. Equation (10.4) now gives

$$\mu(\psi)=\mathrm{gr}(\Theta^+_{\xi,\sigma},\Theta)=0.$$

Hence, it remains to show that

$$\sum_{\substack{\psi_0\in\pi_2(\Theta^+_{\xi,\zeta},\Theta^+_{\zeta,\sigma},\Theta^+_{\xi,\sigma})\\ n_{p_0}(\psi_0)=k}} \#\mathcal{M}(\psi,\mathbf{d})\equiv 1, \tag{10.5}$$

for a generic $\mathbf{d}\in\Delta^k$, which is disjoint from the fat diagonal. Equation (10.5) is proven by considering a path $(\mathbf{d}_t)_{t\in[0,\infty)}$, satisfying the following:

(1) $\mathbf{d}_0=\mathbf{d}$.
(2) The k components of $\mathbf{d}_t$ approach ∞ in the α-β cylindrical end of Δ. Furthermore, with respect to an identification of the cylindrical end with $[0,1]\times[0,\infty)$, the points of $\mathbf{d}_t$ approach some fixed

$$\mathbf{d}'\in((0,1)\times\mathbb{R})^k,$$

modulo overall translation by $\mathbb{R}$. Furthermore, $\mathbf{d}'$ lies in the complement of the fat diagonal.

If $\mathbf{z}\in\mathbb{T}_\xi\cap\mathbb{T}_\sigma$, we consider the 1-dimensional moduli space

$$\mathcal{M}:=\bigcup_{t\in[0,\infty)}\coprod_{\substack{\psi\in\pi_2(\Theta^+_{\xi,\zeta},\Theta^+_{\zeta,\sigma},\Theta^+_{\xi,\sigma})\\ n_{p_0}(\psi)=k}}\mathcal{M}(\psi,\mathbf{d}_t).$$

The count of the ends of $\mathcal{M}$ at $t=0$ coincides with the left-hand side of (10.5). The ends of $\mathcal{M}$ at finite t occur in canceling pairs, since the differentials vanish on $\widehat{CF}(\Sigma_0,\boldsymbol{\xi},\boldsymbol{\zeta})$, $\widehat{CF}(\Sigma_0,\boldsymbol{\zeta},\boldsymbol{\sigma})$ and $\widehat{CF}(\Sigma_0,\boldsymbol{\xi},\boldsymbol{\zeta})$. The remaining ends of $\mathcal{M}$ occur as $t\to\infty$, and are identified with the Cartesian product

$$\left(\coprod_{\substack{\psi\in\pi_2(\Theta^+_{\xi,\zeta},\Theta^+_{\zeta,\sigma},\Theta^+_{\xi,\sigma})\\ n_{p_0}(\psi)=0\\ \mu(\psi)=0}}\mathcal{M}(\psi)\right)\times\left(\coprod_{\substack{\phi\in\pi_2(\Theta^+_{\xi,\zeta},\Theta^+_{\xi,\zeta})\\ n_{p_0}(\psi_0)=k}}\mathcal{M}(\phi,\mathbf{d}')\right). \tag{10.6}$$

The left-hand side of (10.6), is the $\Theta^+_{\xi,\sigma}$ coefficient of $\hat{f}_{\xi,\zeta,\sigma}(\Theta^+_{\xi,\zeta},\Theta^+_{\zeta,\sigma})$. The right-hand factor of (10.6) has total count 1 (modulo 2) by (10.2).

The main claim thus amounts to showing that the left-hand factor of (10.6) has total count congruent to 1. This is equivalent to showing

$$\hat{f}_{\xi,\zeta,\sigma}(\Theta^+_{\xi,\zeta},\Theta^+_{\zeta,\sigma})=\Theta^+_{\xi,\sigma}, \tag{10.7}$$

where $\hat{f}_{\xi,\zeta,\sigma}$ denotes the map which counts triangles on $\mathcal{T}_0$ which do not cross the basepoints. Equation (10.7) is verified in the subsequent Lemma 10.4. □

Remark 10.3. Note that if we were to verify the first two statements of Proposition 10.2 directly, the main difference would be that $\mathrm{gr}(\Theta^-_{\xi,\sigma},\Theta)$ may be negative, allowing for the existence of curves with $\mu(\psi)\geq 1$.

This is a free offprint provided to the author by the publisher. Copyright restrictions may apply.

LEMMA 10.4. *Suppose that $\mathcal{T}_0 = (\Sigma_0, \boldsymbol{\xi}, \boldsymbol{\zeta}, \boldsymbol{\tau}, \mathbf{p}_0)$ is a multi-stabilizing Heegaard triple.*

(1) *If $m_1(\mathcal{T}_0) = 0$, then*

$$\hat{f}_{\mathcal{T}_0}(\Theta^-_{\xi,\zeta}, \Theta^+_{\zeta,\sigma}) = \Theta^-_{\xi,\sigma} + \sum_{\Theta \in \mathbb{T}_\xi \cap \mathbb{T}_\sigma \setminus \{\Theta^-_{\xi,\sigma}\}} C_\Theta \cdot \Theta,$$

for some $C_\Theta \in \mathbb{F}$.

(2) *If $m_2(\mathcal{T}_0) = 0$, then*

$$\hat{f}_{\mathcal{T}_0}(\Theta^+_{\xi,\zeta}, \Theta^-_{\zeta,\sigma}) = \Theta^-_{\xi,\sigma} + \sum_{\Theta \in \mathbb{T}_\xi \cap \mathbb{T}_\sigma \setminus \{\Theta^-_{\xi,\sigma}\}} C_\Theta \cdot \Theta,$$

for some $C_\Theta \in \mathbb{F}$.

(3) *If $m_3(\mathcal{T}_0) = 0$, then*

$$\hat{f}_{\mathcal{T}_0}(\Theta^+_{\xi,\zeta}, \Theta^+_{\zeta,\sigma}) = \Theta^+_{\xi,\sigma}.$$

PROOF. We focus on the third claim, when $m_3(\mathcal{T}_0) = 0$, since it is the simplest notationally, and all claims are equivalent upon dualizing, as in (10.9).

According to Definition 9.3, a multi-stabilizing triple is built by inductively attaching elementary stabilizing triples. Hence, we prove the claim by induction on the number n of elementary stabilizing triples used in the construction. If $n = 1$, the computation is easy to perform directly. We suppose now that the claim holds for all multi-stabilizing triples built with n or fewer elementary triples. This implies that Proposition 10.2 holds whenever the stabilizing triple is built with n or fewer elementary triples. In particular, Proposition 10.2 holds when $\mathcal{T}_0$ is an elementary stabilizing triple.

We suppose now that $\mathcal{T}$ is a general multi-stabilizing triple. It is sufficient to show the present claim for some almost complex structure, since if J and J' are two almost complex structures on $\Sigma \times \Delta$, then we may pick a stratified family of almost complex structures $(J_s)_{s\in[0,1]}$ on $\Sigma_0 \times \Delta$ such that $J_0 = J$, and as $s \to 1$, the family J_s limits to J' on $\Sigma \times \Delta$, as well as three non-cylindrical almost complex structures on the ends of $\Sigma \times \Delta$. Counting the ends of index 0 families of J_s-holomorphic triangles, we obtain

$$\begin{aligned} &\hat{f}_{\mathcal{T}_0,J}(\Theta^+_{\xi,\zeta}, \Theta^+_{\zeta,\sigma}) + \Psi_{J'\to J}(f_{\mathcal{T}_0,J'}(\Psi_{J\to J'}(\Theta^+_{\xi,\zeta}), \Psi_{J\to J'}(\Theta^+_{\zeta,\sigma}))) \\ &+ \hat{\partial}_{\xi,\sigma} H(\Theta^+_{\xi,\zeta}, \Theta^+_{\zeta,\sigma}) + H(\hat{\partial}_{\xi,\zeta}(\Theta^+_{\xi,\zeta}), \Theta^+_{\zeta,\sigma}) + H(\Theta^+_{\xi,\zeta}, \hat{\partial}_{\zeta,\sigma}(\Theta^+_{\zeta,\sigma})) = 0, \end{aligned} \tag{10.8}$$

where $\Psi_{J\to J'}$ denotes the change of almost complex structure map, and H is the map which counts index -1 triangles which are J_s-holomorphic for some $s \in (0,1)$. (Note that we are abusing notation slightly by writing $\Psi_{J\to J'}$ and writing J for an almost complex structure on $\Sigma_0 \times \Delta$, as well as an almost complex structure on the cylindrical ends).

Since the change of almost complex structure maps are graded, they must fix $\Theta^+_{\xi,\zeta}$, $\Theta^+_{\zeta,\sigma}$ and $\Theta^+_{\xi,\sigma}$. Since also the differentials on $\widehat{CF}(\Sigma_0, \boldsymbol{\xi}, \boldsymbol{\zeta})$, $\widehat{CF}(\Sigma_0, \boldsymbol{\zeta}, \boldsymbol{\sigma})$ and $\widehat{CF}(\Sigma_0, \boldsymbol{\xi}, \boldsymbol{\sigma})$ all vanish, we conclude from (10.8) that if the main claim holds using J, then it also holds using J'.

Suppose now that $\mathcal{T}_0$ is a multi-stabilizing triple with $m_3(\mathcal{T}_0) = 0$, obtained by adjoining $n+1$ elementary stabilizations. Let us say that $\mathcal{T}_0$ is obtained by adjoining the elementary triple $\mathcal{E}$ to a triple $\mathcal{T}'$, obtained from n elementary stabilizations.

This is a free offprint provided to the author by the publisher. Copyright restrictions may apply.

We pick the almost complex structure to be infinitely degenerated between $\mathcal{E}$ and $\mathcal{T}'$. By the inductive hypothesis, the present claim holds for $\mathcal{T}'$. We now view $\mathcal{T}_0$ as an elementary stabilization of $\mathcal{T}'$, using the triple $\mathcal{E}$, and apply Proposition 10.2 to obtain the claim for $\mathcal{T}_0$. The proof is complete. □

REMARK 10.5. If we symmetrize the triangle map, by viewing it instead as a map

(10.9)
$$f_{\alpha,\beta,\gamma;\mathfrak{s}} : \boldsymbol{CF}^-(\Sigma,\boldsymbol{\alpha},\boldsymbol{\beta},\mathfrak{s}|_{Y_{\alpha,\beta}})\otimes \boldsymbol{CF}^-(\Sigma,\boldsymbol{\beta},\boldsymbol{\gamma},\mathfrak{s}|_{Y_{\beta,\gamma}})\otimes \boldsymbol{CF}^-(\Sigma,\boldsymbol{\gamma},\boldsymbol{\alpha},\mathfrak{s}|_{Y_{\gamma,\alpha}})\to \mathbb{F}[\![U]\!],$$

then the three statements of Proposition 10.2 become equivalent.

10.3. Stabilizations and holomorphic quadrilaterals

We now describe the analogs of the stabilization results from Section 10.2 for holomorphic quadrilaterals.

PROPOSITION 10.6. *Suppose that $\mathcal{Q} = (\Sigma,\boldsymbol{\alpha},\boldsymbol{\beta},\boldsymbol{\gamma},\boldsymbol{\delta},w)$ is a Heegaard quadruple, and $\mathcal{Q}_0 = (\Sigma_0,\boldsymbol{\xi},\boldsymbol{\zeta},\boldsymbol{\sigma},\boldsymbol{\tau},p_0)$ is a multi-stabilizing Heegaard quadruple. We form the wedge sum $\Sigma\wedge\Sigma_0$ at p_0 and a point in $\Sigma\setminus(\boldsymbol{\alpha}\cup\boldsymbol{\beta}\cup\boldsymbol{\gamma}\cup\boldsymbol{\delta})$. Suppose and $J = (J_s)_{s\in[0,1]}$ and $I = (I_s)_{s\in[0,1]}$ are stratified families of almost complex structures on $\Sigma\times\square$ and $\Sigma_0\times\square$, respectively, for counting rectangles. With respect to the families J and $J\wedge I$, we have the following:*

(1) *If $m_1(\mathcal{Q}_0) = 0$, then*

$$\begin{aligned}&h_{\mathcal{Q}\wedge\mathcal{Q}_0;\mathfrak{s}\#\mathfrak{s}_0}(\mathbf{x}\times\Theta^-_{\xi,\zeta},\mathbf{y}\times\Theta^+_{\zeta,\sigma},\mathbf{z}\times\Theta^+_{\sigma,\tau})\\ =&h_{\mathcal{Q};\mathfrak{s}}(\mathbf{x},\mathbf{y},\mathbf{z})\otimes\Theta^-_{\xi,\tau}+\sum_{\substack{\mathbf{w}\in\mathbb{T}_\alpha\cap\mathbb{T}_\delta\\ \Theta\in\mathbb{T}_\xi\cap\mathbb{T}_\tau\setminus\Theta^-_{\xi,\tau}}} C_{\mathbf{x},\mathbf{y},\mathbf{z},\mathbf{w},\Theta}\cdot\mathbf{w}\times\Theta,\end{aligned}$$

for some $C_{\mathbf{x},\mathbf{y},\mathbf{z},\mathbf{w},\Theta}\in\mathbb{F}[U]$.

(2) *If $m_2(\mathcal{Q}_0) = 0$, then*

$$\begin{aligned}&h_{\mathcal{Q}\wedge\mathcal{Q}_0;\mathfrak{s}\#\mathfrak{s}_0}(\mathbf{x}\times\Theta^+_{\xi,\zeta},\mathbf{y}\times\Theta^-_{\zeta,\sigma},\mathbf{z}\times\Theta^+_{\sigma,\tau})\\ =&h_{\mathcal{Q};\mathfrak{s}}(\mathbf{x},\mathbf{y},\mathbf{z})\otimes\Theta^-_{\xi,\tau}+\sum_{\substack{\mathbf{w}\in\mathbb{T}_\alpha\cap\mathbb{T}_\delta\\ \Theta\in\mathbb{T}_\xi\cap\mathbb{T}_\tau\setminus\Theta^-_{\xi,\tau}}} C_{\mathbf{x},\mathbf{y},\mathbf{z},\mathbf{w},\Theta}\cdot\mathbf{w}\times\Theta,\end{aligned}$$

for some $C_{\mathbf{x},\mathbf{y},\mathbf{z},\mathbf{w},\Theta}\in\mathbb{F}[U]$.

(3) *If $m_3(\mathcal{Q}_0) = 0$, then*

$$\begin{aligned}&h_{\mathcal{Q}\wedge\mathcal{Q}_0;\mathfrak{s}\#\mathfrak{s}_0}(\mathbf{x}\times\Theta^+_{\xi,\zeta},\mathbf{y}\times\Theta^+_{\zeta,\sigma},\mathbf{z}\times\Theta^-_{\sigma,\tau})\\ =&h_{\mathcal{Q};\mathfrak{s}}(\mathbf{x},\mathbf{y},\mathbf{z})\otimes\Theta^-_{\xi,\tau}+\sum_{\substack{\mathbf{w}\in\mathbb{T}_\alpha\cap\mathbb{T}_\delta\\ \Theta\in\mathbb{T}_\xi\cap\mathbb{T}_\tau\setminus\Theta^-_{\xi,\tau}}} C_{\mathbf{x},\mathbf{y},\mathbf{z},\mathbf{w},\Theta}\cdot\mathbf{w}\times\Theta,\end{aligned}$$

for some $C_{\mathbf{x},\mathbf{y},\mathbf{z},\mathbf{w},\Theta}\in\mathbb{F}[U]$.

(4) *If $m_4(\mathcal{Q}_0) = 0$, then*

$$h_{\mathcal{Q}\wedge\mathcal{Q}_0;\mathfrak{s}\#\mathfrak{s}_0}(\mathbf{x}\times\Theta^+_{\xi,\zeta},\mathbf{y}\times\Theta^+_{\zeta,\sigma},\mathbf{z}\times\Theta^+_{\sigma,\tau}) = h_{\mathcal{Q},J,\mathfrak{s}}(\mathbf{x},\mathbf{y},\mathbf{z})\otimes\Theta^+_{\xi,\tau}.$$

This is a free offprint provided to the author by the publisher. Copyright restrictions may apply.

PROOF. We focus on the proof of the fourth claim, since it is notationally the simplest. The proof follows similarly to the proof of Proposition 10.2, until (10.5) therein. The necessary substitute is

$$\sum_{\substack{\psi_0\in\pi_2(\Theta^+_{\xi,\zeta},\Theta^+_{\zeta,\sigma},\Theta^+_{\sigma,\tau},\Theta^+_{\xi,\tau})\\ n_{p_0}(\psi_0)=k}} \#\mathcal{M}(\psi_0,\widetilde{\mathbf{d}}) \equiv 1 \pmod 2, \tag{10.10}$$

for generic $\widetilde{\mathbf{d}} \in \mathrm{int}(\square)^k \times (0,1)$.

Write $\mathcal{M}(\widetilde{\mathbf{d}})$ for the union over such ψ_0 of the matched moduli spaces $\mathcal{M}(\psi_0,\widetilde{\mathbf{d}})$ so $\#\mathcal{M}(\widetilde{\mathbf{d}})$ is equal to the left side of (10.10). We will use a cobordism argument to show (10.10).

We consider a path $(\widetilde{\mathbf{d}}_t)_{t\in[0,\infty]}$ in $(\mathrm{int}(\square))^k \times (0,1)$ satisfying the following:

(1) $\widetilde{\mathbf{d}}_0 = \widetilde{\mathbf{d}}$.
(2) The $(0,1)$-component (i.e. the almost complex structure parameter) of $\widetilde{\mathbf{d}}_t$ approaches 1 as $t \to \infty$.
(3) The k $\square$-components of $\widetilde{\mathbf{d}}_t$ approach ∞ in the α-β cylindrical end of $\square$. Furthermore, with respect to an identification of the cylindrical end with $[0,1]\times[0,\infty)$, the points of $\widetilde{\mathbf{d}}_t$ approach some fixed, generic

$$\mathbf{d} \in ((0,1)\times\mathbb{R})^k,$$

modulo overall translation by $\mathbb{R}$.

There are three types of ends of the 1-dimensional moduli space

$$\bigcup_{t\in[0,\infty)} \mathcal{M}(\widetilde{\mathbf{d}}_t).$$

The first type are the curves in $\mathcal{M}(\widetilde{\mathbf{d}})$ (i.e. the ones we want to count). The next type of end is curves which break off at finite $t \in (0,\infty)$. The final type is curves which appear as $t \to \infty$.

The degenerations appearing at finite t can only correspond to strips breaking off (degenerations into a pair of triangles are prohibited since the aspect ratio is determined by $\widetilde{\mathbf{d}}_t$ and is finite for $t \in [0,\infty)$). Ends corresponding to strip breaking occur in canceling pairs, since $\Theta^+_{\xi,\zeta}$, $\Theta^+_{\zeta,\sigma}$, $\Theta^+_{\sigma,\tau}$ and $\Theta^+_{\xi,\tau}$ are all cycles in the hat version of the complexes which contain them.

As $t \to \infty$, a family of curves approaches a pair of triangles not crossing the basepoints, as well as a holomorphic disk which matches $\mathbf{d}$. As such, these ends correspond to the space

$$\left(\coprod_{\mathbf{z}\in\mathbb{T}_\xi\cap\mathbb{T}_\sigma}\left(\coprod_{\substack{\psi_{\xi,\zeta,\sigma}\in\pi_2(\Theta^+_{\xi,\zeta},\Theta^+_{\zeta,\sigma},\mathbf{z})\\ \mu(\psi_{\xi,\zeta,\sigma})=0\\ n_{p_0}(\psi_{\xi,\zeta,\sigma})=0}} \mathcal{M}(\psi_{\xi,\zeta,\sigma})\right)\times\left(\coprod_{\substack{\psi_{\xi,\sigma,\tau}\in\pi_2(\mathbf{z},\Theta^+_{\sigma,\tau},\Theta^+_{\xi,\tau})\\ \mu(\psi_{\xi,\sigma,\tau})=0\\ n_{p_0}(\psi_{\xi,\sigma,\tau})=0}} \mathcal{M}(\psi_{\xi,\sigma,\tau})\right)\right) \times\left(\coprod_{\substack{\phi\in\pi_2(\Theta^+_{\xi,\zeta},\Theta^+_{\xi,\zeta})\\ n_{p_0}(\phi)=k}} \mathcal{M}(\phi,\mathbf{d})\right). \tag{10.11}$$

This is a free offprint provided to the author by the publisher. Copyright restrictions may apply.

We wish to show the above space has an odd number of points. An identical argument to [**Zem21**, Equation 24] establishes that the last factor of (10.11) has an odd number of elements.

The first pair of factors corresponds exactly to the $\Theta^+_{\xi,\tau}$ component of

$$\hat{f}_{\xi,\sigma,\tau}(\hat{f}_{\xi,\zeta,\sigma}(\Theta^+_{\xi,\zeta},\Theta^+_{\zeta,\sigma}),\Theta^+_{\sigma,\tau}),$$

where $\hat{f}_{\xi,\sigma,\tau}$ denotes the map which counts index 0 holomorphic triangles with zero multiplicity on p_0. Consequently, it is sufficient to show that

$$\hat{f}_{\xi,\sigma,\tau}(\hat{f}_{\xi,\zeta,\sigma}(\Theta^+_{\xi,\zeta},\Theta^+_{\zeta,\sigma}),\Theta^+_{\sigma,\tau}) = \Theta^+_{\xi,\tau}. \tag{10.12}$$

To prove (10.12) it is sufficient to prove

$$\hat{f}_{\xi,\sigma,\tau}(\Theta^+_{\xi,\sigma},\Theta^+_{\sigma,\tau}) = \Theta^+_{\xi,\tau}, \quad \text{and} \quad \hat{f}_{\xi,\zeta,\sigma}(\Theta^+_{\xi,\zeta},\Theta^+_{\zeta,\sigma}) = \Theta^+_{\zeta,\sigma}, \tag{10.13}$$

which is proven in Lemma 10.4. □

10.4. Lens space stabilizations of Heegaard diagrams

Let $\mathcal{H}$ be a Heegaard diagram, and let $\mathcal{H}_0 = (\mathbb{T}^2, c_1, c_2, p_0)$ be a standard genus 1 diagram for $L(m,1)$. Let J be an almost complex structure for $\mathcal{H}$, and let J_0 be an almost complex structure on $\mathbb{T}^2 \times [0,1] \times \mathbb{R}$.

If $i \in \mathbb{Z}/m$, we define a map

$$\sigma_i \colon \boldsymbol{CF}^-_J(\mathcal{H}, \mathfrak{s}) \to \boldsymbol{CF}^-_{J\wedge J_0}(\mathcal{H}, \mathcal{H}_0, \mathfrak{s}\#\mathfrak{s}_i),$$

via the formula

$$\sigma_i(\mathbf{x}) := \mathbf{x} \times x_i,$$

extended equivariantly over U.

Lemma 10.7. *For each i, σ_i is a chain map.*

Proof. Note that each intersection point on $\mathcal{H}_0$ represents a different Spin^c structure. Hence any class of disks on $(\mathbb{T}^2, c_1, c_2, p_0)$ must have the same incoming and outgoing intersection point. Furthermore, as $H_2(L(m,1);\mathbb{Z}) = 0$, the set of doubly periodic domains vanishes, so $\pi_2(x_i, x_i) \cong \mathbb{Z}$. Furthermore, every class in $\pi_2(x_i, x_i)$ is of the form $k \cdot [\mathbb{T}_2] + e_{x_i}$, where e_{x_i} denotes the constant class. Write ϕ_{k,x_i} for this class. We note

$$\mu(\phi_{k,x_i}) = 2k.$$

Write p for the connected sum point on $\mathcal{H}$. If $\phi \in \pi_2(\mathbf{x}, \mathbf{y})$ is a class on $\mathcal{H}$, and $n_p(\phi) = k$,

$$\mu(\phi \# \phi_{k,x_i}) = \mu(\phi),$$

using Lipshitz's formula for the Maslov index [**Lip06**, Corollary 4.3].

Hence, the main claim follows if we can show

$$\#\mathcal{M}\mathcal{M}(\phi, \phi_{k,x_i})/\mathbb{R} \equiv \#\mathcal{M}(\phi)/\mathbb{R}$$

for any index 1 class ϕ with $n_p(\phi) = k$.

Hence, it is sufficient to show that if $\mathbf{d} = (d_1, \dots, d_k)$ is a k-tuple of distinct points in $[0,1] \times \mathbb{R}$, then

$$\#\mathcal{M}(\phi_{k,x_i}, \mathbf{d}) \equiv 1 \pmod 2, \tag{10.14}$$

where $\mathcal{M}(\phi_{k,x_i}, \mathbf{d})$ denotes the disjoint union of the moduli spaces $\{u \in \mathcal{M}(S^{\mathbf{q}}, \phi_{k,x_i}) : \mathrm{ev}_{q_i}(u) = d_i\}$, over equivalence classes of source curves S with k marked points $\mathbf{q}$.

This is a free offprint provided to the author by the publisher. Copyright restrictions may apply.

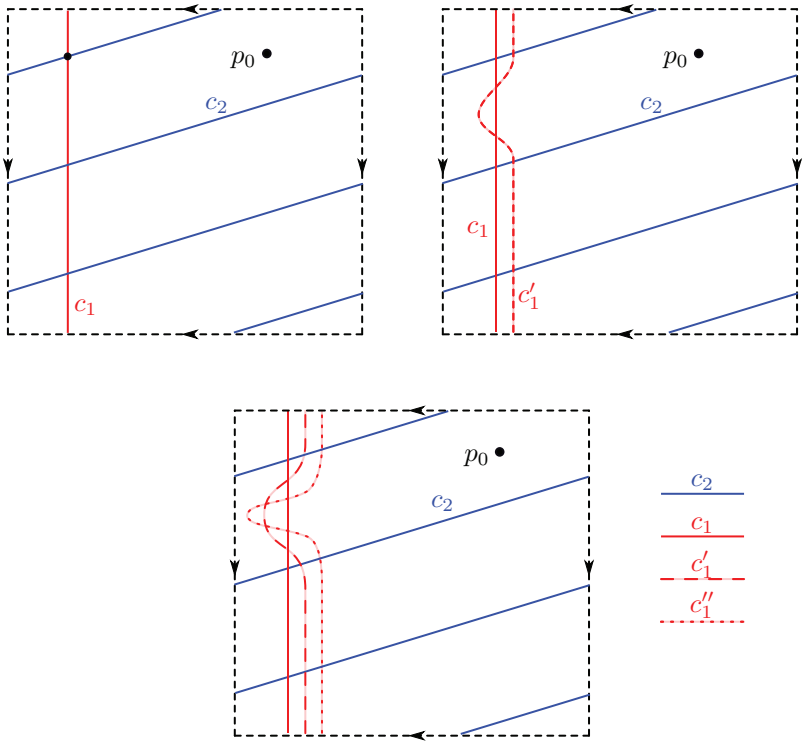


FIGURE 10.1. Top left: a diagram for $L(m,1)$. Top right: a triple obtained by adding an isotopic copy of the alpha curve. Bottom: a triple obtained by adding two isotopic alpha curves.

Equation (10.14) may be established using the same argument as in the $k=1$ case (i.e. ordinary stabilizations), as described by Lipshitz [**Lip06**, Appendix A]. Alternatively, one may establish (10.14) by degenerating $\mathbf{d}$ towards k distinct points along $\{0\}\times\mathbb{R}$, and using the count of index 2 boundary degenerations for generic almost complex structures given in Proposition 7.9. □

10.5. Lens space stabilizations and holomorphic triangles

Next, we consider triangles and lens space stabilizations. We consider taking the connected sum of a Heegaard triple with a triple of the form shown in Figure 10.1.

LEMMA 10.8. *Suppose that c_1', c_1 and c_2 are the three curves on the torus shown in Figure* 10.1*, and suppose that $\mathcal{T}=(\Sigma,\boldsymbol{\alpha},\boldsymbol{\beta},\boldsymbol{\gamma},w)$ is an arbitrary Heegaard triple. Write $\mathcal{T}_{c_1',c_1,c_2}$ for the triple $(\mathbb{T}^2,c_1',c_1,c_2,p_0)$, and write $\mathcal{T}_{c_1,c_2,c_1'}$ and $\mathcal{T}_{c_2,c_1',c_1}$ for the triples obtained by cyclically permuting the attaching curves. Suppose J and J_0 are almost complex structures on $\Sigma\times\Delta$ and $\Sigma_0\times\Delta$, and let $J\wedge J_0$ denote their wedge. Then, counting triangles with respect to J and $J\wedge J_0$, we have the following:*

$$f_{\mathcal{T}\wedge\mathcal{T}_{c_1',c_1,c_2};\mathfrak{s}\#\mathfrak{s}_i}(\mathbf{x}\times\Theta^+_{c_1',c_1},\mathbf{y}\times x_i)=f_{\mathcal{T},\mathfrak{s}}(\mathbf{x},\mathbf{y})\otimes x_i';$$
$$f_{\mathcal{T}\wedge\mathcal{T}_{c_1,c_2,c_1'};\mathfrak{s}\#\mathfrak{s}_i}(\mathbf{x}\times x_i,\mathbf{y}\times x_i')=f_{\mathcal{T};\mathfrak{s}}(\mathbf{x},\mathbf{y})\otimes\Theta^-_{c_1,c_1'}$$

This is a free offprint provided to the author by the publisher. Copyright restrictions may apply.

$$+\sum_{\mathbf{z}\in\mathbb{T}_\alpha\cap\mathbb{T}_\gamma} C_{\mathbf{x},\mathbf{y},\mathbf{z}}\cdot\mathbf{z}\times\Theta^+_{c_1,c_1'},\quad \textit{and}$$

$$f_{\mathcal{T}\wedge\mathcal{T}_{c_2,c_1',c_1};\mathfrak{s}\#\mathfrak{s}_i}(\mathbf{x}\times x_i',\mathbf{y}\times\Theta^+_{c_1',c_1})=f_{\mathcal{T};\mathfrak{s}}(\mathbf{x},\mathbf{y})\otimes x_i,$$

for some $C_{\mathbf{x},\mathbf{y},\mathbf{z}}\in\mathbb{F}[U]$, and where x_i' is the unique intersection point in the corresponding Spin^c *structure.*

PROOF. All of the equations are equivalent, by reordering the attaching curves, and dualizing, so we focus on the first one. The $m=1$ case is used in the proof that the cobordism maps are invariants [**OS06**, Theorem 2.14]. Our proof is a modification of the proof of an analogous result in the cylindrical setting [**Zem15**, Theorem 9.7].

Suppose $\psi_0\in\pi_2(\Theta,x_i,x_i')$ is a class of triangles on $\mathcal{T}_{c_1',c_1,c_2}$. We have

$$\mu(\psi_0)=2n_{p_0}(\psi_0)+\mathrm{gr}(\Theta^+_{c_1',c_1},\Theta).$$

If $\psi\in\pi_2(\mathbf{x},\mathbf{y},\mathbf{z})$ is a class, it follows that

$$\mathrm{ind}_{\mathrm{emb}}(\psi,\psi_0,M_\#)=\mu(\psi)+\mathrm{gr}(\Theta^+_{c_1',c_1},\Theta). \tag{10.15}$$

If the matched moduli space $\mathcal{MM}(\psi,\psi_0)$ is non-empty, then $\mathcal{M}(\psi)$ is non-empty, so we may assume $\mu(\psi)\geq 0$, by transversality. Equation (10.15) implies that if (ψ,ψ_0) has a matched representative, then $\Theta=\Theta^+_{c_1',c_1}$ and $\mu(\psi)=0$. The proof now follows by showing that if $\mathbf{d}\in(\mathrm{int}\,(\Delta))^k$ is generic, then

$$\sum_{\substack{\psi_0\in\pi_2(\Theta^+_{c_1',c_1},x_i,x_i')\\ n_{p_0}(\psi_0)=k}}\#\mathcal{M}(\psi_0,\mathbf{d})\equiv 1\pmod 2. \tag{10.16}$$

Equation (10.16) is obtained by degenerating $\mathbf{d}$ into one of the cylindrical ends of $\mathbb{T}^2\times\Delta$, as in the proof of (10.5). Equation (10.16) then follows from (10.2), as well as the computation for the hat-triangle map (i.e. the count of holomorphic triangles not covering the basepoint), which is straightforward to perform by hand. The proof is complete. □

10.6. Lens space stabilizations and holomorphic rectangles

We will also need a version of the previous lens space stabilization results for rectangles.

LEMMA 10.9. *Suppose that $\mathcal{Q}$ is a Heegaard quadruple. Write $\mathcal{Q}_{c_1'',c_1',c_1,c_2}$ for the genus 1 quadruple shown in Figure* 10.1. *Suppose that $J=(J_s)_{s\in[0,1]}$ and $I=(I_s)_{s\in[0,1]}$ are stratified families of almost complex structures, for counting rectangles on $\mathcal{Q}$ and $\mathcal{Q}_0$, respectively. With respect to the families of almost complex structures J and $J\wedge I$, we have*

$$\begin{aligned}&h_{\mathcal{Q}\wedge\mathcal{Q}_{c_1',c_1,c_2,c_1''};\mathfrak{s}\#\mathfrak{s}_0}(\mathbf{x}\times\Theta^+_{c_1',c_1},\mathbf{y}\times\Theta^{\mathrm{can}}_{c_1,c_2},\mathbf{z}\times\Theta^+_{c_2,c_1''})\\ =&h_{\mathcal{Q};\mathfrak{s}}(\mathbf{x},\mathbf{y},\mathbf{z})\otimes\Theta^-_{c_1',c_1''}+\sum_{\mathbf{w}\in\mathbb{T}_\alpha\cap\mathbb{T}_\delta}C_{\mathbf{x},\mathbf{y},\mathbf{z},\mathbf{w}}\cdot\mathbf{w}\times\Theta^+_{c_1',c_1''},\end{aligned}$$

for $C_{\mathbf{x},\mathbf{y},\mathbf{z},\mathbf{w}}\in\mathbb{F}[U]$. Similar statements hold for quadruples which are stabilized by the genus 1 diagrams obtained by cyclically permuting c_1'', c_1', c_1 and c_2.

The proof is not substantially different than the proof of Lemma 10.8, so we leave it as an exercise to the reader.

This is a free offprint provided to the author by the publisher. Copyright restrictions may apply.

This is a free offprint provided to the author by the publisher. Copyright restrictions may apply.

CHAPTER 11

Holomorphic triangles and nearest point maps

In this chapter, we consider Heegaard triples where one set of attaching curves is obtained via a small isotopy of another. We show that in favorable circumstances, the counts of holomorphic triangles are appropriately simple. The main result is known to experts. An extremely similar statement and argument was given in a closely related context by Lipshitz, Ozsváth and Thurston [**LOT16**, Section 3.4], on which our argument is modeled.

PROPOSITION 11.1. *Suppose that* $(\Sigma, \boldsymbol{\alpha}', \boldsymbol{\alpha}, \boldsymbol{\beta})$ *is a Heegaard triple and* $\boldsymbol{\alpha}'$ *are Hamiltonian isotopies of* $\boldsymbol{\alpha}$*, such that*

$$|\alpha' \cap \alpha| = 2\delta_{ij}.$$

If $\boldsymbol{\alpha}'$ *are sufficiently close to* $\boldsymbol{\alpha}$*, then the holomorphic triangle map* $f_{\alpha',\alpha,\beta}(\Theta^+_{\alpha',\alpha}, -)$ *counts only small triangles, and is equal to the nearest point map.*

11.1. Vertex multiplicities

We now review some basic facts about the domains of triangle classes. Suppose that $(\Sigma, \boldsymbol{\gamma}_1, \boldsymbol{\gamma}_2, \boldsymbol{\gamma}_3)$ is a Heegaard triple. If $\psi \in \pi_2(\mathbf{x}, \mathbf{y}, \mathbf{z})$ is a homology class of triangles, then we write $D(\psi)$ for the *domain* of ψ, which is an integral 2-chain on Σ, with boundary on $\boldsymbol{\gamma}_1 \cup \boldsymbol{\gamma}_2 \cup \boldsymbol{\gamma}_3$.

The domain $D(\psi)$ satisfies *vertex relations* at the intersection points on the Heegaard diagram, which we now describe. Suppose $x \in \Sigma$ is in the intersection of a curve in $\boldsymbol{\gamma}_j$ and a curve in $\boldsymbol{\gamma}_k$. We can label the multiplicities of the four quadrants near x by a, b, c and d, as shown in Figure 11.1.

The vertex relations are

$$a + d = c + b + \delta_x(\mathbf{x}) + \delta_x(\mathbf{y}) - \delta_x(\mathbf{z}),$$

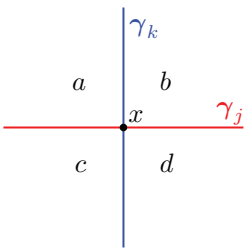


FIGURE 11.1. Multiplicities near an intersection point x. We assume $j < k$.

This is a free offprint provided to the author by the publisher. Copyright restrictions may apply.

where

$$\delta_x(\mathbf{x}) = \begin{cases} 1 & \text{if } x \in \mathbf{x} \\ 0 & \text{otherwise,} \end{cases}$$

and similarly for $\delta_x(\mathbf{y})$ and $\delta_x(\mathbf{z})$.

Any domain which satisfies the vertex relations is a homology class of triangles.

11.2. Approximating triangle classes

Suppose $(\boldsymbol{\alpha}', \boldsymbol{\alpha}, \boldsymbol{\beta})$ is a Heegaard triple where $\boldsymbol{\alpha}'$ consists of Hamiltonian isotopies of $\boldsymbol{\alpha}$, satisfying

$$|\alpha_i' \cap \alpha_j| = 2\delta_{ij}.$$

We assume all intersections of the attaching curves are transverse. Furthermore, we assume that each curve in $\boldsymbol{\beta}$ intersects the small regions between α_k and α_k' in a collection of arcs which each connect α_k and α_k'.

If $\mathbf{x} \in \mathbb{T}_\alpha \cap \mathbb{T}_\beta$, then there is a nearest point $\mathbf{x}_{np} \in \mathbb{T}_{\alpha'} \cap \mathbb{T}_\beta$. Given a homology class of triangles $\psi \in \pi_2(\Theta, \mathbf{x}, \mathbf{y}_{np})$, there is a unique domain $D_{\mathrm{app}}(\psi)$ on $(\Sigma, \boldsymbol{\alpha}, \boldsymbol{\beta})$ which agrees with $D(\psi)$ outside of the regions between $\boldsymbol{\alpha}$ and $\boldsymbol{\alpha}'$.

The following is a straightforward computation:

LEMMA 11.2. *If $\mathbf{x} \in \mathbb{T}_\alpha \cap \mathbb{T}_\beta$ and $\Theta \in \mathbb{T}_{\alpha'} \cap \mathbb{T}_\alpha$, and $\psi \in \pi_2(\Theta, \mathbf{x}, \mathbf{y}_{np})$, then the domain $D_{\mathrm{app}}(\psi)$ satisfies the vertex relations for a class in $\pi_2(\mathbf{x}, \mathbf{y})$.*

Hence, $D_{\mathrm{app}}(\psi)$ determines a class of disks $\psi_{\mathrm{app}} \in \pi_2(\mathbf{x}, \mathbf{y})$. The following index formula is key to proving Proposition 11.1:

LEMMA 11.3. *Suppose that $(\Sigma, \boldsymbol{\alpha}', \boldsymbol{\alpha}, \boldsymbol{\beta}, w)$ is a Heegaard triple, and $\boldsymbol{\alpha}'$ are small Hamiltonian isotopies of $\boldsymbol{\alpha}$, as above. Let $\psi \in \pi_2(\Theta, \mathbf{x}, \mathbf{y}_{np})$ be a homology class of triangles, and $\psi_{\mathrm{app}} \in \pi_2(\mathbf{x}, \mathbf{y})$ be its approximation. Then*

$$\mu(\psi_{\mathrm{app}}) = \mu(\psi) + \mathrm{gr}(\Theta^+_{\alpha',\alpha}, \Theta).$$

PROOF. Firstly, it is sufficient to show the claim when $\Theta = \Theta^+_{\alpha',\alpha}$, since the general claim follows by splicing bigons into ψ to reduce to this case. Hence, we assume $\Theta = \Theta^+_{\alpha',\alpha}$.

Noting that $\psi_{\mathrm{app}} \in \pi_2(\mathbf{x}, \mathbf{y})$, we may splice to obtain a triangle class

$$\psi_0 := \psi - \psi_{\mathrm{app}} \in \pi_2(\Theta^+_{\alpha',\alpha}, \mathbf{y}, \mathbf{y}_{np}). \tag{11.1}$$

The class ψ_0 is supported in the regions between $\boldsymbol{\alpha}$ and $\boldsymbol{\alpha}'$. The difference between ψ_0 and a canonical small triangle class is a doubly periodic domain which is contained in the region between $\boldsymbol{\alpha}$ and $\boldsymbol{\alpha}'$. See Figure 11.2. Such doubly periodic domains have index 0, so

$$\mu(\psi_0) = 0.$$

Using additivity of the index and (11.1), we obtain $\mu(\psi) = \mu(\psi_0)$, completing the proof. □

In Figure 11.3, we give an example of a Maslov index 0 class of triangles whose approximation is a Maslov index 1 class of disks.

This is a free offprint provided to the author by the publisher. Copyright restrictions may apply.

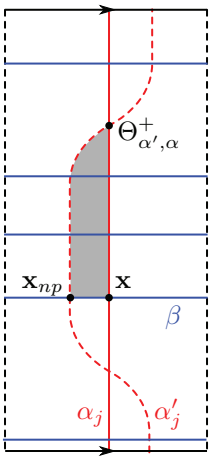


FIGURE 11.2. A small triangle class.

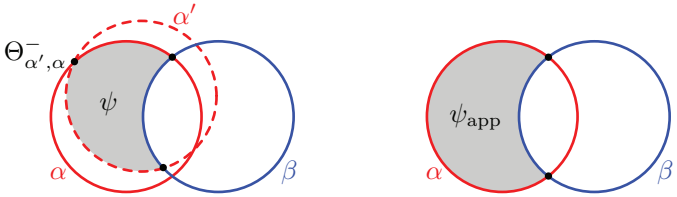


FIGURE 11.3. A Maslov index 0 triangle class (left), whose approximation has Maslov index 1 (right). Note that the triangle has a vertex at $\Theta^-_{\alpha',\alpha}$, and not $\Theta^+_{\alpha',\alpha}$.

11.3. Proof of Proposition 11.1

PROOF. The proof follows from essentially the same argument as [**LOT16**, Lemma 3.38], as we now sketch. Let $\boldsymbol{\alpha}'_i$ be a sequence of Hamiltonian translates of $\boldsymbol{\alpha}$, each of which is sufficiently close to $\boldsymbol{\alpha}$ for the nearest point map to be well defined, and such that $\boldsymbol{\alpha}'_i \to \boldsymbol{\alpha}'$ as $i \to \infty$.

By picking $\boldsymbol{\alpha}_i$ suitably, we may assume that the sets of homology classes of triangles on $(\Sigma, \boldsymbol{\alpha}'_i, \boldsymbol{\alpha}, \boldsymbol{\beta})$ are canonically identified for different i. Let Θ^+_i denote the top intersection point of $\mathbb{T}_{\alpha'_i} \cap \mathbb{T}_\alpha$. Suppose that $\mathbf{y}'_i \in \mathbb{T}_{\alpha'_i} \cap \mathbb{T}_\beta$ are similarly identified, and $\mathbf{x} \in \mathbb{T}_\alpha \cap \mathbb{T}_\beta$. Suppose that $\psi \in \pi_2(\Theta^+_i, \mathbf{x}, \mathbf{y}'_i)$ is a Maslov index 0 class of triangles, which has a holomorphic representative for all i.

Let us label the edges of the triangle Δ as $e_{\alpha'}$, e_α and e_β. Analogously to the argument in [**LOT16**, Lemma 3.38], we may extract a Gromov limit of u_i, consisting of a collection of curves mapping into $\Sigma \times \Delta$, with boundary on $\boldsymbol{\alpha} \times e_{\alpha'}$, $\boldsymbol{\alpha} \times e_\alpha$ and $\boldsymbol{\beta} \times e_\beta$, as well as a collection of curves mapping into $\Sigma \times [0,1] \times \mathbb{R}$, corresponding to the three cylindrical ends. We organize all of the components whose sources are not closed, and which project non-constantly to Δ into a collection u. If u is a J-holomorphic curve mapping into $\Sigma \times \Delta$ (or $\Sigma \times [0,1] \times \mathbb{R}$) for some J satisfying (J-1)–(J-5), and $\pi_\Delta \circ u$ is locally non-constant, then it follows from [**Lip06**, Lemma 3.1] that $\pi_\Delta \circ u$ is an open map (in the notation therein, $\Sigma \times \Delta$ is

This is a free offprint provided to the author by the publisher. Copyright restrictions may apply.

E and Σ is B). Hence any closed components or components with constant projection to Σ contribute domain $k[\Sigma]$ for some $k \in \mathbb{Z}$. Positivity of intersections implies that $k \geq 0$. Similarly, the curves mapping into the cylindrical ends also have to consist of curves satisfying (M-1)–(M-7), as well as curves whose domain consists of nonnegative multiples of $[\Sigma]$. Using transversality for holomorphic disks, we may conclude that curves mapping into $\Sigma \times [0,1] \times \mathbb{R}$ have nonnegative Maslov index.

We may view the curve u, mapping into $\Sigma \times \Delta$, as instead mapping into $\Sigma \times [0,1] \times \mathbb{R} \setminus \Sigma \times \{(1,0)\}$, with additional punctures which are asymptopic to points along $\boldsymbol{\alpha} \times \{(1,0)\}$. Using removal of singularities [**MS12**, Theorem 4.1.2], u may be completed over $\Sigma \times \{(1,0)\}$, to obtain a holomorphic curve mapping into $\Sigma \times [0,1] \times \mathbb{R}$, satisfying ($M$-1)–($M$-7). We write u also for this holomorphic curve. We write ϕ_0 for the class of u. The domain of ϕ_0 differs from ψ_{app} by $k[\Sigma]$, for some $k \geq 0$, as well as a collection of disk classes corresponding to the curves in the α-β and α'-β cylindrical ends of $\Sigma \times \Delta$, which have nonnegative Maslov index. By Lemma 11.3, $\mu(\psi_{\mathrm{app}}) = 0$. We conclude that $\mu(\phi_0) \leq 0$, with equality if and only if the remaining classes have trivial domain. Since ϕ_0 has a holomorphic representative, $\phi(\phi_0) \geq 0$. Transversality considerations imply that ϕ_0 has trivial domain, and that the remaining curves also have trivial domain.

It follows that the original triangle class ψ had domain supported in the thin regions between $\boldsymbol{\alpha}'$ and $\boldsymbol{\alpha}$, and consequently must be a small triangle class. On the other hand, it is straightforward to enumerate small triangles by hand, and see that the count of small triangles gives exactly the nearest point map. It follows that $f_{\alpha',\alpha,\beta}(\Theta^+_{\alpha',\alpha}, -)$ is the nearest point map. □

Remark 11.4. The nearest point count of Proposition 11.1 will be used in the construction of the central hypercube in Sections 16 and 19. We note that a result of Lipshitz [**Lip06**, Proposition 11.4] implies that the nearest point map is chain homotopic to the transition map obtained by counting triangles. It is possible to describe our argument without the nearest point map counts, by adding these homotopies as length 2 maps in the central hypercube. However, a tradeoff to including these homotopies in the central hypercube is a further increase in complexity of the hypercube in Section 19. Hence, we opt to use the nearest point map to simplify the presentation.

11.4. Small isotopies and Heegaard quadruples

Proposition 11.1 has a natural analog for higher counts of holomorphic curves, and the proof is essentially the same.

Proposition 11.5. *Suppose that $(\Sigma, \boldsymbol{\alpha}', \boldsymbol{\alpha}, \boldsymbol{\beta}, \boldsymbol{\gamma}, w)$ is a Heegaard quadruple such that $\boldsymbol{\alpha}'$ are small Hamiltonian translates of $\boldsymbol{\alpha}$, satisfying*

$$|\alpha' \cap \alpha| = 2\delta_{ij}.$$

If $\boldsymbol{\alpha}'$ are sufficiently small translates of $\boldsymbol{\alpha}$, then for a suitable family of almost complex structures on $\Sigma \times \square$, we have $h_{\alpha',\alpha,\beta,\gamma;\mathfrak{s}}(\Theta^+_{\alpha',\alpha}, \mathbf{x}, \mathbf{y}) = 0$, for all $\mathbf{x}$ and $\mathbf{y}$. In fact, the moduli spaces counted by $h_{\alpha',\alpha,\beta,\gamma;\mathfrak{s}}(\Theta^+_{\alpha',\alpha}, \mathbf{x}, \mathbf{y})$ are empty.

The proof of Proposition 11.5 is largely the same as the proof of Proposition 11.1, as we sketch presently. We consider a sequence $\boldsymbol{\alpha}'_i$ which approaches $\boldsymbol{\alpha}$. The moduli space of rectangles may be identified with the moduli space of triangles

This is a free offprint provided to the author by the publisher. Copyright restrictions may apply.

with an extra marked point on one of the boundary components. Hence, from a sequence of Maslov index -1 rectangles which have boundary on $\boldsymbol{\alpha}'_i$, $\boldsymbol{\alpha}$, $\boldsymbol{\beta}$ and $\boldsymbol{\gamma}$, we may extract a Gromov limit, which consists of a broken triangle on $(\Sigma, \boldsymbol{\alpha}, \boldsymbol{\beta}, \boldsymbol{\gamma}, w)$, with Maslov index -1. Generically, no such triangles exist, by transversality, so the moduli spaces counted by $h_{\alpha'_i,\alpha,\beta,\gamma;\mathfrak{s}}(\Theta^+_{\alpha'_i,\alpha}, \mathbf{x}, \mathbf{y})$ must be empty for large i.

This is a free offprint provided to the author by the publisher. Copyright restrictions may apply.

This is a free offprint provided to the author by the publisher. Copyright restrictions may apply.

CHAPTER 12

Input from Ozsváth and Szabó's surgery exact sequence

In this chapter, we review some background on Ozsváth and Szabó's surgery exact sequence [**OS08b**]. In particular, we describe the maps which appear along the top and bottom faces of our main hypercube.

12.1. Surgery quadruples

DEFINITION 12.1. Suppose K is a null-homologous knot in a 3-manifold Y. We say a doubly pointed Heegaard quadruple $(\Sigma, \boldsymbol{\alpha}_3, \boldsymbol{\alpha}_2, \boldsymbol{\alpha}_1, \boldsymbol{\beta}, w, z)$ is an $(n, n+m, \infty)$-*surgery quadruple diagram* for (Y, K) if the following are satisfied:

(D-1) We can write

$$\boldsymbol{\alpha}_1 = \boldsymbol{\alpha} \cup \{c_1\}, \quad \boldsymbol{\alpha}_2 = \boldsymbol{\alpha}' \cup \{c_2\}, \quad \text{and} \quad \boldsymbol{\alpha}_3 = \boldsymbol{\alpha}'' \cup \{c_3\},$$

where $\boldsymbol{\alpha}$, $\boldsymbol{\alpha}'$ and $\boldsymbol{\alpha}''$ are pairwise Hamiltonian translates of each other. Furthermore,

$$|\alpha_i \cap \alpha'_j| = |\alpha'_i \cap \alpha''_j| = |\alpha_i \cap \alpha''_j| = 2\delta_{ij}.$$

(D-2) There is a once punctured torus $F \subseteq \Sigma$, which contains c_1, c_2 and c_3 and is disjoint from $\boldsymbol{\alpha}$, $\boldsymbol{\alpha}'$ and $\boldsymbol{\alpha}''$. We call F the *surgery region*.

(D-3) The diagram $(\Sigma, \boldsymbol{\alpha}_1, \boldsymbol{\beta}, w, z)$ represents a doubly based unknot in $Y_n(K)$. Furthermore, w and z are immediately adjacent.

(D-4) The diagram $(\Sigma, \boldsymbol{\alpha}_2, \boldsymbol{\beta}, w, z)$ represents a doubly based unknot in $Y_{n+m}(K)$. Furthermore, w and z are immediately adjacent.

(D-5) The diagram $(\Sigma, \boldsymbol{\alpha}_3, \boldsymbol{\beta}, w, z)$ represents K in Y, decorated with two basepoints.

(D-6) The curves c_1, c_2 and c_3 may be oriented so that

$$\#(c_1 \cap c_2) = m, \quad \text{and} \quad \#(c_2 \cap c_3) = \#(c_3 \cap c_1) = 1.$$

See Figure 12.1 for a schematic of the surgery region of Σ.

12.2. Heegaard Floer homology of lens spaces

In this section, we recall some facts about the Floer homology of lens spaces, which Ozsváth and Szabó use to build their exact sequence in [**OS08b**].

DEFINITION 12.2. View $L(m,1)$ as the boundary of a disk bundle $D(m,1)$ over S^2 with Euler number m. The *canonical* Spin^c *structure*, $\mathfrak{s}_0 \in \text{Spin}^c(L(m,1))$, is the restriction to $L(m,1)$ of the two Spin^c structures $\mathfrak{t} \in \text{Spin}^c(D(m,1))$ satisfying

$$\langle c_1(\mathfrak{t}), S^2 \rangle = \pm m.$$

This is a free offprint provided to the author by the publisher. Copyright restrictions may apply.

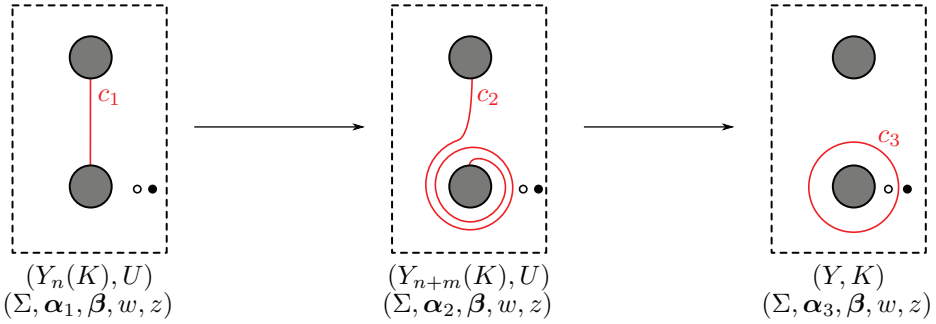


FIGURE 12.1. The genus 1 surgery region of an $(n, n+m, \infty)$-surgery quadruple $(\Sigma, \boldsymbol{\alpha}_3, \boldsymbol{\alpha}_2, \boldsymbol{\alpha}_1, \boldsymbol{\beta}, w, z)$. The curves $\boldsymbol{\beta}$ are not shown.

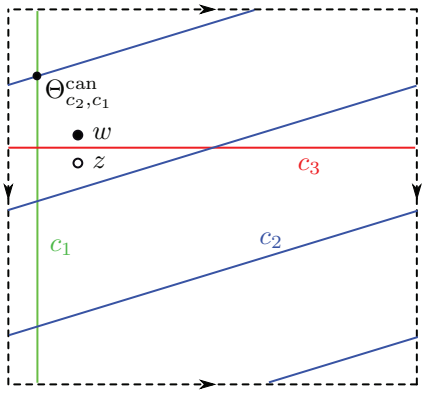


FIGURE 12.2. The triple $(\mathbb{T}^2, c_3, c_2, c_1, w, z)$. The generator of the canonical Spin^c structure is labeled.

The Floer homology of a lens space has a simple form:

$$HF^-(L(m,1), \mathfrak{s}) \cong \mathbb{F}[U],$$

for each $\mathfrak{s} \in \mathrm{Spin}^c(L(m,1))$. We write Θ^{can} for the generator of $HF^-(L(m,1), \mathfrak{s}_0)$.

12.3. Cobordism maps for disk bundles over S^2

Let m be a positive integer. We recall that the induced map on Heegaard Floer homology for $-m$ surgery on an unknot has a simple form. See [**OS08b**, Section 3]. The blow-up formula corresponds to $m = 1$ [**OS06**, Theorem 3.7].

LEMMA 12.3. *Let $(\mathbb{T}^2, c_3, c_2, c_1, w, z)$ denote the genus 1 Heegaard triple shown in Figure 12.2. The twisted triangle map satisfies*

$$f_{c_3,c_2,c_1;\mathfrak{s}_k^{\pm}}(\Theta_{c_3,c_2}, \Theta^{\mathrm{can}}_{c_2,c_1}) = U^{mk(k+1)/2} \cdot T^0 \cdot \Theta_{c_3,c_1},$$

where $\mathfrak{s}_k^{\pm}$ satisfies $\langle c_1(\mathfrak{s}_k^{\pm}), S\rangle = \pm(2k+1)m$, for $k \geq 0$. In particular, the sum over all $\mathfrak{s}_k^+$ and $\mathfrak{s}_k^-$ is 0.

This is a free offprint provided to the author by the publisher. Copyright restrictions may apply.

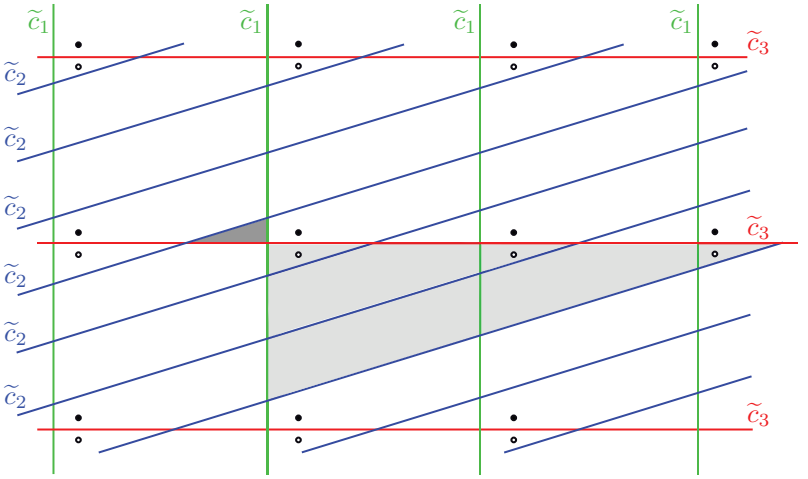


FIGURE 12.3. The universal cover of Figure 12.2, as well as the lifts of two triangle classes. The curves $\widetilde{c}_1$, $\widetilde{c}_2$ and $\widetilde{c}_3$ are the lifts of c_1, c_2 and c_3.

PROOF. A holomorphic triangle counted by $f_{c_3,c_2,c_1,\mathfrak{s}_k^{\pm}}$ may be lifted to the universal cover of $\mathbb{T}^2$, where the count is easy to perform. See Figure 12.3. □

It will sometimes be helpful to index Spin^c structures by the odd integers $s \in 2\mathbb{Z}+1$. If u_s denotes the triangle representing the Spin^c structure with $\langle c_1(\mathfrak{s}), S\rangle = sm$, then one may compute directly that

$$n_w(u_s) = \frac{m(s^2-1)}{8} \quad \text{and} \quad n_z(u_s) = \frac{m((s+2)^2-1)}{8}.$$

12.4. The length 1 maps on the top and bottom of the main hypercube

We now describe the length 1 maps along the top and bottom of the involutive hypercube of a triad in Theorem 1.14. Suppose that $(\Sigma, \boldsymbol{\alpha}_3, \boldsymbol{\alpha}_2, \boldsymbol{\alpha}_1, \boldsymbol{\beta}, w, z)$ is an $(n, n+m, \infty)$ surgery quadruple for $K \subseteq Y$. We will write $f^{\beta}_{\alpha_1\to\alpha_2}$ for the map labeled f_1 in Theorem 1.14, which we define to be

$$f^{\beta}_{\alpha_1\to\alpha_2}(\mathbf{x}) = \sum_{\substack{\mathbf{y}\in\mathbb{T}_{\alpha_2}\cap\mathbb{T}_{\beta}\\ \psi\in\pi_2(\Theta^{\mathrm{can}}_{\alpha_2,\alpha_1},\mathbf{x},\mathbf{y})\\ \mu(\psi)=0}} \#\mathcal{M}(\psi)\cdot U^{n_w(\psi)}\cdot\mathbf{y},$$

extended equivariantly over the action of U.

Similarly, we write $f^{\beta}_{\alpha_2\to\alpha_3}$ for the map labeled f_2, which we define as

$$f^{\beta}_{\alpha_2\to\alpha_3}(\mathbf{x}) = \sum_{\substack{\mathbf{y}\in\mathbb{T}_{\alpha_3}\cap\mathbb{T}_{\beta}\\ \psi\in\pi_2(\Theta^{+}_{\alpha_3,\alpha_2},\mathbf{x},\mathbf{y})\\ \mu(\psi)=0}} \#\mathcal{M}(\psi)\cdot U^{n_w(\psi)}T^{n_z(\psi)-n_w(\psi)}\cdot\mathbf{y}.$$

If we wish to emphasize the almost complex structure, we will write

$${}^{J}f^{\beta}_{\alpha_1\to\alpha_2} \quad \text{and} \quad {}^{J}f^{\beta}_{\alpha_2\to\alpha_3}.$$

This is a free offprint provided to the author by the publisher. Copyright restrictions may apply.

12.5. The length 2 maps along the top and bottom of the main hypercube

The following is a well known fact about Heegaard Floer homology; see, e.g., [**OS08b**]:

LEMMA 12.4. *Suppose that* $(\Sigma, \boldsymbol{\alpha}_3, \boldsymbol{\alpha}_2, \boldsymbol{\alpha}_1, \boldsymbol{\beta}, w, z)$ *is an* $(n, n+m, \infty)$*-surgery quadruple. Let* S *denote the boundary of the surgery region. If* $J = (J_t)_{t\in[0,1]}$ *is a stratified family of almost complex structures on* $\Sigma \times \square$ *which is maximally pinched along* S*, then the diagram in* (12.1) *is a 2-dimensional hypercube of chain complexes:*

$$\begin{array}{ccc} \boldsymbol{CF}^-_J(\boldsymbol{\alpha}_1, \boldsymbol{\beta}) & & \\ \Big\downarrow {\scriptstyle {}^J f^{\beta}_{\alpha_1\to\alpha_2}} & \searrow {\scriptstyle {}^J h^{\beta}_{\alpha_1\to\alpha_2\to\alpha_3}} & \\ \boldsymbol{CF}^-_J(\boldsymbol{\alpha}_2, \boldsymbol{\beta}) & \xrightarrow{{}^J f^{\beta}_{\alpha_2\to\alpha_3}} & \underline{\boldsymbol{CF}}^-_J(\boldsymbol{\alpha}_3, \boldsymbol{\beta}). \end{array} \tag{12.1}$$

Here ${}^J h^{\beta}_{\alpha_1\to\alpha_2\to\alpha_3}$ *denotes the twisted rectangle counting map*

$${}^J h^{\beta}_{\alpha_1\to\alpha_2\to\alpha_3}(\mathbf{x}) := h^J_{\alpha_3,\alpha_2,\alpha_1,\beta}(\Theta^+_{\alpha_3,\alpha_2}, \Theta^{\mathrm{can}}_{\alpha_2,\alpha_1}, \mathbf{x}).$$

PROOF. Using the associativity relations for quadrilaterals, it is sufficient to show

$$f^J_{\alpha_3,\alpha_2,\alpha_1}(\Theta^+_{\alpha_3,\alpha_2}, \Theta^{\mathrm{can}}_{\alpha_2,\alpha_1}) = 0. \tag{12.2}$$

Equation (12.2) is proven as follows. Write $\boldsymbol{\alpha}_3 = \{c_3\} \cup \boldsymbol{\alpha}''$, $\boldsymbol{\alpha}_2 = \{c_2\} \cup \boldsymbol{\alpha}'$ and $\boldsymbol{\alpha}_1 = \{c_1\} \cup \boldsymbol{\alpha}$, where $\boldsymbol{\alpha}$, $\boldsymbol{\alpha}'$ and $\boldsymbol{\alpha}''$ are small Hamiltonian translates of each other. Using Proposition 10.2 we obtain

$$f^J_{\alpha_3,\alpha_2,\alpha_1}(\Theta^+_{\alpha_3,\alpha_2}, \Theta^{\mathrm{can}}_{\alpha_2,\alpha_1}) = f^J_{c_3,c_2,c_1}(\Theta^+_{c_3,c_2}, \Theta^{\mathrm{can}}_{c_2,c_1}) \otimes \Theta^+_{\alpha'',\alpha},$$

which implies (12.2) when combined with Lemma 12.3. □

REMARK 12.5. Lemma 12.4 holds without the family J being maximally pinched, though the proof is easier if we assume that J is maximally pinched. Despite being unnecessary for Lemma 12.4, the maximally pinched condition makes the construction of other portions of the main hypercube substantially easier. As a specific example, see the change of almost complex structure hypercube in Section 13, where the maximally pinched condition prevents curves from appearing along the left side of Figure 13.1.

12.6. Heegaard quadruples related to disk bundles

Analogous to Lemma 12.3, we will need a model count of holomorphic rectangles appearing on quadruples related to those in Figure 12.3.

LEMMA 12.6. *Suppose that* $\mathcal{Q} = (\mathbb{T}^2, c_3, c_2, c_1, c_1', w, z)$ *is the quadruple obtained from the triple* $(\mathbb{T}^2, c_3, c_2, c_1, w, z)$ *shown in Figure* 12.2 *by adding a curve* c_1' *which is a small Hamiltonian translate of* c_1*, and intersects* c_1 *in two points. Then*

$$h_{\mathcal{Q};\mathfrak{s}}(\Theta_{c_3,c_2}, \Theta^{\mathrm{can}}_{c_2,c_1}, \Theta^+_{c_1,c_1'}) = 0,$$

This is a free offprint provided to the author by the publisher. Copyright restrictions may apply.

for all $\mathfrak{s} \in \mathrm{Spin}^c(X_{c_3,c_2,c_1,c_1'})$. *In fact, there are no classes of index* -1 *in*

$$\pi_2(\Theta_{c_3,c_2}, \Theta^{\mathrm{can}}_{c_2,c_1'}, \Theta^+_{c_1,c_1'}, \Theta_{c_3,c_1'}).$$

Analogous claims hold for the quadruples $(\mathbb{T}^2, c_3, c_2', c_2, c_1)$ *and* $(\mathbb{T}^2, c_3', c_3, c_2, c_1)$.

PROOF. First, we note that if we fill the (c_3, c_2), (c_1, c_1') and (c_3, c_1') ends of $X_{c_3,c_2,c_1,c_1'}$ with 3- and 4-handles, we obtain a disk bundle over S^2 with Euler number $-m$. Hence, there is a natural isomorphism between the Spin^c structures on $X_{c_3,c_2,c_1,c_1'}$ which have torsion restrictions to the boundary, and $\mathrm{Spin}^c(D(-m,1))$. Hence, writing $\mathfrak{s}_k^{\pm}$ for the Spin^c structures in Lemma 12.4, we have that

$$h_{\mathbb{Q};\mathfrak{s}_k^{\pm}}(\Theta_{c_3,c_2}, \Theta^{\mathrm{can}}_{c_2,c_1}, \Theta^+_{c_1,c_1'})$$

is of homogeneous grading

$$-mk(k+1)+1,$$

which is always odd. However $CF^-(\mathbb{T}^2, c_3, c_1) \cong \mathbb{F}[U]$ is supported in even gradings, so we conclude that $h_{\mathbb{Q};\mathfrak{s}}(\Theta_{c_3,c_2}, \Theta^{\mathrm{can}}_{c_2,c_1}, \Theta^+_{c_1,c_1'}) = 0$ for all $\mathfrak{s}$ (and in fact, there are no rectangle classes of index -1 spanning the given intersection points). □

This is a free offprint provided to the author by the publisher. Copyright restrictions may apply.

This is a free offprint provided to the author by the publisher. Copyright restrictions may apply.

CHAPTER 13

Hypercubes for changing the almost complex structure

We now construct a 3-dimensional hypercube for changing the almost complex structure. We can think of this 3-dimensional hypercube as relating the 2-dimensional ones considered in Lemma 12.4, for different 1-dimensional families of almost complex structures.

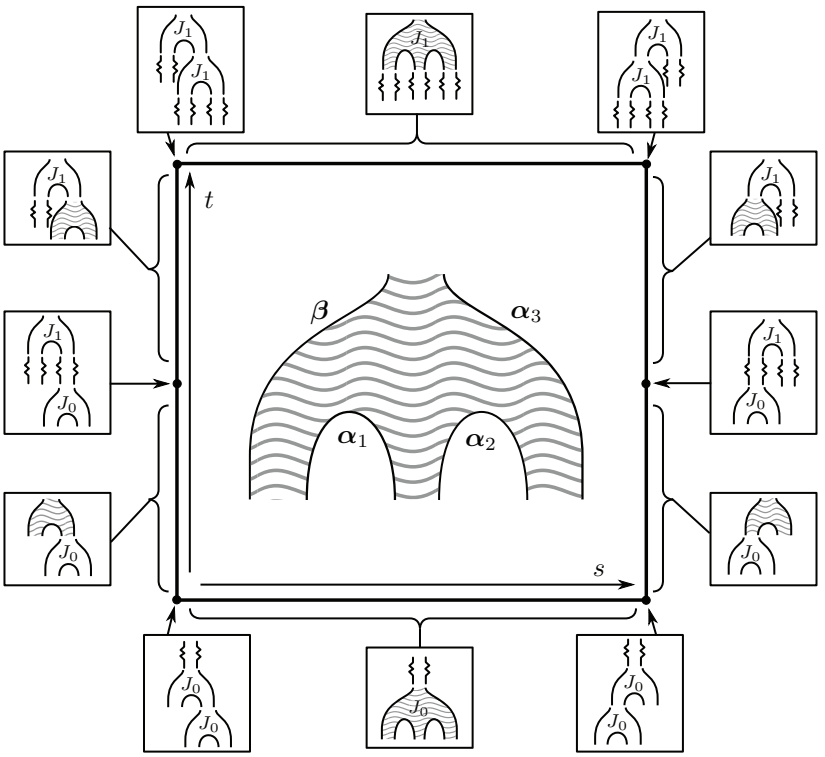
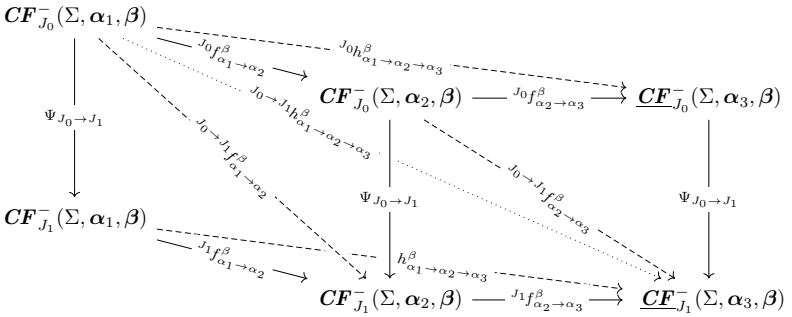


FIGURE 13.1. A 2-parameter stratified family $(J_{s,t})_{(s,t)\in[0,1]\times[0,1]}$ of almost complex structures on $\Sigma \times \square$ used to relate two 1-parameter families of almost complex structures. The behavior of $J_{s,t}$ along the codimension 1 and 2 strata is illustrated. Wavy gray lines along the interior of an n-gon indicate where the almost complex structure may vary along a given strata. Wavy boundary lines indicate non-cylindrical almost complex structures on $\Sigma\times[0,1]\times\mathbb{R}$.

This is a free offprint provided to the author by the publisher. Copyright restrictions may apply.

LEMMA 13.1. *Suppose* $(\Sigma, \boldsymbol{\alpha}_3, \boldsymbol{\alpha}_2, \boldsymbol{\alpha}_1, \boldsymbol{\beta}, w, z)$ *is an* $(n, n+m, \infty)$*-surgery quadruple for a knot* $K \subseteq Y$*, and* $J_0 = (J_{s,0})_{s\in[0,1]}$ *and* $J_1 = (J_{s,1})_{s\in[0,1]}$ *are two stratified families of almost complex structures on* $\Sigma \times \square$*, for counting holomorphic rectangles, which are maximally pinched along the boundary of the surgery region. There are maps which make the following diagram a hypercube of chain complexes:*

(13.1)



PROOF. We pick a family $\widetilde{J} = (J_{s,t})_{(s,t)\in[0,1]\times[0,1]}$ which has the schematic behavior illustrated in Figure 13.1, and which is maximally pinched along S.

In equation (13.1), $\Psi_{J_0\to J_1}$ counts index 0 holomorphic strips for a non-cylindrical almost complex structure (the choice of non-cylindrical almost complex structure is determined by the value of $J_{s,t}$ on the codimension 1 strata of $[0,1] \times [0,1]$). Similarly, the maps ${}^{J_0\to J_1}f^{\beta}_{\alpha_1\to\alpha_2}$ and ${}^{J_0\to J_1}f^{\beta}_{\alpha_2\to\alpha_3}$ count index -1 triangles which are $J_{s,t}$-holomorphic for (s,t) in a particular subset of $\partial([0,1]\times[0,1])$, and ${}^{J_0\to J_1}h^{\beta}_{\alpha_1\to\alpha_2\to\alpha_3}$ counts index -2, $J_{s,t}$-holomorphic rectangles, for $(s,t) \in (0,1)\times(0,1)$.

The length 0, 1 and 2 hypercube relations are easy to verify, so we focus on the length 3 relation. If $\psi \in \pi_2(\Theta^+_{\alpha_3,\alpha_2}, \Theta^{\mathrm{can}}_{\alpha_2,\alpha_1}, \mathbf{x})$ is a Maslov index -1 class of rectangles on the quadruple $(\Sigma, \boldsymbol{\alpha}_3, \boldsymbol{\alpha}_2, \boldsymbol{\alpha}_1, \boldsymbol{\beta})$, then we consider the 1-dimensional moduli space of rectangles

$$\mathcal{M}_{\widetilde{J}}(\psi) := \bigcup_{(s,t)\in(0,1)\times(0,1)} \mathcal{M}_{J_{s,t}}(\psi) \times \{(s,t)\}. \tag{13.2}$$

The boundary of the compactification of $\mathcal{M}_{\widetilde{J}}(\psi)$ consists of the following broken curves:

(1) An index 1 holomorphic strip in one of the cylindrical ends, and an index -2, $J_{s,t}$-holomorphic quadrilateral for some $(s,t) \in (0,1)\times(0,1)$.
(2) A broken curve consisting of $J_{s,t}$-holomorphic curves for (s,t) in the codimension 1 strata of $[0,1]\times[0,1]$. Such a curve consists of an index -1 curve in the portion with interior wavy lines in Figure 13.1, and index 0 curves in all of the remaining regions.

The count of the ends of the moduli spaces $\mathcal{M}_{\widetilde{J}}(\psi)$ at $(s,t) \in (0,1)\times(0,1)$ give

$$\left[\partial, {}^{J_0\to J_1}h^{\beta}_{\alpha_1\to\alpha_2\to\alpha_3}\right](\mathbf{x}). \tag{13.3}$$

Ends of $\mathcal{M}_{\widetilde{J}}(\psi)$ which occur along $\{1\}\times(0,1)$ contribute the expression

$$\left({}^{J_0\to J_1}f^{\beta}_{\alpha_2\to\alpha_3} \circ {}^{J_0}f^{\beta}_{\alpha_1\to\alpha_2} + {}^{J_1}f^{\beta}_{\alpha_2\to\alpha_3} \circ {}^{J_0\to J_1}f^{\beta}_{\alpha_1\to\alpha_2}\right)(\mathbf{x}). \tag{13.4}$$

Ends which occur along $(0,1)\times\{0,1\}$ contribute

$$\left(\Psi_{J_0\to J_1} \circ {}^{J_0}h^{\beta}_{\alpha_1\to\alpha_2\to\alpha_3} + {}^{J_1}h^{\beta}_{\alpha_1\to\alpha_2\to\alpha_3} \circ \Psi_{J_0\to J_1}\right)(\mathbf{x}). \tag{13.5}$$

This is a free offprint provided to the author by the publisher. Copyright restrictions may apply.

The sum of equations (13.3), (13.4) and (13.5) is exactly the length 3 hypercube relation, so it remains to show that the count of ends appearing along $\{0\} \times (0,1)$ make no total contribution.

The ends appearing along $\{0\} \times (0,1/2)$ contribute

$$f^{J_0 \to J_1}_{\alpha_3,\alpha_1,\beta}\left(f^{J_0}_{\alpha_3,\alpha_2,\alpha_1}\left(\Theta^{+}_{\alpha_3,\alpha_2}, \Theta^{\mathrm{can}}_{\alpha_2,\alpha_1}\right), \mathbf{x}\right).$$

Proposition 10.2 implies

$$f^{J_0}_{\alpha_3,\alpha_2,\alpha_1}\left(\Theta^{+}_{\alpha_3,\alpha_2}, \Theta^{\mathrm{can}}_{\alpha_2,\alpha_1}\right) = f_{c_3,c_3,c_1}\left(\Theta^{+}_{c_3,c_2}, \Theta^{\mathrm{can}}_{c_2,c_1}\right) \otimes \Theta_{\alpha'_3,\alpha'_1}, \tag{13.6}$$

where $\boldsymbol{\alpha}'_i = \boldsymbol{\alpha}_i \setminus \{c_i\}$. By Lemma 12.3, the right side of equation (13.6) vanishes. Hence the count of curves along $\{0\} \times (0,1/2)$ makes no total contribution.

We now consider the ends which occur along $\{0\} \times (1/2,1)$, which contribute the expression

$$f^{J_1}_{\alpha_3,\alpha_1,\beta}\left(f^{J_0 \to J_1}_{\alpha_3,\alpha_2,\alpha_1}\left(\Theta^{+}_{\alpha_3,\alpha_2}, \Theta^{\mathrm{can}}_{\alpha_2,\alpha_1}\right), \Psi_{J_0 \to J_1}(\mathbf{x})\right).$$

We claim that

$$f^{J_0 \to J_1}_{\alpha_3,\alpha_2,\alpha_1}\left(\Theta^{+}_{\alpha_3,\alpha_2}, \Theta^{\mathrm{can}}_{\alpha_2,\alpha_1}\right) = 0. \tag{13.7}$$

By definition, $f^{J_0 \to J_1}_{\alpha_3,\alpha_2,\alpha_1}(\Theta^{+}_{\alpha_3,\alpha_2}, \Theta^{\mathrm{can}}_{\alpha_2,\alpha_1})$ counts index -1, matched triangles over a 1-parameter family of almost complex structures. Since the family $\widetilde{J}$ is maximally pinched, the $(\boldsymbol{\alpha}_3, \boldsymbol{\alpha}_2, \boldsymbol{\alpha}_1)$-component of the family $(J_{0,t})_{t\in[0,1]}$ has infinite neck length along S, i.e., it is the wedge of a family $(I_t)_{t\in[0,1]}$ on $\Sigma \times \Delta$, and a family $(I'_t)_{t\in[0,1]}$ on $\mathbb{T}^2 \times \Delta$, and by construction, the moduli spaces appearing along $\{0\} \times (0,1)$ are fibered products over the evaluation map at the connected sum point, as well as the parameter $t \in [0,1]$. We claim that the matched moduli spaces counted by $f^{J_0 \to J_1}_{\alpha_3,\alpha_2,\alpha_1}(\Theta^{+}_{\alpha_3,\alpha_2}, \Theta^{\mathrm{can}}_{\alpha_2,\alpha_1})$ are always empty. To see this, suppose that $(\psi, \psi_0) \in \pi_2(\Theta^{+}_{\alpha'',\alpha'}, \Theta^{+}_{\alpha',\alpha}, \mathbf{z}) \times \pi_2(\Theta_{c_3,c_2}, \Theta^{\mathrm{can}}_{c_2,c_1}, \Theta_{c_3,c_1})$ is a pair of classes, which have the same multiplicity at the connected sum point. The matched index is given by

$$\mathrm{ind}_{\mathrm{emb}}(\psi, \psi_0, M_{\#}) = \mu(\psi_0) + \mathrm{gr}(\Theta^{+}_{\alpha'',\alpha}, \mathbf{z}) \tag{13.8}$$

Transversality for the family I_s implies that if (ψ, ψ_0) has a matched representative, then $\mu(\psi_0) \geq -1$. Hence equation (13.8) implies that if (ψ, ψ_0) has a representative and $\mathrm{ind}_{\mathrm{emb}}(\psi, \psi_0, M_{\#}) = -1$, then

$$\mu(\psi_0) = -1 \quad \text{and} \quad \mathbf{z} = \Theta^{+}_{\alpha'',\alpha}.$$

However the diagram $(\mathbb{T}^2, c_3, c_2, c_1)$ has only triangles of even index, so $\mu(\psi_0) \neq -1$. Hence

$$f^{J_0 \to J_1}_{\alpha_3,\alpha_2,\alpha_1}\left(\Theta^{+}_{\alpha_3,\alpha_2}, \Theta^{\mathrm{can}}_{\alpha_2,\alpha_1}\right) = 0,$$

implying equation (13.7), and completing the proof. □

This is a free offprint provided to the author by the publisher. Copyright restrictions may apply.

This is a free offprint provided to the author by the publisher. Copyright restrictions may apply.

CHAPTER 14

Hypercubes for stabilization

We now describe 3-dimensional hypercubes for stabilization and destabilization. Suppose that

$$\mathcal{Q} = (\Sigma, \boldsymbol{\alpha}_3, \boldsymbol{\alpha}_2, \boldsymbol{\alpha}_1, \boldsymbol{\beta}, w, z) \quad \text{and} \quad \mathcal{Q}_0 = (\Sigma_0, \boldsymbol{\xi}, \boldsymbol{\zeta}, \boldsymbol{\sigma}, \boldsymbol{\tau}, p_0)$$

are Heegaard quadruples, such that $\mathcal{Q}$ is an $(n, n+m, \infty)$-surgery quadruple, as in Definition 12.1, and $\mathcal{Q}_0$ is a multi-stabilizing Heegaard quadruple, as defined in Chapter 9. In this chapter, we describe a 3-dimensional hypercube of chain complexes relating the 2-dimensional hypercubes for $\mathcal{Q}$ and $\mathcal{Q}\#\mathcal{Q}_0$.

The hypercube for stabilization is constructed as the compression of two hypercubes:

(1) A *singular stabilization hypercube*, which involves stabilizing using singularized almost complex structures.
(2) A *desingularization hypercube*, which is a combination of the change of almost complex structure hypercube from Chapter 13, and the transition maps for desingularizing the almost complex structure from Lemma 8.2.

14.1. Singular stabilization hypercubes

We first construct a stabilization hypercube relating $\mathcal{Q}$ and $\mathcal{Q}\#\mathcal{Q}_0$ which involves singular almost complex structures.

Let $J = (J_s)_{s\in[0,1]}$ be a stratified family of almost complex structures on $\Sigma \times \square$, for counting rectangles, which is maximally pinched along ∂F, where $F \subseteq \Sigma$ denotes the surgery region. Let $I = (I_s)_{s\in[0,1]}$ be a stratified family of maximally pinched almost complex structures on $\Sigma_0 \times \square$, for counting rectangles. We write $J \wedge I = (J_s \wedge I_s)_{s\in[0,1]}$ for the wedge product family. We will always assume that the almost complex structures are split in a neighborhood of the connected sum points.

Similar to section 8.2, we may define the matched moduli spaces of triangles and rectangles. The matched moduli spaces of triangles may be defined by an easy adaptation of the construction for disks, in (8.1). The matched moduli space of rectangles is defined similarly, however we also require the rectangles to be matched with respect to the aspect ratio parameter. More concretely, if $S^{\mathbf{q}}$ and $S_0^{\mathbf{q}_0}$ are two source curves for rectangles, and ψ and ψ_0 are two classes of rectangles on $\mathcal{Q}$ and

This is a free offprint provided to the author by the publisher. Copyright restrictions may apply.

$\mathcal{Q}_0$, then we define the matched moduli space of rectangles to be

(14.1)

$$\mathcal{MM}_{J\wedge I}(S^{\mathbf{q}}, S_0^{\mathbf{q}_0}, \psi, \psi_0)$$
$$:= \left\{ (u, s, u_0, s_0) \in \mathcal{M}_J(S^{\mathbf{q}}, \phi) \times \mathcal{M}_I(S_0^{\mathbf{q}_0}, \psi_0) \;\middle|\; \begin{array}{c} (\pi_\Sigma \circ u)(q_i) = p, \\ (\pi_{\Sigma_0} \circ u_0)(q_{0,i}) = p_0, \\ (\pi_\square \circ u)(q_i) = (\pi_\square \circ u)(q_{i,0}), \\ \text{for } i = 1, \dots, k, \\ s = s_0 \end{array} \right\}$$

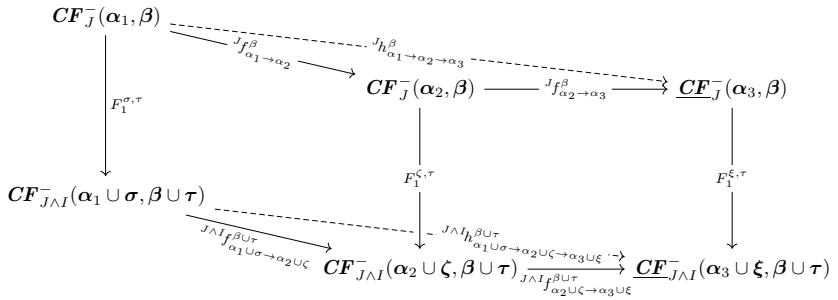
We write $\mathcal{MM}_{J\wedge I}(\psi, \psi_0)$ for the disjoint union of the moduli spaces in (14.1), over pairs of equivalence classes of marked sources.

Recall that in Section 9.4, to a multi-stabilizing quadruple $\mathcal{Q}_0$, we associated a 4-tuple of integers $\mathbf{m}(\mathcal{Q}_0) = (m_1(\mathcal{Q}_0), m_2(\mathcal{Q}_0), m_3(\mathcal{Q}_0), m_4(\mathcal{Q}_0))$, which we called the *index tuple*.

LEMMA 14.1. *Suppose $\mathcal{Q} = (\Sigma, \boldsymbol{\alpha}_3, \boldsymbol{\alpha}_2, \boldsymbol{\alpha}_1, \boldsymbol{\beta}, w, z)$ is an $(n, n+m, \infty)$-surgery quadruple, with genus 1 surgery region bounded by a curve S, and $\mathcal{Q}_0 = (\Sigma_0, \boldsymbol{\xi}, \boldsymbol{\zeta}, \boldsymbol{\sigma}, \boldsymbol{\tau}, \mathbf{p}_0)$ is a multi-stabilization quadruple, satisfying*

$$m_4(\mathcal{Q}_0) = 0.$$

Suppose $J = (J_s)_{s\in[0,1]}$ and $I = (I_s)_{s\in[0,1]}$ are stratified families of almost complex structures on $\Sigma \times \square$ and $\Sigma_0 \times \square$, both for counting rectangles, and J is maximally pinched along S. The following diagram is a hypercube:



PROOF. We verify the hypercube relations. The length 0 hypercube relations are immediate. We now consider the length 1 hypercube relations. For the horizontal length 1 maps, the hypercube relations follow by counting the ends of moduli spaces of triangles of index 1. For the vertical length 1 maps, the hypercube relations follow from Lemma 10.1.

We now consider the length 2 relations. Lemma 12.4 imples that ${}^J h^{\beta}_{\alpha_1\to\alpha_2\to\alpha_3}$ is a null-homotopy of ${}^J f^{\beta}_{\alpha_2\to\alpha_3} \circ {}^J f^{\beta}_{\alpha_1\to\alpha_2}$. The same argument, applied to matched triangles and rectangles, implies that ${}^{J\wedge I} h^{\beta\cup\tau}_{\alpha_1\cup\sigma\to\alpha_2\cup\zeta\to\alpha_3\cup\xi}$ is a null-homotopy of ${}^{J\wedge I} f^{\beta\cup\tau}_{\alpha_2\cup\zeta\to\alpha_3\cup\xi} \circ {}^{J\wedge I} f^{\beta\cup\tau}_{\alpha_1\cup\sigma\to\alpha_2\cup\zeta}$. Additionally, we need to show that

$$\begin{aligned} F_1^{\zeta,\tau} \circ {}^J f^{\beta}_{\alpha_1\to\alpha_2} &= {}^{J\wedge I} f^{\beta\cup\tau}_{\alpha_1\cup\sigma\to\alpha_2\cup\zeta} \circ F_1^{\sigma,\tau}, \quad \text{and} \\ F_1^{\sigma,\tau} \circ {}^J f^{\beta}_{\alpha_2\to\alpha_3} &= {}^{J\wedge I} f^{\beta\cup\tau}_{\alpha_2\cup\zeta\to\alpha_3\cup\xi} \circ F_1^{\zeta,\tau}. \end{aligned} \tag{14.2}$$

By hypothesis, $m_4(\mathcal{Q}_0) = 0$. By Lemma 9.9, we have

$$m_4(\mathcal{Q}) = m_3(\mathcal{T}_{\zeta,\sigma,\tau}) + m_3(\mathcal{T}_{\xi,\zeta,\tau}). \tag{14.3}$$

This is a free offprint provided to the author by the publisher. Copyright restrictions may apply.

Using Lemma 9.7 and (14.3), we obtain

$$0 = m_3(\mathcal{T}_{\zeta,\sigma,\tau}) = m_3(\mathcal{T}_{\xi,\zeta,\tau}).$$

Proposition 10.2 now gives (14.2).

Lastly, we consider the length 3 hypercube relation. The length 3 hypercube relation is equivalent to

$$F_1^{\xi,\tau} \circ {}^{J}h^{\beta}_{\alpha_1\to\alpha_2\to\alpha_3} = {}^{J\wedge I}h^{\beta\cup\tau}_{\alpha_1\cup\sigma\to\alpha_2\cup\zeta\to\alpha_3\cup\xi} \circ F_1^{\xi,\tau},$$

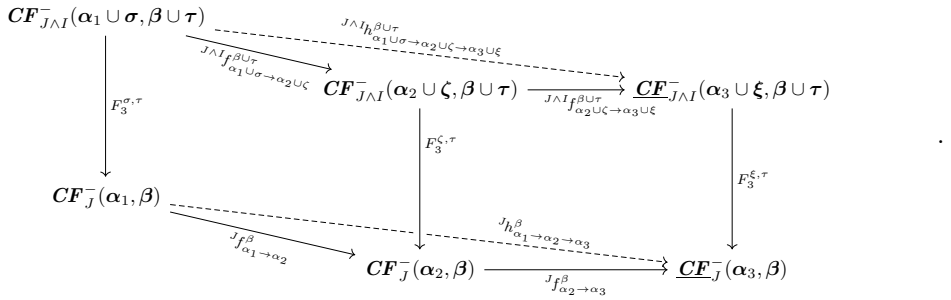
which follows from Proposition 10.6. □

Dually, we obtain the following:

LEMMA 14.2. *Suppose that $\mathcal{Q} = (\Sigma, \boldsymbol{\alpha}_3, \boldsymbol{\alpha}_2, \boldsymbol{\alpha}_1, \boldsymbol{\beta}, w, z)$ is an $(n, n+m, \infty)$-surgery quadruple, with a genus 1 surgery region bounded by the curve S. Suppose that $\mathcal{Q}_0 = (\Sigma_0, \boldsymbol{\xi}, \boldsymbol{\zeta}, \boldsymbol{\sigma}, \boldsymbol{\tau}, \mathbf{p}_0)$ is a multi-stabilizing quadruple with*

$$m_3(\mathcal{Q}_0) = 0.$$

Suppose $J = (J_s)_{s\in[0,1]}$ is a family of almost complex structures on $\Sigma \times \square$ which is maximally pinched along S, and $I = (I_s)_{s\in[0,1]}$ is a family of almost complex structures on $\Sigma_0 \times \square$, both for counting holomorphic rectangles. The following diagram is a hypercube of chain complexes



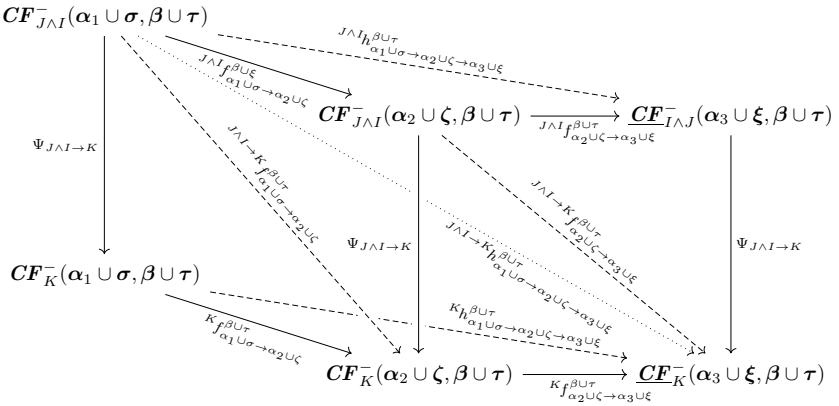
14.2. Desingularization hypercubes

In Section 14.1 we described a hypercube for stabilization which involved matched moduli spaces (i.e. fibered products along evaluation maps). We now relate construct a hypercube which relates the singular almost complex structures to ordinary ones:

LEMMA 14.3. *Suppose that $\mathcal{Q} = (\Sigma, \boldsymbol{\alpha}_3, \boldsymbol{\alpha}_2, \boldsymbol{\alpha}_1, \boldsymbol{\beta}, \mathbf{w})$ is an $(n, n+m, \infty)$ surgery quadruple, with a genus 1 surgery region bounded by a curve S, and $\mathcal{Q}_0 = (\Sigma_0, \boldsymbol{\xi}, \boldsymbol{\zeta}, \boldsymbol{\sigma}, \boldsymbol{\tau}, p)$ is a multi-stabilizing Heegaard quadruple. Suppose that $J = (J_s)_{s\in[0,1]}$ and $I = (I_s)_{s\in[0,1]}$ are stratified families of almost complex structures on $\Sigma \times \square$ and $\Sigma_0 \times \square$, and J is maximally pinched along S. Suppose further that $K = (K_s)_{s\in[0,1]}$ is a family of almost complex structure on $\Sigma\#\Sigma_0 \times \square$ which is maximally pinched along S. Then there is a stratified family of almost complex structures $L = (L_{s,t})_{(s,t)\in[0,1]\times[0,1]}$ on $\Sigma\#\Sigma_0 \times \square$, whose associated moduli spaces*

This is a free offprint provided to the author by the publisher. Copyright restrictions may apply.

give the following hypercube of chain complexes:



PROOF. The proof follows from the same reasoning as the proof of Lemma 13.1, which covers more general changes of the almost complex structure. □

By stacking and compressing the hypercubes in Lemmas 14.1 and 14.3, we obtain the general hypercube for stabilization. Dualizing, as in Lemma 14.2, yields a hypercube for destabilization.

This is a free offprint provided to the author by the publisher. Copyright restrictions may apply.

CHAPTER 15

The first 2-handle hypercube

We now construct the first 2-handle hypercube, $\mathcal{C}^1_{2\text{-h}}$. For all of the complexes appearing in this hypercube, we use the underlying Heegaard surface $\Sigma\#\overline{\Sigma}$. We make the following definitions:

- We write $D(F)$ for the genus 2 subset of $\Sigma\#\overline{\Sigma}$ consisting of the surgery region on Σ, and its image on $\overline{\Sigma}$.
- We write $\boldsymbol{\Delta} \subseteq \Sigma\#\overline{\Sigma}$ for a collection of curves which are obtained by doubling a basis of arcs $d_1, \dots, d_{2g}$ for $H_1(\Sigma \setminus N(w), I; \mathbb{Z})$. Furthermore, we assume that $\boldsymbol{\Delta}$ is adapted to $\boldsymbol{\alpha}_3$, in the sense of Definition 6.6.
- We write Δ_1 and Δ_2 for the two curves of $\boldsymbol{\Delta}$ which are in $D(F)$. And we write $\hat{\boldsymbol{\Delta}}$ for $\boldsymbol{\Delta} \setminus \{\Delta_1, \Delta_2\}$.

We consider the pentuple

$$\mathcal{P} = \left(\Sigma\#\overline{\Sigma}, \boldsymbol{\alpha}_3 \cup \overline{\boldsymbol{\beta}}''', \boldsymbol{\alpha}_2 \cup \overline{\boldsymbol{\beta}}'', \boldsymbol{\alpha}_1 \cup \overline{\boldsymbol{\beta}}', \boldsymbol{\beta} \cup \overline{\boldsymbol{\beta}}, \boldsymbol{\Delta}, w\right),$$

where $\overline{\boldsymbol{\beta}}$, $\overline{\boldsymbol{\beta}}'$, $\overline{\boldsymbol{\beta}}''$, $\overline{\boldsymbol{\beta}}'''$ are small Hamiltonian translates.

LEMMA 15.1. *If $\boldsymbol{\beta}$ are sufficiently wound on Σ (with the winding also performed on $\overline{\boldsymbol{\beta}}$ and its small translates), and Δ_1 and Δ_2 are sufficiently wound on $D(F)$, then $\mathcal{P}$ is weakly admissible.*

PROOF. Let $\Pi^{\mathbb{Q}}_{\mathcal{P}}$ denote the set of rational periodic domains on $\mathcal{P}$. Let $\Pi^{\mathbb{Q}}_{\mathcal{P},L}$ denote the set of periodic domains with boundary equal to a rational linear combination of the curves in

$$\boldsymbol{\alpha} \cup \{c_1, c_2, c_3\} \cup \boldsymbol{\beta} \cup \overline{\boldsymbol{\beta}} \cup \boldsymbol{\Delta}.$$

(That is, we remove all but one curve in any collection of pairwise isotopic curves). There is a canonical map

$$L\colon \Pi^{\mathbb{Q}}_{\mathcal{P}} \to \Pi^{\mathbb{Q}}_{\mathcal{P},L}.$$

The map L is clearly surjective. See Figure 15.1 for a schematic of L.

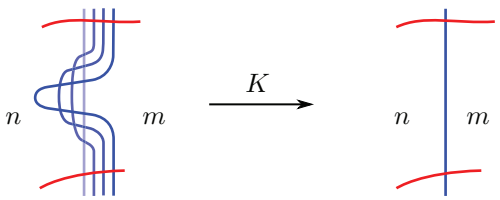


FIGURE 15.1. A schematic of the homomorphism L. The isotopic curves denote $\overline{\boldsymbol{\beta}}$, $\overline{\boldsymbol{\beta}}'$, $\overline{\boldsymbol{\beta}}''$ and $\overline{\boldsymbol{\beta}}'''$. The numbers n and m denote the multiplicities of a domain D. On the right is the domain $L(D)$.

This is a free offprint provided to the author by the publisher. Copyright restrictions may apply.

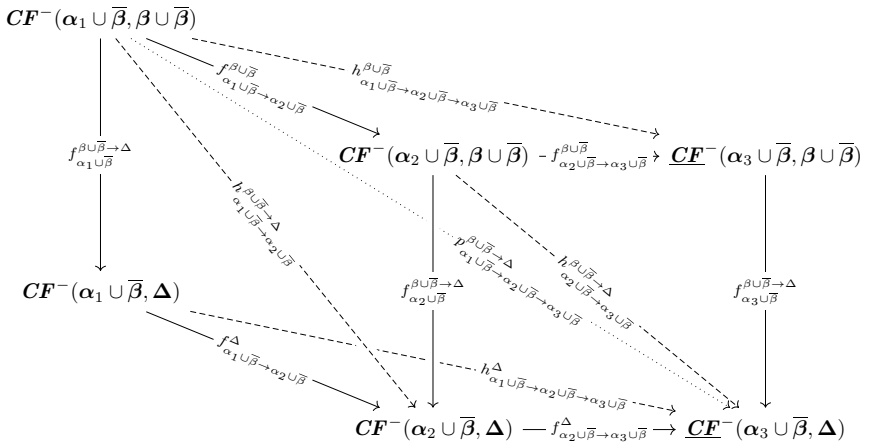


FIGURE 15.2. The hypercube $\mathcal{C}^1_{2\text{-h}}$. The Heegaard surface is $\Sigma\#\overline{\Sigma}$, for all Floer complexes. We have dropped the primes on the various copies of $\overline{\boldsymbol{\beta}}$, to simplify the notation.

We will show that every non-zero element of $\Pi^{\mathbb{Q}}_{\mathcal{P},L}$ has both positive and negative multiplicities. This will imply that any nonnegative periodic domains in $\Pi^{\mathbb{Q}}_{\mathcal{P}}$ must be in the kernel of L. By picking the small Hamiltonian translations which appear in the construction of $\mathcal{P}$ appropriately, one can ensure that any elements in the kernel of L have both positive and negative multiplicities, which will imply the desired result.

By applying the same argument as in Lemma 6.5, for sufficiently wound $\boldsymbol{\beta}$, $\overline{\boldsymbol{\beta}}$, Δ_1 and Δ_2 it is sufficient to show that there are no non-zero periodic domains in $\Pi^{\mathbb{Q}}_{\mathcal{P},L}$ with only nonnegative coefficients, whose boundary is a linear combination of only the curves in $\boldsymbol{\alpha} \cup \{c_1, c_2, c_3\} \cup \hat{\boldsymbol{\Delta}}$. Write $\Pi^{\mathbb{Q}}_{\boldsymbol{\alpha}\cup\{c_1,c_2,c_3\}\cup\hat{\Delta}}$ for the set of such periodic domains.

Note that $\{c_1, c_2, c_3\}$ are contained on a genus 1 summand of $\Sigma\#\overline{\Sigma}$, and $\boldsymbol{\alpha} \cup \hat{\boldsymbol{\Delta}}$ are contained on a disjoint, genus $2g-2$ summand. Hence the subspace $\mathrm{Span}([c_1], [c_2], [c_3]) \in H_1(\Sigma\#\overline{\Sigma}; \mathbb{Q})$ has trivial intersection with each of $\mathrm{Span}([\alpha] : \alpha \in \boldsymbol{\alpha})$ and $\mathrm{Span}([\Delta] : \Delta \in \hat{\boldsymbol{\Delta}})$. Furthermore, the subspaces $\mathrm{Span}([\alpha] : \alpha \in \boldsymbol{\alpha})$ and $\mathrm{Span}([\Delta] : \Delta \in \hat{\boldsymbol{\Delta}})$ have trivial intersection in $H_1(\Sigma\#\overline{\Sigma}; \mathbb{Q})$ by the definition of a doubled diagram. Since $\mathrm{Span}([\alpha] : \alpha \in \boldsymbol{\alpha})$ and $\mathrm{Span}([\Delta] : \Delta \in \hat{\boldsymbol{\Delta}})$ each have dimension $|\boldsymbol{\alpha}|$ and $|\hat{\boldsymbol{\Delta}}|$, it follows that an element of $\Pi^{\mathbb{Q}}_{\boldsymbol{\alpha}\cup\{c_1,c_2,c_3\}\cup\hat{\Delta}}$ must have boundary equal to a linear combination of the curves c_1, c_2 and c_3, so $\Pi^{\mathbb{Q}}_{\boldsymbol{\alpha}\cup\{c_1,c_2,c_3\}\cup\hat{\Delta}}$ is naturally isomorphic to $\Pi^{\mathbb{Q}}_{\{c_1,c_2,c_3\}}$. The main claim now follows from the fact that the diagram $(\mathbb{T}^2, c_3, c_2, c_1, w)$ is weakly admissible, as can be seen by explicit examination of the diagram in Figure 12.2. □

Using the pentuple $\mathcal{P}$, we build the hypercube $\mathcal{C}^1_{2\text{-h}}$, as shown in Figure 15.2.

PROPOSITION 15.2. *The diagram $\mathcal{C}^1_{2\text{-h}}$ is a hypercube of chain complexes.*

This is a free offprint provided to the author by the publisher. Copyright restrictions may apply.

PROOF. The hypercube $\mathcal{C}^1_{2\text{-h}}$ may equivalently be described as the pairing of the following two hypercubes of attaching curves:
(15.1)

$$\mathcal{L}_\alpha := \begin{array}{c} \boldsymbol{\alpha}_1 \cup \overline{\boldsymbol{\beta}}' \\ \Big\downarrow {\scriptstyle \Theta^{\mathrm{can}}_{\boldsymbol{\alpha}_2 \cup \overline{\boldsymbol{\beta}}'', \boldsymbol{\alpha}_1 \cup \overline{\boldsymbol{\beta}}'}} \\ \boldsymbol{\alpha}_2 \cup \overline{\boldsymbol{\beta}}'' \end{array} \qquad \mathcal{L}_\beta := \boldsymbol{\beta} \cup \overline{\boldsymbol{\beta}} \xrightarrow{\Theta^+_{\boldsymbol{\beta} \cup \overline{\boldsymbol{\beta}}, \boldsymbol{\Delta}}} \boldsymbol{\Delta}.$$

$$\boldsymbol{\alpha}_2 \cup \overline{\boldsymbol{\beta}}'' \xrightarrow{\Theta^+_{\boldsymbol{\alpha}_3 \cup \overline{\boldsymbol{\beta}}''', \boldsymbol{\alpha}_2 \cup \overline{\boldsymbol{\beta}}''}} \boldsymbol{\alpha}_3 \cup \overline{\boldsymbol{\beta}}'''$$

Using Lemma 5.10, it remains only to show the hypercube relations for $\mathcal{L}_\alpha$ and $\mathcal{L}_\beta$. The only non-trivial relation is the length 2 relation for $\mathcal{L}_\alpha$, which follows from Lemma 12.4, completing the proof. □

This is a free offprint provided to the author by the publisher. Copyright restrictions may apply.

This is a free offprint provided to the author by the publisher. Copyright restrictions may apply.

CHAPTER 16

The central hypercube

In this chapter, we construct the central hypercube. We construct three hypercubes, $\mathcal{C}^{(1)}_{\text{cen}}$, $\mathcal{C}^{(2)}_{\text{cen}}$ and $\mathcal{C}^{(3)}_{\text{cen}}$, which we stack and compress to obtain a hypercube $\hat{\mathcal{C}}_{\text{cen}}$. In Section 16.6, we describe how to modify $\hat{\mathcal{C}}_{\text{cen}}$ to obtain the hypercube $\mathcal{C}_{\text{cen}}$.

16.1. Almost complex structures

Let S_1 and S_2 be the two closed curves on $\Sigma\#\overline{\Sigma}$ shown in Figure 16.1. The curve S_1 bounds the surgery region of Σ, and S_2 bounds this region as well as its image on $\overline{\Sigma}$. Throughout this section, we assume that all almost complex structures are maximally pinched along S_1 and S_2 (Definition 8.4).

16.2. Standard curves in the surgery region

We will encounter the curves c_1, c_2 and c_3 on Σ, as well as their images on $\overline{\Sigma}$. We label the curves on $\overline{\Sigma}$ by $\overline{c}_1$, $\overline{c}_2$ and $\overline{c}_3$, as shown in Figure 16.2. Note that to achieve admissibility, we do not pick $\overline{c}_i$ to be an exact mirror of c_i, but instead to have the configuration shown in Figure 16.2.

Let $\mathcal{P}_{D(F)}$ denote the set of rational 2-chains D on $D(F)$ which have boundary equal to a linear combination of the c_i and $\overline{c}_i$ curves, and which have $n_w(D) = 0$. The following lemma is helpful to achieve admissibility on the multi-diagrams appearing in the central hypercube:

LEMMA 16.1. *All non-zero domains $\mathcal{P}_{D(F)}$ have both positive and negative coefficients.*

PROOF. The proof is by direct inspection. The set of triply periodic domains in $\mathcal{P}_{D(F)}$ is isomorphic to $\mathbb{Z}\oplus\mathbb{Z}$. The first $\mathbb{Z}$ summand is supported on the left side of $D(F)$, while the second $\mathbb{Z}$ summand is supported on the right. Furthermore, both

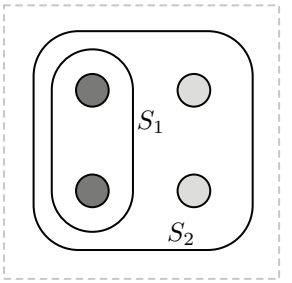


FIGURE 16.1. The closed curves S_1 and S_2, along which we assume all almost complex structures are maximally pinched (Definition 8.4).

This is a free offprint provided to the author by the publisher. Copyright restrictions may apply.

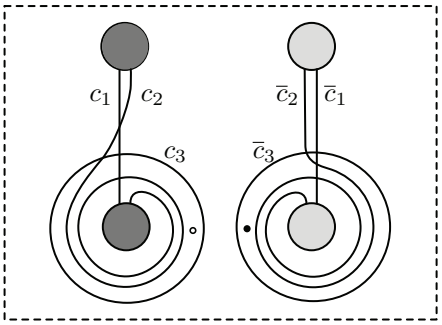


FIGURE 16.2. The curves c_1, c_2, c_3, $\overline{c}_1$, $\overline{c}_2$ and $\overline{c}_3$ in the genus 2 region $D(F)$. (Notice the slight asymmetry between the left and right hand sides). The basepoint w is the solid dot on the left, and z is the open dot on the right.

generators have both positive and negative coefficients, so any linear combination does as well. □

16.3. The hypercube $\mathcal{C}^{(1)}_{\text{cen}}$

We begin by constructing an auxiliary hypercube, $\mathcal{C}^{(1)}_{\text{aux}}$, shown in Figure 16.3, which is built from a pentuple $(\Sigma\#\overline{\Sigma}, \boldsymbol{\gamma}'', \boldsymbol{\gamma}', \boldsymbol{\gamma}, \boldsymbol{\delta}, \boldsymbol{\delta}')$. In the notation of Figure 6.3, the attaching curves of $\mathcal{P}^{(1)}$ are as follows:

- $\boldsymbol{\gamma} = \boldsymbol{\alpha}_1 \cup \overline{\boldsymbol{\beta}}$, $\boldsymbol{\gamma}' = \boldsymbol{\alpha}_2 \cup \overline{\boldsymbol{\beta}}$, and $\boldsymbol{\gamma}'' = \boldsymbol{\alpha}_3 \cup \overline{\boldsymbol{\beta}}$.
- $\boldsymbol{\delta}$ coincide with the curves $\boldsymbol{\Delta}$, described in Chapter 15.
- $\boldsymbol{\delta}'$ coincides with small translates of $\hat{\boldsymbol{\Delta}}$ outside of the special genus 2 region $D(F)$, and is equal to small translates of $c_3 \cup \overline{c}_3$ in the special genus two region.

Recall that we write Δ_1 and Δ_2 for the two curves of $\boldsymbol{\Delta}$ appearing in $D(F)$. We assume that the curves, c_1, c_2, c_3 and $\overline{c}_3$ are in standard position in $D(F)$, i.e. they appear with the configuration of Figure 12.1. The curves Δ_1 and Δ_2 will be wound in $D(F)$, so in general will not be in a simple configuration. Note that we will usually omit the winding of Δ_1 and Δ_2 from the figures.

The maps labeled in Figure 16.3 count all triangles, quadrilaterals and pentagons which have special inputs equal to cycles which induce the top graded or canonical elements of the Floer homology of $L(m,1)\#(S^1 \times S^2)^{\#k}$ or $(S^1 \times S^2)^{\#k}$. For $(\boldsymbol{\gamma}, \boldsymbol{\gamma}')$ and $(\boldsymbol{\gamma}', \boldsymbol{\gamma}'')$, the top graded and canonical cycles are each represented by a unique intersection point. For $(\boldsymbol{\delta}, \boldsymbol{\delta}')$, this will usually not be the case, since we wind $\Delta_1, \Delta_2 \subseteq D(F)$ to achieve admissibility.

LEMMA 16.2. *If $\overline{\boldsymbol{\beta}}$ are sufficiently wound on $\overline{\Sigma}$, and Δ_1 and Δ_2 are sufficiently wound in $D(F)$, then the tuple $(\Sigma\#\overline{\Sigma}, \boldsymbol{\gamma}'', \boldsymbol{\gamma}', \boldsymbol{\gamma}, \boldsymbol{\delta}, \boldsymbol{\delta}', w)$ is weakly admissible.*

PROOF. Following the proof of Lemma 15.1, if we wind $\overline{\boldsymbol{\beta}}$, Δ_1 and Δ_2 sufficiently, we reduce the main claim to showing that every non-zero rational periodic domain with boundary equal to a linear combination of the curves in $\boldsymbol{\alpha} \cup \{c_1, c_2, c_3, \overline{c}_3\} \cup \hat{\boldsymbol{\Delta}}$ has both positive and negative multiplicities. Since $\hat{\boldsymbol{\Delta}}$ are adapted to $\boldsymbol{\alpha}$, it is easy to see that this is equivalent to showing that any non-zero domain

This is a free offprint provided to the author by the publisher. Copyright restrictions may apply.

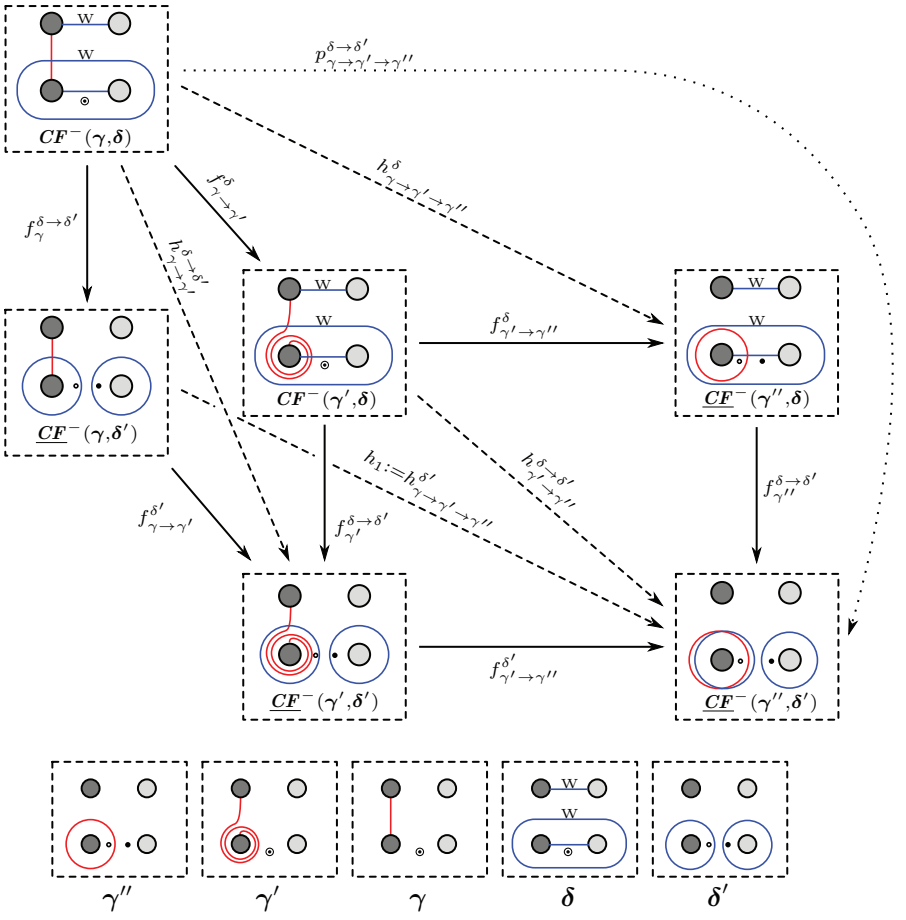


FIGURE 16.3. The auxiliary hypercube $\mathcal{C}^{(1)}_{\text{aux}}$. A W along a curve indicates that it is wound.

with equal to a linear combination of c_1, c_2, c_3, and $\overline{c}_3$ has positive and negative coefficients. This follows immediately from Lemma 16.1. □

We may equivalently think of $\mathcal{C}^{(1)}_{\text{aux}}$ as the pairing of alpha and beta hypercubes of attaching curves shown below:

$$\mathcal{L}^{(1)}_{\alpha} := \begin{array}{ccc} \boldsymbol{\gamma} & & \\ \downarrow{\scriptstyle \Theta^{\text{can}}_{\gamma',\gamma}} & & \\ \boldsymbol{\gamma}' & \xrightarrow{\Theta^{+}_{\gamma'',\gamma'}} & \boldsymbol{\gamma}'' \end{array} \qquad \mathcal{L}^{(1)}_{\beta} := \boldsymbol{\delta} \xrightarrow{\Theta^{+}_{\delta,\delta'}} \boldsymbol{\delta}' \tag{16.1}$$

LEMMA 16.3. *The diagram $\mathcal{C}^{(1)}_{\text{aux}}$ is a hypercube of chain complexes.*

PROOF. Given the description of $\mathcal{C}^{(1)}_{\text{aux}}$ as the pairing of the two diagrams in equation (16.1), by Lemma 5.10 it remains only to show that the diagrams $\mathcal{L}^{(1)}_{\alpha}$

This is a free offprint provided to the author by the publisher. Copyright restrictions may apply.

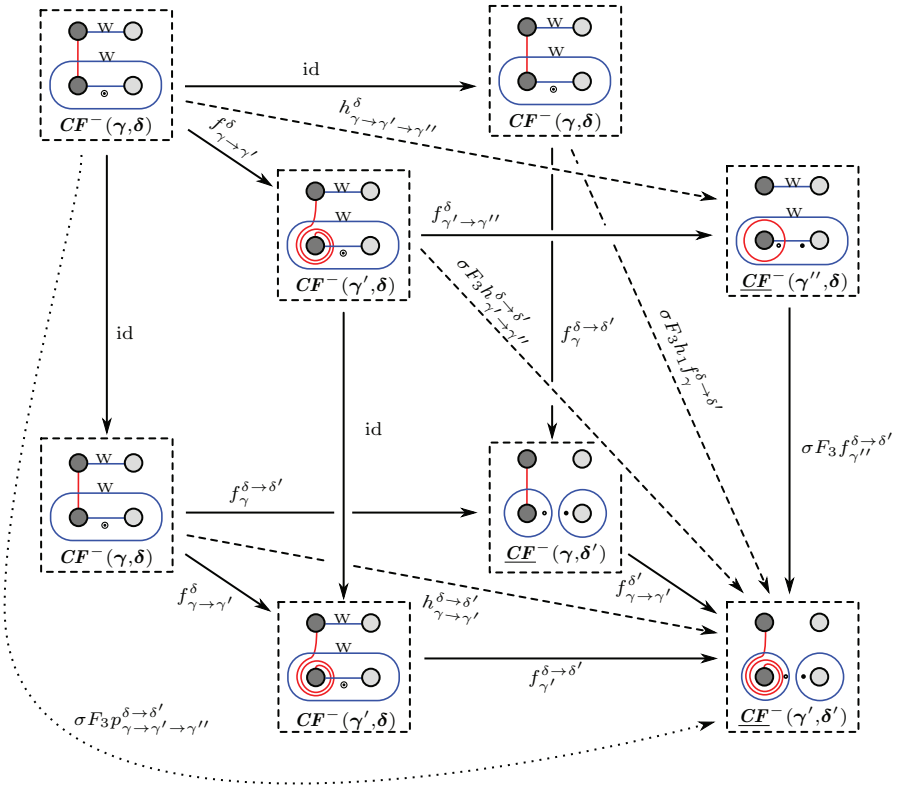


FIGURE 16.4. The hypercube $\mathcal{C}^{(1)}_{\text{cen}}$. The character W indicates winding.

and $\mathcal{L}^{(1)}_{\beta}$ are hypercubes of attaching curves. The only non-trivial relation is

$$f_{\gamma'',\gamma',\gamma}(\Theta^{+}_{\gamma'',\gamma'},\Theta^{\text{can}}_{\gamma',\gamma}) = 0,$$

which follows from Lemma 12.3. □

Let Σ_0 denote Σ with the surgery region removed, and let $\boldsymbol{\gamma}_0$ denote the curves obtained from $\boldsymbol{\gamma}'$ by removing the surgery region. Let $\boldsymbol{\delta}_0$ denote the curves on Σ_0 obtained from $\boldsymbol{\delta}'$ by removing the surgery region. There is a stabilization map on the twisted complexes

$$\sigma\colon \underline{\boldsymbol{CF}}^-(\Sigma_0\#\overline{\Sigma},\boldsymbol{\gamma}_0,\boldsymbol{\delta}_0) \to \underline{\boldsymbol{CF}}^-(\Sigma\#\overline{\Sigma},\boldsymbol{\gamma}',\boldsymbol{\delta}'),$$

defined in the same manner as on the untwisted complexes. The hypercube $\mathcal{C}^{(1)}_{\text{cen}}$ is shown in Figure 16.4.

LEMMA 16.4. *The diagram $\mathcal{C}^{(1)}_{\text{cen}}$ in Figure 16.4 is a hypercube of chain complexes.*

PROOF. Before proving the hypercube relations, we make the following claim:

$$\sigma F_3 f^{\delta'}_{\gamma'\to\gamma''} = \text{id}_{\underline{\boldsymbol{CF}}^-(\boldsymbol{\gamma}',\boldsymbol{\delta}')} \tag{16.2}$$

This is a free offprint provided to the author by the publisher. Copyright restrictions may apply.

Equation (16.2) is proven by using Proposition 10.2 to identify the composition $\sigma F_3 f^{\delta'}_{\gamma'\to\gamma''}$ with the count of triangles after destabilizing the triple for $f^{\delta'}_{\gamma'\to\gamma''}$. Proposition 11.1 identifies this count with a nearest point map.

We now verify the hypercube relations. The length 0 and 1 relations are straightforward. The length 2 relation along the left and back faces are trivial. The length 2 relation along the top face follows from Lemma 12.4. The length 2 relation along the bottom face is a consequence of the hypercube relations for $\mathcal{C}^{(1)}_{\mathrm{aux}}$.

We now consider the length 2 relation for the front face. The desired relation reads

$$\left[\partial, \sigma F_3 h^{\delta\to\delta'}_{\gamma'\to\gamma''}\right] = \sigma F_3 f^{\delta\to\delta'}_{\gamma''} f^{\delta}_{\gamma'\to\gamma''} + f^{\delta\to\delta'}_{\gamma'}. \tag{16.3}$$

To establish (16.3), we note that associativity of holomorphic rectangles gives

$$\left[\partial, h^{\delta\to\delta'}_{\gamma'\to\gamma''}\right] = f^{\delta'}_{\gamma'\to\gamma''} f^{\delta\to\delta'}_{\gamma'} + f^{\delta\to\delta'}_{\gamma''} f^{\delta}_{\gamma'\to\gamma''}. \tag{16.4}$$

We compose (16.4) with σF_3, and then apply (16.2), and immediately obtain (16.3).

Next, we verify the length 2 hypercube relation along the right face. The desired relation is

$$\left[\partial, \sigma F_3 h_1 f^{\delta\to\delta'}_{\gamma}\right] = f^{\delta'}_{\gamma\to\gamma'} f^{\delta\to\delta'}_{\gamma}. \tag{16.5}$$

To prove (16.5), we begin with by the associativity relations, applied to the map $h_1 := h^{\delta'}_{\gamma\to\gamma'\to\gamma''}$, which read

$$[\partial, h_1] = f^{\delta'}_{\gamma'\to\gamma''} f^{\delta'}_{\gamma\to\gamma'}. \tag{16.6}$$

We now postcompose (16.6) with σF_3, and precompose with $f^{\delta\to\delta'}_{\gamma}$ to obtain

$$\left[\partial, \sigma F_3 h_1 f^{\delta\to\delta'}_{\gamma}\right] = \sigma F_3 f^{\delta'}_{\gamma'\to\gamma''} f^{\delta'}_{\gamma\to\gamma'} f^{\delta\to\delta'}_{\gamma}. \tag{16.7}$$

Applying (16.2) to (16.7) gives the desired (16.5).

Finally, we note by post-composing the length 3 hypercube relation of $\mathcal{C}^{(1)}_{\mathrm{aux}}$ with σF_3, we obtain

$$\begin{aligned} &\sigma F_3 f^{\delta'}_{\gamma'\to\gamma''} h^{\delta\to\delta'}_{\gamma\to\gamma'} \\ &+\sigma F_3 f^{\delta\to\delta'}_{\gamma''} h^{\delta}_{\gamma\to\gamma'\to\gamma''} \\ &+\sigma F_3 h^{\delta\to\delta'}_{\gamma'\to\gamma''} f^{\delta}_{\gamma\to\gamma'} \\ &+\sigma F_3 h^{\delta'}_{\gamma\to\gamma'\to\gamma''} f^{\delta\to\delta'}_{\gamma} \\ &= \left[\partial, \sigma F_3 p^{\delta\to\delta'}_{\gamma\to\gamma'\to\gamma''}\right], \end{aligned} \tag{16.8}$$

which is exactly the desired length 3 relation for $\mathcal{C}^{(1)}_{\mathrm{cen}}$ (we remind the reader that $h^{\delta'}_{\gamma\to\gamma'\to\gamma''} := h_1$). □

16.4. The hypercube $\mathcal{C}^{(2)}_{\mathrm{cen}}$

We consider the attaching curves $\boldsymbol{\gamma}'$, $\boldsymbol{\gamma}$, $\boldsymbol{\delta}$, $\boldsymbol{\delta}'$, $\widetilde{\boldsymbol{\delta}}'$ and $\boldsymbol{\delta}''$, shown in Figure 16.5. We build an auxiliary hypercube $\mathcal{C}^{(2)}_{\mathrm{aux}}$, shown schematically in Figure 16.5. Using the maps therein, we build the hypercube $\mathcal{C}^{(2)}_{\mathrm{cen}}$, shown in Figure 16.7.

This is a free offprint provided to the author by the publisher. Copyright restrictions may apply.

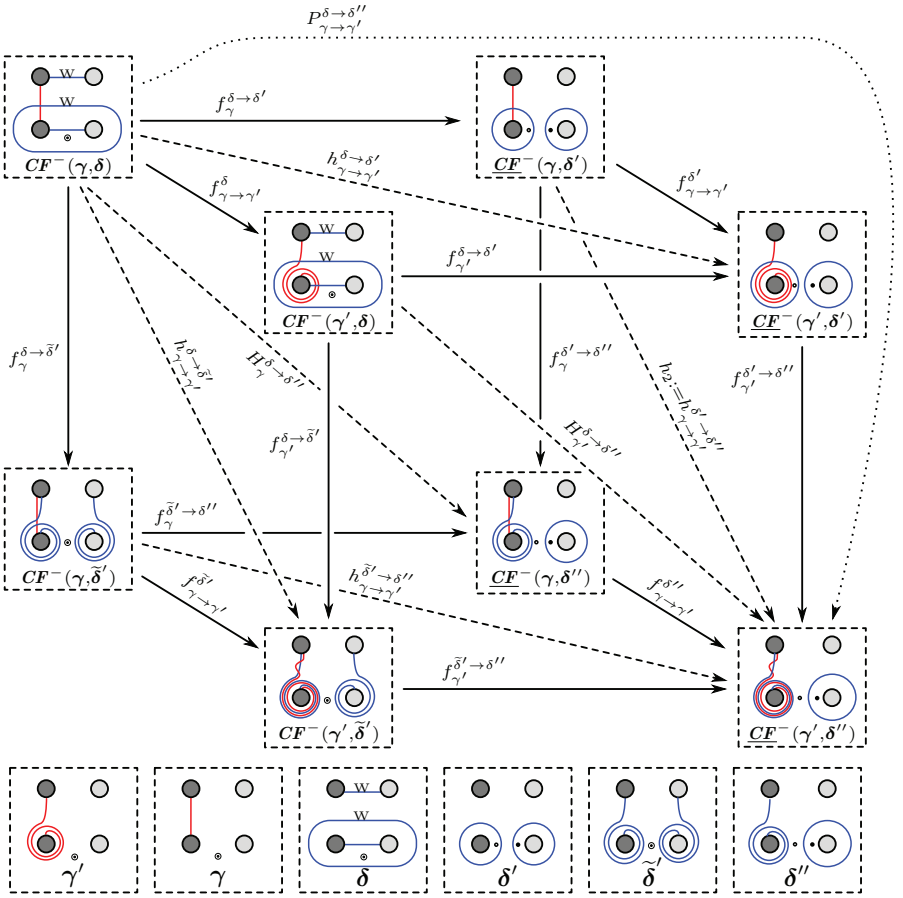


FIGURE 16.5. The auxiliary hypercube $\mathcal{C}^{(2)}_{\mathrm{aux}}$. The character W indicates winding.

LEMMA 16.5. *If $\overline{\boldsymbol{\beta}} \subseteq \overline{\Sigma}$ and $\Delta_1, \Delta_2 \subseteq D(F)$ are sufficiently wound, then the tuple*

$$(\Sigma \# \overline{\Sigma}, \boldsymbol{\gamma}', \boldsymbol{\gamma}, \boldsymbol{\delta}, \boldsymbol{\delta}', \widetilde{\boldsymbol{\delta}}', \boldsymbol{\delta}'', w)$$

is weakly admissible.

PROOF. The proof is not substantially different than the proof of Lemma 16.2. □

We will define $\mathcal{C}^{(2)}_{\mathrm{aux}}$ as the pairing of two hypercubes of attaching curves, taking the following forms:

$$\mathcal{L}^{(2)}_{\alpha} := \boldsymbol{\gamma} \xrightarrow{\Theta^{\mathrm{can}}_{\boldsymbol{\gamma}',\boldsymbol{\gamma}}} \boldsymbol{\gamma}' \quad \text{and} \quad \mathcal{L}^{(2)}_{\beta} := \begin{array}{ccc} \boldsymbol{\delta} & \xrightarrow{\Theta^+_{\delta,\delta'}} & \boldsymbol{\delta}' \\ \downarrow{\scriptstyle \Theta^+_{\delta,\widetilde{\delta}'}} & \searrow{\scriptstyle \lambda_{\delta,\delta''}} & \downarrow{\scriptstyle \Theta^+_{\delta',\delta''}} \\ \widetilde{\boldsymbol{\delta}}' & \xrightarrow{\Theta^+_{\widetilde{\delta}',\delta''}} & \boldsymbol{\delta}'' \end{array} \tag{16.9}$$

This is a free offprint provided to the author by the publisher. Copyright restrictions may apply.

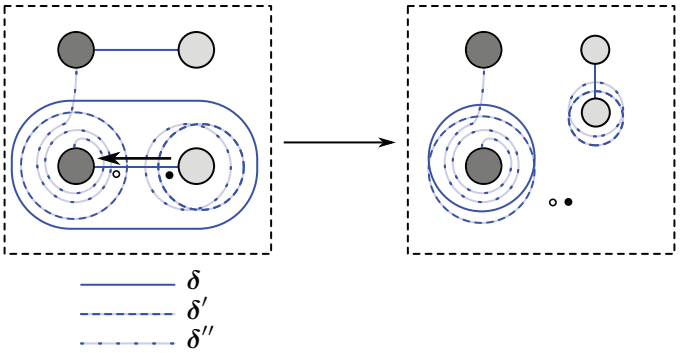


FIGURE 16.6. Manipulating the triple $(\Sigma\#\overline{\Sigma}, \boldsymbol{\delta}, \boldsymbol{\delta}', \boldsymbol{\delta}'', w, z)$. The arrow indicates that we move the bottom right handle (light gray), across the bottom left handle (dark gray), via a sequence of handleslides.

We now explain how to pick the chains appearing in (16.9). First, we pick cycles

$$\Theta^{\text{can}}_{\gamma',\gamma}, \quad \Theta^{+}_{\delta,\delta'}, \quad \Theta^{+}_{\delta',\delta''}, \quad \Theta^{+}_{\delta,\widetilde{\delta}'}, \quad \Theta^{+}_{\widetilde{\delta}',\delta''}, \quad \text{and} \quad \Theta^{+}_{\delta,\delta''},$$

each representing the top degree or canonical elements of their homology groups. Note that since we wound the curves Δ_1 and Δ_2, the chains $\Theta^{+}_{\delta,\delta'}$, $\Theta^{+}_{\delta,\widetilde{\delta}'}$ and $\Theta^{+}_{\delta,\delta''}$ may not be represented by a canonical intersection point. For these chains, we pick a cycle which represents the top degree or canonical class arbitrarily.

LEMMA 16.6.

$$\left[f_{\delta,\delta',\delta''}\left(\Theta^{+}_{\delta,\delta'}, \Theta^{+}_{\delta',\delta''}\right)\right] = \left[f_{\delta,\widetilde{\delta}',\delta''}\left(\Theta^{+}_{\delta,\widetilde{\delta}'}, \Theta^{+}_{\widetilde{\delta}',\delta''}\right)\right] = \left[\Theta^{+}_{\delta,\delta''}\right]. \tag{16.10}$$

In (16.10)*, the brackets denote the induced elements of the homology group* $\underline{\boldsymbol{HF}}^{-}(\boldsymbol{\delta}, \boldsymbol{\delta}'')$.

PROOF. The triple $(\Sigma\#\overline{\Sigma}, \boldsymbol{\delta}, \boldsymbol{\delta}', \boldsymbol{\delta}'', w)$ may be interpreted as corresponding to the link cobordism obtained by attaching a 2-handle to $((S^1 \times S^2)^{\#2g-1}, U)$, (where U denotes an unknot), which cancels one of the $S^1 \times S^2$ summands, and is unlinked from the unknot. This can be seen by handlesliding curves and manipulating the diagram as illustrated in Figure 16.6. A similar manipulation works for the triple $(\Sigma\#\overline{\Sigma}, \boldsymbol{\delta}, \widetilde{\boldsymbol{\delta}}', \boldsymbol{\delta}'')$. □

Lemma 16.6 implies that there is a chain $\lambda_{\delta,\delta''} \in \underline{\boldsymbol{CF}}^{-}(\boldsymbol{\delta}, \boldsymbol{\delta}'')$, with grading 1 higher than $\Theta^{+}_{\delta,\delta''}$, such that

$$\partial(\lambda_{\delta,\delta''}) = f_{\delta,\delta',\delta''}\left(\Theta^{+}_{\delta,\delta'}, \Theta^{+}_{\delta',\delta''}\right) + f_{\delta,\widetilde{\delta}',\delta''}\left(\Theta^{+}_{\delta,\widetilde{\delta}'}, \Theta^{+}_{\widetilde{\delta}',\delta''}\right). \tag{16.11}$$

The chain $\lambda_{\delta,\delta''}$ satisfying equation (16.11) is the one which features in the hypercube $\mathcal{L}^{(2)}_{\beta}$ in (16.9). We define the maps in $\mathcal{C}^{(2)}_{\text{aux}}$ to be the ones obtained by pairing $\mathcal{L}^{(2)}_{\alpha}$ and $\mathcal{L}^{(2)}_{\beta}$, via (5.7).

LEMMA 16.7. *The diagram* $\mathcal{C}^{(2)}_{\text{aux}}$ *in Figure* 16.5 *is a hypercube of chain complexes.*

This is a free offprint provided to the author by the publisher. Copyright restrictions may apply.

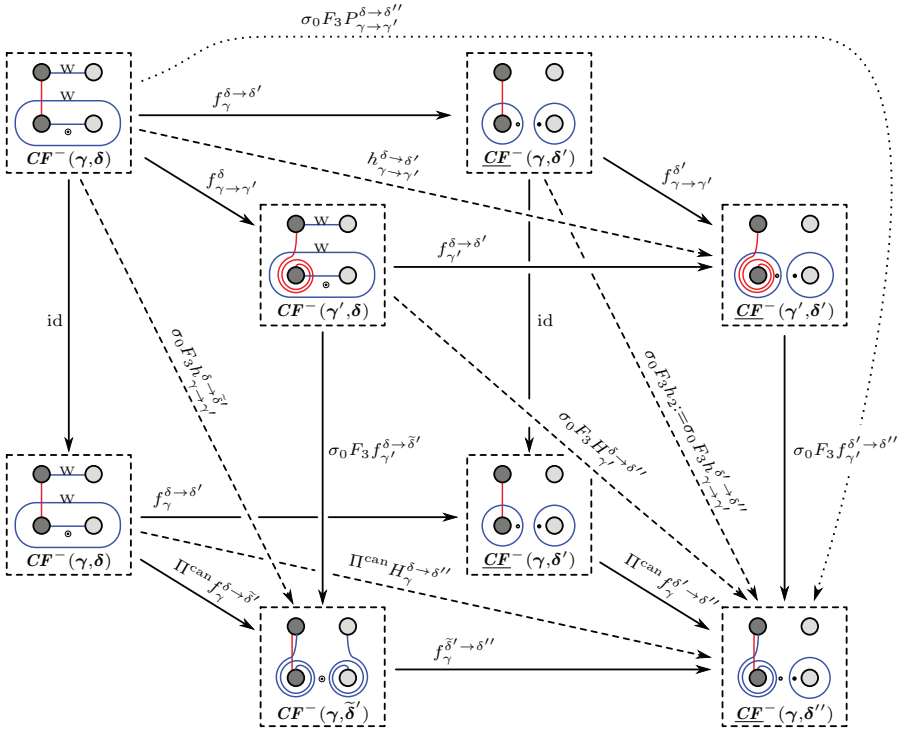


FIGURE 16.7. The central hypercube $\mathcal{C}^{(2)}_{\mathrm{cen}}$.

Lemma 16.7 follows immediately from the hypercube relations for $\mathcal{L}^{(2)}_{\alpha}$ and $\mathcal{L}^{(2)}_{\beta}$, as well as Lemma 5.10.

We now give a more concrete description of the maps appearing in $\mathcal{C}^{(2)}_{\mathrm{aux}}$. All of the length 1 maps are elementary triangle maps. For example,

$$f^{\delta\to\delta'}_{\gamma} = f_{\gamma,\delta,\delta'}(-,\Theta^{+}_{\delta,\delta'}).$$

The length 2 maps $h^{\delta\to\widetilde{\delta}'}_{\gamma\to\gamma'}$, $h^{\delta\to\delta'}_{\gamma\to\gamma'}$, $h^{\delta\to\delta'}_{\gamma\to\gamma'}$ and $h^{\widetilde{\delta}'\to\delta''}_{\gamma\to\gamma'}$ are each given by a single quadrilateral counting map.

The maps $H^{\delta\to\delta''}_{\gamma}$ and $H^{\delta\to\delta''}_{\gamma'}$ are more complicated. They are given by the formulas

$$H^{\delta\to\delta''}_{\gamma} = h^{\delta\to\delta'\to\delta''}_{\gamma} + h^{\delta\to\widetilde{\delta}'\to\delta''}_{\gamma} + f^{\delta\to\delta''}_{\gamma},$$

where $f^{\delta\to\delta''}_{\gamma} := f_{\gamma,\delta,\delta''}(-,\lambda_{\delta,\delta''})$. The map $H^{\delta\to\delta''}_{\gamma'}$ is defined similarly.

Finally, the length 3 map is given by

$$P^{\delta\to\delta''}_{\gamma\to\gamma'} = p^{\delta\to\delta'\to\delta''}_{\gamma\to\gamma'} + p^{\delta\to\widetilde{\delta}'\to\delta''}_{\gamma\to\gamma'} + h^{\delta\to\delta''}_{\gamma\to\gamma'},$$

where $h^{\delta\to\delta''}_{\gamma\to\gamma'} = h_{\gamma',\gamma,\delta,\delta''}(\Theta^{\mathrm{can}}_{\gamma',\gamma},-,\lambda_{\delta,\delta''})$.

This is a free offprint provided to the author by the publisher. Copyright restrictions may apply.

In Figure 16.7, we define $\mathcal{C}^{(2)}_{\mathrm{cen}}$ using the maps from $\mathcal{C}^{(2)}_{\mathrm{aux}}$. The map F_3 is the 3-handle map, and σ_0 is the lens space stabilization map. Also, Π^{can} denotes projection onto the canonical Spin^c structure of the $L(m,1)$ summand. More explicitly,

$$\Pi^{\mathrm{can}}(\mathbf{x}\times x_i)=\begin{cases}\mathbf{x}\times x_i & \text{if } i=0\\ 0 & \text{otherwise,}\end{cases} \tag{16.12}$$

extended equivariantly over T and U.

LEMMA 16.8. *The diagram $\mathcal{C}^{(2)}_{\mathrm{cen}}$ in Figure 16.5 is a hypercube of chain complexes.*

PROOF. There are two main inputs to the proof. The first is, naturally, the hypercube relations for $\mathcal{C}^{(2)}_{\mathrm{aux}}$. The second input consists of several results concerning the simplicity of the maps appearing along the bottom face of the hypercube $\mathcal{C}^{(2)}_{\mathrm{aux}}$. More precisely, we claim

$$\begin{aligned}\sigma_0F_3f^{\widetilde{\delta}'}_{\gamma\to\gamma'}&=\Pi^{\mathrm{can}}\colon \boldsymbol{CF}^-(\boldsymbol{\gamma},\widetilde{\boldsymbol{\delta}}')\to\boldsymbol{CF}^-(\boldsymbol{\gamma},\widetilde{\boldsymbol{\delta}}'),\\ \sigma_0F_3f^{\delta''}_{\gamma\to\gamma'}&=\Pi^{\mathrm{can}}\colon \underline{\boldsymbol{CF}}^-(\boldsymbol{\gamma},\boldsymbol{\delta}'')\to\underline{\boldsymbol{CF}}^-(\boldsymbol{\gamma},\boldsymbol{\delta}''),\end{aligned} \tag{16.13}$$

$$f^{\widetilde{\delta}'\to\delta''}_{\gamma}\sigma_0F_3=\sigma_0F_3f^{\widetilde{\delta}'\to\delta''}_{\gamma'}\colon \boldsymbol{CF}^-(\boldsymbol{\gamma}',\widetilde{\boldsymbol{\delta}}')\to\boldsymbol{CF}^-(\boldsymbol{\gamma},\boldsymbol{\delta}''), \tag{16.14}$$

and

$$F_3h^{\widetilde{\delta}'\to\delta''}_{\gamma\to\gamma'}=0. \tag{16.15}$$

Equation (16.13) is proven by using Lemma 10.8 to relate the triangle counts for $f^{\widetilde{\delta}'}_{\gamma\to\gamma'}$ and $f^{\delta''}_{\gamma\to\gamma'}$ with triangle counts on the destabilized complex. Proposition 11.1 identifies the destabilized triangle counts with nearest point maps, giving the stated formula. Equation (16.14) is similarly proven by applying Lemma 10.8 and Proposition 10.2 to the genus 1 region bounded by the curve S_1 to identify both compositions with a triangle count on the same genus $2g(\Sigma)-1$ Heegaard triple. Finally, (16.15) is proven by using Lemma 10.9 to identify the map $F_3h^{\widetilde{\delta}'\to\delta''}_{\gamma\to\gamma'}$ with the count of quadrilaterals on the quadruple obtained by removing the genus 1 region bounded by S_1. Note that outside of the genus 1 region bounded by S, the curves $\boldsymbol{\gamma}$ and $\boldsymbol{\gamma}'$ are pairwise Hamiltonian isotopic (they coincide with small translates of $\boldsymbol{\alpha}\cup\overline{\boldsymbol{\beta}}$). Hence Proposition 11.5 implies that the count is zero, for $\boldsymbol{\gamma}$ and $\boldsymbol{\gamma}'$ chosen to be suitably small translates of each other outside of the surgery region.

We now prove the hypercube relations. The length 0 and 1 hypercube relations are immediate. The length 2 relations along the top and back faces follow immediately from the hypercube relations for $\mathcal{C}^{(2)}_{\mathrm{aux}}$. The length 2 relation along the front face follows by taking the length 2 relation along the front face of $\mathcal{C}^{(2)}_{\mathrm{aux}}$ and post-composing with σ_0F_3.

The length 2 relation along the bottom face follows immediately from the relation

$$f^{\widetilde{\delta}'\to\delta''}_{\gamma}\Pi^{\mathrm{can}}=\Pi^{\mathrm{can}}f^{\widetilde{\delta}'\to\delta''}_{\gamma}, \tag{16.16}$$

which follows because the map $f^{\widetilde{\delta}'\to\delta''}_{\gamma}$ is the cobordism map for a 2-handle whose attaching cycle is disjoint from the $L(m,1)$ summand of $(\boldsymbol{\gamma},\widetilde{\boldsymbol{\delta}}')$, and hence we may use the lens space stabilization result for triangles in Lemma 10.8.

This is a free offprint provided to the author by the publisher. Copyright restrictions may apply.

We now consider the length 2 relation along the left face. The desired relation is

$$\left[\partial, \sigma_0 F_3 h^{\delta\to\widetilde{\delta}'}_{\gamma\to\gamma'}\right] = \sigma_0 F_3 f^{\delta\to\widetilde{\delta}'}_{\gamma'} f^{\delta}_{\gamma\to\gamma'} + \Pi^{\mathrm{can}} f^{\delta\to\widetilde{\delta}'}_{\gamma}. \tag{16.17}$$

To prove equation (16.17), we begin with the relation

$$\left[\partial, h^{\delta\to\widetilde{\delta}'}_{\gamma\to\gamma'}\right] = f^{\delta\to\widetilde{\delta}'}_{\gamma'} f^{\delta}_{\gamma\to\gamma'} + f^{\widetilde{\delta}'}_{\gamma\to\gamma'} f^{\delta\to\widetilde{\delta}'}_{\gamma}. \tag{16.18}$$

Post-composing with $\sigma_0 F_3$, (16.18) becomes

$$\left[\partial, \sigma_0 F_3 h^{\delta\to\widetilde{\delta}'}_{\gamma\to\gamma'}\right] = \sigma_0 F_3 f^{\delta\to\widetilde{\delta}'}_{\gamma'} f^{\delta}_{\gamma\to\gamma'} + \sigma_0 F_3 f^{\widetilde{\delta}'}_{\gamma\to\gamma'} f^{\delta\to\widetilde{\delta}'}_{\gamma}.$$

Applying (16.13) immediately gives (16.17). The length 2 relation along the right face of $\mathcal{C}^{(2)}_{\mathrm{cen}}$ is proved entirely analogously.

We now consider the length 3 relation. The desired relation is

$$\begin{aligned}\left[\partial, \sigma_0 F_3 P^{\delta\to\delta''}_{\gamma\to\gamma'}\right] &= f^{\widetilde{\delta}'\to\delta''}_{\gamma} \sigma_0 F_3 h^{\delta\to\widetilde{\delta}'}_{\gamma\to\gamma'} \\ &\quad + \sigma_0 F_3 f^{\delta'\to\delta''}_{\gamma'} h^{\delta\to\delta'}_{\gamma\to\gamma'} \\ &\quad + \Pi^{\mathrm{can}} H^{\delta\to\delta''}_{\gamma} \\ &\quad + \sigma_0 F_3 H^{\delta\to\delta''}_{\gamma'} f^{\delta}_{\gamma\to\gamma'} \\ &\quad + \sigma_0 F_3 h^{\delta'\to\delta''}_{\gamma\to\gamma'} f^{\delta\to\delta'}_{\gamma}\end{aligned} \tag{16.19}$$

To obtain (16.19), we post-compose the length 3 relation of $\mathcal{C}^{(2)}_{\mathrm{aux}}$ with $\sigma_0 F_3$ to obtain

$$\begin{aligned}\left[\partial, \sigma_0 F_3 P^{\delta\to\delta''}_{\gamma\to\gamma'}\right] &= \sigma_0 F_3 f^{\widetilde{\delta}'\to\delta''}_{\gamma'} h^{\delta\to\widetilde{\delta}'}_{\gamma\to\gamma'} + \sigma_0 F_3 f^{\delta'\to\delta''}_{\gamma'} h^{\delta\to\delta'}_{\gamma\to\gamma'} \\ &\quad + \sigma_0 F_3 h^{\delta'\to\delta''}_{\gamma\to\gamma'} f^{\delta\to\delta'}_{\gamma} + \sigma_0 F_3 h^{\widetilde{\delta}'\to\delta''}_{\gamma\to\gamma'} f^{\delta\to\widetilde{\delta}'}_{\gamma} \\ &\quad + \sigma_0 F_3 f^{\delta''}_{\gamma\to\gamma'} H^{\delta\to\delta''}_{\gamma} \\ &\quad + \sigma_0 F_3 H^{\delta\to\delta''}_{\gamma'} f^{\delta}_{\gamma\to\gamma'}.\end{aligned} \tag{16.20}$$

The equivalence of (16.20) and (16.19) follows quickly from (16.13), (16.15) and (16.14). □

16.5. The hypercube $\mathcal{C}^{(3)}_{\mathrm{cen}}$

In this section, we construct the hypercube $\mathcal{C}^{(3)}_{\mathrm{cen}}$. We first construct an auxiliary hypercube $\mathcal{C}^{(3)}_{\mathrm{aux}}$, shown schematically in Figure 16.8.

LEMMA 16.9. *If $\overline{\boldsymbol{\beta}}$ are sufficiently wound on $\overline{\Sigma}$, and Δ_1 and Δ_2 are sufficiently wound on $\overline{\Sigma}$, then the diagram*

$$(\Sigma \# \overline{\Sigma}, \boldsymbol{\gamma}, \boldsymbol{\delta}, \boldsymbol{\delta}', \boldsymbol{\delta}'', \widetilde{\boldsymbol{\delta}}', \boldsymbol{\delta}_1, \boldsymbol{\delta}_2, \boldsymbol{\delta}_3, w)$$

is weakly admissible.

The proof of Lemma 16.9 is essentially the same as the proof of Lemma 16.2, so we omit it.

The hypercube $\mathcal{C}^{(3)}_{\mathrm{aux}}$ is the pairing of the 0-dimensional hypercube $\mathcal{L}^{(3)}_{\alpha}$ of alpha attaching curves consisting of $\boldsymbol{\gamma}$, as well the following 3-dimensional hypercube of

This is a free offprint provided to the author by the publisher. Copyright restrictions may apply.

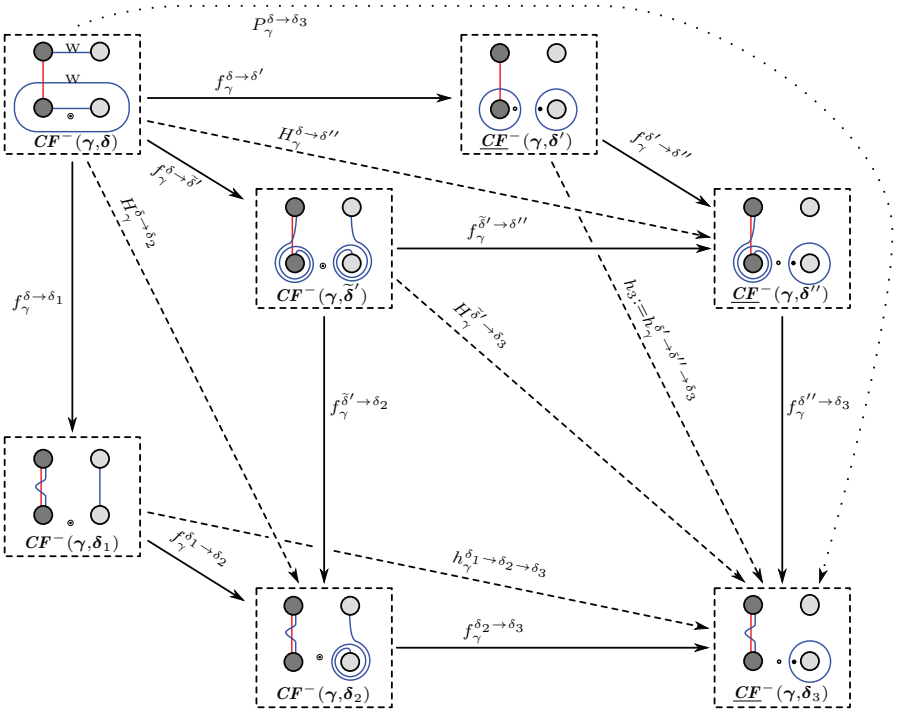


FIGURE 16.8. The auxiliary hypercube $\mathcal{C}^{(3)}_{\mathrm{aux}}$.

beta attaching curves:

(16.21)
$$\mathcal{L}^{(3)}_\beta := \quad \begin{array}{ccccc} \boldsymbol{\delta} & \xrightarrow{\Theta^+_{\delta,\delta'}} & \boldsymbol{\delta}' & & \\ & \searrow^{\Theta^+_{\delta,\widetilde{\delta}'}} & \downarrow{\scriptstyle \lambda_{\delta,\delta_2}} & \searrow^{\Theta^+_{\delta',\delta''}} & \\ \downarrow{\scriptstyle \Theta^+_{\delta,\delta_1}} & & \widetilde{\boldsymbol{\delta}}' & \xrightarrow{\Theta^+_{\widetilde{\delta}',\delta''}} & \boldsymbol{\delta}'' \\ & \swarrow{\scriptstyle \lambda_{\delta,\delta_2}} & \downarrow{\scriptstyle \Theta^{\mathrm{can}}_{\widetilde{\delta}',\delta_2}} & \swarrow{\scriptstyle \omega_{\delta,\delta_3}}\ \swarrow{\scriptstyle \lambda_{\widetilde{\delta}',\delta_3}} & \downarrow{\scriptstyle \Theta^{\mathrm{can}}_{\delta'',\delta_3}} \\ \boldsymbol{\delta}_1 & \xrightarrow{\Theta^{\mathrm{can}}_{\delta_1,\delta_2}} & \boldsymbol{\delta}_2 & \xrightarrow{\Theta^+_{\delta_2,\delta_3}} & \boldsymbol{\delta}_3 \end{array}$$

We now describe the chains appearing in $\mathcal{L}^{(3)}_\beta$. First, we pick a collection of cycles

$$\Theta^+_{\delta,\widetilde{\delta}'},\quad \Theta^+_{\delta,\delta'},\quad \Theta^+_{\delta',\delta''},\quad \Theta^+_{\widetilde{\delta}',\delta''},\quad \Theta^+_{\delta,\delta_1},\quad \Theta^{\mathrm{can}}_{\delta',\delta_2},\quad \Theta^{\mathrm{can}}_{\delta'',\delta_3},\quad \Theta^{\mathrm{can}}_{\delta_1,\delta_2},\quad \text{and}\quad \Theta^+_{\delta_2,\delta_3},$$

which each represent the top degree generator or canonical generator of their homology groups. We use these cycles for the length 1 cycles in (16.21).

This is a free offprint provided to the author by the publisher. Copyright restrictions may apply.

LEMMA 16.10. *Suppose* $\boldsymbol{\delta}$, $\widetilde{\boldsymbol{\delta}}'$, $\boldsymbol{\delta}'$, $\boldsymbol{\delta}''$, $\boldsymbol{\delta}_1$, $\boldsymbol{\delta}_2$ *and* $\boldsymbol{\delta}_3$ *are the attaching curves appearing in* $\mathcal{L}_\beta^{(3)}$. *Then*

$$\begin{aligned}\left[f_{\delta,\delta',\delta''}\left(\Theta^+_{\delta,\delta'},\Theta^+_{\delta',\delta''}\right)\right] &= \left[\Theta^+_{\delta,\delta''}\right],\\ f_{\delta',\delta'',\delta_3}\left(\Theta^+_{\delta',\delta''},\Theta^{\mathrm{can}}_{\delta'',\delta_3}\right) &= 0,\end{aligned}$$

$$\begin{aligned}\left[f_{\delta,\widetilde{\delta}',\delta''}\left(\Theta^+_{\delta,\widetilde{\delta}'},\Theta^+_{\widetilde{\delta}',\delta''}\right)\right] &= \left[\Theta^+_{\delta,\delta''}\right],\\ \left[f_{\widetilde{\delta}',\delta'',\delta_3}\left(\Theta^+_{\widetilde{\delta}',\delta''},\Theta^{\mathrm{can}}_{\delta'',\delta_3}\right)\right] &= \left[\Theta^{\mathrm{can}}_{\widetilde{\delta}',\delta_3}\right],\end{aligned}$$

$$\begin{aligned}\left[f_{\delta,\widetilde{\delta}',\delta_2}\left(\Theta^+_{\delta,\widetilde{\delta}'},\Theta^{\mathrm{can}}_{\widetilde{\delta}',\delta_2}\right)\right] &= \left[\Theta^{\mathrm{can}}_{\delta,\delta_2}\right],\\ \left[f_{\widetilde{\delta}',\delta_2,\delta_3}\left(\Theta^{\mathrm{can}}_{\widetilde{\delta}',\delta_2},\Theta^+_{\delta_2,\delta_3}\right)\right] &= \left[\Theta^{\mathrm{can}}_{\widetilde{\delta}',\delta_3}\right],\end{aligned}$$

$$\begin{aligned}\left[f_{\delta,\delta_1,\delta_2}\left(\Theta^+_{\delta,\delta_1},\Theta^{\mathrm{can}}_{\delta_1,\delta_2}\right)\right] &= \left[\Theta^{\mathrm{can}}_{\delta,\delta_2}\right],\\ f_{\delta_1,\delta_2,\delta_3}\left(\Theta^{\mathrm{can}}_{\delta_1,\delta_2},\Theta^+_{\delta_2,\delta_3}\right) &= 0,\end{aligned}$$

where the brackets denote the induced elements of homology.

PROOF. First, recall that all almost complex structures in this section are maximally pinched along S_1 and S_2. Furthermore, outside of the genus two region pictured in Figure 16.8, all of the attaching curves appearing in the statement coincide with small translates of the $\hat{\boldsymbol{\Delta}}$ curves. Hence, we can view all triples appearing in the claim as being stabilizations of the genus two region shown. Furthermore, the stabilizations have index tuple $(0,0,0)$. Hence, using Proposition 10.2, it suffices to prove the claim for the corresponding genus 2 triples.

The computations are handled by one of three cases.

The first case occurs when the associated Heegaard triple represents surgery on $S^1\times\{pt\}\subseteq S^1\times S^2$, yielding S^3. The triples $(\boldsymbol{\delta},\boldsymbol{\delta}',\boldsymbol{\delta}'')$, $(\boldsymbol{\delta},\widetilde{\boldsymbol{\delta}}',\boldsymbol{\delta}_2)$, and $(\boldsymbol{\delta},\widetilde{\boldsymbol{\delta}}',\boldsymbol{\delta}'')$ have this configuration. By invariance of the cobordism maps under index 1 and 2 handle cancelations, the top degree generator is preserved, on homology. The triple $(\boldsymbol{\delta},\boldsymbol{\delta}',\boldsymbol{\delta}'')$ is shown in Figure 16.9.

The second case occurs when the triple represents surgery on $S^1\times\{pt\}\subseteq(S^1\times S^2)\#L(m,1)$. By the same argument as in the first case, the element Θ^{can} is preserved. The triples $(\widetilde{\boldsymbol{\delta}}',\boldsymbol{\delta}'',\boldsymbol{\delta}_3)$, $(\boldsymbol{\delta},\boldsymbol{\delta}_1,\boldsymbol{\delta}_2)$ and $(\widetilde{\boldsymbol{\delta}}',\boldsymbol{\delta}_2,\boldsymbol{\delta}_3)$ satisfy this configuration.

The third case is when the triple represents $-m$-framed surgery on an unknot in S^3, giving $L(m,1)$. The triples $(\boldsymbol{\delta}_1,\boldsymbol{\delta}_2,\boldsymbol{\delta}_3)$ and $(\boldsymbol{\delta}',\boldsymbol{\delta}'',\boldsymbol{\delta}_3)$ satisfy this condition. Furthermore, these triples are in standard position (i.e. the triples are not wound), so holomorphic triangles cancel modulo 2 by Lemma 12.4. □

This is a free offprint provided to the author by the publisher. Copyright restrictions may apply.

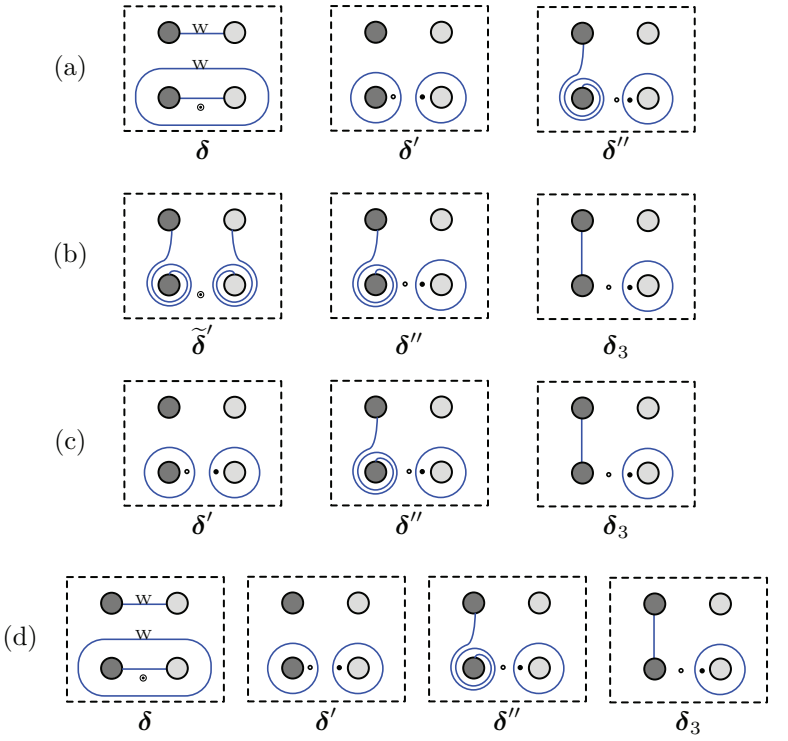


FIGURE 16.9. Examples of the triples and quadruples from Lemma 16.10. (a) The triple $(\boldsymbol{\delta}, \boldsymbol{\delta}', \boldsymbol{\delta}'')$, which represents surgery on $S^1 \times \{pt\} \subseteq S^1 \times S^2$. (b) The triple $(\widetilde{\boldsymbol{\delta}}', \boldsymbol{\delta}'', \boldsymbol{\delta}_3)$ represents surgery on $S^1 \times \{pt\} \subseteq S^1 \times S^2 \# L(m,1)$. (c) The triple $(\boldsymbol{\delta}', \boldsymbol{\delta}'', \boldsymbol{\delta}_3)$ represents surgery on a knot in $L(m,1)$ which gives S^3. (d) The quadruple $(\boldsymbol{\delta}, \boldsymbol{\delta}', \boldsymbol{\delta}'', \boldsymbol{\delta}_3)$.

Lemma 16.10 implies that there are chains $\lambda_{\delta,\delta''}$, $\lambda_{\widetilde{\delta}',\delta_3}$, and $\lambda_{\delta,\delta_2}$ satisfying

$$\begin{aligned}
\partial(\lambda_{\delta,\delta''}) &= f_{\delta,\delta',\delta''}\left(\Theta^+_{\delta,\delta'}, \Theta^+_{\delta',\delta''}\right) + f_{\delta,\widetilde{\delta}',\delta''}\left(\Theta_{\delta,\widetilde{\delta}'}, \Theta^+_{\widetilde{\delta}',\delta''}\right), \\
\partial(\lambda_{\widetilde{\delta}',\delta_3}) &= f_{\widetilde{\delta}',\delta'',\delta_3}\left(\Theta^+_{\widetilde{\delta}',\delta''}, \Theta^{\text{can}}_{\delta'',\delta_3}\right) + f_{\widetilde{\delta}',\delta_2,\delta_3}\left(\Theta^{\text{can}}_{\widetilde{\delta}',\delta_2}, \Theta^+_{\delta_2,\delta_3}\right), \\
\partial(\lambda_{\delta,\delta_2}) &= f_{\delta,\widetilde{\delta}',\delta_2}\left(\Theta^+_{\delta,\widetilde{\delta}'}, \Theta^{\text{can}}_{\widetilde{\delta}',\delta_2}\right) + f_{\delta,\delta_1,\delta_2}\left(\Theta^+_{\delta,\delta_1}, \Theta^{\text{can}}_{\delta_1,\delta_2}\right).
\end{aligned} \tag{16.22}$$

Furthermore, since all of the triangles maps in (16.22) are homogeneously graded with respect to the Maslov grading, we can assume these chains live in Maslov grading one greater than $\Theta^{\text{can}}_{\delta,\delta_2}$, $\Theta^+_{\delta,\delta''}$ and $\Theta^{\text{can}}_{\widetilde{\delta}',\delta_3}$. We use the chains from (16.22) for the length 2 chains in $\mathcal{L}^{(3)}_\beta$, appearing in (16.21).

Next, we describe how to construct the length 3-chain ω_{δ,δ_3} appearing in $\mathcal{L}^{(3)}_\beta$. To make our analysis of gradings easier, we will define ω_{δ,δ_3} as an infinite sum

$$\omega_{\delta,\delta_3} = \sum_{k=0}^{\infty} \omega_{\delta,\delta_3;\mathfrak{s}^+_k}, \tag{16.23}$$

This is a free offprint provided to the author by the publisher. Copyright restrictions may apply.

where each $\omega_{\delta,\delta_3;\mathfrak{s}_k^+}$ is homogeneously graded. Here, $\mathfrak{s}_k^+$ denotes the element of $\mathrm{Spin}^c(D(-m,1))$ defined in Lemma 12.3. We think of $\omega_{\delta,\delta_3;\mathfrak{s}_k^-}$ as also being defined, but being 0. We write $\mathfrak{u}_k$ for $\{\mathfrak{s}_k^+,\mathfrak{s}_k^-\}$.

Consider the four-ended 4-manifolds constructed from the genus 2 surgery regions of the Heegaard quadruples $(\boldsymbol{\delta},\boldsymbol{\delta}',\boldsymbol{\delta}'',\boldsymbol{\delta}_3)$, $(\boldsymbol{\delta},\widetilde{\boldsymbol{\delta}}',\boldsymbol{\delta}'',\boldsymbol{\delta}_3)$, $(\boldsymbol{\delta},\widetilde{\boldsymbol{\delta}}',\boldsymbol{\delta}_2,\boldsymbol{\delta}_3)$ and $(\boldsymbol{\delta},\boldsymbol{\delta}_1,\boldsymbol{\delta}_2,\boldsymbol{\delta}_3)$. Note that outside of the special genus 2 subregion, the attaching curves are all small translations of $\hat{\boldsymbol{\Delta}}$. It is a straightforward exercise to see that each of the aforementioned 4-manifolds is obtained by attaching two 2-handles along a 2-component unlink in S^3, with framings 0 and $-m$, and then removing the neighborhood of two 4-dimensional genus 1 handlebodies. Phrased another way, each of the 4-manifolds above have 2 boundary components equal to $S^1\times S^2$, such that when we fill in those components with 3 and 4-handles, we obtain the 2-handle cobordism described above. In particular, Spin^c structures on the 4-manifolds above, which restrict to the torsion and canonical Spin^c structures on the boundary, are naturally identified with Spin^c structures on the disk bundle $D(-m,1)$ which restrict to the canonical one on the boundary.

LEMMA 16.11. *For each $k\geq 0$, the chain*

$$\begin{aligned}C_{\delta,\delta_3;\mathfrak{u}_k} :=& h_{\delta,\delta',\delta'',\delta_3;\mathfrak{u}_k}\left(\Theta^+_{\delta,\delta'},\Theta^+_{\delta',\delta''},\Theta^{\mathrm{can}}_{\delta'',\delta_3}\right)+h_{\delta,\widetilde{\delta}',\delta'',\delta_3;\mathfrak{u}_k}\left(\Theta^+_{\delta,\widetilde{\delta}'},\Theta^+_{\widetilde{\delta}',\delta''},\Theta^{\mathrm{can}}_{\delta'',\delta_3}\right)\\&+h_{\delta,\widetilde{\delta}',\delta_2,\delta_3;\mathfrak{u}_k}\left(\Theta^+_{\delta,\widetilde{\delta}'},\Theta^{\mathrm{can}}_{\widetilde{\delta}',\delta_2},\Theta^+_{\delta_2,\delta_3}\right)+h_{\delta,\delta_1,\delta_2,\delta_3;\mathfrak{u}_k}\left(\Theta^+_{\delta,\delta_1},\Theta^{\mathrm{can}}_{\delta_1,\delta_2},\Theta^+_{\delta_2,\delta_3}\right)\\&+f_{\delta,\delta'',\delta_3;\mathfrak{u}_k}(\lambda_{\delta,\delta''},\Theta^{\mathrm{can}}_{\delta'',\delta_3})+f_{\delta,\widetilde{\delta}',\delta_3;\mathfrak{u}_k}\left(\Theta^+_{\delta,\widetilde{\delta}'},\lambda_{\widetilde{\delta}',\delta_3}\right)\\&+f_{\delta,\delta_2,\delta_3;\mathfrak{u}_k}\left(\lambda_{\delta,\delta_2},\Theta^+_{\delta_2,\delta_3}\right)\end{aligned}$$

is a boundary in $\underline{\boldsymbol{CF}}^-(\boldsymbol{\delta},\boldsymbol{\delta}_3)$.

PROOF. First, note that using our stabilization formulas for triangles and quadrilaterals in Proposition 10.2 and 10.6, it is sufficient to show the claim for the genus 2 regions shown in Figure 16.8. Next, we claim $C_{\delta,\delta_3;\mathfrak{u}_k}$ is a cycle. This is proven by an easy associativity argument, together with the definition of the chains $\lambda_{\delta,\delta''}$, $\lambda_{\widetilde{\delta}',\delta_3}$ and $\lambda_{\delta,\delta_2}$ in (16.22). The absolute grading formula of [**OS03**] implies that $C_{\delta,\delta_3;\mathfrak{u}_k}$ has grading

$$-mk(k+1)+1.$$

(Compare Lemma 12.3). However $\underline{\boldsymbol{HF}}^-(\boldsymbol{\delta},\boldsymbol{\delta}_3)\cong\mathbb{F}[\![U]\!]\otimes\mathbb{F}[\mathbb{Z}/m]$ is non-trivial only in even gradings. Hence $C_{\delta,\delta_3;\mathfrak{u}_k}$ must be a boundary. □

Let $\omega_{\delta,\delta_3;\mathfrak{s}_k^+}\in\underline{\boldsymbol{CF}}^-(\boldsymbol{\delta},\boldsymbol{\delta}_3)$ be any chain satisfying

$$\partial(\omega_{\delta,\delta_3;\mathfrak{s}_k^+})=C_{\delta,\delta_3;\mathfrak{u}_k}, \tag{16.24}$$

which has homogeneous grading 1 greater than $C_{\delta,\delta_3;\mathfrak{u}_k}$. As indicated in (16.23), we define ω_{δ,δ_3} to be the sum over $k\geq 0$ of $\omega_{\delta,\delta_3;\mathfrak{s}_k^+}$. We use ω_{δ,δ_3} as the length 3 chain in the construction of $\mathcal{L}^{(3)}_\beta$.

LEMMA 16.12. *The diagram $\mathcal{L}^{(3)}_\beta$ is a hypercube of beta attaching curves. Furthermore, $\mathcal{C}^{(3)}_{\mathrm{aux}}$ is a hypercube of chain complexes.*

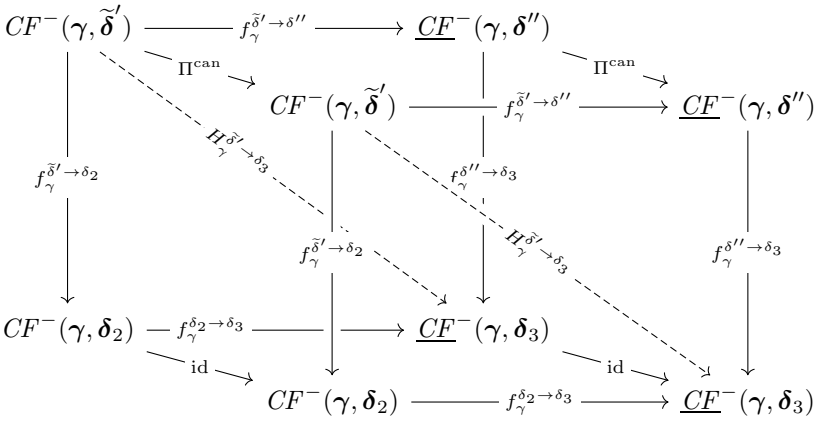
This is a free offprint provided to the author by the publisher. Copyright restrictions may apply.

PROOF. The length 1 relations for $\mathcal{L}^{(3)}_{\beta}$ are immediate. Lemma 16.10 and (16.22) together give the length 2 relations. Lemma 16.11 and (16.24) give the length 3 relations of $\mathcal{L}^{(3)}_{\beta}$, concluding the proof. □

REMARK 16.13. Our construction of the chains appearing in $\mathcal{L}^{(3)}_{\beta}$ is similar to the procedure of *filling* an empty β-hyperbox, in the terminology of Manolescu and Ozsváth [**MO10**, Section 8].

Next, we modify $\mathcal{C}^{(3)}_{\mathrm{aux}}$ slightly, and construct a hypercube $\mathcal{C}^{(3)}_{\mathrm{aux},\Pi^{\mathrm{can}}}$. The hypercube $\mathcal{C}^{(3)}_{\mathrm{aux},\Pi^{\mathrm{can}}}$ has the same complexes as $\mathcal{C}^{(3)}_{\mathrm{aux}}$, except the maps along the top face are composed with Π^{can}, as in the bottom face of $\mathcal{C}^{(2)}_{\mathrm{cen}}$. We claim that $\mathcal{C}^{(3)}_{\mathrm{aux},\Pi^{\mathrm{can}}}$ is also a hypercube of chain complexes. To establish this, we note that $\mathcal{C}^{(3)}_{\mathrm{aux},\Pi^{\mathrm{can}}}$ coincides with the hypercube obtained by stacking $\mathcal{C}^{(3)}_{\mathrm{aux}}$ with the hypercube shown in (16.25), and then compressing. Hence, it is sufficient to show the hypercube relations for the diagram in (16.25). The length 1 relations are clear. The length 2 relations along the back, front and bottom faces are also clear. The length 2 relation along the top face follows from (16.16). For the length 2 relations on the left and right faces, we note that the intersection points in the non-canonical Spin^c structures are in the kernel of $f^{\widetilde{\delta}'\to\delta_2}_{\gamma}$ and $f^{\delta''\to\delta_3}_{\gamma}$. Indeed these two maps count holomorphic triangles on Heegaard triples which have a genus 1 lens space stabilizations, and by construction they have the intersection point in the canonical Spin^c structure as a special input, so there are no homology classes which could be counted unless the other input is also in the canonical Spin^c structure. The length 3 relation follows from the same argument, applied to the rectangle counting map for the front and back face.

(16.25)



Next, we construct the additional hypercube $\mathcal{C}^{(3)}_{\mathrm{cen,3\text{-}h}}$ shown in Figure 16.10. Note that $\mathcal{C}^{(3)}_{\mathrm{cen,3\text{-}h}}$ is a hypercube for destabilization, as constructed in Section 14.

Finally, we define $\mathcal{C}^{(3)}_{\mathrm{cen}}$ by stacking and then compressing $\mathcal{C}^{(3)}_{\mathrm{aux},\Pi^{\mathrm{can}}}$ and $\mathcal{C}^{(3)}_{\mathrm{cen,3\text{-}h}}$.

This is a free offprint provided to the author by the publisher. Copyright restrictions may apply.

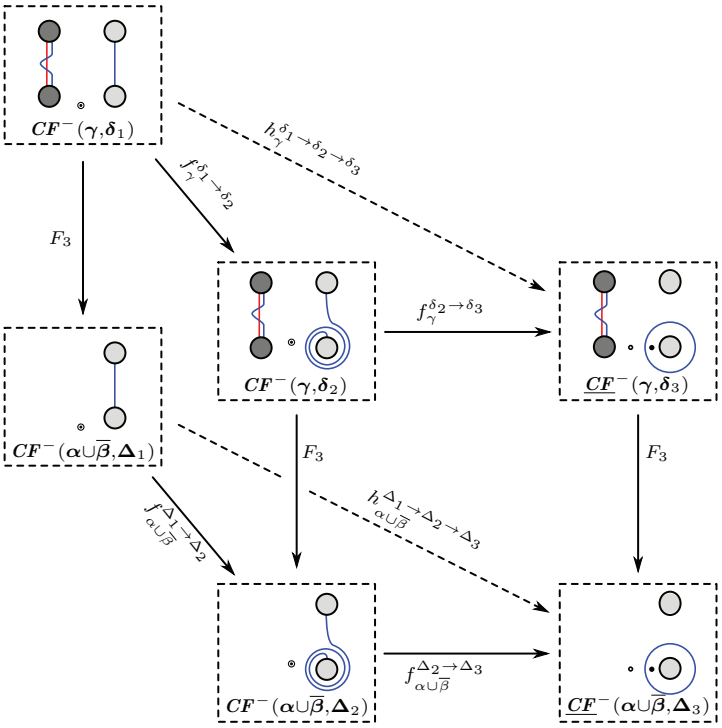


FIGURE 16.10. The 3-handle hypercube $\mathcal{C}^{(3)}_{\text{cen,3-h}}$.

16.6. Constructing $\mathcal{C}_{\text{cen}}$

We now stack and compress $\mathcal{C}^{(1)}_{\text{cen}}$, $\mathcal{C}^{(2)}_{\text{cen}}$ and $\mathcal{C}^{(3)}_{\text{cen}}$. Let us write $\hat{\mathcal{C}}_{\text{cen}}$ for the hypercube obtained by stacking $\mathcal{C}^{(1)}_{\text{cen}}$, $\mathcal{C}^{(2)}_{\text{cen}}$ and $\mathcal{C}^{(3)}_{\text{cen}}$, and then compressing. The hypercube $\hat{\mathcal{C}}_{\text{cen}}$ has the form shown in Figure 16.11.

In the cube $\hat{\mathcal{C}}_{\text{cen}}$, we would like to delete the extra complex labeled $\boldsymbol{CF}^-(\boldsymbol{\alpha}_1\cup\overline{\boldsymbol{\beta}},\boldsymbol{\Delta})$ along the top face. If we remove this complex, the length 0, 1 and 2 relations are preserved, though the length 3 relation may not be. However if $\hat{E}$ is itself null-homotopic, i.e. $\hat{E}=\partial H+H\partial$, for some H, then H may be added to the length 3 arrow of $\hat{\mathcal{C}}_{\text{cen}}$, and the hypercube relations will be satisfied. By examination of the compression operation, the map $\hat{E}$ is given by

$$\begin{aligned}\hat{E} &= F_3 f_\gamma^{\delta''\to\delta_3}\sigma_0 F_3 f_{\gamma'}^{\delta'\to\delta''}\sigma F_3 h_1 f_\gamma^{\delta\to\delta'}\\ &\quad + F_3 f_\gamma^{\delta''\to\delta_3}\sigma_0 F_3 h_2 f_\gamma^{\delta\to\delta'}\\ &\quad + F_3 h_3 f_\gamma^{\delta\to\delta'}.\end{aligned}\tag{16.26}$$

Equation (16.26) can be simplified as follows. Note first that (16.2) is equivalent to

$$F_3 f_{\gamma'}^{\delta'\to\delta''}\sigma=\mathrm{id},\tag{16.27}$$

since σ is a chain isomorphism. Similarly (16.13) implies

$$F_3 f_\gamma^{\delta''\to\delta_3}\sigma_0=\mathrm{id}\,.\tag{16.28}$$

This is a free offprint provided to the author by the publisher. Copyright restrictions may apply.

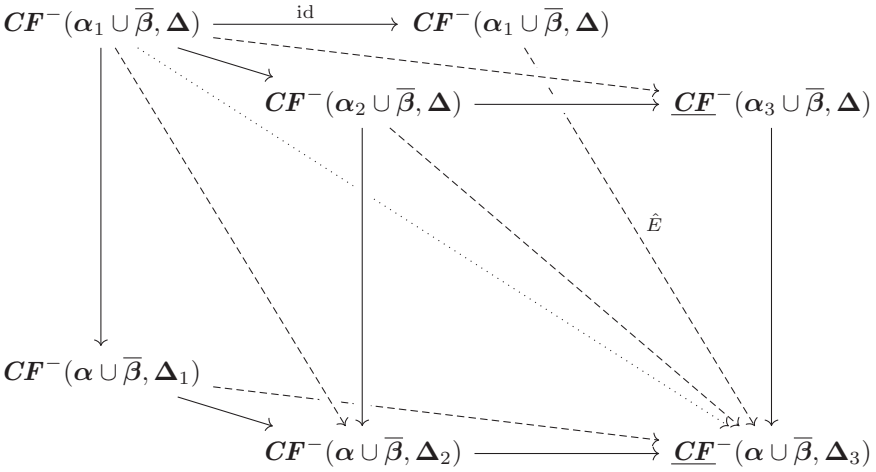


FIGURE 16.11. The hypercube $\hat{\mathcal{C}}_{\text{cen}}$.

Hence (16.26) simplifies to

$$\hat{E} = (F_3h_1 + F_3h_2 + F_3h_3)\, f_\gamma^{\delta\to\delta'}. \tag{16.29}$$

It turns out that the most natural object of study is the map

$$E := F_3h_1 + F_3h_2 + F_3h_3.$$

In Chapter 19, we will construct a map H_E satisfying

$$E = \partial H_E + H_E\partial,$$

which, of course, also gives a null-homotopy $H = H_E f_\gamma^{\delta\to\delta'}$ of $\hat{E}$. We define $\mathcal{C}_{\text{cen}}$ to be the hypercube obtained by deleting the extra copy of $\boldsymbol{CF}^-(\boldsymbol{\alpha}_1 \cup \overline{\boldsymbol{\beta}}, \boldsymbol{\Delta})$ from $\hat{\mathcal{C}}_{\text{cen}}$, and adding H to the length 3 map of $\hat{\mathcal{C}}_{\text{cen}}$.

16.7. Compatibility with the involution

In this section, we verify the following:

LEMMA 16.14. *The vertical maps in the central hypercube coincide with the change of diagram maps from naturality.*

PROOF. Let us write Φ_1, Φ_2 and Φ_3 for the vertical maps (in the same order as the central hypercube). By construction,

$$\begin{aligned}
\Phi_1 &= F_3 f_\gamma^{\delta\to\delta'}\\
\Phi_2 &= F_3 f_\gamma^{\widetilde{\delta'}\to\delta_2}\sigma_0 F_3 f_{\gamma'}^{\delta\to\widetilde{\delta'}}\\
\Phi_3 &= F_3 f_\gamma^{\delta''\to\delta_3}\sigma_0 F_3 f_{\gamma'}^{\delta'\to\delta''}\sigma F_3 f_{\gamma''}^{\delta\to\delta'}
\end{aligned} \tag{16.30}$$

We first consider Φ_1. Note that $f_\gamma^{\delta\to\delta'}$ represents the cobordism map for a 0-framed unknot, so the formula for Φ_1 consists of the cobordism map for surgery on a 0-framed unknot, followed by a canceling 3-handle. Hence, Φ_1 represents the map from naturality.

This is a free offprint provided to the author by the publisher. Copyright restrictions may apply.

Next, we consider Φ_2. Firstly, we claim that $F_3 f_\gamma^{\widetilde{\delta}' \to \delta_2} \sigma_0 = \mathrm{id}$, which is proven by using Lemma 10.8 and Proposition 11.1, similar to equation (16.13). Hence the formula reduces to

$$\Phi_2 = F_3 f_{\gamma'}^{\delta \to \widetilde{\delta}'}.$$

As with Φ_1, this expression for Φ_2 represents the cobordism map for surgery on a 0-framed unknot, followed by the 3-handle map. Hence Φ_2 coincides with the map from naturality.

Finally, we consider Φ_3. Using (16.27) and (16.28), the expression for Φ_3 in (16.30) reduces to

$$\Phi_3 = F_3 f_{\gamma''}^{\delta \to \delta'},$$

which similarly represents the cobordism map for a canceling pair of index 2 and 3 handles. The proof is complete. □

This is a free offprint provided to the author by the publisher. Copyright restrictions may apply.

CHAPTER 17

The second 2-handle hypercube

We now construct the second 2-handle hypercube, $\mathcal{C}^2_{2\text{-h}}$. We first describe the Heegaard diagrams that appear therein, and then subsequently define the maps, and prove the hypercube relations.

17.1. Heegaard diagrams for $\mathcal{C}^2_{2\text{-h}}$

All of the complexes used to construct $\mathcal{C}^2_{2\text{-h}}$ use the Heegaard surface

$$\Sigma_0 \# \overline{\Sigma},$$

where Σ_0 denotes the surface obtained by removing the genus 1 surgery region from Σ. We define the following sets of attaching curves:

- $\boldsymbol{\alpha} \subseteq \Sigma_0$ denotes the original alpha curves which are outside of the genus 1 surgery region of Σ.
- $\widehat{\boldsymbol{\Delta}} \subseteq \Sigma_0 \# \overline{\Sigma}_0$ denotes the curves obtained by taking the curves $\boldsymbol{\Delta}$ constructed in Chapter 15, and deleting the two curves which intersect the surgery region of Σ.
- We define
$$\boldsymbol{\Delta}_i := \widehat{\boldsymbol{\Delta}} \cup \overline{c}_i,$$
where $\overline{c}_i$ denotes the image of c_i on $\overline{\Sigma}$.
- $\overline{\boldsymbol{\alpha}}^H$ denotes the curves obtained by handlesliding each curve in $\overline{\boldsymbol{\alpha}}$ over the corresponding curve in $\boldsymbol{\alpha}$. Furthermore, we choose each curve in $\overline{\boldsymbol{\alpha}}^H$ to be a small translate of a curve in $\widehat{\boldsymbol{\Delta}}$.
- We define
$$\overline{\boldsymbol{\alpha}}^H_i := \overline{\boldsymbol{\alpha}}^H \cup \overline{c}_i.$$

See Figure 17.1 for a schematic of the curves $\boldsymbol{\Delta}_i$, $\boldsymbol{\alpha}$ and $\overline{\boldsymbol{\alpha}}^H_i$ outside of the genus 1 surgery region of $\Sigma_0 \# \overline{\Sigma}$.

LEMMA 17.1. *If the $\overline{\boldsymbol{\beta}}$ curves are sufficiently wound, then the tuple*

$$(\Sigma_0 \# \overline{\Sigma}, \boldsymbol{\alpha} \cup \overline{\boldsymbol{\beta}}, \boldsymbol{\Delta}_1, \boldsymbol{\Delta}_2, \boldsymbol{\Delta}_3, \boldsymbol{\alpha}' \cup \overline{\boldsymbol{\alpha}}^H_1, \boldsymbol{\alpha}'' \cup \overline{\boldsymbol{\alpha}}^H_2, \boldsymbol{\alpha}''' \cup \overline{\boldsymbol{\alpha}}^H_3, w)$$

is weakly admissible, where $\boldsymbol{\alpha}'$, $\boldsymbol{\alpha}''$ and $\boldsymbol{\alpha}'''$ are appropriately chosen, Hamiltonian translates of $\boldsymbol{\alpha}$.

The proof of Lemma 17.1 is an easy adaptation of the proof of Lemma 15.1.

This is a free offprint provided to the author by the publisher. Copyright restrictions may apply.

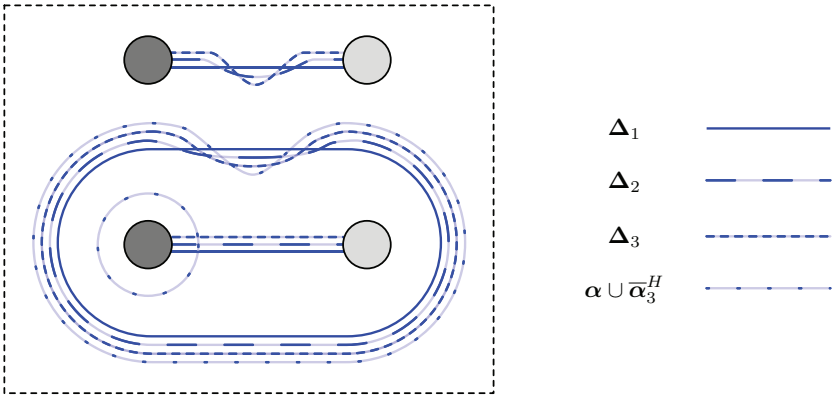


FIGURE 17.1. A generic genus 2 region of the quadruple $(\Sigma_0 \# \overline{\Sigma}, \boldsymbol{\Delta}_1, \boldsymbol{\Delta}_2, \boldsymbol{\Delta}_3, \boldsymbol{\alpha} \cup \overline{\boldsymbol{\alpha}}_3^H)$.

17.2. Constructing $\mathcal{C}^2_{2\text{-h}}$

We first construct a diagram $\mathcal{L}^2_{2\text{-h},\beta}$ of beta attaching curves:

$$\mathcal{L}^2_{2\text{-h},\beta} := \quad \begin{array}{ccccc} \boldsymbol{\Delta}_1 & \xrightarrow{\Theta^{can}_{\Delta_1,\Delta_2}} & \boldsymbol{\Delta}_2 & \xrightarrow{\Theta^+_{\Delta_2,\Delta_3}} & \boldsymbol{\Delta}_3 \\ \downarrow{\scriptstyle \Theta^+_{\Delta_1,\alpha\cup\overline{\alpha}_1^H}} & & \downarrow{\scriptstyle \Theta^+_{\Delta_2,\alpha\cup\overline{\alpha}_2^H}} & & \downarrow{\scriptstyle \Theta^+_{\Delta_3,\alpha\cup\overline{\alpha}_3^H}} \\ \boldsymbol{\alpha} \cup \overline{\boldsymbol{\alpha}}_1^H & \xrightarrow{\Theta^{can}_{\alpha\cup\overline{\alpha}_1^H,\alpha\cup\overline{\alpha}_2^H}} & \boldsymbol{\alpha} \cup \overline{\boldsymbol{\alpha}}_2^H & \xrightarrow{\Theta^+_{\alpha\cup\overline{\alpha}_2^H,\alpha\cup\overline{\alpha}_3^H}} & \boldsymbol{\alpha} \cup \overline{\boldsymbol{\alpha}}_3^H \end{array} .$$

Here, we are omitting writing primes on the various curves labeled $\boldsymbol{\alpha}$.

A generic, genus 2 region of the quadruple $(\Sigma_0 \# \overline{\Sigma}, \boldsymbol{\Delta}_1, \boldsymbol{\Delta}_2, \boldsymbol{\Delta}_3, \boldsymbol{\alpha} \cup \overline{\boldsymbol{\alpha}}_3^H)$ is shown in Figure 17.1.

LEMMA 17.2. *The diagram $\mathcal{L}^2_{2\text{-h},\beta}$ is a hypercube of attaching curves.*

PROOF. The length 1 relations are equivalent to each length 1 class being a cycle, which is straightforward from the construction.

There are four length 2 relations to verify, which follow from the relations

$$\begin{aligned} f_{\Delta_1,\Delta_2,\Delta_3}\left(\Theta^{\text{can}}_{\Delta_1,\Delta_2}, \Theta^+_{\Delta_2,\Delta_3}\right) &= 0, \\ f_{\alpha\cup\overline{\alpha}_1^H,\alpha\cup\overline{\alpha}_2^H,\alpha\cup\overline{\alpha}_3^H}\left(\Theta^{\text{can}}_{\alpha\cup\overline{\alpha}_1^H,\alpha\cup\overline{\alpha}_2^H}, \Theta^+_{\alpha\cup\overline{\alpha}_2^H,\alpha\cup\overline{\alpha}_3^H}\right) &= 0, \\ f_{\Delta_1,\alpha\cup\overline{\alpha}_1^H,\alpha\cup\overline{\alpha}_2^H}\left(\Theta^+_{\Delta_1,\alpha\cup\overline{\alpha}_1^H}, \Theta^{\text{can}}_{\alpha\cup\overline{\alpha}_1^H,\alpha\cup\overline{\alpha}_2^H}\right) &= \Theta^{\text{can}}_{\Delta_1,\alpha\cup\overline{\alpha}_2^H}, \\ f_{\Delta_1,\alpha\cup\overline{\alpha}_1^H,\alpha\cup\overline{\alpha}_2^H}\left(\Theta^+_{\Delta_1,\alpha\cup\overline{\alpha}_1^H}, \Theta^{\text{can}}_{\alpha\cup\overline{\alpha}_1^H,\alpha\cup\overline{\alpha}_2^H}\right) &= \Theta^{\text{can}}_{\Delta_1,\alpha\cup\overline{\alpha}_2^H}, \\ f_{\Delta_2,\Delta_3,\alpha\cup\overline{\alpha}_3^H}\left(\Theta^+_{\Delta_2,\Delta_3}, \Theta^+_{\Delta_3,\alpha\cup\overline{\alpha}_3^H}\right) &= \Theta^+_{\Delta_2,\alpha\cup\overline{\alpha}_3^H}, \\ f_{\Delta_2,\alpha\cup\overline{\alpha}_2^H,\alpha\cup\overline{\alpha}_3^H}\left(\Theta^+_{\Delta_2,\alpha\cup\overline{\alpha}_2^H}, \Theta^+_{\alpha\cup\overline{\alpha}_2^H,\alpha\cup\overline{\alpha}_3^H}\right) &= \Theta^+_{\Delta_2,\alpha\cup\overline{\alpha}_3^H}. \end{aligned} \tag{17.1}$$

This is a free offprint provided to the author by the publisher. Copyright restrictions may apply.

The first two lines of (17.1) follow from Lemma 12.4. We now focus on the third equation. The triple $(\Sigma_0\#\overline{\Sigma}, \boldsymbol{\Delta}_1, \boldsymbol{\alpha}\cup\overline{\boldsymbol{\alpha}}_1, \boldsymbol{\alpha}\cup\overline{\boldsymbol{\alpha}}_2^H)$ is a genus $2g(\Sigma)-2$ stabilization of the genus 1 triple $(\mathbb{T}^2, \overline{c}_1', c_1, c_2)$ (where $\overline{c}_1'$ denotes an isotopic copy of $\overline{c}_1$). The index tuple of this stabilization is $(0, -g(\Sigma_0), 0)$, by Lemma 9.7 and Figure 9.4. By Proposition 10.2, it suffices to show the claim for the destabilized, genus 1 triple. For the genus 1 triple, the count is immediate. The fourth through sixth model computations are proven similarly.

The length 3 relation fo the diagram $\mathcal{L}^2_{2\text{-h},\beta}$ is reads

$$\begin{aligned} 0 &= h_{\Delta_1,\Delta_2,\Delta_3,\alpha\cup\overline{\alpha}_3^H}\left(\Theta^{\text{can}}_{\Delta_1,\Delta_2}, \Theta^+_{\Delta_2,\Delta_3}, \Theta^+_{\Delta_3,\alpha\cup\overline{\alpha}_3^H}\right) \\ &+ h_{\Delta_1,\Delta_2,\alpha\cup\overline{\alpha}_2^H,\alpha\cup\overline{\alpha}_3^H}\left(\Theta^{\text{can}}_{\Delta_1,\Delta_2}, \Theta^+_{\Delta_2,\alpha\cup\overline{\alpha}_2^H}, \Theta^+_{\alpha\cup\overline{\alpha}_2^H,\alpha\cup\overline{\alpha}_3^H}\right) \\ &+ h_{\Delta_1,\alpha\cup\overline{\alpha}_1^H,\alpha\cup\overline{\alpha}_2^H,\alpha\cup\overline{\alpha}_3^H}\left(\Theta^+_{\Delta_1,\alpha\cup\overline{\alpha}_1^H}, \Theta^{\text{can}}_{\alpha\cup\overline{\alpha}_1^H,\alpha\cup\overline{\alpha}_2^H}, \Theta^+_{\alpha\cup\overline{\alpha}_2^H,\alpha\cup\overline{\alpha}_3^H}\right). \end{aligned} \tag{17.2}$$

To prove (17.2), we will show that each quadrilateral count vanishes. We focus on the count which occurs on $(\Sigma_0\#\overline{\Sigma}, \boldsymbol{\Delta}_1, \boldsymbol{\Delta}_2, \boldsymbol{\Delta}_3, \boldsymbol{\alpha}\cup\overline{\boldsymbol{\alpha}}_3^H)$. This quadruple is a genus $2g(\Sigma)-2$ stabilization of the genus 1 quadruple $(\mathbb{T}^2, c_1, c_2, c_3, c_3')$. Furthermore, the index tuple of this stabilization is $(-g(\Sigma_0), -g(\Sigma_0), 0, 0)$, by Lemma 9.7 and Figure 9.5. By Proposition 10.6 it is sufficient to show that the associated count of quadrilaterals on $(\mathbb{T}^2, c_1, c_2, c_3, c_3')$ vanishes, which is proven in Lemma 12.6. The other two quadrilateral counts are proven by an easy modification of this arguement. □

We define $\mathcal{C}^2_{2\text{-h}}$ as the pairing of the $\mathcal{L}^2_{2\text{-h},\beta}$, and the 0-dimensional hypercube of alpha attaching curves consisting of $\boldsymbol{\alpha}\cup\overline{\boldsymbol{\beta}}$. The hypercube is schematically shown below:

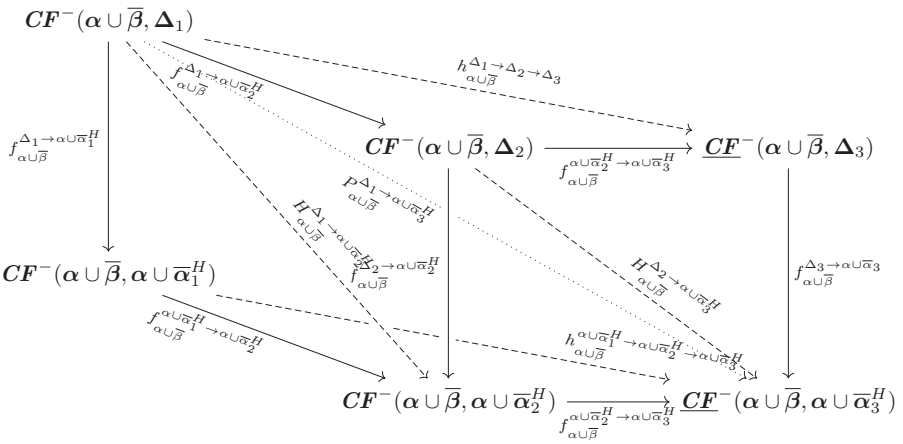


FIGURE 17.2. The hypercube $\mathcal{C}^2_{2\text{-h}}$. We omit writing the primes on the various copies of $\boldsymbol{\alpha}$.

This is a free offprint provided to the author by the publisher. Copyright restrictions may apply.

This is a free offprint provided to the author by the publisher. Copyright restrictions may apply.

CHAPTER 18

The tautological and flip-map hypercubes

18.1. The tautological hypercube

The bottom face of the hypercube $\mathcal{C}_{3\text{-h}}$ reads

$$\begin{array}{ccc} \boldsymbol{CF}^-\left(\overline{\Sigma},\overline{\boldsymbol{\beta}},\overline{\boldsymbol{\alpha}}_1\right) & & \\ \Big\downarrow{\scriptstyle f^{\overline{\alpha}_1\to\overline{\alpha}_2}_{\overline{\beta}}} & \searrow^{h^{\overline{\alpha}_1\to\overline{\alpha}_2\to\overline{\alpha}_3}_{\overline{\beta}}} & \\ \boldsymbol{CF}^-(\overline{\Sigma},\overline{\boldsymbol{\beta}},\overline{\boldsymbol{\alpha}}_2) & \xrightarrow{f^{\overline{\alpha}_2\to\overline{\alpha}_3}_{\overline{\beta}}} & \underline{\boldsymbol{CF}}^-(\overline{\Sigma},\overline{\boldsymbol{\beta}},\overline{\boldsymbol{\alpha}}_3,\hat{z},w). \end{array} \tag{18.1}$$

The diagram in (18.1) is very similar to the top of the main hypercube, as described in Chapter 12. There are two subtle differences:

(1) The point z is now the special basepoint of the third complex, whereas at the top of the main hypercube, w is the special basepoint
(2) To achieve admissibility for triangles and rectangles, the curves $\overline{c}_1$, $\overline{c}_2$ and $\overline{c}_3$ must have slightly different position than c_1, c_2 and c_3. (Compare the two sides of Figure 16.2).

We will assume that $\overline{c}_1$ and $\overline{c}_2$ are the mirrors of c_1 and c_2, but that $\overline{c}_3$ differs slightly from the mirror of c_3. We write $\overline{\overline{c}}_3$ for the image of $\overline{c}_3$ on Σ. We may view $\overline{\overline{c}}_3$ as being obtained by sliding c_3 across the intersection of c_1 and c_2. Compare Figure 16.2. We will write

$$\overline{\overline{\boldsymbol{\alpha}}}_3 := \boldsymbol{\alpha} \cup \overline{\overline{c}}_3.$$

As defined in Section 2.2, there are tautological isomorphism

$$\begin{aligned} \eta_1 &\colon \boldsymbol{CF}^-(\overline{\Sigma},\overline{\boldsymbol{\beta}},\overline{\boldsymbol{\alpha}}_1) \to \boldsymbol{CF}^-(\Sigma,\boldsymbol{\alpha}_1,\boldsymbol{\beta}) \\ \eta_2 &\colon \boldsymbol{CF}^-(\overline{\Sigma},\overline{\boldsymbol{\beta}},\overline{\boldsymbol{\alpha}}_2) \to \boldsymbol{CF}^-(\Sigma,\boldsymbol{\alpha}_2,\boldsymbol{\beta}) \\ \underline{\eta}_3 &\colon \underline{\boldsymbol{CF}}^-(\overline{\Sigma},\overline{\boldsymbol{\beta}},\overline{\boldsymbol{\alpha}}_3,\hat{z},w) \to \underline{\boldsymbol{CF}}^-(\Sigma,\overline{\overline{\boldsymbol{\alpha}}}_3,\boldsymbol{\beta},w,\hat{z}). \end{aligned}$$

Furthermore, the following diagram is tautologically a hypercube of chain complexes:

This is a free offprint provided to the author by the publisher. Copyright restrictions may apply.

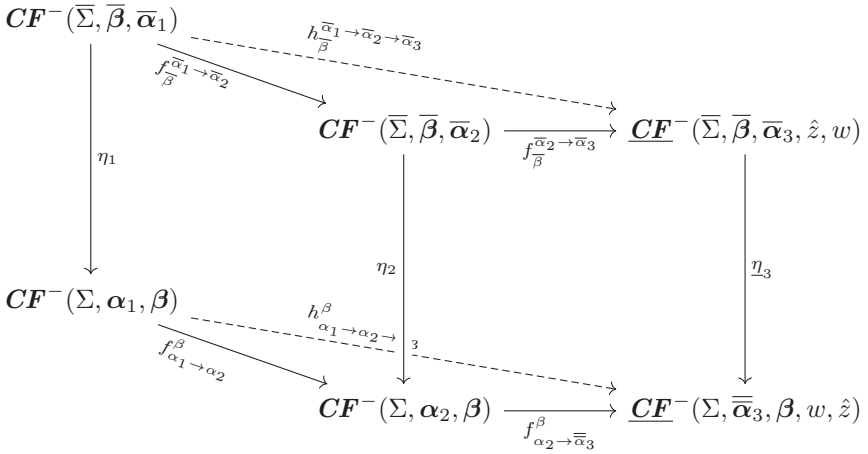


FIGURE 18.1. The tautological hypercube $\mathcal{C}_\eta$.

18.2. The flip-map

In this section, we investigate the *flip-map*

$$\mathfrak{F}_{z\to w}\colon \underline{\boldsymbol{CF}}^-(\Sigma,\overline{\overline{\boldsymbol{\alpha}}}_3,\boldsymbol{\beta},w,\hat{z})\to\underline{\boldsymbol{CF}}^-(\Sigma,\boldsymbol{\alpha}_3,\boldsymbol{\beta},\hat{w},z),$$

in detail. Note that the distinction between $\overline{\overline{\boldsymbol{\alpha}}}_3$ and $\boldsymbol{\alpha}_3$ makes no difference to the complexes described above (if $\overline{\overline{c}}_3$ is sufficiently close to c_3), however it will make a difference for the triangle and quadrilateral maps appearing in the flip-map hypercube. (Compare Figure 16.2).

We recall from (2.10) that the flip-map $\mathfrak{F}_{z\to w}$ is the composition

$$\mathfrak{F}_{z\to w}:=\theta_w^{-1}\circ(\Psi_{(\Sigma,\overline{\overline{\alpha}}_3,\beta,z)\to(\Sigma,\alpha_3,\beta,w)}\otimes T^n)\circ\theta_z,$$

where $\Psi_{(\Sigma,\overline{\overline{\alpha}}_3,\beta,z)\to(\Sigma,\alpha_3,\beta,w)}$ is the naturality map induced by moving z to w along a fixed subarc of K.

For the purpose of constructing the flip map hypercube, it is helpful to have a concrete model for the naturality map $\Psi_{(\Sigma,\overline{\overline{\alpha}}_3,\beta,z)\to(\Sigma,\alpha_3,\beta,w)}$. Let us write $(\Sigma,\boldsymbol{\alpha}_3',\boldsymbol{\beta},z)$ for the diagram obtained by moving c_3 over the basepoint z (this may be achieved by a sequence of handleslides, away from z). There is a canonical diffeomorphism

$$\phi_*\colon(\Sigma,\boldsymbol{\alpha}_3',\boldsymbol{\beta},z)\to(\Sigma,\boldsymbol{\alpha}_3,\boldsymbol{\beta},w),$$

which may be identified with the diffeomorphism map which moves z to w, along a subarc of K.

The map $\Psi_{(\Sigma,\overline{\overline{\alpha}}_3,\beta,z)\to(\Sigma,\alpha_3,\beta,w)}$ is equal to the composition

$$\Psi_{(\Sigma,\overline{\overline{\alpha}}_3,\beta,z)\to(\Sigma,\alpha_3,\beta,w)}=\phi_*\circ\Psi^{\beta}_{\overline{\overline{\alpha}}_3\to\alpha_3'},$$

where $\Psi^{\beta}_{\overline{\overline{\alpha}}_3\to\alpha_3'}\colon\boldsymbol{CF}^-(\Sigma,\boldsymbol{\alpha}_3,\boldsymbol{\beta},z)\to\boldsymbol{CF}^-(\Sigma,\boldsymbol{\alpha}_3',\boldsymbol{\beta},z)$ is the ordinary map from naturality.

The map $\Psi^{\beta}_{\overline{\overline{\alpha}}_3\to\alpha_3'}$ cannot in general be computed using a single triangle count, because of admissibility issues. Instead, we pick an intermediate choice of alpha-curves, $\boldsymbol{\alpha}_3^{\mathrm{W}}$, by winding $\boldsymbol{\alpha}_3'$ in the genus 1 surgery region along a curve which is

This is a free offprint provided to the author by the publisher. Copyright restrictions may apply.

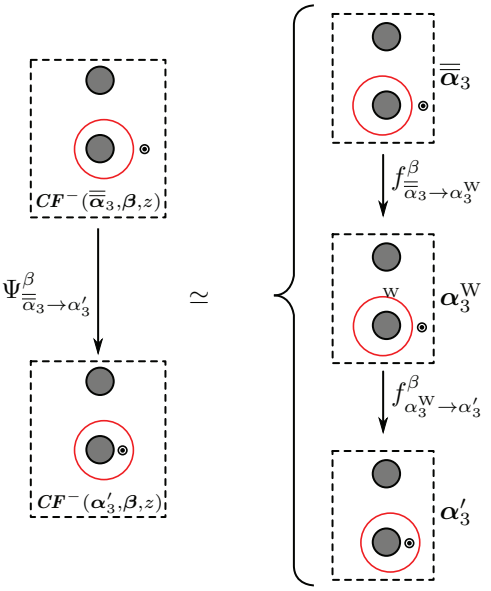


FIGURE 18.2. Decomposing $\Psi^{\beta}_{\alpha_3\to\alpha_3'}$ as the composition $f^{\beta}_{\alpha_3^{\mathrm{W}}\to\alpha_3'}\circ f^{\beta}_{\alpha_3\to\alpha_3^{\mathrm{W}}}$. We continue our convention of denoting wound curves with a W.

dual to c_3. We decompose $\Psi^{\beta}_{\overline{\overline{\alpha}}_3\to\alpha_3'}$ as

$$\Psi^{\beta}_{\overline{\overline{\alpha}}_3\to\alpha_3'} = f^{\beta}_{\alpha_3^{\mathrm{W}}\to\alpha_3'}\circ f^{\beta}_{\overline{\overline{\alpha}}_3\to\alpha_3^{\mathrm{W}}},$$

where $f^{\beta}_{\alpha_3^{\mathrm{W}}\to\alpha_3'}$ and $f^{\beta}_{\overline{\overline{\alpha}}_3\to\alpha_3^{\mathrm{W}}}$ are holomorphic triangle maps. See Figure 18.2. Compare [**MO10**, Section 8.7].

18.3. More hypercubes with twisted coefficients

In this section, we describe a construction of hypercubes with twisted coefficients, which is similar to the one from Section 5.7, but appears in the flip-map hypercube.

Let Σ be a compact, oriented surface, equipped with two points, $p, q \in \Sigma$, as well as a special basepoint w (which may be different from p and q). Suppose that $\boldsymbol{\alpha}_n, \dots, \boldsymbol{\alpha}_1$ is a collection of attaching curves on Σ, and suppose that $\gamma_n, \dots, \gamma_1$ is a collection of integral 1-chains in $U_{\alpha_n}, \dots, U_{\alpha_1}$, respectively, such that $\partial\gamma_i = p - q$. The 1-chains $\gamma_n, \dots, \gamma_1$ determine a relative 2-cycle

$$S_{\gamma_n,\dots,\gamma_1} \in C_2(X_{\alpha_n,\dots,\alpha_1}, \partial X_{\alpha_n,\dots,\alpha_1}).$$

The 2-chain $S_{\gamma_n,\dots,\gamma_1}$ is the sum of $\gamma_i \times [0,1] \subseteq U_{\alpha_i} \times [0,1]$, as well as $\{p,q\} \times D_n \subseteq \Sigma \times D_n$. If ψ is a homology class of n-gons on $(\Sigma, \boldsymbol{\alpha}_n, \dots, \boldsymbol{\alpha}_1, w)$ and $\widehat{S} \in H_2(X;\mathbb{Z})$, we define

$$\mathfrak{m}(w, \widehat{S}, \psi) = \frac{\left\langle c_1(\mathfrak{s}_w(\psi)), [\widehat{S}]\right\rangle - [\widehat{S}]\cdot[\widehat{S}]}{2}.$$

Note that $\mathfrak{m}(w, \widehat{S}, \psi)$ is an integer, since $c_1(\mathfrak{s}_w(\psi))$ is a characteristic vector.

This is a free offprint provided to the author by the publisher. Copyright restrictions may apply.

We say $\underline{\mathcal{L}}_\alpha$ is a hypercube of alpha attaching curves with a *cube of singular twisting chains* on (Σ, p, q, w), if $\underline{\mathcal{L}}_\alpha$ consists of the following:

(1) For each $\varepsilon \in \mathbb{E}_n$, a set of curves $\boldsymbol{\alpha}^\varepsilon$ on Σ.
(2) For each pair $\varepsilon', \varepsilon \in \mathbb{E}_n$ such that $\varepsilon' > \varepsilon$, a choice of chain $\Theta_{\alpha^{\varepsilon'}, \alpha^\varepsilon} \in \boldsymbol{CF}^-(\Sigma, \boldsymbol{\alpha}^{\varepsilon'}, \boldsymbol{\alpha}^\varepsilon, w) \otimes \mathbb{F}[\mathbb{Z}/m]$.
(3) For each $\varepsilon \in \mathbb{E}_n$, a choice of integral 1-chain $\gamma^\varepsilon \subseteq U_{\alpha^\varepsilon}$ such that $\partial \gamma^\varepsilon = p - q$.
(4) For each pair $\varepsilon, \varepsilon' \in \mathbb{E}_n$ such that $\varepsilon' > \varepsilon$, a choice of integral 2-chain $C_{\varepsilon', \varepsilon} \subseteq -U_{\alpha^{\varepsilon'}} \cup U_{\alpha^\varepsilon}$ such that $\partial C_{\varepsilon', \varepsilon} = \gamma_{\varepsilon'} \cup -\gamma_\varepsilon$.

Furthermore, there is a compatibility condition, as we now describe. Write $\underline{\mathfrak{f}}_{\alpha^{\varepsilon_n}, \ldots, \alpha^{\varepsilon_1}}$ for the map which counts holomorphic n-gons of index $3-n$, weighted by $U^{n_w(\psi)} T^{\mathfrak{m}(w, \widehat{S}_{\gamma_n, \ldots, \gamma_1}, \psi)}$. Here, $\widehat{S}_{\gamma_n, \ldots, \gamma_1}$ is the closed, integral 2-chain

$$\widehat{S}_{\gamma_n, \ldots, \gamma_1} = S_{\gamma_n, \ldots, \gamma_1} - C_{\varepsilon_n, \varepsilon_{n-1}} - \cdots - C_{\varepsilon_2, \varepsilon_1} + C_{\varepsilon_n, \varepsilon_1}.$$

We assume that the twisted polygon counting maps satisfy (5.6) (the compatibility condition for a hypercube of attaching curves). A hypercube of *beta* attaching curves with a cube of singular twisting chains is defined by the natural modification.

Suppose $\underline{\mathcal{L}}_\alpha$ and $\underline{\mathcal{L}}_\beta$ are two hypercubes of attaching curves on $(\Sigma, p, q, \hat{w})$ which are equipped with cubes of singular twisting chains. If we additionally pick a collection of 2-chains $C_{\varepsilon, \nu}$, ranging over $\varepsilon \in \mathbb{E}_n$ and $\nu \in \mathbb{E}_{n'}$, we may pair them to form a hypercube $\underline{\underline{\boldsymbol{CF}}}^-(\underline{\mathcal{L}}_\alpha, \underline{\mathcal{L}}_\beta)$. The complex at any (ε, ν) is the Floer complex $\boldsymbol{CF}^-(\boldsymbol{\alpha}^\varepsilon, \boldsymbol{\beta}^\nu) \otimes \mathbb{F}[\mathbb{Z}/m]$. The hypercube maps are defined as in (5.7), but using the twisted polygon counting maps.

Suppose additionally that whenever $\varepsilon' \in \mathbb{E}_n$ has the property that the homology class of $\widehat{S}_{\varepsilon_j, \ldots, \varepsilon_1}$ is trivial for all sequences $\varepsilon_1 < \cdots < \varepsilon_j$ such that $\varepsilon_j \leq \varepsilon'$, the chain $\Theta_{\alpha^{\varepsilon'}, \alpha^\varepsilon}$ is in $\boldsymbol{CF}^-(\boldsymbol{\alpha}^{\varepsilon'}, \boldsymbol{\alpha}^\varepsilon) \otimes T^0$, for all $\varepsilon < \varepsilon'$. We assume a similar condition holds for the beta-chains. In this situation there is a subcomplex $\underline{\boldsymbol{CF}}^-(\underline{\mathcal{L}}_\alpha, \underline{\mathcal{L}}_\beta) \subseteq \underline{\underline{\boldsymbol{CF}}}^-(\underline{\mathcal{L}}_\alpha, \underline{\mathcal{L}}_\beta)$, as follows. If $(\varepsilon, \nu) \in \mathbb{E}_n \times \mathbb{E}_{n'}$ has the property that

$$\widehat{S}_{\alpha^{\varepsilon_i}, \ldots, \alpha^{\varepsilon_1}, \beta^{\nu_1}, \ldots, \beta^{\nu_j}} = 0 \in H_2(X_{\alpha^{\varepsilon_i}, \ldots, \alpha^{\varepsilon_1}, \beta^{\nu_1}, \ldots, \beta^{\nu_j}}),$$

whenever $\varepsilon_1 < \cdots < \varepsilon_i \leq \varepsilon$ and $\nu_1 < \cdots < \nu_j \leq \nu$, then we set

$$\underline{\boldsymbol{CF}}^-(\underline{\mathcal{L}}_\alpha, \underline{\mathcal{L}}_\beta)^{(\varepsilon, \nu)} = \boldsymbol{CF}^-(\boldsymbol{\alpha}^\varepsilon, \boldsymbol{\beta}^\nu).$$

Otherwise, we set $\underline{\boldsymbol{CF}}^-(\underline{\mathcal{L}}_\alpha, \underline{\mathcal{L}}_\beta)^{(\varepsilon, \nu)} = \boldsymbol{CF}^-(\boldsymbol{\alpha}^\varepsilon, \boldsymbol{\beta}^\nu) \otimes \mathbb{F}[\mathbb{Z}/m]$. It is straightforward to see that $\underline{\boldsymbol{CF}}^-(\underline{\mathcal{L}}_\alpha, \underline{\mathcal{L}}_\beta)^{(\varepsilon, \nu)}$ is a subcomplex of $\underline{\underline{\boldsymbol{CF}}}^-(\underline{\mathcal{L}}_\alpha, \underline{\mathcal{L}}_\beta)$.

For hypercubes of dimension 3 and lower, we use the following analog of the notation from Section 5.8. We use lower case letters $\underline{\mathfrak{f}}$, $\underline{\mathfrak{h}}$ and $\underline{\mathfrak{p}}$ to indicate triangle, quadrilateral, and pentagon counting maps, which are weighted using by the quantity $U^{n_w(\psi)} T^{\mathfrak{m}(w, \widehat{S}, \psi)}$. We use the upper case letters $\underline{\mathfrak{H}}$ and $\underline{\mathfrak{P}}$ to indicate length 2 and 3 maps in a hypercube, when they involve more than just a single count of quadrilaterals or pentagons.

18.4. The flip-map hypercube

In this section, we construct the *flip-map hypercube*, shown in Figure 18.3.

This is a free offprint provided to the author by the publisher. Copyright restrictions may apply.

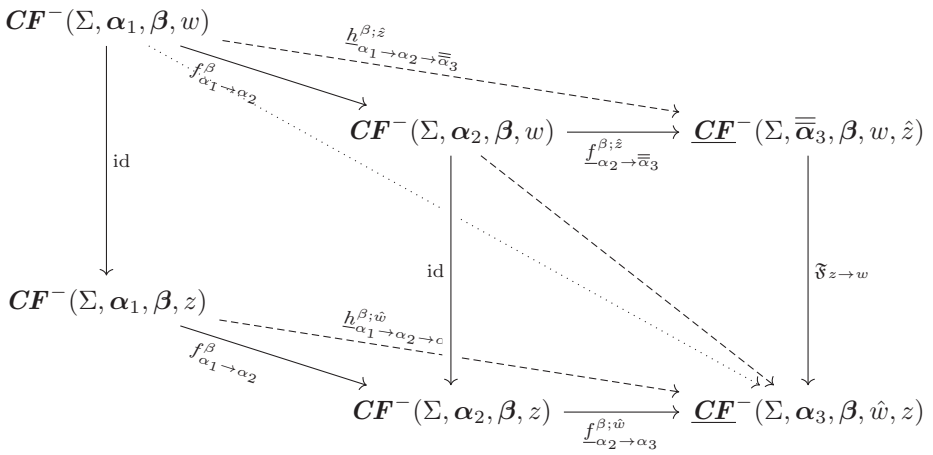


FIGURE 18.3. The flip-map hypercube $\mathcal{C}_{\mathfrak{F}}$. A superscript containing $\hat{w}$ or $\hat{z}$ indicates which basepoint contributes the power of U.

We define the hypercube $\mathcal{C}_{\mathfrak{F}}$ as the compression of a hyperbox of size $(1, 1, 5)$, outlined in Figure 18.4. We explain presently the maps and complexes therein, and then will prove that the diagram satisfies the hyperbox relations.

Let W_{n+m} denote the 2-handle cobordism from Y to $Y_{n+m}(K)$, and let W'_{n+m} denote the cobordism from $Y_{n+m}(K)$ to Y, obtained by reversing the orientation. Let $S_{n+m} \subseteq W'_{n+m}$ denote the induced link cobordism from $(Y_{n+m}(K), U)$ to (Y, K). We orient S_{n+m} so that the chosen orientation of $K \subseteq Y$ coincides with the boundary orientation of ∂S_{n+m}. Write $\widehat{S}_{n+m} \subseteq W'_{n+m}$ for the closed surface obtained by capping S_{n+m} with Seifert surfaces on both ends.

We now describe the maps appearing in the hyperbox in Figure 18.4. The maps $\underline{f}^{\beta;\hat{w}}_{\alpha_2\to\alpha_3}$ and $\underline{f}^{\beta;\hat{z}}_{\alpha_2\to\overline{\alpha}_3}$ are the ones which count triangles weighted by $U^{n_w(\phi)}T^{n_z(\psi)-n_w(\psi)}$, and $U^{n_z(\psi)}T^{n_z(\psi)-n_w(\psi)}$, respectively. These are the maps we have already encountered in the exact triangle.

We view the hyperbox in Figure 18.4 as being obtained by stacking 5 hypercubes $\mathcal{C}^{(1)}_{\mathfrak{F}}, \dots, \mathcal{C}^{(5)}_{\mathfrak{F}}$, ordered from top to bottom. We now explain in more detail the maps which appear in $\mathcal{C}^{(2)}_{\mathfrak{F}}$ and $\mathcal{C}^{(3)}_{\mathfrak{F}}$. The maps appearing in $\mathcal{C}^{(2)}_{\mathfrak{F}}$ are easiest to define if we define them as a pairing of slightly generalized hypercubes of alpha and beta attaching curves, which are equipped with singular twisting chains. We write down

This is a free offprint provided to the author by the publisher. Copyright restrictions may apply.

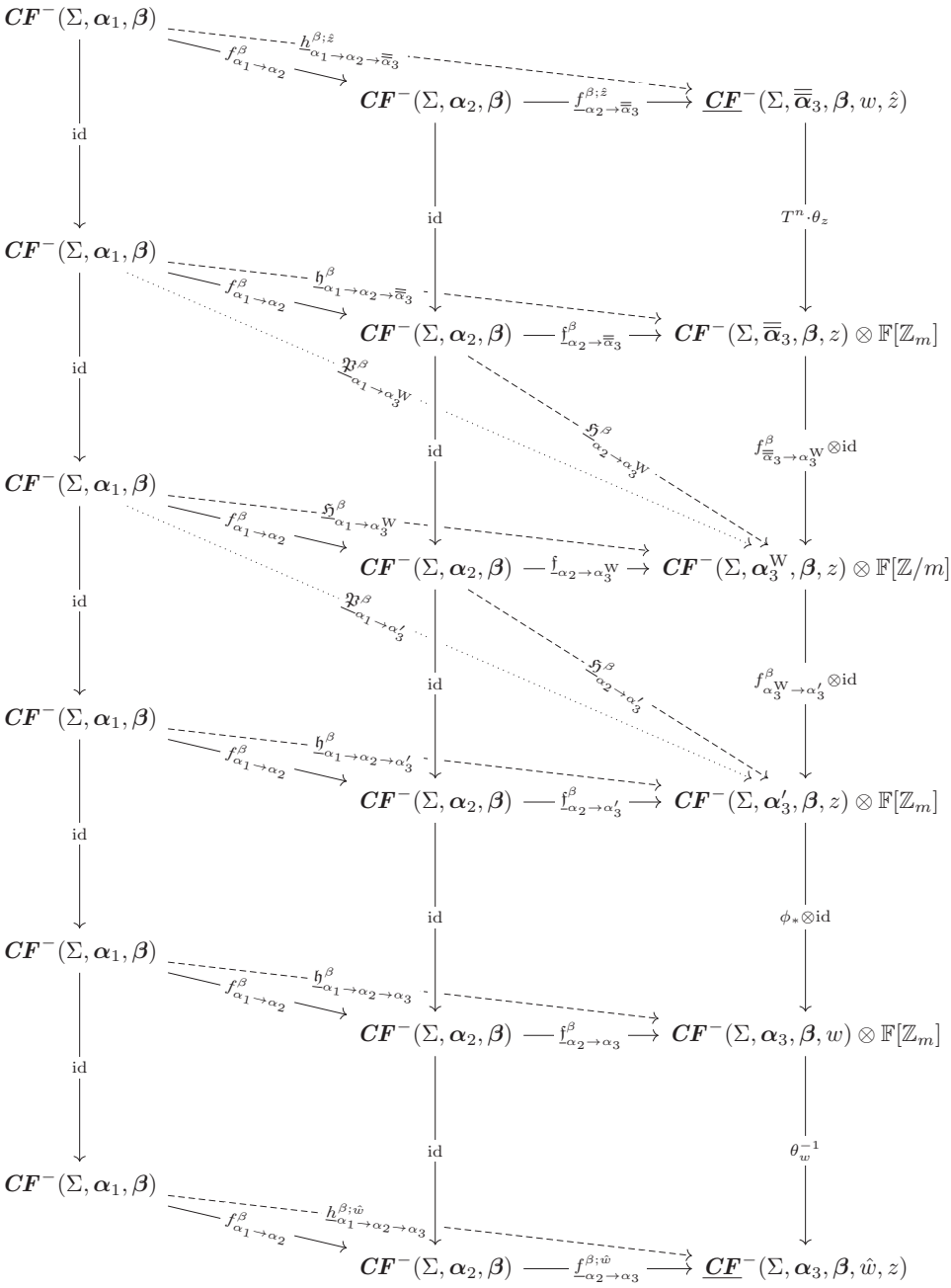
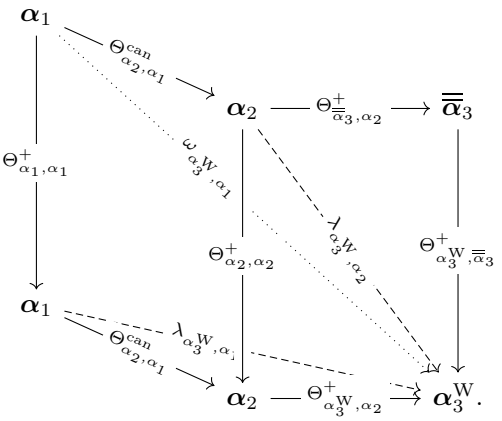


FIGURE 18.4. The hyperbox of chain complexes whose compression is $\mathcal{C}_{\mathfrak{F}}$. We write $\mathcal{C}_{\mathfrak{F}}^{(1)},\dots,\mathcal{C}_{\mathfrak{F}}^{(5)}$ for these hypercubes, ordered top-to-bottom.

This is a free offprint provided to the author by the publisher. Copyright restrictions may apply.

the following non-admissible diagram of alpha attaching curves:

(18.2) $\mathcal{L}_{\alpha}^{(2)} :=$



Equation (18.2) is not a genuine diagram of attaching curves, since $\boldsymbol{\alpha}_1$ and $\boldsymbol{\alpha}_2$ are both repeated. In particular, the classes $\Theta^+_{\alpha_1,\alpha_1}$ and $\Theta^+_{\alpha_2,\alpha_2}$ are not genuine elements of a chain complex. Nonetheless, we may still define polygon counting maps which have them as inputs, by adopting the *strict unality* convention that a triangle map with input $\Theta^+_{\alpha_i,\alpha_i}$ is the identity map, and a quadrilateral or pentagon map with $\Theta^+_{\alpha_i,\alpha_i}$ as input vanishes. (Alternatively, one could just replace the second copies of $\boldsymbol{\alpha}_1$ and $\boldsymbol{\alpha}_2$ with small Hamiltonian translates).

We now wish to promote $\mathcal{L}^2_\alpha$ to a hypercube of attaching curves with a cube of singular twisting chains, as follows. We consider the diagram $(\Sigma, \boldsymbol{\alpha}_3, \boldsymbol{\alpha}_2, \boldsymbol{\alpha}_1, w, z)$. Each set of attaching curves determines a 1-chain γ_3, γ_2 or γ_1, as follows. Pick an embedded arc on Σ which avoids $\boldsymbol{\alpha}_3$, $\boldsymbol{\alpha}_2$ or $\boldsymbol{\alpha}_1$ and connects w to z. Then γ_i is obtained by pushing the interior of this arc into the handlebody U_{α_3}, U_{α_2} or U_{α_1}. For $\boldsymbol{\alpha}_1$ and $\boldsymbol{\alpha}_2$, we pick the canonical short path on Σ. We pick the 2-chains C_{α_2,α_1} to be a disk in the neighborhood of the canonical short path. The choice of C_{α_3,α_2} and C_{α_3,α_1} is not important, though we assume they are supported in the summands of Y_{α_3,α_2} and Y_{α_2,α_1} corresponding to the special genus 1 region of the Heegaard triple. Additionally, we construct 2-chains C_{α_1,α_1}, C_{α_2,α_2} and C_{α_3,α_3}, as follows. Since the arc γ_i is obtained by pushing an arc off of Σ, we may push this arc off in both directions to obtain a disk in Y_{α_i,α_i}.

To equip $\mathcal{L}^2_\alpha$ with a cube of singular twisting chains, we use the arcs γ_i whenever a set of attaching curves is related to $\boldsymbol{\alpha}_i$ by a sequence of handleslides and isotopies. For example, we decorate $\overline{\overline{\boldsymbol{\alpha}}}_3$ and $\boldsymbol{\alpha}_3^{\mathrm{W}}$ both by γ_3. Similarly, if $\boldsymbol{\delta}$ and $\boldsymbol{\xi}$ are a pair of attaching curves in the cube, we use the 2-chains C_{α_i,α_j} if $\boldsymbol{\delta}$ (resp. $\boldsymbol{\xi}$) is related to $\boldsymbol{\alpha}_i$ (resp. $\boldsymbol{\alpha}_j$) by a sequence of handleslides and isotopies.

We now pick the length 1 chains in Equation (18.2) arbitrarily, so that they are homogeneously grades cycles and represent the top degree or canonical elements of homology.

LEMMA 18.1. *The cycles in Equation* (18.2) *satisfy*

$$\underline{f}_{\overline{\overline{\alpha}}_3,\alpha_2,\alpha_1}\left(\Theta^+_{\overline{\overline{\alpha}}_3,\alpha_2}, \Theta^{\mathrm{can}}_{\alpha_2,\alpha_1}\right) = 0,$$
$$\left[f_{\alpha_3^{\mathrm{W}},\overline{\overline{\alpha}}_3,\alpha_2}\left(\Theta^+_{\alpha_3^{\mathrm{W}},\overline{\overline{\alpha}}_3}, \Theta^+_{\overline{\overline{\alpha}}_3,\alpha_2}\right)\right] = \left[\Theta^+_{\alpha_3^{\mathrm{W}},\alpha_2}\right],$$
$$\left[\underline{f}_{\alpha_3^{\mathrm{W}},\alpha_2,\alpha_1}\left(\Theta^+_{\alpha_3^{\mathrm{W}},\alpha_2}, \Theta^{\mathrm{can}}_{\alpha_2,\alpha_1}\right)\right] = 0.$$

This is a free offprint provided to the author by the publisher. Copyright restrictions may apply.

PROOF. The second equality follows since $\boldsymbol{\alpha}_3^{\mathrm{W}}$ are isotopic to $\overline{\overline{\boldsymbol{\alpha}}}_3$, so the corresponding transition map preserves the top degree generator. We turn our attention to the first equation. Equation 12.3 implies that triangle classes appear in pairs which have the same U power, and represent conjugate Spin^c structures. It remains to see that the T-powers coincide, for each pair. The surface $\widehat{S}_{\overline{\overline{\alpha}}_3,\alpha_2,\alpha_1}$ is $\widehat{S}_m$, a sphere of self-interestion $-m$. Using the notation of Lemma 12.3, the difference of the T-powers representing $\mathfrak{s}_k^+$ and $\mathfrak{s}_k^-$ is $\pm\langle c_1(\mathfrak{s}_k^+), \widehat{S}_m\rangle = \pm(2k+1)m$, which is divisible by m. The third equation follows from the first, together with the well-definedness of the cobordism maps. □

We pick $\lambda_{\alpha_3^{\mathrm{W}},\alpha_2}$ and $\lambda_{\alpha_3^{\mathrm{W}},\alpha_1}$ so that

$$\begin{aligned}\partial(\lambda_{\alpha_3^{\mathrm{W}},\alpha_2}) &= f_{\alpha_3^{\mathrm{W}},\overline{\overline{\alpha}}_3,\alpha_2}\left(\Theta^+_{\alpha_3^{\mathrm{W}},\overline{\overline{\alpha}}_3}, \Theta^{\pm}_{\overline{\overline{\alpha}}_3,\alpha_2}\right) + \Theta^+_{\alpha_3^{\mathrm{W}},\alpha_2},\\ \partial(\lambda_{\alpha_3^{\mathrm{W}},\alpha_1}) &= \underline{\mathfrak{f}}_{\alpha_3^{\mathrm{W}},\alpha_2,\alpha_1}\left(\Theta^+_{\alpha_3^{\mathrm{W}},\alpha_2}, \Theta^{\mathrm{can}}_{\alpha_2,\alpha_1}\right).\end{aligned} \tag{18.3}$$

Furthermore, we assume that $\lambda_{\alpha_3^{\mathrm{W}},\alpha_2}$ is of homogenous grading one higher than $\Theta^+_{\alpha_3^{\mathrm{W}},\alpha_2}$. This is not possible for $\lambda_{\alpha_3^{\mathrm{W}},\alpha_1}$, since $\underline{\mathfrak{f}}_{\alpha_3^{\mathrm{W}},\alpha_2,\alpha_1}$ sums over infinitely many Spin^c structures. Instead, we assume that $\lambda_{\alpha_3^{\mathrm{W}},\alpha_1}$ is decomposed as a sum

$$\lambda_{\alpha_3^{\mathrm{W}},\alpha_1} := \sum_{k=0}^{\infty} \lambda_{\alpha_3^{\mathrm{W}},\alpha_1;\mathfrak{s}_k^+},$$

where $\mathfrak{s}_k^+$ is the Spin^c structure on $X_{\alpha_3^{\mathrm{W}},\alpha_2,\alpha_1}$ defined in Section 12.3. We will think of $\lambda_{\alpha_3^{\mathrm{W}},\alpha_1;\mathfrak{s}_k^-}$ as also being defined, but being 0. (The asymmetry is somewhat arbitrary, but makes our discussion of gradings in Section 20 simpler). Write

$$\mathfrak{u}_k := \{\mathfrak{s}_k^+, \mathfrak{s}_k^-\} \subseteq \mathrm{Spin}^c(X_{\alpha_3^{\mathrm{W}},\alpha_2,\alpha_1}).$$

We assume $\lambda_{\alpha_3^{\mathrm{W}},\alpha_1;\mathfrak{s}_k^+}$ is chosen so that

$$\partial\left(\lambda_{\alpha_3^{\mathrm{W}},\alpha_1;\mathfrak{s}_k^+}\right) = \underline{\mathfrak{f}}_{\alpha_3^{\mathrm{W}},\alpha_2,\alpha_1;\mathfrak{u}_k}\left(\Theta^+_{\alpha_3^{\mathrm{W}},\alpha_2}, \Theta^{\mathrm{can}}_{\alpha_2,\alpha_1}\right), \tag{18.4}$$

and also so that $\lambda_{\alpha_3^{\mathrm{W}},\alpha_1;\mathfrak{s}_k^+}$ is of homogeneous grading one greater than the expected grading of the right hand side of (18.4).

Next, we construct the length 3 cycle $\omega_{\alpha_3^{\mathrm{W}},\alpha_1}$. Note that there is a restriction map

$$r\colon \mathrm{Spin}^c\left(X_{\alpha_3^{\mathrm{W}},\overline{\overline{\alpha}}_3,\alpha_2,\alpha_1}\right) \to \mathrm{Spin}^c\left(X_{\alpha_3^{\mathrm{W}},\alpha_2,a_1}\right),$$

which is an isomorphism on the set of Spin^c structures which have torsion restriction to the boundary. Abusing notation slightly, write $\mathfrak{u}_k$ also for $r(\mathfrak{u}_k)$.

LEMMA 18.2. *For each $k \geq 0$, the chain*

$$\begin{aligned}C_{\alpha_3^{\mathrm{W}},\alpha_1;\mathfrak{u}_k} := {}& \underline{\mathfrak{h}}_{\alpha_3^{\mathrm{W}},\overline{\overline{\alpha}}_3,\alpha_2,\alpha_1;\mathfrak{u}_k}\left(\Theta^+_{\alpha_3^{\mathrm{W}},\overline{\overline{\alpha}}_3}, \Theta^{\pm}_{\overline{\overline{\alpha}}_3,\alpha_2}, \Theta^{\mathrm{can}}_{\alpha_2,\alpha_1}\right)\\ &+ \underline{\mathfrak{f}}_{\alpha_3^{\mathrm{W}},\alpha_2,\alpha_1;\mathfrak{u}_k}\left(\lambda_{\alpha_3^{\mathrm{W}},\alpha_2}, \Theta^{\mathrm{can}}_{\alpha_2,\alpha_1}\right) + \lambda_{\alpha_3^{\mathrm{W}},\alpha_1;\mathfrak{s}_k^+}\end{aligned}$$

is a boundary in $\boldsymbol{CF}^-(\boldsymbol{\alpha}_1, \boldsymbol{\alpha}_3^{\mathrm{W}}) \otimes \mathbb{F}[\mathbb{Z}/m]$.

PROOF. The proof is similar to the proof of Lemma 16.11. An easy computation using associativity shows that $C_{\alpha_3^{\mathrm{W}},\alpha_1;\mathfrak{u}_k}$ is a cycle. Note also that since we use almost complex structures which are maximally pinched along the connected

This is a free offprint provided to the author by the publisher. Copyright restrictions may apply.

sum neck, it is sufficient to consider the case then $g(\Sigma) = 1$, by Propositions 10.2 and 10.6. In the genus 1 case, each chain $C_{\alpha_3^{\mathrm{W}},\alpha_1;\mathfrak{u}_k}$ is of homogeneous grading $-mk(k+1)+1$ in a chain complex whose homology is $\mathbb{F}[\![U]\!] \otimes \mathbb{F}[\mathbb{Z}_m]$, which is supported in even gradings. Hence $C_{\alpha_3^{\mathrm{W}},\alpha_1;\mathfrak{u}_k}$ is a boundary. □

For each k, we let $\omega_{\alpha_3^{\mathrm{W}},\alpha_1;\mathfrak{s}_k^+}$ be a chain of homogeneous grading one higher than $C_{\alpha_3^{\mathrm{W}},\alpha_1;\mathfrak{u}_k}$, such that

$$\partial\left(\omega_{\alpha_3^{\mathrm{W}},\alpha_1;\mathfrak{s}_k^+}\right) = C_{\alpha_3^{\mathrm{W}},\alpha_1;\mathfrak{u}_k}.$$

Finally, we define

$$\omega_{\alpha_3^{\mathrm{W}},\alpha_1} := \sum_{k=0}^{\infty} \omega_{\alpha_3^{\mathrm{W}},\alpha_1;\mathfrak{s}_k^+}. \tag{18.5}$$

Finally, we define the maps in $\mathcal{C}_{\mathfrak{F}}^{(2)}$ by pairing $\mathcal{L}_{\alpha}^{(2)}$ with the 0-dimensional hypercube of beta attaching curves consisting of $\boldsymbol{\beta}$ (using the strict unality convention to adapt the construction from Section 5.6). The pairing also requires a choice of 2-chains $C_{\alpha_1,\beta}$, $C_{\alpha_2,\beta}$ and $C_{\alpha_3,\beta}$. We pick $C_{\alpha_1,\beta}$ and $C_{\alpha_2,\beta}$ to be the disks traced out by push-offs of the canonical short paths on the diagram. We pick $C_{\alpha_3,\beta}$ to be a Seifert surface for K.

Concretely,

$$\begin{aligned}
\underline{\mathfrak{H}}^{\beta}_{\alpha_1\to\alpha_3^{\mathrm{W}}} &:= \underline{\mathfrak{h}}^{\beta}_{\alpha_1\to\alpha_2\to\alpha_3^{\mathrm{W}}} + \underline{\mathfrak{f}}^{\beta}_{\alpha_1\to\alpha_3^{\mathrm{W}}} \\
\underline{\mathfrak{H}}^{\beta}_{\alpha_2\to\alpha_3^{\mathrm{W}}} &:= \underline{\mathfrak{h}}^{\beta}_{\alpha_2\to\overline{\overline{\alpha}}_3\to\alpha_3^{\mathrm{W}}} + \underline{\mathfrak{f}}^{\beta}_{\alpha_2\to\alpha_3^{\mathrm{W}}}, \\
\underline{\mathfrak{P}}^{\beta}_{\alpha_1\to\alpha_3^{\mathrm{W}}} &:= \underline{\mathfrak{p}}^{\beta}_{\alpha_1\to\alpha_2\to\overline{\overline{\alpha}}_3\to\alpha_3^{\mathrm{W}}} + \underline{\mathfrak{h}}^{\beta}_{\alpha_1\to\alpha_2\to\alpha_3^{\mathrm{W}}} + \underline{\mathfrak{f}}^{\beta}_{\alpha_1\to\alpha_3^{\mathrm{W}}}.
\end{aligned} \tag{18.6}$$

In the first line of (18.6), $\underline{\mathfrak{h}}^{\beta}_{\alpha_1\to\alpha_2\to\alpha_3^{\mathrm{W}}}$ counts rectangles weighted by $U^{n_w(\psi)}T^{\mathfrak{m}(w,\widehat{S}_{n+m},\psi)}$, with special inputs $\Theta^{\mathrm{can}}_{\alpha_2,\alpha_1}$ and $\Theta^{+}_{\alpha_3^{\mathrm{W}},\alpha_3}$. The map labeled $\underline{\mathfrak{f}}^{\beta}_{\alpha_1\to\alpha_3^{\mathrm{W}}}$ in the first line counts triangles with special input $\lambda_{\alpha_3^{\mathrm{W}},\alpha_1}$, weighted by $U^{n_w(\psi)}T^{\mathfrak{m}(w,\widehat{S}_{n+m},\psi)}$ where $\widehat{S}_{n+m}$ denotes the connected sum of $\widehat{S}_n \subseteq W_n'(K)$ and $\widehat{S}_m \subseteq D(-m,1)$. We note that there is a minor ambiguity in our notation, because the map labeled $\underline{\mathfrak{f}}^{\beta}_{\alpha_1\to\alpha_3^{\mathrm{W}}}$ on the bottom line counts triangles with special input $\omega_{\alpha_3^{\mathrm{W}},\alpha_1}$, and the same T and U weighting as the top line.

The maps for $\mathcal{C}_{\mathfrak{F}}^{(3)}$ are constructed analogously.

Proposition 18.3. *The diagram shown in Figure* 18.4 *forms a 3-dimensional hyperbox of chain complexes of size* $(1,1,5)$.

Proof. It is sufficient to show that each of $\mathcal{C}_{\mathfrak{F}}^{(i)}$ is a 3-dimensional hypercube, for $i \in \{1,2,3,4,5\}$.

Firstly, the diagram $\mathcal{C}_{\mathfrak{F}}^{(4)}$ is obviously a hypercube. Next, the diagrams $\mathcal{C}_{\mathfrak{F}}^{(2)}$ and $\mathcal{C}_{\mathfrak{F}}^{(3)}$ are hypercubes because they are obtained by pairing two hypercubes of attaching curves with cubes of singular twisting chains, as in Section 18.3.

Next, we consider $\mathcal{C}_{\mathfrak{F}}^{(1)}$ and $\mathcal{C}_{\mathfrak{F}}^{(5)}$. We claim

$$T^n \cdot \theta_z \circ \underline{f}^{\beta;\hat{z}}_{\alpha_2\to\overline{\overline{\alpha}}_3} = \underline{\mathfrak{f}}^{\beta}_{\alpha_2\to\overline{\overline{\alpha}}_3} \quad \text{and} \quad \theta_w^{-1} \circ \underline{\mathfrak{f}}^{\beta}_{\alpha_2\to\alpha_3} = \underline{f}^{\beta;\hat{w}}_{\alpha_2\to\alpha_3}. \tag{18.7}$$

This is a free offprint provided to the author by the publisher. Copyright restrictions may apply.

Equation (18.7) follows similarly to [**OS08b**, pg. 18], as we now describe. For the equation involving θ_z, it suffices to show that if $\psi \in \pi_2(\Theta^+_{\overline{\overline{\boldsymbol{\alpha}}}_3,\boldsymbol{\alpha}_2}, \mathbf{x}, \mathbf{y})$ is a class of triangles, then

$$(n_z - n_w)(\psi) + A_{w,z}(\mathbf{y}) = \mathfrak{m}(z, \widehat{S}_{n+m}, \psi) - n. \tag{18.8}$$

Equation (18.8) can be verified by interpreting the triple $(\Sigma, \overline{\overline{\boldsymbol{\alpha}}}_3, \boldsymbol{\alpha}_2, \boldsymbol{\beta}, w, z)$ as determining the link cobordism (W'_{n+m}, S_{n+m}) from $(Y_{n+m}(K), U)$ to (Y, K). Noting that $A_{w,z}(\mathbf{x}) = 0$ for all $\mathbf{x} \in \mathbb{T}_{\alpha_2} \cap \mathbb{T}_\beta$, since $(\Sigma, \boldsymbol{\alpha}_2, \boldsymbol{\beta}, w, z)$ represents an unknot in $Y_{n+m}(K)$, the left hand side of (18.8) is the Alexander grading change of the link cobordism map, which coincides with $\mathfrak{m}(w, \widehat{S}_{n+m}, \psi)$ by [**Zem19b**, Theorem 1.4]. On the other hand,

$$\mathfrak{m}(w, \widehat{S}_{n+m}, \psi) - \mathfrak{m}(z, \widehat{S}_{n+m}, \psi) = \frac{\left\langle c_1(\mathfrak{s}_w(\psi)) - c_1(\mathfrak{s}_z(\psi)), [\widehat{S}_{n+m}] \right\rangle}{2} = -(n+m). \tag{18.9}$$

The first equality of (18.9) is from the definition, while the second follows from the relation $\mathfrak{s}_w(\psi) - \mathfrak{s}_z(\psi) = PD[\widehat{S}_{n+m}]$; see [**OS08b**, pg. 11] or more generally [**Zem19b**, Lemma 3.9].

The equality involving θ_w in (18.7) is proven by the same reasoning. Similarly,

$$\begin{aligned} T^n \cdot \theta_z \circ \underline{h}^{\beta;\hat{z}}_{\alpha_1\to\alpha_2\to\overline{\overline{\alpha}}_3} &= \underline{\mathfrak{h}}^{\beta}_{\alpha_1\to\alpha_2\to\overline{\overline{\alpha}}_3} \quad \text{and} \\ \theta_w^{-1} \circ \underline{\mathfrak{h}}^{\beta}_{\alpha_1\to\alpha_2\to\alpha_3} &= \underline{h}^{\beta;\hat{w}}_{\alpha_1\to\alpha_2\to\alpha_3}. \end{aligned} \tag{18.10}$$

Equations (18.7) and (18.10) imply the length 2 and 3 hypercube relations for $\mathcal{C}^{(1)}_{\mathfrak{F}}$ and $\mathcal{C}^{(5)}_{\mathfrak{F}}$. The length 0 and 1 relations are easy to verify, so we conclude that $\mathcal{C}^{(1)}_{\mathfrak{F}}$ and $\mathcal{C}^{(5)}_{\mathfrak{F}}$ are hypercubes. The proof is complete. □

This is a free offprint provided to the author by the publisher. Copyright restrictions may apply.

CHAPTER 19

Constructing the null-homotopy H_E

In Section 16.6, we showed that to finish the construction of the central hypercube, it is sufficient to construct a map

$$H_E\colon \underline{\boldsymbol{CF}}^-(\Sigma\#\overline{\Sigma},\boldsymbol{\gamma},\boldsymbol{\delta}')\to \underline{\boldsymbol{CF}}^-(\Sigma_0\#\overline{\Sigma},\boldsymbol{\alpha}\cup\overline{\boldsymbol{\beta}},\boldsymbol{\Delta}_3)$$

satisfying

$$[\partial, H_E] = F_3h_1 + F_3h_2 + F_3h_3.$$

We recall that the domain and codomain of H_E are both complexes for $\underline{\boldsymbol{CF}}^-(Y)$. In this section, we describe the construction of the map H_E.

19.1. The endomorphism E

In this section, we describe a more general way to organize the maps h_1, h_2 and h_3 from the central hypercube. We consider genus 1, doubly pointed quadruples

$$\mathcal{Q}_1^0 = (\mathbb{T}^2, c_3, c_2, c_1, c_3', w_0, z_0), \quad \mathcal{Q}_2^0 = (\mathbb{T}^2, c_2, c_1, c_3', c_2', w_0, z_0)$$
$$\text{and} \quad \mathcal{Q}_3^0 = (\mathbb{T}^2, c_1, c_3', c_2', c_1', w_0, z_0).$$

The quadruple $\mathcal{Q}_1^0$ is shown in Figure 19.1, and $\mathcal{Q}_2^0$ and $\mathcal{Q}_3^0$ are obtained similarly.

The doubly pointed quadruple $\mathcal{Q}_1^0$ determines a properly embedded surface $S_{c_3,c_2,c_1,c_3'} \subseteq X_{c_3,c_2,c_1,c_3'}$, as described in Section 18.3. The 4-manifold $X_{c_3,c_2,c_1,c_3'}$ has four boundary components. Two of these boundary components are S^3, one is $S^1\times S^2$, and the other is $L(m,1)$. The surface $S_{c_3,c_2,c_1,c_3'}$ intersects each component of $\partial X_{c_3,c_2,c_1,c_3'}$ in an unknot. Upon attaching 3- and 4-handles to $\partial X_{c_3,c_2,c_1,c_3'}$,

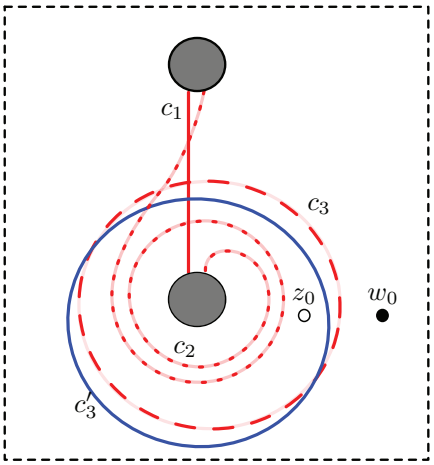


FIGURE 19.1. The Heegaard quadruple $\mathcal{Q}_1^0$.

This is a free offprint provided to the author by the publisher. Copyright restrictions may apply.

and filling in $\partial S_{c_3,c_2,c_1,c_3'}$ with disks, we obtain a sphere of self-intersection $-m$ in the disk bundle $D(-m,1)$. The quadruples $\mathcal{Q}_2^0$ and $\mathcal{Q}_3^0$ determine surfaces and 4-manifolds with the same description.

Suppose that $(\Sigma,\boldsymbol{\alpha},\boldsymbol{\beta},w,z)$ is a doubly pointed diagram for (Y,K). We form the connected sum $\Sigma\#\mathbb{T}^2$ near the points $w_0\in\mathbb{T}^2$ and $z\in\Sigma$. We define the following sets of attaching curves on $\Sigma\#\mathbb{T}^2$:

$$\boldsymbol{\alpha}_1=\boldsymbol{\alpha}\cup\{c_1\},\quad \boldsymbol{\alpha}_2=\boldsymbol{\alpha}'\cup\{c_2\},\quad \boldsymbol{\alpha}_3=\boldsymbol{\alpha}''\cup\{c_3\},$$
$$\boldsymbol{\beta}_3=\boldsymbol{\beta}\cup\{c_3'\},\quad \boldsymbol{\beta}_2:=\boldsymbol{\beta}'\cup\{c_2'\},\quad \text{and}\quad \boldsymbol{\beta}_1:=\boldsymbol{\beta}''\cup\{c_1'\}.$$

Here $\boldsymbol{\alpha}'$ and $\boldsymbol{\alpha}''$ are small Hamiltonian translates of $\boldsymbol{\alpha}$. Similarly $\boldsymbol{\beta}'$ and $\boldsymbol{\beta}''$ are small Hamiltonian translates of $\boldsymbol{\beta}$, and c_i' denotes a translate of c_i.

We define the quadruples

$$\mathcal{Q}_1:=(\Sigma\#\mathbb{T}^2,\boldsymbol{\alpha}_3,\boldsymbol{\alpha}_2,\boldsymbol{\alpha}_1,\boldsymbol{\beta}_3,w,z_0)$$
$$\mathcal{Q}_2:=(\Sigma\#\mathbb{T}^2,\boldsymbol{\alpha}_2,\boldsymbol{\alpha}_1,\boldsymbol{\beta}_3,\boldsymbol{\beta}_2,w,z_0)$$
$$\mathcal{Q}_3:=(\Sigma\#\mathbb{T}^2,\boldsymbol{\alpha}_1,\boldsymbol{\beta}_3,\boldsymbol{\beta}_2,\boldsymbol{\beta}_1,w,z_0).$$

We view $\mathcal{Q}_1$ as being obtained by taking the connected sum of $\mathcal{Q}_1^0$ with the quadruple $(\Sigma,\boldsymbol{\alpha}'',\boldsymbol{\alpha}',\boldsymbol{\alpha},\boldsymbol{\beta},w,z)$ at points p_0 and p, very near w_0 and z, respectively. Then we delete the basepoints w_0 and z.

In this general setting, we define maps h_1, h_2 and h_3 as rectangle counts

$$h_1:=h^{\beta_3}_{\alpha_1\to\alpha_2\to\alpha_3},\quad h_2:=h^{\beta_3\to\beta_2}_{\alpha_1\to\alpha_2},\quad\text{and}\quad h_3:=h^{\beta_3\to\beta_2\to\beta_1}_{\alpha_1}, \tag{19.1}$$

where we weight a rectangle class by $U^{n_w(\psi)}T^{(n_{z_0}-n_w)(\psi)}$. Here, we also use almost complex structures which are maximally pinched along a circle bounding the genus 1 region shown in Figure 19.2. The maps labeled h_1, h_2 and h_3 in Section 16.6 coincide with the maps defined in (19.1), for a particular choice of Heegaard diagram $(\Sigma,\boldsymbol{\alpha},\boldsymbol{\beta},w,z)$.

The maps h_1, h_2 and h_3 fit into the diagram of chain complexes shown in Figure 19.2. In fact, this diagram satisfies all of the hypercube relations except for the length 3 relation. (To see the length 2 relations along the bottom and right faces, we use Proposition 10.2 to destabilize the triples, and Proposition 11.1 to identify the resulting triangle maps with nearest point maps).

We now define

$$E:=F_3\circ h_1+F_3\circ h_2+F_3\circ h_3,$$

where F_3 denotes a 3-handle map. In light of the discussion in Section 16.6, to finish the construction of $\mathcal{C}_{\text{cen}}$, it is sufficient to show the following:

PROPOSITION 19.1. *The map E is chain homotopic to zero. Equivalently, there is a length 3 map H_E which makes the diagram in Figure* 19.2 *into a hypercube of chain complexes.*

In the remainder of this section, we construct a null-homotopy of E, via a holomorphic deformation.

19.2. Vector fields for deformations

In this section, we define several vector fields on $[0,1]\times\mathbb{R}$, Δ and $\square$, which we will use in our proof of Proposition 19.1. We will use these vector fields to deform the quadrilateral maps appearing in the definition of the map E.

This is a free offprint provided to the author by the publisher. Copyright restrictions may apply.

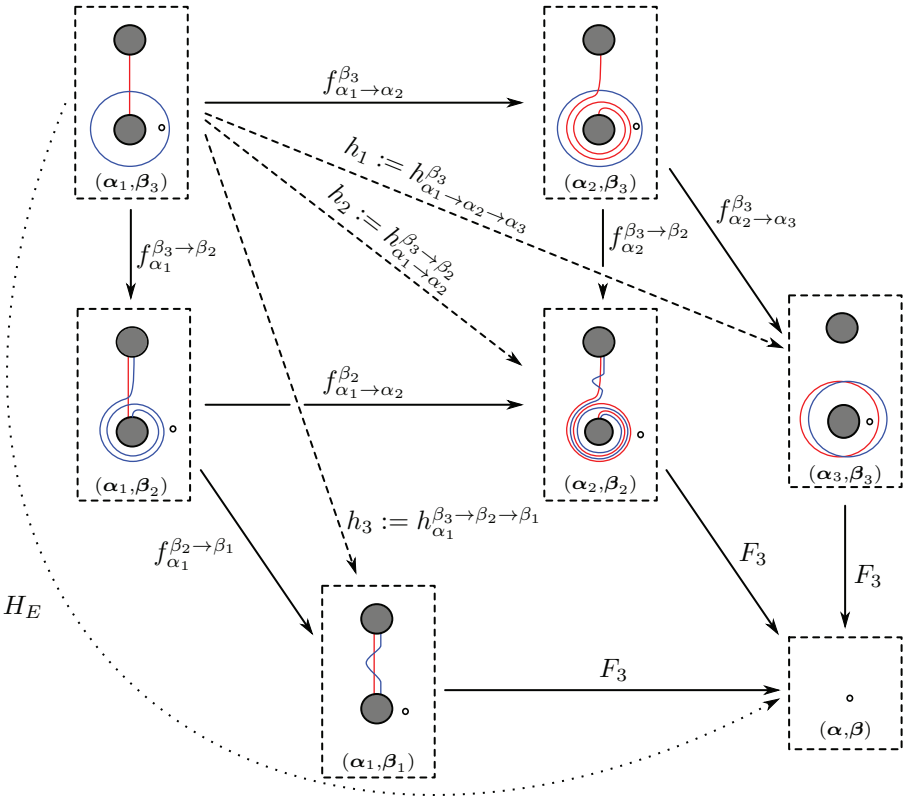


FIGURE 19.2. A null-homotopy H_E of E gives a length 3 arrow which makes this diagram a hypercube of chain complexes.

We begin by defining two vector fields on $[0,1]\times\mathbb{R}$, for which we write v_Y and v_H. Let $f\colon\mathbb{R}\to\mathbb{R}$ be a smooth function, such that $f(0)=0$, $f(1)=0$ and $f(s)>0$ for $s\in(0,1)$. We define v_H to be

$$(v_H)_{(s,t)} := f(s)\cdot\partial/\partial s. \tag{19.2}$$

Next, we construct a vector field v_Y on $[0,1]\times\mathbb{R}$ which satisies the following:

(v_Y-1) v_Y is invariant under the $\mathbb{R}$ action.
(v_Y-2) v_Y is 0 on $\{0,1\}\times\mathbb{R}$, and is non-zero on $(0,1)\times\mathbb{R}$.
(v_Y-3) v_Y extends smoothly to a vector field on $\mathbb{R}\times\mathbb{R}$.
(v_Y-4) There is an $\mathbb{R}$-invariant neighborhood of the line $s=1/2$ such that

$$v_Y = \partial/\partial t + (s-1/2)\cdot\partial/\partial s. \tag{19.3}$$

(v_Y-5) The closure of each flowline of v_Y, except for $s=1/2$, has one transverse intersection point with $\{0,1\}\times\mathbb{R}$.

Equation (19.3) is useful in controlling the level structure of degenerations of matched combs. The two vector fields v_H and v_Y are schematically shown in Figure 19.3.

We now discuss two important vector fields for deforming the holomorphic triangle maps. We call these $v_{\Delta,1}$ and $v_{\Delta,2}$. These are shown in Figure 19.4. We assume that $v_{\Delta,1}$ satisfies the following:

This is a free offprint provided to the author by the publisher. Copyright restrictions may apply.

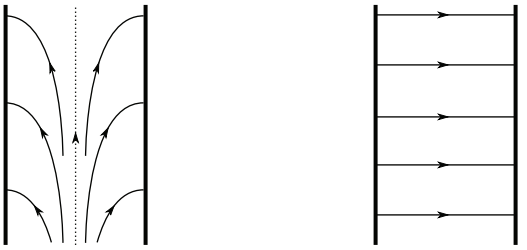


FIGURE 19.3. The $\mathbb{R}$-invariant vector fields v_Y (left) and v_H (right) on $[0,1]\times\mathbb{R}$.

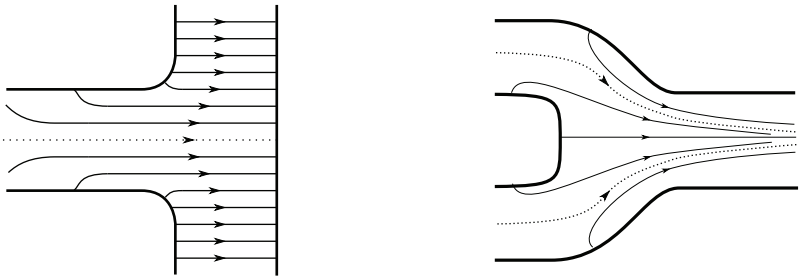


FIGURE 19.4. The vector fields $v_{\Delta,1}$ (left) and $v_{\Delta,2}$ (right).

($v_{\Delta,1}$-1) $v_{\Delta,1}$ vanishes on $\partial\Delta$ and extends to a smooth vector field on $\mathbb{C}$.
($v_{\Delta,1}$-2) $v_{\Delta,1}$ is non-vanishing on $\mathrm{int}(\Delta)$.
($v_{\Delta,1}$-3) $v_{\Delta,1}$ is $\mathbb{R}$-invariant on each of the cylindrical ends of Δ.
($v_{\Delta,1}$-4) $v_{\Delta,1}$ coincides with v_H on two cylindrical ends, and $-v_Y$ on the remaining end.
($v_{\Delta,1}$-5) The closure of all but one flowline of $v_{\Delta,1}$ has two transverse intersection points with $\partial\Delta$. The remaining flowline has just one intersection.

We construct the vector field $v_{\Delta,2}$ shown in Figure 19.4, except we require $v_{\Delta,2}$ to coincide with v_Y in all three ends of Δ. Furthermore, all but two flowlines have closures with exactly one transverse intersection with $\partial\Delta$, while two flowlines have closures which are bounded away from $\partial\Delta$.

We now describe three families of vector fields on $\square$. To meaningfully deform the quadrilateral maps, we need to describe pairs consisting of families of vector fields and almost complex structures on $\square$. We think of these families as being associated to the Heegaard quadruples $\mathcal{Q}_1$, $\mathcal{Q}_2$ and $\mathcal{Q}_3$.

For $i\in\{1,2,3\}$, we pick smooth families of vector fields $v_i := (v_{i,s})_{s\in(0,1)}$ and almost complex structures $j_i = (j_{i,s})_{s\in(0,1)}$, on $\square$, which have the configuration shown in Figure 19.5. We assume v_1 and j_1 satisfy the following:

(v_1-1) In each cylindrical end of $\square$, $v_{1,s}$ and $j_{1,s}$ are constant in s and $v_{1,s}$ coincides with v_H or v_Y.
(v_1-2) Near $s=0$, the vector field $v_{1,s}$ is obtained by inserting copies of $([0,1]\times(-R,R),v_Y)$, for increasing R, into the $(\boldsymbol{\alpha}_1,\boldsymbol{\alpha}_3)$-subregion. Similarly, $j_{1,s}$ is obtained by inserting copies of $[0,1]\times(-R,R)$, equipped with the

This is a free offprint provided to the author by the publisher. Copyright restrictions may apply.

standard almost complex structure. The limiting vector field consists of one copy of $v_{\Delta,1}$ and one copy of $v_{\Delta,2}$.

(v_1-3) Near $s = 1$, $v_{1,s}$ is obtained by inserting copies of $([0,1] \times (-R, R), v_H)$, for increasing R, into the $(\boldsymbol{\alpha}_2, \boldsymbol{\beta}_3)$-subregion. The analogous statement holds for j_1. The limiting vector field consists of two copies of $\pm v_{\Delta,1}$.

(v_1-4) $v_{1,s}|_{\partial\square} = 0$ for each s.

We assume that the families (v_2, j_2) and (v_3, j_3) satisfy the analogous conditions.

REMARK 19.2. Families v_1 and j_1 satisfying (v_1-1)–(v_1-4) may be constructed as follows. We may identify the moduli space of complex rectangles with the space of configurations of two marked points along $\{1\} \times \mathbb{R} \subseteq [0,1] \times \mathbb{R}$ (with the constant family of almost complex structures j_1). The family v_1 may be constructed by rescaling the vector field $\partial/\partial s$ on $[0,1] \times \mathbb{R}$, similar to (19.2).

REMARK 19.3. Many of the vector fields have one or two non-generic flowlines. For example, v_Y has a single flowline ($s = 1/2$) whose closure is bounded away from $\{0,1\} \times \mathbb{R}$. Similarly $v_{\Delta,1}$ has one flowline whose closure intersects $\partial\Delta$ only once. We refer to these flowlines, and their natural analogs on $v_{\Delta,2}$ and v_i, as the *special lines*.

19.3. Local degree theory

In this section, we frequently obtain algebraic relations by counting the ends of 1-dimensional matched moduli spaces. A natural strategy for such an argument is to show that each point in the boundary of the 1-dimensional moduli space in question has a neighborhood modeled on $[0, \infty)$. Proving such a claim usually requires defining a smooth structure on the compactification of the moduli space of unmatched curves, and proving that the relevant evaluation maps extend smoothly. Instead we opt to use degree theory argument of [**LOT18**], which is sufficient for the purpose of determining algebraic relations. In this section, we collect several background results which we will subsequently use.

We refer the reader to [**LOT18**, Definition 5.36] for the definition of a stratified space which we use. We now recall [**LOT18**, Definition 5.37]:

DEFINITION 19.4. Let X be a stratified space so that the top stratum is a smooth m-manifold, and suppose that $f\colon X \to [0,\infty)^m$ is a stratified map so that $f^{-1}((0,\infty)^m)$ is the top stratum of X. Let $p \in [0,\infty)^m$ and assume f is proper near p. We say that f is *odd degree near* p if there is an open neighborhood U of p such that for any regular value $p' \in U \cap (0,\infty)^m$, the set $f^{-1}(p')$ consists of an odd number of points.

In practice, we will say a broken holomorphic curve appearing in the boundary of a 1-dimensional moduli space *makes odd algebraic contribution*, if the closure of the 1-dimensional moduli space admits a stratified map to $[0,\infty)$, which is locally proper and odd degree near 0, such that the preimage of 0 is the broken curve.

The following lemma is a helpful criterion for constructing stratified spaces as fibered products which have an evaluation map to $[0,\infty)$ which is odd degree near 0:

LEMMA 19.5. *Suppose that X^j and Y^k are topological manifolds without boundary, and suppose $X \times [0,\infty)$ and $Y \times [0,\infty)$ are given the structure of stratified*

This is a free offprint provided to the author by the publisher. Copyright restrictions may apply.

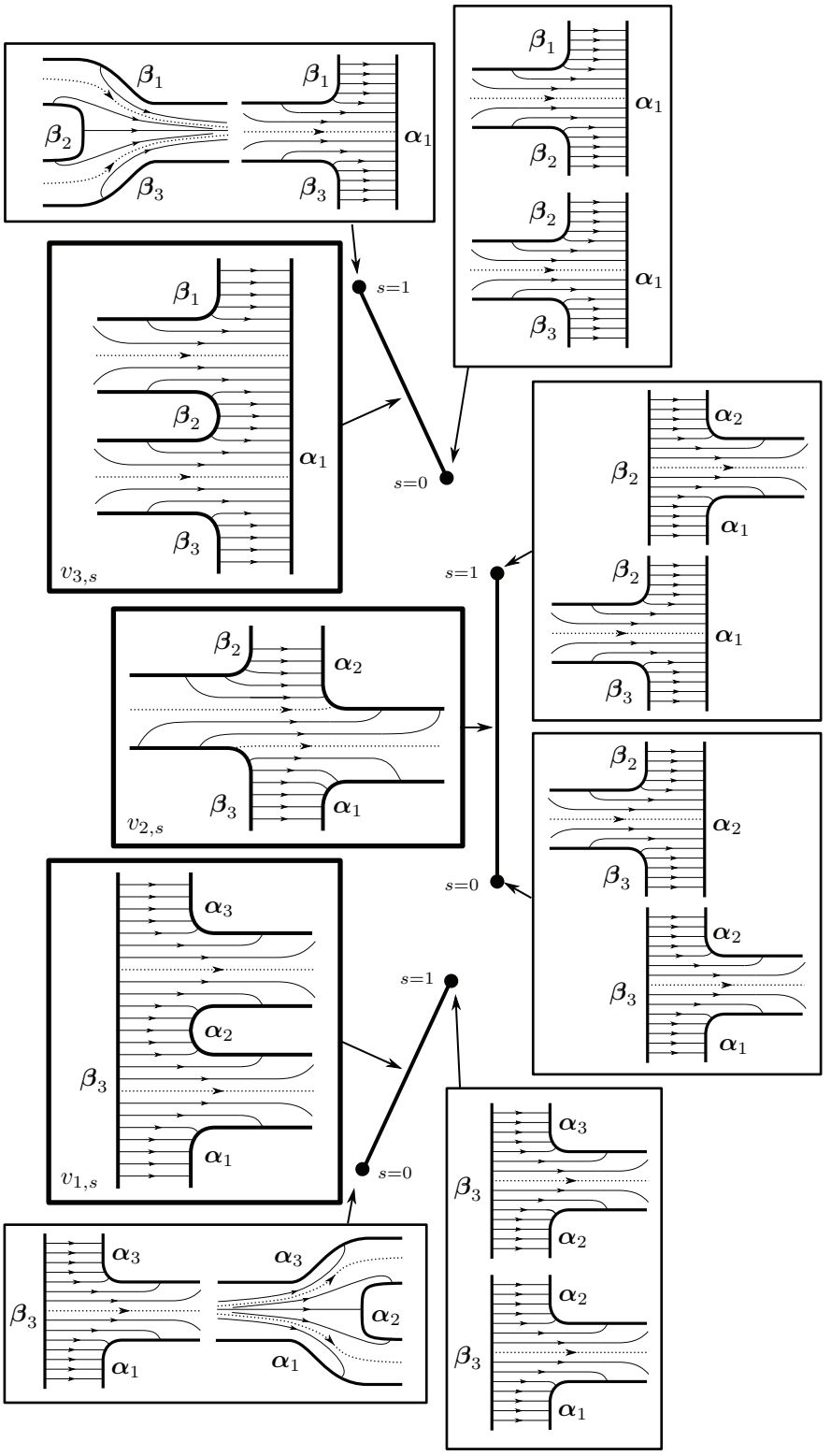


FIGURE 19.5. The 1-parameter families (v_1, j_1), (v_2, j_2) and (v_3, j_3).

This is a free offprint provided to the author by the publisher. Copyright restrictions may apply.

spaces (i.e. given a choice of smooth structure on $\{0\} \times X$, $(0,\infty) \times X$, $\{0\} \times Y$ *and* $(0,\infty) \times Y$*). Suppose that*

$$f\colon [0,\infty) \times X \to [0,\infty) \times \mathbb{R}^{j+k} \quad \text{and} \quad g\colon [0,\infty) \times Y \to [0,\infty) \times \mathbb{R}^{j+k}$$

are proper, stratified maps (i.e. continuous maps which are smooth on the interior of each strata). Furthermore, suppose that $f^{-1}(0 \times \mathbb{R}^{j+k}) = 0 \times X$ *and similarly for* g*. Finally, suppose that* $f|_{0\times X}$ *and* $g|_{0\times Y}$ *have transverse intersection at a single point* $\mathbf{0} = 0 \times \mathbf{0} \in 0 \times \mathbb{R}^{j+k} \subseteq [0,\infty) \times \mathbb{R}^{j+k}$*, and that* f *and* g *are transverse on the top strata. Then projection onto* $[0,\infty)$ *of the fibered product of* f *and* g *is odd degree near* $\mathbf{0}$*.*

PROOF. Let $\pi_1\colon [0,\infty) \times \mathbb{R}^{j+k} \to [0,\infty)$ denote projection onto $[0,\infty)$, and let π_2 denote projection onto $\mathbb{R}^{j+k}$. We first claim that the map

$$E := (\pi_1 \circ f, \pi_1 \circ g, \pi_2 \circ f - \pi_2 \circ g)\colon [0,\infty)^2 \times X \times Y \to [0,\infty)^2 \times \mathbb{R}^{j+k}$$

is odd degree near $\mathbf{0}$. To see this, note that $E|_{0\times 0\times X\times Y}$ is proper near $\mathbf{0}$ and also odd degree near $\mathbf{0}$, since $f|_{0\times X}$ and $g|_{0\times Y}$ are transverse, and hence $E|_{[0,\infty)\times 0\times X\times Y}$ is also odd degree near 0 by [**LOT18**, Lemma 5.38 (2)]. The proof of [**LOT18**, Lemma 5.38 (2)] implies that E is odd degree near $\mathbf{0}$ on $[0,\infty)^2 \times X \times Y$. Transversality on the top stratum to $\Delta \times \mathbb{R}^{j+k}$, where $\Delta \subseteq [0,\infty)^2$ is the diagonal, guarantees that the fiber over $\Delta \times \mathbf{0} \subseteq [0,\infty)^2 \times \mathbb{R}^{j+k}$, with its projection to $[0,\infty)$, is proper and odd-degree near zero. But that is equivalent to the projection onto $[0,\infty)$ of the fibered product of f and g being odd-degree near zero. □

19.4. The connected sum formula by deforming the matching

As a warmup to the holomorphic degeneration we use to analyze E, we describe a deformation of the matched moduli spaces in Section 8.1 which gives the connected sum formula for CF^-. The deformation is inspired by the time-dilation degeneration described in [**LOT18**], as well as Ozsváth and Szabó's bordered version of knot Floer homology [**OS18**] [**OS19**] [**OS04**], and the forthcoming minus version of bordered Floer homology [**LOT**]. Our argument deforms the matching in the $[0,1]$-direction.

We are interested in the following two connected sum operations:

(#-1) Suppose $\mathcal{H}_1 = (\Sigma_1, \boldsymbol{\alpha}_1, \boldsymbol{\beta}_1, w_1)$ and $\mathcal{H}_2 = (\Sigma_2, \boldsymbol{\alpha}_2, \boldsymbol{\beta}_2, w_2)$ are two singly pointed Heegaard diagrams. Let p_1 and p_2 be two points on Σ_1 and Σ_2, in the complement of the alpha and beta curves, and suppose that p_2 is immediately adjacent to w_2. Let $\mathcal{H}_1 \# \mathcal{H}_2$ denote their connected sum, taken at p_1 and p_2. In forming $\mathcal{H}_1 \# \mathcal{H}_2$, we delete w_2, and leave w_1.

(#-2) There is a version of the previous operation for knots, as follows. Suppose $\mathcal{H}_1 = (\Sigma_1, \boldsymbol{\alpha}_1, \boldsymbol{\beta}_1, w_1, z_1)$ and $\mathcal{H}_2 = (\Sigma_2, \boldsymbol{\alpha}_2, \boldsymbol{\beta}_2, w_2, z_2)$ are two doubly based knot diagrams. We take the connected sum $\mathcal{H}_1 \# \mathcal{H}_2$ at z_1 and w_2. We delete z_1 and w_2, but leave w_1 and z_2.

We now describe a deformation of the matched complexes from Section 7.3. If $\tau \in \mathbb{R}$, let $\rho_\tau\colon [0,1] \to [0,1]$ be the flow of v_H. Note that ρ_τ fixes $\{0,1\}$ for all τ, but has no fixed points on $(0,1)$ for $\tau \neq 0$.

The map ρ_τ determines a diffeomorphism

$$R^\tau\colon [0,1] \times \mathbb{R} \to [0,1] \times \mathbb{R},$$

This is a free offprint provided to the author by the publisher. Copyright restrictions may apply.

given by

$$R^\tau(s,t) = (\rho_\tau(s), t). \tag{19.4}$$

The diffeomorphism R^τ also gives a map

$$R^\tau \colon ([0,1]\times\mathbb{R})^k \to ([0,1]\times\mathbb{R})^k,$$

given by

$$R^\tau(x_1,\dots,x_k) = (R^\tau(x_1),\dots,R^\tau(x_k)), \tag{19.5}$$

which fixes the fat-diagonal setwise.

Similar to the matched moduli spaces from (8.1), if $S_1^{\mathbf{q}_1}$ and $S_2^{\mathbf{q}_2}$ are two k-pointed source curves, we define the τ-matched moduli spaces as

(19.6)

$$\mathcal{MM}^\tau_{J_1\wedge J_2}(S_1^{\mathbf{q}_1}, S_2^{\mathbf{q}_2}, \phi_1, \phi_2) := \left\{ (u_1,u_2) \in \mathcal{M}_{J_1}(S_1^{\mathbf{q}_1},\phi_1)\times\mathcal{M}_{J_2}(S_2^{\mathbf{q}_2},\phi_2) \;\middle|\; \begin{array}{c} (\pi_{\Sigma_1}\circ u_1)(q_{1,i}) = p_1, \\ (\pi_{\Sigma_2}\circ u_2)(q_{2,i}) = p_2, \\ R^\tau((\pi_{\mathbb{D}}\circ u_1)(q_{1,i})) = (\pi_{\mathbb{D}}\circ u_2)(q_{2,i}), \\ \text{for } i = 1,\dots,k \end{array} \right\}.$$

We define a τ-matched differential on the complex $CF^-(\mathcal{H}_1,\mathcal{H}_2)$ from Section 8.2 via the formula

$$\partial^\tau(\mathbf{x}_1\times\mathbf{x}_2) := \sum_{\substack{\phi_1\in\pi_2(\mathbf{x}_1,\mathbf{y}_1)\\ \phi_2\in\pi_2(\mathbf{x}_2,\mathbf{y}_2)\\ n_{p_1}(\phi_1)=n_{p_2}(\phi_2)\\ \mathrm{ind}_{\mathrm{emb}}(\phi_1,\phi_2,M_\#)=1}} \#(\mathcal{MM}^\tau_{J_1\wedge J_2}(\phi_1,\phi_2)/\mathbb{R})\cdot U^{n_{w_1}(\phi_1)}\cdot(\mathbf{y}_1\times\mathbf{y}_2).$$

We weight the counts by $n_{w_1}(\phi_1)$ since we delete w_2 in the operation (#-1). Note that if we instead used the construction in (#-2), we would use w_1 and z_2 to form the weights.

Lemma 19.6.

(1) *The endomorphism ∂^τ is a differential.*
(2) *If $\tau_1,\tau_2\in\mathbb{R}$, then $(CF^-(\mathcal{H}_1,\mathcal{H}_2),\partial^{\tau_1})\simeq(CF^-(\mathcal{H}_1,\mathcal{H}_2),\partial^{\tau_2})$.*

Proof. The proof that ∂^τ squares to zero is not substantially different than the proof of Lemma 8.1.

The proof of the second claim is similar to the proof of [**LOT18**, Proposition 9.22], and follows by defining an appropriate continuation map, as we now describe. Let $\theta\colon\mathbb{R}\to\mathbb{R}$ be a monotonic, smooth function such that there are $a,b\in\mathbb{R}$ such that $\theta(t)=\tau_1$ if $t\le a$, and $\theta(t)=\tau_2$ if $t\ge b$. The map θ determines a diffeomorphism

$$R^\theta\colon[0,1]\times\mathbb{R}\to[0,1]\times\mathbb{R},\quad \text{defined by}\quad R^\theta(s,t)=(\rho_{\theta(t)}(s),t),$$

where ρ_τ denotes the time τ flow of the vector field v in (19.2). The map R^θ induces an automorphism of $([0,1]\times\mathbb{R})^k$, which fixes the fat-diagonal, setwise.

We define a transition map

$$\Psi^{\tau_1\to\tau_2}\colon(CF^-(\mathcal{H}_1,\mathcal{H}_2),\partial^{\tau_1})\to(CF^-(\mathcal{H}_1,\mathcal{H}_2),\partial^{\tau_2})$$

This is a free offprint provided to the author by the publisher. Copyright restrictions may apply.

by counting index 0 holomorphic curves which are θ-matched, i.e., counting elements of the moduli spaces

(19.7)
$$\mathcal{MM}^{\theta}_{J_1\wedge J_2}(S_1^{\mathbf{q}_1}, S_2^{\mathbf{q}_2}, \phi_1, \phi_2) := \left\{ (u_1,u_2)\in \mathcal{M}_{J_1}(S_1^{\mathbf{q}_1},\phi_1)\times\mathcal{M}_{J_2}(S_2^{\mathbf{q}_2},\phi_2) \;\middle|\; \begin{array}{c} (\pi_{\Sigma_1}\circ u_1)(q_{1,i}) = p_1,\\ (\pi_{\Sigma_2}\circ u_2)(q_{2,i}) = p_2,\\ R^{\theta}((\pi_{\mathbb{D}}\circ u_1)(q_{2,i})) = (\pi_{\mathbb{D}}\circ u_2)(q_{1,i}),\\ \text{for } i=1,\dots,k \end{array} \right\},$$

when $\mathrm{ind}_{\mathrm{emb}}(\phi_1,\phi_2,M_{\#}) = 0$.

To see that $\Psi^{\tau_1\to\tau_2}$ is a chain map, one counts the ends of the ϕ-matched moduli spaces for pairs (ϕ_1,ϕ_2) with $\mathrm{ind}_{\mathrm{emb}}(\phi_1,\phi_2,M_{\#}) = 1$. It is easily checked, using expected dimensions, as in Proposition 7.3, that for generically chosen almost complex structures, the ends of index 1 moduli spaces correspond exactly to broken curves with two stories, where one story has index 1 and is τ_1 or τ_2 matched, and the other story has index 0 and is ϕ-matched.

To see that $\Psi^{\tau_1\to\tau_2}$ is a chain homotopy equivalence, one argues that $\Psi^{\tau_2\to\tau_1}$ is a homotopy inverse, by showing that $\Psi^{\tau_2\to\tau_1}\circ\Psi^{\tau_1\to\tau_2}$ and $\Psi^{\tau_1\to\tau_2}\circ\Psi^{\tau_2\to\tau_1}$ are chain homotopic to the identity. The chain homotopy is constructed by counting index -1 curves which are matched over a 2-parameter family of matching conditions. □

We now show that the τ-matched complex is chain homotopic to the ordinary tensor product complex $CF^-(\mathcal{H}_1)\otimes_{\mathbb{F}[U]} CF^-(\mathcal{H}_2)$, by letting $\tau\to\infty$. Write

$$\partial^{\otimes} = \partial_1\otimes \mathrm{id} + \mathrm{id}\otimes\partial_2$$

for the differential on $CF^-(\mathcal{H}_1)\otimes CF^-(\mathcal{H}_2)$.

If $S^{\mathbf{q}}$ is a marked source, and $q\in\mathbf{q}$, then we define *stable* and *unstable* evaluation maps

$$\mathrm{ev}_q^{\mathrm{st}}\colon \mathcal{M}_J(S^{\mathbf{q}},\phi)\to\{1\}\times\mathbb{R} \quad\text{and}\quad \mathrm{ev}_q^{\mathrm{un}}\colon \mathcal{M}_J(S^{\mathbf{q}},\phi)\to\{0\}\times\mathbb{R},$$

via the formulas

$$\mathrm{ev}_q^{\mathrm{st}}(u) := \lim_{\tau\to+\infty}(R^{\tau}\circ\pi_{\mathbb{D}}\circ u)(q) \quad\text{and}\quad \mathrm{ev}_q^{\mathrm{un}}(u) := \lim_{\tau\to-\infty}(R^{\tau}\circ\pi_{\mathbb{D}}\circ u)(q)$$

where R^{τ} denotes the flow of v_H.

Definition 19.7. An *∞-matched holomorphic disk* representing $(\phi_1,\phi_2)\in \pi_2(\mathbf{x}_1,\mathbf{y}_1)\times\pi_2(\mathbf{x}_2,\mathbf{y}_2)$ consists of a pair $(\mathcal{U}_1,\mathcal{U}_2)$ of 1-story holomorphic combs on $\mathcal{H}_1$ and $\mathcal{H}_2$, respectively, satisfying the following:

(1) $\mathcal{U}_1 = (u_1,a)$, where $u_1\in\mathcal{M}_{J_1}(S_1^{\mathbf{q}_1},\phi_1')$ satisfies (M-1)–(M-7), and a is the disjoint union of n boundary degenerations $a_1,\dots,a_n$, which each have Maslov index 2. Furthermore $\phi_1 = \phi_1' + n\cdot[\Sigma_1]$, and $n = n_{p_2}(\phi_2)$.
(2) $\mathcal{U}_2 = (b,u_2)$ where $u_2\in\mathcal{M}_{J_2}(S_2^{\mathbf{q}_2},\phi_2')$ satisfies (M-1)–(M-7), and b is the disjoint union of m beta-boundary degenerations $b_1,\dots,b_m$ which each have Maslov index 2. Furthermore, $\phi_2 = \phi_2' + m\cdot[\Sigma_2]$, and $m = n_{p_1}(\phi_1)$.

This is a free offprint provided to the author by the publisher. Copyright restrictions may apply.

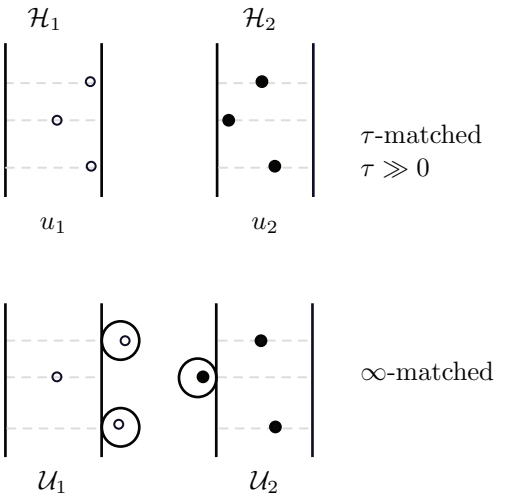


FIGURE 19.6. A schematic of a τ-matched curve (top), and a nearby ∞-matched curve (bottom). The dots represent the image under of the marked points under the evaluation map to $[0,1] \times \mathbb{R}$.

(3) The collection $\mathbf{q}_1$ consists of m marked points $(q_{1,1}, \dots, q_{1,m})$ and $\mathbf{q}_2$ consists of n marked points $(q_{2,1}, \dots, q_{2,n})$. Furthermore, for all i and j,

$$(\pi_{\Sigma_i} \circ u_i)(q_{i,j}) = p_i,$$
$$(\pi_{\Sigma_2} \circ u_2)\left((\pi_{\mathbb{D}} \circ u_2)^{-1}\left(\mathrm{ev}^{\mathrm{un}}_{q_{1,j}}(u_1)\right)\right) = \mathrm{ev}^{\infty}(b_j), \quad \text{and}$$
$$(\pi_{\Sigma_1} \circ u_1)\left((\pi_{\mathbb{D}} \circ u_1)^{-1}\left(\mathrm{ev}^{\mathrm{st}}_{q_{2,j}}(u_2)\right)\right) = \mathrm{ev}^{\infty}(a_j).$$

A schematic of a τ-matched disk and a nearby ∞-matched disk is shown in Figure 19.6. If $(\mathcal{U}_1, \mathcal{U}_2)$ is an ∞-matched disk, we define the *trimming* of $(\mathcal{U}_1, \mathcal{U}_2)$ to be the pair (u_1, u_2).

Given two classes ϕ_1 and ϕ_2, on $\mathcal{H}_1$ and $\mathcal{H}_2$, respectively, satisfying $n_{p_1}(\phi_1) = n_{p_2}(\phi_2)$, we write $\mathcal{MM}^{\infty}_{J_1 \wedge J_2}(\phi_1, \phi_2)$ for the moduli space of ∞-matched disks representing (ϕ_1, ϕ_2).

We write $M_{\otimes}$ for the matching condition

$$M_{\otimes} := \left(([0,1] \times \mathbb{R})^{k_1} \times ([0,1] \times \mathbb{R})^{k_2}, (0, \dots, 0)\right).$$

Note that being $M_{\otimes}$-matched is a vacuous condition: any two curves are $M_{\otimes}$-matched. Also, $M_{\otimes}$ depends on the integers k_1 and k_2, though we suppress this from the notation.

We define a *formal expansion* map

$$\mathscr{E} \colon \pi_2(\mathbf{x}_1, \mathbf{y}_1) \times \pi_2(\mathbf{x}_2, \mathbf{y}_2) \to \pi_2(\mathbf{x}_1, \mathbf{y}_1) \times \pi_2(\mathbf{x}_2, \mathbf{y}_2),$$

via the formula

$$\mathscr{E}(\phi_1, \phi_2) = (\phi_1 + n_{p_2}(\phi_2) \cdot [\Sigma_1], \phi_2 + n_{p_1}(\phi_1) \cdot [\Sigma_2]). \tag{19.8}$$

If $(\phi_1, \phi_2) \in \pi_2(\mathbf{x}_1, \mathbf{y}_1) \times \pi_2(\mathbf{x}_2, \mathbf{y}_2)$, then

$$\mathrm{ind}_{\mathrm{emb}}(\phi_1, \phi_2, M_{\otimes}) = \mathrm{ind}_{\mathrm{emb}}(\mathscr{E}(\phi_1, \phi_2), M_{\#}).$$

This is a free offprint provided to the author by the publisher. Copyright restrictions may apply.

The tensor product differential $\partial^{\otimes} = \partial_1 \otimes \mathrm{id} + \mathrm{id} \otimes \partial_2$ coincides with the map obtained by counting $\#(\mathcal{M}_{J_1}(\phi_1') \times \mathcal{M}_{J_2}(\phi_2'))/\mathbb{R}$ for all pairs $(\phi_1', \phi_2') \in \pi_2(\mathbf{x}_1, \mathbf{y}_1) \times \pi_2(\mathbf{x}_2, \mathbf{y}_2)$ with

$$\mathrm{ind}_{\mathrm{emb}}(\phi_1', \phi_2', M_{\otimes}) = 1.$$

On the other hand, the count of boundary degenerations from Proposition 7.9 implies that if $\phi_1 \in \pi_2(\mathbf{x}_1, \mathbf{y}_1)$ and $\phi_2 \in \pi_2(\mathbf{x}_2, \mathbf{y}_2)$ are classes which have the same multiplicity at the connected sum points, and $\mathrm{ind}_{\mathrm{emb}}(\phi_1, \phi_2, M_{\#}) = 1$, then

(19.9)

$$\#\left(\mathcal{MM}^{\infty}_{J_1 \wedge J_2}(\phi_1, \phi_2)/\mathbb{R}\right) \equiv \sum_{\substack{(\phi_1', \phi_2') \in \pi_2(\mathbf{x}_1, \mathbf{y}_1) \times \pi_2(\mathbf{x}_2, \mathbf{y}_2) \\ \mathscr{E}(\phi_1', \phi_2') = (\phi_1, \phi_2)}} \#\left(\mathcal{M}_{J_1}(\phi_1') \times \mathcal{M}_{J_2}(\phi_2')\right)/\mathbb{R}.$$

In particular, (19.9) implies that $\partial^{\otimes}$ coincides with the differential obtained by counting ∞-matched holomorphic disks representing pairs (ϕ_1', ϕ_2') with $\mathrm{ind}_{\mathrm{emb}}(\phi_1', \phi_2', M_{\#}) = 1$.

We define a transition map

$$\Psi^{\tau \to \infty} \colon (CF^-(\mathcal{H}_1, \mathcal{H}_2), \partial^{\tau}) \to (CF^-(\mathcal{H}_1) \otimes CF^-(\mathcal{H}_2), \partial^{\otimes}),$$

as follows. Pick a smooth function $\theta \colon \mathbb{R} \to \mathbb{R}$ such that $\theta'(t) \geq 0$ for all $t \in \mathbb{R}$, $\theta(t) = \tau$ for all $t \ll 0$, and $\theta(t) \to \infty$ as $t \to \infty$. We define a moduli space $\mathcal{MM}^{\theta}(\phi_1, \phi_2)$ as in (19.7). The map $\Psi^{\tau \to \infty}$ counts elements of the θ-matched moduli spaces ranging over pairs (ϕ_1, ϕ_2) satisfying $\mathrm{ind}_{\mathrm{emb}}(\phi_1, \phi_2, M_{\#}) = 0$ and $n_{p_1}(\phi_1) = n_{p_2}(\phi_2)$. We may similarly define a map $\Psi^{\infty \to \tau}$ in the opposite direction.

Lemma 19.8.

(1) *The map $\Psi^{\tau \to \infty}$ is a chain map.*
(2) *The map $\Psi^{\tau \to \infty}$ is a chain homotopy equivalence.*

Proof. The first is proven by counting the ends of index 1 families of θ-matched flowlines. Using transversality, the ends are constrained into the following 2-story holomorphic combs:

(1) A τ-matched holomorphic disk with $\mathrm{ind}_{\mathrm{emb}}(\phi_1, \phi_2, M_{\#}) = 1$, and a θ-matched holomorphic disk with $\mathrm{ind}_{\mathrm{emb}}(\phi_1, \phi_2, M_{\#}) = 0$.
(2) An ∞-matched disk, whose trimming represents a pair (ϕ_1', ϕ_2') with $\mathrm{ind}_{\mathrm{emb}}(\phi_1', \phi_2', M_{\otimes}) = 1$, and a θ-matched holomorphic disk with $\mathrm{ind}_{\mathrm{emb}}(\phi_1, \phi_2, M_{\#}) = 0$.

We claim that in the latter case, the matched moduli space admits a map to $[0, \infty)$, defined on a small neighborhood of the broken curve, which is locally proper and odd degree near 0. We sketch the argument, which is very similar to [**OS04**, Section 7.8]. Suppose (u_1, u_2) is such a limiting comb, and suppose further that u_1 consists of an index 1 disk with k marked points, and u_2 consists of k index 2 boundary degenerations, as well as a constant flowline. Let $c_1 < c_2 < \cdots < c_k$ denote the $\mathbb{R}$-values of the marked points of u_1. Let V_0 denote $(c_1 - \varepsilon, c_1 + \varepsilon) \times \cdots \times (c_k - \varepsilon, c_k + \varepsilon)$, and let V denote the image of V under the diagonal $\mathbb{R}$-action. For some small $\varepsilon > 0$, gluing gives a map

$$\gamma \colon [0, \varepsilon)^k \times V \to \overline{\mathcal{M}}(\phi_2),$$

which is a homeomorphism onto its image. Let $\overline{U}$ denote the image of γ. The $(c_i - \varepsilon, c_i + \varepsilon)$ components correspond to the height at which a boundary degeneration is glued, and the $[0, \varepsilon)$ components are the gluing parameters. There is an evaluation

This is a free offprint provided to the author by the publisher. Copyright restrictions may apply.

map $\overline{\mathrm{ev}}_2\colon \overline{U} \to [0,1)^k \times \mathbb{R}^k$. Similarly there is an evaluation map $\mathrm{ev}_1\colon \mathcal{M}(\phi_1) \to (0,1)^k \times \mathbb{R}^k$. The θ-matched moduli space is the fibered product of $\mathcal{M}(\phi_1)$ and $\mathcal{M}(\phi_2)$ under ev_1 and $R^\theta \circ \mathrm{ev}_2$.

If q_i is an arbitrarily chosen marked point of u_1, then the map $\mathrm{ev}_{\mathbb{R}}\colon \mathcal{M}(\phi_1) \to \mathbb{R}$ given by $u \mapsto \pi_{\mathbb{R}}(u(q_i))$ restricts to a diffeomorphism on a neighborhood of u_1. Furthermore, we may view the map as extending to a continuous map $\overline{\mathrm{ev}}_{\mathbb{R}}\colon \overline{\mathcal{M}}(\phi_1) \to [-\infty,\infty]$. We claim that on the θ-matched moduli spaces, the map $\overline{\mathrm{ev}}_{\mathbb{R}}$ is locally proper and odd degree near ∞. To see this, we note that a small modification of [**LOT18**, Lemma 5.38 (2)] implies that the map $\overline{\mathrm{ev}}_2$ is proper and odd degree near $\mathbf{0} \times c_1 \times \cdots \times c_k$. In particular, if $t \in \mathbb{R}$ is fixed, and $u_t := \mathrm{ev}_{\mathbb{R}}^{-1}(t) \in \mathcal{M}(\phi_1)$, and $R^{-\theta}\,\mathrm{ev}_1(u_t)$ is a regular value of ev_2, then there are an odd number of curves in the θ-matched moduli space which have $\mathrm{ev}_{\mathbb{R}} = t$. It follows that $\mathrm{ev}_{\mathbb{R}}$ is locally odd degree near ∞. In particular, combs satisfying (2) make odd algebraic contribution, so

$$\Psi^{\tau\to\infty} \circ \partial^\tau + \partial^\otimes \circ \Psi^{\tau\to\infty} = 0,$$

where we are identifying $\partial^\otimes$ with the map which counts ∞-matched holomorphic disks, using (19.9).

The second claim follows from the same reasoning as the corresponding claim of Lemma 19.6. □

19.5. Deformed stabilizations

In our construction of H_E, we will encounter some additional variations of the matching deformation considered in Section 19.4. Suppose $\mathcal{H}_1$ and $\mathcal{H}_2$ are two Heegaard diagrams with chosen connected sum points, and v is an $\mathbb{R}$-invariant vector field on $[0,1] \times \mathbb{R}$ which vanishes on $\{0,1\} \times \mathbb{R}$. We may define a (v,τ)-deformed differential $\partial^{v,\tau}_{\mathcal{H}_1 \wedge \mathcal{H}_2}$, by counting holomorphic disks which are matched by the time τ flow of v.

We will need the following fact:

LEMMA 19.9. *Suppose that $\mathcal{H} = (\Sigma, \boldsymbol{\alpha}, \boldsymbol{\beta}, w)$ is a Heegaard diagram with a special point $p \in \Sigma \setminus (\boldsymbol{\alpha} \cup \boldsymbol{\beta})$, and v is a vector field on $[0,1] \times \mathbb{R}$, as above.*

(1) *Suppose $\mathcal{H}_0 = (\mathbb{T}^2, \alpha, \beta)$ is a standard diagram for S^3 or $L(m,1)$ and $x \in \alpha \cap \beta$. If $\tau \in \mathbb{R}$ is generic, then*

$$\partial^{v,\tau}_{\mathcal{H} \wedge \mathcal{H}_0}(\mathbf{x} \times x) = \partial_{\mathcal{H}}(\mathbf{x}) \otimes x.$$

Furthermore, if ϕ and ϕ_0 are a pair of classes of disks such that $\mathrm{ind}_{\mathrm{emb}}(\phi, \phi_0, M_\#) = 0$, and

$$\mathcal{MM}^{v,\tau \in [\tau_1,\tau_2]}(\phi, \phi_0) \neq \emptyset,$$

then ϕ and ϕ_0 represent constant classes.

(2) *Suppose $\mathcal{H}_0 = (\mathbb{T}^2, \alpha, \beta)$ is a standard diagram for $S^1 \times S^2$. Write $\{\theta^+, \theta^-\} = \alpha \cap \beta$. Then, for generic $\tau \in \mathbb{R}$,*

$$\partial^{v,\tau}_{\mathcal{H} \wedge \mathcal{H}_0}(\mathbf{x} \times \theta^+) = \partial_{\mathcal{H}}(\mathbf{x}) \otimes \theta^+, \quad \text{and}$$
$$\partial^{v,\tau}_{\mathcal{H} \wedge \mathcal{H}_0}(\mathbf{x} \times \theta^-) = \partial_{\mathcal{H}}(\mathbf{x}) \otimes \theta^- + \sum_{\mathbf{y} \in \mathbb{T}_\alpha \cap \mathbb{T}_\beta} C_{\mathbf{x},\mathbf{y}} \cdot \mathbf{y} \times \theta^+,$$

for some $C_{\mathbf{x},\mathbf{y}} \in \mathbb{F}[U]$. Furthermore, suppose ϕ and ϕ_0 are classes of disks, such that $\mathrm{ind}_{\mathrm{emb}}(\phi, \phi_0, M_\#) = 0$. Write $\phi_0 \in \pi_2(\theta_1, \theta_2)$, for $\theta_1, \theta_2 \in \alpha \cap \beta$.

This is a free offprint provided to the author by the publisher. Copyright restrictions may apply.

If $\mathrm{gr}(\theta_1,\theta_2)\geq 0$, *and*

$$\mathcal{MM}^{v,\tau\in[\tau_1,\tau_2]}(\phi,\phi_0)\neq\emptyset,$$

then ϕ *and* ϕ_0 *both represent constant classes.*

PROOF. The computation of the differential follows from the same argument as the ordinary proof of stabilization invariance [**OS04b**, Section 10]. See Lemma 10.7 for details in our present context.

We now consider the claim about index 0 classes. We focus on the claim when $\mathcal{H}_0$ is a diagram for $S^1\times S^2$, since the other cases follow a similar argument. If $\phi_0\in\pi_2(\theta_1,\theta_2)$ is a class on $\mathcal{H}_0$, then

$$\mu(\phi_0)=2n_{p_0}(\phi_0)+\mathrm{gr}(\theta_1,\theta_2).$$

Hence, if ϕ is a class on $\mathcal{H}$, then

$$\mathrm{ind}_{\mathrm{emb}}(\phi,\phi_0,M_\#)=\mu(\phi)+\mu(\phi_0)-2n_{p_0}(\phi_0)=\mu(\phi)+\mathrm{gr}(\theta_1,\theta_2).$$

If $\mathcal{MM}^{v,\tau\in[\tau_1,\tau_2]}(\phi,\phi_0)\neq\emptyset$, then $\mu(\phi)\geq 0$ by transversality. Hence, if $\mathrm{gr}(\theta_1,\theta_2)\geq 0$ we must have $\mu(\phi)=0$. By transversality, ϕ must be the constant class. It is straightforward to see that this also implies that ϕ_0 is a constant class. □

19.6. Deformed stabilizations and holomorphic triangles

We need several results about deformed stabilizations and holomorphic triangles, similar to those stated in Section 19.5 for disks.

We now consider deforming the triangle maps using a smooth vector field v on Δ which vanishes on $\partial\Delta$ and is $\mathbb{R}$-invariant on the cylindrical ends of Δ. (We only have need to consider the vector fields $v_{\Delta,1}$ and $v_{\Delta,2}$ from Figure 19.4). Suppose that $\mathcal{T}=(\Sigma,\boldsymbol{\alpha},\boldsymbol{\beta},\boldsymbol{\gamma},w)$ is a Heegaard triple with a distinguished point $p\in\Sigma\backslash(\boldsymbol{\alpha}\cup\boldsymbol{\beta}\cup\boldsymbol{\gamma})$, and suppose that $\mathcal{T}_0=(\mathbb{T}^2,\alpha,\beta,\alpha',p_0)$ is a genus 1 lens space stabilizing triple, as in Section 10.5. If ψ and ψ_0 are two classes of triangles on $\mathcal{T}$ and $\mathcal{T}_0$, then we may define their τ-matched moduli space $\mathcal{MM}^{\tau}(S^{\mathbf{q}},S_0^{\mathbf{q}_0},\psi,\psi_0)$ by adapting (19.6).

We define a matched triangle map $f^{\tau}_{\mathcal{T}\wedge\mathcal{T}_0}$ by counting τ-matched triangles representing pairs (ψ_1,ψ_2) with $\mathrm{ind}_{\mathrm{emb}}(\psi_1,\psi_2,M_\#)=0$. Given $\tau_1,\tau_2\in\mathbb{R}$ with $\tau_1<\tau_2$, we may also count representatives of pairs (ψ,ψ_0) with $\mathrm{ind}_{\mathrm{emb}}(\psi,\psi_0)=-1$, which are τ-matched for some $\tau\in[\tau_1,\tau_2]$. We write $f^{\tau_1\to\tau_2}_{\mathcal{T}\wedge\mathcal{T}_0}$ for this map.

We have the following analog of Lemma 10.8:

LEMMA 19.10. *Suppose that* $\mathcal{T}=(\Sigma,\boldsymbol{\alpha},\boldsymbol{\beta},\boldsymbol{\gamma},w)$ *is a Heegaard triple with a distinguished point* $p\in\Sigma\setminus(\boldsymbol{\alpha}\cup\boldsymbol{\beta}\cup\boldsymbol{\gamma})$, *and* $\mathcal{T}_0=(\mathbb{T}^2,\alpha,\beta,\alpha',p_0)$ *is a triple such that* $(\mathbb{T}^2,\alpha,\beta)$ *is a standard diagram for* $L(m,1)$, *and* α' *is a small Hamiltonian translate of* α *satisfying* $|\alpha\cap\alpha'|=2$. *See Figure* 10.1.

(1) *If* $\tau\in\mathbb{R}$ *is generic* $c_{\alpha,\beta}\in\alpha\cap\beta$ *and* $c_{\beta,\alpha'}\in\beta\cap\alpha'$, *then*

$$f^{\tau}_{\mathcal{T}\wedge\mathcal{T}_0}(\mathbf{x}\times c_{\alpha,\beta},\mathbf{y}\times c_{\beta,\alpha'})=f_{\mathcal{T}}(\mathbf{x},\mathbf{y})\otimes\Theta^-_{\alpha,\alpha'}+\sum_{\mathbf{z}\in\mathbb{T}_\alpha\cap\mathbb{T}_\gamma}C^{\tau}_{\mathbf{x},\mathbf{y},\mathbf{z}}\cdot\mathbf{z}\otimes\Theta^+_{\alpha,\alpha'},$$

for some $C^{\tau}_{\mathbf{x},\mathbf{y},\mathbf{z}}\in\mathbb{F}[U]$.

(2) *If* $\tau_1,\tau_2\in\mathbb{R}$ *are generic, and* $c_{\alpha,\beta}\in\alpha\cap\beta$ *and* $c_{\beta,\alpha'}\in\beta\cap\alpha'$, *then*

$$f^{\tau_1\to\tau_2}_{\mathcal{T}\wedge\mathcal{T}_0}(\mathbf{x}\times c_{\alpha,\beta},\mathbf{y}\times c_{\beta,\alpha'})$$

This is a free offprint provided to the author by the publisher. Copyright restrictions may apply.

$$= \begin{cases} \displaystyle\sum_{\mathbf{z}\in\mathbb{T}_\alpha\cap\mathbb{T}_\gamma} C^{[\tau_1,\tau_2]}_{\mathbf{x},\mathbf{y},\mathbf{z}} \cdot \mathbf{z}\otimes\Theta^+_{\alpha,\alpha'} & \text{if } \mathfrak{s}_{p_0}(c_{\alpha,\beta}) = \mathfrak{s}_{p_0}(c_{\beta,\alpha'}), \\ 0 & \text{otherwise,} \end{cases}$$

for some $C^{[\tau_1,\tau_2]}_{\mathbf{x},\mathbf{y},\mathbf{z}} \in \mathbb{F}[U]$.

PROOF. The first claim is proven no differently than Lemma 10.8, using (10.16).

The second claim is proven as follows. Suppose ψ is a class on $(\Sigma,\boldsymbol{\alpha},\boldsymbol{\beta},\boldsymbol{\gamma})$ and $\psi_0 \in \pi_2(c_{\alpha,\beta}, c_{\beta,\alpha'}, \Theta)$ is a class on $(\mathbb{T}^2,\alpha,\beta,\alpha')$, where $\Theta \in \alpha\cap\alpha'$. Adapting (10.15) to our present situation, we obtain

$$\operatorname{ind}_{\mathrm{emb}}(\psi,\psi_0,M_\#) = \mu(\psi) + \operatorname{gr}(\Theta^+_{\alpha,\alpha'},\Theta) - 1. \tag{19.10}$$

Note that any holomorphic curve counted by $f^{\tau_1\to\tau_2}_{\mathcal{T}\wedge\mathcal{T}_0}$ contains an ordinary holomorphic triangle on $\mathcal{T}$. In particular, if (ψ,ψ_0) is a pair of classes which admit a τ-matched representative for some τ, then $\mu(\psi)\geq 0$, by transversality for curves on $\mathcal{T}$. Combined with (19.10), we see that if $\Theta = \Theta^-_{\alpha,\alpha'}$, and (ψ,ψ_0) has a τ-matched index -1 representative, then $\mu(\psi) = -1$, which violates transversality. Hence we may only have representatives if $\Theta = \Theta^+_{\alpha,\alpha'}$, proving the stated formula. □

19.7. Deforming E

In this section, we describe our null-homotopy of E, by deforming the holomorphic quadrilateral maps using the families of vector fields v_1, v_2 and v_3 on $\square$ described in Section 19.2.

The time τ flow of $v_{i,s}$ gives a 2-parameter family of diffeomorphisms,

$$R^\tau_{i,s}\colon \square \to \square,$$

for each $i\in\{1,2,3\}$.

Suppose v_i and j_i satisfy the analogs of (v_1-1)–(v_1-4). If $J\wedge I = (J_s\wedge I_s)_{s\in[0,1]}$ is a stratified family of almost complex structures on $(\Sigma\wedge\mathbb{T}^2)\times\square$, which covers a family j_i on $\square$, we define the (v_i,τ)-matched moduli space of rectangles as follows:

(19.11)

$$\mathcal{MM}^{v_i,\tau}_{I\wedge J}(S^{\mathbf{q}_0}_0, S^{\mathbf{q}}, \psi_0, \psi)$$

$$:= \left\{ (u,s,u_0,s_0)\in\mathcal{M}_J(S^{\mathbf{q}},\psi)\times\mathcal{M}_I(S^{\mathbf{q}_0}_0,\psi_0) \;\middle|\; \begin{array}{c} (\pi_\Sigma\circ u)(q_j) = p, \\ (\pi_{\mathbb{T}^2}\circ u_0)(q_{0,j}) = p_0, \\ R^\tau_{i,s}((\pi_\square\circ u_0)(q_{0,j})) = (\pi_\square\circ u)(q_j), \\ \text{for } j=1,\dots,k, \\ s = s_0 \end{array} \right\}.$$

We define maps h^τ_1, h^τ_2 and h^τ_3 with the same domain and range as h_1, h_2 and h_3, by counting (v_i,τ)-matched quadrilaterals on $\mathcal{Q}_1$, $\mathcal{Q}_2$ and $\mathcal{Q}_3$. We define

$$E^\tau := F_3\circ h^\tau_1 + F_3\circ h^\tau_2 + F_3\circ h^\tau_3.$$

LEMMA 19.11. *For generic $\tau\geq 0$, the map E^τ is a chain map.*

PROOF. The proof follows by counting the ends of index 0, (v_i,τ)-matched rectangles, representing classes (ψ,ψ_0) in

$$\begin{gathered} \pi_2(\Theta^+_{\alpha_3,\alpha_2},\Theta^{\mathrm{can}}_{\alpha_2,\alpha_1},\mathbf{x}\times x,\mathbf{y}\times\theta^-), \quad \pi_2(\Theta^{\mathrm{can}}_{\alpha_2,\alpha_1},\mathbf{x}\times x,\Theta^+_{\beta_3,\beta_2},\mathbf{y}\times\theta^-), \\ \text{and} \quad \pi_2(\mathbf{x}\times x,\Theta^+_{\beta_3,\beta_2},\Theta^{\mathrm{can}}_{\beta_2,\beta_1},\mathbf{y}\times\theta^-). \end{gathered} \tag{19.12}$$

This is a free offprint provided to the author by the publisher. Copyright restrictions may apply.

Here, $\{x\} = c_1 \cap c_3'$, and θ^- denotes the bottom generator of either $c_1 \cap c_1'$, $c_2 \cap c_2'$ or $c_3 \cap c_3'$.

We claim that for generic, fixed $\tau \in [0, \infty)$, the moduli spaces of index 0, (v_1, τ)-matched quadrilaterals on $\mathcal{Q}_1$ have ends corresponding exactly to the following 2-story combs:

(h_1-1) $s \in (0, 1)$:
- An index 1, (v, τ)-matched holomorphic disk in one of the four cylindrical ends, where $v \in \{v_H, v_Y\}$, and
- a $(v_{1,s}, \tau)$-matched holomorphic rectangle on $\mathcal{Q}_1$ of index -1.

(h_1-2) $s = 0$:
- A $(v_{1,0}, \tau)$-matched triangle on $(\Sigma \wedge \mathbb{T}^2, \boldsymbol{\alpha}_3, \boldsymbol{\alpha}_1, \boldsymbol{\beta}_3)$ of index 0, and
- a $(v_{1,0}, \tau)$-matched triangle on $(\Sigma \wedge \mathbb{T}^2, \boldsymbol{\alpha}_3, \boldsymbol{\alpha}_2, \boldsymbol{\alpha}_1)$ of index 0.

(h_1-3) $s = 1$:
- A $(v_{1,1}, \tau)$-matched triangle on $(\Sigma \wedge \mathbb{T}^2, \boldsymbol{\alpha}_3, \boldsymbol{\alpha}_2, \boldsymbol{\beta}_3)$ of index 0, and
- a $(v_{1,1}, \tau)$-matched triangle on $(\Sigma \wedge \mathbb{T}^2, \boldsymbol{\alpha}_2, \boldsymbol{\alpha}_1, \boldsymbol{\beta}_3)$ of index 0.

Similarly, the ends of the moduli spaces of (v_2, τ)-matched quadrilaterals on $\mathcal{Q}_2$ have one of the following forms:

(h_2-1) $s \in (0, 1)$:
- An index 1, (v, τ)-matched holomorphic disk in one of the 4 cylindrical ends, where $v \in \{v_H, v_Y\}$, and
- a $(v_{2,s}, \tau)$-matched holomorphic rectangle on $\mathcal{Q}_2$ of index -1.

(h_2-2) $s = 0$:
- A $(v_{2,0}, \tau)$-matched triangle on $(\Sigma \wedge \mathbb{T}^2, \boldsymbol{\alpha}_2, \boldsymbol{\beta}_3, \boldsymbol{\beta}_2)$ of index 0, and
- a $(v_{2,0}, \tau)$-matched triangle $(\Sigma \wedge \mathbb{T}^2, \boldsymbol{\alpha}_2, \boldsymbol{\alpha}_1, \boldsymbol{\beta}_3)$ of index 0.

(h_2-3) $s = 1$:
- A $(v_{2,1}, \tau)$-matched triangle on $(\Sigma \wedge \mathbb{T}^2, \boldsymbol{\alpha}_2, \boldsymbol{\alpha}_1, \boldsymbol{\beta}_2)$ of index 0, and
- a τ-matched triangle on $(\Sigma \wedge \mathbb{T}^2, \boldsymbol{\alpha}_1, \boldsymbol{\beta}_3, \boldsymbol{\beta}_2)$ of index 0.

Finally, the ends of the moduli spaces of (v_3, τ)-matched quadrilaterals on $\mathcal{Q}_3$ take one of the following forms:

(h_3-1) $s \in (0, 1)$:
- An index 1, (v, τ)-matched holomorphic disk in one of the 4 cylindrical ends, where $v \in \{v_H, v_Y\}$, and
- a $(v_{3,s}, \tau)$-matched holomorphic rectangle on $\mathcal{Q}_3$ of index -1.

(h_3-2) $s = 0$:
- A $(v_{3,0}, \tau)$-matched triangle on $(\Sigma \wedge \mathbb{T}^2, \boldsymbol{\alpha}_1, \boldsymbol{\beta}_3, \boldsymbol{\beta}_2)$ of index 0, and
- a $(v_{3,0}, \tau)$-matched triangle on $(\Sigma \wedge \mathbb{T}^2, \boldsymbol{\alpha}_1, \boldsymbol{\beta}_2, \boldsymbol{\beta}_1)$ of index 0.

(h_3-3) $s = 1$:
- A $(v_{3,1}, \tau)$-matched triangle on $(\Sigma \wedge \mathbb{T}^2, \boldsymbol{\alpha}_1, \boldsymbol{\beta}_3, \boldsymbol{\beta}_1)$ of index 0, and
- A $(v_{3,1}, \tau)$-matched triangle on $(\Sigma \wedge \mathbb{T}^2, \boldsymbol{\beta}_3, \boldsymbol{\beta}_2, \boldsymbol{\beta}_1)$ of index 0.

Furthermore, an argument similar to the one in Lemma 19.8 implies that each broken curve labeled (h_i-j) makes odd algebraic contribution to the count of ends of its moduli space.

The ends of the moduli spaces in (19.12), of type (h_1-1), (h_2-1) and (h_3-1), where additionally the index 1 disk occurs in the $(\boldsymbol{\alpha}_1, \boldsymbol{\beta}_3)$ end or the $(\boldsymbol{\alpha}_i, \boldsymbol{\beta}_i)$ end, give the $\mathbf{y}$ component of

$$(\partial E^\tau + E^\tau \partial)(\mathbf{x}).$$

This is a free offprint provided to the author by the publisher. Copyright restrictions may apply.

The remaining ends of type (h_1-1), (h_2-1) and (h_3-1) have a disk component which is $\pm(v_Y, \tau)$-matched and occurs in one of the ends labeled $(\boldsymbol{\alpha}_2, \boldsymbol{\alpha}_1)$, $(\boldsymbol{\alpha}_3, \boldsymbol{\alpha}_2)$, $(\boldsymbol{\beta}_3, \boldsymbol{\beta}_2)$ or $(\boldsymbol{\beta}_2, \boldsymbol{\beta}_1)$. The total count of these ends is zero, since $\Theta^{\mathrm{can}}_{\boldsymbol{\alpha}_2,\boldsymbol{\alpha}_1}$, $\Theta^{+}_{\boldsymbol{\alpha}_3,\boldsymbol{\alpha}_2}$, $\Theta^{\mathrm{can}}_{\boldsymbol{\beta}_1,\boldsymbol{\beta}_2}$ and $\Theta^{+}_{\boldsymbol{\beta}_2,\boldsymbol{\beta}_3}$ are cycles in the $\pm(v_Y, \tau)$-matched complexes by Lemma 19.9.

Next, the moduli spaces (h_1-2) and (h_3-3) make total contribution zero, by Lemma 12.3 and a τ-matched version of Proposition 10.2.

We now claim that the ends labeled (h_1-3) cancel the ends labeled (h_2-2). This follows since both ends feature a count of triangles on $(\boldsymbol{\alpha}_2, \boldsymbol{\alpha}_1, \boldsymbol{\beta}_3)$, and a count on either $(\boldsymbol{\alpha}_3, \boldsymbol{\alpha}_2, \boldsymbol{\beta}_3)$ or $(\boldsymbol{\alpha}_2, \boldsymbol{\alpha}_1, \boldsymbol{\beta}_2)$. The counts of triangles on $(\Sigma \wedge \mathbb{T}^2, \boldsymbol{\alpha}_3, \boldsymbol{\alpha}_2, \boldsymbol{\beta}_3)$ and $(\Sigma \wedge \mathbb{T}^2, \boldsymbol{\alpha}_2, \boldsymbol{\alpha}_1, \boldsymbol{\beta}_2)$ coincide, since we may destabilize using Lemma 10.8, and then identify both destabilized counts with nearest point maps by Proposition 11.1. Hence, the counts of the ends (h_1-3) cancel those of (h_2-2), as claimed. The ends (h_2-3) cancel the ends of (h_3-2) in a similar manner.

Summing over all of the above ends, we obtain $\partial E^\tau + E^\tau \partial = 0$, completing the proof. □

We now describe a candidate limiting map, E^∞, which has the same domain and range as E^τ. We define

$$E^\infty := F_3 \circ h_1^\infty + F_3 \circ h_2^\infty + F_3 \circ h_3^\infty,$$

where h_i^∞ counts *aspect ratio matched*, holomorphic quadrilaterals on $\mathcal{Q}_i$ of index -1, i.e. E^∞ counts elements of the moduli spaces

$$\mathcal{MM}^{\infty,\mathrm{a.r.}}_{J\wedge I}(\psi, \psi_0) := \{(u, s, u_0, s_0) \in \mathcal{M}_J(\psi) \times \mathcal{M}_I(\psi_0) : s = s_0\},$$

ranging over pairs with

$$\mathrm{ind}_{\mathrm{emb}}(\psi, \psi_0, M_\otimes) := \mu(\psi) + \mu(\psi_0) = -1.$$

Note that in the definition of $\mathcal{MM}^{\infty,\mathrm{a.r.}}_{J\wedge I}(\psi, \psi_0)$, we do not require $n_p(\psi) = n_{p_0}(\psi_0)$, and also there is no matching condition at the connected sum points.

In the map h_i^∞, an aspect ratio matched pair (u, u_0) representing (ψ, ψ_0) is counted with a factor of

$$U^{n_{p_0}(\psi_0)+n_w(\psi)} T^{n_p(\psi)+n_{z_0}(\psi_0)-n_{p_0}(\psi_0)-n_w(\psi)}. \tag{19.13}$$

The weight in (19.13) is the ordinary weight of the formal expansion $\mathscr{E}(\psi, \psi_0)$, as in (19.8).

We will show the following:

PROPOSITION 19.12. *If τ is generic, then $E^\tau \simeq E^\infty$.*

The proof of Proposition 19.12 is technical, and is delayed until Section 19.8. The proof is in the same spirit as the proof of Lemma 19.8. Before embarking upon the proof of Proposition 19.12, we prove the following, which, together with Proposition 19.12, implies Proposition 19.1.

LEMMA 19.13. *The map E^∞ satisfies $E^\infty \simeq 0$.*

PROOF. The proof follows by deforming the aspect ratio matching. For $T \in \mathbb{R}$, we consider the deformed moduli spaces

$$\mathcal{MM}^{\infty,\mathrm{a.r.},T}_{J\wedge I}(\psi, \psi_0) := \{(u, s, u_0, s_0) \in \mathcal{M}_J(\psi) \times \mathcal{M}_I(\psi_0) : \rho_T(s) = s_0\},$$

where $\rho_T \colon [0,1] \to [0,1]$ denotes the time T flow of the vector field from (19.2).

This is a free offprint provided to the author by the publisher. Copyright restrictions may apply.

We consider the ends of the parametrized moduli spaces

$$\mathcal{MM}^{\infty,\text{a.r.},T\in[0,\infty)}(\psi,\psi_0) := \bigcup_{T\in[0,\infty)} \mathcal{MM}^{\infty,\text{a.r.},T}_{J\wedge I}(\psi,\psi_0)\times\{T\}, \tag{19.14}$$

ranging over the classes in (19.12), with $\text{ind}_{\text{emb}}(\psi,\psi_0,M_\otimes) = -1$.

Firstly, there are ends at $T=0$, which contribute

$$E^\infty(\mathbf{x}).$$

We claim that any end at $T\in(0,\infty)$ must have $s\in(0,1)$. Indeed, an end with $T\in(0,\infty)$ and $s\in\{0,1\}$ would necessarily contain four holomorphic triangles, as well as potentially a collection of holomorphic disks and boundary degenerations. By transversality, every holomorphic triangle, disk or boundary degeneration must have nonnegative Maslov index. However, the total Maslov index must be -1, since such a curve appears in the boundary of the moduli space of Maslov index -1 rectangles, leading to a contradiction.

Hence, the ends at finite T are restricted to consist of holomorphic strips breaking off into the 4 cylindrical ends. Furthermore, strips breaking off into the ends labeled $(\boldsymbol{\alpha}_3,\boldsymbol{\alpha}_2)$, $(\boldsymbol{\alpha}_2,\boldsymbol{\alpha}_1)$, $(\boldsymbol{\beta}_3,\boldsymbol{\beta}_2)$ or $(\boldsymbol{\beta}_2,\boldsymbol{\beta}_1)$ cancel modulo 2, since $\Theta^+_{\boldsymbol{\alpha}_3,\boldsymbol{\alpha}_2}$, $\Theta^{\text{can}}_{\boldsymbol{\alpha}_2,\boldsymbol{\alpha}_1}$, $\Theta^+_{\boldsymbol{\beta}_3,\boldsymbol{\beta}_2}$ and $\Theta^{\text{can}}_{\boldsymbol{\beta}_2,\boldsymbol{\beta}_1}$ are cycles. Hence, the ends at finite T contribute

$$(H\circ\partial+\partial\circ H)(\mathbf{x}),$$

where H counts index -2 curves (u,s,u_0,s_0), which satisfy $\rho_T(s)=s_0$ for some $T\in(0,\infty)$.

Finally, it remains to count the ends appearing as $T\to\infty$. By transversality, these ends consist of two holomorphic triangles, and one holomorphic rectangle. Furthermore, since there is no matching condition, the triangles must have index 0, and the rectangle index -1.

More concretely, the broken curves appearing on $\mathcal{Q}_1$ as $T\to\infty$ have one of the following configurations:

($h_1^{\infty,\infty}$-1) $s\in(0,1)$, $T\to\infty$:
- An index 0 triangle on $(\mathbb{T}^2,c_3,c_1,c_3')$,
- an index 0 triangle on $(\mathbb{T}^2,c_3,c_2,c_1)$, and
- an index -1 rectangle on $(\Sigma,\boldsymbol{\alpha}'',\boldsymbol{\alpha}',\boldsymbol{\alpha},\boldsymbol{\beta})$.

($h_1^{\infty,\infty}$-2) $s=0$, $T\to\infty$:
- An index -1 rectangle on $(\mathbb{T}^2,c_3,c_2,c_1,c_3')$,
- an index 0 triangle on $(\Sigma,\boldsymbol{\alpha}'',\boldsymbol{\alpha},\boldsymbol{\beta})$, and
- an index 0 triangle on $(\Sigma,\boldsymbol{\alpha}'',\boldsymbol{\alpha}',\boldsymbol{\alpha})$.

Similarly, the broken curves arising on $\mathcal{Q}_2$ have one of the following configurations:

($h_2^{\infty,\infty}$-1) $s\in(0,1)$, $T\to\infty$:
- An index 0 triangle on $(\mathbb{T}^2,c_1,c_3',c_2')$,
- an index 0 triangle on $(\mathbb{T}^2,c_2,c_1,c_2')$, and
- an index -1 rectangle on $(\Sigma,\boldsymbol{\alpha}',\boldsymbol{\alpha},\boldsymbol{\beta},\boldsymbol{\beta}')$.

($h_2^{\infty,\infty}$-2) $s=0$, $T\to\infty$:
- An index -1 rectangle on $(\mathbb{T}^2,c_2,c_1,c_3',c_2')$,
- an index 0 triangle on $(\Sigma,\boldsymbol{\alpha}',\boldsymbol{\alpha},\boldsymbol{\beta})$, and
- an index 0 triangle on $(\Sigma,\boldsymbol{\alpha},\boldsymbol{\beta},\boldsymbol{\beta}')$.

Finally, the curves appearing on $\mathcal{Q}_3$ consist of the following:

($h_3^{\infty,\infty}$-1) $s\in(0,1)$, $T\to\infty$:

This is a free offprint provided to the author by the publisher. Copyright restrictions may apply.

- An index 0 triangle on $(\mathbb{T}^2, c_1, c_3', c_1')$,
- an index 0 triangle on $(\mathbb{T}^2, c_3', c_2', c_1')$, and
- an index -1 rectangle on $(\Sigma, \boldsymbol{\alpha}, \boldsymbol{\beta}, \boldsymbol{\beta}', \boldsymbol{\beta}'')$.

($h_3^{\infty,\infty}$-2) $s = 0$, $T \to \infty$:

- An index -1 rectangle on $(\mathbb{T}^2, c_1, c_3', c_2', c_1')$,
- an index 0 triangle on $(\Sigma, \boldsymbol{\alpha}, \boldsymbol{\beta}, \boldsymbol{\beta}')$, and
- an index 0 triangle on $(\Sigma, \boldsymbol{\alpha}, \boldsymbol{\beta}', \boldsymbol{\beta}'')$.

Furthermore, we claim that each of the above broken curves labeled ($h_i^{\infty,\infty}$-j) makes odd algebraic contribution to the count of ends of the moduli spaces in (19.14). By this, we mean that in a neighborhood of a broken curve, the matched moduli spaces admit a continuous, proper map to $[0, \infty)$, with the preimage of 0 being the broken curve, which is odd degree near 0; see Definition 19.4.

The total count of curves satisfying each of the configurations (weighted by powers of U and T), ranging over classes in (19.12), vanishes modulo 2, by Lemmas 12.6 and 12.3.

Counting up all ends, we obtain $E^\infty = [\partial, H]$, completing the proof. □

19.8. Proof of Proposition 19.12

As a warmup to proving Proposition 19.12, we prove the following:

LEMMA 19.14. *If $\tau_1, \tau_2 \in \mathbb{R}$ are generic, then $E^{\tau_1} \simeq E^{\tau_2}$.*

PROOF. We count the ends of the parametrized moduli spaces

$$\mathcal{MM}^{v_i, \tau \in [\tau_1, \tau_2]}(\psi, \psi_0) := \bigcup_{\tau \in [\tau_1, \tau_2]} \mathcal{MM}^{v_i, \tau}(\psi, \psi_0) \times \{\tau\},$$

ranging over pairs of classes (ψ, ψ_0) as in (19.12), which have index -1. These parametrized moduli spaces have ends similar to those described in Lemma 19.11. For example, in addition to the ends at τ_1 and τ_2, the moduli spaces on $\mathcal{Q}_1 = (\Sigma \wedge \mathbb{T}^2, \boldsymbol{\alpha}_3, \boldsymbol{\alpha}_2, \boldsymbol{\alpha}_1, \boldsymbol{\beta}_3)$ have the following ends:

($h_1^{[\tau_1,\tau_2]}$-1) $s \in (0,1)$, $\tau \in (\tau_1, \tau_2)$:

- An index 1, τ-matched holomorphic disk in one of the four cylindrical ends, and
- an index -2, $(v_{1,s}, \tau)$-matched holomorphic quadrilateral.

($h_1^{[\tau_1,\tau_2]}$-2) $s \in (0,1)$, $\tau \in (\tau_1, \tau_2)$:

- An index 0, τ-matched disk in the four cylindrical ends, and
- an index -1, $(v_{1,s}, \tau)$-matched holomorphic quadrilateral.

($h_1^{[\tau_1,\tau_2]}$-3) $s = 0$, $\tau \in (\tau_1, \tau_2)$:

- A $(v_{1,0}, \tau)$-matched triangle on $(\Sigma \wedge \mathbb{T}^2, \boldsymbol{\alpha}_3, \boldsymbol{\alpha}_1, \boldsymbol{\beta}_3)$ of some index $k \in \{-1, 0\}$, and
- a $(v_{1,0}, \tau)$-matched triangle on $(\Sigma \wedge \mathbb{T}^2, \boldsymbol{\alpha}_3, \boldsymbol{\alpha}_2, \boldsymbol{\alpha}_1)$ of index $-1 - k$.

($h_1^{[\tau_1,\tau_2]}$-4) $s = 1$, $\tau \in (\tau_1, \tau_2)$:

- A $(v_{1,1}, \tau)$-matched triangle on $(\Sigma \wedge \mathbb{T}^2, \boldsymbol{\alpha}_3, \boldsymbol{\alpha}_2, \boldsymbol{\beta}_3)$ of index $k \in \{-1, 0\}$, and
- a $(v_{1,1}, \tau)$-matched triangle on $(\Sigma \wedge \mathbb{T}^2, \boldsymbol{\alpha}_2, \boldsymbol{\alpha}_1, \boldsymbol{\beta}_3)$ of some index $-1 - k$.

This is a free offprint provided to the author by the publisher. Copyright restrictions may apply.

Furthermore, a gluing argument similar to Lemma 19.8 implies that each of the ends labeled ($h_1^{[\tau_1,\tau_2]}$-j) makes odd algebraic contribution to the ends of its moduli space.

The only ends which did not have a counterpart in Lemma 19.11 are the ends labeled ($h_1^{[\tau_1,\tau_2]}$-2) above. Note that simple index considerations do not prohibit a similar end consisting of an index -1 rectangle, and a finite collection of index 0 disks. Nonetheless, for generically chosen almost complex structures, the set of τ which support a τ-matched, index 0 disk is discrete, and hence in each end where an index 0 disk appears, we may assume that just one appears. Lemma 19.9 implies that the count of the ends of type ($h_1^{[\tau_1,\tau_2]}$-2), for curves representing the classes shown in (19.12), vanishes.

Part (2) of Lemma 19.10 implies that $k = 0$ in the ends of type ($h_1^{[\tau_1,\tau_2]}$-3) and ($h_1^{[\tau_1,\tau_2]}$-4). Furthermore, we claim that there are no ends with the configuration ($h_1^{[\tau_1,\tau_2]}$-3). By the previous reasoning, such an end would contain a $(v_{1,0},\tau)$-matched triangle on $(\Sigma\wedge\mathbb{T}^2,\boldsymbol{\alpha}_3,\boldsymbol{\alpha}_2,\boldsymbol{\alpha}_1)$ with index $-1-k$. If $\psi\#\psi_0$ is the underlying homology class, this implies that

$$\mathrm{ind}(\psi\#\psi_0,M_\#)=\mu(\psi)+\mu(\psi_0)-2n_p(\psi)=-1.$$

Write $\psi\in\pi_2(\Theta^+_{\alpha'',\alpha'},\Theta^+_{\alpha',\alpha},\mathbf{z})$. By Lemma 9.6 we have $\mu(\psi)=2n_p(\psi)+\mathrm{gr}(\Theta^+_{\alpha'',\alpha},\mathbf{z})$, and hence

$$\mu(\psi_0)+\mathrm{gr}(\Theta^+_{\alpha'',\alpha},\mathbf{z})=-1.$$

In particular, $\mu(\psi_0)\leq -1$. However a $(v_{1,0},\tau)$-matched representative of $\psi\#\psi_0$ contains an ordinary representative of ψ_0, which would violate transversality for curves on $(\mathbb{T}^2,c_3,c_2,c_1)$ with respect to a fixed almost complex structure.

The ends of the moduli spaces $\mathcal{MM}^{v_i,\tau\in[\tau_1,\tau_2]}(\psi,\psi_0)$ on $\mathcal{Q}_2=(\Sigma\wedge\mathbb{T}^2,\boldsymbol{\alpha}_2,\boldsymbol{\alpha}_1,\boldsymbol{\beta}_3,\boldsymbol{\beta}_2)$ and $\mathcal{Q}_3=(\Sigma\wedge\mathbb{T}^2,\boldsymbol{\alpha}_1,\boldsymbol{\beta}_3,\boldsymbol{\beta}_2,\boldsymbol{\beta}_1)$ have a similar description. A cancellation pattern occurs similar to how, in Lemma 19.11, the ends (h_1-3) canceled the ends (h_2-2), and the ends labeled (h_2-3) canceled the ends labeled (h_3-2). In particular, the ends labeled ($h_1^{[\tau_1,\tau_2]}$-4) cancel ends on $\mathcal{Q}_2$, and another family of ends on $\mathcal{Q}_2$ and $\mathcal{Q}_3$ cancel. Counting all the ends, we obtain

$$E^{\tau_1}+E^{\tau_2}=\partial\circ H^{\tau_1\to\tau_2}+H^{\tau_1\to\tau_2}\circ\partial,$$

where $H^{\tau_1\to\tau_2}$ counts index -2 rectangles which are (v_i,τ)-matched for some $\tau\in(\tau_1,\tau_2)$. □

We now move on to prove Proposition 19.12. The proof consists of carefully analyzing the ends of index -1 moduli spaces of rectangles which are (v_i,τ)-matched for some $\tau\in[\tau_0,\infty)$. The ends appearing as $\tau\to\infty$ are more complicated than those which appeared for $\tau\in[\tau_1,\tau_2]$. Unlike in Lemma 19.8, which concerned holomorphic disks, the ends which appear as $\tau\to\infty$ do not correspond exactly to the map E^∞.

Before moving on to consider the ends appearing as $\tau\to\infty$, we first record the ends of (v_i,τ)-matched moduli spaces which are easy to understand. The ends at $\tau=\tau_0$ contribute the term

$$E^{\tau_0}(\mathbf{x}).$$

As in Lemma 19.11, there are ends at finite $\tau\in[\tau_0,\infty)$, similar to ($h_1^{[\tau_1,\tau_2]}$-1),…, ($h_1^{[\tau_1,\tau_2]}$-4), and their analogs on the quadruples $\mathcal{Q}_2$ and $\mathcal{Q}_3$. The total count of

This is a free offprint provided to the author by the publisher. Copyright restrictions may apply.

these ends gives the term

$$(\partial \circ H^{\tau_0 \to \infty} + H^{\tau_0 \to \infty} \circ \partial)(\mathbf{x}),$$

where $H^{\tau_0 \to \infty}$ counts (v_i, τ)-matched, index -2 rectangles, for $\tau \in [\tau_0, \infty)$.

The ends of the (v_i, τ)-matched moduli spaces which appear as $\tau \to \infty$ may be partitioned into two sets:

(e-1) Ends where $\tau \to \infty$ and $s \in (0,1)$.
(e-2) Ends where $\tau \to \infty$ and $s = 0$ or $s = 1$.

To analyze the ends labeled (e-1) and (e-2), we introduce a new type of evaluation map. We first introduce a version of this evaluation map for disks, and then move on to an analog for triangles and quadrilaterals which is relevant to (e-1) and (e-2).

Consider the vector field v_Y on $[0,1] \times \mathbb{R}$, shown in Figure 19.3. Suppose $S^{\mathbf{q}}$ is marked Riemann surface, ϕ is a homology class of disks, and $|\mathbf{q}| = k$. Write $\mathbb{R}^k/\mathbb{R}$ for $\mathbb{R}^k$, modulo the diagonal action of $\mathbb{R}$. There is an *unstable asymptotic evaluation map*

$$\mathrm{ev}^{\mathrm{un}}_{\mathbf{q}} \colon \mathcal{M}_J(S^{\mathbf{q}}, \phi) \to \mathbb{R}^k/\mathbb{R},$$

defined as follows. Write $\mathbf{q} = (q_1, \dots, q_k)$. Let R^τ denote the flow of v_Y. If $u \in \mathcal{M}_J(S^{\mathbf{q}}, \phi)$, we consider the tuple

$$\lim_{\tau \to -\infty} \big((\pi_{\mathbb{R}} \circ R^\tau \circ \pi_{\mathbb{D}} \circ u)(q_1), \dots, (\pi_{\mathbb{R}} \circ R^\tau \circ \pi_{\mathbb{D}} \circ u)(q_k)\big) \in \ell^k/\mathbb{R}. \tag{19.15}$$

Since v_Y is $\mathbb{R}$-invariant, and ℓ is a flowline of v_Y, we obtain a canonical identification of ℓ with $\mathbb{R}$. We define $\mathrm{ev}^{\mathrm{un}}_{\mathbf{q}}(u)$ to be the image of the tuple in (19.15) under the canonical identification of $\ell^k/\mathbb{R}$ with $\mathbb{R}^k/\mathbb{R}$. Note also the existence of the limit in (19.15) follows from (19.3).

Similarly, if ℓ denotes the line $\{\frac{1}{2}\} \times \mathbb{R}$, and $\mathcal{M}_J(S^{\mathbf{q}}, \phi, \ell)$ denotes the set of holomorphic disks u such that $(\pi_{\mathbb{D}} \circ u)(\mathbf{q}) \subseteq \ell$, there is a *stable asymptotic evaluation map*

$$\mathrm{ev}^{\mathrm{st}}_{\mathbf{q}} \colon \mathcal{M}_J(S^{\mathbf{q}}, \phi, \ell) \to \mathbb{R}^k/\mathbb{R},$$

defined similarly. (In fact, in our present setting of holomorphic disks, $\mathrm{ev}^{\mathrm{st}}_{\mathbf{q}}$ is induced by the ordinary evaluation $(\pi_{\mathbb{R}} \circ u)(q_i)$, though this will not be the case for triangles or rectangles).

We now consider analogous evaluation maps for holomorphic triangles and rectangles. Suppose that $S^{\mathbf{q}}$ is a marked Riemann surface, and $u \colon S \to \Sigma \times \Delta$ is a holomorphic triangle for the Heegaard triple $(\Sigma, \boldsymbol{\gamma}_1, \boldsymbol{\gamma}_2, \boldsymbol{\gamma}_3, w)$. Let v denote one of the limiting vector fields on Δ shown in Figure 19.5. (The cyclic identification of $(\boldsymbol{\gamma}_1, \boldsymbol{\gamma}_2, \boldsymbol{\gamma}_3)$ with $(\boldsymbol{\alpha}, \boldsymbol{\beta}, \boldsymbol{\gamma})$ is unimportant for our present purposes). If v coincides with $\pm v_Y$ on the $(\boldsymbol{\gamma}_i, \boldsymbol{\gamma}_{i+1})$-cylindrical end of Δ, then we write write $\ell_{\gamma_i, \gamma_{i+1}}$ for the line $\{\frac{1}{2}\} \times [0, \infty) \subseteq [0,1] \times [0, \infty)$ in the $(\boldsymbol{\gamma}_i, \boldsymbol{\gamma}_{i+1})$ cylindrical end of Δ. Note that $\ell_{\gamma_i, \gamma_{i+1}}$ is a flowline of the vector field v. We refer to $\ell_{\gamma_i, \gamma_{i+1}}$ as the *special line*. We write $\mathcal{W}^s_v(\ell_{\gamma_i, \gamma_{i+1}})$ and (resp. $\mathcal{W}^u_v(\ell_{\gamma_i, \gamma_{i+1}})$) for *stable* (resp. *unstable*) sets of $\ell_{\gamma_i, \gamma_{i+1}}$, by which we mean the set of points of Δ whose positive (resp. negative) flow under v asymptotically approaches the line $\ell_{\gamma_i, \gamma_{i+1}}$. We may similarly define stable and unstable sets associated to other subsets of Δ.

If u is a holomorphic triangle with marked source $S^{\mathbf{q}}$, and $\mathbf{q}_0 \subseteq \mathbf{q}$ is a subset of the marked points such that

$$(\pi_\Delta \circ u)(\mathbf{q}_0) \subseteq \mathcal{W}^s_v(\ell_{\gamma_i, \gamma_{i+1}}), \tag{19.16}$$

This is a free offprint provided to the author by the publisher. Copyright restrictions may apply.

then there is a well defined element

$$\mathrm{ev}^{\mathrm{st}}_{\mathbf{q}_0}(u) \in \mathbb{R}^{|\mathbf{q}_0|}/\mathbb{R},$$

defined similarly to (19.15). The map $\mathrm{ev}^{\mathrm{st}}_{\mathbf{q}_0}$ determines a continuous map on the subspace of $\mathcal{M}_J(S^{\mathbf{q}}, \phi)$ consisting of curves u satisfying (19.16). The above terminology adapts easily for holomorphic quadrilaterals.

With this notation in place, we can now describe the ends of the moduli spaces $\mathcal{MM}^{v_i,\tau\in[\tau_0,\infty)}(\psi,\psi_0)$. We have the following analog of Definition 19.7:

DEFINITION 19.15.

(h_1^∞-*e*-1) We say a pair $\mathcal{U}$ and $\mathcal{U}_0$ of broken $J_s \wedge I_s$-holomorphic quadrilaterals on $\mathcal{Q}_1$ is a *simple,* (v_1,∞)*-matched quadrilateral*, if it satisfies the following:

(a) $\mathcal{U}$ consists of exactly one J_s-holomorphic rectangle $u \in \mathcal{M}_{J_s}(S^{\mathbf{q}}, \psi')$ on $(\Sigma, \boldsymbol{\alpha}'', \boldsymbol{\alpha}', \boldsymbol{\alpha}, \boldsymbol{\beta})$, as well as a collection of index 2 boundary degenerations $b_1, \dots, b_n$. Furthermore $\psi = \psi' + [b_1] + \cdots + [b_n]$.

(b) $\mathcal{U}_0$ consists of exactly one I_s-holomorphic rectangle $u_0 \in \mathcal{M}_{I_s}(S_0^{\mathbf{q}_0}, \psi_0')$ on $(\mathbb{T}^2, c_3, c_2, c_1, c_3')$, as well as a collection of index 2 boundary degenerations $d_1, \dots, d_m$. Furthermore, $\psi_0 = \psi_0' + [d_1] + \cdots [d_m]$.

(c) $n_p(\psi') = m = |\mathbf{q}|$ and $n_{p_0}(\psi_0') = n = |\mathbf{q}_0|$. Furthermore,

$$(\pi_\square \circ u)(\mathbf{q}) \subseteq \mathcal{W}^s_{v_1}(e_{\alpha''} \cup e_{\alpha'} \cup e_\alpha) \quad \text{and} \quad (\pi_\square \circ u_0)(\mathbf{q}_0) \subseteq \mathcal{W}^u_{v_1}(e_{c_3}).$$

(d) The following matching conditions are satisfied:

$$(\pi_\Sigma \circ u)(q_j) = p,$$
$$(\pi_{\mathbb{T}^2} \circ u_0)(q_{0,j}) = p_0,$$
$$(\pi_{\mathbb{T}^2} \circ u_0)\left((\pi_\square \circ u_0)^{-1}\left(\mathrm{ev}^{\mathrm{un}}_{q_j}(u)\right)\right) = \mathrm{ev}^\infty(d_j), \quad \text{and}$$
$$(\pi_\Sigma \circ u)\left((\pi_\square \circ u)^{-1}\left(\mathrm{ev}^{\mathrm{st}}_{q_{0,j}}(u_0)\right)\right) = \mathrm{ev}^\infty(b_j).$$

(h_2^∞-*e*-1) A pair $(\mathcal{U},\mathcal{U}_0)$ is a *simple,* (v_2,∞)*-matched quadrilateral* on $\mathcal{Q}_2$ if it satisfies the analog of (h_1^∞-*e*-1) for $\mathcal{Q}_2$.

(h_3^∞-*e*-1) A pair $(\mathcal{U},\mathcal{U}_0)$ is a *simple,* (v_3,∞)*-matched quadrilateral* on $\mathcal{Q}_3$ if it satisfies the analog of (h_1^∞-*e*-1) for $\mathcal{Q}_3$.

Examples of simple, (v_i,∞)-matched quadrilaterals are shown in Figure 19.7. Note that (h_1^∞-*e*-1), (h_2^∞-*e*-1) and (h_3^∞-*e*-1) are natural analogs of Definition 19.7 for rectangles.

LEMMA 19.16. *The ends of the moduli spaces* $\mathcal{MM}^{v_i,\tau\in[\tau_0,\infty)}(\psi,\psi_0)$ *which appear as* $\tau \to \infty$ *and* $s \to s_0 \in (0,1)$ *(labeled* (*e*-1) *above) generically correspond to simple,* (v_i,∞)*-matched holomorphic rectangles. Furthermore, each such broken curve makes odd algebraic contribution to the ends of the moduli spaces* $\mathcal{MM}^{v_i,\tau\in[\tau_0,\infty)}(\psi,\psi_0)$.

PROOF. We focus on the curves appearing on $\mathcal{Q}_1$. We can view the moduli space $\mathcal{MM}^{v_i,\tau\in[\tau_0,\infty)}(\psi,\psi_0)$ as consisting of holomorphic curves mapping into $(\Sigma \sqcup \mathbb{T}^2) \times \square$, and hence limiting curves may be described in terms of holomorphic combs, via an extension of Definition 7.15 to handle holomorphic polygons. Since we are

This is a free offprint provided to the author by the publisher. Copyright restrictions may apply.

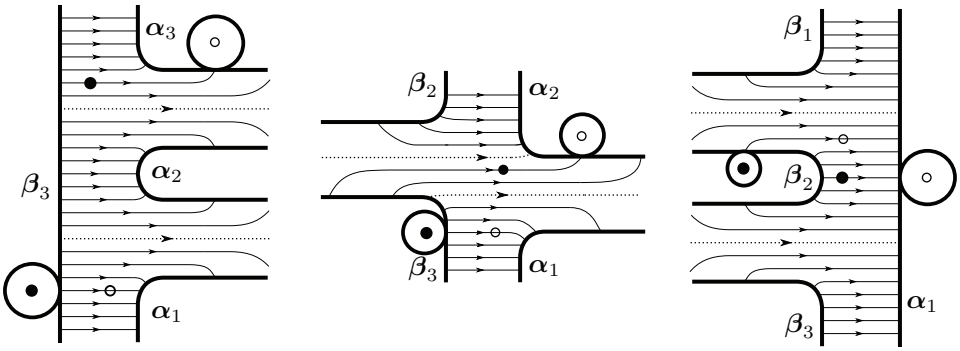


FIGURE 19.7. Simple, (v_i, ∞)-matched quadrilaterals from Definition 19.15. The open dots denote the images of the marked points mapping to $p \in \Sigma$, and the solid dots denote the marked points mapping to $p_0 \in \mathbb{T}^2$.

restricting to the case that $s_0 \in (0,1)$, the limiting collection of curves consists of a pair of holomorphic rectangles (one on each of $\mathbb{T}^2 \times \square$ and $\Sigma \times \square$), as well as a collection of holomorphic curves in the four ends, and also boundary degenerations. Let us write $\mathcal{U}_1, \dots, \mathcal{U}_n$ for the disk levels appearing in the $(\boldsymbol{\alpha}_2, \boldsymbol{\alpha}_3)$ end. Let us write $\mathcal{V}_1, \dots, \mathcal{V}_m$ for the disk levels appearing in the $(\boldsymbol{\alpha}_1, \boldsymbol{\alpha}_2)$ end. (These are not shown in Figure 19.8.) For ease of notation, we group any boundary degenerations into the disk or rectangle level that they originate from.

As a first step, we will show that generically $n \leq 1$ and $m \leq 1$, and that there are no disk levels in the $(\boldsymbol{\alpha}_1, \boldsymbol{\beta}_3)$ or $(\boldsymbol{\alpha}_3, \boldsymbol{\beta}_3)$ ends. To simply the notation, we first show that if $m = 0$, then $n \in \{0, 1\}$. The same argument applies to show that more generally, $n, m \in \{0, 1\}$. Similarly, it is easy to use index considerations to show that generically no curves can appear in the $(\boldsymbol{\alpha}_1, \boldsymbol{\beta}_3)$ or $(\boldsymbol{\alpha}_3, \boldsymbol{\beta}_3)$ ends (since here any disks are v_H-matched).

Write $\mathcal{U}_0$ for the curves in the quadrilateral level (as well as any boundary degenerations branching off of this level), and let $\mathcal{U}_1, \dots, \mathcal{U}_n$ be the disks in the $(\boldsymbol{\alpha}_2, \boldsymbol{\alpha}_3)$ levels, as above. We can further partition these curves into collections $\mathcal{U}_0^\Sigma, \dots, \mathcal{U}_n^\Sigma$ and $\mathcal{U}_0^\mathbb{T}, \dots, \mathcal{U}_n^\mathbb{T}$, depending on whether they map to Σ or $\mathbb{T}^2$. See Figure 19.8.

We now trim off any boundary degenerations from the collections $\mathcal{U}_i^\mathbb{T}$ and $\mathcal{U}_i^\Sigma$ (and we call the remaining collections $\mathcal{U}_i^\mathbb{T}$ and $\mathcal{U}_i^\Sigma$, abusing notation slightly). This leaves two types of marked points on the remaining curves. We say a marked point is *coupled* if it is matched to a marked point which remains after trimming boundary degenerations. We say a marked point is *decoupled* if it was matched to a marked point in a boundary degeneration.

For $i \in \{0, \dots, n\}$, let $d_i \geq 0$ denote the number coupled marked points on the curves in $\mathcal{U}_i^\mathbb{T}$. The marked points of $\mathcal{U}_i^\mathbb{T}$ must be mapped to the special line of $[0,1] \times \mathbb{R}$ or the special line of $\square$ which extends into the $(\boldsymbol{\alpha}_2, \boldsymbol{\alpha}_3)$ end. There is an injection $f \colon \{i : d_i > 0\} \to \{1, \dots, n\}$, which sends an i to the index j such that the d_i marked points of $\mathcal{U}_i^{\mathbb{T}^2}$ are matched with marked points of $\mathcal{U}_j^\Sigma$. Note

This is a free offprint provided to the author by the publisher. Copyright restrictions may apply.

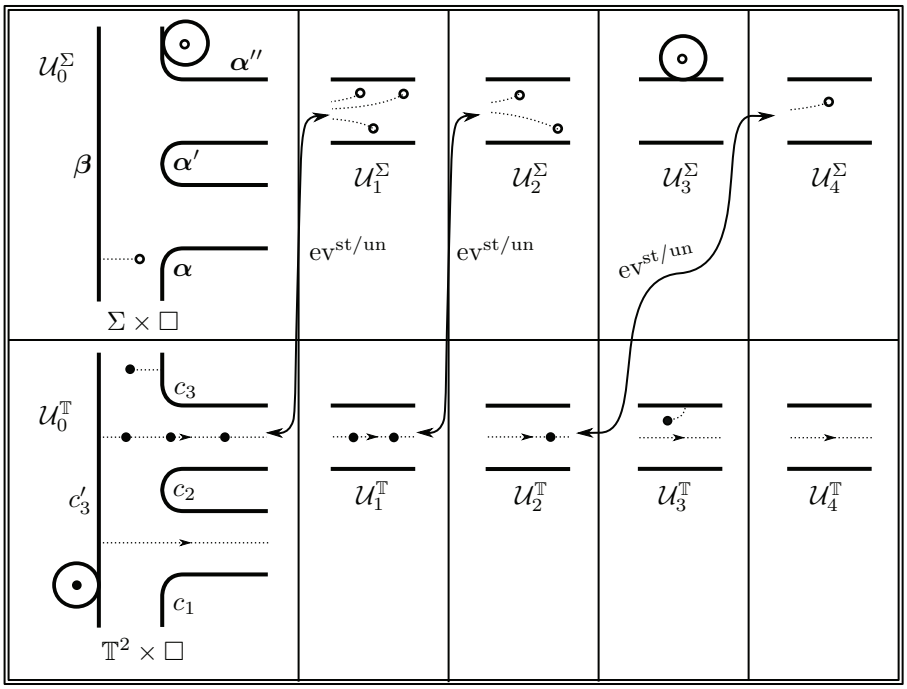


FIGURE 19.8. A non-generic degeneration appearing in (e-1).

that if $d_i > 0$, then the curves of $\mathcal{U}_i^\mathbb{T}$ are matched with the curves of $\mathcal{U}_{f(i)}^\Sigma$ via the asymptotic evaluation map $\mathrm{ev}^{\mathrm{st/un}}$ applied to the coupled marked points. We write

$$\mathbf{d} := \sum_{i=0}^{n} d_i. \tag{19.17}$$

Write $\phi_0^\Sigma, \ldots, \phi_n^\Sigma$ and $\phi_0^\mathbb{T}, \ldots, \phi_n^\mathbb{T}$ for the homology classes of $\mathcal{U}_0^\Sigma, \ldots, \mathcal{U}_n^\Sigma$ and $\mathcal{U}_0^\mathbb{T}, \ldots, \mathcal{U}_n^\mathbb{T}$. Here, $\phi_0^\mathbb{T}$ is a class of rectangles, while $\phi_i^\mathbb{T}$ is a class of disks, for $i > 0$, and similarly for the classes on Σ. By assumption, we are considering curves which appeared in the limit of a 1-parameter family of (v_i, τ)-matched curves representing a pair (ψ, ψ_0) satisfying

$$\mu(\psi) + \mu(\psi_0) = 2n_p(\psi) - 1, \quad \text{and} \quad n_p(\psi) = n_{p_0}(\psi_0). \tag{19.18}$$

Since we have trimmed off boundary degenerations, we obtain

$$\sum_{i=0}^{n} \left(\mu(\phi_i^\Sigma) + \mu(\phi_i^\mathbb{T})\right) = 2\mathbf{d} - 1. \tag{19.19}$$

Write $n^\mathbb{T}$ and n^Σ for the number of non-trivial disk levels amongst the $\mathcal{U}_i^\mathbb{T}$ and $\mathcal{U}_i^\Sigma$, respectively, ranging over $i > 0$. We define

$$\Phi^\mathbb{T} := (\phi_0^\mathbb{T}, \ldots, \phi_n^\mathbb{T}, d_0, \ldots, d_n),$$

an ordered tuple of classes, counts of coupled marked points. We define an ordered tuple Φ^Σ similarly.

This is a free offprint provided to the author by the publisher. Copyright restrictions may apply.

We can consider the collection $\mathcal{U}_0^{\mathbb{T}},\dots,\mathcal{U}_n^{\mathbb{T}},\mathcal{U}_0^{\Sigma},\dots,\mathcal{U}_n^{\Sigma}$ as living in their own moduli space $\mathcal{MM}(\Phi^{\Sigma},\Phi^{\mathbb{T}},f)$, consisting of such collections of curves which are matched under the asymptotic evaluation map. The expected dimension of this moduli space at embedded curves is given by

$$\dim \mathcal{MM}(\Phi^{\Sigma},\Phi^{\mathbb{T}},f) = 1+\sum_{i=0}^{n}\left(\mu(\phi_i^{\Sigma})+\mu(\phi_i^{\mathbb{T}})-d_i-\max(0,d_i-1)\right). \tag{19.20}$$

In (19.20), $\sum_{i=0}^{n}(\mu(\phi_i^{\Sigma})+\mu(\phi_i^{\mathbb{T}}))$ is the expected dimension of the unconstrained moduli space, for a fixed almost complex structure. The $+1$ in (19.20) comes from the parameter s, the summand $-d_i$ is the result of the constraint that the coupled marked points on the $\mathbb{T}^2$-side must lie on the special line, and the summand of $-\max(0,d_i-1)$ given by matching condition involving the asymptotic evaluation map.

The moduli space $\mathcal{MM}(\Phi^{\Sigma},\Phi^{\mathbb{T}},f)$ has a free action of $\mathbb{R}^{n^{\Sigma}+n^{\mathbb{T}}}$, where each component acts by translation on one of the $n^{\Sigma}+n^{\mathbb{T}}$ non-trivial disk components of $\mathcal{MM}(\Phi^{\Sigma},\Phi^{\mathbb{T}},f)$. In particular, for $\mathcal{MM}(\Phi^{\Sigma},\Phi^{\mathbb{T}},f)$ to be non-empty, it must have dimension at least $n^{\Sigma}+n^{\mathbb{T}}$. Hence (19.20) gives

$$1+\sum_{i=0}^{n}\left(\mu(\phi_i^{\Sigma})+\mu(\phi_i^{\mathbb{T}})-d_i-\max(0,d_i-1)\right)\geq n^{\Sigma}+n^{\mathbb{T}}.$$

Applying (19.17) and (19.19) and rearranging, we obtain that if $\mathcal{MM}(\Phi^{\Sigma},\Phi^{\mathbb{T}},f)$ is non-empty, then

$$\mathbf{d}-n^{\Sigma}-n^{\mathbb{T}}-\sum_{i=0}^{n}\max(0,d_i-1)\geq 0. \tag{19.21}$$

Since for each i with $d_i>0$, the level $\mathcal{U}_{f(i)}^{\Sigma}$ is non-trivial, we obtain that

$$n^{\Sigma}+\sum_{i=0}^{n}\max(0,d_i-1)=\mathbf{d}+n_0^{\Sigma},$$

where n_0^{Σ} denotes the number of non-trivial levels of $\mathcal{U}_1^{\Sigma},\dots\mathcal{U}_n^{\Sigma}$ which have no coupled marked points. Hence, from (19.21) we obtain $-n^{\mathbb{T}}-n_0^{\Sigma}\geq 0$, which implies that $n^{\mathbb{T}}=n_0^{\Sigma}=0$. It follows that $n=n^{\Sigma}\in\{0,1\}$, since all coupled marked points must be matched with the rectangle $\mathcal{U}_0^{\mathbb{T}}$, and at most one level can match this level. This completes the proof of the subclaim under the assumption that $m=0$. Furthermore, the argument easily extends to handle the case that m and n are both allowed to be non-zero, and implies that $n,m\in\{0,1\}$.

It follows from the above argument that, after trimming boundary degenerations, the limiting curve consists of up to four levels. There are two holomorphic quadrilaterals, v^{Σ} and $v^{\mathbb{T}}$, as well as potentially two holomorphic disks, $u_{\boldsymbol{\alpha}'',\boldsymbol{\alpha}'}$ and $u_{\boldsymbol{\alpha}',\boldsymbol{\alpha}}$ on $\mathbb{T}^2\times[0,1]\times\mathbb{R}$, which occur in the $(\boldsymbol{\alpha}'',\boldsymbol{\alpha}')$ and $(\boldsymbol{\alpha}',\boldsymbol{\alpha})$ ends, respectively. The curves $u_{\boldsymbol{\alpha}'',\boldsymbol{\alpha}'}$ and $u_{\boldsymbol{\alpha}',\boldsymbol{\alpha}}$ are matched to $v^{\mathbb{T}}$ via the asymptotic evaluation map. See Figure 19.9.

Up until now, we have not used any particular facts about the quadruple $\mathcal{Q}_1$. The key observation that prohibits degenerations like those in Figure 19.9 is that if $\phi\in\pi_2(\Theta^+,\Theta)$ is a class of disks on $(\Sigma,\boldsymbol{\alpha}'',\boldsymbol{\alpha}')$ or $(\Sigma,\boldsymbol{\alpha}',\boldsymbol{\alpha})$, then then

$$\mu(\phi)=2n_p(\phi)+\mathrm{gr}(\Theta^+,\Theta)\geq 2n_p(\phi). \tag{19.22}$$

This is a free offprint provided to the author by the publisher. Copyright restrictions may apply.

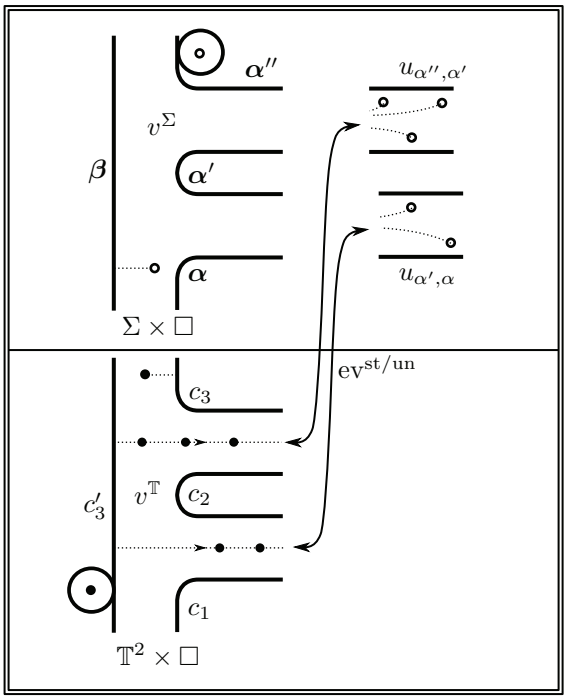


FIGURE 19.9. A more generic configuration, which is still prohibited for $\mathcal{Q}_1$.

Write $d_{\alpha'',\alpha'}$ and $d_{\alpha',\alpha}$ for the number of marked points mapped to the two special lines of $\square$, by the holomorphic rectangle on $\Sigma \times \square$ of a curve appearing in a limiting configuration. Since this curve was obtained in a limit of a path of curves representing a pair (ψ, ψ_0) satisfying (19.18), we obtain, similarly to (19.19), that

$$\mu(v^\Sigma) + \mu(v^{\mathbb{T}}) + \mu(u_{\alpha'',\alpha'}) + \mu(u_{\alpha',\alpha}) = 2d_{\alpha'',\alpha'} + 2d_{\alpha',\alpha} - 1. \tag{19.23}$$

Combining (19.22) and (19.23), we obtain

$$\mu(v^\Sigma) + \mu(v^{\mathbb{T}}) \leq -1. \tag{19.24}$$

However, (19.24) implies that generically there are no representatives of the pair $(v^\Sigma, v^{\mathbb{T}})$, ranging over $s \in (0,1)$, if $v^{\mathbb{T}}$ has one or more coupled marked points which are sent to the special line, since this adds a constraint of codimension at least 1. This completes the proof for $\mathcal{Q}_1$. The proofs for the quadruples $\mathcal{Q}_2$ and $\mathcal{Q}_3$ follow from similar arguments. $\square$

The count of index 2 boundary degenerations in Proposition 7.9 lets us identify the count of curves of type (h_1^∞-e-1), (h_2^∞-e-1) and (h_3^∞-e-1) with the map E^∞.

We now consider the ends labeled (e-2) above, which appear as $\tau \to \infty$ and $s \to 1$ or $s \to 0$. We consider the following two types of broken curves (see Figure 19.10):

(h_1^∞-e-2) A pair of broken holomorphic rectangles $\mathcal{V}$ and $\mathcal{V}_0$ on $\mathcal{Q}_1$, satisfying the following:

This is a free offprint provided to the author by the publisher. Copyright restrictions may apply.

(a) $\mathcal{V}$ consists of a holomorphic triangle $v_{\alpha'',\alpha,\beta}$ on $(\Sigma, \boldsymbol{\alpha}'', \boldsymbol{\alpha}, \boldsymbol{\beta})$ and a holomorphic triangle $v_{\alpha'',\alpha',\alpha}$ on $(\Sigma, \boldsymbol{\alpha}'', \boldsymbol{\alpha}', \boldsymbol{\alpha})$, as well as a collection of index 2 boundary degenerations $d_1, \dots, d_n$.
(b) $\mathcal{V}_0$ consists of a holomorphic triangle $v_{c_3,c_1,c_3'}$ on $(\mathbb{T}^2, c_3, c_1, c_3')$ and a holomorphic triangle v_{c_3,c_2,c_1} on $(\mathbb{T}^2, c_3, c_2, c_1)$, as well as a collection of index 2 boundary degenerations $e_1, \dots e_m$.
(c) The source of the holomorphic triangle $v_{\alpha'',\alpha,\beta}$ has two disjoint collections of marked points $\mathbf{q}^c_{\alpha'',\alpha,\beta}$, $\mathbf{q}^d_{\alpha'',\alpha,\beta}$, which we call the *coupled* and *decoupled* marked points, respectively. The other three holomorphic triangles have analogous collections of marked points.
(d) We have $|\mathbf{q}^d_{\alpha'',\alpha,\beta}|+|\mathbf{q}^d_{\alpha'',\alpha',\alpha}| = m$ and $|\mathbf{q}^d_{c_3,c_1,c_3'}|+|\mathbf{q}^d_{c_3,c_2,c_1}| = n$.
(e) $v_{\alpha'',\alpha,\beta}$ and v_{c_3,c_2,c_1} have no coupled marked points.
(f) $v_{\alpha'',\alpha',\alpha}$ has no decoupled marked points.
(g) $|\mathbf{q}^c_{\alpha'',\alpha',\alpha}| = |\mathbf{q}^c_{c_3,c_1,c_3'}|$.
(h) The coupled marked points of $v_{c_3,c_1,c_3'}$ map to the special line of Δ.
(i) The coupled marked points of $v_{\alpha'',\alpha',\alpha}$ and $v_{c_3,c_1,c_3'}$ are matched under the asymptotic evaluation map $\mathrm{ev}^{\mathrm{st/un}}$, which takes values in $\mathbb{R}^k/\mathbb{R}$, where $k = |\mathbf{q}^c_{\alpha'',\alpha',\alpha}|$.
(j) The decoupled marked points of $v_{\alpha'',\alpha,\beta}$ are matched to the boundary degenerations $e_1, \dots, e_m$, similar to part (d) of (h_1^∞-e-1), in Definition 19.15. Similarly the decoupled marked points of v_{c_3,c_2,c_1} and $v_{c_3,c_1,c_3'}$ are matched to the boundary degenerations $d_1, \dots, d_n$.

(h_3^∞-e-2) A pair of broken holomorphic rectangles $\mathcal{V}$ and $\mathcal{V}_0$ on $\mathcal{Q}_3$, satisfying the analogs of (h_1^∞-e-2).

The argument from Lemma 19.16 adapts to show the following:

LEMMA 19.17. *The ends of $\mathcal{MM}^{\tau\in[\tau_0,\infty),v_i}_{J\wedge I}(\psi,\psi_0)$ labeled (e-2) above (i.e. appearing as $\tau\to\infty$ and $s\to 0$ or $s\to 1$) correspond generically to broken curves which satisfy either (h_1^∞-e-2) or (h_3^∞-e-2). Furthermore, any such broken curve makes odd algebraic contribution to the count of ends of its moduli space.*

Write X_1^∞ and X_3^∞ for the maps which count the elements of 0-dimensional moduli spaces of broken curves satisfying (h_1^∞-e-2) or (h_3^∞-e-2), respectively. Combining Lemma 19.17 with the proof of Lemma 19.14, by counting the ends of $[\tau_0,\infty)$-matched moduli spaces, we obtain the relation

$$E^{\tau_0} + E^\infty + X_1^\infty + X_3^\infty = \partial H^{\tau_0\to\infty} + H^{\tau_0\to\infty}\partial. \tag{19.25}$$

We may trim off the boundary degenerations in the definitions of the maps X_1^∞ and X_3^∞, as in (19.9). Hence X_1^∞ may be identified as the counts of quadruples of holomorphic triangles

$$(v_{\alpha'',\alpha,\beta}, v_{c_3,c_1,c_3'}, v_{\alpha'',\alpha',\alpha}, v_{c_3,c_2,c_1}), \tag{19.26}$$

which are equipped with marked points and satisfy the matching conditions of (h_1^∞-e-2), which furthermore represent a quadruple of triangle classes $(\psi_{\alpha'',\alpha,\beta}, \psi_{c_3,c_1,c_3'}, \psi_{\alpha'',\alpha',\alpha}, \psi_{c_3,c_2,c_1})$ satisfying

$$\mu(\psi_{\alpha'',\alpha,\beta}) + \mu(\psi_{c_3,c_1,c_3'}) + \mu(\psi_{\alpha'',\alpha',\alpha}) + \mu(\psi_{c_3,c_2,c_1}) = 2n_{p_0}(\psi_{\alpha'',\alpha',\alpha}) - 1. \tag{19.27}$$

This is a free offprint provided to the author by the publisher. Copyright restrictions may apply.

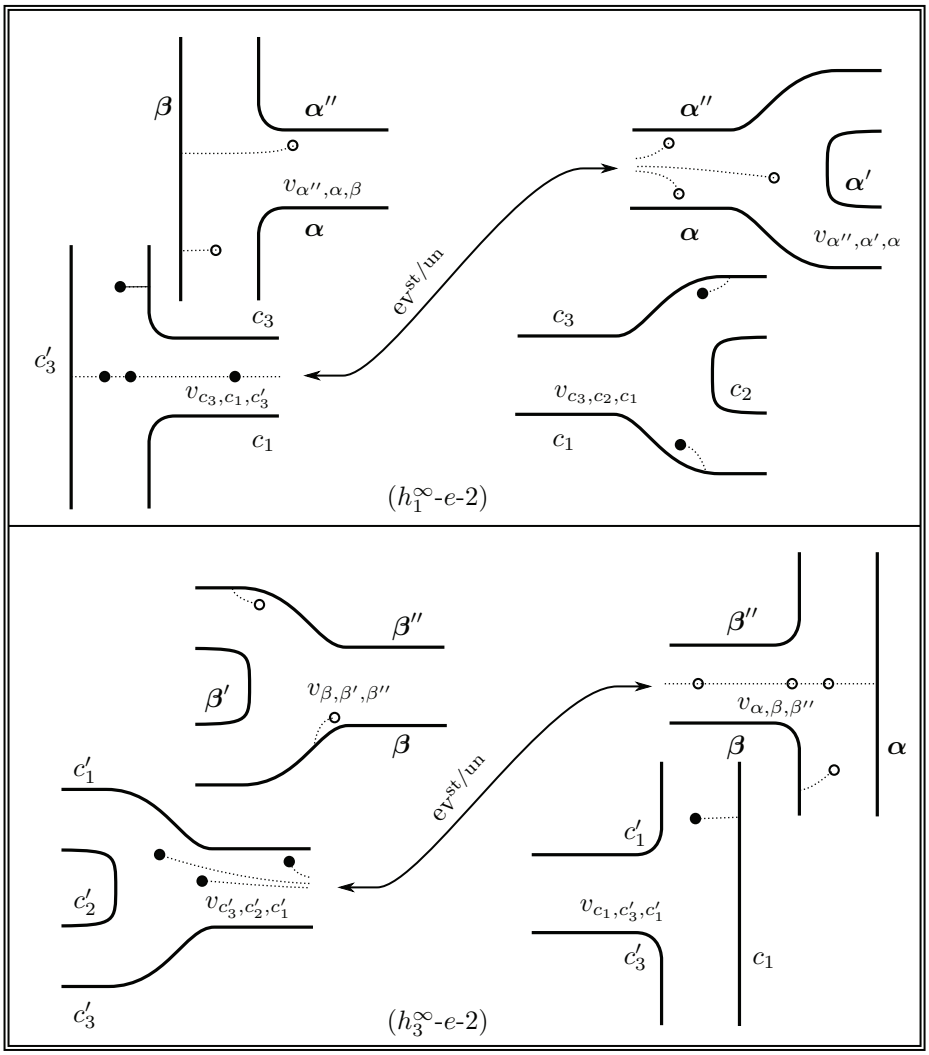


FIGURE 19.10. A schematic of configurations $(h_1^\infty\text{-}e\text{-}2)$ and $(h_3^\infty\text{-}e\text{-}2)$. Open dots indicate marked points which map to Σ. Solid dots indicate marked points mapped to $\mathbb{T}^2$. Boundary degenerations have been trimmed.

The map X_3^∞ has an analogous description. The maps X_1^∞ and X_3^∞ assign U and T weights to quadruples of triangles similarly to (19.13).

Proposition 19.12 now follows from (19.25), together with the following lemma:

LEMMA 19.18.

(1) $X_1^\infty = 0$.
(2) $X_3^\infty \simeq 0$.

Lemma 19.18 is slightly involved, so we prove the two subclaims separately. We begin with the proof for X_1^∞:

This is a free offprint provided to the author by the publisher. Copyright restrictions may apply.

PROOF OF PART (1) OF LEMMA 19.18 . We focus on the trimmed description of X_1^∞, which counts 4-tuples of marked holomorphic triangles, as in (19.26).

The map X_1^∞ counts 4-tuples of holomorphic triangles, representing 4-tuples of classes

$$(\psi_{\alpha'',\alpha,\beta}, \psi_{c_3,c_1,c_3'}, \psi_{\alpha'',\alpha',\alpha}, \psi_{c_3,c_2,c_1}).$$

We write $S^{\mathbf{q}_{\alpha'',\alpha,\beta}}$ for the marked source of the holomorphic triangle $v_{\alpha'',\alpha,\beta})$. The marked points $\mathbf{q}_{\alpha'',\alpha,\beta}$ are partitioned into coupled and decoupled marked points, $\mathbf{q}^c_{\alpha'',\alpha,\beta}$ and $\mathbf{q}^d_{\alpha'',\alpha,\beta}$, respectively, as in ($h_1^\infty$-$e$-2). The same holds for the other three holomorphic triangles, and we use the analogous notation for their marked sources.

Define

$$N := |\mathbf{q}^c_{c_3,c_1,c_3'}|,$$

which we note coincides with $|\mathbf{q}^c_{\alpha'',\alpha',\alpha}|$. Note that $v_{\alpha'',\alpha,\beta}$ and v_{c_3,c_2,c_1} have no coupled marked points. We recall from (19.27) that

$$\mu(\psi_{\alpha'',\alpha,\beta}) + \mu(\psi_{c_3,c_1,c_3'}) + \mu(\psi_{\alpha'',\alpha',\alpha}) + \mu(\psi_{c_3,c_2,c_1}) = 2N - 1. \tag{19.28}$$

The matching condition only involves $\psi_{\alpha'',\alpha',\alpha}$ and $\psi_{c_3,c_1,c_3'}$, and it imposes a codimension $2N-1$ condition, by Proposition 7.3. More explicitly, the restriction that $\mathbf{q}^c_{c_3,c_1,c_3'}$ map to the special line of Δ imposes a codimension N condition, while the matching of $v_{c_3,c_1,c_3'}$ and $v_{\alpha'',\alpha',\alpha}$ under the evaluation maps $\mathrm{ev}^{\mathrm{st/un}}$, which take values in $\mathbb{R}^N/\mathbb{R}$, gives an extra codimension $N-1$ condition.

Hence, for a 4-tuple of marked sources and homology classes to have holomorphic representatives for generic almost complex structures, it is necessary that

$$\mu(\psi_{\alpha'',\alpha,\beta}) \geq 0 \quad \mu(\psi_{c_3,c_2,c_1}) \geq 0, \quad \text{and} \quad \mu(\psi_{\alpha'',\alpha',\alpha}) + \mu(\psi_{c_3,c_1,c_3'}) \geq 2N - 1. \tag{19.29}$$

Equations (19.28) and (19.29) imply that if a 4-tuple of homology classes and marked sources have matched representatives, then

$$\mu(\psi_{\alpha'',\alpha,\beta}) = \mu(\psi_{c_3,c_2,c_1}) = 0 \quad \text{and} \quad \mu(\psi_{\alpha'',\alpha',\alpha}) + \mu(\psi_{c_3,c_1,c_3'}) = 2N - 1. \tag{19.30}$$

In particular, the curves counted by X_1^∞ on $(\mathbb{T}^2, c_3, c_2, c_1)$ are exactly the Maslov index 0 triangles, with no constraints. Consequently, the equality $X_1^\infty = 0$ follows immediately from Lemma 12.3, the ordinary count of index 0 triangles on $(\mathbb{T}^2, c_3, c_2, c_1)$. □

The computation for X_3^∞ is slightly more involved. As in the proof of part (1) of Lemma 19.18, we focus on the trimmed description of X_3^∞, which counts quadruples of marked holomorphic triangles

$$(v_{c_3',c_2',c_1'}, v_{c_1,c_3',c_1'}, v_{\beta,\beta',\beta''}, v_{\alpha,\beta,\beta''}),$$

such that the evaluation under $\mathrm{ev}^{\mathrm{st/un}}$ on the coupled marked points of $v_{c_3',c_2',c_1'}$ and $v_{\alpha,\beta,\beta'}$ coincide.

For the map X_3^∞, the triangles $v_{c_3',c_2',c_1'}$ have only coupled marked points, and hence the classes counted by X_3^∞ satisfy

$$\mu(\psi_{c_1,c_3',c_1'}) + \mu(\psi_{\beta,\beta',\beta''}) + \mu(\psi_{\alpha,\beta,\beta''}) + \mu(\psi_{c_3',c_2',c_1'}) = 2n_{p_0}(\psi_{c_3',c_2',c_1'}) - 1. \tag{19.31}$$

The matching condition satisfied by $v_{\alpha,\beta,\beta''}$ and $v_{c_3',c_2',c_1'}$ consists of the following. Both triangles have exactly $n_{p_0}(\psi_{c_3',c_2',c_1'})$ coupled marked points. The coupled

This is a free offprint provided to the author by the publisher. Copyright restrictions may apply.

marked points of $v_{\alpha,\beta,\beta''}$ occur along the special line of Δ. Furthermore,

$$\mathrm{ev}^{\mathrm{st}}_{\mathbf{q}^c_{c_3',c_2',c_1'}}(v_{c_3',c_2',c_1'}) = \mathrm{ev}^{\mathrm{un}}_{\mathbf{q}^c_{\alpha,\beta,\beta''}}(v_{\alpha,\beta,\beta''}).$$

See Figure 19.10 for a schematic.

To define our null-homotopy of X_3^∞, we investigate expected dimensions further. Let $S^{\mathbf{q}}$ and $S_0^{\mathbf{q}_0}$ denote two marked sources for $\psi_{\alpha,\beta,\beta''}$ and $\psi_{c_3',c_2',c_1'}$, respectively. Generically, the fibered product

$$\mathcal{M}(S^{\mathbf{q}}, \psi_{\alpha,\beta,\beta''}) \times_{\mathrm{ev}^{\mathrm{st/un}}} \mathcal{M}(S_0^{\mathbf{q}_0}, \psi_{c_3',c_2',c_1'})$$

will be a manifold, whose dimension near any embedded curve is given by

$$\begin{aligned}&\dim\left(\mathcal{M}(S^{\mathbf{q}}, \psi_{\alpha,\beta,\beta''}) \times_{\mathrm{ev}^{\mathrm{st/un}}} \mathcal{M}(S_0^{\mathbf{q}_0}, \psi_{c_3',c_2',c_1'})\right)\\ =&\mu(\psi_{\alpha,\beta,\beta''}) + \mu(\psi_{c_3',c_2',c_1'}) - 2n_{p_0}(\psi_{c_3',c_2',c_1'}) + 1.\end{aligned} \tag{19.32}$$

We now deform the evaluation map. Given $r \in [1,\infty)$, we define

$$\mathcal{M}(S^{\mathbf{q}}, \psi_{\alpha,\beta,\beta''}) \times_{r\cdot\mathrm{ev}^{\mathrm{st/un}}} \mathcal{M}(S_0^{\mathbf{q}_0}, \psi_{c_3',c_2',c_1'})$$

to be the set of pairs of marked holomorphic triangles $(v_{c_3',c_2',c_1'}, v_{\alpha,\beta,\beta''})$ which satisfy

$$r \cdot \mathrm{ev}^{\mathrm{st}}_{\mathbf{q}^c_{c_3',c_2',c_1'}}(v_{c_3',c_2',c_1'}) = \mathrm{ev}^{\mathrm{un}}_{\mathbf{q}^c_{\alpha,\beta,\beta''}}(v_{\alpha,\beta,\beta''}). \tag{19.33}$$

In (19.33), r acts diagonally on $\mathbb{R}^k/\mathbb{R}$ by multiplication.

Furthermore, the parametrized moduli space

$$\begin{aligned}&\mathcal{MM}^{r\cdot\mathrm{ev}^{\mathrm{st/un}}, r\in[1,\infty)}(S^{\mathbf{q}}, S_0^{\mathbf{q}_0}, \psi_{\alpha,\beta,\beta''}, \psi_{c_3',c_2',c_1'})\\ :=&\bigcup_{r\in[1,\infty)} \mathcal{M}(S^{\mathbf{q}}, \psi_{\alpha,\beta,\beta''}) \times_{r\cdot\mathrm{ev}^{\mathrm{st/un}}} \mathcal{M}(S_0^{\mathbf{q}_0}, \psi_{c_3',c_2',c_1'}) \times \{r\}\end{aligned} \tag{19.34}$$

will generically be a manifold, whose dimension near any embedded curve is

$$\begin{aligned}&\dim\left(\mathcal{MM}^{r\cdot\mathrm{ev}^{\mathrm{st/un}}, r\in[1,\infty)}(S^{\mathbf{q}}, S_0^{\mathbf{q}_0}, \psi_{\alpha,\beta,\beta''}, \psi_{c_3',c_2',c_1'})\right)\\ =&\mu(\psi_{\alpha,\beta,\beta''}) + \mu(\psi_{c_3',c_2',c_1'}) - 2n_p(\psi_{c_3',c_2',c_1'}) + 2.\end{aligned} \tag{19.35}$$

We define our homotopy $H_3^{\infty,[1,\infty)}$ to count quadruples of marked triangles

$$(v_{c_3',c_2',c_1'}, v_{c_1,c_3',c_1'}, v_{\beta,\beta',\beta''}, v_{\alpha,\beta,\beta''}),$$

satisfying

$$\mu(v_{c_1,c_3',c_1'}) = \mu(v_{\beta,\beta',\beta''}) = 0 \quad \text{and} \quad \mu(v_{\alpha,\beta,\beta''}) + \mu(v_{c_3',c_2',c_1'}) = 2n_{p_0}(v_{c_3',c_2',c_1'}) - 2,$$

and such that $v_{\alpha,\beta,\beta''}$ and $v_{c_3',c_2',c_1'}$ are $r\cdot\mathrm{ev}^{\mathrm{st/un}}$ matched for some $r \in [1,\infty)$. A quadruple of triangles is assigned U and T weights similarly to (19.13).

Part (2) of Lemma 19.18 is a consequence of the following lemma:

LEMMA 19.19. *The maps X_3^∞ and $H_3^{\infty,[1,\infty)}$ satisfy*

$$X_3^\infty = \left[\partial, H_3^{\infty,[1,\infty)}\right].$$

The proof of Lemma 19.19 follows from a careful analysis of the ends of the moduli spaces in (19.34), which we do in the subsequent Lemmas 19.20 and 19.23.

This is a free offprint provided to the author by the publisher. Copyright restrictions may apply.

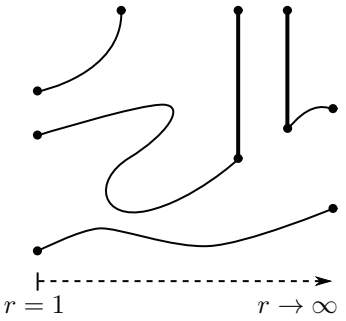


FIGURE 19.11. The union of the moduli spaces $\mathcal{MM}^{r\cdot \mathrm{ev}^{\mathrm{st/un}}}(\Psi)$ over different configurations Ψ. The r-regular subset is shown using thin-solid lines. The r-flat subset is shown with bold-solid lines.

First, we introduce some notation. Suppose Ψ is a tuple consisting of four homology classes of triangles $(\psi_{c_3',c_2',c_1'}, \psi_{c_1,c_3',c_1'}, \psi_{\beta,\beta',\beta''}, \psi_{\alpha,\beta,\beta''})$, as well as four marked sources; $r \geq 1$ is fixed. Write

$$\mathcal{MM}^{r\cdot \mathrm{ev}^{\pm\infty}}(\Psi),$$

for the moduli space of quadruples of marked triangles $(v_{c_3',c_2',c_1'}, v_{c_1,c_3',c_1'}, v_{\beta,\beta',\beta''}, v_{\alpha,\beta,\beta''})$ such that $v_{c_3',c_2',c_1'}$ and $v_{\alpha,\beta,\beta''}$ are matched under $r \cdot \mathrm{ev}^{\mathrm{st/un}}$. Similarly, we write

$$\mathcal{MM}^{r\cdot \mathrm{ev}^{\mathrm{st/un}}, r\in[1,\infty)}(\Psi) \tag{19.36}$$

for the parametrized moduli space, consisting of such quadruples, which are r-matched for some $r \in [1, \infty)$.

Note that the number of coupled marked points in the four homology classes of Ψ is fixed. Namely, the sources of $v_{c_3',c_2',c_1'}$ and $v_{\alpha,\beta,\beta''}$ both have $n_{p_0}(c_3', c_2', c_1')$ coupled marked points. All other marked points are decoupled. We note that Ψ also contains the information of a bijection between the coupled marked points of $v_{c_3',c_2',c_1'}$ and $v_{\alpha,\beta,\beta''}$.

We wish to count the ends of the moduli spaces $\mathcal{MM}^{r\cdot \mathrm{ev}^{\mathrm{st/un}}, r\in[1,\infty)}(\Psi)$, ranging over configurations Ψ which satisfy

$$\mu(\psi_{c_3',c_2',c_1'}) + \mu(\psi_{c_1,c_3',c_1'}) + \mu(\psi_{\beta,\beta',\beta''}) + \mu(\psi_{\alpha,\beta,\beta''}) - 2n_{p_0}(\psi_{c_3',c_2',c_1'}) + 1 = 0. \tag{19.37}$$

These are exactly the configurations Ψ where (19.36) has expected dimension 1. Using (19.35), we see that there are two ways a tuple Ψ can have a 1-dimensional moduli space:

(r-1) *r-regular*:

$$\mu(\psi_{c_1,c_3',c_1'}) = \mu(\psi_{\beta,\beta',\beta''}) = 0 \quad \text{and} \quad \mu(\psi_{\alpha,\beta,\beta''}) + \mu(\psi_{c_3',c_2',c_1'}) = 2n_{p_0}(\psi_{c_3',c_2',c_1'}) - 1.$$

(r-2) *r-flat*:

$$\mu(\psi_{c_1,c_3',c_1'}) + \mu(\psi_{\beta,\beta',\beta''}) = 1 \quad \text{and} \quad \mu(\psi_{\alpha,\beta,\beta''}) + \mu(\psi_{c_3',c_2',c_1'}) = 2n_{p_0}(\psi_{c_3',c_2',c_1'}) - 2.$$

For r-flat configurations Ψ, projection onto r of $\mathcal{MM}^{r\cdot \mathrm{ev}^{\mathrm{st/un}}, r\in[1,\infty)}(\Psi)$ is locally constant. A schematic is shown in Figure 19.11.

We now enumerate the ends of the moduli spaces $\mathcal{MM}^{r\cdot \mathrm{ev}^{\mathrm{st/un}}, r\in[1,\infty)}(\Psi)$ which occur at $r \in [1, \infty)$:

This is a free offprint provided to the author by the publisher. Copyright restrictions may apply.

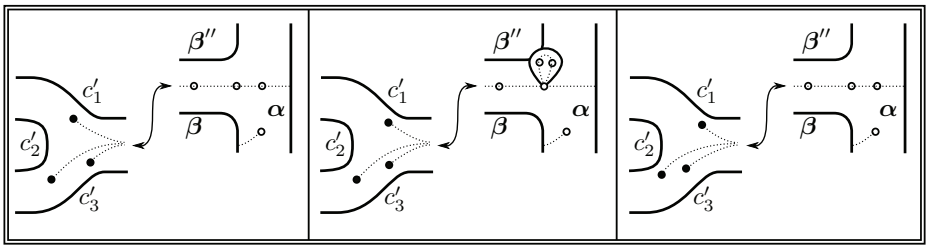


FIGURE 19.12. A collision of evaluation (c-3) (center) appearing in the boundaries of two families of r-matched moduli spaces (left and right).

LEMMA 19.20. *Suppose that Ψ is a configuration of homology classes, decorated sources, and marked point matchings which satisfies* (19.37)*, and has incoming intersection points at a fixed $\mathbf{x} \in \mathbb{T}_{\alpha_1} \cap \mathbb{T}_{\beta_3}$, as well as the canonical inputs, as in* (19.12)*. Let k denote $n_{p_0}(\psi_{c_3',c_2',c_1'})$. Generically, the ends of*

$$\mathcal{MM}^{r\cdot \mathrm{ev}^{\mathrm{st/un}}, r\in[1,\infty)}(\Psi)$$

occurring at finite $r \in [1,\infty)$ correspond to the following configurations:

(c-1) *The curves at $r = 1$.*

(c-2) *(Disk breaking) A 5-tuple of the form $(u, v_{\beta,\beta',\beta''}, v_{\alpha,\beta,\beta''}, v_{c_3',c_2',c_1'}, v_{c_1,c_3',c_1'})$ where u is a holomorphic disk of Maslov index 1, in any of the twelve cylindrical ends of the 4-manifolds corresponding to the triple diagrams $(\Sigma, \boldsymbol{\beta}, \boldsymbol{\beta}', \boldsymbol{\beta}'')$, $(\Sigma, \boldsymbol{\alpha}, \boldsymbol{\beta}, \boldsymbol{\beta}'')$, $(\mathbb{T}^2, c_3', c_2', c_1')$ and $(\mathbb{T}^2, c_1, c_3', c_1')$. The disk u has no coupled marked points, while $v_{c_3',c_2',c_1'}$ and $v_{\alpha,\beta,\beta''}$ each have exactly k coupled marked points. Furthermore, $v_{c_3',c_2',c_1'}$ has no decoupled marked points. Finally,*

$$\mu(v_{\beta,\beta',\beta''}) = \mu(v_{c_1,c_3',c_1'}) = 0 \quad \text{and} \quad \mu(v_{c_3',c_2',c_1'}) + \mu(v_{\alpha,\beta,\beta''}) = 2k - 2.$$

(c-3) *(Collisions of evaluation) A quadruple $(v_{\beta,\beta',\beta''}, v'_{\alpha,\beta,\beta''}, b, v_{c_3',c_2',c_1'}, v_{c_1,c_3',c_1'})$, where $v_{\beta,\beta',\beta''}$, $v_{c_3',c_2',c_1'}$, $v_{c_1,c_3',c_1'}$ are holomorphic triangles satisying the triangular analogs of (M-1)–(M-7). The curve $v'_{\alpha,\beta,\beta''}$, satisfies ($M$-1)–($M$-7), except that it has one additional interior puncture, which matches $p \in \Sigma$ to first order. Furthermore $(\pi_\Delta \circ v_{\alpha',\beta,\beta''})(q)$ is contained in the special line of Δ, and also corresponds with the image of the constant bubble b. The asymptotic evaluations of the coupled marked points of $(v'_{\alpha,\beta,\beta''}, b)$ and $v_{c_3',c_2',c_1'}$ coincide, and furthermore have exactly one repeated entry. Furthermore, the tuple $(\pi_\Delta \circ v_{c_3',c_2',c_1'})(\mathbf{q}_{c_3',c_2',c_1'})$ consists of k distinct points. Finally,*

$$\mu(v_{\beta,\beta',\beta''}) = \mu(v_{c_1,c_3',c_1'}) = 0 \quad \text{and} \quad \mu(v_{c_3',c_2',c_1'}) + \mu(v_{\alpha,\beta,\beta''}) = 2k - 1.$$

PROOF. The degenerations labeled (c-1), (c-2) and (c-3) occur in the correct codimension, so it suffices to prove that there are no additional ends. To prove this, we first describe which degenerations occur generically in the ends of 1-dimensional r-matched moduli spaces, and then use several facts about $\mathcal{Q}_3$ to prohibit degenerations beyond those in the statement.

This is a free offprint provided to the author by the publisher. Copyright restrictions may apply.

We consider a degeneration at some $r \in (1, \infty)$, consisting of a pair of combs, which together consist of two curves on $\Sigma \times \Delta$, two curves on $\mathbb{T}^2 \times \Delta$, as well as a collection of boundary degenerations and curves in the cylindrical ends. To analyze the limiting curves, it is helpful to combine the level structures in the (c_3', c_2') and (c_2', c_1') ends into a single level structure. We view limiting curves in this end as mapping into $\mathbb{T}^2 \times ([0,1] \times \mathbb{R} \sqcup [0,1] \times \mathbb{R})$.

We may assume that a comb is the limit of a r-regular family, since r-flat families involve only degenerations of the curves $v_{\alpha,\beta,\beta''}$ and $v_{c_3',c_2',c_1'}$. For an r-flat family, one of $v_{\alpha,\beta,\beta''}$ and $v_{c_3',c_2',c_1'}$ has Maslov index 1, while the other has index 0. Hence, all degenerations correspond to an index 1 disk breaking off, which contains no coupled marked points; this is a special case of (c-2). Hence, it is sufficient to consider limiting combs involving only degenerations of $v_{c_3',c_2',c_1'}$ and $v_{\alpha,\beta,\beta''}$.

Next, we note that any holomorphic disk appearing in the $(\boldsymbol{\alpha}, \boldsymbol{\beta})$ or $(\boldsymbol{\alpha}, \boldsymbol{\beta}'')$ end has no coupled marked points, by definition of the vector field v_3, and hence must have Maslov index 1 (as the remaining components would otherwise violate transversality). It is easy to see that the resulting configuration satisfies (c-2).

We now consider degenerations which involve non-trivial holomorphic disks breaking off in the $(\boldsymbol{\beta}, \boldsymbol{\beta}'')$, (c_3', c_2'), (c_2', c_1') or (c_3', c_1') ends, or non-trivial boundary degenerations. Suppose that $\mathcal{U}$ and $\mathcal{V}$ are the combs appearing in such a degeneration, and let $\mathcal{U}$ be on the $\mathbb{T}^2$-side, and $\mathcal{V}$ be on the Σ-side. As described above, we may assume that this degeneration was the limit of an r-regular family. For notational convenience, we trim $v_{c_1,c_3',c_1'}$ and $v_{\beta,\beta',\beta''}$ (which are index 0 triangles) from $\mathcal{U}$ and $\mathcal{V}$. Write $\mathcal{U}_1, \ldots, \mathcal{U}_n$ for the levels of $\mathcal{U}$, and $\mathcal{V}_1, \ldots, \mathcal{V}_m$ for the levels of $\mathcal{V}$. See Figure 19.13.

Let d_i denote the number of coupled marked points of $\mathcal{U}_i$, and let

$$\mathbf{d} = \sum_{i=1}^{n} d_i.$$

Define

$$\mathbb{I} := \{i : 1 \leq i \leq m, \quad d_i > 0\}.$$

The matching of marked points descends to an injection

$$f : \mathbb{I} \to \{1, \ldots, n\}.$$

When neither $\mathcal{U}_i$ nor $\mathcal{V}_{f(i)}$ is a boundary degeneration, the curves $\mathcal{U}_i$ and $\mathcal{V}_{f(i)}$ are matched under $r \cdot \mathrm{ev}^{\mathrm{st/un}}$. (When one or both of $\mathcal{U}_i$ or $\mathcal{V}_{f(i)}$ is a boundary degeneration, there is still a matching condition which is satisfied, though it is more subtle and not important for our purposes).

Write $\phi_1^{\mathbb{T}}, \ldots, \phi_n^{\mathbb{T}}$ for the homology classes of $\mathcal{U}_1, \ldots, \mathcal{U}_n$, and $\phi_1^{\Sigma}, \ldots, \phi_m^{\Sigma}$ for the homology classes of $\mathcal{V}_1, \ldots, \mathcal{V}_m$. For each $i \in \mathbb{I}$, we define

$$\kappa_i := \mu(\phi_i^{\mathbb{T}}) + \mu(\phi_{f(i)}^{\Sigma}) - 2d_i.$$

Since $\mathcal{U}$ and $\mathcal{V}$ are the limit of a family of curves representing a pair $(\psi_{\alpha,\beta,\beta''}, \psi_{c_3',c_2',c_1'})$ with

$$\mu(\psi_{\alpha,\beta,\beta''}) + \mu(\psi_{c_3',c_2',c_1'}) - 2\mathbf{d} = -1,$$

we obtain the formula

$$\sum_{i \in \mathbb{I}} \kappa_i + \sum_{i \in \{1,\ldots,n\} \setminus \mathbb{I}} \mu(\phi_i^{\mathbb{T}}) + \sum_{j \in \{1,\ldots,m\} \setminus f(\mathbb{I})} \mu(\phi_j^{\Sigma}) = -1. \tag{19.38}$$

This is a free offprint provided to the author by the publisher. Copyright restrictions may apply.

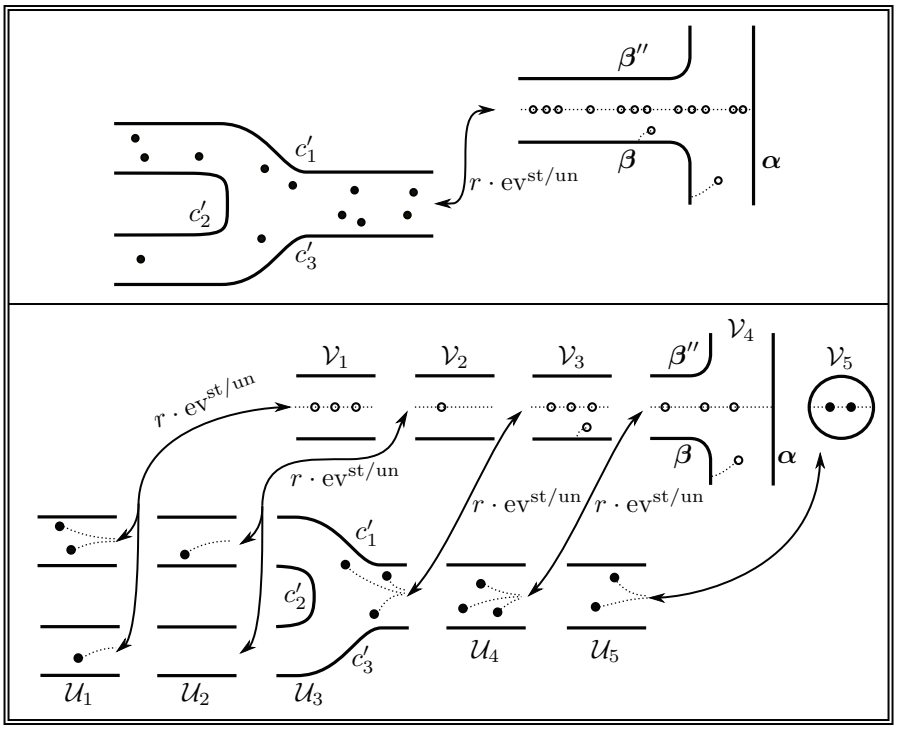


FIGURE 19.13. An $\mathrm{ev}^{\mathrm{st/un}}$-matched pair $(v_{\alpha,\beta,\beta''}, v_{c_3',c_2',c_1'})$ (top) and a nearby comb (bottom). The pictured degeneration occurs in high codimension.

By transversality, if $i \in \{1,\dots,n\} \setminus \mathbb{I}$ and $\phi_i^{\mathbb{T}}$ is a non-trivial homology class of $g_i^{\mathbb{T}}$-gons, then

$$\mu(\phi_i^{\mathbb{T}}) \geq 3 - g_i^{\mathbb{T}}. \tag{19.39}$$

An analogous lower bound holds for each $j \in \{1,\dots,m\} \setminus f(\mathbb{I})$.

We now claim that for each $i \in \mathbb{I}$, if $\mathcal{U}_i$ is a holomorphic $g_i^{\mathbb{T}}$-gon and $\mathcal{V}_{f(i)}$ is a g_i^{Σ}-gon, then

$$\kappa_i \geq \begin{cases} 5 - g_i^{\mathbb{T}} - g_i^{\Sigma} - \delta(i) & \text{if } g_i^{\mathbb{T}} > 1 \text{ and } g_i^{\Sigma} > 1, \\ 3 - g_i^{\Sigma} + d_i & \text{if } g_i^{\mathbb{T}} = 1 \text{ and } g_i^{\Sigma} > 1, \\ 3 - g_i^{\mathbb{T}} & \text{if } g_i^{\mathbb{T}} > 1 \text{ and } g_i^{\Sigma} = 1, \\ 2d_i & \text{if } g_i^{\Sigma} = g_i^{\mathbb{T}} = 1. \end{cases} \tag{19.40}$$

for some function $\delta\colon \mathbb{I} \to \{0,1\}$, satisfying

$$\sum_{i \in \mathbb{I}} \delta(i) \leq 1.$$

We note that the bound in (19.40) is not dependent on the quadruple $\mathcal{Q}_3$ in any way.

We now prove (19.40). Suppose first that $g_i^{\mathbb{T}}, g_i^{\Sigma} > 1$. If r is fixed, then the moduli space of $r \cdot \mathrm{ev}^{\mathrm{st/un}}$-matched pairs of holomorphic curves representing

This is a free offprint provided to the author by the publisher. Copyright restrictions may apply.

the classes $\phi_i^{\mathbb{T}}$ and $\phi_{f(i)}^{\Sigma}$ has expected dimension $\kappa_i + 1$. The expected dimension ranging over $r \in (1,\infty)$ is greater by 1. If an $r \cdot \mathrm{ev}^{\mathrm{st/un}}$-matched moduli space is non-empty for some r, then it must have dimension at least $(3 - g_i^{\Sigma}) + (3 - g_i^{\mathbb{T}})$, since the map $\mathrm{ev}^{\mathrm{st/un}}$ is invariant under the translation action on the moduli spaces of disks.

Note that if $\kappa_i + 2 = (3 - g_i^{\Sigma}) + (3 - g_i^{\mathbb{T}})$, such configurations do not appear for generic r. It follows that there is at most one $i \in \mathbb{I}$ such that $(\mathcal{U}_i, \mathcal{V}_{f(i)})$ contains no boundary degenerations and the r-matched moduli space generated by the homology classes of $\mathcal{U}_i$ and $\mathcal{V}_{f(i)}$, parametrized by $r \in (1,\infty)$, has expected dimension $6 - g_i^{\mathbb{T}} - g_i^{\Sigma}$. This pair corresponds to the $i \in \mathbb{I}$ with $\delta(i) > 0$. The remaining $i \in \mathbb{I}$ such that $(\mathcal{U}_i, \mathcal{V}_{f(i)})$ has no boundary degenerations must live in r-matched moduli spaces (with r ranging over $(1,\infty)$) which are 1-dimensional. Since $\kappa_i + 1$ is the expected dimension, this immediately gives the first line of (19.40).

Suppose now that $g_i^{\mathbb{T}} = 1$ while $g_i^{\Sigma} > 1$, so that $\mathcal{U}_i$ is a boundary degeneration. By definition, $\kappa_i = \mu(\phi_{f(i)}^{\Sigma})$. On the other hand, the curve $\mathcal{V}_{f(i)}$ contains a disk or triangle where the d_i coupled marked points are mapped to the special line. The subspace of $\mathcal{M}(\phi_i^{\Sigma})$ which satisfies this constraint has expected dimension $\mu(\phi_{f(i)}^{\Sigma}) - d_i$. Hence, for a representative to exist, we must have $\kappa_i = \mu(\phi_i^{\Sigma}) \geq (3 - g_i^{\Sigma}) + d_i$, as claimed. This gives the second line of (19.40).

Suppose now that $g_i^{\Sigma} = 1$. In this case, $\kappa_i = \mu(\phi_i^{\mathbb{T}})$. Since $\phi_i^{\mathbb{T}}$ has a holomorphic representative, we know that $\mu(\phi_{f(i)}^{\mathbb{T}}) \geq 3 - g_i^{\mathbb{T}}$. This gives the third line of (19.40). If $g_i^{\Sigma} = g_i^{\mathbb{T}} = 1$, then the fourth line of (19.40) is in fact an equality.

In the setting of a general Heegaard quadruple, (19.40) implies that the generic degenerations of 1-dimensional $r \cdot \mathrm{ev}^{\mathrm{st/un}}$-matched moduli spaces which are parametrized over $r \in (1,\infty)$, and also involve a non-trivial disk or boundary degeneration, must consist of one of the following (see Figure 19.14):

- (g-1) A pair of holomorphic triangles which together have $\kappa_i = -2$, as well as a Maslov index 1 disk in the (c_3', c_1')-end, whose coupled marked points are matched to the coupled marked points on a $(\Sigma, \boldsymbol{\alpha})$ boundary degeneration. The disk and boundary degeneration together have $\kappa_i = 1$.
- (g-2) A pair of holomorphic triangles which together have $\kappa_i = -1$, as well as a pair of disks with a non-zero number of marked points, which together have $\kappa_i = 0$. One disk occurs in the (c_3', c_2')-(c_2', c_1')-end (recall we have collapsed the level structure over these two ends), while the other occurs in the $(\boldsymbol{\beta}, \boldsymbol{\beta}'')$-end.
- (g-3) A pair of holomorphic triangles which together have $\kappa_i = -2$, as well as an index 1 disk in any end, which contains no coupled marked points.

We remark that in (g-1), we have not ruled out the boundary degeneration from containing further ghost curve levels (e.g. resulting from the collision of two marked points).

We claim that the degenerations (g-1) and (g-2) are non-generic for $\mathcal{Q}_3$. The necessary extra fact is that any class of disks ψ on one of the three ends of $(\mathbb{T}^2, c_3', c_2', c_1')$ satisfies

$$\mu(\psi) = 2n_{p_0}(\psi). \tag{19.41}$$

We consider first (g-1). Suppose a limiting comb had a matched level $(\mathcal{U}_i, \mathcal{V}_{f(i)})$ such that $\mathcal{U}_i$ is a holomorphic disk, and $\mathcal{V}_{f(i)}$ is a boundary degeneration. From

This is a free offprint provided to the author by the publisher. Copyright restrictions may apply.

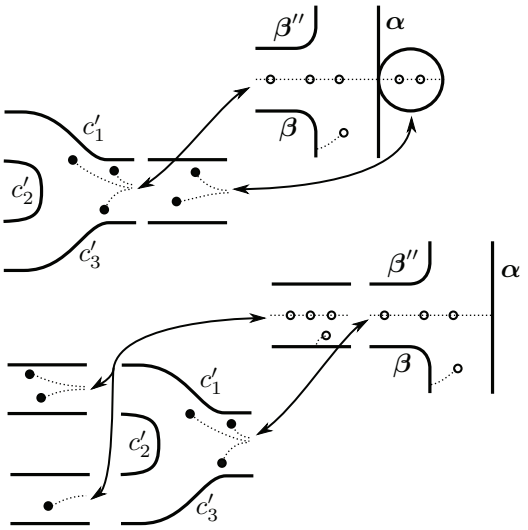


FIGURE 19.14. Codimension 1 degenerations in Lemma 19.20 that are prohibited for $\mathcal{Q}_3$.

(19.41) and the definition of κ_i, we obtain

$$\kappa_i = 2d_i,$$

which can never be 1.

Next, we consider (g-2). Suppose a limiting comb had a matched level $(\mathcal{U}_i, \mathcal{V}_{f(i)})$ consisting of a holomorphic disk in the (c_3', c_2')-(c_2', c_1')-end, matched to a disk in the $(\boldsymbol{\beta}, \boldsymbol{\beta}'')$-end. Furthermore, suppose that $\kappa_i = 0$. Combining the definition of κ_i with (19.41), we obtain $\kappa_i = \mu(\phi^{\Sigma}_{f(i)})$, which must be at least 1 for $\phi^{\Sigma}_{f(i)}$ to have a holomorphic representative. We obtain a contradiction, so ends of the form (g-2) are prohibited. Hence, (g-3) is the only generic degeneration for $\mathcal{Q}_3$ which involves non-trivial disk or boundary degeneration levels. We note (g-3) corresponds to (c-2).

We now consider limiting combs which do not involve a holomorphic disk or boundary degeneration breaking off. Such a limiting comb must contain a ghost curve (i.e. a curve which has constant value), or the formation of a double point. Limiting combs containing a ghost curve and double points on the $\mathbb{T}$-side occur in codimension at least 2, and hence do not feature in codimension 1 degenerations featuring in the statement. This is proven as follows. A standard argument [**LOT18**, Lemma 5.57] implies that double points and ghost curves which do not contain a marked point occur in codimension at least 2. Ghost curves containing one coupled marked point are prohibited by identical reasoning. Ghost curves containing more than one coupled marked point are prohibited by combining [**LOT18**, Lemma 5.57] with the expected dimensions of moduli spaces with tangency constraints using Proposition 7.3. Double points on the Σ-side are prohibited by similar reasoning.

Ghost degenerations on the Σ-side are slightly more subtle, since the coupled marked points are already matched to the special line. Ghost curves containing 0 or 1 marked points are prohibited by identical reasoning to the $\mathbb{T}$-side. More generally, suppose $\mathcal{U}_i$ and $\mathcal{V}_{f(i)}$ are a matched level, as above, and $\mathcal{V}_{f(i)}$ contains a

This is a free offprint provided to the author by the publisher. Copyright restrictions may apply.

ghost curve with $\ell > 1$ marked points. Suppose further that $\mathcal{V}_{f(i)}$ is not a boundary degeneration. We can trim off the ghost curve, and fill in the remaining puncture with a marked point, to obtain a curve with a marked point which matches $p \in \Sigma$ to order $\ell - 1$, and also matches the special line. An easy computation using (19.40) shows that we may increase the lower bound of κ_i appearing in (19.40) by $\ell - 1$. There is exactly one configuration which satisfies this modified (19.40), which is the case that $\mathcal{U}_i$ and $\mathcal{V}_{f(i)}$ are both triangles, $\ell = 2$, and there are no more levels. We restricted above to the case where the topological source of the ghost was a sphere. Ghost curves with more topologically complicated sources can be seen to live in codimension at least 2, by adapting [**LOT18**, Lemma 5.57]. □

The ends labeled (c-1) correspond to the expression

$$X_3^{\infty}(\mathbf{x}).$$

Amongst the ends labeled (c-2), disks breaking into the ends $(\boldsymbol{\alpha}, \boldsymbol{\beta})$ and $(\boldsymbol{\alpha}, \boldsymbol{\beta}'')$ correspond exactly to

$$\left(\partial H_3^{\infty,[1,\infty)} + H_3^{\infty,[1,\infty)}\partial\right)(\mathbf{x}).$$

We claim that the remaining ends occuring at finite $r \in (1, \infty)$ make vanishing total contribution:

LEMMA 19.21. *The total weighted count of the broken curves labeled* (c-2)*, not occuring in the* $(\boldsymbol{\alpha}, \boldsymbol{\beta})$ *or* $(\boldsymbol{\alpha}, \boldsymbol{\beta}'')$*-cylindrical ends, as well as the broken curves labeled* (c-3)*, vanishes.*

PROOF. The total count of broken curves with the configuration (c-2) where the disk occurs in one of the cylindrical ends labeled $(\boldsymbol{\beta}, \boldsymbol{\beta}')$, $(\boldsymbol{\beta}', \boldsymbol{\beta}'')$, (c_3', c_2'), (c_2', c_1') or (c_1, c_3') or (c_1, c_1') vanishes since the special inputs (i.e. $\Theta_{c_1,c_3'}$, $\Theta^+_{\beta,\beta'}$, etc.) are cycles.

The remaining configurations from (c-2) corresponds to a Maslov index 1 holomorphic disk, with no coupled marked points, breaking off in one of the $(\boldsymbol{\beta}, \boldsymbol{\beta}'')$ cylindrical ends. These degenerations occur in canceling pairs: if $\mathcal{U} = (v_{\alpha,\beta,\beta''}, v_{\beta,\beta',\beta''}, v_{c_3',c_2',c_1'}, v_{c_1,c_3',c_1'}, u)$ is such a limiting comb, then we may glue u to either $v_{\beta,\beta',\beta''}$ or $v_{\alpha,\beta,\beta''}$ to obtain a 1-dimensional moduli space with $\mathcal{U}$ in its boundary. (Note that such ends correspond to transitions between the r-flat and r-regular moduli spaces).

We now consider (c-3). Suppose the punctures q_1 and q_2 bubble off in a once punctured sphere, denoted $T_0^{q_1,q_2}$. We write $v'_{\alpha,\beta,\beta''}$ for the holomorphic triangle on $(\Sigma, \boldsymbol{\alpha}, \boldsymbol{\beta}, \boldsymbol{\beta}'')$ obtained by trimming off the bubble, and we write $\mathbf{q}$ for the set of coupled marked points on this level (including q_1 and q_2). We write $v_{c_3',c_2',c_1'}$ for the holomorphic triangle on $(\mathbb{T}^2, c_3', c_2', c_1')$, and $\mathbf{q}_0$ for the coupled marked points if $v_{c_3',c_2',c_1'}$. There are two marked points, $q_1', q_2' \in \mathbf{q}_0$, which are matched with q_1 and q_2, respectively. In the formation of the limiting comb, we may rescale the Σ-component near p, and also rescale the Δ component, to obtain a limiting curve $v_0 \colon T_0^{q_1,q_2} \to \mathbb{C} \times \mathbb{C}$. We view $S^2 \times S^2$ as the compactification of $\mathbb{C} \times \mathbb{C}$. Note that we can complete v_0 to a map from S^2 into $S^2 \times S^2$.

Let us write $\pi_1 \colon \mathbb{C} \times \mathbb{C} \to \mathbb{C}$ for projection onto the first factor, and π_2 for projection onto the second.

The following two properties of v_0 are immediate:

This is a free offprint provided to the author by the publisher. Copyright restrictions may apply.

(v_0-1) v_0 maps q_1 and q_2 to $\{0\} \times \mathbb{R}$ (here we view $\mathbb{R} \subseteq \mathbb{C}$ as the image of the special line in Δ after rescaling).

(v_0-2) v_0 maps the puncture of T_0 to $(\infty, \infty) \in S^2 \times S^2$.

We claim that generically v_0 will also have the following properties:

(v_0-3) The map $\pi_2 \circ v_0$ has degree 1.

(v_0-4) If we identify (T_0, q_0, q_1) with $(\mathbb{C}, -1, 1)$, then the map $\pi_1 \circ v_0$ takes the form

$$(\pi_1 \circ v_0)(z) = \alpha(z+1)(z-1)$$

for some $\alpha \in \mathbb{C}^\times$.

Property (v_0-4) follows from (v_0-3), as well as (v_0-1), (v_0-2) and basic complex analysis. Property (v_0-3) is proven as follows. We can view the source of $v'_{\alpha,\beta,\beta''}$ as having a marked point q, which is mapped to a point $(p, d) \in \Sigma \times \Delta$, which is the same point where the ghost bubble maps. If the degree of $\pi_2 \circ v_0$ was greater than 1, then $v'_{\alpha,\beta,\beta''}$ would have the property that $(\pi_\Sigma \circ v'_{\alpha,\beta,\beta''})(q) = p$ to order 1, $(\pi_\Delta \circ v'_{\alpha,\beta,\beta''})(q)$ is in the special line, and $\pi_\Delta \circ v'_{\alpha,\beta,\beta''}$ has vanishing derivative. Using the dimension counts of Proposition 7.3, we see that the expected dimension of the moduli space of such curves is too small (it drops by 3 instead of by 1), so does not appear in codimension 1 degenerations.

Let us write $\mathcal{U}'$ for the four triangular components of the limit (with the ghost trimmed off). We view $(\mathcal{U}', v_0)$ as being in the compactification of the moduli space $\mathcal{MM}^{r\cdot \mathrm{ev}^{\mathrm{st/un}}, r\in[1,\infty)}(\Phi)$, for some collection of homology classes with marked sources and matching data, which we denote by Φ. There is exactly one other configuration Φ' which contains a canceling broken curve of the form $(\mathcal{U}', v'_0)$. The curve v'_0 is the same as v_0, except with the matching of (q_1, q_2) and (q'_1, q'_2) switched. □

It remains to show that each of the broken curves described above make odd algebraic contribution to the count of the ends of the matched moduli spaces.

LEMMA 19.22. *Near a broken curve labeled* (c-2) *or* (c-3)*, there is a neighborhood in the compactification of the matched moduli spaces which admits a proper continuous map to* $[0, \infty)$ *which is locally odd degree and proper, such that the preimage of* 0 *is the broken curve.*

PROOF. We focus on the ends labeled (c-3), since the ends labeled (c-2) can be handled by a similar argument. Let us write $(\mathcal{U}', v_0)$ for a broken curve satisfying (c-3).

Since the source of v_0 is a once punctured sphere, the map v_0 achieves transversality for any split almost complex structure; see [**MS12**, Lemma 3.3.1]. (Compare [**LOT18**, Proposition 5.16]).

We first establish some notation. First, trim off the curves $v_{\beta,\beta',\beta''}$ and v_{c_1,c'_3,c'_1}, since they are index 0 and have no constraint. Write $v'_{\alpha,\beta,\beta''}$ for the limiting triangle on $(\Sigma, \boldsymbol{\alpha}, \boldsymbol{\beta}, \boldsymbol{\beta''})$ with the bubble trimmed off. By filling in the order two Reeb orbit with a marked point, we can view $v'_{\alpha,\beta,\beta''}$ as being an element of the moduli space of holomorphic triangles representing $\psi_{\alpha,\beta,\beta''}$, which have $n-1$ marked points, $n-2$ of which are order 1 at p, and 1 of which is order two, but which have no constraint with regards to the special line. We write W_0 for a small neighborhood of $v'_{\alpha,\beta,\beta''}$ in this moduli space.

This is a free offprint provided to the author by the publisher. Copyright restrictions may apply.

We write $\mathcal{N}_2$ for the moduli space of holomorphic maps $v_0 \colon T_0 \to S^2 \times S^2$ with 2 marked points, and one puncture, which satisfy the following conditions. We assume that $\pi_1 \circ v_0$ is asymptotic to ∞ with order 2 at the puncture of T_0, and $(\pi_1 \circ v_0)(q_i) = 0$ for $i \in \{1, 2\}$. Finally, we assume that $\pi_2 \circ v_0$ is degree 1.

We write G for the group of transformations of $\mathbb{C}$ given by $\{z \mapsto az + b : a > 0, b \in \mathbb{C}\}$. We write $\widetilde{\mathcal{N}}_2$ for the quotient of $\mathcal{N}_2$ by G (where G acts on the second factor of a map). Note that complex analysis identifies $\widetilde{\mathcal{N}}_2$ with S^1.

Standard gluing results imply that the above neighborhood W_0 of $v'_{\alpha,\beta,\beta''}$ may be chosen so that there is a map

$$\gamma \colon W_0 \times \widetilde{\mathcal{N}}_2 \times [0, \varepsilon) \to \overline{W},$$

which is a homeomorphism onto its image. Here, $\overline{W}$ denotes a neighborhood of $(v'_{\alpha,\beta,\beta''}, v_0)$ in the compactification of holomorphic triangles which have n marked points which each match the point $p \in \Sigma$ to order 1. We write W for the interior of $\overline{W}$. The factor $[0, \varepsilon)$ is the gluing parameter.

Write U for a neighborhood of $v_{c'_3,c'_2,c'_1}$ inside the moduli space of triangles representing $\psi_{c'_3,c'_2,c'_1}$ which have n marked points which match $p_0 \in \mathbb{T}^2$ to order 1.

Let r_0 denote the value of r where the bubble forms. Note that we can view the evaluation map $\mathrm{ev}^{\mathrm{st}}$ on U as taking values in $\Delta^n/\mathbb{R}$, where $\mathbb{R}$ acts diagonally by the flow of $v_{3,1}$. We can pick a diffeomorphism of Δ with $\mathbb{C}$, such that the time t flow of $v_{3,1}$ coincides with the map $z \mapsto z + t$. Hence, we will view the evaluation map as taking values in $\mathbb{C}^n/\mathbb{R}$, and we assume the special line is the real axis. Similarly, $r \cdot \mathrm{ev}^{\mathrm{st}}$ can be thought of as having values in the same space, but taking values in $\mathbb{R}^n/\mathbb{R} \subseteq \mathbb{C}^n/\mathbb{R}$.

Define

$$\mathrm{ev}_{q_1,q_2} := \mathrm{Re}(\mathrm{ev}_{q_2}) - \mathrm{Re}(\mathrm{ev}_{q_1}),$$

and write $\overline{\mathrm{ev}}_{q_1,q_2}$ for the continuous extension to the compactification. Note that near $(\mathcal{U}', v_0)$, $\overline{\mathrm{ev}}_{q_1,q_2}$ is either nonnegative or nonpositive (depending on the ordering of the marked points along the special line), and the only zero is $(\mathcal{U}', v_0)$. For concreteness, assume $\overline{\mathrm{ev}}_{q_1,q_2} \geq 0$. We will show that the map $\overline{\mathrm{ev}}_{q_1,q_2}$ is locally degree 1 near $(\mathcal{U}', v_0)$, which will prove the main claim.

Consider the diagram

$$\begin{array}{ccccc} \mathbb{R} \times U & & & & \mathbb{R} \times \overline{W} \xleftarrow[\mathrm{id} \times \gamma]{\sim} \mathbb{R} \times W_0 \times \widetilde{\mathcal{N}}_2 \times [0, \varepsilon) \\ & \searrow^{\mathrm{ev}_1} & & \swarrow_{\mathrm{ev}_2} & \\ & & \mathbb{R} \times \mathbb{C}^n/\mathbb{R} & & \end{array} \tag{19.42}$$

where

$$\mathrm{ev}_1(r, u) = (r, r \cdot \mathrm{ev}^{\mathrm{st}}(u)) \quad \text{and} \quad \mathrm{ev}_2(r, v) = (r, \overline{\mathrm{ev}}(v)).$$

Near $(\mathcal{U}', v_0)$, the moduli space $\mathcal{MM}^{r \cdot \mathrm{ev}^{\mathrm{st/un}}, r \in [1,\infty)}(\Phi)$ is the fibered product of ev_1 and ev_2. We define $\mathcal{I}_U^{\geq 0}$ (resp. $\mathcal{I}_U^{>0}$ or $\mathcal{I}_U^0$) to be subset of $\mathbb{R} \times U$ where $\mathrm{ev}_{q_1,q_2} \geq 0$ (resp. $\mathrm{ev}_{q_1,q_2} > 0$ or $\mathrm{ev}_{q_1,q_2} = 0$). For generically chosen almost complex structures, the following two statements follow from an adaptation of Proposition 7.3:

- The maps ev_1 and ev_2 are transverse, when restricted to $\mathcal{I}_U^{>0}$ and $\mathbb{R} \times W$, respectively.
- The maps ev_1 and ev_2 are transverse, when restricted to $\mathcal{I}_U^0$ and $\mathbb{R} \times W_0$ are transverse, and have $\mathcal{U}'$ as an intersection of their images.

This is a free offprint provided to the author by the publisher. Copyright restrictions may apply.

Finally, we note that $\mathcal{MM}^{r\cdot \mathrm{ev}^{\mathrm{st/un}}\, r\in[1,\infty)}(\Phi)$ is identified with the intersection of the images of $\mathcal{I}_U^{\geqslant 0}$ and $\mathbb{R}\times\overline{W}$. Lemma 19.5 can be used to show that the map $\overline{\mathrm{ev}}_{q_1,q_2}$ is locally proper and odd degree near 0 on $\mathcal{MM}^{r\cdot \mathrm{ev}^{\mathrm{st/un}}\, r\in[1,\infty)}(\Phi)$, completing the proof. □

It remains to count the ends which appear as $r\to\infty$.

LEMMA 19.23. *The ends appearing as $r\to\infty$ consist exactly of 4-tuples of curves*

$$(v_{c_3',c_2',c_1'}, v_{c_1,c_3',c_1'}, v_{\beta,\beta',\beta''}, v_{\alpha,\beta,\beta''}),$$

as follows.

(1) *The curves $v_{c_3',c_2',c_1'}$, $v_{c_1,c_3',c_1'}$, $v_{\beta,\beta',\beta''}$ all have Maslov index 0, and have no marked point constraints.*
(2) *If $k = n_{p_0}(v_{c_3',c_2',c_1'}) > 0$, then $v_{\alpha,\beta,\beta''}$ has Maslov index $2k-1$. Furthermore, $v_{\alpha,\beta,\beta''}$ has exactly one coupled marked point (and any number of decoupled marked points). This marked point projects to the special line, and matches p to order $k-1$. If $k=0$, then $v_{\alpha,\beta,\beta''}$ has Maslov index 0 and no constraint.*

Furthermore,

(*g*-1) *The total count of such broken curves, weighted by their appropriate powers of U and T, is 0.*
(*g*-2) *Each of the above broken curves has a neighborhood in the compactification of $r\cdot \mathrm{ev}^{\mathrm{st/un}}$-matched curves which admits a map to $[0,1)$ which is degree 1 near 0.*

PROOF. Similar to Lemma 19.20, we first give a general description, and then specialize to the quadruple $\mathcal{Q}_3$. The argument therein adapts without substantial complication to show that the limiting curves as $r\to\infty$ consist of the following configurations:

- An index 0 triangle on $(\Sigma, \boldsymbol{\beta}, \boldsymbol{\beta}', \boldsymbol{\beta}'')$, with only decoupled marked points.
- An index 0 triangle on $(\mathbb{T}^2, c_1, c_3', c_1')$, with only decoupled marked points.
- An index 0 triangle on $(\mathbb{T}^2, c_3', c_2', c_1')$, with only coupled marked points.
- A collection of Maslov index 1 disks in the (c_1', c_3') and (c_3', c_2')-(c_2', c_1')-cylindrical ends of $(\mathbb{T}^2, c_3', c_2', c_1')$. (An index 1 disk in the (c_3', c_2')-(c_2', c_1') consists of an index 1 disk in either of the (c_3', c_2') or (c_2', c_1') ends, and a constant disk in the other). All marked points here are coupled. Suppose there are $n\geq 1$ levels here, and write $k_1,\dots,k_n$ for the number of marked points in each level.
- A broken holomorphic triangle on $(\Sigma, \boldsymbol{\alpha}, \boldsymbol{\beta}, \boldsymbol{\beta}'')$ of Maslov index $2(k_1+\cdots+k_n)-1$, with n interior punctures, which each project to the special line. Furthermore, the i^{th} puncture matches the point $p\in\Sigma$ to order k_i. Additionally, there is one ghost component for each $i\in\{1,\dots,n\}$ such that $k_i>1$. This ghost component consists of a sphere with one puncture, and k_i marked points.

See Figure 19.15 for a schematic. We note that in the limit, we can rescale any ghost bubble to obtain a map of a once punctured sphere into $\mathbb{C}\times\mathbb{C}$, as we did in Lemma 19.20. For the component corresponding to $i\in\{1,\dots,n\}$, the k_i marked points of this rescaled curve are mapped to $\{0\}\times\mathbb{R}\subseteq\mathbb{C}\times\mathbb{C}$. If we identify the source with $\mathbb{C}$, we may identify the marked points with numbers $\alpha_1,\dots,\alpha_{k_i}\in\mathbb{R}$.

This is a free offprint provided to the author by the publisher. Copyright restrictions may apply.

Furthermore $[(\alpha_1, \dots, \alpha_{k_i})] \in \mathbb{R}^{k_i}/\mathbb{R}$ coincides up to an overall scalar factor with the asymptotic evaluation map, applied to the corresponding holomorphic triangle on $(\mathbb{T}, c_3', c_2', c_1')$ or holomorphic disk mapping into one of its cylindrical ends. Gluing gives an identification of a neighborhood of such a configuration with $(0, 1]$.

In the present case, that Maslov index formula from (19.41) implies immediately that $n = 1$, since there are no holomorphic disks in the ends of $(\mathbb{T}^2, c_3', c_2', c_1')$ which have Maslov index 1.

Claim (g-1), the count of such broken curves, follows from Lemma 12.3, since the holomorphic triangles on $(\mathbb{T}^2, c_3', c_2', c_1')$ are unconstrained. Some care is required to verify that the weights of the curves cancel, since Lemma 12.3 holds with the algebra weights $U^{n_{p_0}}(\psi_0)T^{n_{z_0}(\psi_0)-n_{w_0}(\psi_0)}$, and for the curves in the limit, the punctures at p_0 do not contribute any U-weight or T-weight. Instead, a class ψ_0 is given T-weight $T^{n_{z_0}(\psi_0)}$ and no U-weight. We observe that the index 0 triangles on $(\mathbb{T}^2, c_3', c_2', c_1')$ may be indexed by $s \in 2\mathbb{Z} + 1$. The triangle u_s has

$$n_{w_0}(u_s) = \frac{m(s^2-1)}{8} \quad \text{and} \quad n_{z_0}(u_s) = \frac{m((s+2)^2-1)}{8}.$$

In particular,

$$n_{z_0}(u_s) \equiv n_{z_0}(u_{-s}) \pmod{m}.$$

In particular, the two triangles u_s and u_{-s} have the same multiplicity at w_0 and contribute the same U and T-weight. Hence, the curve quadruples appearing as $r \to \infty$ will cancel when counted with U and T weights.

We remark that it is in this model computatation that we use the choice of the involution described in Remark 6.3. Indeed if we had taken the connected sum at $z_0 \in \mathbb{T}^2$ instead of w_0, then the curves u_s and u_{-s-4} would have the same multiplicity at the puncture z_0, but these curves contribute different U-weights since the exponent of U is not taken with values modulo m.

We now consider claim (g-2). The proof is very similar to the proof of Lemma 19.22. We let $\mathcal{N}_n$ denote the moduli space of once punctured spheres with n marked points, which map to $\mathbb{C} \times \mathbb{C}$, have an order n puncture mapping to (∞, ∞), whose projection to the second factor is degree 1. We further assume that each marked point projects to 0 in the first factor. The group G of transformations of $\mathbb{C}$ given by $\{z \mapsto az + b : a > 0, b \in \mathbb{C}\}$ acts on $\mathcal{N}_n$, and we write $\widetilde{\mathcal{N}}_n$ for the quotient. We let q_1 and q_2 be two of the coupled marked points of the curve on $(\Sigma, \boldsymbol{\alpha}, \boldsymbol{\beta}, \boldsymbol{\beta}'')$, and let q_1' and q_2' be the corresponding marked points of the curve of $(\mathbb{T}^2, c_3', c_2', c_1')$. Write $(v'_{\alpha,\beta,\beta''}, v_0)$ for the limiting triangle and marked bubble on $(\Sigma, \boldsymbol{\alpha}, \boldsymbol{\beta}, \boldsymbol{\beta}'')$. Let W_0 denote a neighborhood of $v'_{\alpha,\beta,\beta''}$ in the moduli space of holomorphic curves representing $\psi_{\alpha,\beta,\beta''}$ which have an order n marked points which match $p \in \Sigma$ to order 1, but which do not necessarily map to the special line. Standard gluing results give a homeomorphism

$$\gamma \colon W_0 \times \widetilde{\mathcal{N}}_n \times [0, \varepsilon) \to \overline{W},$$

where $\overline{W}$ is a neighborhood of $(v'_{\alpha,\beta,\beta''}, v_0)$ in the compactification triangles on $(\Sigma, \boldsymbol{\alpha}, \boldsymbol{\beta}, \boldsymbol{\beta}'')$, with n marked points which each match p to order 1.

We let U denote a neighborhood of the limiting representative of $\psi_{c_3',c_2',c_1'}$. In the present case, U consists of a single point, since $\psi_{c_3',c_2',c_1'}$ has Maslov index 0. In particular, we may assume that $\mathrm{Re}(\mathrm{ev}_{q_1'} - \mathrm{ev}_{q_2'})$ is non-zero. Let V denote a

This is a free offprint provided to the author by the publisher. Copyright restrictions may apply.

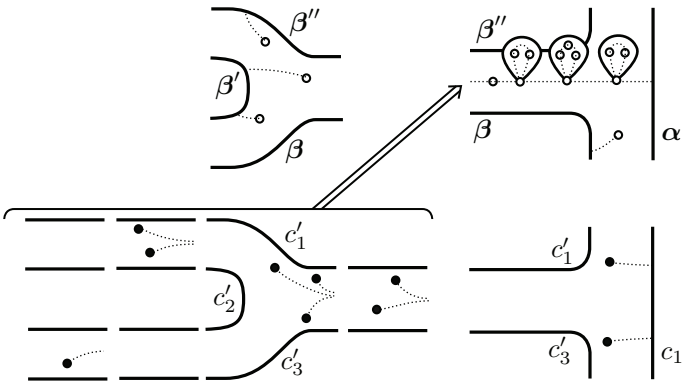


FIGURE 19.15. A curve appearing as $r \to \infty$. For $\mathcal{Q}_3$, the only generic configuration occurs when there are no disk levels.

neighborhood in $\widetilde{\mathcal{N}}_n$ of the bubble curve v_0. We assume that on V, any curve satisfies $\mathrm{Re}(\mathrm{ev}_{q_1} - \mathrm{ev}_{q_2}) \geq 0$. Let $\overline{W}_V$ denote the image under γ of $W_0 \times V \times [0, \varepsilon)$.

It is helpful to consider the parameter $r \in (0, \infty]$ as instead taking values in $[0, \infty)$, which we do by the change of variables $s = 1/r$. We consider the diagram

$$\begin{array}{ccccc} [0,\infty) \times U & & & & \mathbb{R} \times \overline{W}_V \xleftarrow[\mathrm{id} \times \gamma]{\sim} \mathbb{R} \times W_0 \times V \times [0,\varepsilon) \\ & \searrow^{\mathrm{ev}_1} & & \swarrow_{\mathrm{ev}_2} & \\ & & \mathbb{R} \times \mathbb{C}^n/G \times \mathbb{R} \times [0,\infty) & & \end{array} \tag{19.43}$$

In (19.43),

$$\mathrm{ev}_1(s, u) = (s, \mathrm{ev}^{\mathrm{st}}(u), 0, s \cdot \mathrm{Re}(\mathrm{ev}_{q_1}(u) - \mathrm{ev}_{q_2}(u))),$$

and

$$\mathrm{ev}_2(s, v) = (s, \overline{\mathrm{ev}}(v), \mathrm{im}(\mathrm{ev}_{q_1'}(v)), \mathrm{Re}(\mathrm{ev}_{q_1'}(v) - \mathrm{ev}_{q_2'}(v))).$$

The images of the codimension 1 facets $\{0\} \times U$ and $\mathbb{R} \times \partial\overline{W}_V$ have a transverse intersection point corresponding to $(v_{c_{3'}, c_2', c_1'}, v_{\alpha,\beta,\beta''}, v_0)$, so Lemma 19.5 implies that the map $\mathrm{Re}(\mathrm{ev}_{q_1'} - \mathrm{ev}_{q_2'})$ is locally proper and odd degree near 0 on the fibered product of the diagram in (19.43), which one may easily show coincides with $\mathcal{MM}^{r \cdot \mathrm{ev}^{\mathrm{st/un}}, r \in [1,\infty)}(\Phi)$ near the limiting curve. □

Lemma 19.19 now follows from Lemmas 19.20 and 19.23. As a consequence, Proposition 19.12 follows, and hence from Lemma 19.13 we obtain Proposition 19.1.

This is a free offprint provided to the author by the publisher. Copyright restrictions may apply.

This is a free offprint provided to the author by the publisher. Copyright restrictions may apply.

CHAPTER 20

The involutive mapping cone formula and surgery exact sequence

In this chapter, we prove Theorem 1.4 of the introduction. Let

$$\mathbb{A} = \prod_{s\in\mathbb{Z}} \boldsymbol{A}_s \quad \text{and} \quad \mathbb{B} := \prod_{s\in\mathbb{Z}} \boldsymbol{B}_s.$$

Ozsváth and Szabó describe a map $D_n\colon \mathbb{A} \to \mathbb{B}$ so that $\boldsymbol{CF}^-(Y_n)$ is quasi-isomorphic to $\mathbb{X}_n := \mathrm{Cone}(D_n\colon \mathbb{A} \to \mathbb{B})$.

It is also helpful to consider a smaller model of the mapping cone. If $b \in \mathbb{N}$, we define the *horizontal truncation* of $\mathbb{X}_n$, denoted $\mathbb{X}_n\langle b\rangle$, to be the submodule

$$\bigoplus_{-b\le s\le b} \boldsymbol{A}_s \oplus \bigoplus_{-b+n\le s\le b} \boldsymbol{B}_s. \tag{20.1}$$

We endow $\mathbb{X}_n\langle b\rangle$ with a differential D_n by viewing $\mathbb{X}_n\langle b\rangle$ as a quotient of $\mathbb{X}_n$ if $n > 0$, and viewing $\mathbb{X}_n\langle b\rangle$ as a subcomplex if $n < 0$. We write $\mathbb{A}_n\langle b\rangle$ and $\mathbb{B}_n\langle b\rangle$ for the two summands of $\mathbb{X}_n\langle b\rangle$.

If $n > 0$, then for large b, the quotient map

$$\Pi\colon \mathbb{X}_n \to \mathbb{X}_n\langle b\rangle$$

is a homotopy equivalence. For $n < 0$, the inclusion from $\mathbb{X}_n\langle b\rangle$ to $\mathbb{X}_n$ is a homotopy equivalence for negative n. See [**OS08b**, Lemma 4.3].

In this chapter, we prove the following:

THEOREM 20.1. *Suppose $n \in \mathbb{Z}\setminus\{0\}$, Y is an integer homology 3-sphere, and $K \subseteq Y$ is a knot. The involutive Heegaard Floer homology $\boldsymbol{CFI}^-(Y_n)$ is homotopy equivalent over the ring $\mathbb{F}[\![U]\!][Q]/Q^2$ to a complex $\mathbb{F}[Q]/(Q^2)\otimes_{\mathbb{F}}(\mathbb{A}\oplus\mathbb{B})$ with differential specified by some $\mathbb{F}[\![U]\!]$-linear maps as below:*

$$\mathbb{XI}_n = \begin{array}{ccccc} \mathbb{A} & & \xrightarrow{\quad D_n \quad} & & \mathbb{B} \\ \downarrow{\scriptstyle Q\cdot(\mathrm{id}+\iota_{\mathbb{A}})} & \searrow & & & \downarrow{\scriptstyle Q\cdot(\mathrm{id}+\iota_{\mathbb{B}})} \\ & & Q\cdot H & \searrow & \\ Q\cdot\mathbb{A} & & \xrightarrow{\quad D_n \quad} & & Q\cdot\mathbb{B}. \end{array}$$

In fact, the ι-complex $(\boldsymbol{CF}^-(Y_n),\iota)$ is ι-homotopy equivalent to the complex $\mathbb{X}_n := \mathrm{Cone}(D_n\colon \mathbb{A}\to\mathbb{B})$, with involution $\iota_{\mathbb{X}} := \iota_{\mathbb{A}} + H + \iota_{\mathbb{B}}$. Furthermore, the following hold:

(1) *$D_n = v + h$, where v sends $\boldsymbol{A}_s$ to $\boldsymbol{B}_s$, and h sends $\boldsymbol{A}_s$ to $\boldsymbol{B}_{s+n}$.*

This is a free offprint provided to the author by the publisher. Copyright restrictions may apply.

(2) $\iota_{\mathbb{A}}$ *sends* $\boldsymbol{A}_s$ *to* $\boldsymbol{A}_{-s}$. *Furthermore,* $\iota_{\mathbb{A}}$ *coincides with* $x \mapsto U^s \cdot \iota_K(x)$, *where* ι_K *is the knot involution.*
(3) $H = k + j$, *where* k *maps* $\boldsymbol{A}_s$ *to* $\boldsymbol{B}_{-s+n}$ *and* j *maps* $\boldsymbol{A}_s$ *to* $\boldsymbol{B}_{-s}$.

The analogous claims hold for the truncated complexes $\mathbb{XI}_n\langle b\rangle$, *provided* b *is sufficiently large.*

REMARK 20.2. It is an easy consequence of Theorem 20.1 that the uncompleted complex $CFI^-(Y_n(K))$ is ι-homotopy equivalent to the truncated complex $\mathbb{XI}_n\langle b\rangle$, taken with coefficients in $\mathbb{F}[U,Q]/Q^2$. This holds since every free, finitely generated, relatively $\mathbb{Z}$-graded chain complex C over $\mathbb{F}[\![U]\!]$ is chain isomorphic to $C' \otimes_{\mathbb{F}[U]} \mathbb{F}[\![U]\!]$, for some free, finitely generated, relatively $\mathbb{Z}$-graded chain complex C' over $\mathbb{F}[U]$. Furthermore, the chain complex C' is unique up to chain isomorphism. Indeed, if C and D are free, finitely generated, relatively $\mathbb{Z}$ graded chain complexes over $\mathbb{F}[\![U]\!]$, then C and D are homotopy equivalent over $\mathbb{F}[\![U]\!]$ if and only if the corresponding complexes C' and D' are homotopy equivalent over $\mathbb{F}[U]$.

The complex $\mathbb{XI}_n$ splits over conjugacy classes of Spin^c structures, as we now describe. Suppose $\varpi = \{\mathfrak{s}, \overline{\mathfrak{s}}\}$ is a conjugacy class of Spin^c structures on Y_n. Using the standard identification $\mathrm{Spin}^c(Y_n) \cong \mathbb{Z}_n$, we write $\varpi_i := \{\mathfrak{s}_i, \overline{\mathfrak{s}}_i\}$, which consists of either one or two elements. We define

$$\mathbb{A}_{\{i,-i\}} := \prod_{\substack{s\in\mathbb{Z}\\ s\equiv\pm i \mod n}} \boldsymbol{A}_s,$$

and we define $\mathbb{B}_{\{i,-i\}}$ similarly. The complex $\mathbb{XI}_n$ splits as

$$\mathbb{XI}_n = \bigoplus_{\{i,-i\}\in\mathbb{Z}_n/\mathrm{conj}} \mathbb{XI}_{n;\{i,-i\}},$$

where $\mathbb{XI}_{n;\{i,-i\}}$ has underlying group $\mathbb{F}[Q]/Q^2 \otimes (\mathbb{A}_{\{i,-i\}} \oplus \mathbb{B}_{\{i,-i\}})$. Furthermore,

$$\mathbb{XI}_{n;\{i,-i\}} \simeq \boldsymbol{CFI}^-(Y_n, \varpi_i).$$

20.1. Truncations

Following [**OS08b**] and [**MO10**], we define several truncation operations.

DEFINITION 20.3. Suppose (C,∂) is a finitely generated, free complex over $\mathbb{F}[U]$ or $\mathbb{F}[\![U]\!]$ and $\delta \in \mathbb{N}$. The *vertical trunction* of (C,∂) is the complex $C^\delta := C \otimes_{\mathbb{F}[U]} \mathbb{F}[U]/U^\delta$, with differential induced by ∂.

The following algebraic lemma is a variation of a standard result (see [**OS08b**, Section 4.1], [**MO10**, Section 10.2]):

LEMMA 20.4. *Suppose* $\mathcal{R}$ *is* $\mathbb{F}[U]$ *or* $\mathbb{F}[\![U]\!]$. *Suppose that* (C_1,∂_1) *and* (C_2,∂_2) *are two chain complexes over* $\mathcal{R}$ *or* $\mathcal{R}[Q]/Q^2$, *which are homotopy equivalent to finitely generated, free chain complexes over* $\mathcal{R}$ *or* $\mathcal{R}[Q]/Q^2$, *which are relatively* $\mathbb{Z}$*-graded. Then* (C_1,∂_1) *and* (C_2,∂_2) *are homotopy equivalent if and only if* $(C_1^\delta,\partial_1^{\delta_1})$ *and* $(C_2^\delta,\partial_2^{\delta_2})$ *are homotopy equivalent for all* δ.

We have also encountered the *horizontal truncation* operation in (20.1), denoted $\mathbb{X}_n\langle b\rangle$. We will use the following result:

LEMMA 20.5. *If* $\mathscr{C}$ *is an* ι_K*-complex, equipped with a choice of flip-map, then* $\mathbb{X}_n(\mathscr{C})\langle b\rangle$ *and* $\mathbb{X}_n(\mathscr{C})$ *are homotopy equivalent over the ring* $\mathbb{F}[\![U]\!]$, *for sufficiently large* b.

This is a free offprint provided to the author by the publisher. Copyright restrictions may apply.

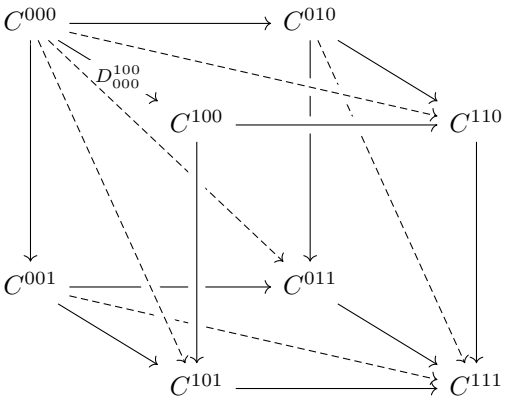
Ozsváth and Szabó prove that $\mathbb{X}_n(\mathscr{C})\langle b\rangle$ and $\mathbb{X}_n(\mathscr{C})$ are quasi-isomorphic, by exhibiting a quasi-isomorphism from $\mathbb{X}_n(\mathscr{C})$ to $\mathbb{X}_n(\mathscr{C})\langle b\rangle$ if $n > 0$ (projection), and a quasi-isomorphism from $\mathbb{X}_n(\mathscr{C})\langle b\rangle$ to $\mathbb{X}_n(\mathscr{C})$ if $n < 0$ (inclusion) [**OS08b**, Lemma 4.3]. For bounded, free complexes, being quasi-isomorphic is equivalent to being homotopy equivalent (cf. [**Wei94**, Lemma 10.4.6]). However, $\mathbb{X}_n(\mathscr{C})$ is not free (it is an infinite direct product), and the set of gradings of the generators is not bounded. Nonetheless, it is not too hard to construct homotopy inverses by hand, using the fact that v_s and (resp. h_s) admits a homotopy inverse if $s \gg 0$ (resp. $s \ll 0$). In slightly more detail, if $n > 0$, one first constructs a map from $\mathbb{X}_n(\mathscr{C})\langle b\rangle$ to $\mathbb{X}_n(\mathscr{C})\langle b+1\rangle$, which is a homotopy inverse to projection, and which is furthermore a genuine one-sided inverse to projection (such a map may be chosen to have a similar shape to Figure 3.4). By composing, we obtain a map $\mathbb{X}_n(\mathscr{C})\langle b\rangle \to \mathbb{X}_n(\mathscr{C})\langle b+k\rangle$, for any k. This construction naturally gives a limiting map, from $\mathbb{X}_n(\mathscr{C})\langle b\rangle$ to $\mathbb{X}_n(\mathscr{C})$, which is a homotopy inverse to projection. We leave the details to the reader.

20.2. Filling hypercubes

A key lemma for passing from the involutive hypercube to the involutive mapping cone formula is the following algebraic lemma:

LEMMA 20.6. *Suppose that we have a diagram of chain complexes*

(20.2)



consisting of the maps shown and the internal differentials of the complexes, with maps denoted as in Definition 5.1. *Suppose that all faces, except for the front face, satisfy the 2-dimensional hypercube relation. Further, assume that*

$$D^{100}_{000}\colon C^{000} \to C^{100}$$

is a chain homotopy equivalence. Then there exist maps

$$D^{011}_{100} : C^{100} \to C^{111}$$
$$D^{111}_{000} : C^{000} \to C^{111}$$

which make (C, D) into a three dimensional hypercube. In particular, if G_{back}, G_{bottom}, and G_{top} are the filtered maps

$$G_{\mathrm{back}}\colon \mathrm{Cone}\left(C^{000} \to C^{010}\right) \to \mathrm{Cone}\left(C^{001} \to C^{011}\right)$$
$$G_{\mathrm{bottom}}\colon \mathrm{Cone}\left(C^{001} \to C^{011}\right) \to \mathrm{Cone}\left(C^{101} \to C^{111}\right)$$
$$G_{\mathrm{top}}\colon \mathrm{Cone}\left(C^{000} \to C^{010}\right) \to \mathrm{Cone}\left(C^{100} \to C^{110}\right)$$

This is a free offprint provided to the author by the publisher. Copyright restrictions may apply.

and G_{front} *is the induced filtered map*

$$G_{\text{front}}\colon \operatorname{Cone}\left(C^{100} \to C^{110}\right) \to \operatorname{Cone}\left(C^{101} \to C^{111}\right),$$

then the compositions $G_{\text{front}} \circ G_{\text{top}}$ *and* $G_{\text{bottom}} \circ G_{\text{back}}$ *are chain homotopy equivalent.*

PROOF. Let $E : C^{100} \to C^{000}$ be a homotopy inverse to D^{100}_{000}. Choose homotopies

$$H\colon C^{000} \to C^{000}, \quad \text{and}$$
$$J\colon C^{100} \to C^{100}$$

such that $\partial H + H\partial = \mathrm{Id} + E \circ D^{100}_{000}$ and $\partial J + J\partial = \mathrm{Id} + D^{100}_{000} \circ E$. Observe that the sum $f = D^{100}_{000} \circ H + J \circ D^{100}_{000}$ is a chain map, since

$$\begin{aligned}
\partial f + f\partial &= \partial(D^{100}_{000} \circ H + J \circ D^{100}_{000}) + (D^{100}_{000} \circ H + J \circ D^{100}_{000})\partial \\
&= D^{100}_{000} \circ (\partial H + H\partial) + (\partial J + J\partial) \circ D^{100}_{000} \\
&= D^{100}_{000}(\mathrm{Id} + E \circ D^{100}_{000}) + (\mathrm{Id} + D^{100}_{000} \circ E) \circ D^{100}_{000} \\
&= 0
\end{aligned}$$

Let K denote the sum of all of the length two compositions of maps from C^{000} to C^{111} appearing in the diagram (20.2), so that

$$K = D^{100}_{011} \circ D^{011}_{000} + D^{101}_{010} \circ D^{010}_{000} + D^{110}_{001} \circ D^{001}_{000} + D^{010}_{101} \circ D^{101}_{000} + D^{001}_{110} \circ D^{110}_{000}.$$

Observe that

$$\partial K + K\partial = \left(D^{010}_{101} \circ D^{001}_{100} + D^{001}_{110} \circ D^{010}_{100}\right) \circ D^{100}_{000}$$

Using this notation, we claim that the following maps complete the hypercube

$$\begin{aligned}
D^{011}_{100} &= K \circ E + \left(D^{010}_{101} \circ D^{001}_{100} + D^{001}_{110} \circ D^{010}_{100}\right) \circ J. \\
D^{111}_{000} &= K \circ H + D^{011}_{100} \circ f
\end{aligned}$$

There are two relations to check: the 2-dimensional hypercube relation on the front face and the 3-dimensional hypercube relation for the entire cube. We see that

$$\begin{aligned}
\partial D^{011}_{100} + D^{011}_{100}\partial &= (\partial K + K\partial) \circ E + \left(D^{010}_{101} \circ D^{001}_{100} + D^{001}_{110} \circ D^{010}_{100}\right) \circ (\partial J + J\partial) \\
&= \left(D^{010}_{101} \circ D^{001}_{100} + D^{001}_{110} \circ D^{010}_{100}\right) \circ D^{100}_{000} \circ E \\
&\quad + \left(D^{010}_{101} \circ D^{001}_{100} + D^{001}_{110} \circ D^{010}_{100}\right) \circ (\mathrm{Id} + D^{100}_{000} \circ E) \\
&= D^{010}_{101} \circ D^{001}_{100} + D^{001}_{110} \circ D^{010}_{100}
\end{aligned}$$

which confirms the length 2 hypercube relation on the front face. We also have that

$$\begin{aligned}
\partial D^{111}_{000} + D^{111}_{000}\partial &= (\partial K + K\partial) \circ H + K \circ (\partial H + H\partial) + \left(\partial D^{011}_{100} + D^{011}_{100}\partial\right) \circ f \\
&= \left(\left(D^{010}_{101} \circ D^{001}_{100} + D^{001}_{110} \circ D^{010}_{100}\right) \circ D^{100}_{000}\right) \circ H \\
&\quad + K \circ \left(\mathrm{Id} + E \circ D^{100}_{000}\right) + \left(D^{010}_{101} \circ D^{001}_{100} + D^{001}_{110} \circ D^{010}_{100}\right) \circ f \\
&= K + K \circ E \circ D^{100}_{000} + \left(D^{010}_{101} \circ D^{001}_{100} + D^{001}_{110} \circ D^{010}_{100}\right) \\
&\quad \circ (D^{100}_{000} \circ H + f) \\
&= K + K \circ E \circ D^{100}_{000} + \left(D^{010}_{101} \circ D^{001}_{100} + D^{001}_{110} \circ D^{010}_{100}\right) \circ (J \circ D^{100}_{000}) \\
&= K + D^{011}_{100} \circ D^{100}_{000}
\end{aligned}$$

This is a free offprint provided to the author by the publisher. Copyright restrictions may apply.

This is exactly the length 3 hypercube relation. □

REMARK 20.7. If the map D^{100}_{000} is a chain isomorphism, then the maps D^{011}_{100} and D^{111}_{000} have a particularly simple form. In this case, $D^{011}_{100} = K \circ (D^{100}_{000})^{-1}$ and $D^{111}_{000} \equiv 0$.

REMARK 20.8. Lemma 20.6 can also be viewed as a consequence of the fact that $\mathbb{F}[U]$-chain complexes form an infinity category in the sense of Lurie [**Lur09**]. The defining property of an infinity category $\mathcal{C}$ is that diagrams on "inner horns" Λ^n_i for $0 < i < n$ in $\mathcal{C}$ extend to diagrams on the standard simplex Δ^n. There is a precise sense in which cube (or other diagrammatic) extension problems are related to extension problems along simplices: this is the idea of anodyne extensions. From this perspective, the diagram in Lemma 20.6 is not analogous to an inner horn, but to a horn $\Lambda^3_0 \subseteq \Delta^3$. However, an early result in the theory [**Joy02**] shows that if the "first arrow" in a horn Λ^n_0 is an equivalence, then the horn extends. The proof of Lemma 20.6 can be viewed as writing down the map explicitly that Joyal constructs (inductively), slightly modified to treat cubes in place of simplices.

20.3. Gradings

In this section, we describe how the maps in the involutive surgery hypercube decompose with respect to Spin^c structures, and their associated gradings. Consider the vertical truncation of the main hypercube:

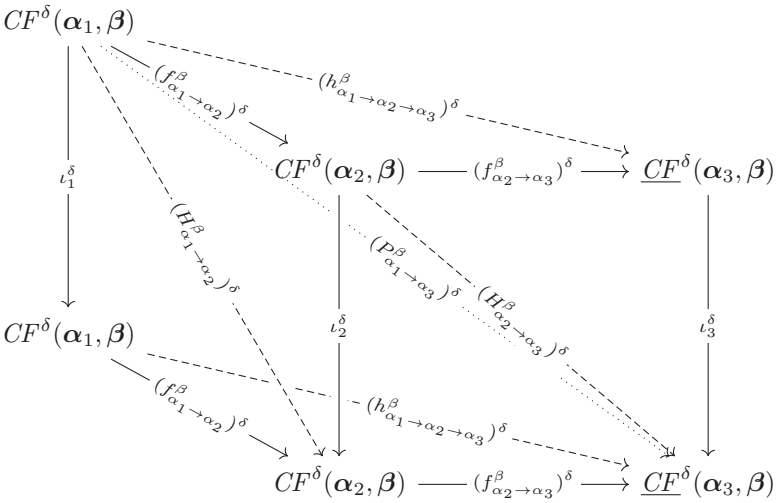


FIGURE 20.1. Vertically truncating the main hypercube.

We give the complexes in Figure 20.1 the absolute grading induced by $CF^-(Y)$, $CF^-(Y_n)$ and $CF^-(Y_{n+m})$. For $\underline{CF}^\delta(\boldsymbol{\alpha}_3, \boldsymbol{\beta})$, we give T grading 0. (Ozsváth and Szabó refer to these as the *old* gradings in [**OS08b**]).

We write

$$\begin{aligned} W_n &\colon Y \to Y_n(K), \\ W_{n,m+n} &\colon Y_n(K) \# L(m,1) \to Y_{n+m}(K), \quad \text{and} \\ W_{n+m} &\colon Y \to Y_{n+m}(K) \end{aligned}$$

This is a free offprint provided to the author by the publisher. Copyright restrictions may apply.

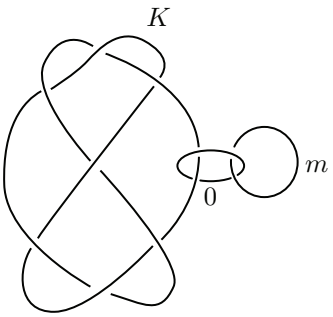


FIGURE 20.2. The cobordism $W_m\colon Y_n(K)\#L(m,1)\to Y_{n+m}(K)$ is obtained by attaching a 2-handle along the 0-framed unknot.

for the standard 2-handle cobordisms. We write $W_n'\colon Y_n(K)\to Y$ (and so forth) for the cobordism obtained by turning around and reversing the orientation of W_n. We note that $W_{n,m+n}$ is obtained by attaching a 0-framed 2-handle to $Y_n(K)\#L(m,1)$, which clasps K and an m-framed unknot corresponding to the $L(m,1)$-summand. See Figure 20.2.

A straightforward computation (see, e.g. [**MO10**, Lemma 11.1]) shows that $H_2(W_{n,m+n};\mathbb{Z})$ is free, of rank 1, and is generated by a surface Σ with

$$\Sigma^2=-\frac{mn(m+n)}{\gcd(m,n)^2}. \tag{20.3}$$

Note that W_n coincides with $X_{\alpha_3,\alpha_1,\beta}$, after filling in Y_{α_3,α_1} with 3-handles and a 4-handle. Similarly, $W_{n,n+m}$ is obtained from $X_{\alpha_2,\alpha_1,\beta}$ by filling in the $S^1\times S^2$ summands of Y_{α_2,α_1}, and removing a neighborhood of an arc connecting $Y_{\alpha_1,\beta}$ and Y_{α_2,α_1}. Finally, the 4-manifold $X_{\alpha_3,\alpha_2,\alpha_1,\beta}$ may be identified with $W_n'\#D(-m,1)$, after filling in $S^1\times S^2$ summands.

The maps in the main hypercube are not homogeneously graded, but instead decompose as sums of homogeneously graded maps, indexed by Spin^c structures. The following lemma describes how the maps in the main hypercube decompose into homogeneously graded maps:

LEMMA 20.9.

(1) *The maps $f^\beta_{\alpha_1\to\alpha_2}$ and $H^\beta_{\alpha_1\to\alpha_2}$ decompose as*

$$f^\beta_{\alpha_1\to\alpha_2}=\sum_{\substack{\mathfrak{s}\in\mathrm{Spin}^c(W_{n,m+n})\\ \mathfrak{s}|_{L(m,1)}=\mathfrak{s}_0}} f^\beta_{\alpha_1\to\alpha_2;\mathfrak{s}} \quad\text{and}\quad H^\beta_{\alpha_1\to\alpha_2}=\sum_{\substack{\mathfrak{s}\in\mathrm{Spin}^c(W_{n,m+n})\\ \mathfrak{s}|_{L(m,1)}=\mathfrak{s}_0}} H^\beta_{\alpha_1\to\alpha_2;\mathfrak{s}}.$$

Furthermore, $f^\beta_{\alpha_1\to\alpha_2;\mathfrak{s}}$ and $H^\beta_{\alpha_1\to\alpha_2;\mathfrak{s}}$ are of homogeneous degrees

$$\frac{c_1^2(\mathfrak{s})+m}{4} \quad\text{and}\quad \frac{c_1^2(\mathfrak{s})+m}{4}+1,$$

respectively.

(2) *The maps $f^\beta_{\alpha_2\to\alpha_3}$ and $H^\beta_{\alpha_2\to\alpha_3}$ decompose as*

$$f^\beta_{\alpha_2\to\alpha_3}=\sum_{\mathfrak{s}\in\mathrm{Spin}^c(W'_{n+m})} f^\beta_{\alpha_2\to\alpha_3;\mathfrak{s}} \quad\text{and}\quad H^\beta_{\alpha_2\to\alpha_3}=\sum_{\mathfrak{s}\in\mathrm{Spin}^c(W'_{n+m})} H^\beta_{\alpha_2\to\alpha_3;\mathfrak{s}}.$$

This is a free offprint provided to the author by the publisher. Copyright restrictions may apply.

Furthermore, $f^{\beta}_{\alpha_2\to\alpha_3;\mathfrak{s}}$ and $H^{\beta}_{\alpha_2\to\alpha_3;\mathfrak{s}}$ have homogeneous degree

$$\frac{c_1^2(\mathfrak{s})+1}{4} \quad \text{and} \quad \frac{c_1^2(\mathfrak{s})+1}{4}+1,$$

respectively.

(3) *The maps $h^{\beta}_{\alpha_1\to\alpha_2\to\alpha_3}$ and $P^{\beta}_{\alpha_1\to\alpha_3}$ decompose as*

$$h^{\beta}_{\alpha_1\to\alpha_2\to\alpha_3} = \sum_{\substack{\mathfrak{s}\in\mathrm{Spin}^c(W_n'\#D(-m,1))\\ \mathfrak{s}|_{L(m,1)}=\mathfrak{s}_0}} h^{\beta}_{\alpha_1\to\alpha_2\to\alpha_3;\mathfrak{s}} \quad \text{and}$$

$$P^{\beta}_{\alpha_1\to\alpha_2} = \sum_{\substack{\mathfrak{s}\in\mathrm{Spin}^c(W_n'\#D(-m,1))\\ \mathfrak{s}|_{L(m,1)}=\mathfrak{s}_0}} P^{\beta}_{\alpha_1\to\alpha_3;\mathfrak{s}}.$$

Furthermore, $h^{\beta}_{\alpha_1\to\alpha_2\to\alpha_3;\mathfrak{s}}$ and $P^{\beta}_{\alpha_1\to\alpha_3;\mathfrak{s}}$ are of homogeneous degree

$$\frac{c_1^2(\mathfrak{s}|_{W_{n,n+m}})+c_1^2(\mathfrak{s}|_{W'_{n+m}})+m+1}{4}+1$$

$$\text{and} \quad \frac{c_1^2(\mathfrak{s}|_{W_{n,n+m}})+c_1^2(\mathfrak{s}|_{W'_{n+m}})+m+1}{4}+2,$$

respectively.

PROOF. For the maps along the top and bottom of the hypercube, the claim is immediate. The proof is slightly more subtle for the maps $H^{\beta}_{\alpha_1\to\alpha_2}$, $H^{\beta}_{\alpha_2\to\alpha_3}$ and $P^{\beta}_{\alpha_1\to\alpha_3}$, as they are not defined via a single count of holomorphic polygons. These maps are defined via the compression operation for hyperboxes, and hence involve many different maps.

We focus our attention first on the map $H^{\beta}_{\alpha_2\to\alpha_3}$. This map is the diagonal map in the compression of a hyperbox of size $(1,d)$ for some large $d\geq 0$. The compression operation for such hyperboxes is illustrated in Figure 5.1. Each of the vertical maps represents either a change of diagram map, the cobordism map for a collection of 1-handles which are canceled in a later step by a collection of 2-handles, or the cobordism map for surgery on 0-framed unlink which is canceled by a collection of 3-handles in a later step. Each summand of $H^{\beta}_{\alpha_1\to\alpha_2}$ contains exactly one length 2 map from a constituent hypercube. Each of these length 2 maps counts holomorphic triangles or rectangles on a triple or quadruple which topologically represents the 2-handle cobordism $W'_{n+m}\colon Y_{m+n}\to Y$, or a small modification of this cobordism. For example, the corresponding length 2 map in $\mathcal{C}^{(3)}_{\mathrm{cen}}$ counts holomorphic triangles and rectangles on diagrams which represent a cobordism from $L(m,1)\#Y_{m+n}$ to $S^1\times S^2\#Y$, obtained by surgery on the dual of K in Y_{m+n}, as well as a knot in $L(m,1)$. By direct inspection, the maps decompose over Spin^c structures on W'_{m+n} into a sum of maps which have the stated grading. The claim for $H^{\beta}_{\alpha_1\to\alpha_2}$ is not substantially different.

The argument for the length 3 map $P^{\beta}_{\alpha_1\to\alpha_3}$, is similar, but is slightly more involved. The compression operation for hyperboxes of size $(1,1,d)$ is illustrated in Figure 5.2. The summands of $P^{\beta}_{\alpha_1\to\alpha_3}$ each consist either of a composition of numerous length 1 maps and exactly two length 2 maps, or numerous length 1 maps and exactly one length 3 map. For the summands of $P^{\beta}_{\alpha_1\to\alpha_3}$ which contain two length 2 maps, the argument is not substantially different than the above argument for the length 2 maps $H^{\beta}_{\alpha_1\to\alpha_2}$ and $H^{\beta}_{\alpha_2\to\alpha_3}$. For the summands containing a length

This is a free offprint provided to the author by the publisher. Copyright restrictions may apply.

3 map, the situation is similar, but in principle there are more checks to be done, as we now describe. Most of the length 3 maps which contribute to $P^{\beta}_{\alpha_1\to\alpha_3}$ count pentagons on a Heegaard pentuple which represents surgery on the dual knot in Y_n, as well as a $-m$-framed unknot which is unlinked from K (the associated 2-handle cobordism is $W_n'\#D(-m,1)$). There are also additional triangle and quadrilateral counts which arise from the higher compositions in a pairing of hypercubes of Lagrangians. For example, in the construction of $\mathcal{C}^{(3)}_{\mathrm{cen}}$ in Section 16.5, the length 3 map has summands which count rectangles with one input labeled λ and one input labeled Θ, and also a summand corresponding to counting triangles with the special input ω_{δ,δ_3}. There is a small subtlety in that the triangle map with special input ω_{δ,δ_3} counts triangles on a triple representing the cobordism W_n'. However we constructed the chain ω_{δ,δ_3} to decompose over Spin^c structures on $D(-m,1)$ (see (16.23)), and hence the corresponding triangle map decomposes over $\mathrm{Spin}^c(W_n'\#D(-m,1))$, as claimed. Finally, as described in Section 16.6, the length 3 map of $\mathcal{C}_{\mathrm{cen}}$ has an additional contribution of $H_E f^{\delta\to\delta'}_{\gamma}$. The map $f^{\delta\to\delta'}_{\gamma}$ is the 2-handle map from Y_n to Y, while H_E counts more complicated holomorphic curves on quadruples which themselves represent $([0,1]\times Y)\#D(-m,1)$ (followed by a cobordism for 0-surgery on an unknot). Hence, it is straightforward to verify that H_E decomposes over $\mathrm{Spin}^c(D(-m,1))$ into summands of the expected grading. □

Ozsváth and Szabó additionally proved several strong restrictions on some of the vertically truncated maps appearing in Figure 20.1, when m is sufficiently large. To state their results, and how they adapt to our present situation, we first recall some background and notation. There is a standard identification $\mathrm{Spin}^c(Y_{m+n}(K))\cong\mathbb{Z}/(m+n)$, as follows. Let F be a Seifert surface in Y for K, and let $\hat{F}\subseteq W'_{m+n}(K)$ be the surface which is capped off by the core of the 2-handle. If $i\in\mathbb{Z}/(m+n)$, we define $\mathfrak{s}_i\in\mathrm{Spin}^c(Y_{m+n}(K))$ to be the Spin^c structure which admits an extension $\mathfrak{t}_i$ over $W'_{m+n}(K)$ satisfying

$$\langle c_1(\mathfrak{t}_i),[\hat{F}]\rangle\equiv n+m+2i \mod 2(n+m).$$

We write $\mathfrak{x}_s$ and $\mathfrak{y}_s$ for the two Spin^c structures on $W'_{n+m}(K)$ which satisfy

$$\langle c_1(\mathfrak{x}_s),[\hat{F}]\rangle=2s-m-n \quad\text{and}\quad \langle c_1(\mathfrak{y}_s),[\hat{F}]\rangle=2s+m+n, \tag{20.4}$$

respectively. If $-(m+n)/2\le s<(m+n)/2$, then $\mathfrak{x}_s$ and $\mathfrak{y}_s$ are the Spin^c structures with maximal and second to maximal c_1^2. (See [**OS08b**, Lemma 4.4]).

PROPOSITION 20.10. *Suppose δ is fixed.*

(1) *If m is sufficiently large, then for each $\mathfrak{t}\in\mathrm{Spin}^c(Y_{n+m})$, there is at most one Spin^c structure $\mathfrak{s}$ on $W_{n,m+n}$ which restricts to $\mathfrak{t}$ on Y_{n+m}, for which the map $(f^{\beta}_{\alpha_1\to\alpha_2;\mathfrak{s}})^{\delta}$ is non-trivial. This is also the only Spin^c structure for which $(H^{\beta}_{\alpha_1\to\alpha_2;\mathfrak{s}})^{\delta}$ may be non-trivial.*

(2) *There is an integer $b>0$ with the following property. If m is sufficiently large, and $-(m+n)/2\le s<(m+n)/2$, then the maps $(f_{\alpha_2\to\alpha_3;\mathfrak{s}})^{\delta}$ are non-vanishing on $\boldsymbol{CF}^-(\boldsymbol{\alpha}_2,\boldsymbol{\beta},[s])$ only if $\mathfrak{s}=\mathfrak{x}_s$ or $\mathfrak{s}=\mathfrak{y}_s$. Furthermore, if $s>b$, then $(f^{\beta}_{\alpha_2\to\alpha_3;\mathfrak{s}})^{\delta}$ is non-vanishing only if $\mathfrak{s}=\mathfrak{x}_s$. If $s<-b$, then $(f^{\beta}_{\alpha_2\to\alpha_3;\mathfrak{s}})^{\delta}$ is non-vanishing only if $\mathfrak{s}=\mathfrak{y}_s$. The same statements hold for the maps $(H^{\beta}_{\alpha_2\to\alpha_3;\mathfrak{s}})^{\delta}$.*

This is a free offprint provided to the author by the publisher. Copyright restrictions may apply.

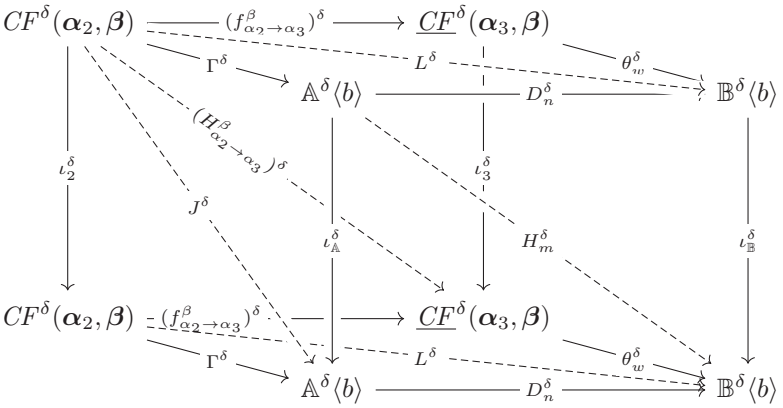


FIGURE 20.3. A hypercube which relates the 3-manifold complexes with the knot Floer complexes. There is a length 3 map, which is not shown.

(3) *If m is sufficiently large, then $(h^\beta_{\alpha_1\to\alpha_2\to\alpha_3;\mathfrak{s}})^\delta$ is non-vanishing only if $\mathfrak{s}|_{W_{n,n+m}}$ and $\mathfrak{s}|_{W'_{n+m}}$ are contained on the list of* Spin^c *structures described in parts* (1) *and* (2)*. The same holds for the maps $(P^\beta_{\alpha_1\to\alpha_3;\mathfrak{s}})^\delta$.*

Proposition 20.10 is proven by Ozsváth and Szabó for the maps $(f^\beta_{\alpha_1\to\alpha_2;\mathfrak{s}})^\delta$, $(f^\beta_{\alpha_2\to\alpha_3;\mathfrak{s}})^\delta$, and $(h^\beta_{\alpha_1\to\alpha_2\to\alpha_3;\mathfrak{s}})^\delta$ when $n>0$. See specifically [**OS08b**, Lemma 4.4, Proposition 4.6, and Lemma 4.8]. Note that Ozsváth and Szabó focus on the case that $m=nk$, for $k\in\mathbb{N}$, which simplifies equation (20.3), though their proof extends to the more general case. They argued by showing that for sufficiently large m, the maps $(f^\beta_{\alpha_1\to\alpha_2;\mathfrak{s}})^\delta$, $(f^\beta_{\alpha_2\to\alpha_3;\mathfrak{s}})^\delta$ and $(h^\beta_{\alpha_1\to\alpha_2\to\alpha_3;\mathfrak{s}})^\delta$ land outside of the range of gradings supported by the vertically truncated complexes appearing in Figure 20.1, except for the Spin^c structures described in the statement of Proposition 20.10. Using the grading change formulas described in Lemma 20.9, it is easy to check that Ozsváth and Szabó's argument implies the same statement for the maps $H^\beta_{\alpha_1\to\alpha_2;\mathfrak{s}}$, $H^\beta_{\alpha_2\to\alpha_3;\mathfrak{s}}$ and $P^\beta_{\alpha_1\to\alpha_3;\mathfrak{s}}$.

For negative n, Ozsváth and Szabó's proof does not immediately apply (the main challenge being part (3); note that for negative surgeries they instead built a map from Cone(D_n) to $\boldsymbol{CF}^-(Y_n)$ whose grading properties are easier to analyze). We delay our proof for negative n until later, where we cover it in greater generality in Chapter 22. See specifically Lemmas 22.1, 22.2, 22.3 and 22.4.

20.4. Proof of Theorem 20.1

In this section, we prove the mapping cone formula, as stated in Theorem 20.1.

PROOF OF THEOREM 20.1. Proposition 20.10 implies that if $\delta>0$ is fixed, and m is sufficiently large, then the maps $(f^\beta_{\alpha_2\to\alpha_3;\mathfrak{s}})^\delta$ and $(H^\beta_{\alpha_2\to\alpha_3;\mathfrak{s}})^\delta$ will be non-zero only if $\mathfrak{s}$ is one of $\mathfrak{x}_s$ or $\mathfrak{y}_s$ for some $-(m+n)/2<s\le(m+n)/2$. We consider the hypercube in Figure 20.3, which relates the 3-manifold complexes to the knot Floer complexes.

We now explain the terms appearing in Figure 20.3. The truncation $\mathbb{A}\langle b\rangle$ is the direct sum of the complexes A_s, ranging over $-b\le s\le b$. Similarly $\mathbb{B}\langle b\rangle$ is the

This is a free offprint provided to the author by the publisher. Copyright restrictions may apply.

direct sum of complexes B_s ranging over $-b+n \le s \le b$. We are assuming here that

$$0 < b < (m+n)/2. \tag{20.5}$$

The map Γ is the direct sum of the maps

$$\Gamma_s \colon CF^-(\boldsymbol{\alpha}_2, \boldsymbol{\beta}, [s]) \to A_s,$$

described by Ozsváth and Szabó [**OS04a**, Theorem 4.4] [**OS08b**, Theorem 2.3], ranging over $-b \le s \le b$. The map Γ_s counts holomorphic triangles on $(\Sigma, \boldsymbol{\alpha}_3, \boldsymbol{\alpha}_2, \boldsymbol{\beta}, w, z)$ which satisfy $\mathfrak{s}_w(\psi) = \mathfrak{x}_s$.

Note that if $m+n$ is even and positive, then $Y_{n+m}(K)$ has two self-conjugate Spin^c structures, corresponding to $s = 0$ and $s = (m+n)/2$. The condition in (20.5) ensures that the one corresponding to $s = (m+n)/2$ is sent to zero by Γ^δ. Similarly, in the map θ_w^δ, we are implicitly projecting $\underline{CF}^\delta(\boldsymbol{\alpha}_3, \boldsymbol{\beta}, [s])$ to zero unless $-b+n \le s \le b$.

We recall from [**HM17**, Section 6.6] that there is a map J_0 making the following diagram a hypercube:

$$\begin{array}{ccc} CF^-(\boldsymbol{\alpha}_2, \boldsymbol{\beta}, [0]) & \xrightarrow{\Gamma_0} & A_0 \\ \downarrow{\scriptstyle \iota_2} & \swarrow{\scriptstyle J_0} & \downarrow{\scriptstyle \iota_{\mathbb{A},0}} \\ CF^-(\boldsymbol{\alpha}_2, \boldsymbol{\beta}, [0]) & \xrightarrow{\Gamma_0} & A_0, \end{array} \tag{20.6}$$

where $\iota_{\mathbb{A},0}$ is the map induced by the knot involution ι_K. Applying the same argument, but to other Spin^c structures, gives a map J_s which makes the following diagram a hypercube of chain complexes:

$$\begin{array}{ccc} CF^-(\boldsymbol{\alpha}_2, \boldsymbol{\beta}, [s]) & \xrightarrow{\Gamma_s} & A_s \\ \downarrow{\scriptstyle \iota_2} & \swarrow{\scriptstyle J_s} & \downarrow{\scriptstyle \iota_{\mathbb{A},s}} \\ CF^-(\boldsymbol{\alpha}_2, \boldsymbol{\beta}, [-s]) & \xrightarrow{\Gamma_{-s}} & A_{-s}, \end{array} \tag{20.7}$$

where $\iota_{\mathbb{A},s} \colon A_s \to A_{-s}$ denotes the map

$$x \mapsto U^s \cdot \iota_K(x).$$

We define J to be the direct sum of the maps J_s, and define the map J^δ appearing along the left side of Figure 20.3 to be the truncation, summed only over s satisfying $-b \le s \le b$.

In Figure 20.3, we define D_n, L and H as follows. Let I_s be a homotopy inverse of Γ_s. We defined D_n on A_s via the formula

$$D_{n,s} := \theta_w \circ (f^\beta_{\alpha_2 \to \alpha_3; \mathfrak{x}_s} + f^\beta_{\alpha_2 \to \alpha_3; \mathfrak{y}_s}) \circ I_s. \tag{20.8}$$

To construct L, we pick a homogeneous null-homotopy h of $\mathrm{id} + I \circ \Gamma$, and set

$$L = \theta_w \circ f^\beta_{\alpha_2 \to \alpha_3} \circ h.$$

Along the right face, we define $\iota_{\mathbb{B}}$ to be $\theta_w \circ \iota_3 \circ \theta_w^{-1}$, so that the right face commutes as well.

This is a free offprint provided to the author by the publisher. Copyright restrictions may apply.

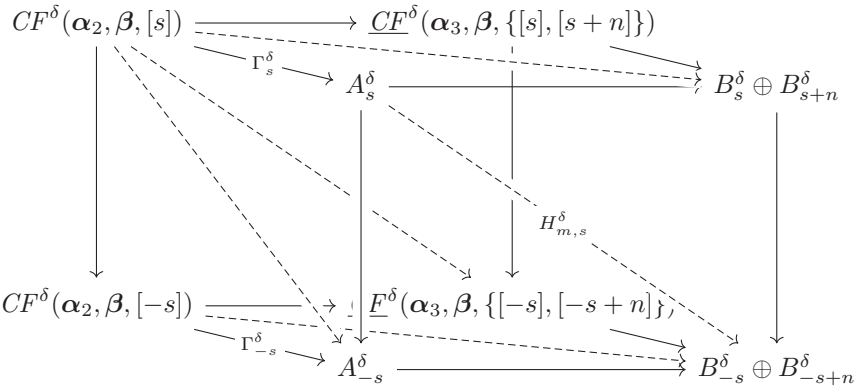


FIGURE 20.4. A subdiagram of Figure 20.3.

We define the map

$$H_m \colon \mathbb{A}_n\langle m\rangle \to \mathbb{B}_n\langle m\rangle$$

appearing along the front face of Figure 20.3 to be similar to the one constructed in Lemma 20.6. The only caveat here is that the map labeled Γ^δ is not in general a homotopy equivalence, because of the projection maps. However, Lemma 20.6 may be applied to a restricted version of the hypercube, shown in Figure 20.4. Lemma 20.6 also gives a length 3 map, which turns the diagram into a hypercube, though we have omitted this from the figure.

We claim that the resulting diagram in Figure 20.3 is a hypercube of chain complexes. This mostly follows immediately from the hypercube relations in Figure 20.4. For positive surgeries, the hypercube relations are actually satisfied on the full minus version (i.e. with no vertical truncations), as long as we restrict each map on the back face to the Spin^c structures of the form $\mathfrak{x}_s$ and $\mathfrak{y}_s$. For negative n, the hypercube relations will only hold on the vertically truncated complexes. The possibility that requires checking is if $s > b$ but $s + n \leq b$. In this case, the hypercube relations follow from the fact that $f^\delta_{2,\mathfrak{y}_s}$ vanishes if s is sufficiently large, relative to δ, by Proposition 20.10.

Note that claims (1) and (3) hold for D_n and H_m, since by construction we are only using the contributions from the Spin^c structures $\mathfrak{x}_s$ and $\mathfrak{y}_s$.

We stack and compress the hypercubes shown in Figures 20.1, and 20.3. The maps along the top and bottom faces of the resulting hypercube coincide. Hence, we may add the identity to each vertical map, and the hypercube relations are preserved. We obtain a hypercube of the form shown in Figure 20.5.

The diagram in Figure 20.5 determines a $\mathbb{F}[U,Q]/Q^2$ equivariant map from $CFI^\delta(Y_n)$ to the chain complex associated to the 2-dimensional hypercube on the front side of Figure 20.5. The maps along the top and bottom faces coincide with Ozsváth and Szabó's homotopy equivalence between $CF^\delta(\boldsymbol{\alpha}_1, \boldsymbol{\beta})$ and $\mathrm{Cone}(D^\delta_n \colon \mathbb{A}^\delta_n\langle b\rangle \to \mathbb{A}^\delta_n\langle b\rangle)$.

We now claim that we can obtain from the diagram in Figure 20.5 both finite and infinite models of the involutive mapping cone, with maps which satisfy the conditions outlined in Theorem 20.1.

The required m, necessary for a hypercube as in Figure 20.5 to exist, depends on δ. We let δ_i be a sequence approaching $+\infty$, and we m_i be a sequence of

This is a free offprint provided to the author by the publisher. Copyright restrictions may apply.

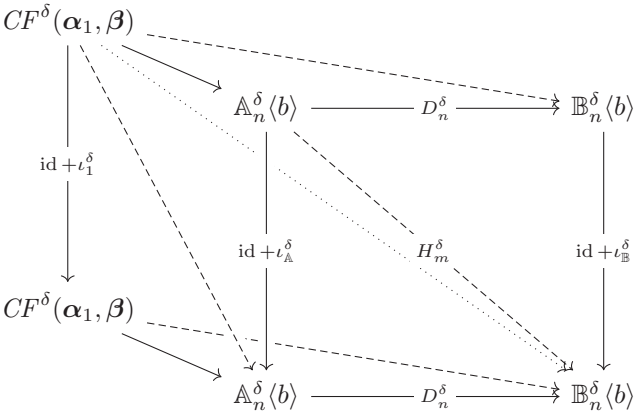


FIGURE 20.5. A hypercube relating $CFI^\delta(Y_n)$ and a truncated mapping cone.

integers, such that m_i is sufficiently large for the hypercube in Figure 20.5 to exist. For convenience, take $b = \lfloor \frac{m+n-1}{2} \rfloor$, which ensures (20.5) is satisfied.

Since we are working over $\mathbb{F} = \mathbb{Z}/2$, the set of elements of A_s and B_s in each grading is finite. Consequently, by picking a subsequence, we may assume that $H_{m_i}(x)$ is eventually constant, for each $x \in A_s$. Consequently, we obtain a limiting map, which we call $\widetilde{H}$, which we extend $\mathbb{F}[\![U]\!]$-equivariantly. The map $\widetilde{H}$ clearly makes the untruncated analog of the front of the hypercube in Figure 20.5 into a 2-dimensional hypercube of chain complexes. Analogously, we may assume that the maps labeled D_n are eventually constant on each $x \in A_s$, for each s. Hence, we obtain a limiting map, for which we write $\widetilde{D}_n$.

Let us write $\widetilde{\mathbb{XI}}_n$ for the infinite involutive mapping cone, constructed with the maps $\widetilde{D}_n$ and $\widetilde{H}$. There are also several horizontal truncations to consider, namely the one appearing in Figure 20.5, constructed for m_i, for which we write $\mathbb{XI}_n(m_i)$ (it is easy to check that the hypercube relations are satisfied without vertically truncating). We may also horizontally truncate $\widetilde{\mathbb{XI}}_n$. We write $\widetilde{\mathbb{XI}}_n\langle m\rangle$ for this complex.

We make the following subclaims:

(t-1) If m is large, then $\widetilde{\mathbb{XI}}_n$ and $\widetilde{\mathbb{XI}}_n\langle m\rangle$ are homotopy equivalent over $\mathbb{F}[\![U]\!][Q]/Q^2$.

(t-2) If m_i is large, then $\widetilde{\mathbb{XI}}_n\langle m_i\rangle$ and $\mathbb{XI}_n(m_i)$ are homotopy equivalent over $\mathbb{F}[\![U]\!][Q]/Q^2$.

The proof of claim (t-1) is as follows. Let us assume $n > 0$, for the sake of demonstration. In this case, projection from $\widetilde{\mathbb{XI}}_n$ to $\widetilde{\mathbb{XI}}_n\langle m\rangle$ is an $\mathbb{F}[\![U]\!][Q]/Q^2$-equivariant chain map. Furthermore, the map obtained by setting $Q = 0$ is a homotopy equivalence, by Lemma 20.5. Hence, Lemma 5.5 implies that the involutive version is an $\mathbb{F}[\![U]\!][Q]/Q^2$-equivariant homotopy equivalence. The proof for negative coefficients is essentially the same, except one instead considers the inclusion of $\widetilde{\mathbb{XI}}_n\langle m\rangle$ into $\widetilde{\mathbb{XI}}_n$, which is a homotopy equivalence for large m.

The proof of claim (t-2) is similar. Fix an integer b. For sufficiently large m_i, the complex $\mathbb{XI}_n(m_i)\langle b\rangle$ is equal to $\widetilde{\mathbb{XI}}_n\langle b\rangle$ (since $\widetilde{\mathbb{XI}}_n$ is obtained as a limit). As before, let us focus on the case that n is positive. Hence if b is sufficiently large, and

This is a free offprint provided to the author by the publisher. Copyright restrictions may apply.

m_i is chosen sufficiently large, relative to b, then the projection for $\widetilde{\mathbb{XI}}_n$ onto $\widetilde{\mathbb{XI}}_n\langle b\rangle$ is an $\mathbb{F}[\![U]\!][Q]/Q^2$-equivariant homotopy equivalence, and projection of $\mathbb{XI}_n(m_i)$ onto $\widetilde{\mathbb{XI}}_n\langle b\rangle$ is also an $\mathbb{F}[\![U]\!][Q]/Q^2$-equivariant homotopy equivalence. Claim (t-2) now follows.

The diagram in Figure 20.5 induces an $\mathbb{F}[U,Q]/Q^2$-equivariant chain map between $CFI^{\delta_i}(Y_n(K))$ and $\mathbb{XI}_n^{\delta_i}(m_i)$, for each i, which we see is an $\mathbb{F}[U,Q]/Q^2$-homotopy equivalence, by combining the fact that the $Q=0$ specializing is an $\mathbb{F}[U]$-equivariant homotopy equivalence with Lemma 5.5. By claims (t-1) and (t-2), we obtain also that $CFI^{\delta}(Y_n(K))$ and $\widetilde{\mathbb{XI}}_n^{\delta}$ are homotopy equivalent over $\mathbb{F}[U,Q]/Q^2$, for all δ. Lemma 20.4 now implies the claim for the complexes without the vertical truncations. □

20.5. Proof of Theorems 1.2 and 1.3

We now prove the exact sequences described in the introduction:

Proof of Theorem 1.3. The front face of the involutive surgery hypercube of Theorem 1.14 determines an $\mathbb{F}[\![U]\!][Q]/Q^2$-equivariant chain map

$$F_2\colon \boldsymbol{CFI}^-(Y_{n+m}(K)) \to \underline{\boldsymbol{CFI}}^-(Y).$$

Furthermore, the remaining maps in the hypercube determine an $\mathbb{F}[\![U]\!][Q]/Q^2$-equivariant chain map

$$F_1\colon \boldsymbol{CFI}^-(Y_n(K)) \to \mathrm{Cone}(F_2).$$

Furthermore, F_1 is a homotopy equivalence of $\mathbb{F}[\![U]\!][Q]/Q^2$-modules by Lemma 5.5, since Ozsváth and Szabó proved that the map obtained by setting $Q=0$ is a homotopy equivalence of $\mathbb{F}[\![U]\!]$-modules [**OS08b**, Theorem 3.1]. The long exact sequence of a mapping cone now gives the exact sequence

$$\cdots \to \boldsymbol{HFI}^-(Y_n(K)) \to \boldsymbol{HFI}^-(Y_{n+m}(K)) \to \underline{\boldsymbol{HFI}}^-(Y) \to \cdots.$$

It remains only to prove the description of $\underline{\boldsymbol{HFI}}^-(Y)$ stated in (1.2). The map θ_w gives a chain isomorphism $\boldsymbol{CFI}^-(Y) \cong \boldsymbol{CF}^-(Y)\otimes\mathbb{F}[\mathbb{Z}/m]$. The map $\underline{\iota}_3$ sends $\boldsymbol{CF}^-(Y)\otimes T^s$ to $\boldsymbol{CF}^-(Y)\otimes T^{-s+n}$, but otherwise coincides with the involution on $\boldsymbol{CF}^-(Y)$ by Proposition 6.1 and Lemma 16.14. It is also important to check the path of the basepoint w in the corresponding loop of Heegaard diagrams. We observe that our model of ι_K moves w to $\overline{z}$ negatively along K, while the flip map moves z to w in the positive direction along K, so the overall path of w is null-homotopic.

Hence,

$$\underline{\boldsymbol{HFI}}^-(Y) \cong \bigoplus_{i=1}^{N} \boldsymbol{HFI}^-(Y) \oplus \bigoplus_{i=1}^{M} (\boldsymbol{HF}^-(Y)[-1] \oplus \boldsymbol{HF}^-(Y)),$$

where N is the number of subsets $\{s,-s+n\}\subseteq\mathbb{Z}/m$ which consist of one element, and M is the number of subsets $\{s,-s+n\}$ which consist of two elements. Note that $\{s,-s+n\}$ consists of one element if and only if $2s\equiv n \mod m$. If m is odd, then the map $\times 2\colon \mathbb{Z}/m\to\mathbb{Z}/m$ is a bijection. If m is even, then $\times 2$ has image exactly equal to the even numbers, and the fiber of each even number has cardinality 2. Hence, if m is odd, then $N=1$ and $M=(m-1)/2$. If m is even, and n is odd, then $N=0$ and $M=m/2$. If m and n are even, then $N=2$ and $M=(m-2)/2$. □

This is a free offprint provided to the author by the publisher. Copyright restrictions may apply.

PROOF OF THEOREM 1.2. The proof is very similar to the proof of Theorem 1.3. We build a hypercube similar to the hypercube in Theorem 1.14, but which has $m = 1$. The construction is essentially the same as Figure 6.3, except we only keep track of the basepoint labeled with a hat, and we use no twisted coefficients. With this hypercube in hand, the proof follows no differently than the proof of Theorem 1.3. □

This is a free offprint provided to the author by the publisher. Copyright restrictions may apply.

CHAPTER 21

The strong cone formula for L-spaces

In this chapter, we prove the strong version of the mapping cone formula, for knots in L-spaces:

THEOREM 21.1. *Suppose $n \neq 0$ and K is a knot in an L-space integer homology 3-sphere. Then $\boldsymbol{CFI}^-(Y_n(K))$ is homotopy equivalent over $\mathbb{F}[\![U]\!][Q]/Q^2$ to a complex of the form*

$$\mathbb{XI}_n(Y,K) := \begin{array}{ccc} \mathbb{A} & \xrightarrow{\quad D_n \quad} & \mathbb{B} \\ \downarrow{\scriptstyle Q\cdot(\mathrm{id}+\iota_{\mathbb{A}})} & \swarrow{\scriptstyle Q\cdot H\widetilde{v}} & \downarrow{\scriptstyle Q\cdot(\mathrm{id}+\iota_{\mathbb{B}})} \\ Q\cdot\mathbb{A} & \xrightarrow{\quad D_n \quad} & Q\cdot\mathbb{B}, \end{array}$$

for some $\mathbb{F}[\![U]\!]$-equivariant maps D_n, $\iota_{\mathbb{A}}$, $\iota_{\mathbb{B}}$ and H. Furthermore, the following hold:

1. *H sends $\widetilde{B}_s$ to B_{-s}.*
2. *$D_n = v + \mathfrak{F}\widetilde{v}$, where v denotes the inclusion of A_s into B_s, and $\widetilde{v}$ denotes inclusion of A_s into $\widetilde{B}_s$.*
3. *$\iota_{\mathbb{B}} = \mathfrak{F}\iota_K$.*
4. *$\iota_{\mathbb{A}}$ coincides with the conjugation of ι_K by the shift isomorphism in* (3.5).

In particular, $(\boldsymbol{CF}^-(Y_n(K)), \iota)$ is ι-homotopy equivalent to $\mathbb{XI}_n^{\mathrm{alg}}(CFK^\infty(Y,K), \iota_K)$.

Interestingly, our argument does not seem to work unless Y is an L-space. See Remark 21.2.

21.1. Overview of the proof of Theorem 21.1

We begin by outlining the proof of Theorem 21.1. We describe more details in the subsequent sections. We begin by considering a vertical truncation of the involutive surgery hypercube involving $Y_n(K)$, $Y_{n+m}(K)$ and Y, as shown in Figure 20.1. It follows from Lemma 20.9 that for sufficiently large m, the only Spin^c structures which contribute to the front face are $\mathfrak{x}_s$ or $\mathfrak{y}_s$, ranging over $-(m+n)/2 \leq s \leq (m+n)/2$. Here $\mathfrak{x}_s$ and $\mathfrak{y}_s$ are characterized by (20.4).

The key technical step of our proof of Theorem 21.1 is to construct two 3-dimensional hypercubes, $\mathcal{K}_{\mathfrak{x}_s}$ and $\mathcal{K}_{\mathfrak{y}_s}$, for each $s \in \mathbb{Z}$. After restricting Spin^c structures and vertically truncating, the back faces of the hypercubes $\mathcal{K}_{\mathfrak{x}_s}$ and $\mathcal{K}_{\mathfrak{y}_s}$ match the front face of the main involutive surgery hypercube in Figure 20.1. The hypercubes $\mathcal{K}_{\mathfrak{x}_s}$ and $\mathcal{K}_{\mathfrak{y}_s}$ are shown schematically in Figure 21.1. The maps labeled

This is a free offprint provided to the author by the publisher. Copyright restrictions may apply.

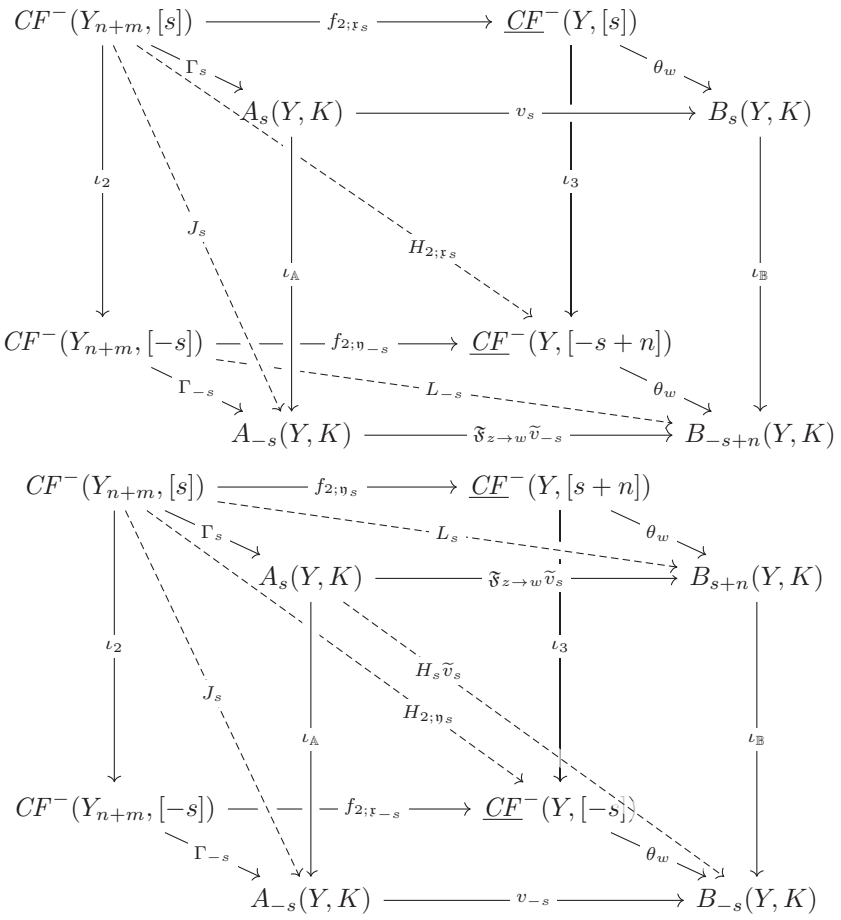


FIGURE 21.1. The hypercubes $\mathcal{K}_{\mathfrak{x}_s}$ (top) and $\mathcal{K}_{\mathfrak{y}_s}$ (bottom). The length 3 arrows are not drawn. The maps labeled L_s coincide in the two diagrams, and similarly for the maps J_s and Γ_s. Both cubes have a length 3 map which is not shown.

L_s coincide in the two diagrams, and similarly for J_s and Γ_s. Therein, the indexing of the maps is consistent with notation in Theorem 1.14 of the introduction, so $f_{2;\mathfrak{x}_s}$ denotes $f^{\beta}_{\alpha_2\to\alpha_3;\mathfrak{x}_s}$, and similarly for the other maps.

We now prove Theorem 21.1, assuming the existence of the hypercubes $\mathcal{K}_{\mathfrak{x}_s}$ and $\mathcal{K}_{\mathfrak{y}_s}$:

PROOF OF THEOREM 21.1. We construct hypercubes $\mathcal{K}_{\mathfrak{X}}\langle b\rangle$ by taking the direct sum of the hypercubes $\mathcal{K}_{\mathfrak{x}_s}$ ranging over $-b \le s \le b$. We define $\mathcal{K}_{\mathfrak{Y}}\langle b\rangle$ similarly by taking the direct sum of the $\mathcal{K}_{\mathfrak{y}_s}$ for $-b \le s \le b$. We now combine $\mathcal{K}_{\mathfrak{X}}\langle b\rangle$ and $\mathcal{K}_{\mathfrak{Y}}\langle b\rangle$ to construct a new cube, $\mathcal{K}_{\{\mathfrak{X},\mathfrak{Y}\}}\langle b\rangle$, the vertical truncation of which is shown in Figure 21.2. Here, b is an integer satisfying

$$0 \ll b < (m+n)/2.$$

This is a free offprint provided to the author by the publisher. Copyright restrictions may apply.

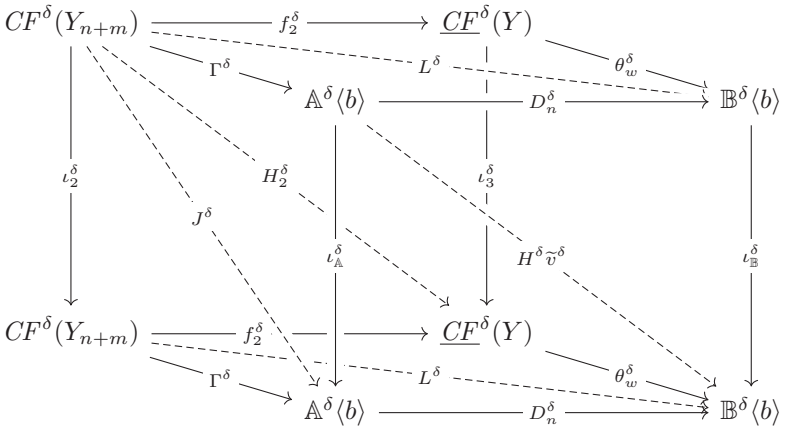


FIGURE 21.2. The hypercube $\mathcal{K}^\delta_{\{\mathfrak{X},\mathfrak{Y}\}}\langle b\rangle$. There is a length 3 map which is not shown.

The maps along the left face of $\mathcal{K}_{\{\mathfrak{X},\mathfrak{Y}\}}\langle b\rangle$ coincide with the ones in $\mathcal{K}_{\mathfrak{X}}\langle b\rangle$ (which themselves coincide with those of $\mathcal{K}_{\mathfrak{Y}}\langle b\rangle$). The maps along the top, front, bottom and back faces of $\mathcal{K}^\delta_{\{\mathfrak{X},\mathfrak{Y}\}}\langle b\rangle$, except for the purely vertical maps (i.e. the involutions), are defined to be the sum of the maps from $\mathcal{K}_{\mathfrak{X}}\langle b\rangle$ and $\mathcal{K}_{\mathfrak{Y}}\langle b\rangle$. The map along the right face of $\mathcal{K}^\delta_{\{\mathfrak{X},\mathfrak{Y}\}}\langle b\rangle$ is zero. The construction of $\mathcal{K}_{\{\mathfrak{X},\mathfrak{Y}\}}\langle b\rangle$ is essentially the same as the operation of *gluing* hypercubes, described by Manolescu and Ozsváth [**MO10**, Proposition 12.10].

By a slight abuse of notation, we define Γ, L and J in Figure 21.2 to project to 0 any summands corresponding to $[s] \in \mathrm{Spin}^c(Y_{n+m})$ for s satisfying $|s| > b$. Similarly, in the map labeled θ_w we are also implicitly post-composing with the map which projects B_s to 0 unless $-b+n \le s \le b$.

For s satisfying $-b \le s \le b$, the map Γ_s coincides with the large surgery map, and hence is a homotopy equivalence. Hence, the same argument as at the end of the proof of Theorem 20.1 (with $\mathcal{K}^\delta_{\{\mathfrak{X},\mathfrak{Y}\}}\langle b\rangle$ replacing the cube in Figure 20.4) shows that $(\boldsymbol{CF}^-(Y_n(K)),\iota)$ is ι-homotopy equivalent to $\mathbb{XI}^{\mathrm{alg}}_n(CFK^\infty(K),\iota_K)$, completing the proof. □

We now outline the construction of the hypercubes $\mathcal{K}_{\mathfrak{x}_s}$ and $\mathcal{K}_{\mathfrak{y}_s}$, which will be described in more detail in the subsequent sections. The main involutive surgery hypercube of Theorem 1.14 is constructed as the compression of the hyperbox of size $(1,1,7)$ shown in Figure 6.3. The hyperbox therein is constructed by stacking the seven hypercubes

$$\mathcal{C}_{1\text{-h}},\quad \mathcal{C}^1_{2\text{-h}},\quad \mathcal{C}_{\mathrm{cen}},\quad \mathcal{C}^2_{2\text{-h}},\quad \mathcal{C}_{3\text{-h}},\quad \mathcal{C}_\eta \quad\text{and}\quad \mathcal{C}_{\mathfrak{F}}. \tag{21.1}$$

The hypercube $\mathcal{K}_{\mathfrak{x}_s}$ is built as the compression of a hyperbox of size $(1,1,7)$, composed of seven 3-dimensional hypercubes

$$\mathcal{K}_{1\text{-h};\mathfrak{x}_s},\quad \mathcal{K}^1_{2\text{-h};\mathfrak{x}_s},\quad \mathcal{K}_{\mathrm{cen};\mathfrak{x}_s},\quad \mathcal{K}^2_{2\text{-h};\mathfrak{x}_s},\quad \mathcal{K}_{3\text{-h};\mathfrak{x}_s},\quad \mathcal{K}_{\eta;\mathfrak{x}_s} \quad\text{and}\quad \mathcal{K}_{\mathfrak{F};\mathfrak{x}_s}. \tag{21.2}$$

The back face of each of the hypercubes in (21.2) matches a Spin^c restriction of the front face of the corresponding hypercube in (21.1). The hypercube $\mathcal{K}_{\mathfrak{y}_s}$ is constructed similarly as the compression of a hyperbox of size $(1,1,7)$, consisting

This is a free offprint provided to the author by the publisher. Copyright restrictions may apply.

of seven hypercubes

$$\mathcal{K}_{\text{1-h};\mathfrak{y}_s}, \quad \mathcal{K}^1_{\text{2-h};\mathfrak{y}_s}, \quad \mathcal{K}_{\text{cen};\mathfrak{y}_s}, \quad \mathcal{K}^2_{\text{2-h};\mathfrak{y}_s}, \quad \mathcal{K}_{\text{3-h};\mathfrak{y}_s}, \quad \mathcal{K}_{\eta;\mathfrak{y}_s} \quad \text{and} \quad \mathcal{K}_{\mathfrak{F};\mathfrak{y}_s}. \tag{21.3}$$

We now introduce some additional notation which will be helpful in this section. Recall that the description of twisted Floer complexes from Section 2.3 involved a choice of orientation $\mathfrak{o}$ for K. In this section, we fix an orientation $\mathfrak{o}$ on K, which never changes in the course of the argument. We will need to frequently change the special basepoint. To simplify the notation, if $\mathcal{H} = (\Sigma, \boldsymbol{\alpha}, \boldsymbol{\beta}, w, z)$ is a doubly pointed diagram for (Y, K), we write $\mathcal{H}_w$ for $\mathcal{H}$, equipped with the enhanced orientation $(\mathfrak{o}, w)$. Similarly, we write $\mathcal{H}_z$ for $\mathcal{H}$ equipped with the enhanced orientation $(\mathfrak{o}, z)$.

21.2. The hypercube $\mathcal{K}_{\mathfrak{x}_s}$

We now describe the construction of $\mathcal{K}_{\mathfrak{x}_s}$ in detail. This amounts to constructing the seven hypercubes shown in (21.2).

First, suppose that $\mathcal{C}_\circ$ is one of the first five hypercubes in (21.1). We will describe the construction of the corresponding hypercube in (21.2), which we will denote by $\mathcal{K}_{\circ;\mathfrak{x}_s}$. Let $\mathcal{H}^1_0$, $\mathcal{H}^2_0$, and $\mathcal{H}^3_0$ denote the diagrams appearing along the top face of $\mathcal{C}_\circ$, and let $\mathcal{H}^1_1$, $\mathcal{H}^2_1$ and $\mathcal{H}^3_1$ denote the diagrams appearing along the bottom face. We will abuse notation slightly and write w and z for the basepoints on $\mathcal{H}^3_0$ and $\mathcal{H}^3_1$, even though they trace a half-twist along K in the doubling model of the involution; see Sections 6.2 and 6.3.

The cube $\mathcal{K}_{\circ;\mathfrak{x}_s}$ is illustrated schematically in Figure 21.3. The cube $\mathcal{K}_{\circ;\mathfrak{x}_s}$ has no length 3 map. The maps $\Psi^2_{0\to1}$ and $\Psi^3_{0\to1}$ appearing along the back face are the same ones which appear along the front face of $\mathcal{C}_\circ$. The maps labeled $\Psi^3_{0\to1}$ appearing along the front face are defined using the same sequence of Heegaard diagrams as for the map $\Psi^3_{0\to1}$ along the back face, as well as the same holomorphic curve counts, but instead using the weights $\mathscr{U}^{n_w(\psi)}\mathscr{V}^{n_z(\psi)}$. Since the map constructed in this manner preserves the Alexander grading (by explicit examination of the construction of each hypercube), we conclude that there is an induced map, also denoted $\Psi^3_{0\to1}$, which sends $A_s(\mathcal{H}^3_0)$ to $A_s(\mathcal{H}^3_1)$, and similarly for the B_s complexes.

The map Γ_s is the composition of the the shift isomorphism between $\mathcal{A}_s$ and A_s, together with the map from $CF^-(\mathcal{H}^2_0, [s])$ to $\mathcal{A}_s(\mathcal{H}^2_0)$, which counts holomorphic triangles representing classes which satisfy $\mathfrak{s}_w(\psi) = \mathfrak{x}_s$, weighted by a factor of $\mathscr{U}^{n_w(\psi)}\mathscr{V}^{n_z(\psi)}$. This map counts the same triangles as $f^{2\to3}_{0;\mathfrak{x}_s}$. Similarly, we define $J_{0\to1;s}$ by composing the shift map from $\mathcal{A}_s$ to A_s with the analogs on $\mathcal{A}_s$ of each constituent map of $H^{2\to3}_{0\to1;\mathfrak{x}_s}$. For example, if $H^{2\to3}_{0\to1;\mathfrak{x}_s}$ had a factor or summand which counted holomorphic rectangles representing classes satisfying $\mathfrak{s}_w(\psi) = \mathfrak{x}_s$, then the map $J_{0\to1;s}$ would also have a constituent map which counted rectangles weighted by $\mathscr{U}^{n_w(\psi)}\mathscr{V}^{n_z(\psi)}$.

To prove that Γ_s and $J_{0\to1;s}$ have codomain in A_s, as claimed, one needs to check that the maps Γ_s and $J_{0\to1;s}$ change Alexander grading by s (viewing $CF^-(\mathcal{H}^2_0, [s])$ and $CF^-(\mathcal{H}^2_1, [s])$ as being concentrated in Alexander grading 0). This follows from [**Zem19b**, Theorem 1.4] (compare [**OS11**, Proposition 2.2]).

Next, we verify the hypercube relations for $\mathcal{K}_{\circ;\mathfrak{x}_s}$. The length 2 relations along the left, back, right and front faces are straightforward. The length 2 relation along the top and bottom faces, as well as the length 3 relation, follow from the fact that Γ_s and $J_{0\to1;s}$ are both given as a map which changes Alexander grading by

This is a free offprint provided to the author by the publisher. Copyright restrictions may apply.

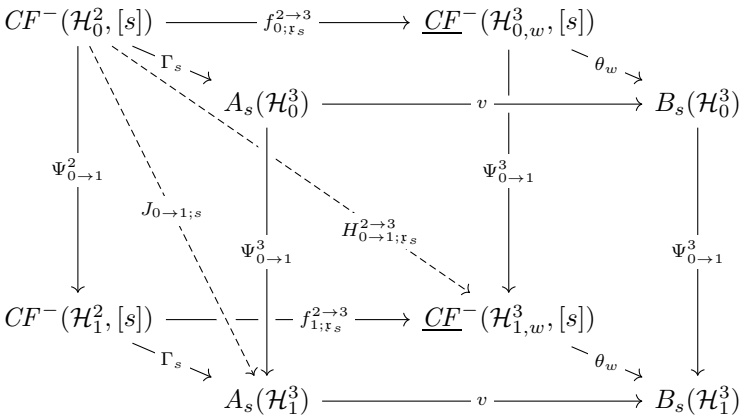


FIGURE 21.3. A schematic of the hypercube $\mathcal{K}_{\circ,\mathfrak{r}_s}$, which is one of the first five hypercubes of (21.2). There is no length 3 map.

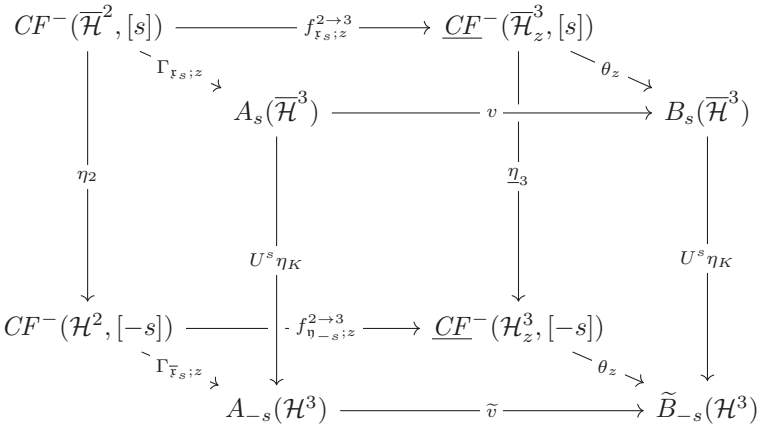


FIGURE 21.4. The hypercube $\mathcal{K}_{\eta;\mathfrak{r}_s}$. There are no length 2 or 3 maps.

s, followed by the shift isomorphism, as well as the fact that they both count the same holomorphic curves as $f^{2\to3}_{0;\mathfrak{r}_s}$ or $f^{2\to3}_{1;\mathfrak{r}_s}$, and $H^{2\to3}_{0\to1;\mathfrak{r}_s}$, respectively.

We now describe the hypercube $\mathcal{K}_{\eta;\mathfrak{r}_s}$, which is shown in Figure 21.4. Therein, we have added some decoration to the map Γ_s to disambiguate terms. We write $\Gamma_{\mathfrak{s};w}$ for the map which counts holomorphic triangles satisfying $\mathfrak{s}_w(\psi)=\mathfrak{s}$, which are weighted by a factor of $\mathscr{U}^{n_w(\psi)}\mathscr{V}^{n_z(\psi)}$, composed with the shift isomorphism between $\mathcal{A}_s$ and A_s. The map Γ_s in Figure 21.3 coincides with $\Gamma_{\mathfrak{r}_s;w}$. The hypercube relations therein are easily checked.

We now describe a helpful conjugation relation for the maps labeled by Γ. We claim that for all $s\in\mathbb{Z}$,

$$\Gamma_{\mathfrak{r}_s;w}=\Gamma_{\mathfrak{y}_s;z} \qquad \text{and} \qquad \overline{\mathfrak{r}}_s=\mathfrak{y}_{-s}, \tag{21.4}$$

This is a free offprint provided to the author by the publisher. Copyright restrictions may apply.

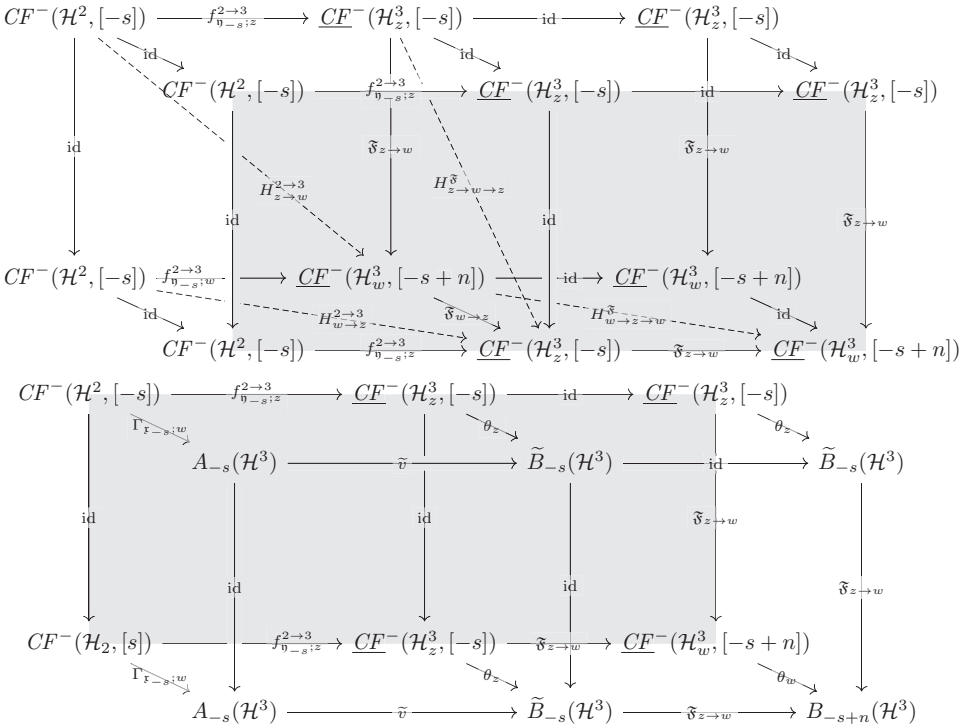


FIGURE 21.5. The hyperbox whose compression is $\mathcal{K}_{\mathfrak{F};\mathfrak{x}_s}$. The top two cubes each have a length 3 map, which is not shown, while the bottom two have no length 3 map. We stack the top and bottom hyperboxes along the gray faces. We think of this hyperbox as being made of four hypercubes, $\mathcal{K}^1_{\mathfrak{F};\mathfrak{x}_s}, \dots \mathcal{K}^4_{\mathfrak{F};\mathfrak{x}_s}$, which are the top-left, top-right, bottom-left, and bottom-right hypercubes, respectively.

The second part of (21.4) is immediate from the definition of $\mathfrak{x}_s$ and $\mathfrak{y}_s$ in (20.4). The first part follows from the relation

$$\mathfrak{s}_w(\psi) - \mathfrak{s}_z(\psi) = PD[\widehat{S}], \tag{21.5}$$

where $\widehat{S}$ is the class in $H_2(W'_{n+m}(K))$ obtained by capping the core of the 2-handle. Equation (21.5) follows from [**Zem19b**, Lemma 3.9]. Hence $\Gamma_{\mathfrak{x}_s;w}$ and $\Gamma_{\mathfrak{y}_s;z}$ count the same triangles, with the same powers of $\mathscr{U}$ and $\mathscr{V}$. (Note that the choice of basepoint in the map $\Gamma_{\mathfrak{y}_s;z}$ affects only which classes are counted, via the choice of Spin^c structure, but not the $\mathscr{U}$ or $\mathscr{V}$ weight). Equation (21.4) follows.

We now construct $\mathcal{K}_{\mathfrak{F};\mathfrak{x}_s}$ by stacking and compressing four hypercubes, $\mathcal{K}^1_{\mathfrak{F};\mathfrak{x}_s}$, $\dots, \mathcal{K}^4_{\mathfrak{F};\mathfrak{x}_s}$, as shown in Figure 21.5. We begin by describing the hypercube $\mathcal{K}^1_{\mathfrak{F};\mathfrak{x}_s}$, which is the top left hypercube in Figure 21.5. Let $\phi\colon \Sigma \to \Sigma$ denote the diffeomorphism which moves z to w along the canonical short path in the Heegaard diagram. We construct $\mathcal{K}^1_{\mathfrak{F};\mathfrak{x}_s}$ as the compression of a hyperbox of size $(1,3,3)$. This hyperbox is shown schematically in Figure 21.6. Therein, we assume that $\boldsymbol{\alpha}_3^{\mathrm{W}}$ is a sufficiently wound copy of $\boldsymbol{\alpha}_3$, which we additionally assume is wound so as not to intersect

This is a free offprint provided to the author by the publisher. Copyright restrictions may apply.

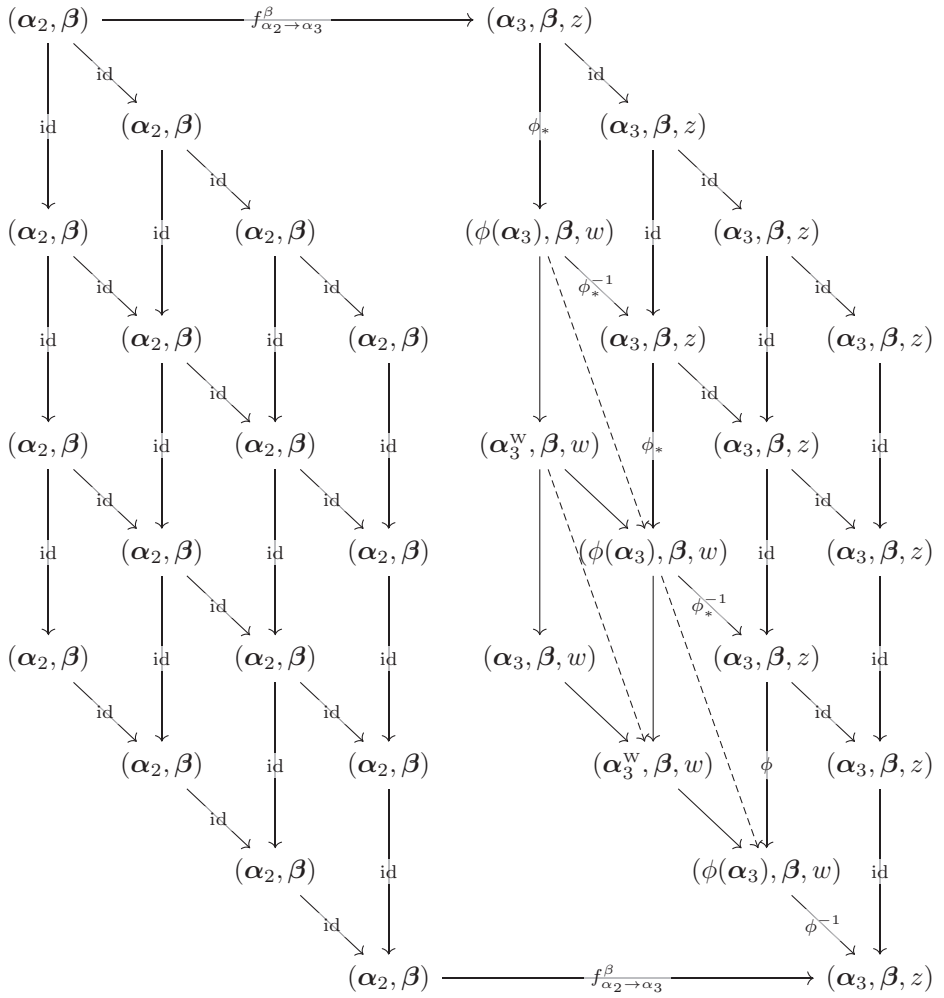


FIGURE 21.6. The hyperbox whose compression is $\mathcal{K}^1_{\mathfrak{F};\mathfrak{r}_s}$. The solid arrows count holomorphic triangles, while the dashed arrows count holomorphic quadrilaterals and holomorphic triangles. Many arrows from the left-side to the right-side are not drawn.

the boundary of the surgery region. We view this hyperbox as consisting of nine hypercubes. Each of these hypercubes may be constructed by pairing a hyperbox of alpha attaching circles with the 0-dimensional hypercube consisting of $\boldsymbol{\beta}$. We also compose some of the maps appearing in these hypercubes with one of the tautological maps ϕ_* or ϕ_*^{-1}. When a single attaching curve appears at different locations in the hyperbox, one would need to replace certain copies with small Hamiltonian translates. Furthermore, we are implicitly using Proposition 11.1 to identity the maps labeled by id with the corresponding small triangle maps.

We now construct the hypercube $\mathcal{K}^2_{\mathfrak{F};\mathfrak{r}_s}$, which is the top right hypercube shown in Figure 21.5. The length 2 map along the left side of $\mathcal{K}^2_{\mathfrak{F};\mathfrak{r}_s}$ is constructed in $\mathcal{K}^1_{\mathfrak{F};\mathfrak{r}_s}$. The map along the bottom is constructed similarly. A length 3 map may be defined

This is a free offprint provided to the author by the publisher. Copyright restrictions may apply.

by noting that every complex appearing at a vertex of $\mathcal{K}^2_{\mathfrak{F};\mathfrak{x}_s}$ is homotopy equivalent to $\mathbb{F}[\![U]\!]$, since Y is an L-space. The expression

$$M := \mathfrak{F}_{z\to w} H^{\mathfrak{F}}_{z\to w\to z} + H^{\mathfrak{F}}_{w\to z\to w}\mathfrak{F}_{z\to w}$$

is an $\mathbb{F}[U]$-equivariant chain map, which is $+1$ graded and hence is chain homotopic to zero. We let the length 3 map in $\mathcal{K}^2_{\mathfrak{F};\mathfrak{x}_s}$ be any null-homotopy of M which is homogeneously graded. (Alternatively, one could define $\mathcal{K}^2_{\mathfrak{F};\mathfrak{x}_s}$ by building a hyperbox of size $(3,3,3)$, similar to the one used to build $\mathcal{K}^1_{\mathfrak{F};\mathfrak{x}_s}$, but with two more layers).

Finally, we consider $\mathcal{K}^3_{\mathfrak{F};\mathfrak{x}_s}$ and $\mathcal{K}^4_{\mathfrak{F};\mathfrak{x}_s}$, the bottom two hypercubes in Figure 21.5. We note that the hypercube relations for these cubes are automatic, since all faces commute on the nose, so no length 2 or 3 arrows are necessary.

21.3. The hypercubes $\mathcal{K}_{1\text{-h};\mathfrak{y}_s}$, $\mathcal{K}^1_{2\text{-h};\mathfrak{y}_s}$, $\mathcal{K}^2_{2\text{-h};\mathfrak{y}_s}$ and $\mathcal{K}_{3\text{-h};\mathfrak{y}_s}$

In this section, we describe the construction of the hypercubes $\mathcal{K}_{1\text{-h};\mathfrak{y}_s}$, $\mathcal{K}^1_{2\text{-h};\mathfrak{y}_s}$, $\mathcal{K}^2_{2\text{-h};\mathfrak{y}_s}$, and $\mathcal{K}_{3\text{-h};\mathfrak{y}_s}$. Let $\mathcal{K}_{\circ;\mathfrak{y}_s}$ denote one of these hypercubes. We will construct $\mathcal{K}_{\circ;\mathfrak{y}_s}$ by stacking and compressing four hypercubes $\mathcal{K}^i_{\circ;\mathfrak{y}_s}$ for $i\in\{1,2,3,4\}$. The hypercubes $\mathcal{K}_{\circ;\mathfrak{y}_s}$ and $\mathcal{K}^i_{\circ;\mathfrak{y}_s}$ are schematically illustrated in Figure 21.7.

In the doubling model of the involution, each of the factors of the involution moves the basepoints slightly, resulting in a cumulative half-twist along K (see Section 6.3). As a consequence, the basepoints on the top faces of some of the hypercubes in (21.1) differ from the basepoints on the bottom face. In this section, we abuse notation slightly, and denote every basepoint by w or z, with the convention that K intersects the Heegaard surface positively (resp. negatively) at z (resp. w).

Let $\mathcal{H}^1_0$, $\mathcal{H}^2_0$ and $\mathcal{H}^3_0$ denote the Heegaard diagrams appearing on the top face of $\mathcal{C}_{\circ;\mathfrak{y}_s}$, and let $\mathcal{H}^1_1$, $\mathcal{H}^2_1$ and $\mathcal{H}^3_1$ denote those appearing along the bottom face. For $i\in\{0,1\}$, let $\mathcal{T}_i$ denote the Heegaard triple used to compute the maps from $\boldsymbol{CF}^-(\mathcal{H}^2_i)$ to $\underline{\boldsymbol{CF}}^-(\mathcal{H}^3_i)$. We have the following cases, depending on the hypercube $\mathcal{K}_{\circ,\mathfrak{y}_s}$:

- (K-1) $\mathcal{T}_1$ is obtained from $\mathcal{T}_0$ by a stabilization or destabilization with index tuple $(0,0,0)$ (i.e. $\mathcal{T}_1$ is obtained by attaching or removing a collection of 1-handle stabilizations from $\mathcal{T}_0$). This configuration appears in $\mathcal{K}_{1\text{-h};\mathfrak{y}_s}$ and $\mathcal{K}_{3\text{-h};\mathfrak{y}_s}$.
- (K-2) $\mathcal{T}_0 = (\Sigma, \boldsymbol{\alpha}^3, \boldsymbol{\alpha}^2, \boldsymbol{\beta}_0, w, z)$ and $\mathcal{T}_1 = (\Sigma, \boldsymbol{\alpha}^3, \boldsymbol{\alpha}^2, \boldsymbol{\beta}_1, w, z)$. Furthermore, for $j\in\{2,3\}$, the triple $(\Sigma, \boldsymbol{\alpha}^j, \boldsymbol{\beta}_0, \boldsymbol{\beta}_1, w, z)$ represents surgery on an ℓ-component link in
$$(Y\setminus N(K))\#(S^1\times S^2)^{\#\ell}$$
which cancels the $S^1\times S^2$-summands. This configuration corresponds to $\mathcal{K}^1_{2\text{-h};\mathfrak{y}_s}$.
- (K-3) $\mathcal{T}_0 = (\Sigma, \boldsymbol{\alpha}, \boldsymbol{\beta}^2_0, \boldsymbol{\beta}^3_0, w, z)$ and $\mathcal{T}_1 = (\Sigma, \boldsymbol{\alpha}, \boldsymbol{\beta}^2_1, \boldsymbol{\beta}^3_1, w, z)$. Furthermore the triples $(\Sigma, \boldsymbol{\alpha}, \boldsymbol{\beta}^2_0, \boldsymbol{\beta}^2_1, w)$ and $(\Sigma, \boldsymbol{\alpha}, \boldsymbol{\beta}^3_0, \boldsymbol{\beta}^3_1, w, z)$ both represent surgery on a 0-framed unlink in $Y\setminus N(K)$. This configuration corresponds to $\mathcal{K}^2_{2\text{-h};\mathfrak{y}_s}$.

Note that the notation of the alpha and beta curves in configurations (K-1), (K-2) and (K-3) does not coincide with the notation of Figure 6.3. We have condensed it for convenience.

This is a free offprint provided to the author by the publisher. Copyright restrictions may apply.

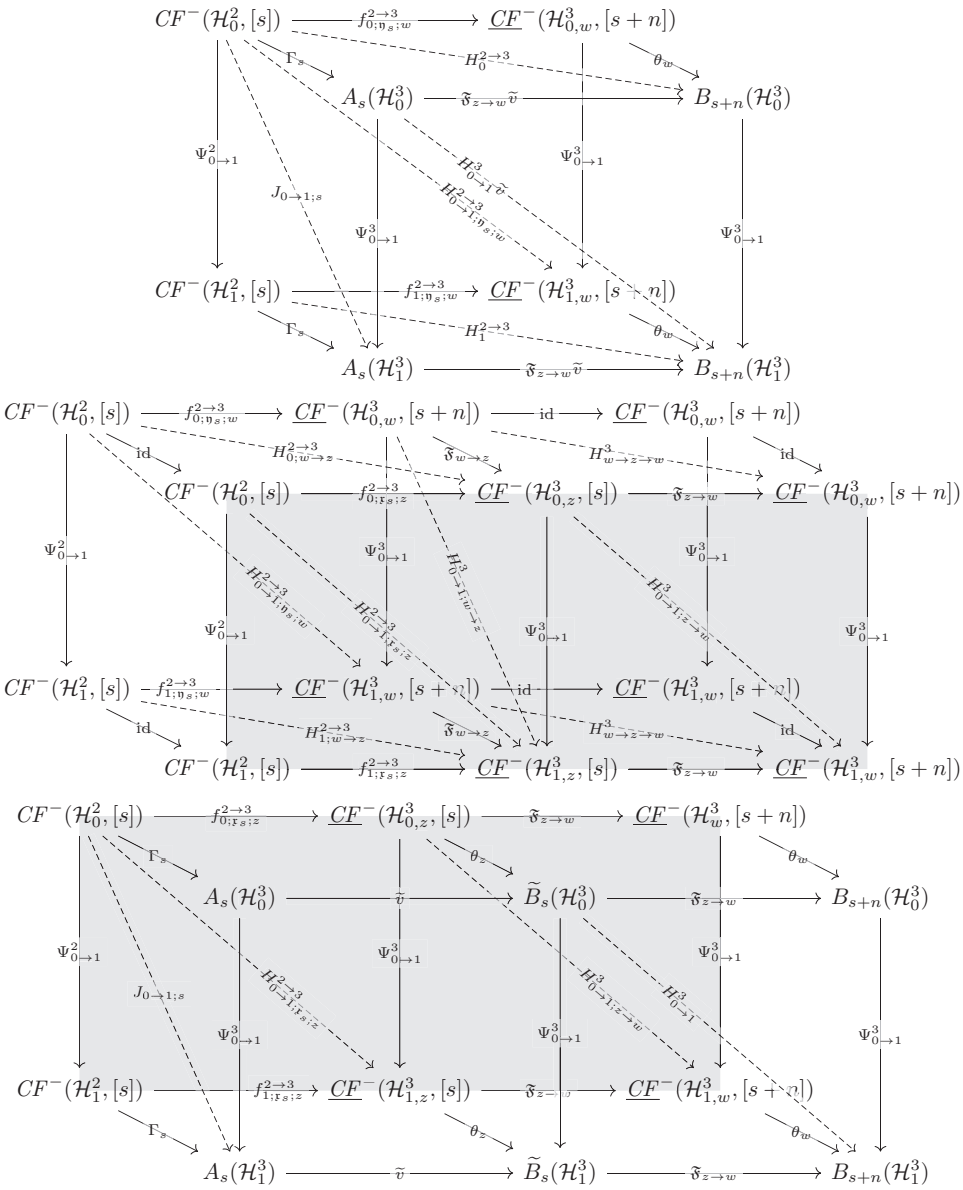


FIGURE 21.7. A schematic of the construction of a hypercube $\mathcal{K}_{\circ;\mathfrak{y}_s} \in \{\mathcal{K}_{1\text{-h};\mathfrak{y}_s}, \mathcal{K}^1_{2\text{-h};\mathfrak{y}_s}, \mathcal{K}^2_{2\text{-h};\mathfrak{y}_s}, \mathcal{K}_{3\text{-h};\mathfrak{y}_s}\}$. We construct $\mathcal{K}_{\circ;\mathfrak{y}_s}$ (top) as the compression of the hyperbox obtained by stacking and compressing the middle and bottom hyperboxes along their gray faces. We write $\mathcal{K}^1_{\circ;\mathfrak{y}_s}$, $\mathcal{K}^2_{\circ;\mathfrak{y}_s}$, $\mathcal{K}^3_{\circ;\mathfrak{y}_s}$ and $\mathcal{K}^4_{\circ;\mathfrak{y}_s}$ for the middle-left, middle-right, bottom-left and bottom-right hypercubes, respectively.

This is a free offprint provided to the author by the publisher. Copyright restrictions may apply.

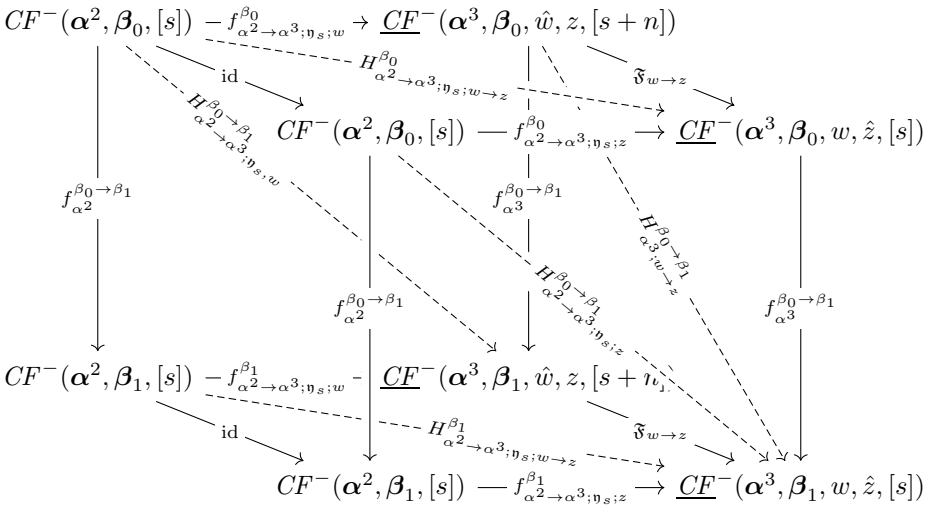


FIGURE 21.8. The hypercube $\mathcal{K}^{1,1}_{\text{2-h};\mathfrak{y}_s}$ (i.e. case (K-2)). There is a length 3 arrow which is not shown.

We describe the construction of $\mathcal{K}^1_{\text{2-h};\mathfrak{y}_s}$ (i.e. case (K-2)) since the other two configurations are handled using similar reasoning. The hypercube $\mathcal{K}^{1,1}_{\text{2-h};\mathfrak{y}_s}$ is depicted schematically in Figure 21.8. We think of this cube as relating 2-dimensional faces of the flip-map hypercubes for the two triples $(\Sigma, \boldsymbol{\alpha}^3, \boldsymbol{\alpha}^2, \boldsymbol{\beta}_0, w, z)$ and $(\Sigma, \boldsymbol{\alpha}^3, \boldsymbol{\alpha}^2, \boldsymbol{\beta}_1, w, z)$, which appear as the top and bottom faces of Figure 21.8.

We begin by describing the maps appearing on the back and front faces of $\mathcal{K}^{1,1}_{\text{2-h};\mathfrak{y}_s}$. We pick cycles $\Theta^+_{\alpha^3,\alpha^2}$ and $\Theta^+_{\beta_0,\beta_1}$, representing the top degree generators. The length 1 maps appearing along the back face are the holomorphic triangle maps with inputs $\Theta^+_{\alpha^3,\alpha^2}$ and $\Theta^+_{\beta_0,\beta_1}$. In the case of $f^{\beta_0}_{\alpha^2\to\alpha^3;\mathfrak{y}_s;w}$, we further restrict to triangles where $\mathfrak{s}_w(\psi) = \mathfrak{y}_s$. The length 2 map $H^{\beta_0\to\beta_1}_{\alpha^2\to\alpha^3;\mathfrak{y}_s;w}$ similarly counts rectangles with the two special inputs $\Theta^+_{\alpha^3,\alpha^2}$ and $\Theta^+_{\beta_0,\beta_1}$, again with the restriction that $\mathfrak{s}_w(\psi) = \mathfrak{y}_s$. Along the back face, we use the weights $U^{n_w(\psi)}T^{n_z(\psi)-n_w(\psi)}$. The maps along the front face are defined similarly, but instead use z as the special basepoint, and are weighted by $U^{n_z(\psi)}T^{n_z(\psi)-n_w(\psi)}$.

The remaining maps in the hypercube $\mathcal{K}^{1,1}_{\text{2-h};\mathfrak{y}_s}$ are constructed by stacking and compressing 5 hypercubes, mirroring the construction of the flip-map hypercube in Chapter 18. In analogy to the construction therein, the five hypercubes are as follows:

(K-2-1) One hypercube involving the map θ_w and T^{-n}.
(K-2-2) One hypercube involving the tautological map for a diffeomorphism ϕ which moves w to z.
(K-2-3) Two hypercubes for changing $\phi(\boldsymbol{\alpha}^3)$ to $\boldsymbol{\alpha}^3$.
(K-2-4) One hypercube involving the map θ_z.

The hypercube labeled (K-2-1), involving θ_w, is shown in Figure 21.9, and the hypercube (K-2-4) involving θ_z is similar, though with no weight by a power of T on the θ_z arrows.

This is a free offprint provided to the author by the publisher. Copyright restrictions may apply.

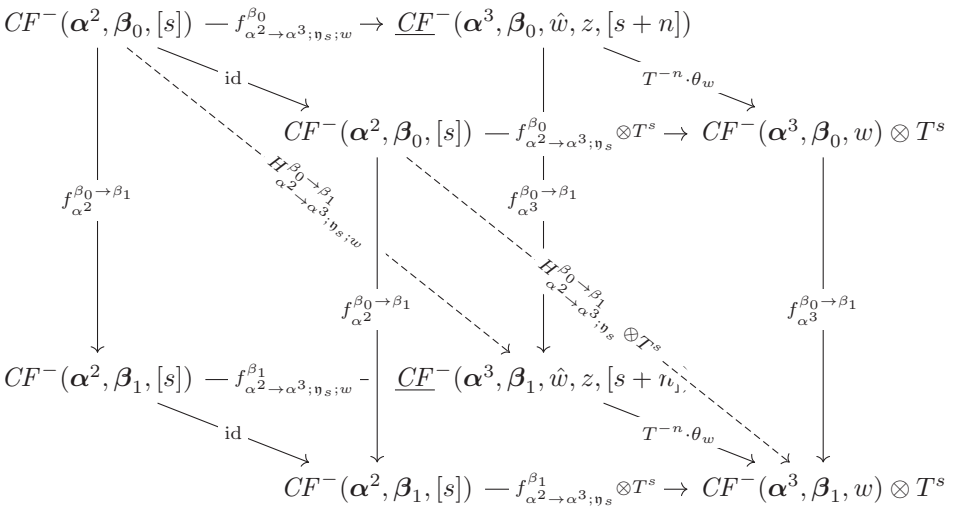
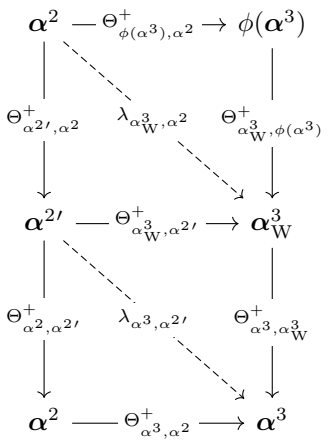


FIGURE 21.9. The hypercube labeled (K-2-1) in the construction of $\mathcal{K}^{1,1}_{2\text{-h};\mathfrak{y}_s}$.

The hypercube involving the tautological map ϕ_*, labeled (K-2-2), is straightforward to construct, and has the map ϕ_* in the direction which comes out of the page, and no length 2 maps except on the front and back faces.

We now describe the two hypercubes which move $\phi(\boldsymbol{\alpha}^3)$ to $\boldsymbol{\alpha}^3$, and are labeled (K-2-3) above. We construct these two hypercubes by pairing a hyperbox of alpha attaching curves $\mathcal{L}_\alpha$ with a hyperbox of beta attaching curves, as shown in (21.6). Therein, $\boldsymbol{\alpha}^{2\prime}$ denotes a small isotopy of $\boldsymbol{\alpha}^2$. The curves $\boldsymbol{\alpha}^3_{\mathrm{W}}$ are obtained by winding $\boldsymbol{\alpha}^3$ to achieve admissibility, in a way which does not intersect the boundary of the 1-handle region.

(21.6)



$\mathcal{L}_\alpha :=$ $\qquad\qquad$ $\mathcal{L}_\beta :=$ $\boldsymbol{\beta}_0 \longrightarrow \Theta^+_{\beta_0,\beta_1} \longrightarrow \boldsymbol{\beta}_1$

Next, we discuss the hypercube $\mathcal{K}^{1,2}_{2\text{-h};\mathfrak{y}_s}$, which is schematically shown in Figure 21.10. The hypercube $\mathcal{K}^{1,2}_{2\text{-h};\mathfrak{y}_s}$ is defined as the compression of a hypercube of size $(5,5,1)$. The top face of this hypercube is shown in Figure 21.11. The bottom face is similar, but has $\boldsymbol{\beta}_1$ instead of $\boldsymbol{\beta}_0$. We leave the remaining details of

This is a free offprint provided to the author by the publisher. Copyright restrictions may apply.

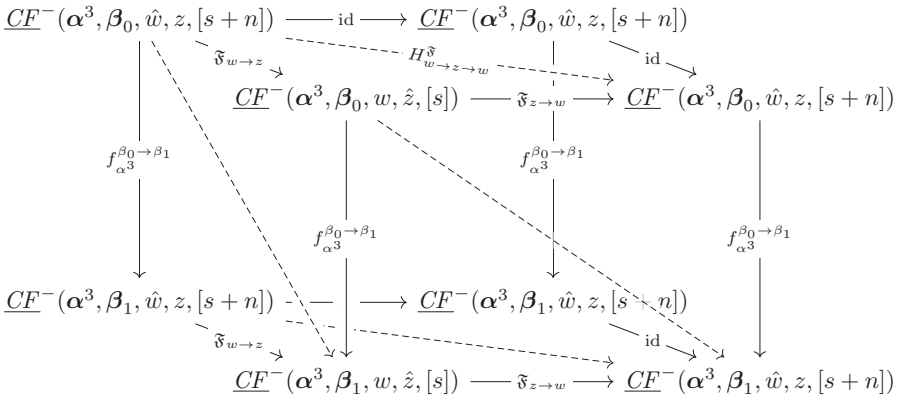


FIGURE 21.10. The hypercube $\mathcal{K}^{1,2}_{\text{2-h};\mathfrak{y}_s}$ from case (K-2). There is a length 3 map, which is not shown.

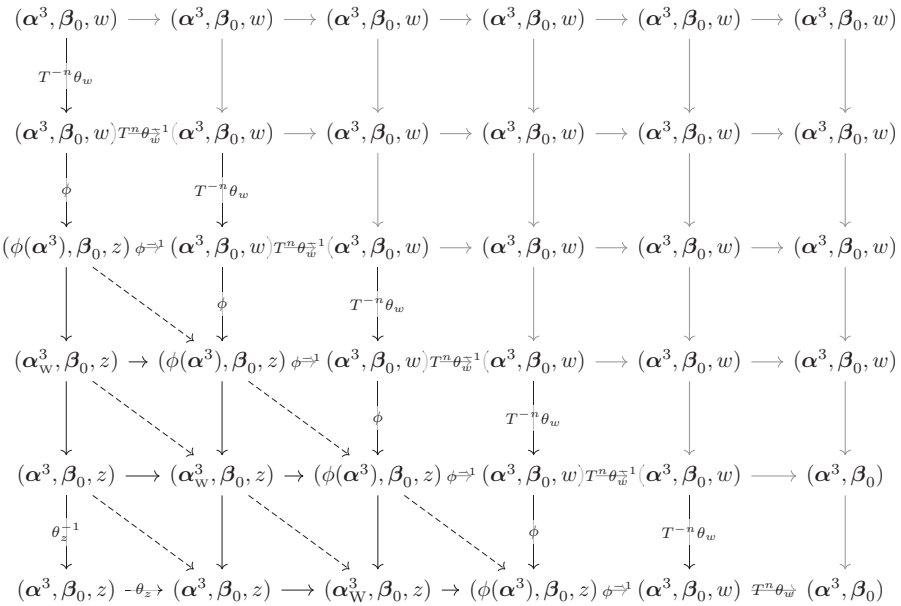


FIGURE 21.11. The top face of the hyperbox used to construct $\mathcal{K}^{1;2}_{\text{2-h};\mathfrak{y}_s}$. The bottom face has $\boldsymbol{\beta}_1$ in place of $\boldsymbol{\beta}_0$. A gray, unmarked arrow indicates the identity map.

the construction of $\mathcal{K}^{1,2}_{\text{2-h};\mathfrak{y}_s}$ to the reader, since the construction is similar to the description of $\mathcal{K}^1_{\mathfrak{F};\mathfrak{x}_s}$ in Figure 21.6. Similarly, we leave the construction of $\mathcal{K}^{1,3}_{\text{2-h};\mathfrak{y}_s}$ and $\mathcal{K}^{1,4}_{\text{2-h};\mathfrak{y}_s}$ to the reader, since they are similar to $\mathcal{K}^3_{\mathfrak{F};\mathfrak{x}_s}$ and $\mathcal{K}^4_{\mathfrak{F};\mathfrak{x}_s}$, respectively.

21.4. The hypercube $\mathcal{K}^{(1)}_{\text{cen};\mathfrak{y}_s}$

We now construct the hypercube $\mathcal{K}^{(1)}_{\text{cen};\mathfrak{y}_s}$. The back face of $\mathcal{K}^{(1)}_{\text{cen};\mathfrak{y}_s}$ will match a Spin^c restriction the front face of the hypercube $\mathcal{C}^{(1)}_{\text{cen}}$ from Chapter 16. The

This is a free offprint provided to the author by the publisher. Copyright restrictions may apply.

hypercube $\mathcal{K}^{(1)}_{\mathrm{cen};\mathfrak{y}_s}$ is constructed as a compression of four hypercubes $\mathcal{K}^{(1),j}_{\mathrm{cen};\mathfrak{y}_s}$, for $j \in \{1,2,3,4\}$, which fit into a similar configuration as the hypercubes $\mathcal{K}^{\Psi,j}_{i;\mathfrak{y}_s}$ in Figure 21.7. As in the previous section, we write w and z for the basepoints on the diagrams in the central hypercube, even though they have moved in the doubling operation from their original positions on $\mathcal{H}^3$ (see Section 6.2).

We focus on the construction of $\mathcal{K}^{(1),1}_{\mathrm{cen};\mathfrak{y}_s}$, since $\mathcal{K}^{(1),2}_{\mathrm{cen};\mathfrak{y}_s}$ is simpler, and furthermore the hypercubes $\mathcal{K}^{(1),3}_{\mathrm{cen};\mathfrak{y}_s}$ and $\mathcal{K}^{(1),4}_{\mathrm{cen};\mathfrak{y}_s}$ involve only the maps which appeared on $\mathcal{K}^{(1),1}_{\mathrm{cen};\mathfrak{y}_s}$ and $\mathcal{K}^{(1),2}_{\mathrm{cen};\mathfrak{y}_s}$, as well as canonical isomorphisms and inclusions. The hypercubes $\mathcal{K}^{(1),1}_{\mathrm{cen},\mathfrak{y}_s}$ and $\mathcal{K}^{(1),2}_{\mathrm{cen};\mathfrak{y}_s}$ take the schematic form shown in Figure 21.12.

We first describe the construction of $\mathcal{K}^{(1),1}_{\mathrm{cen};\mathfrak{y}_s}$. The length 1 and 2 maps along the back face are constructed the same as in $\mathcal{C}^{(1)}_{\mathrm{cen}}$; see Figure 16.4. The length 1 and 2 maps along the front face are similar, except they use z as the special basepoint, instead of w.

The remaining maps in $\mathcal{K}^{(1),1}_{\mathrm{cen};\mathfrak{y}_s}$ are obtained by constructing $\mathcal{K}^{(1),1}_{\mathrm{cen};\mathfrak{y}_s}$ by stacking and compressing two hypercubes $\mathcal{Y}^{(1)}_l$ and $\mathcal{Y}^{(1)}_r$, which we stack and compress along the left face of $\mathcal{Y}^{(1)}_r$ and the right face of $\mathcal{Y}^{(1)}_l$. The hypercube $\mathcal{Y}^{(1)}_r$ is shown in Figure 21.13. The hypercube $\mathcal{Y}^{(1)}_l$ is shown in Figure 21.14.

We now describe the top hypercube of Figure 21.13, which features in the construction of $\mathcal{Y}^{(1)}_r$. This hypercube is constructed similarly to the flip-map hypercube. There is a new subtlety in that the canonical short path between w and z now intersects both an alpha curve and a beta curve. Hence, we define $\mathcal{Y}^{(1)}_r$ as the compression of a hyperbox of size $(1,7,1)$. The first constituent hypercube corresponds to θ_w, the second corresponds to the canonical diffeomorphism moving w to z. Next, there are four hypercubes: two for changing the alpha curves,and two for changing the beta curves. Finally, there is a hypercube involving θ_w.

Next, we describe the bottom hypercube of Figure 21.13. All of the maps except X and Z have already been constructed. Our construction of X and Z requires Y to be an L-space, as follows. Firstly, we pick X to be any homogeneously graded map which is a homotopy between $\sigma F_3 \mathfrak{F}_{w\to z}$ and $\mathfrak{F}_{w\to z}\sigma F_3$. Such a map X exists by the following reasoning. Let $V = \mathbb{F}\oplus\mathbb{F}[1]$ (i.e. two copies of $\mathbb{F}$, with the grading of one copy shifted down by 1). For all s, there are homotopy equivalences

$$\underline{CF}^-(\boldsymbol{\gamma}', \boldsymbol{\delta}', \hat{w}, z, [s]) \simeq \mathbb{F}[U] \quad \text{and} \quad \underline{CF}^-(\boldsymbol{\gamma}'', \boldsymbol{\delta}', \hat{w}, z, [s]) \simeq \mathbb{F}[U]\otimes V, \tag{21.7}$$

and similarly when z is the special basepoint. We note that $\mathrm{Hom}_{\mathbb{F}[U]}(\mathbb{F}[U]\otimes V, \mathbb{F}[U])$ has rank 1 over $\mathbb{F}$ in non-positive gradings (and is (0) in positive gradings). Hence, if two $\mathbb{F}[U]$-equivariant chain maps from $\underline{CF}^-(\boldsymbol{\gamma}'', \boldsymbol{\delta}', \hat{w}, z, [s])$ to $\underline{CF}^-(\boldsymbol{\gamma}'', \boldsymbol{\delta}', \hat{w}, z, [s'])$ have the same homogeneous grading, and induce non-zero elements of $\mathrm{Hom}_{\mathbb{F}[U]}(\mathbb{F}[U]\otimes V, \mathbb{F}[U])$, then they are chain homotopic. This gives the map X.

We now construct Z. Let M denote the sum of compositions of length 1 and 2 maps appearing in the length 3 relation of the cube:

$$M := X f^{\delta'}_{\gamma'\to\gamma''} + \sigma F_3 H^{\mathfrak{F}}_{w\to z}.$$

The map M maps $\underline{CF}^-(\boldsymbol{\gamma}', \boldsymbol{\delta}', \hat{w}, z, [s+n])$ to $\underline{CF}^-(\boldsymbol{\gamma}', \boldsymbol{\delta}', w, \hat{z}, [s])$. Equation (21.7) implies that these chain complexes, which are clearly homotopy equivalent as absolutely graded chain complexes via the map $\mathfrak{F}_{w\to z}$, are also both homotopy equivalent

This is a free offprint provided to the author by the publisher. Copyright restrictions may apply.

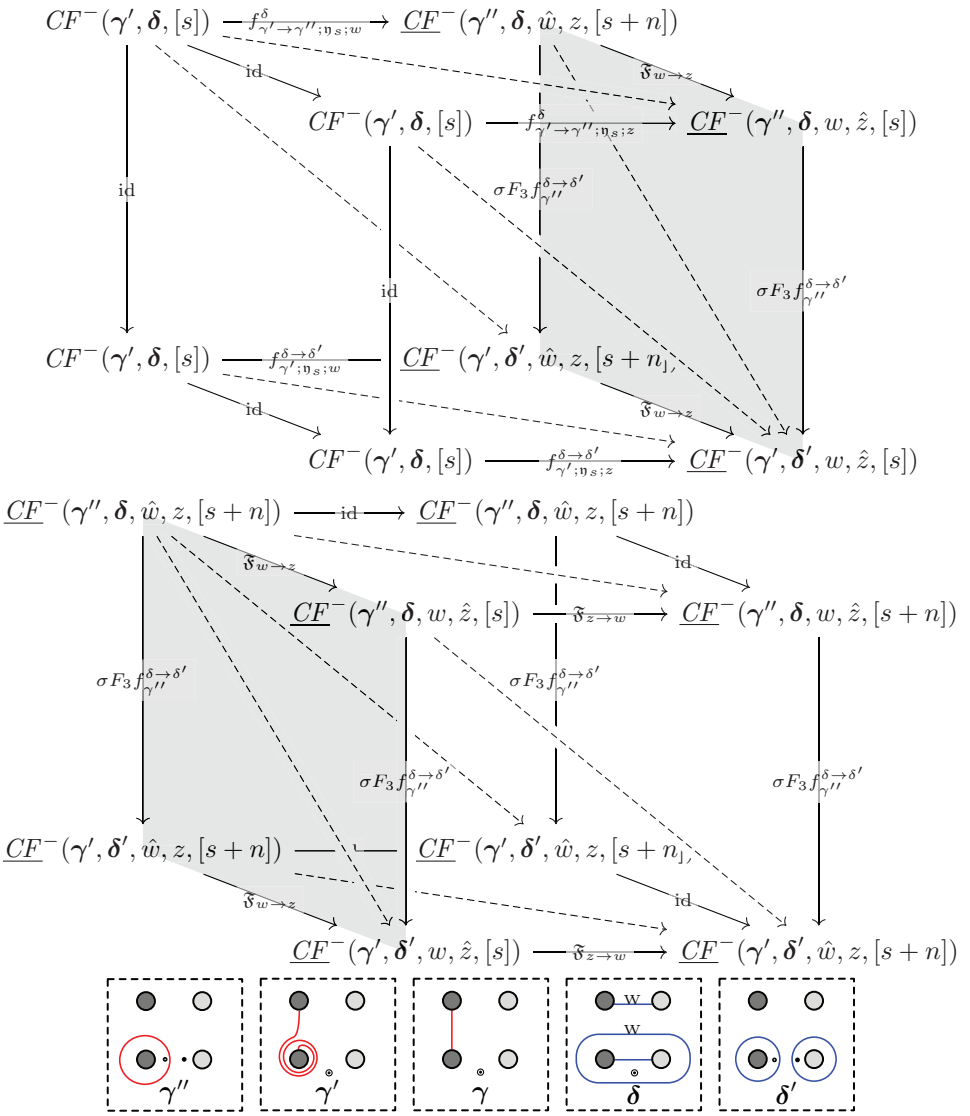


FIGURE 21.12. The hypercubes $\mathcal{K}^{(1),1}_{\mathrm{cen};\mathfrak{y}_s}$ (top) and $\mathcal{K}^{(1),2}_{\mathrm{cen};\mathfrak{y}_s}$ (middle). Both cubes have a length 3 arrow which is not drawn. The cubes are stacked along the gray faces. On the bottom are the attaching curves in the surgery region.

to $\mathbb{F}[U]$. Since M is a chain map and has grading $+1$, it must be chain homotopic to 0. We let Z by any homogeneously graded map satisfying

$$[\partial, Z] = M.$$

Finally, we consider the hypercube $\mathcal{Y}^{(1)}_l$, which is shown in Figure 21.14. In this hypercube, we use the same length 2 map along the right face as along the bottom face. This map was constructed in $\mathcal{Y}^{(2)}_r$.

This is a free offprint provided to the author by the publisher. Copyright restrictions may apply.

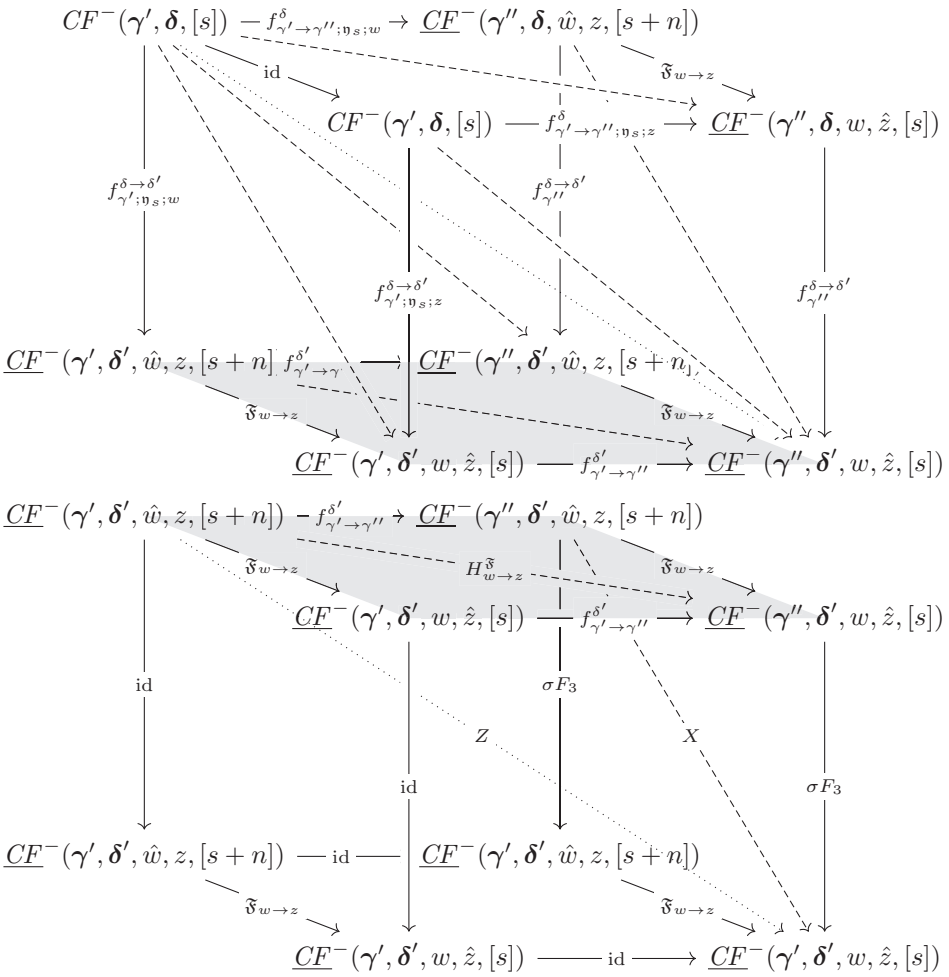


FIGURE 21.13. The hypercube $\mathcal{Y}^{(1)}_r$ is the compression of these two hypercubes, stacked vertically.

REMARK 21.2. The construction of the maps X and Z in $\mathcal{Y}^{(1)}_r$, shown in Figure 21.13, is unusual in that we used the fact that Y was an L-space to algebraically determine the existence of two maps. It does not seem possible to construct these maps by compressing a hypercube analogously to our construction of the flip-map hypercube. The challenge is that the map $\mathfrak{F}_{w \to z}$ on the top right of the bottom cube in Figure 21.13 involves moving w to z along a path which goes through a 3-handle region. See Figure 21.15. The natural algebraic relation involving the 3-handle map does not follow from the framework of stabilizations in Chapter 9.

21.5. The hypercube $\mathcal{K}^{(2)}_{\mathrm{cen};\mathfrak{y}_s}$

We construct $\mathcal{K}^{(2)}_{\mathrm{cen};\mathfrak{y}_s}$ by stacking and compressing 4 hypercubes, $\mathcal{K}^{(2),j}_{\mathrm{cen};\mathfrak{y}_s}$, for $j \in \{1,2,3,4\}$, similarly to Figure 21.7. As in the previous section, we focus on

This is a free offprint provided to the author by the publisher. Copyright restrictions may apply.

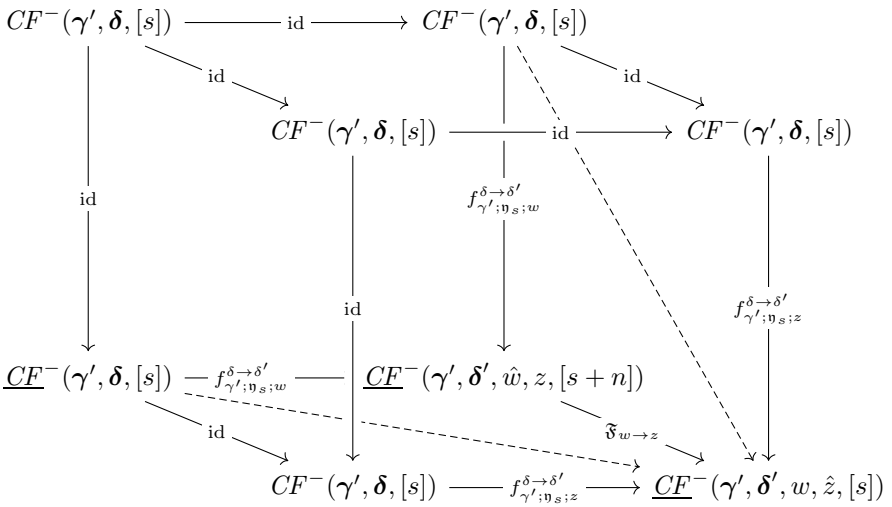


FIGURE 21.14. The hypercube $\mathcal{Y}_l^{(1)}$. The length 2 maps along the bottom and right side coincide, and there is no length 3 map.

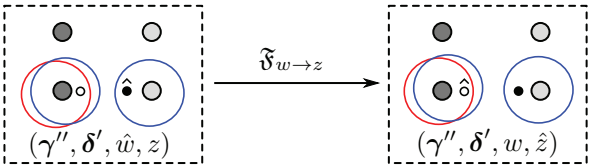


FIGURE 21.15. Moving w to z through the 3-handle region, in the hypercube $\mathcal{Y}_r^{(1)}$. See Remark 21.2.

the hypercubes $\mathcal{K}^{(2),1}_{\mathrm{cen};\mathfrak{y}_s}$ and $\mathcal{K}^{(2),2}_{\mathrm{cen};\mathfrak{y}_s}$. We illustrate these two cubes schematically in Figure 21.16.

The hypercube $\mathcal{K}^{(2),1}_{\mathrm{cen};\mathfrak{y}_s}$ is constructed as the compression of the hyperbox shown in Figure 21.17. We write $\mathcal{Y}_0^{(2)}$ for the top hypercube, therein, and $\mathcal{Y}_1^{(2)}$ for the bottom. The hypercube $\mathcal{Y}_0^{(2)}$ is defined as a compression of a hypercube of size $(1, 5, 1)$, similar to the flip-map hypercube. In the hyperbox for $\mathcal{Y}_0^{(2)}$, there is one hypercube built using θ_w, one using the tautological diffeomorphism map, one hypercube for winding $\boldsymbol{\delta}''$, one cube for unwinding $\boldsymbol{\delta}''$, and a final hypercube involving θ_z.

The hypercube $\mathcal{Y}_1^{(2)}$ is defined by stacking and compressing several hypercubes for destabilization, as we now describe. Since the hypercube $\mathcal{Y}_0^{(2)}$ is the compression of hyperbox of size $(1, 5, 1)$, the bottom face of $\mathcal{Y}_0^{(2)}$ is the compression of a hyperbox of size $(1, 5)$. Each of the 3-dimensional hypercubes comprising $\mathcal{Y}_0^{(2)}$ has along its bottom face only complexes which have a special genus 1 region representing $S^1 \times S^2$, S^3, or $L(m, 1)$. Furthermore, since the canonical path connecting w and z does not cross any of the curves in the special genus 1 region, we may assume that the special genus 1 region is standard for each complex appearing in the construction of the bottom face of $\mathcal{Y}_0^{(2)}$. For each cube used to build $\mathcal{Y}_0^{(2)}$, we

This is a free offprint provided to the author by the publisher. Copyright restrictions may apply.

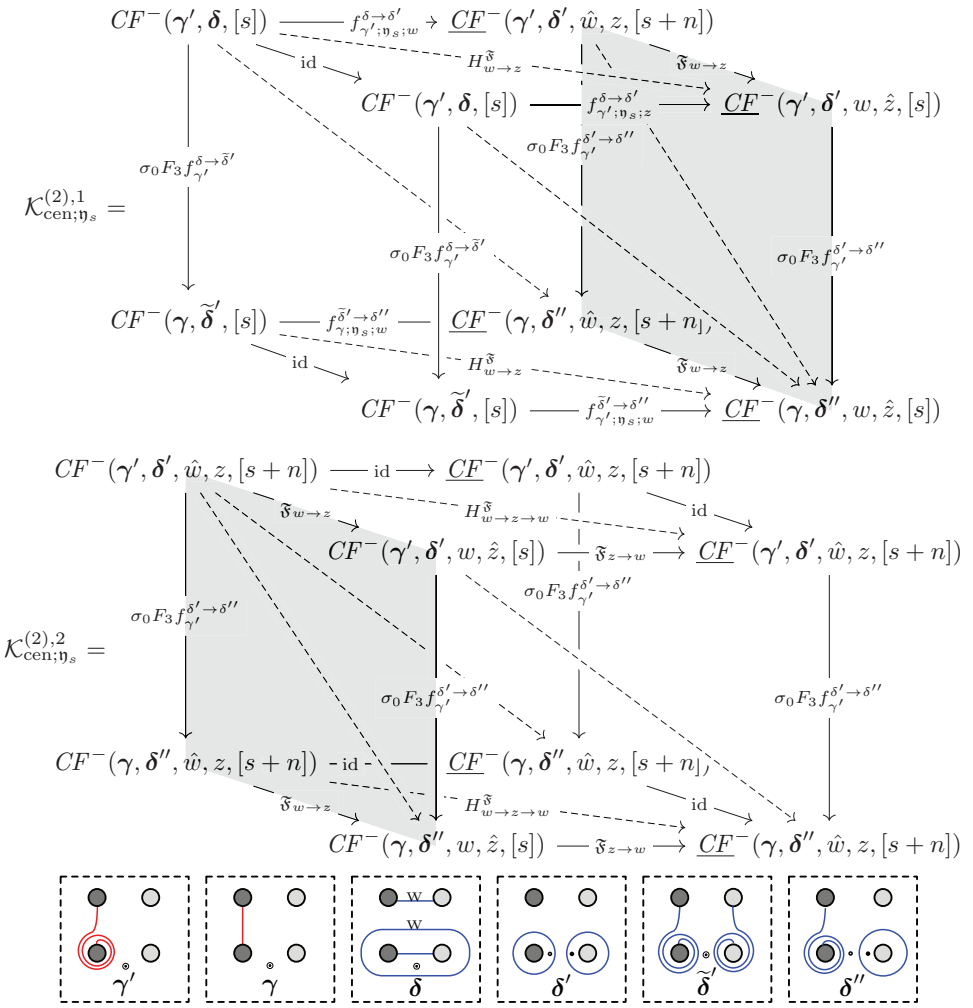


FIGURE 21.16. The hypercubes $\mathcal{K}^{(2),1}_{\mathrm{cen};\mathfrak{y}_s}$ and $\mathcal{K}^{(2),2}_{\mathrm{cen};\mathfrak{y}_s}$. Both have a length 3 arrow (not shown).

build a corresponding hypercube of destabilization in $\mathcal{Y}^{(2)}_1$. The maps along the top face of each of these cubes for $\mathcal{Y}^{(2)}_1$ coincide with the maps appearing along the bottom of the corresponding hypercube used for $\mathcal{Y}^{(2)}_0$. The maps along the bottom are given by the same set of moves used for $\mathcal{Y}^{(2)}_0$, but applied to the diagram obtained by removing the 3-handle region and adding a lens-space stabilization. The length 1 vertical maps are all $\sigma_0 F_3$. Propositions 10.2 and 10.6 imply that the resulting diagram satisfies the hyperbox relations. Finally $\mathcal{Y}^{(2)}_1$ is defined as the compression of this hyperbox of size $(1, 5, 1)$.

The construction of $\mathcal{K}^{(2),2}_{\mathrm{cen};\mathfrak{y}_s}$, shown on the bottom of Figure 21.16, follows from a similar construction. The hypercubes $\mathcal{K}^{(2),3}_{\mathrm{cen};\mathfrak{y}_s}$ and $\mathcal{K}^{(2),4}_{\mathrm{cen};\mathfrak{y}_s}$ are not substantially

This is a free offprint provided to the author by the publisher. Copyright restrictions may apply.

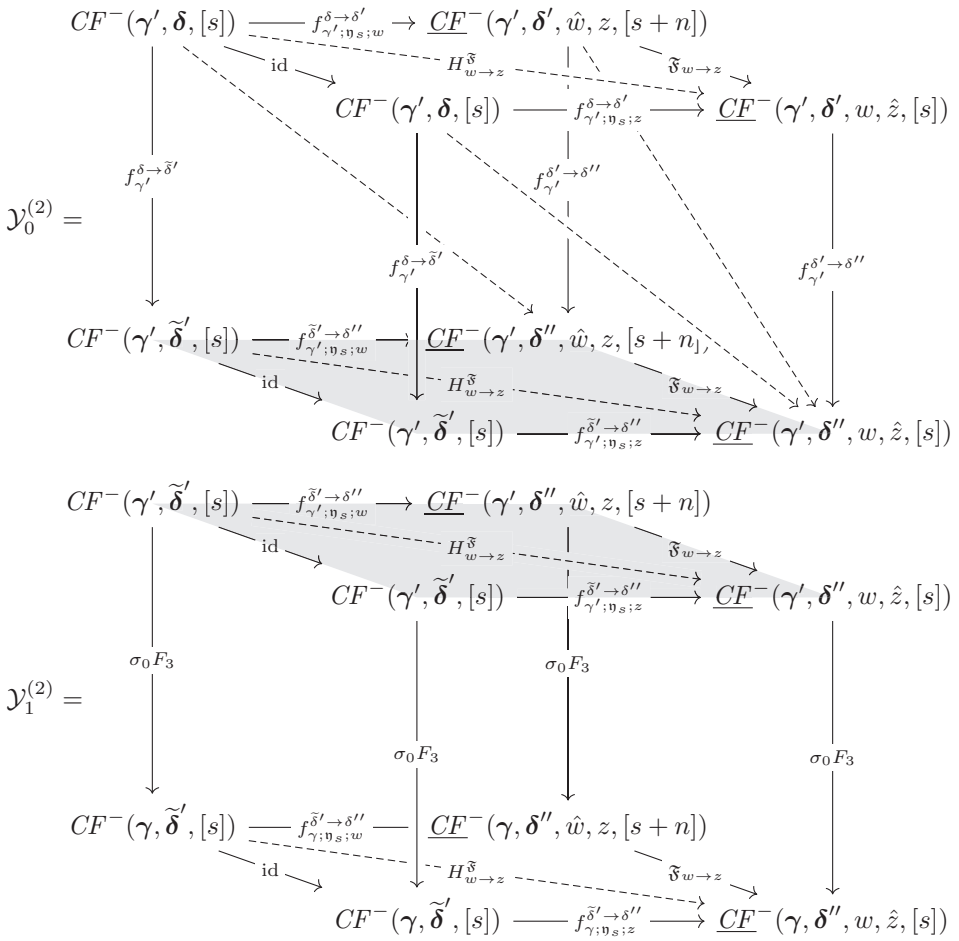


FIGURE 21.17. A hyperbox whose compression is $\mathcal{K}^{(2),1}_{\mathrm{cen};\mathfrak{y}_s}$. The hypercube $\mathcal{Y}_0^{(2)}$ has a length 3 arrow (not shown), whereas $\mathcal{Y}_1^{(2)}$ does not.

different than the corresponding hypercubes of $\mathcal{K}^{1,3}_{\text{2-h};\mathfrak{y}_s}$ and $\mathcal{K}^{1,4}_{\text{2-h};\mathfrak{y}_s}$, shown in Figure 21.7.

21.6. The hypercube $\mathcal{K}^{(3)}_{\mathrm{cen};\mathfrak{y}_s}$

Similar to $\mathcal{K}^{(1)}_{\mathrm{cen};\mathfrak{y}_s}$ and $\mathcal{K}^{(2)}_{\mathrm{cen};\mathfrak{y}_s}$, the hypercube $\mathcal{K}^{(3)}_{\mathrm{cen};\mathfrak{y}_s}$ is defined by stacking and compressing four hypercubes $\mathcal{K}^{(3),j}_{\mathrm{cen};\mathfrak{y}_s}$, for $j \in \{1,2,3,4\}$. The construction is similar to $\mathcal{K}^{(2)}_{\mathrm{cen};\mathfrak{y}_s}$, so we focus on $\mathcal{K}^{(3),1}_{\mathrm{cen};\mathfrak{y}_s}$, and leave the other three hypercubes to the reader. Recall that $\mathcal{C}^{(3)}_{\mathrm{cen}}$ is defined by stacking $\mathcal{C}^{(3)}_{\mathrm{aux},\Pi^{\mathrm{can}}}$ and a hypercube for destabilization $\mathcal{C}^{(3)}_{\text{cen,3-h}}$. The hypercube $\mathcal{K}^{(3),1}_{\mathrm{cen};\mathfrak{y}_s}$ is the compression of the hyperbox shown in Figure 21.18.

The hypercubes in Figure 21.18 are each constructed as the compression of a hypercube of size $(1,4,1)$, similar to the ones appearing in the construction of

This is a free offprint provided to the author by the publisher. Copyright restrictions may apply.

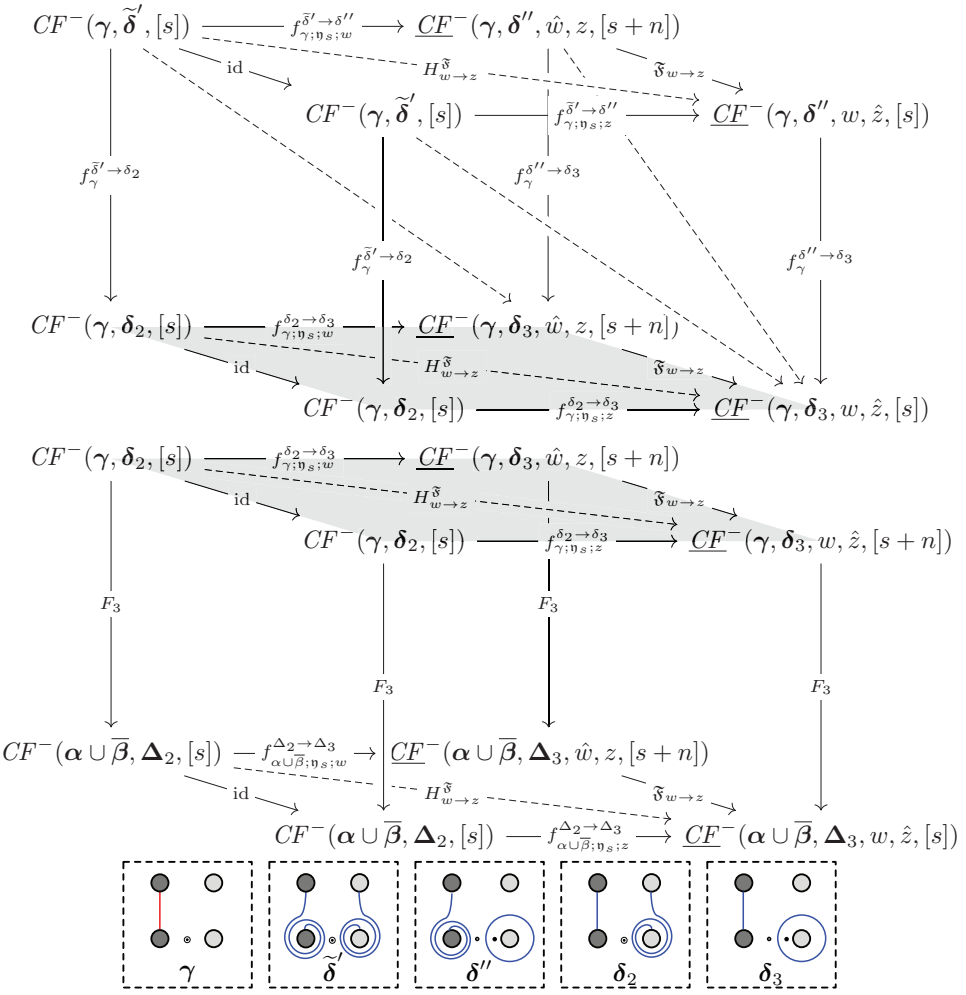


FIGURE 21.18. The two hypercubes used to build $\mathcal{K}^{(3),1}_{\mathrm{cen};\mathfrak{y}_s}$. The cubes are stacked along the gray faces.

the cube $\mathcal{K}^{(2),1}_{\mathrm{cen};\mathfrak{y}_s}$. The construction of the hypercube $\mathcal{K}^{(3),2}_{\mathrm{cen};\mathfrak{y}_s}$ follows from the same line of reasoning used to construct the hypercube $\mathcal{K}^{(2),2}_{\mathrm{cen};\mathfrak{y}_s}$. Hypercubes $\mathcal{K}^{(3),3}_{\mathrm{cen};\mathfrak{y}_s}$ and $\mathcal{K}^{(3),4}_{\mathrm{cen};\mathfrak{y}_s}$ are constructed similarly.

21.7. The hypercubes $\mathcal{K}_{\eta;\mathfrak{y}_s}$ and $\mathcal{K}_{\mathfrak{F};\mathfrak{y}_s}$

We now construct the hypercube $\mathcal{K}_{\eta;\mathfrak{y}_s}$. We define it to be the compression of the hyperbox of size $(2, 2, 1)$ shown in Figure 21.19.

Next, we consider the hypercube $\mathcal{K}_{\mathfrak{F};\mathfrak{y}_s}$. It is obtained by compressing the hyperbox described schematically in Figure 21.20.

We now explain the maps appearing in Figure 21.20. The length 2 maps in the top left cube are constructed in the flip-map hypercube. The map along the top and the map along the back are equal. The hypercube relations are clearly

This is a free offprint provided to the author by the publisher. Copyright restrictions may apply.

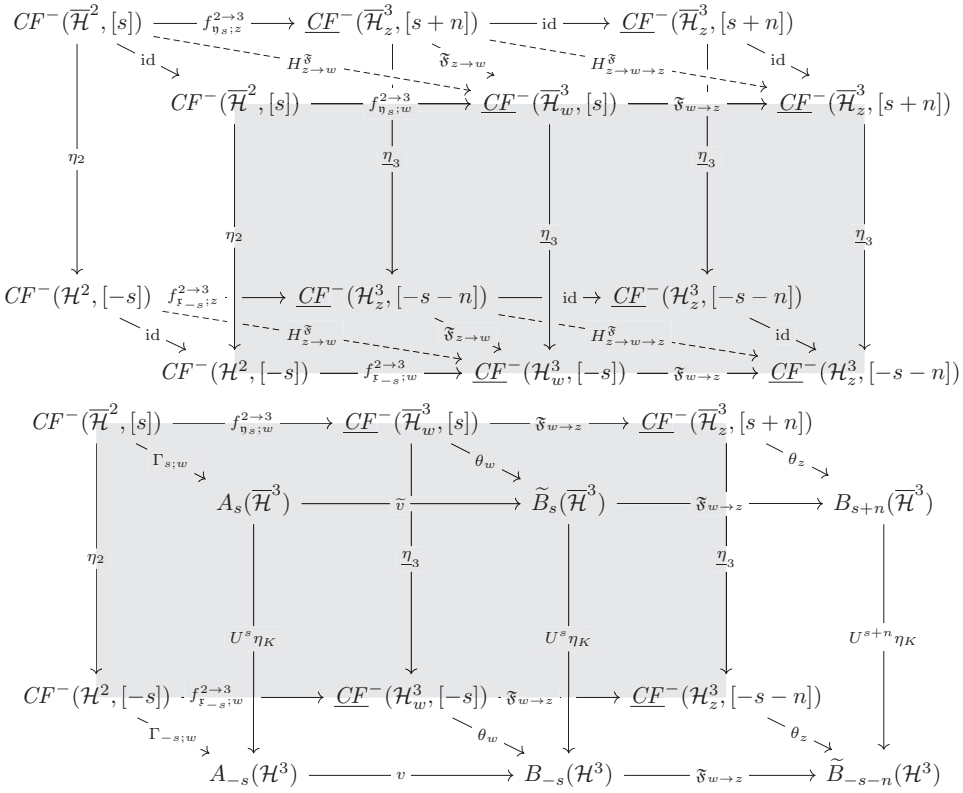


FIGURE 21.19. The hypercube $\mathcal{K}_{\eta;\mathfrak{y}_s}$ is obtained by compressing the above hypercube. The gray faces indicate how the hyperboxes are stacked.

satisfied. The length 2 and 3 maps in the top right cube are constructed in the same manner as those appearing in $\mathcal{K}^2_{\mathfrak{F};\mathfrak{x}_s}$. See Figure 21.5. The bottom left and right cubes of Figure 21.20 are tautological.

This is a free offprint provided to the author by the publisher. Copyright restrictions may apply.

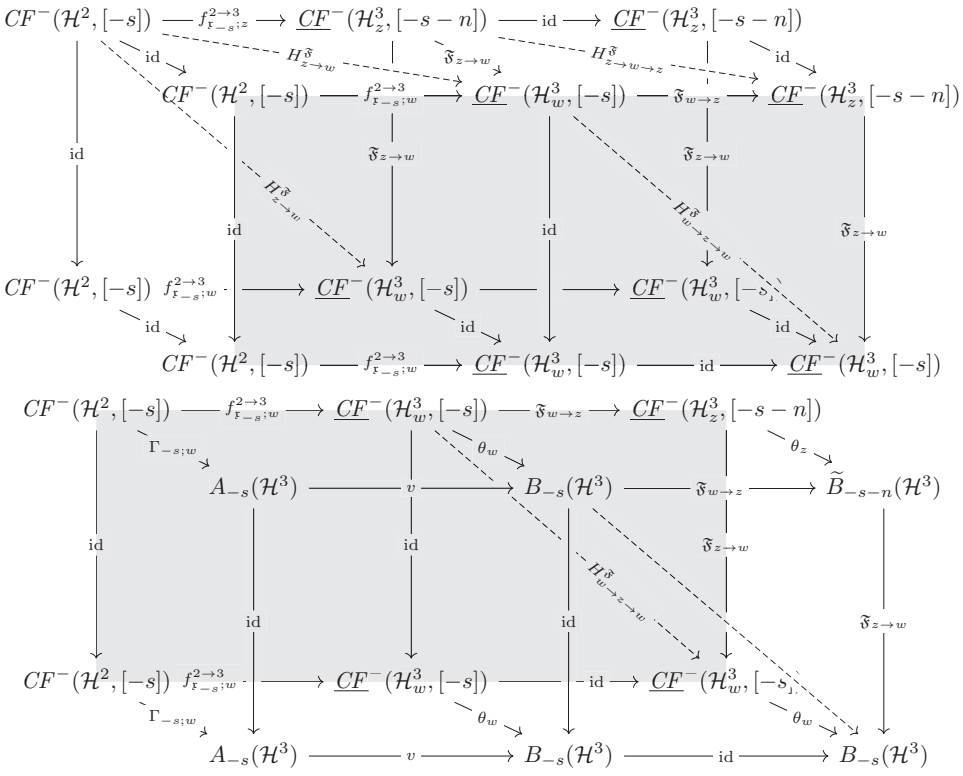


FIGURE 21.20. The hypercube $\mathcal{K}_{\mathfrak{F};\mathfrak{y}_s}$ is obtained by compressing this hyperbox. The gray faces are stacked. The hypercube $\mathcal{K}^2_{\mathfrak{F};\mathfrak{y}_s}$ has a length 3 map, which is not shown, while the other three hypercubes do not.

This is a free offprint provided to the author by the publisher. Copyright restrictions may apply.

This is a free offprint provided to the author by the publisher. Copyright restrictions may apply.

CHAPTER 22

Rational surgeries and 0-surgeries

In this chapter, we prove a version of the involutive surgeries formula for Morse surgeries on rationally null-homologous knots, and as an application, for rational surgeries on knots in S^3. We begin with some basic topology, then state the involutive mapping cone formula in these cases and describe how the proofs differ from the arguments for null-homologous knots. In Section 22.9, we describe a version of the mapping cone formula for 0-surgeries.

22.1. Rationally null-homologous knots

In this section, we describe a few basic topological notions related to rationally null-homologous knots.

Suppose Y is a rational homology 3-sphere and $K \subseteq Y$ is a knot, which has order $d > 0$ in $H_1(Y;\mathbb{Z})$. A *rational Seifert surface* for K is an integral 2-chain F satisfying

$$\partial F = d \cdot [K].$$

We now describe $H_1(Y \setminus K;\mathbb{Z})$. There is a Meyer-Vietoris exact sequence

$$0 \to \mathbb{Z} \xrightarrow{\sigma} H_1(Y \setminus K) \to H_1(Y) \to 0, \tag{22.1}$$

where $\sigma(n) = n \cdot \mu$ and μ is a meridian. Using a rational Seifert surface F, we obtain a map

$$\ell\colon H_1(Y \setminus K) \to \mathbb{Q}$$

given by $\ell(x) = \#(x \cap F)/d$. Note that $\ell \circ \sigma$ gives the standard inclusion of $\mathbb{Z}$ into $\mathbb{Q}$. We obtain an embedding of groups

$$(\ell, i)\colon H_1(Y \setminus K) \to \mathbb{Q} \oplus H_1(Y), \tag{22.2}$$

where i is the inclusion of $H_1(Y \setminus K)$ into $H_1(Y)$. We can explicitly describe the image of (ℓ, i). If $h \in H_1(Y)$, let $\hat{h} \in H_1(Y \setminus K)$ be any lift. We define

$$\hat{A}(h) := [\#(\hat{h} \cap F)/d] \in \mathbb{Q}/\mathbb{Z}. \tag{22.3}$$

The quantity $\hat{A}(h)$ is well defined in $\mathbb{Q}/\mathbb{Z}$, since $\hat{h}$ is well-defined up to addition of an integral multiple of μ, and $\ell(x + \mu) = \ell(x) + 1$. The image of (ℓ, i) consists of all pairs (t, h) where $t \in \hat{A}(h)$ viewed as a subset of $\mathbb{Q}$.

Next, we discuss surgeries on rationally null-homologous knots. We say a framing is *Morse* if it is induced by a simple closed curve on $\partial N(K)$ which intersects the meridian exactly once. For null-homologous knots in an integer homology sphere, there is a canonical identification of the set of Morse framings with $\mathbb{Z}$. For rationally null-homologous knots, the set of Morse framings is canonically identified with $\hat{A}([K])$, viewed as a subset of $\mathbb{Q}$. The correspondence is given by

$$\lambda \mapsto \#(\lambda \cap F)/d. \tag{22.4}$$

This is a free offprint provided to the author by the publisher. Copyright restrictions may apply.

Suppose λ is a Morse framing. Write $W_\lambda(K)\colon Y \to Y_\lambda(K)$ for the corresponding 2-handle cobordism, and write $W'_\lambda(K)\colon Y_\lambda(K) \to Y$ for the 2-handle cobordism with the opposite orientation. Applying Mayer-Vietoris to the attaching region in Y, we obtain an exact sequence

$$0 \to \mathbb{Z} \to H^2(W'_\lambda(K)) \to H^2(Y) \to 0, \tag{22.5}$$

where $\mathbb{Z}$ acts by the Poincaré dual of the co-core of the 2-handle. Similar to (22.2), we obtain an embedding

$$H^2(W'_\lambda(K)) \to \mathbb{Q} \oplus H^2(Y), \tag{22.6}$$

by combining the restriction from $H^2(W'_\lambda(Y)) \to H^2(Y)$ with the map $H^2(W'_\lambda(K)) \to \mathbb{Q}$ given by

$$\eta \mapsto \langle \eta, \hat{\Sigma}_d \rangle / d.$$

Here, $\hat{\Sigma}_d$ is the surface obtained by taking d copies of the core Σ of the 2-handle and capping using a rational Seifert surface.

Since $W'_\lambda(K)$ is also obtained by attaching a 2-handle to $Y_\lambda(K)$, we analogously obtain an exact sequence

$$0 \to \mathbb{Z} \to H^2(W'_\lambda(K)) \to H^2(Y_\lambda(K)) \to 0, \tag{22.7}$$

where $\mathbb{Z}$ now acts by the Poincaré dual of the core of the 2-handle which is attached to K. Combining (22.6) we obtain the description

$$H^2(Y_\lambda(K)) \cong H^2(W'_\lambda(K))/(-\lambda, PD[K]),$$

where we view $H^2(W'_\lambda(K))$ as being a subgroup $\mathbb{Q} \oplus H^2(Y)$.

22.2. Spin^c structures

Similar to (22.5), there is an exact sequence of affine spaces

$$0 \to \mathbb{Z} \to \mathrm{Spin}^c(W'_\lambda(K)) \to \mathrm{Spin}^c(Y) \to 0. \tag{22.8}$$

The fiber of the map from $\mathrm{Spin}^c(W'_\lambda(K))$ to $\mathrm{Spin}^c(Y)$ is generated by the Poincaré dual to the co-core of the 2-handle. There is a natural map $A\colon \mathrm{Spin}^c(W'_\lambda(K)) \to \mathbb{Q}$, given by

$$A(\mathfrak{s}) = \frac{\langle c_1(\mathfrak{s}), [\hat{\Sigma}_d] \rangle - [\Sigma] \cdot [\hat{\Sigma}_d]}{2d}, \tag{22.9}$$

where Σ denotes the core of the 2-handle, and $\hat{\Sigma}_d$ denotes $d[\Sigma]$, capped off using a rational Seifert surface. We obtain an embedding

$$\mathrm{Spin}^c(W'_\lambda(K)) \to \mathbb{Q} \times \mathrm{Spin}^c(Y), \tag{22.10}$$

where $\mathfrak{s} \mapsto (A(\mathfrak{s}), \mathfrak{s}|_Y)$.

We write

$$\mathbb{H}(Y, K) \subseteq \mathbb{Q} \times \mathrm{Spin}^c(Y)$$

for the image of the above embedding. We can describe $\mathbb{H}(Y, K)$ more explicitly. There is a map

$$\hat{A}\colon \mathrm{Spin}^c(Y) \to \mathbb{Q}/\mathbb{Z}, \tag{22.11}$$

obtained by lifting $\mathfrak{s}$ to an element $\mathfrak{u} \in \mathrm{Spin}^c(W'_\lambda(K))$, and setting $\hat{A}(\mathfrak{s}) = A(\mathfrak{u})$. Since adding the Poincaré dual of the co-core of the 2-handle changes L by ± 1, the coset $\hat{A}(\mathfrak{s})$ is well-defined. The image of the map in (22.10) consists of all pairs $(t, \mathfrak{s})$

This is a free offprint provided to the author by the publisher. Copyright restrictions may apply.

where $t \in \hat{A}(\mathfrak{s})$. We write $\mathfrak{u}_{t,\mathfrak{s}}$ for the Spin^c structure on $W'_\lambda(K)$ corresponding to the pair $(t, \mathfrak{s}) \in \mathbb{Q} \times \mathrm{Spin}^c(Y)$.

The set $\mathbb{H}(Y, K)$ is independent of the framing λ. In fact, from the construction of the absolute gradings on $\mathcal{CFK}^-(Y, K)$ (cf. Section 22.5), it is immediate that the Alexander grading on $\mathcal{CFK}^-(Y, K, \mathfrak{s})$ takes values in in $t_0 + \mathbb{Z}$, where t_0 is any element of $\mathbb{Q}$ in the fiber over $\mathfrak{s}$ in the exact sequence of (22.8). (A purely topological proof of this fact may be given by tracing through the proof of the well-definedness of the absolute gradings in [**OS03**]).

Similar to (22.8), there is an exact sequence

$$0 \to \mathbb{Z} \to \mathrm{Spin}^c(W'_\lambda(K)) \to \mathrm{Spin}^c(Y_\lambda(K)) \to 0,$$

where now $\mathbb{Z}$ acts by the Poincaré dual to the core of the 2-handle attached along $K \subseteq Y$. In terms of the embedding in (22.10), the Poincaré dual of the core acts on Spin$^c(Y)$ by $PD[K]$, and on $\mathbb{Q}$ by $\langle PD[\Sigma], \hat{\Sigma}_d\rangle/d = \#(K \cap -F) = -\lambda$. Hence, Spin$^c(Y_\lambda(K))$ is isomorphic to the quotient of $\mathbb{H}(Y, K)$ by the action of $(-\lambda, PD[K])$.

The first Chern class has a simple description in this framework. Namely, if $(t, \mathfrak{s}) \in \mathbb{H}(Y, K)$ and $\mathfrak{u}_{t,\mathfrak{s}} \in \mathrm{Spin}^c(W'_\lambda(K))$ is the corresponding Spin^c structure, then we can rearrange (22.9) to obtain

$$\frac{\langle c_1(\mathfrak{u}_{t,\mathfrak{s}}), [\hat{\Sigma}_d]\rangle}{d} = 2t - \lambda. \tag{22.12}$$

Hence

$$c_1^2(\mathfrak{u}_{t,\mathfrak{s}}) = \frac{(2t-\lambda)^2}{\lambda}. \tag{22.13}$$

In terms of the embedding in (22.10), the conjugation action on $\mathbb{H}(Y, K)$ has the following description:

$$(t, \mathfrak{s}) \mapsto (-t + \lambda, \overline{\mathfrak{s}}). \tag{22.14}$$

There are two families of Spin^c structures on $W'_\lambda(K)$: $Y_\lambda(K) \to Y$ which we are interested in when λ is large. Each element $\mathfrak{t} \in \mathrm{Spin}^c(Y_\lambda(K)) \cong \mathbb{H}(Y, K)/(-\lambda, PD[K])$ has a unique representative $(t_0, \mathfrak{s}_0)$, where $-\lambda/2 < t_0 \leq \lambda/2$. Furthermore, any other Spin^c structure on $W'_\lambda(K)$ which restricts to $\mathfrak{t}$ has the form $(t_0 + k\lambda, \mathfrak{s}_0 - kPD[K])$, for an integer k. We define

$$\mathfrak{x}_\mathfrak{t} = (t_0, \mathfrak{s}_0), \quad \text{and} \quad \mathfrak{y}_\mathfrak{t} = (t_0 + \lambda, \mathfrak{s}_0 - PD[K]).$$

The following is a restatement of [**OS11**, Proposition 4.2] using our present notation:

LEMMA 22.1. *Suppose that K is a rationally null-homologous knot in Y, and C is a fixed number. The following hold:*

(1) *If λ is a sufficiently large Morse framing on K, then the* Spin^c *structures $\mathfrak{x}_\mathfrak{t}$ and $\mathfrak{y}_\mathfrak{t}$ realize the maximal and second maximal squares over all* Spin^c *structures on $W'_\lambda(K)$ which restrict each $\mathfrak{t} \in \mathrm{Spin}^c(Y_\lambda(K))$. Furthermore,*

$$c_1(\mathfrak{z})^2 \leq \max\{c_1^2(\mathfrak{x}_\mathfrak{t}), c_1^2(\mathfrak{y}_\mathfrak{t})\} - C,$$

whenever $\mathfrak{z}|_{Y_\lambda(K)} = \mathfrak{t}$ and $\mathfrak{z} \notin \{\mathfrak{x}_\mathfrak{t}, \mathfrak{y}_\mathfrak{t}\}$.

This is a free offprint provided to the author by the publisher. Copyright restrictions may apply.

(2) *There is a number b such that if $t_0 < -b$ or $b < t_0$ and λ is sufficiently large, then*

$$C \leq \max\{c_1^2(\mathfrak{x}_\mathfrak{t}), c_1^2(\mathfrak{y}_\mathfrak{t})\} - \min\{c_1^2(\mathfrak{x}_\mathfrak{t}), c_1^2(\mathfrak{y}_\mathfrak{t})\},$$

whenever $(t_0, \mathfrak{s}) \in \mathbb{H}(Y, K)$ is the unique representative of $\mathfrak{t}$ with $-\lambda/2 < t_0 \leq \lambda/2$.

PROOF. Suppose $\mathfrak{t} \in Y_\lambda(K)$, and let $(t_0, \mathfrak{s})$ be the unique extension to $W'_\lambda(K)$ with $-\lambda/2 < t_0 \leq \lambda/2$. Any other Spin^c structure on W'_λ which restricts to $\mathfrak{t}$ may be written as $(t_0 + s\lambda, \mathfrak{s} + s \cdot PD[K])$, for some $s \in \mathbb{Z}$. Equation (22.13) implies that

$$c_1^2(t_0 + s\lambda, \mathfrak{s}_0 + sPD[K]) = -\frac{(2t_0 + (2s-1)\lambda)^2}{\lambda}.$$

Ranging over all real x, the function $-(2t_0 + x\lambda)^2$ is a quadratic which is maximized at $x = -2t_0/\lambda$, which by assumption lies in the half open interval $(-1, 1]$. Ranging only over odd integers x, the quadratic function $-(2t_0 + x\lambda)^2$ will take on its two largest values at $x = -1$ and $x = 1$, which correspond to $s = 0$ and $s = 1$. These two values themselves correspond to $\mathfrak{x}_\mathfrak{t}$ and $\mathfrak{y}_\mathfrak{t}$, respectively.

For the stated inequality, suppose first that $t_0 \leq 0$. Then the Spin^c structures with maximal and third to maximal squares are $(t_0, \mathfrak{s})$ and $(t_0 - \lambda, \mathfrak{s} + PD[K])$. Using (22.13), the drop in c_1^2 between these two Spin^c structures is

$$-\frac{(2t_0 - \lambda)^2}{\lambda} + \frac{(2t_0 - 3\lambda)^2}{\lambda} = 8(\lambda - t_0) \geq 4\lambda. \tag{22.15}$$

Similarly, if $t_0 \geq 0$, then the maximal and third to maximal Spin^c structures are $(t_0 + \lambda, \mathfrak{s} - PD[K])$ and $(t_0 + 2\lambda, \mathfrak{s} - 2PD[K])$, the difference of whose squares is

$$-\frac{(2t_0 + \lambda)^2}{\lambda} + \frac{(2t_0 + 3\lambda)^2}{\lambda} = 8(\lambda + t_0) \geq 4\lambda. \tag{22.16}$$

Combining (22.15) and (22.16) easily gives the stated inequality, for sufficiently large λ.

If $t_0 > 0$, then the maximal square is achieved by $\mathfrak{y}_\mathfrak{t}$, and the second maximal is obtained by $\mathfrak{x}_\mathfrak{t}$.

Hence,

$$\begin{aligned} c_1^2(\mathfrak{y}_\mathfrak{t}) - c_1^2(\mathfrak{x}_\mathfrak{t}) =& \frac{(2t_0 + \lambda)^2}{\lambda} - \frac{(2t_0 - \lambda)^2}{\lambda} \\ =& 8t_0. \end{aligned} \tag{22.17}$$

If $t_0 < 0$, then the maximal Spin^c structure is $\mathfrak{x}_\mathfrak{t}$, and the second maximal is $\mathfrak{y}_\mathfrak{t}$. Arguing as in (22.17) shows that $c_1^2(\mathfrak{x}_\mathfrak{t}) - c_1^2(\mathfrak{y}_\mathfrak{t}) = -8t_0$. Combining these, we obtain

$$\max\{c_1^2(\mathfrak{x}_\mathfrak{t}), c_1^2(\mathfrak{y}_\mathfrak{t})\} - \min\{c_1^2(\mathfrak{x}_\mathfrak{t}), c_1^2(\mathfrak{y}_\mathfrak{t})\} = 8|t_0|.$$

Setting $b = C/8$ gives the main claim. □

22.3. The cobordism $W_{\lambda,\lambda+m}$

Suppose K is a knot in a rational homology 3-sphere Y, and let K' and K'' denote two unknots, so that K' is unlinked from K, but K'' links both, as in Figure 20.2. Let $L = K \cup K' \cup K''$ and let $\Lambda = (\lambda, m, 0)$ denote a Morse framing on L, where m is a positive integer. We can view the cobordism $W_{\lambda,\lambda+m}$ as going from $Y_\lambda(K) \# L(m, 1)$ to $Y_{\lambda+m}(K)$, and being obtained by surgery on K'', after already having performed surgery on K and K'.

This is a free offprint provided to the author by the publisher. Copyright restrictions may apply.

Let D' and D'' be Seifert disks of K' and K'', and let F be a rational Seifert surface of K. Let $d>0$ be the order of K in $H_1(Y;\mathbb{Z})$.

We obtain classes $\hat{F}$, $\hat{D}'$, and $\hat{D}''$ in the surgery cobordism $W_\Lambda(L)$ by capping F, D', and D'' with the core of 2-handles. These form a basis of $H_2(W_\Lambda(L);\mathbb{Z})$. The intersection form is clearly

$$Q=\begin{pmatrix} d^2\lambda & 0 & d\\ 0 & m & 1\\ d & 1 & 0\end{pmatrix}$$

The homology of $H_2(W_{\lambda,\lambda+m};\mathbb{Z})$ is the orthogonal complement (over $\mathbb{Z}$) of the span of the first two basis elements. The orthogonal complement is spanned by the vector

$$\hat{\Sigma}=\begin{pmatrix} m/g\\ d\lambda/g\\ -d\lambda m/g\end{pmatrix},$$

where $g=\gcd(m,d\lambda)$. Clearly,

$$\hat{\Sigma}^2=-\frac{d\lambda m(dm+d\lambda)}{g^2}.$$

We now wish to consider gradings on the cobordism map, which will be helpful to prove that the vertical truncation of the main hypercube is homogeneously graded for both positive and negative framings λ.

LEMMA 22.2. *There is a C, such that for all large m and all $\mathfrak{s}\in\mathrm{Spin}^c(Y_{\lambda+m}(K))$, the homogeneous elements of $CF^\delta(Y_{\lambda+m}(K),\mathfrak{t})$ have gradings which lies in the interval $[-C,\frac{\lambda+m}{4}+C]$.*

PROOF. Using the large surgeries theorem [**OS11**, Proposition 4.2], it follows that there is a $C>0$ such that the homogeneous elements of $CF^\delta(Y_{\lambda+m}(K),\mathfrak{t})$ have grading which fall within C of

$$-\max\{(c_1(\mathfrak{u})^2+1)/4:\mathfrak{u}\in\mathrm{Spin}^c(W'_{\lambda+m}(K),\mathfrak{u}|_{Y_{\lambda+m}}=\mathfrak{t}\}.$$

The Chern classes with maximal and second to maximal square are $\mathfrak{x}_\mathfrak{t}$ and $\mathfrak{y}_\mathfrak{t}$, which have squares

$$c_1(\mathfrak{x}_\mathfrak{t})^2=-\frac{(2t_0-\lambda-m)^2}{\lambda+m}\quad\text{and}\quad c_1(\mathfrak{y}_\mathfrak{t})^2=-\frac{(2t_0+\lambda-m)^2}{\lambda+m},$$

where $-(\lambda+m)/2<t_0\le(\lambda+m)/2$. Assuming m is sufficiently large, the maximum of these two quantities always lies in the interval $[-(\lambda+m),0]$, implying the main statement. □

The following is very similar to [**OS11**, Lemma 6.7] (the only difference is that it is stated for negative surgeries as well as positive):

LEMMA 22.3. *Suppose $\lambda\neq0$ and C is some fixed number. For all m sufficiently large, each* Spin^c *structure on $\partial W_{\lambda,\lambda+m}$ has at most one extension $\mathfrak{u}$ to $W_{\lambda,\lambda+m}(K)$ such that $(c_1^2(\mathfrak{u})+m)/4$ lies in the interval $[-C,(\lambda+m)/4+C]$.*

PROOF. The proof is naturally broken into cases, depending on the sign of λ. We consider negative λ first. If λ is negative, the cobordism $W_{\lambda,\lambda+m}$ is positive definite, so it is sufficient to show that for each Spin^c structure on $\partial W_{\lambda,\lambda+m}(K)$, there is at most one extension $\mathfrak{u}$ with

$$c_1^2(\mathfrak{u})\le\lambda+C. \tag{22.18}$$

This is a free offprint provided to the author by the publisher. Copyright restrictions may apply.

We can write $c_1(\mathfrak{u}) = \alpha \cdot PD[\hat{\Sigma}]$ for some $\alpha \in \mathbb{Q}$, and (22.18) implies

$$|\alpha| \leq \sqrt{\frac{C+\lambda}{\hat{\Sigma}^2}}.$$

For sufficiently large m, we may assume that $|\alpha| \leq 1/2$ for all $\mathfrak{u}$ satisfying (22.18). If $\mathfrak{u}'$ is another Spin^c structure on $W_{\lambda,\lambda+m}$ which has the same restriction to $\partial W_{\lambda,\lambda+m}$, then we may write $\mathfrak{u}' = \mathfrak{u} + jPD[\hat{\Sigma}]$, for some $j \in \mathbb{Z}$. We compute that

$$\begin{aligned} c_1^2(\mathfrak{u}') - c_1^2(\mathfrak{u}) &= 4j\langle c_1(\mathfrak{u}), [\hat{\Sigma}]\rangle + 4j^2\hat{\Sigma}^2 \\ &= 4j^2\hat{\Sigma}^2(\alpha/j + 1). \end{aligned}$$

By letting m be sufficiently large, the inequality (22.18) will be violated for $\mathfrak{u}'$.

The case when λ is positive is similar (cf. [**OS11**, Lemma 6.7]). □

22.4. Negative surgeries

The involutive hypercube we have constructed gives a morphism from $CFI^\delta(Y_\lambda(K))$ to $\mathbb{XI}^\delta_\lambda$. For positive λ, the analysis performed by Ozsváth and Szabó [**OS11**, Section 6], together with the obvious analog of Lemma 20.9, show that the map is homogeneously graded, with respect to a relative $\mathbb{Z}$ valued grading on $\mathbb{XI}^\delta_\lambda$. For negative coefficients, our argument thus far shows only that the hypercube determines an ι-homotopy equivalence, but we have not shown it to be homogeneously graded. Note that Ozsváth and Szabó construct a different 2-dimensional hypercube to prove the statement about gradings in the case of negative surgery coefficients. Instead of building another involutive hypercube to mirror Ozsváth and Szabó's approach, we opt to to show that the vertical truncation of the main hypercube is also homogeneously graded for negative surgery coefficients, when m is sufficiently large.

The following is the key new lemma for handling gradings in the main hypercube for negative surgeries:

LEMMA 22.4. *Suppose C is fixed. For sufficiently large m, the following holds: if $\mathfrak{t} \in \text{Spin}^c(Y_\lambda(K))$ and $\mathfrak{s} \in \text{Spin}^c(Y)$, then for each $t \in \mathbb{Q}$, the set of real numbers*

$$G_{\mathbf{w}}(t,\mathfrak{s},\mathfrak{t}) := \left\{ \text{gr}_{\mathbf{w}}(\mathfrak{u}) \;\middle|\; \begin{array}{c} \mathfrak{u} \in \text{Spin}^c(W'_\lambda(K)\#D(-m,1)) \\ \mathfrak{u}|_{Y_\lambda(K)} = \mathfrak{t} \\ \mathfrak{u}|_Y = \mathfrak{s} \\ \mathfrak{u}|_{L(m,1)} = \mathfrak{s}_{\text{can}} \\ A(\mathfrak{u}) - t \in m\mathbb{Z} \end{array} \right\}$$

contains no two elements which have distance less than C.

PROOF. Each Spin^c structure on $W'_\lambda(K)\#D(-m,1)$ decomposes as a connected sum $\mathfrak{w}\#\mathfrak{z}$ where $\mathfrak{w} \in \text{Spin}^c(W'_\lambda(K))$ and $\mathfrak{z} \in \text{Spin}^c(D(-m,1))$. With this notation,

$$A(\mathfrak{w}\#\mathfrak{z}) = \frac{\langle c_1(\mathfrak{w}), \hat{\Sigma}_d\rangle - [\Sigma]\cdot[\hat{\Sigma}_d]}{2d} + \frac{\langle c_1(\mathfrak{z}), S\rangle - S^2}{2},$$

where $\hat{\Sigma}_d \subseteq W'_\lambda(K)$ is d copies of the core Σ of the 2-handle capped off with a rational Seifert surface, and S is the 2-sphere in $D(-m,1)$ of self-intersection $-m$. Suppose that $\mathfrak{u}_0 = \mathfrak{w}_0\#\mathfrak{z}_0$ satisfies $A(\mathfrak{w}_0\#\mathfrak{z}_0) \equiv s_0 \pmod m$. Any other Spin^c structure with the same boundary restrictions may be written as

$$\mathfrak{u}_{i,j} = (\mathfrak{w}_0 + iPD[\hat{\Sigma}_d])\#(\mathfrak{z}_0 + jPD[S]),$$

This is a free offprint provided to the author by the publisher. Copyright restrictions may apply.

for integers i and j. Note that adding $PD[S]$ changes A by m, and adding $\hat{\Sigma}_d$ changes A by $[\hat{\Sigma}_d]^2/d = -d\lambda$. Hence $A(\mathfrak{u}_0) - A(\mathfrak{u}_{i,j}) \in m\mathbb{Z}$ if and only if $id\lambda \equiv 0 \pmod m$. We compute that

$$\begin{aligned} \mathrm{gr}_{\mathbf{w}}(\mathfrak{u}_{i,j}) - \mathrm{gr}_{\mathbf{w}}(\mathfrak{u}_0) &= \frac{c_1^2(\mathfrak{u}_{i,j}) - c_1^2(\mathfrak{u}_0)}{4} \\ &= i\langle c_1(\mathfrak{w}_0), [\hat{\Sigma}_d]\rangle + i^2[\hat{\Sigma}_d]^2 + j\langle c_1(\mathfrak{z}_0), [S]\rangle + j^2 S^2 \\ &= i\langle c_1(\mathfrak{w}_0), [F]\rangle - i^2 d\lambda + jkm - j^2 m, \end{aligned} \tag{22.19}$$

for some $k \in \mathbb{Z}$. Note that since $id\lambda \equiv 0 \pmod m$, the integer i is divisible by $m/\gcd(m, d\lambda)$. Hence $G_{\mathbf{w}}(t, \mathfrak{s}, \mathfrak{t})$ is a subset of a lattice of the form $\alpha + (m/\gcd(m, d\lambda)) \cdot \mathbb{Z})$, where $\alpha \in \mathbb{Q}$. The main claim follows, by picking m so that $m/d\lambda > C$, since $|m/\gcd(m, d\lambda)| \geq |m/d\lambda|$. □

22.5. Knot Floer homology and rationally null-homologous knots

In this section, we consider the Floer homology of rationally null-homologous knots. We focus on knots in rational homology 3-spheres, to simplify the presentation. However, our discussion holds more generally if we focus on torsion Spin^c structures.

Suppose K is a rationally null-homologous knot in a rational homology 3-sphere Y, and $\mathfrak{s} \in \mathrm{Spin}^c(Y)$. We pick a Heegaard diagram $(\Sigma, \boldsymbol{\alpha}, \boldsymbol{\beta}, w, z)$ for (Y, K), and define the full knot Floer complex $\mathcal{CFK}^-(Y, K, \mathfrak{s})$ to be the free $\mathbb{F}[\mathscr{U}, \mathscr{V}]$-module generated by $\mathbf{x} \in \mathbb{T}_\alpha \cap \mathbb{T}_\beta$ satisfying $\mathfrak{s}_w(\mathbf{x}) = \mathfrak{s}$.

The module $\mathcal{CFK}^-(Y, K, \mathfrak{s})$ admits two gradings, $\mathrm{gr}_{\mathbf{w}}$ and $\mathrm{gr}_{\mathbf{z}}$, for which $\mathscr{U}$ and $\mathscr{V}$ having bigradings $(-2, 0)$ and $(0, -2)$. These gradings are obtained from the absolute Maslov gradings on $CF^-(Y, \mathfrak{s})$ and $CF^-(Y, \mathfrak{s} - PD[K])$, via the canonical isomorphisms

$$\mathcal{CFK}^-(Y, K, \mathfrak{s}) \otimes \mathbb{F}[\mathscr{U}, \mathscr{V}]/(\mathscr{V} - 1) \cong CF^-(Y, \mathfrak{s}) \quad \text{and}$$
$$\mathcal{CFK}^-(Y, K, \mathfrak{s}) \otimes \mathbb{F}[\mathscr{U}, \mathscr{V}]/(\mathscr{U} - 1) \cong CF^-(Y, \mathfrak{s} - PD[K]).$$

The difference in Spin^c structures on the right hand side arises from the relation

$$\mathfrak{s}_w(\mathbf{x}) - \mathfrak{s}_z(\mathbf{x}) = PD[K]. \tag{22.20}$$

We take as the definition of the absolute Alexander grading the following:

$$A := \frac{1}{2}(\mathrm{gr}_{\mathbf{w}} - \mathrm{gr}_{\mathbf{z}}). \tag{22.21}$$

The equivalence with other formulations is verified in [**HL24**, Lemma 2.10]. An alternate approach for null-homologous knots may be found in [**Zem19b**, Theorem 2.13 (e); Proposition 8.1]).

The Alexander grading takes values in $\mathbb{Q}$, but is relatively $\mathbb{Z}$ valued. If $s \in \mathbb{Q}$, we define $\mathcal{A}_{(t,\mathfrak{s})}(Y, K)$ to be the subset of $\mathcal{CFK}^-(Y, K, \mathfrak{s})$ in Alexander grading t, and we set $\mathcal{B}_{(t,\mathfrak{s})}(Y, K)$ to be the subset of $\mathscr{V}^{-1} \cdot \mathcal{CFK}^-(Y, K, \mathfrak{s})$ in Alexander grading t.

The construction of an involution on knot Floer homology described in [**HM17**] extends to rationally null-homologous knots. However, there is a new subtlety due to (22.20), in that the involution has the form

$$\iota_K \colon \mathcal{CFK}^-(Y, K, \mathfrak{s}) \to \mathcal{CFK}^-(Y, K, \mathfrak{s} - PD[K]).$$

To streamline the presentation, we find it helpful to consider the grading changes associated to link cobordisms, similar to the presentation of [**Zem19b**].

This is a free offprint provided to the author by the publisher. Copyright restrictions may apply.

The Alexander grading formulas therein are stated for null-homologous links. We now describe how to quickly derive the Alexander grading changes for cobordisms between rationally null-homologous knots from [**Zem19b**]. More generally, one could easily adapt the line of reasoning in [**Zem19b**] to handle cobordisms between rationally null-homologous *links*, but we will not do so here.

Suppose $(W,\Sigma)\colon (Y_1,K_1)\to(Y_2,K_2)$ is an oriented, genus 0 knot cobordism between two rationally null-homologous knots. Further, suppose $\mathfrak{s}\in \mathrm{Spin}^c(W)$ has torsion restriction to Y_1 and Y_2. We consider the link cobordism map $F_{W,\Sigma,\mathfrak{s}}$ for (W,Σ). (The cobordism maps of [**Zem19c**] also require a decoration on Σ; here we assume it consists of two parallel arcs running from K_1 to K_2). According to [**Zem19b**, Theorem 1.4], the $\mathrm{gr}_{\mathbf{w}}$ and $\mathrm{gr}_{\mathbf{z}}$ grading changes are given by

$$\begin{aligned}\mathrm{gr}_{\mathbf{w}}(F_{W,\Sigma,\mathfrak{s}}(\mathbf{x}))-\mathrm{gr}_{\mathbf{w}}(\mathbf{x})&=\frac{c_1^2(\mathfrak{s})-2\chi(W)-3\sigma(W)}{4},\\ \mathrm{gr}_{\mathbf{z}}(F_{W,\Sigma,\mathfrak{s}}(\mathbf{x}))-\mathrm{gr}_{\mathbf{z}}(\mathbf{x})&=\frac{c_1^2(\mathfrak{s}-PD[\Sigma])-2\chi(W)-3\sigma(W)}{4}\end{aligned}\tag{22.22}$$

Here, we are viewing $[\Sigma]$ as a class in $H_2(W,\partial W)$. From (22.21), we obtain

$$A(F_{W,\Sigma,\mathfrak{s}}(\mathbf{x}))-A(\mathbf{x})=\frac{c_1^2(\mathfrak{s})-c_1^2(\mathfrak{s}-PD[\Sigma])}{2}.\tag{22.23}$$

If N is an integer such that $N\cdot[K_1]=0$ and $N\cdot[K_2]=0$, as elements of $H_1(Y_1)$ and $H_1(Y_2)$, then it is easy to rearrange (22.23) to obtain

$$A(F_{W,\Sigma,\mathfrak{s}}(\mathbf{x}))-A(\mathbf{x})=\frac{\langle c_1(\mathfrak{s}),[\hat{\Sigma}_N]\rangle-[\Sigma]\cdot[\hat{\Sigma}_N]}{2N},\tag{22.24}$$

where $\hat{\Sigma}_N$ denotes a class in $H_2(W)$, which is a preimage of $N\cdot[\Sigma]$ under the map $H_2(W)\to H_2(W,\partial W)$.

Note that given the construction of the absolute gradings in [**OS03**], as well as our definition in (22.21), we see that that $\hat{A}(\mathfrak{s})$ is exactly the subset of $\mathbb{Q}$ that the Alexander grading on $\mathcal{CFK}^-(Y,K,\mathfrak{s})$ takes values in.

22.6. Ozsváth and Szabó's mapping cone formula for rationally null-homologous knots

We now restate Ozsváth and Szabó's mapping cone formula using the notation from Sections 22.1 and 22.2. We set

$$\mathfrak{A}(Y,K)=\prod_{(t,\mathfrak{s})\in\mathbb{H}(Y,K)}\boldsymbol{\mathcal{A}}_{(t,\mathfrak{s})}(Y,K)\quad\text{and}\quad\mathfrak{B}(Y,K)=\prod_{(t,\mathfrak{s})\in\mathbb{H}(Y,K)}\boldsymbol{\mathcal{B}}_{(t,\mathfrak{s})}(Y,K),$$

where $\boldsymbol{\mathcal{A}}_{(t,\mathfrak{s})}(Y,K)$ denotes $\mathcal{A}_{(t,\mathfrak{s})}(Y,K)\otimes_{\mathbb{F}[U]}\mathbb{F}[\![U]\!]$, and similarly for $\boldsymbol{\mathcal{B}}_{(t,\mathfrak{s})}(Y,K)$.

The differential D_λ is the sum of two maps, v and h. The map v restricts to the inclusion of $\boldsymbol{\mathcal{A}}_{(t,\mathfrak{s})}(Y,K)$ into $\boldsymbol{\mathcal{B}}_{(t,\mathfrak{s})}(Y,K)$. Similarly,

$$h_{(t,\mathfrak{s})}=\mathfrak{F}_{z\to w}\circ\widetilde{v}_{(t,\mathfrak{s})},$$

where $\widetilde{v}_{(t,\mathfrak{s})}$ is the inclusion of $\boldsymbol{\mathcal{A}}_t(Y,K,\mathfrak{s})$ into $\widetilde{\boldsymbol{\mathcal{B}}}_t(Y,K,\mathfrak{s})$, and

$$\mathfrak{F}_{z\to w}\colon\widetilde{\boldsymbol{\mathcal{B}}}_t(Y,K,\mathfrak{s})\to\boldsymbol{\mathcal{B}}_{t+\lambda}(Y,K,\mathfrak{s}-PD[K]),$$

This is a free offprint provided to the author by the publisher. Copyright restrictions may apply.

is the the canonical homotopy equivalence, as follows. Write w and z for the two basepoints of K. We consider the canonical isomorphisms

$$\theta_z\colon \widetilde{\boldsymbol{\mathcal{B}}}_{(t,\mathfrak{s})}(Y,K,w,z) \to \boldsymbol{CF}^-(Y,z,\mathfrak{s}-PD[K])\otimes T^t \quad \text{and}$$
$$\theta_w\colon \boldsymbol{\mathcal{B}}_{(t+\lambda,\mathfrak{s}-PD[K])}(Y,K,w,z) \to \boldsymbol{CF}^-(Y,w,\mathfrak{s}-PD[K])\otimes T^{t+\lambda}.$$

The change in Spin^c structure appearing in the definition of θ_z is due to the relation

$$\mathfrak{s}_w(\mathbf{x})-\mathfrak{s}_z(\mathbf{x}) = PD[K].$$

We let ϕ be a diffeomorphism which moves z to w along a subarc of K. We define

$$\mathfrak{F}_{z\to w} := \theta_w^{-1}\circ(\phi_*\otimes T^\lambda)\circ\theta_z.$$

REMARK 22.5. We have defined $h_{(t,\mathfrak{s})}$ to take $\boldsymbol{\mathcal{A}}_{(t,\mathfrak{s})}(Y,K)$ to $\boldsymbol{\mathcal{B}}_{(t+\lambda,\mathfrak{s}-PD[K])}(Y,K)$. The sign of $PD[K]$ in our formula differs from Ozsváth and Szabó's [**OS11**]. This is due to inconsistencies in the literature regarding the string orientation of a knot associated to a doubly pointed Heegaard diagram. A discussion may be found in [**HL24**, Section 2.2]. Note that our convention on string orientation is opposite to the one advocated for therein. Our reason is that when considering knot cobordisms, it is natural to define the Alexander grading using a Seifert surface whose oriented boundary is $-K$, so that one can cap off the knot cobordism to obtain a class $H_2(W;\mathbb{Z})$. In [**HL24**], the authors define the Alexander grading using a Seifert surface whose boundary is K.

Ozsváth and Szabó's mapping cone formula can be restated in our notation as saying that

$$\boldsymbol{CF}^-(Y_\lambda(K)) \simeq \mathrm{Cone}(D_\lambda\colon \mathfrak{A}\to\mathfrak{B}).$$

We now sketch the proof of Ozsváth and Szabó's mapping cone formula, stated in terms of our notation. Understanding the proof will allow us to efficiently understand the proof of the involutive version.

We consider the Floer complexes $\boldsymbol{CF}^-(Y_\lambda(K))$, $\boldsymbol{CF}^-(Y_{\lambda+m}(K))$ and $\underline{\boldsymbol{CF}}^-(Y)$, as before. Here the twisted complex $\underline{\boldsymbol{CF}}^-(Y)$ has coefficients in $\mathbb{Z}[\mathbb{Z}/m]$, exactly as in the proof for null-homologous knots. The proof that $\boldsymbol{CF}^-(Y_\lambda(K))$ is homotopy equivalent to the mapping cone of

$$f_2\colon \boldsymbol{CF}^-(Y_{\lambda+m}(K)) \to \underline{\boldsymbol{CF}}^-(Y)$$

is no different than the proof for null-homologous knots. Taking vertical truncations presents no additional complications.

One now claims that there is a natural grading on $\mathrm{Cone}(f_2^\delta)$ with respect to which the homotopy equivalence is homogeneously graded. Ozsváth and Szabó proved that for positive λ, the map from $CF^\delta(Y_\lambda(K))$ to $\mathrm{Cone}(f_2^\delta)$ is homogeneously graded, and for negative surgery coefficients, the map from $\mathrm{Cone}(f_2^\delta)$ to $CF^\delta(Y_\lambda(K))$ is homogenously graded. When we consider the involutive version, it is helpful also to know that the map from $CF^\delta(Y_\lambda(K))$ to $\mathrm{Cone}(f_2^\delta)$ is also homogeneously graded for negative λ, whenever m is sufficiently large, compared to δ. To this end, Lemma 22.1, 22.2 and 22.3 imply that the length 1 maps are homogeneously graded, and Lemma 22.4 implies that the length 2 map is homogeneously graded, when m is sufficiently large compared with δ. We note that the argument for the length 1 maps is not substantially different than Ozsváth and Szabó's argument, though the argument for the length 2 map is new to our present work.

This is a free offprint provided to the author by the publisher. Copyright restrictions may apply.

Next, one builds a 2-dimensional hypercube which relates $\mathrm{Cone}(f_2^\delta)$ with a horizontal truncation of the mapping cone complex. To this end, we first note that θ_w should be viewed as an injection

$$\theta_w\colon \underline{\boldsymbol{CF}}^-(Y) \to \boldsymbol{CF}^-(Y)\otimes_{\mathbb{F}} \mathbb{F}[\mathbb{Q}/m\mathbb{Z}].$$

The image of θ_w consists of the $\mathbb{F}[\![U]\!]$-span of elements of the form $\mathbf{x}\otimes T^t$ where $t\in \hat{A}(\mathfrak{s}_w(\mathbf{x}))$, where $\hat{A}$ is defined in (22.11).

The hypercube one builds has the following form:

(22.25)
$$\begin{array}{ccc} CF^\delta(Y_{\lambda+m}(K)) & \xrightarrow{\ f_2^\delta\ } & \underline{CF}^\delta(Y) \\ \downarrow{\scriptstyle \Gamma^\delta} & \searrow^{L^\delta} & \downarrow{\scriptstyle \kappa^\delta} \\ \mathfrak{A}^\delta\langle b\rangle & \xrightarrow{\ v^\delta+h^\delta\ } & \mathfrak{B}^\delta\langle b\rangle \end{array}$$

We now explain the expressions in (22.25). First, the complex $\mathfrak{A}\langle b\rangle$ is the direct sum over all $\mathcal{A}_{(t,\mathfrak{s})}(Y,K)$ where $-b\le t\le b$, and $\mathfrak{B}\langle b\rangle$ denotes the direct sum over all $\mathcal{B}_{(t,\mathfrak{s})}$ where $-b+\lambda\le t\le b$. Similar to (20.5), we assume

$$0<b<(\lambda+m)/2.$$

Next, we describe κ. There is a canonical map from the image of θ_w to $\mathfrak{B}^\delta\langle b\rangle$, which sends $CF^-(Y)\otimes T^\alpha$ to $\mathfrak{B}_{[\alpha]_m}(Y,K)$, where $[\cdot]_m\colon \mathbb{Q}/m\mathbb{Z}\to\mathbb{Q}$ is the map which sends an element t to its unique representative t_0 in $\mathbb{Q}$ which satisfies $-m/2\le t_0<m/2$. We write

$$\kappa\colon \underline{\boldsymbol{CF}}^-(Y)\to \mathfrak{B}^-(Y,K)\langle b\rangle,$$

for the composition of θ_w with this map, followed by projection onto $\mathfrak{B}^-\langle b\rangle$. Concretely

(22.26)
$$\kappa(T^jU^i\cdot\mathbf{x}) = \begin{cases} \mathscr{U}^i\mathscr{V}^{i+[j+A_{w,z}(\mathbf{x})]_m-A_{w,z}(\mathbf{x})}\cdot\mathbf{x}, & \text{if } -b+\lambda\le [j+A_{w,z}(\mathbf{x})]_m\le b \\ 0 & \text{otherwise.}\end{cases}$$

In (22.25), the map Γ^δ counts holomorphic triangles representing the Spin^c structures of the form $\mathfrak{r}_{t,\mathfrak{s}}$, where $-b\le t\le b$. Note that, essentially by definition, the triangle-counting map, restricted to the Spin^c structure $\mathfrak{r}_{t,\mathfrak{s}}$ induces Alexander grading change t (viewed as a knot cobordism map from the unknot in $Y_{\lambda+m}(K)$ to K in Y), and hence has image in $\mathcal{A}^\delta_{(t,\mathfrak{s})}$.

By Lemma 22.1, the only Spin^c structures which contribute to f_2^δ for sufficiently large m are of the form $\mathfrak{r}_{t,\mathfrak{s}}$ or $\mathfrak{y}_{t,\mathfrak{s}}$, for $-(\lambda+m)/2\le t\le(\lambda+m)/2$. Furthermore, $\theta_w\circ f_{2;\mathfrak{r}_{t,\mathfrak{s}}}$ has image in $CF^-(Y,\mathfrak{s})\otimes T^t$, since $A(\mathfrak{r}_{t,\mathfrak{s}})=t$, and $\theta_w\circ f_{2;\mathfrak{y}_{t,\mathfrak{s}}}$ has image in $CF^-(Y,\mathfrak{s}-PD[K])\otimes T^{t+\lambda}$, since $A(\mathfrak{y}_{t,\mathfrak{s}})=t+\lambda+m$. The map L^δ appearing in (22.25) is constructed similarly to the analogous map in Figure 20.3.

Since $b<(\lambda+m)/2$, the truncations $\mathfrak{A}^\delta\langle b\rangle$ and $\mathfrak{B}^\delta\langle b\rangle$ are not themselves homotopy equivalent to $CF^\delta(Y_{\lambda+m}(K))$ and $\underline{CF}^\delta(Y)$, since Γ^δ projects Spin^c structures outside of the range $-b\le t\le b$ to 0, and a similar statement holds for κ^δ. Nonetheless, it follows from part 2 of Lemma 22.1 that the map determined by Γ^δ, L^δ and κ^δ_w is a homotopy equivalence. Compare the proof of Theorem 20.1. Letting m and δ become sufficiently large, we obtain, in the same manner as mapping cone for

This is a free offprint provided to the author by the publisher. Copyright restrictions may apply.

null-homologous knots, a homotopy equivalence between $\mathrm{Cone}(f_2)$ and the infinite mapping cone $\mathrm{Cone}(D_\lambda\colon \mathfrak{A} \to \mathfrak{B})$. Compare the proof of Theorem 20.1.

Finally, we make one comment on gradings. Ozsváth and Szabó proved that the map from $CF^\delta(Y_\lambda(K))$ to $\mathrm{Cone}(f_2^\delta)$ is homogeneously graded when λ is positive. When λ is negative, they instead showed that the homotopy equivalence, which goes from $\mathrm{Cone}(f_2^\delta)$ to $CF^\delta(Y_\lambda(K))$, is homogeneously graded. We note it follows from Lemma 22.4 that the map from $CF^\delta(Y_\lambda(K))$ to $\mathrm{Cone}(f_2^\delta)$ is homogeneously graded, even when λ is negative, provided m is sufficiently large.

22.7. The involutive mapping cone formula for rationally null-homologous knots

Given our sketch of Ozsváth and Szabó's mapping cone formula for rationally null-homologous knots in Section 22.6, it is clear that our proof of Theorem 20.1 extends without any complication to prove the following:

THEOREM 22.6. *Suppose λ is a Morse framing on a rationally null-homologous knot K in an rational homology 3-sphere Y (we view λ as an element of $\mathbb{Q}$), such that $Y_\lambda(K)$ is also a rational homology 3-sphere. The involutive Heegaard Floer homology $\boldsymbol{CFI}^-(Y_\lambda(K))$ is homotopy equivalent over the ring $\mathbb{F}[\![U]\!][Q]/Q^2$ to a complex $\mathbb{F}[Q]/(Q^2)\otimes_{\mathbb{F}}(\mathfrak{A}\oplus\mathfrak{B})$ with differential specified by some $\mathbb{F}[\![U]\!]$-linear maps as below:*

$$\begin{array}{ccccc} \mathfrak{A} & & \xrightarrow{\quad D_\lambda \quad} & & \mathfrak{B} \\ \Big\downarrow{\scriptstyle Q\cdot(\mathrm{id}+\iota_{\mathbb{A}})} & \searrow & & & \Big\downarrow{\scriptstyle Q\cdot(\mathrm{id}+\iota_{\mathbb{B}})} \\ Q\cdot\mathfrak{A} & & \xrightarrow{\quad D_\lambda \quad} & & Q\cdot\mathfrak{B}. \end{array} \qquad \mathbb{XI}_\lambda = \begin{array}{c} \\ \\ \\ \\ \\ \end{array} \begin{array}{c} \\ \\ Q\cdot H \\ \\ \\ \end{array}$$

In fact, the ι-complex $(\boldsymbol{CF}^-(Y_\lambda(K)),\iota)$ is ι-homotopy equivalent to the complex

$$\mathbb{X}_\lambda := \mathrm{Cone}\left(D_\lambda\colon \mathfrak{A}\to\mathfrak{B}\right),$$

with involution $\iota_{\mathbb{X}} := \iota_{\mathbb{A}} + H + \iota_{\mathbb{B}}$. Furthermore, the following hold:

1. *$D_\lambda = v + h$, where v sends $\boldsymbol{\mathcal{A}}_{(t,\mathfrak{s})}$ to $\boldsymbol{\mathcal{B}}_{(t,\mathfrak{s})}$, and h sends $\boldsymbol{\mathcal{A}}_{(t,\mathfrak{s})}$ to $\boldsymbol{\mathcal{B}}_{(t+\lambda,\mathfrak{s}-PD[K])}$.*
2. *$\iota_{\mathbb{A}}$ sends $\boldsymbol{\mathcal{A}}_{(t,\mathfrak{s})}$ to $\boldsymbol{\mathcal{A}}_{(-t,\overline{\mathfrak{s}}+PD[K])}$. Furthermore, $\iota_{\mathbb{A}}$ coincides with the knot involution.*
3. *$\iota_{\mathbb{B}}$ sends $\boldsymbol{\mathcal{B}}_{(t,\mathfrak{s})}$ to $\boldsymbol{\mathcal{B}}_{(-t+\lambda,\overline{\mathfrak{s}})}$, and coincides with the map induced by $\iota_{\mathbb{A}}$, composed with $\mathfrak{F}_{z\to w}$.*
4. *$H = k + j$, where k maps $\boldsymbol{\mathcal{A}}_{(t,\mathfrak{s})}$ to $\boldsymbol{\mathcal{B}}_{(-t+\lambda,\overline{\mathfrak{s}})}$ and j maps $\boldsymbol{\mathcal{A}}_{(t,\mathfrak{s})}$ to $\boldsymbol{\mathcal{B}}_{(-t,\overline{\mathfrak{s}}+PD[K])}$.*

Given an knot K in a rational homology 3-sphere Y, which is also an L-space, the construction of Proposition 3.15 carries over without substantial change to give an algebraic involutive mapping cone

$$\mathbb{XI}^{\mathrm{alg}}_\lambda(\mathcal{CFK}^-(Y,K),\iota_K),$$

whenever λ is a non-zero Morse framing on K, which is well-defined up to ι-homotopy equivalence. The ι-complex $\mathbb{XI}^{\mathrm{alg}}_\lambda$ is characterized by the property that

This is a free offprint provided to the author by the publisher. Copyright restrictions may apply.

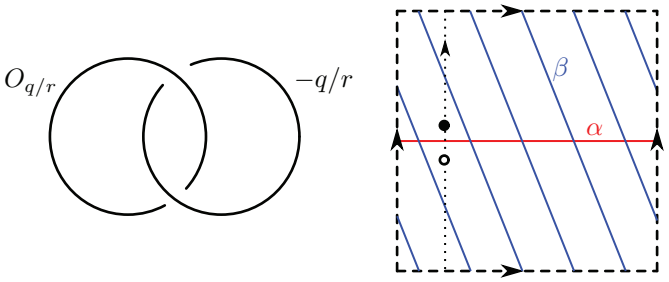


FIGURE 22.1. Left: The knot $O_{q/r}$ inside of $-L(q,r)$. Right: A Heegaard diagram for $O_{5/2}$. The knot $O_{5/2}$ is shown (dotted), with the orientation from the Heegaard diagram.

h and H factor through the inclusion map of $\mathcal{A}_{(t,\mathfrak{s})}(Y,K)$ into $\widetilde{\mathcal{B}}_{(t,\mathfrak{s})}(Y,K)$. The proof of Theorem 21.1 adapts with only notational changes to give the following:

THEOREM 22.7. *Suppose K is a rationally null-homologous knot in a rational homology 3-sphere Y, with non-zero Morse framing. If Y is an L-space, then $\mathbb{XI}^{\mathrm{alg}}_{\lambda}(CFK^{\infty}(Y,K),\iota_K)$ is ι-homotopy equivalent to $\boldsymbol{CFI}^{-}(Y_{\lambda}(K))$.*

22.8. Rational surgeries

We now apply Theorem 22.6 to compute rational surgeries. By using the involutive connected sum formula for knots, the proof follows from the same line of reasoning as [**OS11**, Theorem 1.1]. We now describe the proof, using our present notation.

Suppose that $\lambda = p/q$ is a non-zero rational framing on $K \subseteq S^3$, such that $\gcd(p,q) = 1$. Let n denote $\lfloor p/q \rfloor$. Define $r/q = p/q - n$. We will take the connected sum of K with the knot $O_{q/r} \subseteq -L(q,r)$. See Figure 22.1. Ozsváth and Szabó call $O_{q/r}$ a *U-knot*, since $\widehat{HFK}$ has rank 1 in each Spin^c structure.

We write $x_0,\dots,x_{q-1}$ for the intersection points, ordered left to right (for some choice of starting points). It is easy to check that $\epsilon(x_i,x_{i+r}) = PD[O_{q/r}]$, where $O_{q/r}$ is oriented as in Figure 22.1, and ϵ is defined in [**OS04b**, Section 2.4]. According to [**OS04b**, Lemma 2.19], $\mathfrak{s}_w(x_{i+r}) - \mathfrak{s}_w(x_i) = \epsilon(x_i,x_{i+r}) = PD[O_{q/r}]$. On the other hand $\mathfrak{s}_w(x_i) - \mathfrak{s}_z(x_i) = PD[O_{q/r}]$, so $\mathrm{gr}_z(x_i) = \mathrm{gr}_w(x_{i-r})$.

We have

$$A(x_i) = \frac{1}{2}(\mathrm{gr}_w(x_i) - \mathrm{gr}_z(x_i)) = \frac{1}{2}(\mathrm{gr}_w(x_i) - \mathrm{gr}_w(x_{i-r})). \tag{22.27}$$

According to [**LL08**, Proposition 5.3] (cf. [**OS03**, Proposition 4.8]), there is an identification of Spin$^c(-L(q,r)) \cong \mathbb{Z}/q$, such that if $r \le i \le r+q-1$, then

$$\mathrm{gr}_w(x_i) - \mathrm{gr}_w(x_{i-r}) = \frac{1}{q}(q-1-2i), \tag{22.28}$$

(with subscripts taken modulo q). Combining (22.27) and (22.28), it follows that

$$A(x_i) = \frac{1}{2q}(q-1-2i),$$

for $0 \le i < q$.

This is a free offprint provided to the author by the publisher. Copyright restrictions may apply.

On the Heegaard diagram for $O_{q/r} \subseteq -L(q,r)$, the β curve satisfies $[\beta] = q \cdot O_{q/r} + r \cdot [\alpha]$. This relation gives a rational Seifert surface, by taking a 2-chain F which satisfies $\partial F = q \cdot O_{q/r} + r \cdot \alpha - \beta$, and capping with compressing disks for α and β. Furthermore, $O_{q/r}$, pushed into the alpha handlebody, has intersection number r with this 2-chain, and hence $O_{q/r}$ has rational self-linking number r/q.

The framing p/q on K corresponds to a Morse framing on $K \# O_{q/r}$, as follows. Let $n = \lfloor p/q \rfloor$ and $r/q = p/q - n$, as above. We view K as having integral framing $n = \lfloor p/q \rfloor$ and the knot $O_{q/r}$ as having the Morse framing induced by the 0-framing in (22.29), if we ignore the $-q/r$-framed unknot. These two choices induce a Morse framing on $K \# O_{q/r} \subseteq -L(q,r)$, which corresponds to the rational number p/q, under the map in (22.4).

In particular, the intersection points have Alexander gradings

$$\frac{-q+1}{2q}, \frac{-q+3}{2q}, \dots, \frac{q-3}{2q}, \frac{q-1}{2q}. \tag{22.29}$$

Now, if x_i is the intersection point in Spin^c structure $\mathfrak{s}_i$, then $\mathcal{A}_{(t,\mathfrak{s}_i)}(K \# O_{q/r}) \simeq \mathcal{A}_{t-A(x_i)}(K)$, by the connected sum formula. Note that the projection map from $\mathrm{Spin}^c(W'_\lambda(K)) \to \mathbb{Q}$ is an injection (i.e. all Spin^c structures on $-L(q,r)$ have different values under $\hat{A}$), so we lose no information in writing just $\mathcal{A}_t(K \# O_{q/r})$ instead of $\mathcal{A}_{(t,\mathfrak{s}_i)}(K \# O_{q/r})$. By the Künneth theorem, we have

$$\mathcal{A}_t(K \# O_{q/r}) \cong \mathcal{A}_{[t]}(S^3, K), \tag{22.30}$$

where $[t]$ denotes the closest integer to t. The value of $[t]$ on half-integers is not important, since we never need to apply it there. Note also that the knot involution $\iota_{K \# O_{q/r}}$ coincides with ι_K under the isomorphism in (22.30), by the connected sum formula for involutive knot Floer homology [**Zem19a**] as well as the fact that $O_{q/r}$ is a U-knot (so the maps Φ and Ψ thereon vanish).

We define

$$\begin{aligned} \mathbb{A}_{p/q}(K) &:= \mathfrak{A}(-L(q,r), K \# O_{q/r}) \cong \prod_{s \in \mathbb{Z}} \boldsymbol{\mathcal{A}}_{[\frac{q+2s+1}{2q}]}(K) \quad \text{and} \\ \mathbb{B}_{p/q}(K) &:= \mathfrak{B}(-L(q,r), K \# O_{q/r}) \cong \prod_{s \in \mathbb{Z}} \boldsymbol{\mathcal{B}}_{[\frac{q+2s+1}{2q}]}(K). \end{aligned} \tag{22.31}$$

We think of each $\boldsymbol{\mathcal{A}}_{[\frac{q+2s+1}{2q}]}(K)$ as actually being $\boldsymbol{\mathcal{A}}_{[\frac{q+2s+1}{2q}]}(K) \times \{q+2s+1\}$ (so as to remember index s), but we suppress this from the notation.

Of course, there are canonical isomorphisms $\boldsymbol{\mathcal{A}}_s(K) \cong \boldsymbol{A}_s(K)$ and $\boldsymbol{\mathcal{B}}_s(K) \cong \boldsymbol{B}_s(K)$, so we may translate (22.31) into the more familiar versions of complexes, as in [**OS04a**].

Applying Theorem 22.6, we obtain the following:

THEOREM 22.8. *Suppose that K is a knot in S^3, and p and q are relatively prime integers, neither of which is 0. Then $\boldsymbol{CFI}^-(S^3_{p/q}(K))$ is homotopy equivalent over the ring $\mathbb{F}[\![U]\!][Q]/Q^2$ to a complex $\mathbb{F}[Q]/(Q^2) \otimes_{\mathbb{F}} (\mathbb{A}_{p/q} \oplus \mathbb{B}_{p/q})[-1]$, where $\mathbb{A}_{p/q}$ and $\mathbb{B}_{p/q}$ are as in* (22.31)*, with differential specified by some $\mathbb{F}[\![U]\!]$-linear maps as*

This is a free offprint provided to the author by the publisher. Copyright restrictions may apply.

below:

$$\mathbb{XI}_{p/q} = \begin{array}{ccccc} \mathbb{A}_{p/q} & & \xrightarrow{D_{p/q}} & & \mathbb{B}_{p/q} \\ \downarrow{\scriptstyle Q\cdot(\mathrm{id}+\iota_{\mathbb{A}})} & \searrow{\scriptstyle Q\cdot H} & & & \downarrow{\scriptstyle Q\cdot(\mathrm{id}+\iota_{\mathbb{B}})} \\ Q\cdot\mathbb{A}_{p/q} & & \xrightarrow{D_{p/q}} & & Q\cdot\mathbb{B}_{p/q}, \end{array}$$

Equivalently, the ι-complex $(\boldsymbol{CF}^-(S^3_{p/q}(K)),\iota)$ is ι-homotopy equivalent to the complex $\mathbb{X}_{p/q} := \mathrm{Cone}\left(D_{p/q}\colon \mathbb{A}_{p/q}\to\mathbb{B}_{p/q}\right)$, with involution $\iota_{\mathbb{X}} := \iota_{\mathbb{A}} + H + \iota_{\mathbb{B}}$. Furthermore, the following hold:

1. *$D_{p/q} = v + h$, where v sends $\boldsymbol{A}_{[t]}(K)$ to $\boldsymbol{B}_{[t]}(K)$, and h sends $\boldsymbol{A}_{[t]}(K)$ to $\boldsymbol{B}_{[t+p/q]}$.*
2. *$\iota_{\mathbb{A}}$ sends $\boldsymbol{A}_{[t]}$ to $\boldsymbol{A}_{[-t]}$. Furthermore, $\iota_{\mathbb{A}}$ is the map induced by the knot involution under the isomorphism $\mathcal{A}_n(K)\cong A_n(K)$.*
3. *$\iota_{\mathbb{B}}$ sends $\boldsymbol{B}_{[t]}$ to $\boldsymbol{B}_{[-t+p/q]}$, and coincides with the map induced by $\iota_{\mathbb{A}}$, composed with $\mathfrak{F}_{z\to w}$.*
4. *$H = k + j$, where k maps $\boldsymbol{A}_{[t]}$ to $\boldsymbol{B}_{[-t+p/q]}$ and j maps $\boldsymbol{A}_{[t]}$ to $\boldsymbol{B}_{[-t]}$.*

There is an algebraic ι-complex $\mathbb{XI}^{\mathrm{alg}}_{p/q}(CFK^\infty(K),\iota_K)$, characterized by the property that the maps H and h factor through $\widetilde{v}$, which is well-defined up to ι-homotopy equivalence. Furthermore

$$(\boldsymbol{CFI}^-(S^3_{p/q}(K)),\iota)\simeq\mathbb{XI}^{\mathrm{alg}}_{p/q}(CFK^\infty(K),\iota_K).$$

We make several basic comments about the rational surgeries mapping cone. Our rational surgeries involutive mapping cone is indexed slightly differently than Ozsváth and Szabó's mapping cone [**OS11**]. In their notation

$$\mathbb{A}_{p/q} := \prod_{s\in\mathbb{Z}} A_{\lceil s/q\rceil}\times\{s\} \quad\text{and}\quad \mathbb{B}_{p/q} := \prod_{s\in\mathbb{Z}} B_{\lceil s/q\rceil}\times\{s\}.$$

That is, $\mathbb{A}_{p/q}$ and $\mathbb{B}_{p/q}$ each consist of q copies of each A_s and B_s. In the differential $D_{p/q} := v+h$, the map v sends $A_{\lceil s/q\rceil}\times\{s\}$ to $B_{\lceil s/q\rceil}\times\{s\}$, and h sends $A_{\lceil s/q\rceil}\times\{s\}$ to $B_{\lceil s+p/q\rceil}\times\{s+p\}$.

Next, we discuss the decomposition of the two cones over Spin^c structures. We have $\mathrm{Spin}^c(S^3_{p/q}(K))\cong\mathbb{Z}/p$. In Ozsváth and Szabó's indexing, the cone decomposes over $\mathbb{Z}/p$ congruence classes of the s index.

The conjugation action on Spin^c structures is a bit more natural with respect to the description in Theorem 22.8. Define

$$\mathbb{H} := \left\{\frac{q+2s+1}{2q} : s\in\mathbb{Z}\right\}.$$

There is an isomorphism $\mathrm{Spin}^c(S^3_{p/q}(K))\cong\mathbb{H}/(p/q)$, and analogous to (22.14) the conjugation action sends $x\in\mathbb{H}/(p/q)$ to $-x$. Each element $(q+2s+1)/2q\in\mathbb{H}/(p/q)$ has a representative in the interval $[-p/2q, p/2q]$. The representative is unique, unless p and q differ in parity, in which case the Spin^c structure corresponding to $-p/2q$ has two representatives in the inteveral (the other being $p/2q$). The self-conjugate Spin^c structures are as follows:

This is a free offprint provided to the author by the publisher. Copyright restrictions may apply.

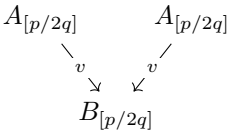
- If p and q are both odd, then there is one self-conjugate Spin^c structure, which corresponds to $0 \in \mathbb{H}$.
- If q is odd and p is even, then there are two self-conjugate Spin^c structures, which are the ones which correspond to $0, p/2q \in \mathbb{H}$
- If q is even and p is odd, then there is one self-conjugate Spin^c structure, which corresponds to $p/2q$.

The techniques of Section 3.7 extend without complication to compute the local class of rational surgeries on knots, as follows:

PROPOSITION 22.9. *Suppose that K is a knot in S^3, and p, q are relatively prime, positive integers.*

(1) *If p and q are both odd, then there is only one self-conjugate* Spin^c *structure on $S^3_{p/q}$, corresponding to $0 \in \mathbb{H}$. Moreover, $CFI^-(S^3_{p/q}(K), [0])$ is locally equivalent to $(A_0(K), \iota_K)$.*

(2) *If q is odd and p is even, then there are two self-conjugate* Spin^c *structures, corresponding to 0 and $p/2q \in \mathbb{H}$. Then, $CFI^-(S^3_{p/q}(K), [0])$ is locally equivalent to $(A_0(K), \iota_K)$, while $CFI^-(S^3_{p/q}(K), [p/2q])$ is locally equivalent to*

(22.32)


equipped with the involution which interchanges the two copies of $A_{[p/2q]}$, and fixes $B_{[p/2q]}$.

(3) *If q is even and p is odd, then there is one self-conjugate* Spin^c *structure, which corresponds to $p/2q \in \mathbb{H}$. Moreover, $CFI^-(S^3_{p/q}(K), [p/2q])$ is locally equivalent to the complex shown in* (22.32).

The proof of Proposition 22.9 follows the same strategy as the proof of Proposition 3.22. Namely, that proof implies that the local class of $\mathbb{XI}^{\mathrm{alg}}_{p/q}(\mathscr{C})$ coincides with the minimal truncation of $\mathbb{XI}^{\mathrm{alg}}_{p/q}(\mathscr{C})$, which is exactly the claim of Proposition 22.9. As a corollary of Proposition 22.9, together with the proof of Proposition 3.25, we obtain the following (stated as Proposition 1.7 in the introduction):

PROPOSITION 22.10. *Suppose that $p, q > 0$ are relatively prime integers and K is a knot in S^3.*

(1) *If p and q are odd, then there is one self-conjugate* Spin^c *structure $[0]$ on $S^3_{p/q}(K)$, and furthermore*

$$\underline{d}(S^3_{p/q}(K), [0]) = d(L(p,q), [0]) - 2\underline{V}_0(K),$$
$$\overline{d}(S^3_{p/q}(K), [0]) = d(L(p,q), [0]) - 2\overline{V}_0(K).$$

(2) *If p is even and q is odd, there are two self-conjugate* Spin^c *structures, which we denote $[0]$ and $[p/2q]$. The correction terms for $[0]$ are the same as the previous case, while*

$$\underline{d}(S^3_{p/q}(K), [p/2q]) = d(S^3_{p/q}(K), [p/2q]),$$
$$\overline{d}(S^3_{p/q}(K), [p/2q]) = d(L(p,q), [p/2q]).$$

This is a free offprint provided to the author by the publisher. Copyright restrictions may apply.

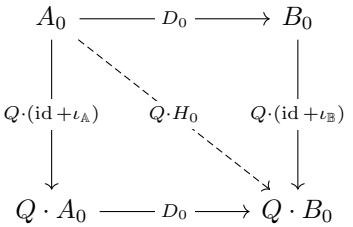
(3) *If q is even and p is odd, then there is just one self-conjugate* Spin^c *structure $[p/2q]$, and*

$$\underline{d}(S^3_{p/q}(K),[p/2q]) = d(S^3_{p/q}(K),[p/2q]),$$
$$\overline{d}(S^3_{p/q}(K),[p/2q]) = d(L(p,q),[p/2q]).$$

22.9. 0-surgeries

As a final variation on the surgery formula, we discuss 0-surgeries. Suppose K is a null-homologous knot in an integer homology 3-sphere Y. It follows from [**OS08b**, Section 4.8] that $CF^-(Y_0(K),[0]) \simeq \mathrm{Cone}(v_0+h_0\colon A_0 \to B_0)$. There is also a simple analog of Theorem 20.1 which holds for 0-surgeries. The proof of Theorem 20.1 carries over to show that $CFI^-(Y_0(K),[0])$ is homotopy equivalent over the ring $\mathbb{F}[U,Q]/Q^2$ to a chain complex of the form

(22.33)



where

$$D_0 = v_0 + h_0,$$
$$\iota_{\mathbb{A}} = \iota_K,$$
$$\iota_{\mathbb{B}} = \mathfrak{F}_0\iota_K.$$

Mirroring this, if $\mathscr{C}$ is an ι_K-complex of L-space type, we can construct an algebraic version of the involutive mapping cone complex $\mathbb{XI}^{\mathrm{alg}}_0(\mathscr{C})$, with underlying chain complex as in (22.33), which is characterized by the additional requirement that $h_0 = \mathfrak{F}_0\widetilde{v}_0$ and $H_0 = H\widetilde{v}$, for an $\mathbb{F}[U]$-equivariant map $H\colon \widetilde{B}_0 \to B_0$. Theorem 21.1 extends into this setting to show that if K is a knot in S^3, then

$$CFI^-(S^3_0(K),[0]) \simeq \mathbb{XI}^{\mathrm{alg}}_0(CFK^\infty(K),\iota_K).$$

This is a free offprint provided to the author by the publisher. Copyright restrictions may apply.

Bibliography

[BEH+03] F. Bourgeois, Y. Eliashberg, H. Hofer, K. Wysocki, and E. Zehnder, *Compactness results in symplectic field theory*, Geom. Topol. **7** (2003), 799–888, DOI 10.2140/gt.2003.7.799. MR2026549

[CM07] K. Cieliebak and K. Mohnke, *Symplectic hypersurfaces and transversality in Gromov-Witten theory*, J. Symplectic Geom. **5** (2007), no. 3, 281–356, DOI 10.4310/jsg.2007.v5.n3.a2. MR2399678

[Dai19] I. Dai, *Connected Heegaard Floer homology of sums of Seifert fibrations*, Algebr. Geom. Topol. **19** (2019), no. 5, 2535–2574, DOI 10.2140/agt.2019.19.2535. MR4023322

[DHST23] I. Dai, J. Hom, M. Stoffregen, and L. Truong, *An infinite-rank summand of the homology cobordism group*, Duke Math. J. **172** (2023), no. 12, 2365–2432, DOI 10.1215/00127094-2022-0082. MR4654053

[DHST21] I. Dai, J. Hom, M. Stoffregen, and L. Truong, *More concordance homomorphisms from knot Floer homology*, Geom. Topol. **25** (2021), no. 1, 275–338, DOI 10.2140/gt.2021.25.275. MR4226231

[DM19] I. Dai and C. Manolescu, *Involutive Heegaard Floer homology and plumbed three-manifolds*, J. Inst. Math. Jussieu **18** (2019), no. 6, 1115–1155, DOI 10.1017/s1474748017000329. MR4021102

[DS19] I. Dai and M. Stoffregen, *On homology cobordism and local equivalence between plumbed manifolds*, Geom. Topol. **23** (2019), no. 2, 865–924, DOI 10.2140/gt.2019.23.865. MR3939054

[EGH00] Y. Eliashberg, A. Givental, and H. Hofer, *Introduction to symplectic field theory*, Geom. Funct. Anal. **Special Volume** (2000), 560–673, DOI 10.1007/978-3-0346-0425-3_4. GAFA 2000 (Tel Aviv, 1999). MR1826267

[FS85] R. Fintushel and R. J. Stern, *Pseudofree orbifolds*, Ann. of Math. (2) **122** (1985), no. 2, 335–364, DOI 10.2307/1971306. MR808222

[FS90] R. Fintushel and R. J. Stern, *Instanton homology of Seifert fibred homology three spheres*, Proc. London Math. Soc. (3) **61** (1990), no. 1, 109–137, DOI 10.1112/plms/s3-61.1.109. MR1051101

[Fur90] M. Furuta, *Homology cobordism group of homology* 3*-spheres*, Invent. Math. **100** (1990), no. 2, 339–355, DOI 10.1007/BF01231190. MR1047138

[GS80] D. E. Galewski and R. J. Stern, *Classification of simplicial triangulations of topological manifolds*, Ann. of Math. (2) **111** (1980), no. 1, 1–34, DOI 10.2307/1971215. MR558395

[Hed09] M. Hedden, *On knot Floer homology and cabling. II*, Int. Math. Res. Not. IMRN **12** (2009), 2248–2274, DOI 10.1093/imrn/rnp015. MR2511910

[HHL21] K. Hendricks, J. Hom, and T. Lidman, *Applications of involutive Heegaard Floer homology*, J. Inst. Math. Jussieu **20** (2021), no. 1, 187–224, DOI 10.1017/S147474801900015X. MR4205781

[HL19] K. Hendricks and R. Lipshitz, *Involutive bordered Floer homology*, Trans. Amer. Math. Soc. **372** (2019), no. 1, 389–424, DOI 10.1090/tran/7557. MR3968773

[HL24] M. Hedden and A. S. Levine, *A surgery formula for knot Floer homology*, Quantum Topol. **15** (2024), no. 2, 229–336, DOI 10.4171/qt/188. MR4725826

[HM17] K. Hendricks and C. Manolescu, *Involutive Heegaard Floer homology*, Duke Math. J. **166** (2017), no. 7, 1211–1299, DOI 10.1215/00127094-3793141. MR3649355

[HMZ18] K. Hendricks, C. Manolescu, and I. Zemke, *A connected sum formula for involutive Heegaard Floer homology*, Selecta Math. (N.S.) **24** (2018), no. 2, 1183–1245, DOI 10.1007/s00029-017-0332-8. MR3782421

This is a free offprint provided to the author by the publisher. Copyright restrictions may apply.

[Hom11] J. Hom, *A note on cabling and L-space surgeries*, Algebr. Geom. Topol. **11** (2011), no. 1, 219–223, DOI 10.2140/agt.2011.11.219. MR2764041

[HTT09] J. Hass, A. Thompson, and W. Thurston, *Stabilization of Heegaard splittings*, Geom. Topol. **13** (2009), no. 4, 2029–2050, DOI 10.2140/gt.2009.13.2029. MR2507114

[Joy02] A. Joyal, *Quasi-categories and Kan complexes*, J. Pure Appl. Algebra **175** (2002), no. 1-3, 207–222, DOI 10.1016/S0022-4049(02)00135-4. Special volume celebrating the 70th birthday of Professor Max Kelly. MR1935979

[JTZ21] A. Juhász, D. Thurston, and I. Zemke, *Naturality and mapping class groups in Heegaard Floer homology*, Mem. Amer. Math. Soc. **273** (2021), no. 1338, v+174, DOI 10.1090/memo/1338. MR4337438

[JZ20] A. Juhász and I. Zemke, *Contact handles, duality, and sutured Floer homology*, Geom. Topol. **24** (2020), no. 1, 179–307, DOI 10.2140/gt.2020.24.179. MR4080483

[JZ24] A. Juhász and I. Zemke, *Stabilization distance bounds from link Floer homology*, J. Topol. **17** (2024), no. 2, Paper No. e12338, 112, DOI 10.1112/topo.12338. MR4821354

[Lin17] F. Lin, *The surgery exact triangle in* Pin(2)*-monopole Floer homology*, Algebr. Geom. Topol. **17** (2017), no. 5, 2915–2960, DOI 10.2140/agt.2017.17.2915. MR3704248

[Lip06] R. Lipshitz, *A cylindrical reformulation of Heegaard Floer homology*, Geom. Topol. **10** (2006), 955–1096, DOI 10.2140/gt.2006.10.955. [Paging previously given as 955–1097]. MR2240908

[Lip14] R. Lipshitz, *Correction to the article: A cylindrical reformulation of Heegaard Floer homology [MR2240908]*, Geom. Topol. **18** (2014), no. 1, 17–30, DOI 10.2140/gt.2014.18.17. MR3158771

[Liv81] C. Livingston, *Homology cobordisms of* 3*-manifolds, knot concordances, and prime knots*, Pacific J. Math. **94** (1981), no. 1, 193–206. MR625818

[LL08] D. A. Lee and R. Lipshitz, *Covering spaces and* $\mathbb{Q}$*-gradings on Heegaard Floer homology*, J. Symplectic Geom. **6** (2008), no. 1, 33–59, `http://projecteuclid.org/euclid.jsg/1215032732`. MR2417439

[LOT16] R. Lipshitz, P. S. Ozsváth, and D. P. Thurston, *Bordered Floer homology and the spectral sequence of a branched double cover II: the spectral sequences agree*, J. Topol. **9** (2016), no. 2, 607–686, DOI 10.1112/jtopol/jtw003. MR3509974

[LOT18] R. Lipshitz, P. S. Ozsvath, and D. P. Thurston, *Bordered Heegaard Floer homology*, Mem. Amer. Math. Soc. **254** (2018), no. 1216, viii+279, DOI 10.1090/memo/1216. MR3827056

[LOT] R. Lipshitz, P. Ozsváth, and D. Thurston, *Bordered* HF^- *modules for the torus*. In preparation.

[Low08] A. M. Lowrance, *On knot Floer width and Turaev genus*, Algebr. Geom. Topol. **8** (2008), no. 2, 1141–1162, DOI 10.2140/agt.2008.8.1141. MR2443110

[Lur09] J. Lurie, *Higher topos theory*, Annals of Mathematics Studies, vol. 170, Princeton University Press, Princeton, NJ, 2009, DOI 10.1515/9781400830558. MR2522659

[Man16] C. Manolescu, *Pin(2)-equivariant Seiberg-Witten Floer homology and the triangulation conjecture*, J. Amer. Math. Soc. **29** (2016), no. 1, 147–176, DOI 10.1090/jams829. MR3402697

[Mat78] T. Matumoto, *Triangulation of manifolds*, Algebraic and geometric topology (Proc. Sympos. Pure Math., Stanford Univ., Stanford, Calif., 1976), Proc. Sympos. Pure Math., XXXII, Amer. Math. Soc., Providence, RI, 1978, pp. 3–6. MR520517

[MO10] C. Manolescu and P. S. Ozsváth, *Heegaard Floer homology and surgeries on links*, 2010. `arXiv:1011.1317`.

[Mon75] J. M. Montesinos, *Surgery on links and double branched covers of* S^3, Knots, groups, and 3-manifolds (Papers dedicated to the memory of R. H. Fox), Ann. of Math. Stud., No. 84, Princeton Univ. Press, Princeton, NJ, 1975, pp. 227–259. MR380802

[MS12] D. McDuff and D. Salamon, *J-holomorphic curves and symplectic topology*, 2nd ed., American Mathematical Society Colloquium Publications, vol. 52, American Mathematical Society, Providence, RI, 2012. MR2954391

[Mye83] R. Myers, *Homology cobordisms, link concordances, and hyperbolic* 3*-manifolds*, Trans. Amer. Math. Soc. **278** (1983), no. 1, 271–288, DOI 10.2307/1999315. MR697074

[Ném05] A. Némethi, *On the Ozsváth-Szabó invariant of negative definite plumbed 3-manifolds*, Geom. Topol. **9** (2005), 991–1042, DOI 10.2140/gt.2005.9.991. MR2140997

This is a free offprint provided to the author by the publisher. Copyright restrictions may apply.

[NW15] Y. Ni and Z. Wu, *Cosmetic surgeries on knots in S^3*, J. Reine Angew. Math. **706** (2015), 1–17, DOI 10.1515/crelle-2013-0067. MR3393360

[OS03] P. Ozsváth and Z. Szabó, *Absolutely graded Floer homologies and intersection forms for four-manifolds with boundary*, Adv. Math. **173** (2003), no. 2, 179–261, DOI 10.1016/S0001-8708(02)00030-0. MR1957829

[OS04a] P. Ozsváth and Z. Szabó, *Holomorphic disks and knot invariants*, Adv. Math. **186** (2004), no. 1, 58–116, DOI 10.1016/j.aim.2003.05.001. MR2065507

[OS04b] P. Ozsváth and Z. Szabó, *Holomorphic disks and topological invariants for closed three-manifolds*, Ann. of Math. (2) **159** (2004), no. 3, 1027–1158, DOI 10.4007/annals.2004.159.1027. MR2113019

[OS04c] P. Ozsváth and Z. Szabó, *Holomorphic disks and three-manifold invariants: properties and applications*, Ann. of Math. (2) **159** (2004), no. 3, 1159–1245, DOI 10.4007/annals.2004.159.1159. MR2113020

[OS05] P. Ozsváth and Z. Szabó, *On knot Floer homology and lens space surgeries*, Topology **44** (2005), no. 6, 1281–1300, DOI 10.1016/j.top.2005.05.001. MR2168576

[OS06] P. Ozsváth and Z. Szabó, *Holomorphic triangles and invariants for smooth four-manifolds*, Adv. Math. **202** (2006), no. 2, 326–400, DOI 10.1016/j.aim.2005.03.014. MR2222356

[OS08a] P. Ozsváth and Z. Szabó, *Holomorphic disks, link invariants and the multi-variable Alexander polynomial*, Algebr. Geom. Topol. **8** (2008), no. 2, 615–692, DOI 10.2140/agt.2008.8.615. MR2443092

[OS08b] P. S. Ozsváth and Z. Szabó, *Knot Floer homology and integer surgeries*, Algebr. Geom. Topol. **8** (2008), no. 1, 101–153, DOI 10.2140/agt.2008.8.101. MR2377279

[OS11] P. S. Ozsváth and Z. Szabó, *Knot Floer homology and rational surgeries*, Algebr. Geom. Topol. **11** (2011), no. 1, 1–68, DOI 10.2140/agt.2011.11.1. MR2764036

[OS18] P. Ozsváth and Z. Szabó, *Kauffman states, bordered algebras, and a bigraded knot invariant*, Adv. Math. **328** (2018), 1088–1198, DOI 10.1016/j.aim.2018.02.017. MR3771149

[OS04] P. Ozsváth and Z. Szabó, *Knot Floer homology, genus bounds, and mutation*, Topology Appl. **141** (2004), no. 1-3, 59–85, DOI 10.1016/j.topol.2003.09.009. MR2058681

[OS19] P. Ozsváth and Z. Szabó, *Bordered knot algebras with matchings*, Quantum Topol. **10** (2019), no. 3, 481–592, DOI 10.4171/QT/127. MR4002230

[OSS17] P. S. Ozsváth, A. I. Stipsicz, and Z. Szabó, *Concordance homomorphisms from knot Floer homology*, Adv. Math. **315** (2017), 366–426, DOI 10.1016/j.aim.2017.05.017. MR3667589

[Sak86] M. Sakuma, *On strongly invertible knots*, Algebraic and topological theories (Kinosaki, 1984), Kinokuniya, Tokyo, 1986, pp. 176–196. MR1102258

[Sar11] S. Sarkar, *Maslov index formulas for Whitney n-gons*, J. Symplectic Geom. **9** (2011), no. 2, 251–270, DOI 10.4310/jsg.2011.v9.n2.a5. MR2811652

[Sar15] S. Sarkar, *Moving basepoints and the induced automorphisms of link Floer homology*, Algebr. Geom. Topol. **15** (2015), no. 5, 2479–2515, DOI 10.2140/agt.2015.15.2479. MR3426686

[SS22] A. I. Stipsicz and Z. Szabó, *A note on thickness of knots*, Gauge theory and low-dimensional topology—progress and interaction, Open Book Ser., vol. 5, Math. Sci. Publ., Berkeley, CA, 2022, pp. 299–308. MR4600730

[Sto17] M. Stoffregen, *Manolescu invariants of connected sums*, Proc. Lond. Math. Soc. (3) **115** (2017), no. 5, 1072–1117, DOI 10.1112/plms.12060. MR3733559

[Sto20] M. Stoffregen, *Pin(2)-equivariant Seiberg-Witten Floer homology of Seifert fibrations*, Compos. Math. **156** (2020), no. 2, 199–250, DOI 10.1112/s0010437x19007620. MR4044465

[Wat11] L. Watson, *A surgical perspective on quasi-alternating links*, Low-dimensional and symplectic topology, Proc. Sympos. Pure Math., vol. 82, Amer. Math. Soc., Providence, RI, 2011, pp. 39–51, DOI 10.1090/pspum/082/2768652. MR2768652

[Wei94] C. A. Weibel, *An introduction to homological algebra*, Cambridge Studies in Advanced Mathematics, vol. 38, Cambridge University Press, Cambridge, 1994, DOI 10.1017/CBO9781139644136. MR1269324

This is a free offprint provided to the author by the publisher. Copyright restrictions may apply.

[Wen10a] C. Wendl, *Automatic transversality and orbifolds of punctured holomorphic curves in dimension four*, Comment. Math. Helv. **85** (2010), no. 2, 347–407, DOI 10.4171/CMH/199. MR2595183

[Wen10b] C. Wendl, *Lectures on holomorphic curves in symplectic and contact geometry*, 2010. `arXiv:1011.1690`, v 3.3.

[Wen23] C. Wendl, *Transversality and super-rigidity for multiply covered holomorphic curves*, Ann. of Math. (2) **198** (2023), no. 1, 93–230, DOI 10.4007/annals.2023.198.1.2. MR4593732

[ZZ15] K. Zehmisch and K. Zehmisch, *Holomorphic jets in symplectic manifolds*, J. Fixed Point Theory Appl. **17** (2015), no. 2, 379–402, DOI 10.1007/s11784-014-0178-z. MR3397123

[Zem15] I. Zemke, *Graph cobordisms and Heegaard Floer homology*, 2015. `arXiv:1512.01184`.

[Zem17] I. Zemke, *Quasistabilization and basepoint moving maps in link Floer homology*, Algebr. Geom. Topol. **17** (2017), no. 6, 3461–3518, DOI 10.2140/agt.2017.17.3461. MR3709653

[Zem19a] I. Zemke, *Connected sums and involutive knot Floer homology*, Proc. Lond. Math. Soc. (3) **119** (2019), no. 1, 214–265, DOI 10.1112/plms.12227. MR3957835

[Zem19b] I. Zemke, *Link cobordisms and absolute gradings on link Floer homology*, Quantum Topol. **10** (2019), no. 2, 207–323, DOI 10.4171/QT/124. MR3950650

[Zem19c] I. Zemke, *Link cobordisms and functoriality in link Floer homology*, J. Topol. **12** (2019), no. 1, 94–220, DOI 10.1112/topo.12085. MR3905679

[Zem21] I. Zemke, *Duality and mapping tori in Heegaard Floer homology*, J. Topol. **14** (2021), no. 3, 1027–1112, DOI 10.1112/topo.12206. MR4503956

This is a free offprint provided to the author by the publisher. Copyright restrictions may apply.

Editorial Information

To be published in the *Memoirs*, a paper must be correct, new, nontrivial, and significant. Further, it must be well written and of interest to a substantial number of mathematicians. Piecemeal results, such as an inconclusive step toward an unproved major theorem or a minor variation on a known result, are in general not acceptable for publication.

Papers appearing in *Memoirs* are generally at least 80 and not more than 200 published pages in length. Papers less than 80 or more than 200 published pages require the approval of the Managing Editor of the Transactions/Memoirs Editorial Board. Published pages are the same size as those generated in the style files provided for $\mathcal{AMS}$-LaTeX.

Information on the backlog for this journal can be found on the AMS website starting from `http://www.ams.org/memo`.

A Consent to Publish is required before we can begin processing your paper. After a paper is accepted for publication, the Providence office will send a Consent to Publish and Copyright Agreement to all authors of the paper. By submitting a paper to the *Memoirs*, authors certify that the results have not been submitted to nor are they under consideration for publication by another journal, conference proceedings, or similar publication.

Information for Authors

Memoirs is an author-prepared publication. Once formatted for print and on-line publication, articles will be published as is with the addition of AMS-prepared frontmatter and backmatter. Articles are not copyedited; however, confirmation copy will be sent to the authors.

Initial submission. The AMS uses Centralized Manuscript Processing for initial submissions. Authors should submit a PDF file using the Initial Manuscript Submission form found at `www.ams.org/submission/memo`, or send one copy of the manuscript to the following address: Centralized Manuscript Processing, MEMOIRS OF THE AMS, 201 Charles Street, Providence, RI 02904-2294 USA. If a paper copy is being forwarded to the AMS, indicate that it is for *Memoirs* and include the name of the corresponding author, contact information such as email address or mailing address, and the name of an appropriate Editor to review the paper (see the list of Editors below).

The paper must contain a *descriptive title* and an *abstract* that summarizes the article in language suitable for workers in the general field (algebra, analysis, etc.). The *descriptive title* should be short, but informative; useless or vague phrases such as "some remarks about" or "concerning" should be avoided. The *abstract* should be at least one complete sentence, and at most 300 words. Included with the footnotes to the paper should be the 2020 *Mathematics Subject Classification* representing the primary and secondary subjects of the article. The classifications are accessible from `www.ams.org/msc/`. The Mathematics Subject Classification footnote may be followed by a list of *key words and phrases* describing the subject matter of the article and taken from it. Journal abbreviations used in bibliographies are listed in the latest *Mathematical Reviews* annual index. The series abbreviations are also accessible from `www.ams.org/msnhtml/serials.pdf`. To help in preparing and verifying references, the AMS offers MR Lookup, a Reference Tool for Linking, at `www.ams.org/mrlookup/`.

Electronically prepared manuscripts. The AMS encourages electronically prepared manuscripts, with a strong preference for $\mathcal{AMS}$-LaTeX. To this end, the Society has prepared $\mathcal{AMS}$-LaTeX author packages for each AMS publication. Author packages include instructions for preparing electronic manuscripts, samples, and a style file that generates the particular design specifications of that publication series.

Authors may retrieve an author package for *Memoirs of the AMS* from `www.ams.org/journals/memo/memoauthorpac.html`. The *AMS Author Handbook* is available in PDF format from the author package link. The author package can also be obtained free of charge by sending email to `tech-support@ams.org` or from the Publication Division,

This is a free offprint provided to the author by the publisher. Copyright restrictions may apply.

American Mathematical Society, 201 Charles St., Providence, RI 02904-2294, USA. When requesting an author package, please specify the publication in which your paper will appear. Please be sure to include your complete mailing address.

After acceptance. The source files for the final version of the electronic manuscript should be sent to the Providence office immediately after the paper has been accepted for publication. The author should also submit a PDF of the final version of the paper to the editor, who will forward a copy to the Providence office.

Accepted electronically prepared files can be submitted via the web at `www.ams.org/submit-book-journal/`, sent via FTP, or sent on CD to the Electronic Prepress Department, American Mathematical Society, 201 Charles Street, Providence, RI 02904-2294 USA. TEX source files and graphic files can be transferred over the Internet by FTP to the Internet node `ftp.ams.org` (130.44.1.100). When sending a manuscript electronically via CD, please be sure to include a message indicating that the paper is for the *Memoirs*.

Electronic graphics. Comprehensive instructions on preparing graphics are available at `www.ams.org/authors/journals.html`. A few of the major requirements are given here.

Submit files for graphics as EPS (Encapsulated PostScript) files. This includes graphics originated via a graphics application as well as scanned photographs or other computer-generated images. If this is not possible, TIFF files are acceptable as long as they can be opened in Adobe Photoshop or Illustrator.

Authors using graphics packages for the creation of electronic art should also avoid the use of any lines thinner than 0.5 points in width. Many graphics packages allow the user to specify a "hairline" for a very thin line. Hairlines often look acceptable when proofed on a typical laser printer. However, when produced on a high-resolution laser imagesetter, hairlines become nearly invisible and will be lost entirely in the final printing process.

Screens should be set to values between 15% and 85%. Screens which fall outside of this range are too light or too dark to print correctly. Variations of screens within a graphic should be no less than 10%.

Any graphics created in color will be rendered in grayscale for the printed version unless color printing is authorized by the Managing Editor and the Publisher. In general, color graphics will appear in color in the online version.

Inquiries. Any inquiries concerning a paper that has been accepted for publication should be sent to `memo-query@ams.org` or directly to the Electronic Prepress Department, American Mathematical Society, 201 Charles St., Providence, RI 02904-2294 USA.

This is a free offprint provided to the author by the publisher. Copyright restrictions may apply.

Editors

The AMS uses Centralized Manuscript Processing for initial submissions to AMS journals. Authors should follow instructions listed on the Initial Submission page found at www.ams.org/tran/transubmit.html.

This journal is designed particularly for long research papers, normally at least 80 pages in length, and groups of cognate papers in pure and applied mathematics. Papers intended for publication in the *Memoirs* should be addressed to one of the following editors. The AMS uses Centralized Manuscript Processing for initial submissions to AMS journals. Authors should follow instructions listed on the Initial Submission page found at www.ams.org/memo/memosubmit.html

Managing Editor: Radha Kessar, Department of Mathematics, The Alan Turing Building, The University of Manchester, Oxford Road, Manchester M13 9PL United Kingdom; e-mail: radha.kessar@manchester.ac.uk

1. GEOMETRY, TOPOLOGY & LOGIC
Coordinating Editor: Mariya Ivanova Soskova, Department of Mathematics, University of Wisconsin–Madison, Madison, WI 53706 USA; e-mail: msoskova@math.wisc.edu

Algebraic topology, Bob Oliver, LAGA, Institut Galilée, Université Sorbonne Paris Nord, 99, Av. J-B Clément, 93430 Villetaneuse, France; e-mail: bobol@math.univ-paris13.fr

Arithmetic geometry and number theory, Megumi Harada, Department of Mathematics and Statistics, McMaster University, 1280 Main Street West, Hamilton, Ontario L8S 4K1, Canada; e-mail: haradam@mcmaster.ca

Geometric group theory and low-dimensional geometry and topology, Christopher Leininger, Department of Mathematics, Rice University, Houston, TX 77005 USA; e-mail: cjl12@rice.edu

Geometric topology, Jennifer Hom, School of Mathematics, Georgia Institute of Technology, 686 Cherry Street, Atlanta, GA 30332 USA; e-mail: jhom6@gatech.edu

Homotopy theory, higher category theory, and geometric applications, Clark Barwick, School of Mathematics, University of Edinburgh, James Clerk Maxwell Building, Peter Guthrie Tait Road, Edinburgh, EH9 3FD, United Kingdom; e-mail: clarkbarAMS@pm.me

Logic, Mariya Ivanova Soskova

2. ALGEBRA & NUMBER THEORY
Coordinating Editor: Daniel Krashen, 3E6 David Rittenhouse Lab., University of Pennsylvania, Department of Mathematics, 209 South 33rd Street, Philadelphia, PA 19104 USA; e-mail: daniel.krashen@gmail.com

Algebra, algebraic and arithmetic geometry, Daniel Krashen

Arithmetic algebraic geometry, Jennifer Balakrishnan, Department of Mathematics and Statistics, 665 Commonwealth Avenue, Boston University, Boston, MA 02215 USA; e-mail: jbala@bu.edu

Algebraic geometry, Renzo Cavalieri, Department of Mathematics, Colorado State University, Weber Building, Fort Collins, CO 80523 USA; e-mail: renzo@colostate.edu

Analytic number theory, Dimitris Koukoulopoulos, Université de Montréal, Pavillon André-Aisenstadt, 2920, chemin de la Tour, H3T 1J4, Montréal, QC, Canada; e-mail: dimitris.koukoulopoulos@umontreal.ca

Arithmetic geometry and number theory, David Loeffler, Faculty of Mathematics and Computer Science, UniDistance Suisse, Schinerstrasse 18, 3900 Brig-Glis, Switzerland; e-mail: david.loeffler@unidistance.ch

Associative rings and algebras, category theory, homological algebra, group theory and generalizations, Daniel Nakano, Department of Mathematics, University of Georgia, Athens, Georgia 30602 USA; e-mail: nakano@uga.edu

Commutative algebra, Henry Schenck, Department of Mathematics and Statistics, Auburn University, 315 Roosevelt Concourse, Auburn, AL 36849 USA; e-mail: hks0015@auburn.edu

Representation theory and group theory, Radha Kessar, Department of Mathematics, The Alan Turing Building, The University of Manchester, Oxford Road, Manchester M13 9PL United Kingdom; e-mail: radha.kessar@manchester.ac.uk

3. GEOMETRIC ANALYSIS & PDE
Coordinating Editor: Joachim Krieger, Bâtiment de Mathématiques, École Polytechnique Fédérale de Lausanne, Station 8, 1015 Lausanne Vaud, Switzerland; e-mail: joachim.krieger@epfl.ch

Elliptic and parabolic PDEs, geometric analysis, Yannick Sire, Department of Mathematics, Johns Hopkins University, 404 Krieger Hall, 3400 N. Charles Street, Baltimore, MD 21218 USA; e-mail: ysire1@jhu.edu

Elliptic and parabolic PDEs, geometric analysis, Ben Weinkove, Mathematics Department, Northwestern University, 2033 Sheridan Rd, Evanston, IL 60201 USA; e-mail: weinkove@math.northwestern.edu

Harmonic analysis and partial differential equations, Monica Visan, Department of Mathematics, University of California Los Angeles, 520 Portola Plaza, Los Angeles, CA 90095 USA; e-mail: visan@math.ucla.edu

Nonlinear Fourier and harmonic analysis and partial differential equations, Andrea R. Nahmod, Department of Mathematics and Statistics, University of Massachusetts Amherst, 710 N. Pleasant St. Lederle GRT, Amherst, MA 01003 USA; e-mail: nahmod@umass.edu

Partial differential equations, calculus of variations, optimizations and control theory, dynamical systems, Wilfrid Gangbo, College of Physical Sciences, UCLA, 520 Portola Plaza, Los Angeles, CA 90095 USA; e-mail: wgangbo@math.ucla.edu

Real analysis and partial differential equations, Joachim Krieger

4. ANALYSIS & DYNAMICS
Coordinating Editor: Krzysztof Frączek Faculty of Math and Computer Science, Nicolaus Copernicus University, Ul. Chopina 12/18 87-100 Toruń, Poland; e-mail: fraczek@mat.umk.pl

Functional analysis, probability and ergodic theory, Tim Austin, Department of Mathematics, University of California, Los Angeles, Los Angeles, CA 90095 USA; e-mail: tim@math.ucla.edu

Ergodic theory and dynamical systems, Krzysztof Frączek

Ergodic theory, applications to combinatorics and number theory, Nikos Frantzikinakis, University of Crete, Rethymno, Crete, Greece; e-mail: frantzikinakis@gmail.com

Functional analysis, groups and operator algebras, analysis in quantum information theory, Magdalena Musat, Department of Mathematical Sciences, University of Copenhagen, Universitetsparken 5, 2100 Copenhagen, Denmark; e-mail: musat@math.ku.dk

Operator algebras and ergodic theory, David Kerr, Mathematisches Institut, University of Münster, Einsteinstrasse 62, 48149 Münster, Germany; e-mail: kerrd@uni-muenster.de

5. PROBABILITY & COMBINATORICS
Coordinating Editor: Davar Khoshnevisan, Department of Mathematics, The University of Utah, Salt Lake City, UT 84112 USA; e-mail: davar@math.utah.edu

Combinatorics, Jacob Fox, Department of Mathematics, 450 Jane Stanford Way, Building 380, Stanford, CA 94305 USA; e-mail: jacobfox@stanford.edu

Enumeration, algebraic combinatorics, integrable probability, symmetric functions, Sylvie Corteel, Department of Mathematics, University of California, Berkeley, Berkeley, CA 94720 USA; CNRS, IRIF et Université Paris Cité, Paris, France; e-mail: corteel@berkeley.edu

Probability theory and statistical physics, Jian Ding, School of Mathematical Sciences, Peking University, Beijing 100871, China; e-mail: dingjian@math.pku.edu.cn

Probability theory and stochastic analysis, Davar Khoshnevisan

Probability theory, probabilistic combinatorics, statistical physics, Eyal Lubetzky, Department of Mathematics, Courant Institute of Mathematical Sciences, New York University, New York, NY 10012 USA; e-mail: eyal@courant.nyu.edu

This is a free offprint provided to the author by the publisher. Copyright restrictions may apply.

1644 **Mike Miller Eismeier,** Equivariant Instanton Homology, 2026

1643 **Matthew Cordes, Tobias Hartnick, Vera Tonić, and Simon Machado,** Foundations of Geometric Approximate Group Theory, 2026

1642 **Leonor Godinho, Grace T. Mwakyoma-Oliveira, and Daniele Sepe,** Classification of Hamiltonian S^1-Actions on Compact Symplectic Orbifolds with Isolated Cyclic Singular Points in Dimension Four, 2026

1641 **Antoine Jego, Titus Lupu, and Wei Qian,** Conformally Invariant Fields Out of Brownian Loop Soups, 2026

1640 **Qi Chen, Shijin Ding, Zhilin Lin, and Zhifei Zhang,** Nonlinear Stability for 3-D Plane Poiseuille Flow in a Finite Channel, 2026

1639 **Hezi Halawi and Avner Segal,** Poles, Residues and Siegel-Weil Identities of Degenerate Eisenstein Series on Split Exceptional Groups of Type E_n, 2026

1638 **Eusebio Gardella and Martino Lupini,** The Complexity of Conjugacy, Orbit Equivalence, and von Neumann Equivalence of Actions of Nonamenable Groups, 2026

1637 **Kim Morrison, Noah Snyder, and Dylan P. Thurston,** Towards the Quantum Exceptional Series, 2026

1636 **Irakli Patchkoria and Piotr Pstrągowski,** Adams Spectral Sequences and Franke's Algebraicity Conjecture, 2026

1635 **Denis Benois and Kâzım Büyükboduk,** Arithmetic of Critical p-Adic L-Functions, 2026

1634 **Damian Dąbrowski and Xavier Tolsa,** The Measures with L^2-Bounded Riesz Transform and the Painlevé Problem, 2026

1633 **Adam Gyenge, Clemens Koppensteiner, and Timothy Logvinenko,** The Heisenberg Category of a Category, 2026

1632 **J. R. Frisch, A. S. Kechris, F. Shinko, and Z. Vidnyánszky,** Realizations of Countable Borel Equivalence Relations, 2026

1631 **Yu Deng and Zaher Hani,** Derivation of the Wave Kinetic Equation: Full Range of Scaling Laws, 2026

1630 **Andrea Merlo, Mihalis Mourgoglou, and Carmelo Puliatti,** On the Density Problem in the Parabolic Space, 2026

1629 **Jieliang Hong,** Rescaled SIR Epidemic Processes Converge to Super-Brownian Motion in Four or More Dimensions, 2026

1628 **Nikolay Konovalov,** Algebraic Goodwillie Spectral Sequence, 2026

1627 **Kaiwen Sun, Haowu Wang, and Brandon Williams,** Hyperbolization of Affine Lie Algebras, 2026

1626 **Brian Lehmann, Eric Riedl, and Sho Tanimoto,** Non-Free Sections of Fano Fibrations, 2026

1625 **Johannes Carmesin,** Embedding Simply Connected 2-Complexes in 3-Space, 2026

1624 **Bjoern Bringmann and Sky Cao,** A Para-Controlled Approach to the Stochastic Yang-Mills Equation in Two Dimensions, 2026

1623 **Ben Elias,** Gaitsgory's Central Sheaves via the Diagrammatic Hecke Category, 2026

1622 **Ruyong Feng and Michael Wibmer,** Differential Galois Groups, Specializations and Matzat's Conjecture, 2026

1621 **Mikhail Borovoi, Tasho Kaletha, and Vladimir Hinich,** Galois Cohomology of Reductive Groups over Global Fields, 2026

1620 **Jian Ding, Zherui Fan, and Lu-Jing Huang,** Uniqueness of the Critical Long-Range Percolation Metrics, 2026

For a complete list of titles in this series, visit the
AMS Bookstore at **www.ams.org/bookstore/memoseries/**.

This is a free offprint provided to the author by the publisher. Copyright restrictions may apply.